TITLE:

STUDY OF THE EFFECT OF THERMAL ALTERATION ON CONFORMANCE EFFICIENCY IN IN-SITU THERMAL RECOVERY PROCESS [Part of Energy, Mines and Resources 50/50 Cost Shared Program and part of the Program of the Federal Panel on Energy Research and Development (PERD)]

Final Report
by:

B.P. Erno
R. Saetre
C. Tsang

Work on the project was conducted under the auspices of the Canada Centre for Mineral and Energy Technology, Energy, Mines and Resources Canada.

DSS File No. 06SQ.23440-7-9060
DSS Contract Serial No. 23440-7-9060/01-SQ
CANMET Scientific Authority: A. George

Date: March 1989

MICROMEDIA

89-05083/

EXECUTIVE SUMMARY

In accordance with the project description as given in the contract, experimental work has been completed in several different areas all related to understanding and improving thermal recovery of heavy oil.

Consistent with the diversity of the various topics, the results have been presented as five separately bound reports. The first of these, completed in March 1988, (Progress Report) collected the work included under Tasks 1,2 5 and 7. The remainder of the work, under Tasks 3&4, 6, 8 and 9, is reported in the 4 additional volumes.

In Task 1, an extensive review of relevant literature was completed. Topics reviewed included oil viscosity variability, thermal alteration of oil, relationship of oil viscosity to asphaltene content, steam distillation, and applications of instrumental thermal analysis techniques.

Task 2 involved a study of the natural variability of oil within a single heavy oil reservoir. In three different reservoirs, oil viscosity was found to increase with increasing depth of origin of the sample. Possible reasons for this variability, and potential impacts of it on thermal recovery processes, are discussed in the report. Results of this work have also been prepared as a paper to be presented at the Annual Technical Meeting of the Petroleum Society of C.I.M., in May 1989.

The relationship between asphaltene content and oil viscosity was investigated in Task 5. Asphaltene content was varied by mixing together different amounts of asphaltenes and maltenes, using a specialized procedure. For two heavy oils originating from Lloydminster reservoirs, oil viscosity increased almost logarithmically with increasing asphaltene content. This behavior, which is not predicted by any simple theoretical models, is nevertheless consistent with results from analogous systems reported by others, and has been attributed to aggregation of the heavier components within the mixture. Variations in the concentration of asphaltenes can account for the viscosity variations observed both in native oil and thermally produced oil samples from a single reservoir.

The contribution of steam distillation to thermal oil recovery was explored in Task 7. A series of linear corefloods was performed in an attempt to assess the relative contribution of this potential recovery mechanism. The results of these experiments did not show any significant contribution from steam distillation. Oil of reduced viscosity was produced, however, confirming that steam distillation/evaporation was taking place. Calculations based on oil properties and published correlations predict that steam distillation could recover as much as 15 % of the oil in place. These

discrepancies, together with the problems encountered in performing the experiments, add considerable uncertainty to the conclusions.

Thermal alteration of two Lloydminster heavy oils was investigated in Tasks 3 and 4. Oil samples were heated in a sealed reactor for various times and temperatures, and changes in oil properties and composition were determined. Heating at 270 C for periods of hours to days causes a slow increase in oil viscosity, whereas heating at temperatures above 300 C, results in rapid and large viscosity reductions. The former changes are suspected to be due to polymerization of reactive components within the oil, whereas the latter changes are attributed to thermal cracking. Thermal cracking was confirmed by compositional analyses of the products. The presence of water or steam in the reactor appears to suppress thermal cracking reactions. Partial oxidation of the oil prior to heating increases the amount of coke formed, but has little effect on the liquid or gas composition.

In Task 6, the potential impact of thermal alteration of oil on flow behavior was explored. No changes in permeability were detected during flow of heavy oil, or oil plus steam, through a sandpack at 200 C and elevated pressure. Abrupt changes in oil viscosity had only very minor affect on oil recovery by hot water or gas.

Applications, of instrumental thermal analysis methods were explored and evaluated in Task 8. Thermogravimetric (TG) curves were collected for oil samples under a variety of conditions. Since the relative importance of different reactions changes with heating rate, complete and consistent explanation of the variations in the curves was possible only by including experiments at various heating rates. TG analysis was found to be fairly insensitive to the thermal history of the sample, although a correlation with sample viscosity was apparent. It was confirmed that partial oxidation increases coke production during subsequent thermal cracking. Attempts to identify an "ignition" temperature for a heavy oil were unsuccessful, in contrast to reports of others. Although the usefulness of TG for gaining certain information about the thermal behavior of heavy oils was confirmed, the lack of fundamental numerical description of the curves prevents quantitative interpretation.

Task 9 gives a review of the numerical simulators which have been developed over the past 20 years to help understand and predict the performance of thermal recovery processes. The report focuses on simulation of in situ combustion, because this process is the most complex, and because almost all oil recovery mechanisms could be operative in a reservoir undergoing insitu combustion. Weaknesses in existing numerical models are identified, and some suggestions are made on how they might be overcome. More significantly, however, it is concluded that development of better thermal simulators is presently restricted by the lack of experimental data needed to describe processes such as thermal cracking and emulsification, and better theoretical descriptions of unstable multi-phase flow. The results of Tasks 2 through 8 begin to address some of these needs, but much additional work will be required before numerical models can be built which correctly describe the chemical and physical processes occurring in a reservoir during in situ combustion.

Summarie Executif

Suite à la description du projet donner dans le contrat, la recherche experimentale est completée dans plusieurs domaines qui sont tous liés à comprendre et à améliorer la récupération du pétrole lourd.

En accordance la diversité des sujets différents, les résultats sont presente dans cinq rapports. Le premier rapport, complete en mars 1988, contient les travaux fournis dans les tâches 1,2,5 et 7. Les restes des travaux, fournis dans les tâches 3,4,6,8 et 9, sont rapporte en quartre volumes additionels.

Une revue des litèratures à propos a été presente dans la tâche 1. La variabilité de la viscosité et le changement thérmique du pétrole, dépendence de sa viscosité sur le contenue en asphaltène, distillation à vapeur, et applications des techniques thérmiques ont été examiner dans la tâche 1.

Tâche 2 contient une étude de la variabilité naturelle de la viscosité du pétrole dans trois reservoirs pétroliers. La viscosité du pétrole semble à augmenter avec la profondeur de l' échantillon. Les courbes de cette variation, et son effet sur la récupération thérmique ont été discuté dans ce rapport. Ces résultats sont aussi utilise pour une publication à presenter à la rencontre Annuelle Technicale de la Société de Pétrole en mai, 1989.

La relation entre le contenue d'asphaltène et la viscosité du pétrole est investiguer dans la tâche 5. Pour deux échantillons des reservoirs à Lloydminster, la viscosité du pétrole augmente presque logarithmiquement. Cela est attribuér à l'aggregation des composants lourds dans un mélange. La variation en concentration des asphaltènes contribue à la variation de la viscosité du pétrole.

La contribution de la distillation à vapeur est explorer dans la tâche 7. Une series d'essais était conduite à fin d'évaluer la contribution de cette mécanisme de récupération. Les résultats indiquent que la distillation à vapeur ne joue pas un rôle important. Méme si la distillation était en place, la récupération était seulement 15% de l'huile en place.

L'altèration thérmique de deux échantillions du pétrole de Lloydminster était investiguer en Tâches 3 et 4. Les échantillons étaient chaufer dans un reacteur pour une durée et a températures variées, et le changement en composition était déterminer. Chauffage à 270°C pendant une période de quelques heures à plusieurs jours tendait à augmenter la viscosité. Au dessus de 300°C, la viscosité chute rapidement. Une augmention en viscosité est peutêtre due à polymerization des composants reactifs, tandis que la chute au dessus de 300°C est due au craquage thérmique. Cela était confirmer par l'analyse des produits. La presence de l'eau ou la vapeur dans le reacteur semble à diminuer les taux de réaction de craquage. Oxidation partiale avant le chauffage augmente la quantité du coke produit, mais ne fait rien à la phase liquide ou gazeuse.

Dans la tâche 6, l'effet de l'alteration thérmique sur l'écoulement du pétrole était explorer. Aucun changement en permeabilité était remarquer pendant l'écoulement du pétrole lourd, ou l'huille et vapeur combinés dans un mileu poreux à 200°C et à une pression élevée. Changement brusque en viscosité d'huile avait un effet négligeable sur la récupération d'huile par du gaz ou de l'eau chaude.

L'application des techniques d'analyse thérmique était explorer et évaluer dans la Tâche 8. Les courbes de gravimétrie thérmique étaient obtenues pour les échantillons du pétrole sous conditions variées. L'analyse de gravimétrie thérmique a prouvé indiffèrent à l'histoire de l'échantillonage, méme qu'une correlation avec la viscosité de l'échantillon soit apparent. Le fait que l'oxidation partiale augmente la production du coke pendent le craquage thérmique a été confirmer.

La tâche 9 présente une revue des modèles mathématiques dévelopés pendent les derniers ans. Ce rapport concentre sur la combustion in situ, parce que cela est le plus complex et les autres mécanismes thérmiques font partis de ceçi. Les problèmes reliés à ces modéles sont remarquér et quelques suggestions sont donners à fin de les résondre. De plus importance, il est conclu que la manque de données experimentales en craquage thérmique et l'émulsification est plus sévère que les autres problems numèriques. Les résultats de Tâche 2 à 8 avancent ces données, même si la modèle mathématique décrivant les phénomènes chimiques et physiques dans une combustion in situ soit loin d'être établie.

NOVA HUSKY
RESEARCH
CORPORATION

**CLASSIFICATION: NHRC, NOVA, Husky
and Subsidiaries
REPORT NUMBER: 00320**

A STUDY OF THE EFFECT OF THERMAL ALTERATION ON CONFORMANCE EFFICIENCY IN IN-SITU THERMAL RECOVERY PROCESSES

PROGRESS REPORT

March, 1988

Authors

B. Erno
R. Saetre
C. Tsang

168 pp

Department: Enhanced Oil Recovery/Analytical/Chemical Process Development
Project No: 687-048
Prepared for: Roger Lafleur - ENERGY MINES RESOURCES

Keywords: heavy oil, cracking, distillation, viscosity, asphaltenes, coreflooding, steam stimulation, fireflood

This report contains the valuable proprietary and confidential information of the NOVA HUSKY RESEARCH CORPORATION, and may not be used, disclosed or reproduced without permission in writing from NOVA HUSKY RESEARCH CORPORATION.

(C) 1988 NOVA HUSKY RESEARCH CORPORATION

MICROMEDIA

DISTRIBUTION LIST

	Copies
EMR:	
Dr. Roger Lafleur,	2
NOVA HUSKY RESEARCH CORPORATION:	
B. Erno	3
R. Saetre	1
C. Tsang	1
Library	2
Total Number of Copies	9

TABLE OF CONTENTS

Page

1.0 SUMMARY 1

2.0 LITERATURE REVIEW (TASK 1)

2.1 Oil Viscosity Variability 2
2.2 Thermal Alteration of Petroleum 3

2.2.1 Temperature Range of 200°-330°C
2.2.2 Temperature Range of 330°-500°C 7
2.2.3 Effects of Pressure 10
2.2.4 Effects of Reservoir Minerals
2.2.5 Effects of Air 11
2.2.6 Kinetics of Thermal Alteration 12

2.3 Influence of Asphaltenes on Oil Viscosity 25
2.4 Contribution of Steam Distillation to Thermal Recovery 27
2.5 Instrumental Thermal Analysis Techniques 32
2.6 References 38

2.6.1 Oil Viscosity Variability
2.6.2 Thermal Alteration of Petroleum
2.6.3 Influence of Asphaltenes on Oil Viscosity 39
2.6.4 Steam Distillation
2.6.5 Instrumental Thermal Analysis Techniques 40

3.0 OIL VISCOSITY VARIABILITY IN THE CARIBOU RESERVOIR (TASK 2)

3.1 Summary 44
3.2 Introduction
3.3 Methods 45

3.3.1 Oil Sample Preparation
3.3.2 Measurements

3.4 Results and Discussion 46
3.5 Conclusions 48
3.6 Tables 50
3.7 Figures 56

4.0 INVESTIGATION OF THE INFLUENCE OF ASPHALTENES ON OIL VISCOSITY (TASK 5)

4.1 Summary 78
4.2 Introduction
4.3 Materials and Methods 79
4.4 Results 82
4.5 Conclusions 88
4.6 Tables 89
4.7 Figures 94
4.8 Appendices 99

5.0 STEAM DISTILLATION STUDIES (TASK 7)

5.1 Summary 114
5.2 Introduction
5.3 Experimental 115

5.3.1 Materials
5.3.2 Methods 116

5.3.2.1 Vapour Pressure Measurements
5.3.2.2 Sandpack Flood Experiments 117

5.4 Results and Discussion 121

5.4.1 Vapour Pressure Measurements
5.4.2 Flood Experiments

5.4.2.1 Initial Sandpack Characteristics 122
5.4.2.3 Heat-up to 200C
5.4.2.4 Hot Waterfloods 123
5.4.2.5 Steam and Gas Floods 124
5.4.2.5 Comparison of Production Data 125
5.4.2.6 Evidence of Steam Distillation 126
5.4.2.7 Comparisons with Earlier Work 127

5.5 Conclusions 128
5.6 Tables 129
5.7 Figures 146

ACKNOWLEDGEMENTS

The laboratory experiments described in this Report were carried out by Dwayne Davis and Janet Chriest, with analytical support from Karen Black and Lori Blight, all of NHRC.

We thank Husky Oil for providing samples of oil and reservoir sand, and particularly thank Alberta Energy Co. and Husky Oil for making available samples of preserved core from Caribou Lake.

Our appreciation is also extended to Ruth Glover and Sonja Bender for their efforts in assembling and typing this report.

1.0 SUMMARY

This Progress Report collects together work completed in four of the Tasks included in the Project description.

Section 2.0 is a review of relevant literature in five different areas all related to understanding thermal recovery processes.

Results of a study of the variability of native oil viscosity in the Caribou Lake heavy oil area are given in Section 3.0. Oil viscosity was found to increase significantly with depth in a number of wells completed in the Clearwater B formation. The viscosity variations were confirmed to be a reflection of compositional variability in the heavy oil.

In Section 4.0, the relationship between asphaltene content and viscosity is explored for two Lloydminster heavy oils. Viscosity increases by about 20% for every 1% increase in asphaltene concentration.

The experiments described in Section 5.0 attempted to determine the contribution of steam distillation to oil recovery by steam. Although definite evidence of distillation was seen in some of the produced oil, the recovery data suggest that the contribution from distillation was small. Further experiments in this area are required to better define the variables, particularly the effect of a condensing front.

2.0 LITERATURE REVIEW (TASK 1)

2.1 Oil Viscosity Variability

Compositional variability within an individual reservoir has been observed all over the world. Hunt [1] cites a number of examples, including the Coalinga field in California, the Lagunillas field in Venezuela, the Sakhalin field in the U.S.S.R., and the Burgan field in Kuwait which show dramatic variations in oil viscosity and density with location and/or depth. In some reservoirs, sharp transitions from light oil to heavy asphaltic oil occur near the oil-water contact. In other fields, there is a more gradual change from light to heavy oil, as for example, in the Seria field in Borneo, where the oil varies from 19 to 37 API as the depth increases from 300 to 3000 m [1], or in the Lagunillas field in Venezuela, where oil varies from 10 to 36 API in different locations in the reservoir.

Hirschberg [2] has discussed the processes believed to be responsible for compositional variation. In many light oil reservoirs, compositional gradation is attributed to gravitational segregation among hydrocarbons, which leads to oil having increasing amounts of higher molecular weight compounds towards the bottom of the reservoir. This process and its implications have also been discussed by Schulte [3], using the Brent reservoir in the North Sea as an example. A gravitational equilibrium model was developed which accounted for some of the observed variations in composition and PVT behavior. From the modelling it was concluded that compositional gradation increased with increasing aromatics fraction and decreasing pressure. Observed variations in oil bubble point, gas dew point, and gas-oil miscibility could be explained.

Compositional gradation in moderately heavy oil reservoirs (20-30 API) has also been attributed to gravitational effects. Hirschberg [2] gives data from a North African field, in which oil viscosity varies from 2 to 12 mPa.s as the elevation decreases 60 m. In this case, modelling results suggest that settling of asphalt (asphaltenes plus resins) aggregates, rather than asphaltenes alone, is the primary cause of the variation. Consideration is also given to the extreme case of a tar mat at the bottom of a formation. Two types of behavior are predicted by the model. When the asphalt and oil are miscible in any proportions, a gradual transition from light to heavy oil is predicted. Alternatively, if solubility of asphalt in the oil is limited, a phase transition from oil to tar is expected.

Tar mats present some unique reservoir engineering problems. Their presence in several Middle East reservoirs appears to impede natural basal water drive [4, 5].

Compositional variability in heavy oils may also be caused by selective degradation of the oil by a variety of processes. Many reservoirs allow oil to seep to surface, where oxidation and biodegradation convert it to tar or asphaltite deposits. Similar processes occur when oil comes into contact with oxygenated near-surface "meteoric" waters. Light components may also be lost by dissolution into water, or be lost to a leaking gas cap. These and other degradation processes have been described in detail by others [1].

In a study of two reservoirs within the Sakhalin oilfields of the Soviet Union, Amosov and Kozina [6] concluded that oxidation was more important than either water-washing or gravity in causing the variation in oil density between the edges and crests of the pools.

2.2 Thermal Alteration of Petroleum

This part of the literature review will focus on the chemical transformation of petroleum in the temperature range of 200° to 500°C. Beyond this range, very little research work has been reported. The entire range of temperature is relevant to fireflood operation, whereas the range of 200° to 300°C is also relevant to steam stimulation operation.

Besides reviewing the effect of heat on petroleum, the influence of pressure, water, and minerals on heated hydrocarbon systems will also be discussed.

2.2.1 Temperature Range of 200° - 330°C

As will be discussed in more detail, the main observable changes in oil systems heated to this temperature range were the production of a small amount (usually less than 1 wt % of the heated oil) of gas and permanent changes in the viscosity of the oil after heat treatment. In all reported cases, changes in the distillation behavior of the heated oil were small.

Gas Production: At temperatures near 200°C, gas evolution has been observed by various researchers. Hyne and coworkers [1] observed the evolution of CO_2, H_2, CH_4, H_2S, and CO from Athabasca oil sand and Venezuelan heavy oil when these materials were heated in the presence of water. Over a period of 30 days, the cumulative amounts of the first four components increased with time (Figure 1); however, the cumulative production of CO went through a maximum, followed by a gradual decline to almost complete disappearance (Figure 2). Hyne explained, with supporting evidence, that the disappearance of CO was caused by its reaction with water to form H_2 and CO_2.

$$CO + H_2O \text{ -------> } CO_2 + H_2$$

Hyne also suggested that reactions between oil, water, and core materials play the most important role in determining the composition of the product gas in this temperature range. Carbon dioxide, H_2S, and H_2 are important components in the temperature region of 200°C to 325°C. He labelled this temperature range as the "aquathermolysis window". At temperatures higher than 325°C, thermal cracking of oil becomes increasingly important and the hydrocarbon content of the produced gas also increases significantly.

Akstinat [2] also reported the evolution of CO_2, H_2S, and light hydrocarbons (C1 to C3) from a viscous German oil heated to this temperature range. Instantaneous evolution of these gases was observed at around 240°C. The rate of gas production increased slowly with increasing temperature. However, at temperatures above the level of approximately 320°C, the rate of gas production -- particularly for the hydrocarbons as shown in Figure 3 --increased rapidly, suggesting an accelerated rate of thermal cracking. Hesp *et al* [3], in their study on an Australian crude, also observed a sudden increase in gas production at around 350°C. Based on the studies mentioned above, there appears to be an agreement on a narrow temperature range of 320°C to 350°C, around which thermal cracking reactions become dominant in determining the produced gas composition.

Akstinat [2] and Monin *et al* [4-6] found that H_2S was produced from crude oil regardless of whether steam was present in the system. Akstinat also found that the presence of quartz sand, silicic acid, and pyrite (FeS_2) did not in any way affect the production of H_2S. In contrast, Hyne [1] claimed that H_2S was not produced in his experiments when bitumen was heated with steam over this temperature range, whereas H_2S production was observed when bitumen, water, and core material were heated together. He did not mention any experiments in which bitumen was heated alone.

Akstinat [2], with the support of considerable experimental evidence and other published research, claimed that the generation of H_2S in the lower temperature region was mainly caused by the presence of elemental as well as organic sulfur species in petroleum. The conversion of elemental sulfur to H_2S started at 140°C and reached a maximum at 200°C. Experiments involving the addition of FeS_2 showed that the latter had no influence on the evolution of H_2S at temperatures up to 320°C.

In a system containing petroleum, water, and core material, Hyne suggested that CO_2 was produced from the following reactions:

- decarboxylation of mineral carbonates in the core material
- decomposition of oxygenated organic compounds in the oil
- chemical reactions between oil and water
- water shift reaction between CO and water.

Both Akstinat [2] and Monin *et al* [4-6] supported the validity of the first three reactions.

Viscosity Changes: Hyne's work on Athabasca bitumen showed that the level of temperature had an important bearing on the viscosity of oil after thermal treatment. When bitumen was heated to 200°C in the presence of water, the viscosity of the recovered bitumen increased with increasing heat treatment period (Figure 4). Hyne suggested that polymerization of organic compounds was responsible for the increase in viscosity. The generation of CO_2 by the oil was speculated as a potential catalyst in enhancing the production of polymer. However, Hyne did not present any evidence that support the formation of polymer in the heat-treated bitumen. Determination of molecular weight of the whole fluid did not show any relationship to viscosity.

Similar experiments by Hyne at 240°C showed that viscosity increased in the first 30 days of heat treatment followed by a slow decline (Figure 4). He suggested this behavior was the result of the interplay between polymerization and molecular cleavage reactions. At 300°C, viscosity decreased as a function of time due to the strong influence of molecular scission.

Venkatesan *et al* [7], in their study of Cold Lake, Celtic, and San Ardo crudes at 300°C, recorded the changes in viscosity as a function of heating time up to a maximum of 480 hours. In those experiments, the oils were heated individually in the absence of water. The pressure of the reactor was maintained at 100 psig with the use of an inert gas. At 300°C, the viscosities of all three oils decreased with increasing heating time (Figure 5), particularly in the first 24 hours of heating. The asphaltene contents of the Cold Lake and San Ardo crudes also decreased with increasing heating time. With the Celtic crude, the asphaltene content in the produced oil went through a maximum with increasing heating time (Figure 6). In an earlier report [8] by the same authors, Cold Lake crude heated at 285°C was found to display the same behavior with regard to a maximum asphaltene content at a certain point of time during the heating period.

Venkatesan *et al* [7] discussed the viscosity behavior of heated oil in simple terms, in which oil contains only two solubility fractions: maltenes (n-pentane soluble) and asphaltenes(n-pentane insoluble, toluene soluble). When oil is heated, the asphaltene fraction may be cracked to form maltenes. On the other hand, the maltene fraction may undergo polymerization and condensation reactions to form asphaltenes; therefore the following global reaction is reversible:

asphaltenes <------> maltenes

The continuous decline in asphaltene concentration observed in experiments involving San Ardo and Cold Lake crudes at 300°C may be explained by a strong forward reaction. The behavior of the Celtic crude may be explained by a strong reverse reaction at the beginning, followed by a strong forward reaction in the later part of the experiment.

Venkatesan *et al* [7] suggested that the viscosity of oil is controlled by the viscosity of the maltene fraction, the concentration of asphaltene, and the solvation power of the maltene fraction according to the following relationship:

$$u = u_m (1 + kc) \qquad (1)$$

where u = viscosity of heavy oil
u_m = viscosity of maltenes
k = Einstein intrinsic viscosity, which varies with the size, shape, and rheological behavior of the suspended particle (asphaltenes)
c = concentration of asphaltene

In this study by Venkatesan *et al* [7], maltene viscosity decreased progressively with increasing heating times for all three crudes. This was interpreted as being caused by the formation of lower molecular weight compounds during thermal cracking.

The intrinsic viscosity was also found to decrease with increasing heating times for all three crudes. This was explained as being caused by the reduction in asphaltene molecular size (supported by gel permeation data) and change to a more spherical molecular shape (supported by C^{13}-nmr data) which offers less resistance to flow.

As discussed earlier, the concentration of asphaltene may vary depending on the stage of the reaction. A delicate balance of the three factors listed in equation (1) determines the viscosity of oil. This viscosity model may also be used to explain the data obtained by Hyne shown in Figure 3. However, Hyne's argument regarding polymerization caused by the presence of CO_2 is still debatable.

2.2.2 Temperature Range of 330° - 500°C

As temperature approaches 330°C, most researchers reported sudden increases in the rate of thermal cracking. Since changes to the oil properties as well as the product yield occur quickly at high temperatures, a proper description of these changes has to accompany a good specification of reaction temperature and time.

Besides producing gaseous products rapidly, coke is also formed in significant quantities. As well, the produced oil exhibits very different distillation and solubility characteristics in comparison with the unheated oil. A more detailed discussion of the three products-- gas, oil, and coke -- follows:

Gas Production: McNab *et al* [9] monitored the production of gas from Athabasca bitumen over a temperature range of 246°C to 309°C. They reported that at 307°C, approximately 0.2 wt. % of the original bitumen was converted to gas over a period of 111 hours. Shu *et al* [8] conducted similar experiments on Cold Lake crude over a temperature range of 260°C to 325°C. At 300°C, they observed a conversion of oil to gas of 0.2 wt % in 480 hours. At the higher temperature end, for example around 500°C -- a temperature region at which most commercial coking processes are operated -- approximately 8 wt % of Athabasca bitumen is converted to gas (propane and lighter) in three to five minutes. These data illustrate the importance of temperature on the rate of gas production.

As discussed in the section 2.2.1, the gas produced at the lower temperature range (200°C to 330°C) is mainly composed of CO_2, H_2, and H_2S, along with minor amounts of light hydrocarbons. However, as the temperature increases, the ratio of hydrocarbon to non-hydrocarbon also increases as shown by Hesp *et al* [3] in Figure 7. According to Hyne [1], Akstinat [2], and Hesp *et al* [3], the gas products observed at lower temperatures were derived from cleavage of weaker bonds (such as C-S and C-O bonds) and reactions between water and hydrocarbons. The rates of these reactions increase with temperature; but such increases are not as fast as those involving C-C bonds once temperature exceeds about 300°C. Above this level, the main hydrocarbon components are ethylene and methane. The theoretical aspects of these cracking reactions have been discussed by Kossiakoff and Rice [10].

Liquid Product:

- Viscosity reduction -

All reported data relating to oil treated in this temperature region showed drastic reduction in viscosity in comparison with the untreated oil. Venkatesan *et al* [7] reported close to 80% reduction in viscosity of Cold Lake crude heated at 300°C for 120 hours. Other data showed that the viscosity of Athabasca bitumen was reduced by more than 99% (viscosity determined at 35°C) after heating for five minutes at 500°C. The reduction in viscosity was mainly caused by the production of low molecular weight species in the liquid phase via a complex set of sequential as well as parallel reaction paths [10,11].

- Solubility changes -

Some of the most common ways to describe the changes to oil after heat treatment are to compare the distillation and solubility behaviors of the thermally altered oil with the original oil. The changes in distillation behavior are significant in this temperature range (330-500°C), and the rate of change will be discussed in the next section. In this section, the focus is on the changes in the solubility behavior.

Erdman *et al* [12] described oil and thermally cracked products using five solubility classes:

1. oil (propane soluble fraction)
2. resin (propane insoluble, pentane soluble)

3. asphaltene (pentane insoluble, benzene soluble)
4. benzene insoluble
5. coke (solid residue obtained prior to solvent extraction)

On heat treatment of each of the first 3 fractions, varying amounts of material with different solubility characteristics were generated. Experiments with Baxterville oil heated to 375°C for 24 hours gave the results presented in Table 1. The propane soluble fraction yielded 4.4 wt % of resin and less than 1 wt % of asphaltenes. The resin fraction yielded 35.6 wt % of oil, 36.6 wt % of asphaltenes, and 9.3 wt % of benzene insoluble. The asphaltene fraction yielded 2.0 wt % of oil and resin combined, and 17.6 wt % of benzene insoluble. Of the three fractions heated, the resin showed the highest percentage of solubility change. The substantial conversion of resin into classes -- oil and asphaltene -- that are less soluble in each other, sets the stage for asphaltene precipitation.

The phenomenon of asphaltene precipitation during thermal treatment of the heavy fraction of oil has been repeatedly observed by refiners who operate visbreaking units. Such units are typically operated in the vicinity of 400°C. Hus [13] discussed the precipitation process by considering oil as a colloidal system containing micelles of asphaltenes. The asphaltenes are not soluble in the light oil phase. However, attached to these micelles are high molecular weight hydrocarbons commonly referred to as resins. Since the resins are soluble in the light oil phase, they serve the purpose of suspending the asphaltenes in the oil matrix. During the visbreaking process, low molecular weight species with high hydrogen contents are formed along with asphaltenes which have low hydrogen contents, causing a net depletion in resins. Eventually, the phase equilibrium is disturbed, and precipitation of asphaltenes occurs as a result of insufficient resin to keep the asphaltenes in solution.

Coke: The formation of coke is influenced by a variety of factors such as the characteristics of the oil, temperature, and the concentration of H_2 in the system during thermal alteration. It is inappropriate to make generalized statements about the lowest temperature at which coking begins, partly because the rate of coke formation at such temperatures is so low that, in many instances, it cannot be properly detected. Lin *et al* [14] reported that 0.3 wt % of Athabasca bitumen was converted to coke after the bitumen was heated for 115.7 hours at 303°C. At higher temperatures, a larger amount of coke is formed in a much shorter time; for example, 3.3 wt % was formed at 452°C after 2.2 hours of heating. Data on commercial coking reactors show that approximately 16 wt % of coke is formed from bitumen within 3 minutes of heating at 500°C.

2.2.3 Effects of Pressure

Henderson *et al* [15] and McNab *et al* [9] conducted similar thermal alteration experiments with Athabasca bitumen and concluded that pressure had no observable effect on the overall conversion of the heavy fraction into lighter materials. However, neither group closely monitored the amount of gas produced under different pressures.

Hesp *et al* [3] presented data of well-controlled experiments with an Australian crude under various pressures developed by helium. Heating the oil at 375° for one week showed that there was a marked reduction in gas yield as pressure was increased up to 3600 psi. This was particularly marked in the 30-1030 psi range (see Figure 8). There was also a good agreement between these results and those from experiments in which pressure was developed by steam. The authors concluded that high pressure, regardless of whether it is developed by steam or gas, reduced the production of gas during thermal cracking.

Hesp *et al* [3] presented very little data on the effect of pressure on the produced oil quality. They noted that there was an increase in the relative concentration of n-alkanes in the C10-C16 range, and a decrease in the decomposition of the C17-C24 hydrocarbons as the inert pressure was increased.

2.2.4 Effects of Reservoir Minerals

This is a very difficult topic for experimental study because of the large variety of components involved in any particular core. It is even more difficult to review this topic because of the variety of cores used by different research groups. The use of model compounds in a few reported studies helped, to a small extent, the understanding of the role of the selected compounds in thermal cracking. However, those studies do not exclude the importance of the large number of compounds that are not yet studied. A few observations related to the role of minerals in thermal cracking are noted in the following paragraphs.

There seems to be a consensus [1,2] on the importance of mineral carbonate(s) in contributing CO_2 to the gas phase. The amount of CO_2 is also enhanced by the presence of water either through reactions with the carbonates, hydrocarbons, and/or CO. However, there is no firm evidence on the relative importance of the various mineral carbonates commonly found in cores.

Akstinat [2] showed that pyrite (FeS_2) generates H_2S when heated to 320°C-400°C in the presence of water, and hence speculated that pyrite might be a source of H_2S in thermal recovery.

Henderson *et al* [15] and McNab *et al* [9] claimed that the presence of core materials did not have any impact on the kinetics of heavy hydrocarbon conversion to lighter liquids. However, it is felt that the analytical procedures used in describing conversion, as well as the experimental techniques used were quite outdated. New studies in this area are needed to confirm the role of minerals in hydrocarbon conversion.

2.2.5 Effects of Air

In the scenario of a fireflood operation, the reservoir system consists of oil, water, minerals, and air. The first three components have been discussed in the previous sections; this section focuses on the role of air.

Romanowski *et al* [16] conducted a series of experiments using a tubular reactor [3.3 inches id x 32 inches long) packed with Utah tar sand. The tar sand was heated to 93° - 121°C prior to injection of a heated air stream. The temperature of the air stream was not reported. Under such an arrangement, the heat supplied by the air stream as well as the heat generated by low temperature oxidation increased the temperature of the tar sand pack.

There was a negligible amount of oxygen uptake by the bitumen at temperatures below 150°C. Between 177° - 315°C, low temperature oxidation accounted for a gradual decrease in oxygen content of the vent gas to less than 1 vol%. As the temperature reached between 343°-399°C, the bitumen ignited and oxygen consumption was close to 100% (see Figure 9). Varying the air flux over a range of 16-111 scf/h-ft^2 did not seem to affect the high efficiency of oxygen consumption. The air stream was not preheated after the top 5-6 inches of the tar sand pack was burning at an average temperature of 482°C. After ignition, combustion temperatures in the range of 815° - 1035°C were observed.

After studying a range of air flux (16-111 scf/h-ft^2), Romanowski *et al* [16] found that low air flux gave a significantly higher volumetric oil recovery (Table 2). The produced oil quality from low air flux experiments was also better in terms of viscosity, molecular weight, and distillation behavior (Table 3). These observations might have been caused by the slow rate of temperature increase in the low air flux experiments, hence the oil was exposed to moderate cracking temperature for a longer period of time resulting in substantial alteration of oil properties. In the case of high air flux, the lighter fraction of the oil was rapidly driven away, mainly unconverted, to the cooler zone. The heavy materials that were left behind underwent a more rapid increase in temperature. The period within which the heavy materials experienced moderate cracking temperature was short, prior to the onset of higher temperatures. Since high cracking temperature gives a lower liquid yield and higher coke yield, the oil recovery of the high air flux case was lower.

2.2.6 Kinetics of Thermal Alteration

The reaction mechanisms of petroleum cracking are very complex: an enormous number of reactants are involved in reactions of different rates. Even finding suitable parameters to describe the extent of changes caused by thermal cracking has proved to be very difficult. This is, in part, caused by the fact that the products of some reactions may also serve as reactants of other reactions. The most common parameters used are distillation behavior and viscosity. The kinetics of thermal cracking using distillation behavior as correlating factor could be quite different from that using viscosity as correlating factor. For example, heating an oil at 300°C produces a rapid change in viscosity but negligible change in distillation behavior.

Lin *et al* [14] have recently done a comprehensive literature review of the various kinetic analyses of thermal cracking. Fassihi *et al* [17] summarized the kinetic parameters (activation energy, reaction order, and Arrhenius constants) collected by various research groups studying different and similar crudes.

TABLE 1
THERMAL TREATMENT OF BAXTERVILLE CRUDE OIL AND ITS SOLVENT FRACTIONS[a]
375°C for 24 hours

Fraction	Treatment	Propane-soluble Oil	Resin	Asphaltene	Benzene Insoluble
Crude Oil	unheated	75.9	8.9	17.2	-
	heated	66.6	5.1	19.3	9.3
Propane-soluble Oil	heated	94.8	4.4	< 1.0	-
Resin	heated	35.6	18.5	36.6	9.3
Asphaltene	heated	[--------2.0--------]		80.4	17.6

a) Taken from reference 12. Values given in mass percent.

TABLE 2: FORWARD COMBUSTION EXPERIMENTAL RESULTS[a]

Air flux, scf/h-ft^2	111	54	33	16	15
Steam flux, scf/h-ft^2	--	--	--	--	--
Product gas comp., vol.%					
O_2	0.5	0.0	0.0	0.0	--
CO	4.4	6.6	9.6	13.3	--
CO_2	15.1	15.7	13.6	9.2	--
Oxygen utilization, %	98	100	100	100	--
Calculated fuel composition equivalent H/C ratio	0.7	0.3	0.4	0.8	--
Oil recovery					
wt. % initial bitumen	39	41	42	43	38
% OOIP	40	44	46	49	43
vol. % Fischer assay	66	72	76	81	71

a) Taken from reference 16. Values are averaged over the high temperature oxidation period.

TABLE 3: CHEMICAL AND PHYSICAL PROPERTIES OF ORIGINAL BITUMEN AND COMBUSTION PRODUCT OILS[a]

	Bitumen	Product Oils				
		111	54	33	16	15/20
Elemental analysis, wt. %						
Carbon	83.1	82.8	83.8	84.1	84.3	84.6
Hydrogen	10.0	10.9	11.3	11.1	11.9	11.6
Nitrogen	0.50	0.50	0.58	0.29	0.19	0.21
Sulfur	3.83	3.61	2.77	2.77	2.26	2.35
Oxygen (by diff.)	2.57	2.19	1.55	1.74	1.35	1.24
H/C ratio	1.43	1.57	1.61	1.57	1.68	1.63
Molecular weight	730	400	390	320	270	290
API gravity, (60°F)	4.1	10.0	14.0	16.5	23.1	20.7
Specific gravity	1.044	1.000	0.973	0.956	0.915	0.930
Viscosity, cp						
34°F	-	-	-	-	55	105
60°F	-	-	3975	221	23	35
140°F	7x 10^{10}	5625	80	20	-	-
195°F	5 x 10^{9}	280	-	-	-	-
Distillation data, vol. %						
200-600°F	1.7	17.6	18.8	24.9	35.1	35.6
600-1000°F	32.0	47.4	56.2	55.9	56.8	55.9
>1000°F	66.3	35.0	25.0	19.2	8.1	8.5

a) Taken from reference 16.

FIGURE 1 - MAIN GASES FROM AQUATHERMOLYSIS AT 300°C (Ref. 1)

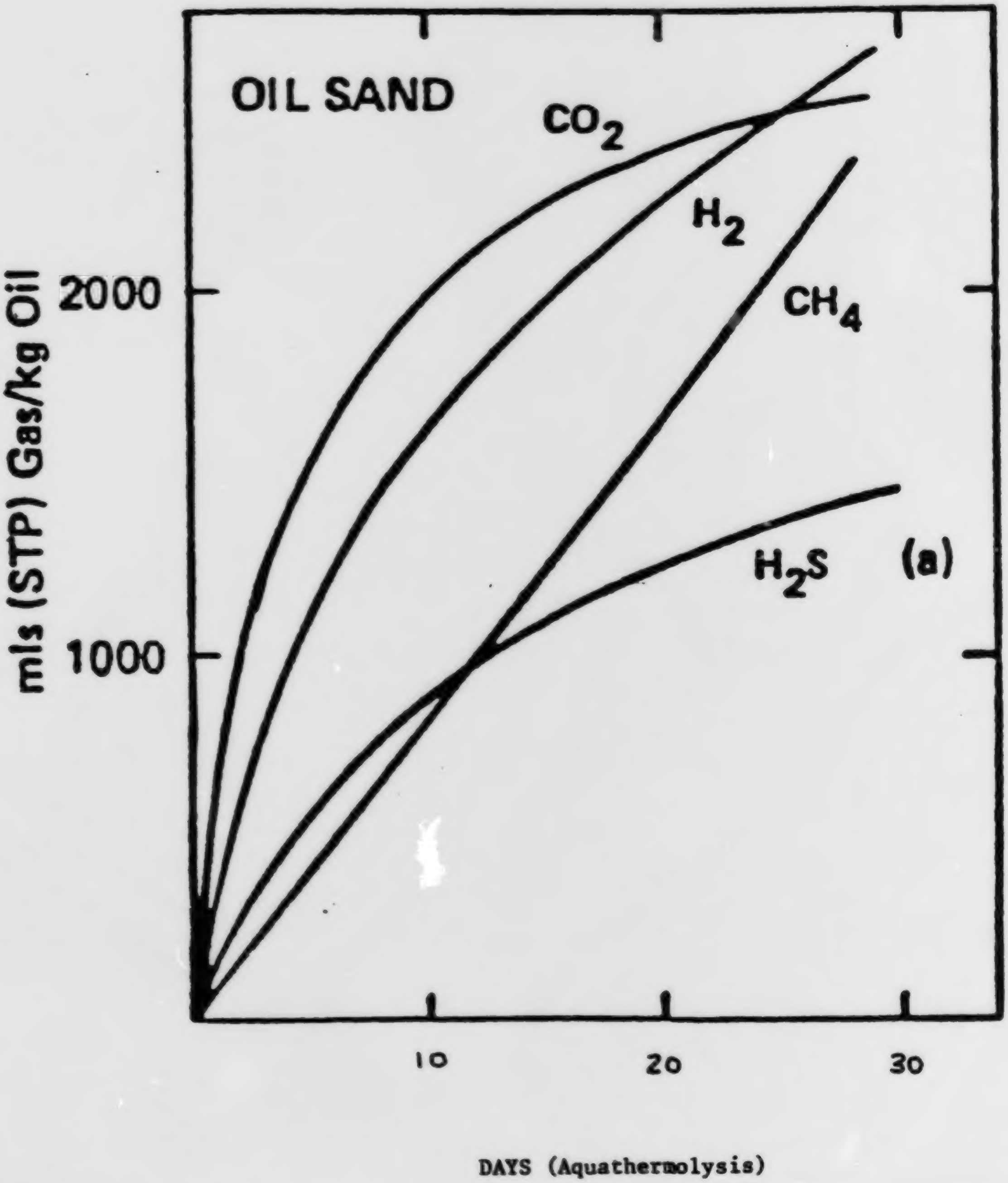

FIGURE 2 - CO PRODUCTION AND DEPLETION DURING AQUATHERMOLYSIS

(Ref.1)

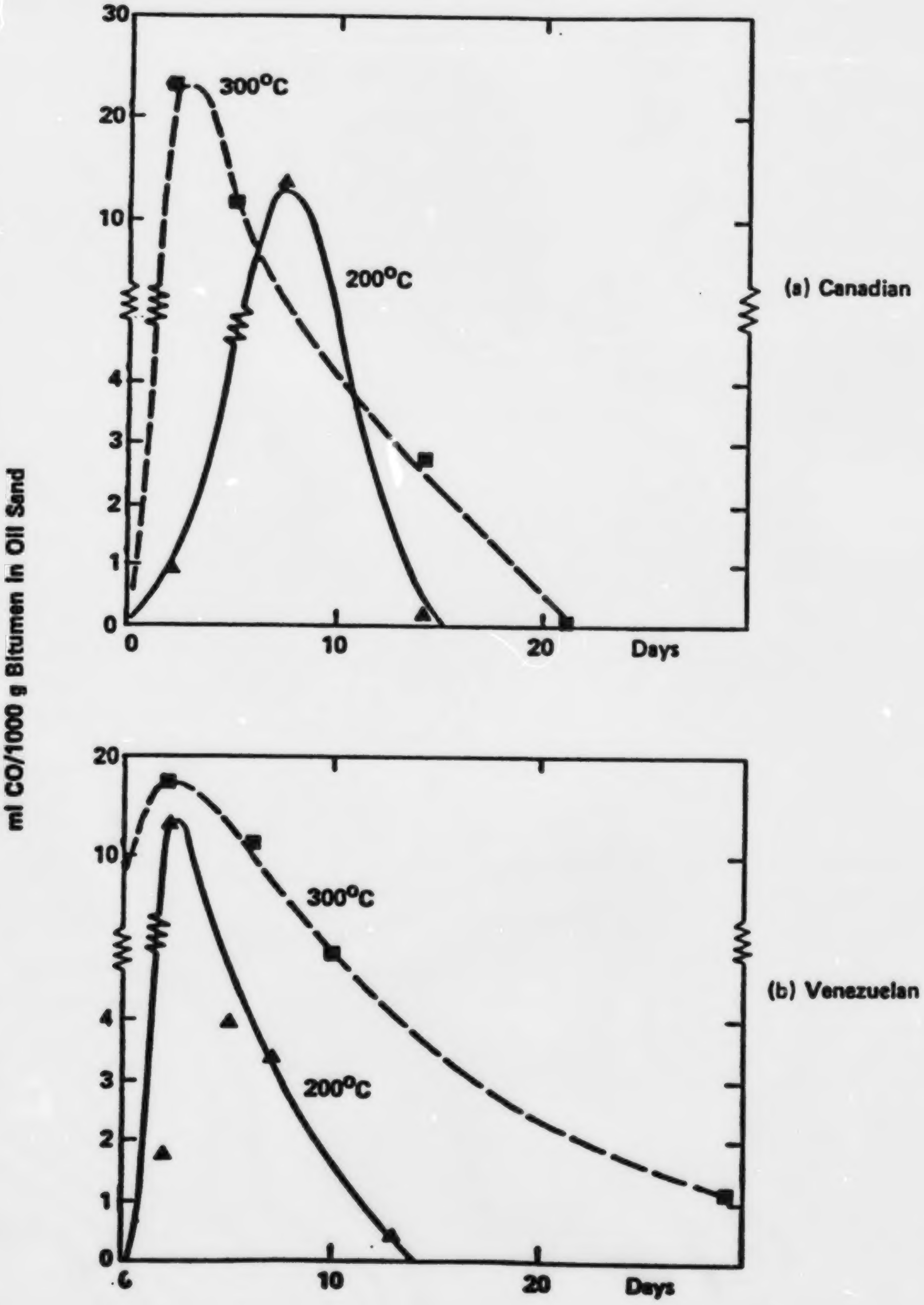

FIGURE 3 - TEMPERATURE V. EVOLUTION OF CH_4 (WITH STEAM) (Ref. 2)

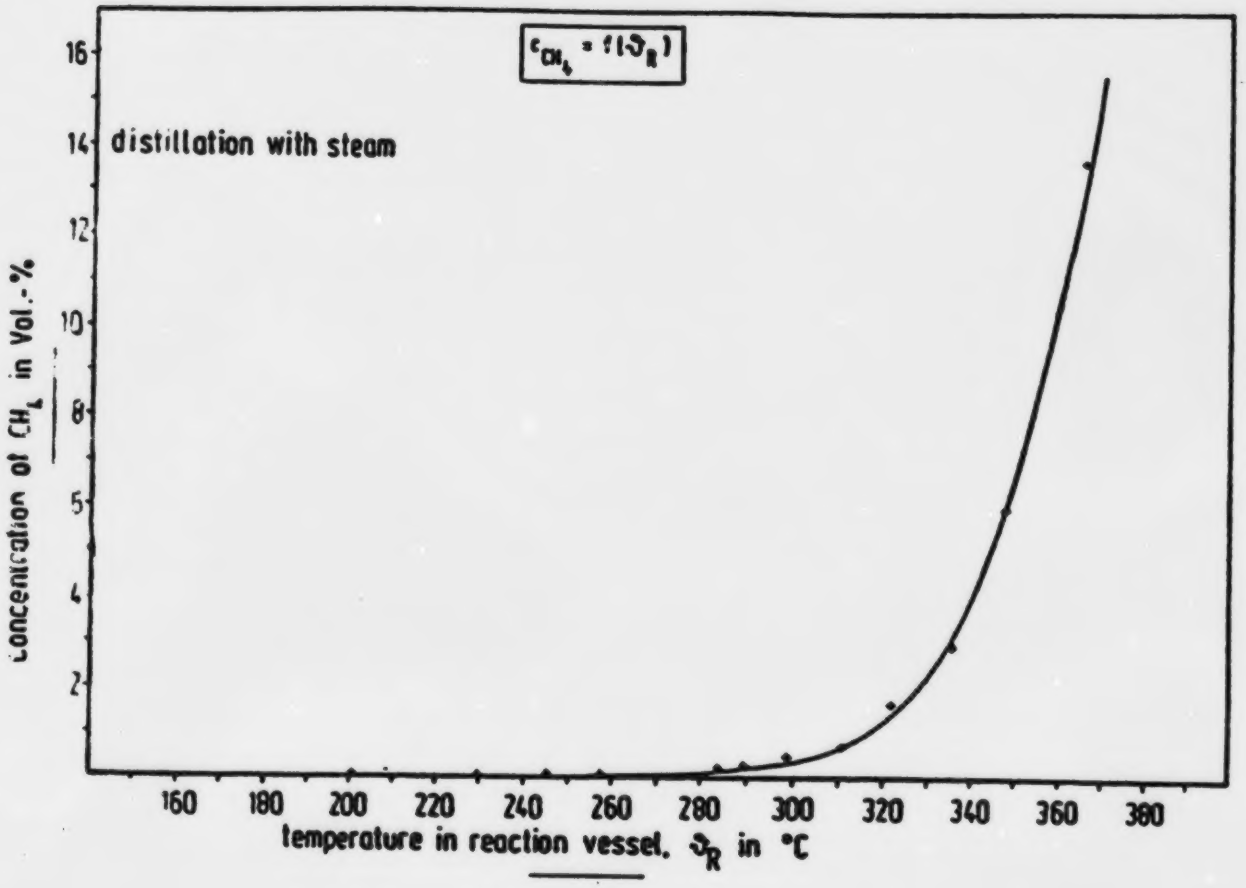

FIGURE 4 - VISCOSITY BEHAVIOUR OF RECOVERED BITUMENS AS FUNCTION OF TEMPERATURE AND DURATION OF AQUATHERMOLYIS (Ref. 1)

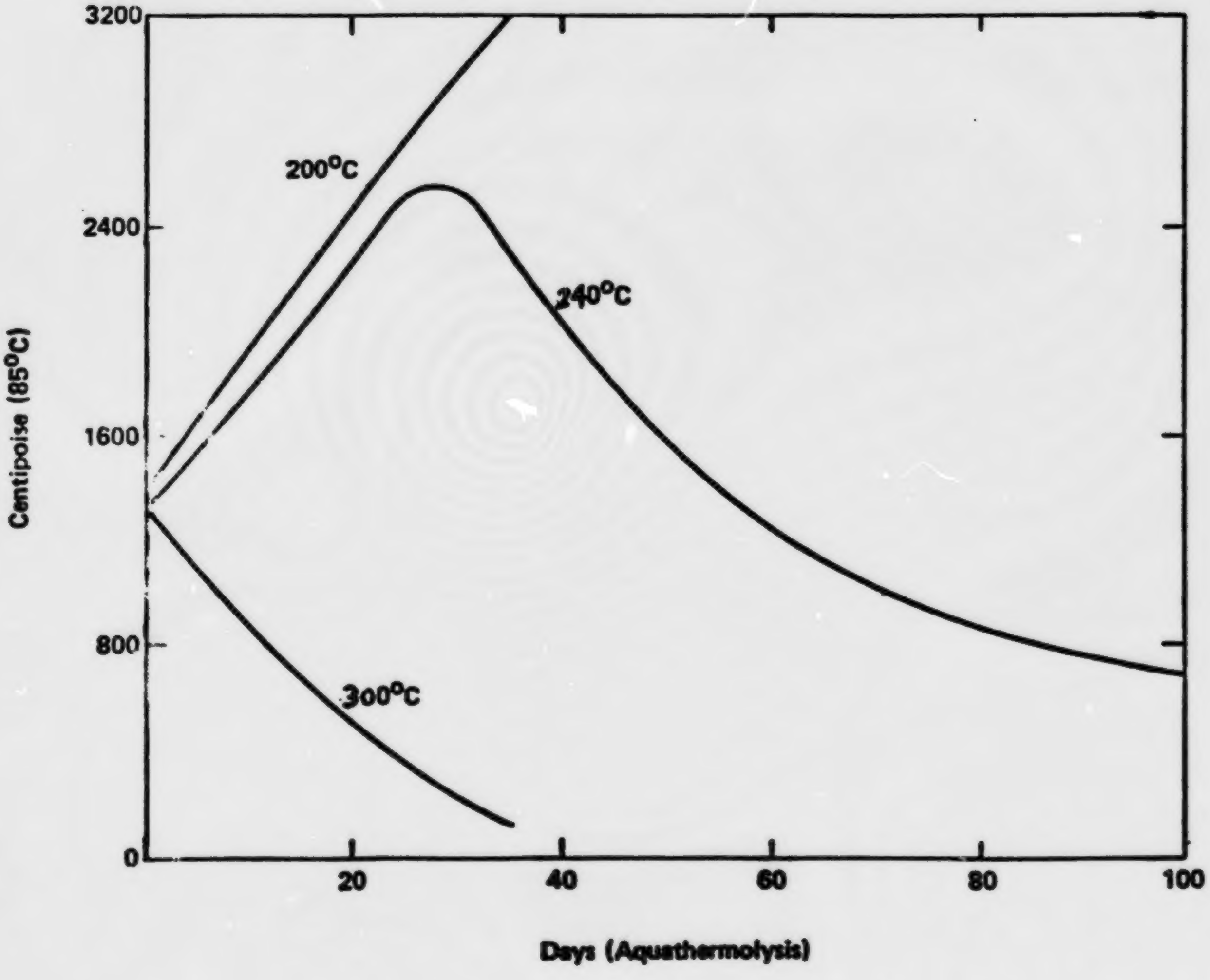

FIGURE 5
VISCOSITY REDUCTION OF HEAVY OILS
REACTOR TEMPERATURE 300°C (Ref. 7)

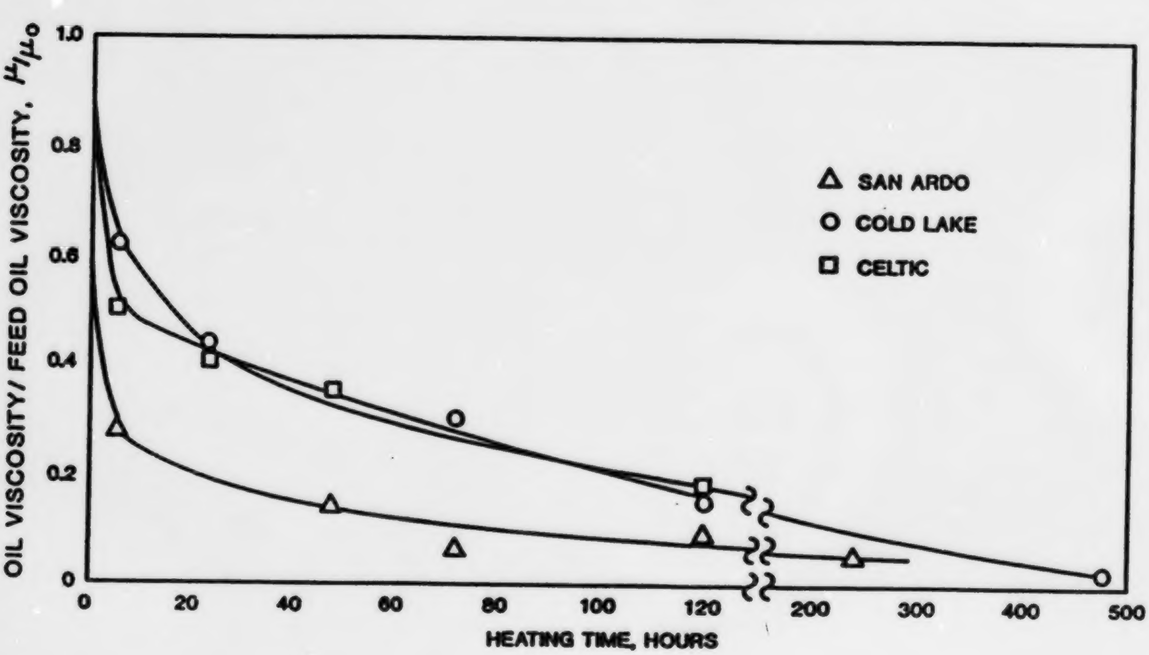

FIGURE 6
ASPHALTENE CONTENT OF VISBROKEN LIQUID PRODUCTS
REACTOR TEMPERATURE 300°C (Ref. 7)

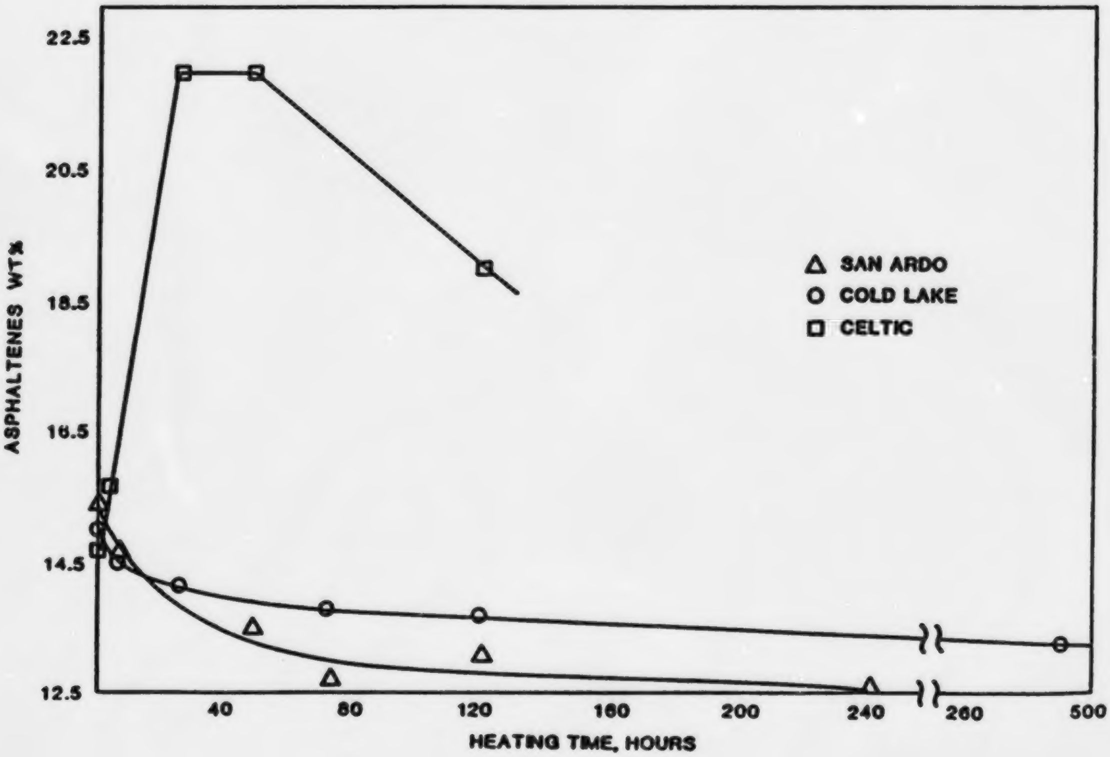

FIGURE 7 - EFFECT OF TEMPERATURE ON REACTION ROUTE (Ref. 3)

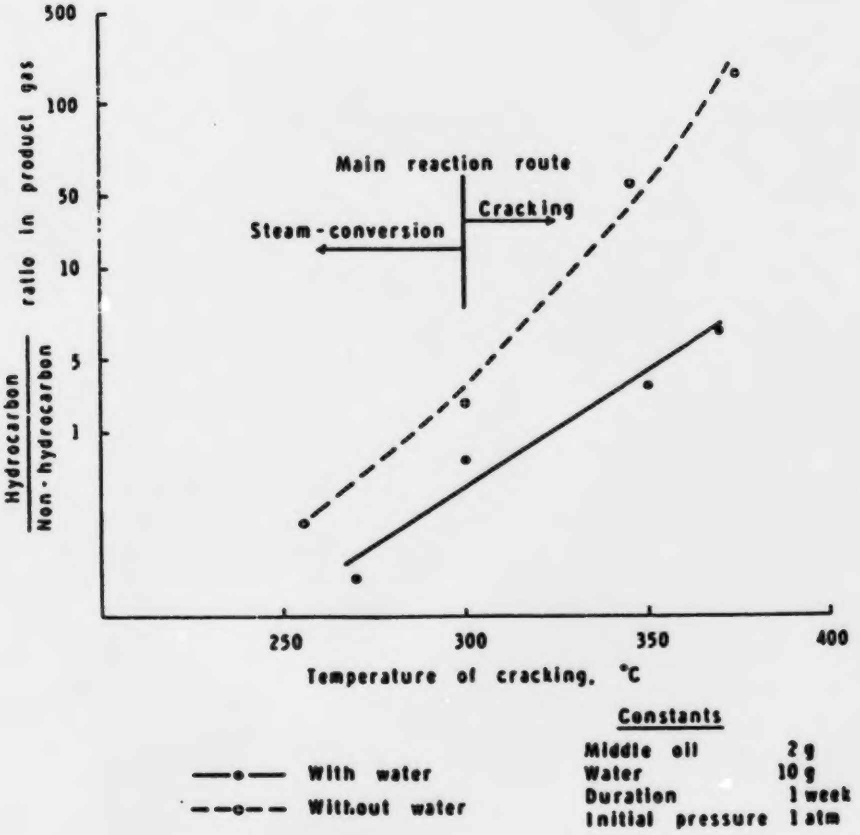

FIGURE 8 - YIELDS OF GAS FROM CRACKING OF MIDDLE OIL UNDER INERT GAS PRESSURE AT 375°C (A) VOLUMETRIC YIELD, (B) WEIGHT YIELD (REF. 3)

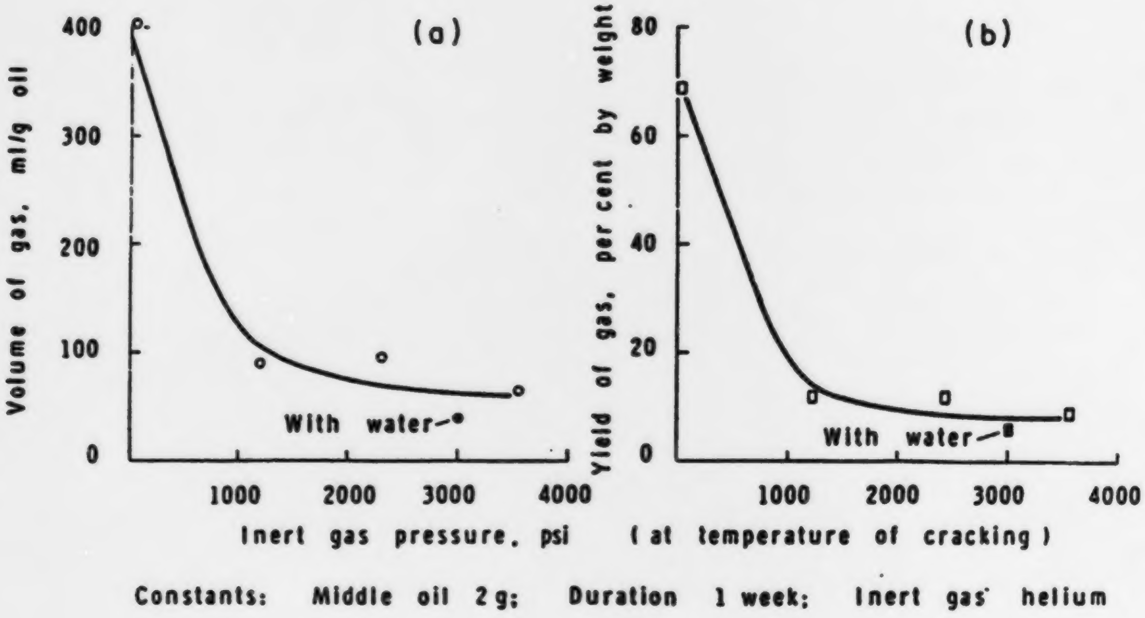

FIGURE 9 - IGNITION TEMPERATURES FOR FORWARD COMBUSTION OF TAR SAND TRIANGLE RESOURCE (Ref. 16)

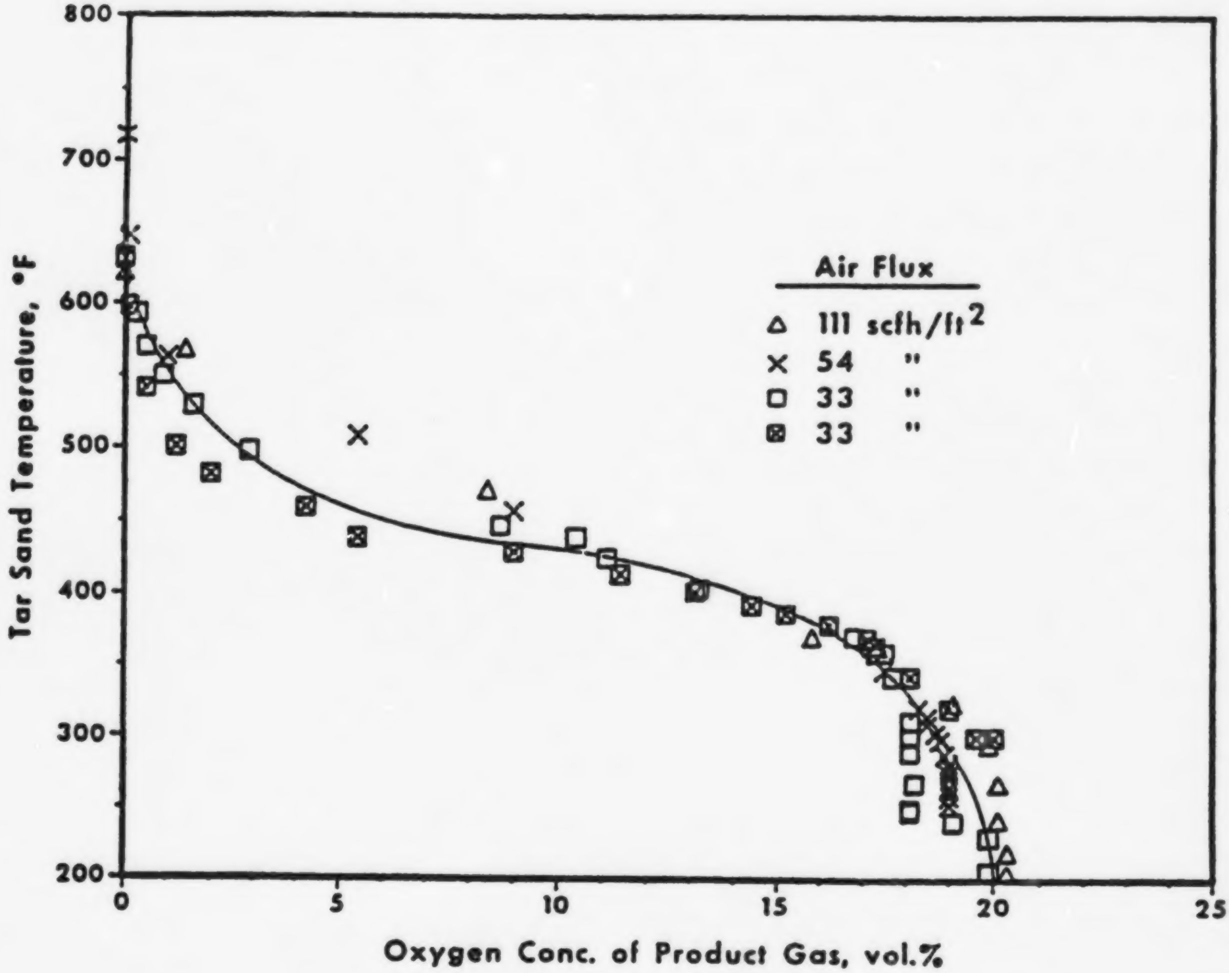

2.3 Influence of Asphaltenes on Oil Viscosity

The effect of asphaltenes on solution viscosity has been studied previously in a variety of ways and with different motivations. Altgelt and Harle [1], using the n-pentane asphaltenes from a Boscan residuum, measured the viscosity of solvent solutions of increasing asphaltene content. They noted that the viscosity of these solutions increased much quicker than analogous solutions of a polymer, and suggested that this was due to aggregation of the asphaltenes in the solvent. The asphaltenes were also fractionated into portions of different average molecular weight. The higher the molecular weight of the asphaltenes, the greater was their effect on viscosity. Viscosity of solutions of the higher molecular weight asphaltenes was very sensitive to the solvent. The viscosifying effect of asphaltenes was greatest in the poorest solvent. This behavior contrasts with that of rigid spheres, for which there is no solvent effect, and that of many polymers, which shrink in poorer solvents reducing the viscosity. The authors conclude that both the effect of molecular weight and of solvent are due to aggregation of the asphaltenes in the solvent.

Altgelt and Harle [1] also measured the viscosity of a series of asphalts of varying composition made by adding maltenes or asphaltenes to asphalt. By comparison with analogous data on asphaltene solutions in various solvents, they assessed the solvent power of the maltenes relative to the solvents. They concluded that asphalt viscosity depends on asphaltene concentration in a similar manner to asphaltenes dissolved in solvents. Thus aggregation of asphaltenes becomes more important with increasing asphaltene concentration, increasing asphaltene molecular weight, and decreasing solvent power of the maltenes.

Reerink [2] made measurements using a variety of techniques on solutions of asphaltenes in toluene. He observed that viscosity of these solutions was 2-5 times higher than expected for spherical, non-solvated, non-aggregated molecules, and tried to determine the reasons for the unusually high values. For concentrated solutions at room temperature, he concluded that aggregation plays a major role, flat elipsoid shape plays a minor role, and the effect of solvation is insignificant. At higher temperatures, aggregation becomes less important and shape begins to be significant in determining the solution viscosity.

Using asphaltenes and maltenes separated from an asphalt with petroleum ether, Mack [3] prepared five mixtures of different composition and measured their viscosity at five temperatures between 0 and 120°C. None of the different mathematical equations that he tried adequately described the relationship between concentration and viscosity. He also compared data reported by other workers giving viscosity of solutions of naphthalene in benzene and in toluene. These data fit the equation:

$$\log (m_r) = k \text{ (molecular weight) (concentration)} \qquad (1)$$

where m_r = viscosity solution/viscosity solvent
and k = constant.

Mack concluded that the asphalt viscosities deviate from Equation (1) because of aggregation of asphaltenes.

Spearot [4] reported on a study of oxidized engine oils, which consist of a solids phase (defined as n-heptane insoluble, benzene soluble) dispersed in a light oil phase. Solutions of the solids in benzene were mixed in different proportions with the solids-free oil, the benzene was removed under vacuum, and the apparent viscosities of the mixtures were measured over a range of shear rate at several temperatures. The viscosity of a sample of oxidized oil from an engine test fits on the curve of viscosity versus solids content obtained from the reconstituted oils.

The viscosity data were not consistent with the theoretically derived expressions of either Einstein or Brinkman. The Brinkman equation has been used successfully for data from a variety of types of suspension, where the solids are non-interacting particles of wide size distribution, at solids contents up to 40%. As an alternative, Spearot [4] presents a model developed by Michaels and Bolger [5] to explain rheology of kaolinite suspensions. The model takes into account the effects of particle aggregation on the viscosity.

Using a simplified version of the theory, which neglects the shear rate dependence, Spearot calculates that about 36% of the solids are aggregated. This value does not appear to change with solids content or with temperature over the range 20 to 80°C. Spearot concludes that the oxidized oils contain structures which break apart with shear to give aggregates of a certain size. These aggregates are composed of solids and a portion of the oil phase.

Extensive studies of four Californian oils were carried out by Datta [6]. As this reference [6] has so far been unavailable, this review is based on a review by Robinson [7]. Several different techniques were used to prepare oils of varying asphaltene content. The procedure usually involved dissolution of asphaltenes in benzene, and vacuum evaporation of the benzene after mixing. As reported by Robinson, none of the samples reconstituted to the same asphaltene content as the original oils had the same rheological behavior. In all cases, the reconstituted samples were more Newtonian in behavior, and had lower apparent viscosity at similar shear rate. Datta apparently explained this difference by suggesting that the native structure had not been recreated, whereas Robinson suggests that some benzene may have remained in the samples.

2.4 Contribution of Steam Distillation to Thermal Recovery

One of the earliest reports of laboratory studies of oil recovery by steam injection is the work of Willman *et al* [1]. Linear floods were performed using consolidated sandstone cores of various origins and ranging from 5 to 15 cm in diameter and 11 to 104 cm long. Five different crude oils, varying in viscosity from 5 to 6500 mPa.s at 26.7°C, as well as several refined oils, were used in the experiments. Cold water (26.7°C), hot water (166°C), or steam (100°C) was injected into the insulated oil-saturated core, and the amount of oil produced was measured during fluid injection of 8 to 12 pore volumes.

From a comparison of cold and hot waterfloods of a sandstone saturated with refined oil, the authors assessed the contributions of thermal expansion and viscosity reduction to overall recovery. Substitution of a refined oil of lower viscosity (4.7 instead of 138 mPa.s, analogous to increasing oil temperature from 26.7 to 166°C) improved recovery by 5% OOIP, and thermal expansion of the oil accounted for another 3% OOIP. These results predict an increase of 8% OOIP of hot water over cold water, in close agreement with the 9% obtained from direct measurements.

A steamflood of the same refined oil from the same core material recovered 67% OOIP, an increase of 11% OOIP over hot water alone. Although the authors do not explain these data, they imply that the additional recovery cannot be due to steam distillation since the refined oil (Primol) is "non-distillable". Based on their later discussion, it appears that this additional recovery may be due to gas flooding effects.

The contributions of other mechanisms to steam recovery were investigated with corefloods using mixtures of "non-distillable" and "completely distillable" refined oils. Recovery with steam increased from 59 to 76% OOIP on changing from 0 to 25% distillable oil, and to 84% OOIP with a 50% distillable oil. While most of this increased recovery was attributed to steam distillation, other mechanisms also contribute. Results from some gasflood experiments indicated that an additional 3% OOIP is recovered as a consequence of 3 phase flow (i.e. steam, water, and oil); comparison of waterflood and steamflood runs using "non-distillable" oil suggests that this component may be more significant in other experiments.

A solvent extraction effect is also discussed. This mechanism results when light components volatilized in the steam zone are condensed in the cooler oil ahead of the steam front. As the steam front moves ahead, the oil bank ahead of the steam becomes progressively richer in light components, until the high temperature reaches the end of the core, and condensation can no longer occur. In the experiments with 25 and 50% distillable oil, changes observed in the composition of the produced oil confirmed that this mechanism was occurring. In another experiment in which steam was injected immediately after the core was flooded with hot water, recovery was lower. The authors explain that in this case, the light components were retained in the gas phase, and thus the solvent extraction mechanism did not occur. This mechanism appears to account for 3 to 8% OOIP in the refined oil floods.

A comparison was also made of the recoveries of two different crude oils, by hot waterflood,and by steamflood at two different pressures. For the heavier crude (6500 mPa.s at 26.7°C), waterflood at 166°C recovered 66 and 69% OOIP at 164° and 271°C, respectively. Another 3% was allocated to gas flood effects, 5 and 9% to steam distillation (based on measured steam distillable fraction), leaving 3-4% to solvent extraction effects. This interpretation is quite consistent with the results from the refined oil experiments.

Other results for the 6500 mPa.s crude oil are of interest. Waterflood at 166°C gave 59.8% OOIP, with an additional 11.2 (total 71) from subsequent steam injection. Values of 73.8 and 77.1% OOIP were obtained from two different cores by steamflooding at 166°C. Note variations of a few percent between runs under similar conditions in different cores. Since no runs are reported under exactly equivalent conditions, the reproducibility cannot be assessed. However, it appears that small changes in the permeability and initial saturation of the core resulted in variations of 5 - 10% OOIP in recovery.

To our knowledge, further work on steam distillation of heavy oils was not reported until 1975, when the first of a series of papers by C.H.Wu and coworkers was published [2]. Wu and Brown were interested in determining steam distillation yields, and thus designed their experiments to prevent oil displacement by any mechanism other than distillation. Their objective was to obtain data needed for improving steamflood simulators by incorporating the effects of steam distillation. They regard steam distillation and steam displacement as the two major recovery mechanisms operating in steamfloods.

In the experiments, steam was injected into the bottom of a heated cylinder containing water, oil, and sand. The fluids produced through a back-pressure valve at the top of the cylinder were condensed, collected, and quantified. The effect of a number of variables on the distillation rate and ultimate amount of distillate was studied. The authors concluded that the distillation yield, compared at the same value of water distilled per gm of initial oil, is insensitive to the amount of oil in the cell, and to whether the cell contains sand or is empty. They observed only a small increase in yield on increasing the temperature of the saturated steam from 197° to 244°C (with a 26 API oil), and no effect of steam injection rate (36 API oil, 197°C steam, 0-360 g/hr steam rates). Yields with superheated steam (500 psig, 316°C) were considerably higher than those with saturated steam (500 psig,244°C), particularly for a 14 API crude. Distillation yield did not correlate in a consistent way with oil density, being determined instead by composition.

Wu and Elder [3,4] extended the previous experiments, reporting steam distillation yields for 16 different crude oils, varying from 12 to 40 API. Initial runs using a 33 API California crude confirmed the reproducibility of the yield at 500 psia, and showed that yield is sensitive to saturated steam pressure above 350 psia. Insensitivity of steam distillation yield to initial oil volume and to injection rate was also confirmed.

Data were obtained for all 16 oils using saturated steam at about 200°C (220 psia). Steam distillation yield increased linearly with oil density, decreased logarithmically with oil viscosity (down to 10 cSt), and increased linearly with simulated distillation yield. More complex correlations between simulated distillation data and yield were also found. Yields varied from 12 to 56% of the initial oil volume, when distilled with steam at 193°C and 1380 kPa.

Duerksen and Hsueh [5] used an apparatus similar to that of Wu and Elder to measure steam distillation yields of 10 crude oils varying in API density from 9.4 to 30. In contrast to the earlier workers, however, Duerksen and Hsueh varied the steam temperature throughout each distillation experiment. At each temperature, the amount of distillate obtained after an arbitrary amount of steam injection was measured. Each distillation curve was thus a composite of 4 different curves of the kind obtained by Wu *et al* [3]. Duerksen and Hsueh carefully explain how the distillation temperature should affect the yield curves, but the correctness of their explanation cannot be proven with their data. Using some estimations, they were able to account for the small changes in yields reported by Wu and Elder for experiments at two temperatures at the same ratio of water injected to initial oil. They define a distillation factor, F, which takes into account variations in steam temperature (and thus pressure), and variations in initial oil volume. For most of the oils studied, the yield increased logarithmically with increasing F.

As a tool for evaluating the importance of steam distillation as an oil recovery mechanism, a correlation between steam distillation yield (at a fixed value of F) and API density was proposed [5]. With the exception of the 3 waxy crudes used in the study, the yield was found to be twice the API gravity.

Initial efforts to include the effects of steam distillation in a numerical simulator were made by Coats [6] and by Ferrer and Farouq Ali [7]. In these models, partial pressures were assumed to be additive (Dalton's Law) and fugacity coefficients in vapour and liquid phases were assumed to be unity (Raoult's Law). According to Hsueh, Hong, and Duerksen [8], both of these assumptions are insufficiently accurate to properly describe steam distillation at the conditions typical of a steamed reservoir (>200°C, >1000 kPa). The latter workers presented a more rigorous approach, in which vapour-liquid equilibrium quotients are determined using the Peng-Robinson equation of state (P-R EOS). Each of the oils was modelled as a mixture of six hypothetical components. The components were defined on the basis of a simulated distillation curve of the oil, from which the average boiling point of each pseudo-component was determined. The authors specifically claim that the simulated distillation curves give volume distilled; we note that the usual approach (the CRUDE procedure [9]), gives mass distilled. The authors give no explanation. Average molecular weights and densities of each pseudo-component were also obtained, by an unspecified method, possibly using a correlation with boiling point. The method of determination of the critical pressure and temperature of each pseudo-component is also not stated, although the Peng-Robinson equations as discussed in the paper require values for these parameters.

The authors give details of a calculation procedure and results of its application to model laboratory steam distillation data. Fairly good matching of the experimental data is achieved, but only by introducing a fitting parameter, the "steam distillation efficiency". It was concluded that the lab apparatus gave an efficiency of 50 to 60%, due to incomplete contact of steam with oil. Sensitivity of the model to some of the input parameters was tested. Pressure, temperature, and steam flow rate have a large effect, as does reducing the number of pseudo-components from six to three. Choice of binary interaction coefficients used in the P-R EOS had a negligible effect; the sensitivity to other input data derived from the simulated distillation curve was not mentioned.

Contrary to the authors conclusion, it is not evident from this work whether the rigorous approach described actually gives better predictions of steam distillation yields than a simpler approach using Dalton's and Raoult's Laws. The introduction of an empirically derived "efficiency factor" to account for non-equilibrium conditions limits the predictive capability of the model.

A different approach to the calculation of steam distillation equilibria has been described recently by Langhoff and Wu [10]. They note that the paucity of 3-phase separation data and critical properties of crude oil fractions introduces considerable uncertainty into methods using an equation of state, such as that used by Hsueh et al [8]. Instead, a method is proposed based on the Holland and Welch model for batch multicomponent steam distillation equilibria [11]. A number of assumptions were made in deriving the Holland and Welch equation, including the approximation that fugacity coefficients are equal to unity (i.e. Raoult's Law). The Holland and Welch approach was previously used by Rhee and Doscher [12] in their numerical model, and has been recommended by several others for steam distillation calculations. The equation requires vapour pressures of each component at the temperature of interest, and the mole fraction of each component in the mixture. To apply this approach to a heavy crude oil, Langhoff and Wu described the oil as a mixture of 12 pseudo-components, defined on the basis of boiling point using data from a simulated distillation. These workers interpret the distillate yield axis as mass percent distilled, but convert mass to volume distilled by assuming the pseudo-components have the same densities as paraffins of comparable boiling point. Presumably they present their data in this manner to make it more similar to data obtained from ASTM D2892 true boiling point analysis. In order to calculate the mole fraction of each pseudo-component, average molecular weights of each are required. For the eleven distillable components, molecular weights were estimated with the Katz and Firoozabadi correlation [13], which uses the average boiling point. The molecular weight of the non-distillable component was calculated from a mass balance using the molecular weights of all the other components and of the whole oil. Vapour pressures of each pseudo-component were determined from measured vapour-liquid equilibrium data reported by others. The authors assumed that the vapour pressure of each pseudo-component is only a function of its average boiling point, and thus used the same vapour pressures for analogous components of all of the oils studied.

Using the Holland and Welch equation, a vaporization efficiency correlation, and previously published data obtained from steam distillation studies of 16 oils (work discussed above), Langhoff and Wu give examples to demonstrate the predictive capability of their approach. They conclude that yields due to steam distillation can be estimated with an average relative error of 12%.

2.5 Instrumental Thermal Analysis Techniques

During the last 10 years, the use of thermogravimetry (TG), derivative thermogravimetry (DTG), differential thermal analysis (DTA), and differential scanning calorimetry (DSC), to provide improved understanding of the mechanisms involved in thermal oil recovery methods, has increased noticeably [1]. Thermal analysis experiments can provide kinetic and thermodynamic information such as activation energies, pre-exponential factors, rate constants, and heats of reaction under a variety of conditions. Parameters such as the amount of coke available to the combustion front, combustion front velocity and combustion temperature are best obtained from combustion tube runs, although it has been claimed that good estimates of these can be obtained from TG/DSC experiments [2-4].

Attempts to use differential thermal analysis to study crude oil combustion date back to 1959 when Tadema [5] showed that DTA curves obtained from the combustion of crude oil in the presence of sand consisted of two distinct regions. These two regions were related to low and high temperature oxidations and started around 200 and 350C, respectively.

Numerous researchers have since used thermal analysis results to develop kinetic models describing oil distillation, cracking, and low and high temperature oxidation (i.e. LTO and HTO). As an extension of the work of Freeman and Carroll [6], Coats and Redfern [7], in a classic paper on using TG to determine kinetic parameters, considered the reaction as representative of solid-state reactions involving weight changes. They suggested the following form for the fractional decomposition , α, as a function of time,t,

$$\frac{d\alpha}{dt} = k(1-\alpha)^n \tag{1}$$

where n is the order of the reaction and **k** the specific reaction rate. The fractional decomposition, α is defined as,

$$\alpha = \frac{w_o - w_t}{w_o - w_f} \tag{2}$$

where w_o is the initial sample weight, w_t the sample weight at time t, and w_f the final weight. The reaction rate, **k**, is given by the Arrhenius equation,

$$k = Ae^{-E/RT} \tag{3}$$

where A is the pre-exponential factor or frequency factor and E is the activation energy. With this kinetic model, Khulbe [8] found, from TG experiments, that the pyrolysis (in a nitrogen atmosphere) of asphaltenes from Cold Lake bitumen followed a second order decomposition. Vossoughi *et al* [9,10] and El Shoubary [11] used TG to study crude oil distillation and cracking/combustion, respectively and calculated reaction orders of 2.2 and between 1 and 2, respectively, for the two mechanisms. A reaction order of 2.2 for distillation was attributed to the complex nature of the crude oil. Less complex samples such as pure components as well as light crude oil follow, according to a TG study by Adonyi [12], a zero order evaporation kinetics. Adonyi and Korosi [13] and Wesolowski [14] have reported that the reaction order and the apparent activation energies of evaporation of volatile substances (water, aromatic, alkylaromatic, paraffin and naphthenic hydrocarbons) from mixtures containing non-volatile components (i.e. residual oil and n-paraffin hydrocarbons with an average molecular weight of 260) are affected by the heating rate used in the TG experiment and also by the kind of non-volatile components. It was, for example, shown that at low temperatures, the volatile substances evaporate from the mixture at a higher rate than from the pure state.

Recently, Skala *et al* [15] reported using the Coats and Redfern model to determine Arrhenius parameters for oil shale from TG curves. In one approach, a single first-order reaction was assumed, while the second approach involved the assumption of parallel first-order reactions. Jha and Verkoczy [3] also found that the Coats and Redfern model was adequate for the kinetic analysis of TG data from cores and extracted oil samples. Three temperature regions were identified from the DTG traces: the first region (40-350C) was attributed to evaporation, distillation, thermolysis, and LTO in the presence of air; the second region (350-500C) to distillation, thermal cracking, and LTO and combustion in air; and the third region (500-850C) to pyrolysis, coking, and combustion. For the distillation/evaporation region, a reaction order of 1 was found as opposed to 2.2 determined by Vossoughi [9,10] and El Shoubary [11]. The reaction orders for the other two regions varied from 0.7 to 2.0. Despite the many successful applications of the Coats and Redfern model, Weckowska and Bogdanow [16] had to use an extension proposed by Zsako [17],

$$\frac{d\alpha}{dt} = k\alpha^{p}(1-\alpha)^{q} \qquad (4)$$

to properly describe the kinetics of thermal decomposition of a crude oil residue. In two later studies, Vossoughi [2,18] used a further extension suggested by Dollimore [19],

$$\frac{d\alpha}{dt} = k\alpha^{m}(1-\alpha)^{n}[-\ln(1-\alpha)]^{p} \qquad (5)$$

to describe the kinetics of crude oil LTO (with m = 0.8, n = 2.0, and p = 3.8) and the two cracking/combustion reaction peaks observed by DTG (1st peak: m = 1.0, n = 2.0, and p = 0.03). Crude oil distillation was described by the following equation,

$$\frac{d\alpha}{dt} = Ae^{b(T_o-T)^2} \qquad (6)$$

where T_o is the temperature at which $d\alpha/dt$ is a maximum and T is the temperature at any time t. Although a reasonable prediction of the *in situ* combustion variables was achieved, the approach used suffered from the lack of the fluid flow and displacement behavior associated with the process.

McCarthy *et al* [20], in a different approach, suggested a method of deriving kinetic data from thermal analysis studies that involved the analysis of the TG curve at a number of isothermal temperatures. An analytical technique was developed in which a single TG plot could be used to determine the pertinent Arrhenius parameters and reaction orders. Phillips [21] determined with a flow-through fixed bed reactor that the LTO reaction of Athabasca bitumen is first order with respect to oxygen concentration and confirmed this finding by DTA [22]. Applying the method of Bae [23] to the determination of kinetic parameters for an n'th order reaction from the solution of DTA equations, Phillips [22] also determined the effect on LTO activation energy/pre-exponential factor of oxygen partial pressure as well as of support materials such as alundum and sand. A very similar approach was taken by Vossoughi and El Shoubary [24] in studying the effect of specific surface area, oxygen partial pressure, and oil content on crude oil coke combustion by TG. The rate of combustion was found to be first order with respect to oxygen partial pressure as well as coke content yet to be burned, while the dependence of the surface area was to the power of 0.14.

Nickle and Meyers [25] confirmed the first order dependency on oxygen partial pressure in a paper discussing a number of shortcomings in the use of TG/DSC to evaluate *in situ* combustion. It was shown that heating rate significantly affects fuel laydown, the heat evolved during LTO and combustion, and the DTG/DSC peak temperatures. The TG sample temperature during combustion was found to be prone to an error which increased with increasing oil saturation, heating rate, purge gas flow rate, and oxygen concentration. Errors as high as 300°C were observed. Also pointed out was the simplistic nature of a single component, single reaction, kinetic model to describe combustion kinetics.

The individual effects of sand surface area and clay catalysis on the combustion process of a 20° API gravity oil have been studied by Vossoughi [18,26]. *In situ* combustion tube experiments were performed with silica sands of different grain size distribution. TG and DSC analysis of samples taken immediately ahead of the combustion front showed that the oil content of this section increased with increasing specific surface area of the porous medium. In addition, the thermograms indicated that the combustion properties of the oil ahead of the combustion front had been altered by the combustion process. Vossoughi [9,10] had also reported the use of TG and DTG to demonstrate that the rate of crude oil weight loss during combustion remained unchanged in the presence of sand, increased slightly in the presence of silica powder, and showed a pronounced increase in the presence of clay. The effect on the distillation region was negligible for all the materials (i.e. the activation energy was unaffected by the presence of clay or silica powder). Identical experiments under nitrogen rather than air showed a reversed clay effect, implying that the crude oil is adsorbed onto the clay surface and cannot be easily removed by a flowing stream of nitrogen. Addition of kaolinite clay or silica powder to the oil changed the shape of the TG/DSC thermograms significantly. The main effect on DSC thermograms was to shift the large amount of heat produced to a lower temperature range.

In addition to the main metal components - silicon and aluminum - a clay may contain a wide variety of trace metals such as potassium, iron, nickel, and more, while the oil may contain various levels of vanadium, nickel, chromium, copper, and others. The catalytic effect of such metals on combustion reactions was reported by Burger [27] in 1968. A few years later, Burger and Sahaquet [28] used an effluent gas TG approach to illustrate catalytic effects of metallic derivatives of copper, iron, nickel, and vanadium. The presence of the selected metal salts caused the oxidation reactions of the 27°API gravity oil to occur at lower temperatures (i.e. with lower activation energy). Also, the amount of coke formed during pyrolysis was found to increase which agrees with the later findings of Verkoczy and Jha [29] that the presence of reservoir minerals can increase coke formation by 37 to 315 percent.

In 1985, Drici and Vossoughi [30] published the results of a more extensive study on the effect of metal oxides on crude oil combustion using DSC and TG. In addition to confirming the findings of Burger and Sahaquet [28], it was found that the effect of a small amount of metal oxides (about 1 wt %) on the crude oil combustion in the presence of silica powder (high surface area) was insignificant. The latter was postulated as resulting from the surface reactions being predominant.
Concurrent with Drici and Vossoughi [30], Al-Sammerrai [31] used TG to show that variations in the nickel and vanadium content of various Iraqi bitumens had no influence on the amount of coke produced during pyrolysis. However, the amount of coke was found to increase from 0.3% of the original bitumen to 14% with an increase in sulfur content from 4 to 8%. Recently, Cardillo and Galtieri [32] demonstrated the TG technique can produce the same results as the Conradson Carbon Residue test.

To determine the relative amount of quartz and kaolinite clay in a matrix for combustion tube runs that best simulated the natural core, Hardy and Raiford [33] chose to use DTA. The basic assumption in their study was that the effect of reservoir rock on *in situ* combustion parameters could be simulated with a quartz - kaolinite mixture in combustion tube experiments if the DTA thermograms of the oil in the presence of the two matrices showed the same profile. Similarly, TG and DSC have been used [34-36] to provide valuable information for the design of field tests. Kharrat and Vossoughi [34-35] made use of TG and DSC to predict a minimum reservoir crude oil content necessary for a self-sustained combustion. A minimum front temperature defined as the temperature at which the total crude oil was consumed was determined from isothermal TG runs, while ΔH values for the crude were obtained from DSC curves. The calculated minimum crude oil content was then used as a criterion in the feasibility study of the *in situ* combustion process. Phillips *et al* [36] also reported the use of DSC to determine enthalpies (i.e. ΔH values) of pyrolysis, and oxidation of Athabasca oil sands, bitumen, and its fractions.

It has been shown [37-40] that TG, DTG, and DSC are useful tools in evaluating *in situ* combustion performed either in the field or in the lab. From DTA analysis of crude oils used in combustion tube experiments, H. Berry [37] estimated an ignition temperature of 500F and a maximum temperature of 700F. In 1977, a careful study by Bae [38] led to the classification of crude oils into three distinctive categories based on their TG thermo-oxidative behaviour. The specific gravity of the oils was found not to correlate well with these categories. Low temperature oxidation was found to drastically change the quality and quantity of fuel available for *in situ* combustion. Bae was also able to use the thermal analysis results to qualitatively predict combustion tube test behaviour. Joseph *et al* [39] used TG and DSC to study core samples from two post-burn evaluation wells in the Bellevue Field where Cities Services Company had applied an *in situ* combustion process. The results of these analyses provided input into the determination of the sweep efficiency of the combustion process, the composition of the oil remaining in the core samples from the various intervals, and the maximum temperatures to which the core material had been subjected. Weyland *et al* [40] used TG and DTG to establish, after having developed baseline data, that considerable LTO occurred ahead of the fire fronts in combustion tube experiments. In addition, very close to, but still ahead of the front, DTG thermograms clearly showed evidence of LTO as well as HTO (i.e. high temperature oxidation). Application of the thermogravimetric techniques to the analysis of post-burn core samples from a field test near Bartlett, Kansas, identified fire front fingering and intervals where only LTO had taken place.

A number of studies [41-46] have used thermal analysis to characterize crude oils and crude oil fractions for reasons other than a better understanding of thermal oil recovery mechanisms. Giavarini and Pochetti [41] and Claudy *et al* [42] have shown that DSC can be used to determine wax content, glass transition temperature, and crystallization temperature of distillates, crude oils, and bitumens. The former [41] also claimed that a correlation existed between the DSC crystallization data and ASTM cloud points (D2500) and pour points (D97). Ciajolo and Barbella [43] and Day and Majid [44] used TG and DTG to evaluate the fuel potential of heavy fuel oils and bitumens. It was found that the thermograms of these samples could be described by two regions as opposed to three reported by Jha and Verkoczy [3]. The first region up to about 400C was assigned to evaporation of low molecular weight species, while the second region between about 400 and 600C was assigned to cracking and degradation of higher molecular weight species. Donbavand *et al* [45] used DTG to characterize a number of asphaltic cements. The technique was sensitive enough to allow detection of changes in the original crude oil or the processing conditions. Recently, Al-Sammerrai [46] showed that TG and DSC can be used to estimate the boiling point range of distillate fractions. This was based on the observation that the onset of the exothermic oxidation increased with molecular weight and total aromatic content.

2.6 References

2.6.1 Oil Viscosity Variability

[1] Hunt, M., "Petroleum Geochemistry and Geology", W.H. Freeman and Co., San Francisco 1979, pp.381-391.

[2] Hirschberg, A., "The Role of Asphaltenes in Compositional Grading of a Reservoir's Fluid Column", SPE 13171, 1984.

[3] Schulte, H.M., "Compositional Variations within a Hydrocarbon Column due to Gravity", SPE 9235, 1980.

[4] Tripathy, B., "Analysis and Evaluation of Alternate Concepts in Modelling Tar Mats to Conform to Laboratory Investigations and Field Conditions", SPE 15689, 1987.

[5] Acharya, U.B., "Effect of Tar Mat on Reservoir Behavior: Reservoir Simulation Case Studies", SPE 15690, 1987.

[6] Amosov, G.A.and Kozina, T.A., "Interaction of Crude Oils and Water in Sakhalin Oilfields", International Geology Review 9(7), 883, (1966).

2.6.2 Thermal Alteration of Petroleum

[1] Hyne, J.B., Synopsis report no. 50, AOSTRA contracts no. 11,103, Apr. 1986.

[2] Akstinat, M.H., J. Pet. Geology, 5(4), 363, 1983.

[3] Hesp, W. and Rigby, D., Erdol and Kohle - Erdgas - Petrochemie rereinigt mit Brennstoff - Chemie 26 (2), 70, 1973.

[4] Monin, J.C. and Audibert, A., Preprint, Div. Pet. Chem (ACS), V29(4), 1223, 1984.

[5] Monin, J.C. and Audibert, A., SPE paper 16269, SPE International Symposium on Oilfield Chem., San Antonio, Feb. 1987.

[6] Monin, J.C. and Audibert, A., 3rd International Conference on Heavy Crude and Tar Sand, Long Beach, July 1985.

[7] Venkatesan, V.N. and Shu, W.R., Preprint no. 84-35-108, 35 Annual Tech. Mtg. CIM, 1984.

[8] Shu, W.R. and Verkatesan, V.N., J. Can. Pet. Tech., 2, P60, 1984.

[9] McNab, J.G., Smith, P.V. and Bette, R.L., Ind. Eng. Chem., 44(11), p 2556, 1952.

[10] Kossiakoff, A and Rice, O., J. Am. Chem. Soc., 65(1), 590, 1943.

[11] Blouri, B. Hamdan, Fadl and Herault, D., Ind. Eng. Chem. Proc. Dev., 24(1), 30, 1985.

[12] Erdman, J.G. and Dickie, J.P., Reprints. Div. Pet. Chem. (ACS), 9(2), PB69, 1964.

[13] Hus, M., Oil & Gas Journal, p. 109, April 13, 1981.

[14] Lin, C.Y., Chen, W.H. and Culham, W.E. SPE paper 13074, 59th Annual Tech. Mtg. of SPE, Sept. 1984.

[15] Henderson, J.H. and Weber, L., J. Can. Pet. Tech., 4, p. 206, 1965.

[16] Romanowski, L.J. and Thomas, K.P., "Laboratory Studies of Forward Combustion in Tar Sand (Tar Sand Triangle)" Laramie, W.Y. report for DOE contract no. DE-FC21-83 FE 60177.

2.6.3 Influence of Asphaltenes on Oil Viscosity

[1] Altgelt, K.H., and Harle, O.L., "The Effect of Asphaltenes on Asphalt Viscosity", *ibid* 14(4).

[2] Reerink, H., "Size and Shape of Asphaltene Particles in Relationship to High Temperature Viscosity", Inc.Eng.Chem.Prod.Res.Dev. 12(1), 81(1973).

[3] Mack, Charles, "Colloid Chemistry of Asphalts", J. Phys.Chem. 36,2901(1932).

[4] Spearot, J.A., "Viscosity of Severely Oxidized Engine Oil", *ibid.* 13(4), 259(1974).

[5] Michaels, A.E. and Bolger, J.C., Ind.Eng.Chem.Fund. 3,14(1964).

[6] Datta, P., "Rheological Studies of Asphaltic Crude Oils of California", M.Sc. Thesis.

[7] Robinson, D.B., and Associates, "The Thermodynamic and Transport Properties of Bitumens and Heavy Oils", AOSTRA Technical Report, July 1984, Chapter 3, pp. 75-76 and 138-146.

[8] Pearson, C.D. *et al.*, "Technique for the Determination of Asphaltenes in Crude Oil Residues", Anal.Chem. 58, 3265 (1986).

2.6.4 Steam Distillation

[1] Willman, B.T., *et al.*, "Laboratory Studies of Oil Recovery by Steam Injection", J. Petr. Tech. July 1961, p. 681.

[2] Wu, C.H., and Brown, Alfred, "A Laboratory Study on Steam Distillation in Porous Media", SPE 5569, (1975).

[3] Wu, C.H., and Elder, R.B., "Crude Oil Steam Distillation in Steam Flooding", DOE/ET/12357-3, August 1980.

[4] Wu, C.H., and Elder, R.B., "Correlation of Crude Oil Steam Distillation Yields with basic Crude Oil Properties", SPEJ, Dec 1983, p. 937.

[5] Duerksen, J.H., and Hsueh, L., "Steam Distillation of Crude Oils", SPEJ, April 1983, p. 265.

[6] Coats, K.H., "Simulation of Steamflooding with Distillation and Solution Gas", SPE 5015 (1974). SPEJ p. 235, Oct. 1976.

[7] Ferrer, J. and Farong Ali, S.M., "A Three Phase Two Dimensional Compositional Thermal Simulator For Steam Injection Processes", J. Can. Pet. Tech., Jan.-Mar., 1977, p. 78.

[8] Hsueh, L., Hong, K.C. and Duerksen, J.H., "Simulation of High Pressure and High Temperature Steam Distillation of Crude Oils", 1982 UNITAR Conference, p. 924.

[9] ASTM Book of Standards, Part 25, 1977.

[10] Langhoff, J.A., and Wu, C.H., "Calculation of High Temperature Crude Oil/Water/Vapor Separations Using Simulated Distillation Data", SPE Res. Eng., Sept. 1986, p. 483.

[11] Holland, C.D., and Welch, N.E., "Steam Batch Distillation Calculations", Petroleum Refiner, May 1957, p. 251.

[12] Rhee, S.W., and Doscher, T.M., "A Method for Predicting Oil Recovery by Steamflooding Including the Effects of Distillation and Gravity Override", SPEJ, Aug. 1980, p. 249.

[13] Katz, D.L., and Firoozabadi, A., "Predicting Phase Behaviour of Condensate/Crude Oil Systems Using Methane Interaction Coefficients", J. Pet. Tech., Nov. 1978, p. 1649.

2.6.5 Instrumental Thermal Analysis Techniques

[1] Vossoughi, S., "TGA/DSC Techniques as Research Tools for the Study of the *In-Situ* Combustion Process", Thermochim. Acta, 106, 63-69, 1986.

[2] Vossoughi, S., Bartlett, G.W., and Willhite, G.P., "Development of a Kinetic Model for *In Situ* Combustion and Prediction of the Process Variables using TGA/DSC Techniques", SPE 11073, presented at the 57th Annual Conference, Sept. 26-29, 1982.

[3] Jha, K.N., and Verkoczy, B., "The Role of Thermal Analysis Techniques in the *In Situ* Combustion Process", SPE 12677, presented at the SPE/DOE Fourth Symposium in Tulsa, Apr. 15-18, 1984.

[4] Saim, S.,"Development and Application of a Fully Implicit One-Dimensional *In-Situ* Combustion Simulator and a Kinetic Model Based on TGA/DTG Experimental Results", M.Sc. Thesis, Univ. of Kansas, 1987.

[5] Tadema, H.J., "Mechanism of Oil Production of Underground Combustion", Proc., Fifth World Petroleum Congress, New York, Sect. II, Paper 22, 279, 1959.

[6] Freeman, E.S., and Carroll, B., "The Application of Thermoanalytical Techniques to Reaction Kinetics; the Thermogravimetric Evaluation of the Kinetices of the Decomposition of Calcium Oxalate Monohydrate", J. Phys. Chem., 62, 394-7, Apr. 1958.

[7] Coats, A.W., and Redfern, J.P., "Kinetic Parameters from Thermogravimetric Data", Nature, 201, 68-69, Jan. 4, 1964.

[8] Khulbe, K.C., Sachdev, A.K., Mann, R.S., and Davis, S., "TGA Studies of Asphaltenes Derived from Cold Lake (Canada) Bitumen", Fuel Proc. Technol., 8, 259-266, 1984.

[9] Vossoughi, S., Willhite, G.P., Kritikos, W.P., Guvenir, I.M., and Shoubary, "Effect of Clay on Crude Oil *In Situ* Combustion Process", SPE 10320, presented at the 56th Annual Conference, Oct. 5-7, 1981.

[10] Vossoughi, S., Willhite, G.P., Shoubary, Y. El, and Bartlett, G., "Study of the Clay Effect on Crude Oil Combustion by Thermogravimetry and Differential Scanning Calorimetry", J. Thermal Anal., 27, 17-36, 1983.

[11] Shoubary, Y. El, "Kinetic Study of the *In Situ* Combustion Process Using Thermal Analysis Technique", Ph.D. Dissertation, Univ. of Kansas, 1986.

[12] Adonyi, Z., Proc., Third Intl. Conf. on Thermal Analysis, Davos, Switzerland, 1, 255, 1971; Birkhauser, Basel, 1972.

[13] Adonyi, Z., and Korosi, G., Period, Polytech., Chem. Eng., 19. 103, 1975.

[14] Wesolowski, M., "Thermal Analysis of Petroleum Products", Thermochim. Acta, 46, 21-45, 1981.

[15] Skala, D., Kopsch, H., Sokic, Neumann, H.J., and Joranovic, J., "Thermogravimetrically and Differential Scanning Calorimetrically Derived Kinetics of Oil Shale Pyrolysis", Fuel, 66, 1185 - 91, Sept. 1987.

[16] Weckowska J., and Bogdanow, "Initial Investigation of the Thermal Decomposition Kinetics of the Vacuum Distillation Residue of Crude Oil", J. Thermal Anal., 17, 39, 1979.

[17] Zsako, J., "Kinetic Analysis of Thermogravimetric Data, "J. Phys. Chem., 72, 2406 - 11, July 1968.

[18] Vossoughi, S., Bartlett, G.W., and Willhite, G.P., "Prediction of *In Situ* Combustion Process Variables by Use of TGA/DSC Techniques and the Effect of Sand-Grain Specific Surface Area on the Process", SPEJ, 656-64, Oct. 1985; Trans., AIME, 279.

[19] Dollimore, D., "Thermal Analysis in Chemical Processing", NBSW Publication 580, 1-31, May 1979.

[20] McCarthy, H., Paiverneker, V.R., and Maycock, J.N., "Determination of Kinetic Parameters from a Single Thermogram", Proc., Third Intl. Conf. on Thermal Analysis, Davos, Switzerland, 1, 355, 1971.

[21] Phillips, C.R., and It-Chin Hsieh, "Oxidation Reaction Kinetics of Athabasca Bitumen", Fuel, 64, 985-9, July 1985.

[22] Yoshiki, K.S., and Phillips, C.R., "Kinetics of the Thermo-oxidative and Thermal Cracking Reactions of Athabasca Bitumen", Fuel, 64, 1591-8, Nov. 1985.

[23] Bae, J.H., "Determination of the Kinetic Parameters from Differential Thermal Analysis", J. Thermal Anal., 4, 261, 1972.

[24] Vossoughi, S., and Shoubary, Y. El, "Kinetics of Crude Oil Coke Combustion", SPE 16268, presented at the Intl. Symposium in San Antonio, Feb. 4-6, 1987.

[25] Nickle, S.K., and Meyers, K.O., "Shortcomings in the Use of TGA/DSC Techniques to Evaluate *In Situ* Combustion", SPE 16867, presented at the 62nd Annual Conference, Sept. 27-30, 1987.

[26] Vossoughi, S., Bartlett, G.W., and Willhite, G.P., "Effect of the Sand-Grain Specific Surface Area on the Performance of the Tube *In-Situ* Combustion Process", SPE 11072, presented at the 57th Annual Conference, Sept. 26-29, 1982.

[27] Hardy, W.C., and Raiford, J.D., "*In Situ* Combustion in a Bartlesville Sand - Allen Count", Proceedings of the Tertiary Oil Recovery Conference, Wichita, Oct. 23-24, Contribution 2, p. 24, 1975.

[28] Kharrat, R., "Development of a New Criterion for a Feasibility Study of the *In Situ* Combustion Process Using TGA/DSC Techniques", J. Pet. Tech., 1441-5, Aug. 1985.

[29] Phillips, C.R., Luymer, R., and Halahel, T.M., "Enthalpies of Pyrolysis and Oxidation of Athabasca Oil Sands", Fuel, 61, 639-46, July 1982.

[30] Joseph, C., Jay, C.B., Eslinger, E.V., and Mundis, C.J., "Evaluation of an *In Situ* Combustion Process by Post Burn Core and Log Analysis", SPE 10766, presented at the 1982 California Regional Meeting, March 24-26, 1982.

[31] Al-Sammerrai, F., and Al Sammerrai, D., "Thermogravimetric Characterization of Some Iraqi Bitumens", Thermochim. Acta, 94, 295-303, 1985.

[32] Cardillo, P., and Galtieri, A., "Determinazione del residuo carbonioso di oli combustibili medianti termogravimetria", La Rivista dei Combustibili, XLI, fasc.1, 1-5, 1987.

[33] Hardy, W.C., and Raiford, J.D., "*In Situ* Combustion in a Bartlesville Sand - Allen Count", Proceedings of the Tertiary Oil Recovery Conference, Wichita, Oct. 23-24, Contribution 2, p. 24, 1975.

[34] Kharrat, R., "Development of a New Criterion for a Feasibility Study of the *In Situ* Combustion Process and Its Implementation for four Kansas Oil Reservoirs", MS Thesis, Univ. of Kansas, Lawrence, KS, 1983.

[35] Kharrat, R., and Vossoughi, S., "Feasibility Study of the *In Situ* Combustion Process Using TGA/DSC Techniques", J. Pet. Tech., 1441-5, Aug. 1985.

[36] Phillips, C.R., Luymer, R., and Halahel, T.M., "Enthalpies of Pyrolysis and Oxidation of Athabasca Oil Sands", Fuel, 61, 639-46, July 1982.

[37] Berry, H.J., "An Experimental Investigation of Forward Combustion Oil Recovery", Ph.D. Dissertation, Univ. of Texas A&M, 1968.

[38] Bae, J.H., "Characterization of Crude Oil for Fireflooding Using Thermal Analysis Methods", Soc. Pet. Eng. J., 17, 211-18, June 1977.

[39] Joseph, C., Jay, C.B., Eslinger, E.V., and Mundis, C.J., "Evaluation of an *In Situ* Combustion Process by Post Burn Core and Log Analysis", SPE 10766, presented at the 1982 California Regional Meeting, March 24-26, 1982.

[40] Weyland, J.R., Lee, D.O., and Massis, T.M., "On the Application of TG Concepts to *In Situ* Combustion Processes", SAND83-0336, Scandia National Laboratories Albuquerque, NM 87185, June 1983.

[41] Giavarini, C., and Pochetti, F., "Characterization of Petroleum Products by DSC Analysis", J. Thermal. Anal., 5, 83-94, 1973.

[42] Claudy, P., Letoffe, J.M., Chaque, B., and Orrit, J., "Crude Oils and Their Distillates" Characterization by Differential Scanning Calorimetry", Fuel, 67, 58-61, Jan. 1988.

[43] Ciajolo, A., and Barbella, R., "Pyrolysis and Oxidation of Heavy Fuel Oils and Their Fractions in a Thermogravimetric Apparatus", Fuel, 63, 657-660, 1984.

[44] Day, M., and Majid, A., "A Thermogravimetric Analysis of some Oil Sand Fractions", J. Thermal. Anal., 29, 1247-58, 1984.

[45] Donbavand, J., Ball, G.F.A., and Patrick, J.E., "A Study of Asphaltic Cements and Their Fracti Thermogravimetry", Thermochim. Acta, 98, 99-109, 1986.

[46] Al-Sammerrai, F., Mohammed, A-H, and Abbas, N., "Thermoanalytical Evaluation of the Thermal Stability of Petroleum Distillates", Fuel, 66, 512-14, 1987.

3.0 OIL VISCOSITY VARIABILITY IN THE CARIBOU LAKE RESERVOIR (TASK 2)

3.1 Summary

Samples of oil were separated from preserved core using a heated centrifugation technique. For a number of wells cored in the Clearwater B reservoir, oil viscosity at 25°C was found to increase with increasing depth of origin of the sample. The areal variation of the viscosity appears to correlate with the structural elevation of the sand. Thus the viscosity depth profiles are shifted towards less viscous oil in locations where the reservoir is structurally high, and towards more viscous oil in structural lows. Distillation curves of selected samples confirm that the oil viscosity variations coincide with compositional differences. Single sets of samples from the McMurray and from the Wabiskaw in the Caribou Lake area also show increasing viscosity with increasing depth. Some discussion of possible causes of these compositional variations and of their significance to thermal recovery is included.

3.2 Introduction

In our early considerations of the effects of thermal alteration on oil recovery processes, questions arose regarding the nature of the unaltered or "native" reservoir oil. Previous in-house studies of fluids produced from thermal projects suggested that oil of differing viscosity is produced from wells in the same reservoir. This variability could result from thermal alteration of the oil, but also could be a consequence of natural compositional variability of the native oil in the reservoir. The present work was initiated to examine the variability in the oil within a heavy oil reservoir.

Since oil viscosity can be measured efficiently and precisely on small samples, is a sensitive indicator of composition, and is an important parameter in recovery processes, it was selected as the primary variable in this study.

Obtaining suitable samples for such a study was problematic; preserved core from the reservoirs of most interest (i.e. located in the Lloydminster area) was not available. However, a drilling program in the Caribou Lake area, located north of Lloydminster in the Primrose Air Weapons Range, made available fresh core for this study.

3.3 Methods

3.3.1 Oil Sample Preparation

Pieces of core material of about 150 g were cut from frozen core in the same way as is used to obtain samples for Dean-Stark oil-water-solids (OWS) determinations (see Figure 1). The V-shaped pieces were cut without lubricant and were transferred from Chemical and Geological Labs to NHRC frozen in sealed bags. Drillers' depths were determined for each sample and marked on the bag. The samples were kept frozen until used.

About one hour before use, a set of six randomly chosen samples was partially thawed at 22°C, and each sample was weighed into a stainless steel centrifuge bottle. The bottle (about 250 cm^3) was then filled to the shoulder with 1 M NaCl, reweighed, and sealed with the lid. Teflon tape was used to seal the threads of the lid.

The six bottles were placed in the centrifuge head, and the head was heated to 90°C in an oven (1 hour). Preheating the head and samples in an oven is more efficient than heating under the vacuum conditions in the centrifuge. The heated head was then transferred to the centrifuge and spun at 14,000 rpm (~30,000 x gravity) for 1.5 hours using a Beckman Model L8/M heated ultracentrifuge kept at 90°C. The head was then cooled to 22°C, and the bottles removed and weighed to assess any leakage.

The oil floating on the top of the brine was transferred to a small vial with as little brine as possible. The measurements were made on portions of the samples within 2 days of separation from the core.

3.3.2 Measurements

The concentration of water remaining in each sample was determined on a 0.5 g subsample using a coulometric Karl-Fischer apparatus.

Viscosity was measured using a Brookfield Model RVT DCP cone and plate viscometer thermostatted at 25°C (35°C for 8D-32). Readings made at three different shear rates (9.6, 3.84, 1.92 s^{-1}) show a slight shear thinning, but it is of such small magnitude compared to other measurement uncertainties that the average of the three readings has been reported.

Overall uncertainty of the sample preparation and measurement technique was evaluated by selecting replicate samples from adjacent locations for one well, 5D-24. The data (which are given in detail in Appendix A) show that overall repeatability is usually better than ± 5% relative.

Simulated distillation data were obtained using the CRUDE procedure and an HP 5880 gas chromatograph with a Level 4 acquisition system.

3.4 Results and Discussion

Viscosity-depth data obtained from samples taken from 15 Caribou Lake wells are collected in Table 1. All of these samples are from the Clearwater "B" reservoir. A quick look at the data shows the variability in the native oil. Plots of the data shown in Figures 2-15 confirm that all but three of the wells studied show a consistent trend of increasing viscosity with increasing depth. In five of the wells, the viscosity increases by a factor of 7 or 8 over the sampled interval; in another five, where the samples cover a more limited portion of the pay, viscosity increases by 2- to 3-fold.

Anomalous viscosity-depth data were obtained from three wells, 9B-12, 8C-9 and 6C-32. In 9B-12, and to a lesser extent in 6C-32, the deepest sample has a lower viscosity than it should to follow the trend (Figures 3, 14). A similar inconsistency is seen in the 8C-9 data (Figure 7). Only the two deepest samples have viscosities which are inconsistent with the upper three. Replicate samples from the same depth confirmed these anomalies. These anomalies in oil viscosity appear to coincide with locations having unusually low oil saturation, as determined from the logs and OWS core analysis data. The reason for this correlation is not apparent.

An overall comparison of the data is obtained by overlaying the plots, as shown in Figure 15. Although there is some scatter, viscosity increases with decreasing mean sea level elevation over the sampled area. Oil viscosity is lower in areas of structural highs (e.g. 6C-32, 8C-36) and increases as structure elevation drops (e.g. 6C-36).

An alternate comparison is shown in Table 2. The viscosity at a point 5 m below the top and at a point 5 m above the bottom of the Clearwater zone was obtained by interpolation from the graphs of the data for each well. It is evident that there is no constancy of viscosity at either of these two relative points in the reservoir. More careful comparison of Table 2 confirms the correlation with structural elevation.

The observed viscosity differences imply that oil composition changes with depth in the reservoir. To support this conclusion, simulated distillation curves were obtained on selected oil samples. In the data presented in Figures 16 to 21, the distillation profiles of samples of lower viscosity from upstructure locations are consistently shifted to lower boiling temperatures compared to those from samples of higher viscosity. The lower viscosity samples are clearly compositionally different from those having higher viscosity. Note that most of the curves are parallel to each other. This suggests that the compositional differences are in the heavy non-distillable fraction rather than in the lighter fraction of the oils.

Table 3 gives some data obtained from oil samples taken from the McMurray and Wabiskaw sand reservoir at Caribou Lake. As for the Clearwater, viscosity increases with increasing depth. These data show that oil property variation is not unique to the Clearwater, but may indeed be a characteristic of many Canadian heavy oil reservoirs.

As noted in the Introduction, the motivation for this work originated with questions arising at several Husky EOR pilots. The availability of fresh core and the interest of project members led to selection of Caribou Lake reservoir for the study. Little thought was initially given to the relevance of oil viscosity variation to the development of the Caribou Lake Cyclic Steam Project. As the work progressed, it was theorized that the higher viscosity oil low in the reservoir would probably enhance steam override. However, with injection above parting pressure, and the likelihood that the viscosity differences will decrease at higher temperatures, the effect on steam override may be insignificant. The correlation of viscosity with structural elevation could potentially impact on Caribou Lake development plans, but again it is not obvious whether oil which is less viscous by a factor of 8 at reservoir conditions will necessarily respond better to cyclic steaming. Other structural considerations such as the presence of gas zones would clearly outweigh any conclusions based on viscosity.

If the higher viscosity oil lower in the reservoir results from an enhanced asphaltene concentration, that oil may be chemically less stable. Upon mobilization by steam, it may be more likely to precipitate asphaltenes, with either good or bad effects depending on where the asphaltenes are deposited. This suggestion is based on the theory that when heavy oils are generated, the concentration of asphaltenes is matched to the dissolving capability of the maltenes. Addition of extra asphaltenes, for example, by gravity settling, would produce an oil with greater than optimum asphaltene content.

The observation of tight streaks in some of the cored wells has raised questions about their impact on fluid flow within the reservoir. At an early point in this work, one well was chosen for more extensive sampling, specifically to look for discontinuities in oil viscosity between samples above and below a tight streak. The data from well 5D-24 in Figure 10 follow a smooth curve, in spite of several tight streaks over the sampled interval. Thus, from the perspective of the process which has caused the oil viscosity variation, the tight streaks had no observable effect.

On the basis of the information reviewed in section 2.1, there appear to be several processes which could have caused the oil compositional variability observed in this study. It could be related to the original migration and trapping processes, or have occurred after the oil was in place. If one accepts the theory that Canadian heavy oils are light oils that have been degraded, the presence of mobile water may have special significance. The correlation with elevation may actually be a correlation with the elevation at which there is an active oil-water contact. It is possible that in a well with a mobile water contact oil degradation may have advanced to the point of forming a tar mat. Such a tar mat may actually impede water coning, a possibility that might be beneficially exploited in heavy oil reservoirs with active bottom water.

3.5 Conclusions

Viscosity of native oil in the Clearwater reservoir at Caribou Lake increases with increasing depth. Furthermore, over the area studied, viscosity appears to correlate with structural elevation. Thus the least viscous oil is found at the top of the Clearwater zone, in locations where the Clearwater is structurally highest.

Distillation curves confirm that the observed viscosity variations are due to compositional rather than physical differences in the oil samples. The curves suggest that the compositional differences are mainly in the heaviest fraction of the oil.

More limited data on samples from the Wabiskaw and McMurray reservoirs in the Caribou Lake area also show increasing oil viscosity with increasing depth. It seems likely that such a phenomenon may be found in all Canadian heavy oil reservoirs. Review of the literature shows that compositional gradation is quite common in oil reservoirs throughout the world, although no reports of such variability in Canadian reservoirs have been found.

The effect of variations in the native oil viscosity on the performance of cyclic steaming is not known. Within a single well, the viscosity trend may enhance steam override, although temperature effects on viscosity will likely dominate. Wells which are structurally higher may show better performance, although there are so many other factors determining performance that original viscosity may be of little significance. The higher viscosity oil low in the reservoir may have more tendency to lose asphaltenes when subjected to changes in temperature and pressure.

3.6 Tables

1. VISCOSITY OF OIL FROM CLEARWATER B RESERVOIR IN CARIBOU LAKE AREA
2. CLEARWATER B STRUCTURAL DATA[a]
3. VISCOSITY OF OIL FROM MCMURRAY AND WABISKAW RESERVOIR IN CARIBOU LAKE AREA

TABLE 1

VISCOSITY OF OIL FROM CLEARWATER B RESERVOIR IN CARIBOU LAKE AREA

WELL	VISCOSITY [a]	DEPTH [b]	RESIDUAL WATER, %	SAMPLE
6C-22	16.5	489.95	1.9	CL124
	17.8	491.40	2.4	CL125
	16.9	491.75	0.01	CL126
9B-12	30.3	438.97	0.1	CL166
	32.2	441.40	0.1	CL167
	38.5	442.12	0.06	CL168
	43.0	444.65	0.05	CL169
	53.4	446.45	0.2	CL170
	28.5	452.62	0.01	CL171
6C-36	43.9	469.15	0.1	CL128
	43.5	469.65	0.01	CL129
	44.7	470.63	0.2	CL130
	50.2	471.20	0.5	CL131
7C-20	20.6	442.53	0.07	CL132
	22.2	444.63	0.01	CL133
	21.1	445.61	0.01	CL134
	23.7	449.08	0.01	CL135
	32.2	454.91	0.06	CL136
	44.5	459.63	0.08	CL137
5D-9	16.9	441.75	0.01	CL119
	21.8	445.17	0.01	CL120
	22.5	448.55	0.01	CL121
	38.3	455.32	0.01	CL122
	37.8	455.95	0.03	CL123
11B-32	26.8	439.33	0.05	CL156
	40.0	442.70	0.04	CL157
8C-9	19.3	453.07	0.07	CL138
	35.5	455.80	0.05	CL139
	61.6	460.37	0.07	CL140
	24.4	466.83	0.01	CL141
	27.2	469.75	0.08	CL143

WELL	VISCOSITY	DEPTH	RESIDUAL WATER, %	SAMPLE
8C-27	13.6	439.40	0.11	CL144
	16.4	443.95	2.1	CL145
	19.1	445.32	0.29	CL146
	25.2	450.97	0.01	CL147
	29.9	454.17	0.12	CL148
	37.7	455.60	0.31	CL149
5C-14	11.8	444.17	0.01	
	19.7	448.85	0.01	CL113
	29.1	452.00	3.6	CL114
	51.5	455.62	0.99	CL115
	73.8	460.20	0.01	CL116
	72.3	460.77	0.01	CL117
8C-36	12.3	449.97	0.68	CL178
	14.4	450.84	3.0	CL179
5D-24	13.2	437.10		1
	12.4	437.75		2
	13.8	438.30		3
	14.2	442.35		4
	13.1	442.70		5
	15.9	444.30		6
	21.4	446.90		7
	28.0	449.90		8
	26.8	452.25		9
	44.2	454.05		10
	45.4	455.40		11
	64.7	458.05		12
	64.6	458.75		13
	79.5	460.35		14
	93.8	461.65		15
	100.0	464.35		16
5C-13	12.6	441.12	0.01	CL106
	13.5	443.37	0.85	CL107
	19.4	445.77	0.8	CL108
	23.5	447.22	0.5	CL109
	70.8	456.90	1.7	CL110
	74.6	460.65	1.0	CL111
7C-12	11.3	454.85	1.0	1
	12.8	459.25	6.6	2
	19.9	464.25	0.6	3
	28.0	467.20	6.2	4
	36.4	470.00	5.3	5
	102.0	476.70	2.2	6

WELL	VISCOSITY	DEPTH	RESIDUAL WATER, %	SAMPLE
11C-6	18.6	480.42	0.01	CL172
	17.0	483.62	0.06	CL173
	28.2	489.20	0.01	CL174
	26.2	492.05	0.01	CL175
	50.5	497.02	0.21	CL176
	92.6	502.10	0.32	CL177
6C-32	14.5	441.79	0.01	CL160
	15.1	443.01	0.02	CL161
	17.2	446.37	0.08	CL162
	23.2	451.79	0.09	CL163
	25.7	458.10	0.05	CL164
	22.2	462.31	0.14	CL165

a) measured at 25°C, reported in Pa.s. 1 Pa.s = 1000 mPa.s = 1000 cP

b) m below KB.

TABLE 2
CLEARWATER B STRUCTURAL DATA [a]

WELL	TOP[b]	BOTTOM[b]	KB, m	ELEVATION OF TOP[c]	ELEVATION OF BOTTOM[c]	VISCOSITY, Pa.s @ 25°C TOP -5m	VISCOSITY, Pa.s @ 25°C BOTTOM +5m
6C-22[d]	481.0	496.0	714.2	233.2	218.2	--	--
9B-12	438.2	456.5	678.6	240.4	222.1	40	--
6C-36	467.0	484.5	696.0	229.0	211.5	52	--
7C-20	436.8	463.5	684.1	247.3	220.6	19	40
5D-9	436.5	457.5	682.0	245.5	224.5	17	31
11B-32	436.2	456.0	671.7	235.5	215.7	--	--
8C-9	450.5	469.0	680.9	230.4	211.9	31	--
8C-27	439.0	462.0	677.5	238.5	215.5	17	38
5C-14	442.7	462.0	677.4	234.7	215.4	18	50
8C-36	441.0	483.0	691.7	250.7	208.7	--	--
5D-24	436.5	463.8	681.5	245.0	217.7	14	56
5C-13	438.1	461.2	680.4	242.3	219.2	13	56
7C-12	454.0	478.4	692.7	238.7	214.3	13	55
11C-6	480.4	505.8	705.3	224.9	199.5	22	71
6C-32	429.9	472.8	689.6	259.7	216.8	--	--

a) Based on printout from LGTF database, October 19, 1987

b) Driller's depth

c) Calculated from driller's depth and KB values.
m above mean sea level.

d) 6C-22-69-6

TABLE 3

VISCOSITY OF OIL FROM McMURRAY AND WABISKAW RESERVOIR IN CARIBOU LAKE AREA

WELL	FORMATION	DEPTH, KB	VISCOSITY [a] Pa.s	Residual Water, %
10B-33-70-6W4	Wabiskaw	453.61	8.5	0.5
		457.15	10.9	0.6
8D-32-69-6W4	McMurray	529.75	72.4	0.4
		530.07	74.9	0.6
		530.30	75.2	1.6
		530.50	77.4	0.9

a) Viscosity measured at 25°C for samples from 10B-33, and at 35°C for samples from 8D-32 (>102 Pa.s at 25°C)

3.7 Figures

1. SAMPLING OF CORE
2. CARIBOU LAKE WELL 6C-22
3. CARIBOU LAKE WELL 9B-12
4. CARIBOU LAKE WELL 6C-36
5. CARIBOU LAKE WELL 7C-20
6. CARIBOU LAKE WELL 5D-9
7. CARIBOU LAKE WELL 8C-9
8. CARIBOU LAKE WELL 8C-27
9. CARIBOU LAKE WELL 5C-14
10. CARIBOU LAKE WELL 5D-24
11. CARIBOU LAKE WELL 5C-13
12. CARIBOU LAKE WELL 7C-12
13. CARIBOU LAKE WELL 11C-6
14. CARIBOU LAKE WELL 6C-32
15. CARIBOU LAKE VISCOSITY
16. DISTILLATION CURVES FOR OIL FROM WELL 5D-24
17. DISTILLATION CURVES FOR OIL FROM WELL 5D-9
18. DISTILLATION CURVES FOR OIL FROM WELL 5C-13
19. DISTILLATION CURVES FOR OIL FROM WELL 8C-9
20. DISTILLATION CURVES FOR OIL FROM WELL 7C-20
21. DISTILLATION CURVES FOR OIL FROM WELL 6C-36

Figure 1 Sampling of Core

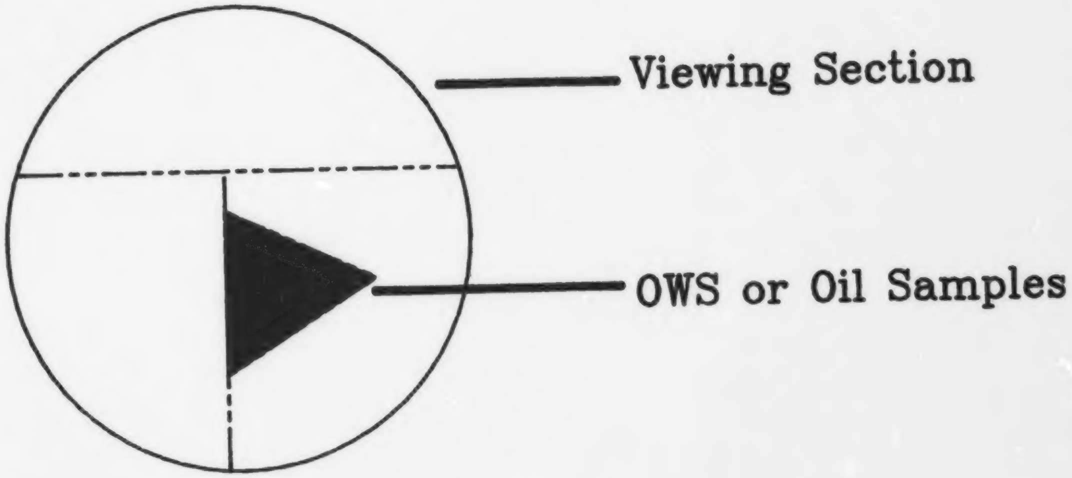
Viewing Section
OWS or Oil Samples

Figure 2
Caribou Lake Well 6C–22

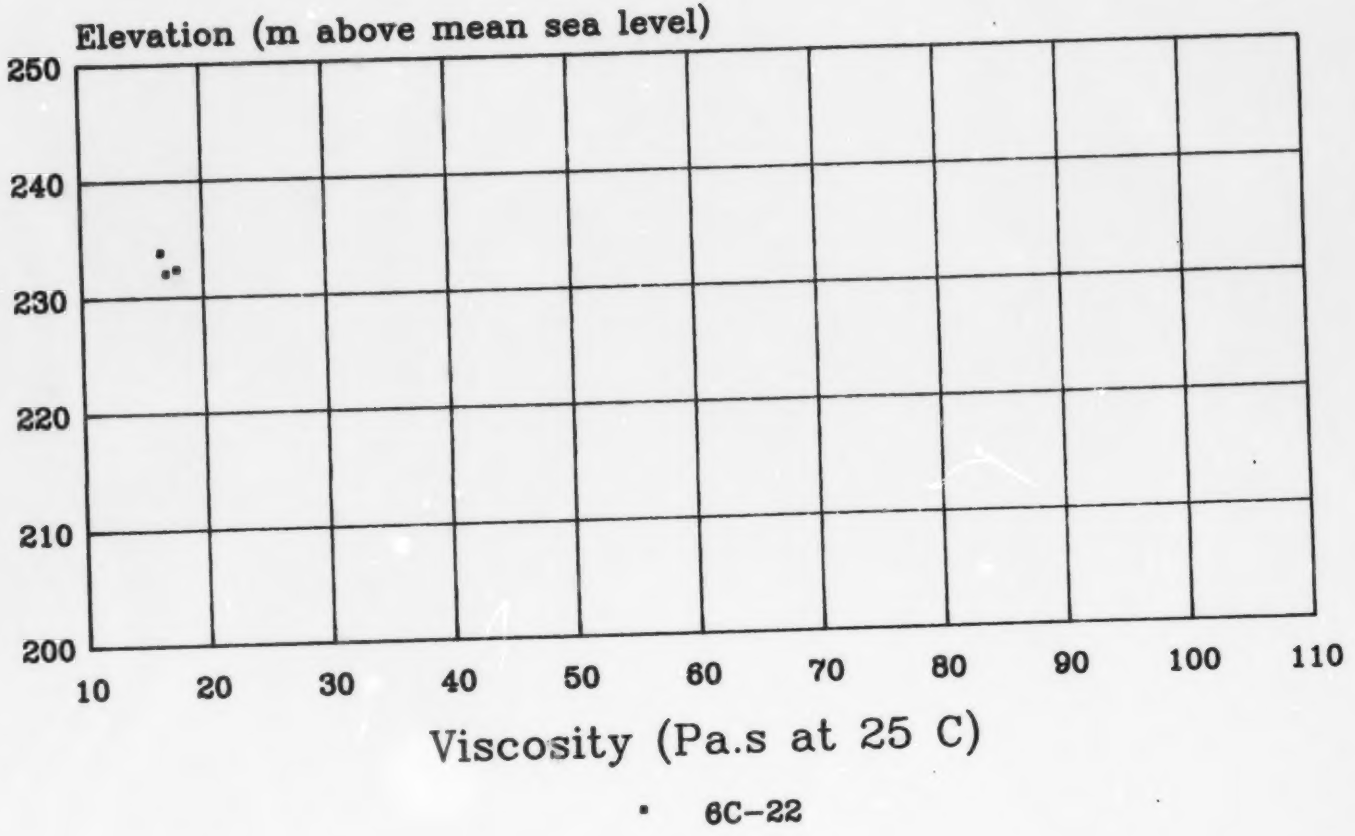

Figure 3
Caribou Lake Well 9B-12

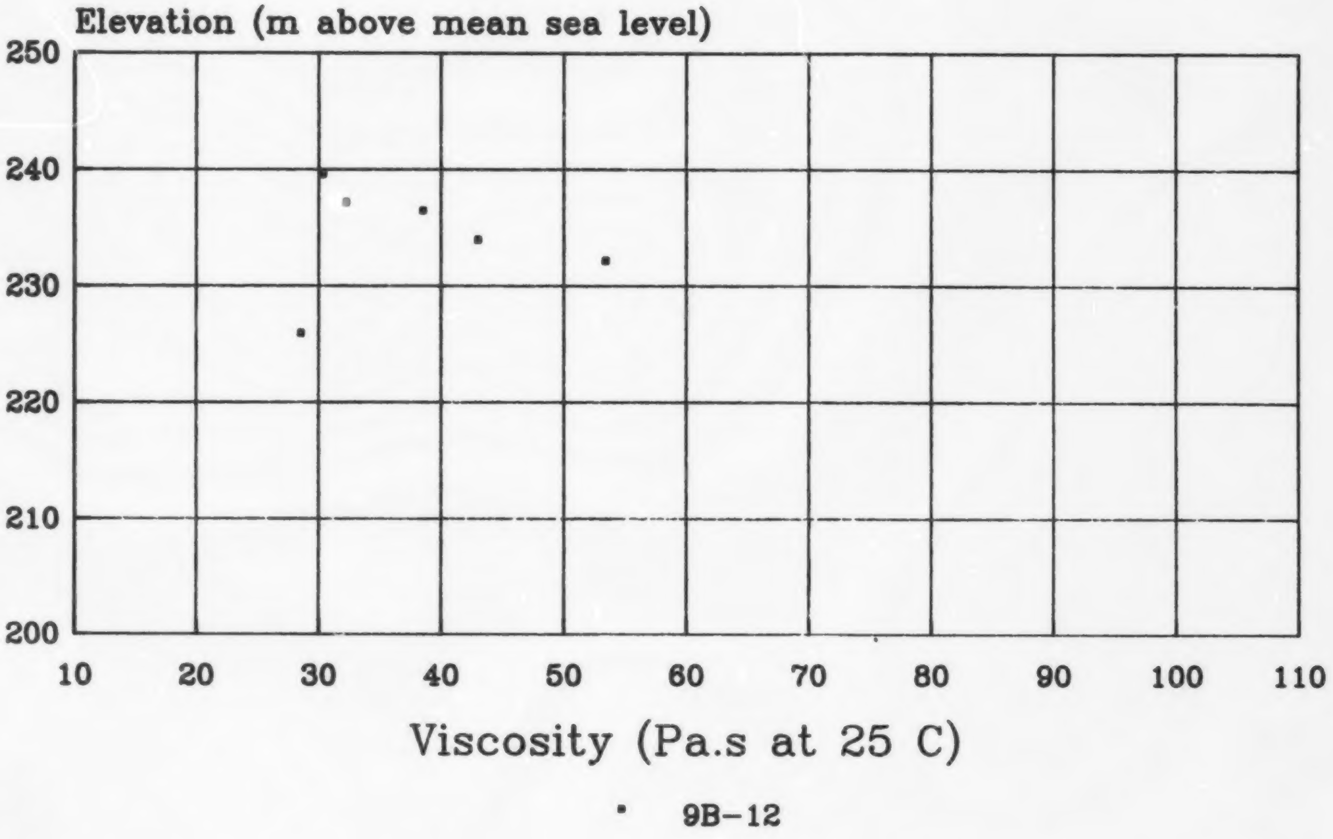

Figure 4
Caribou Lake Well 6C–36

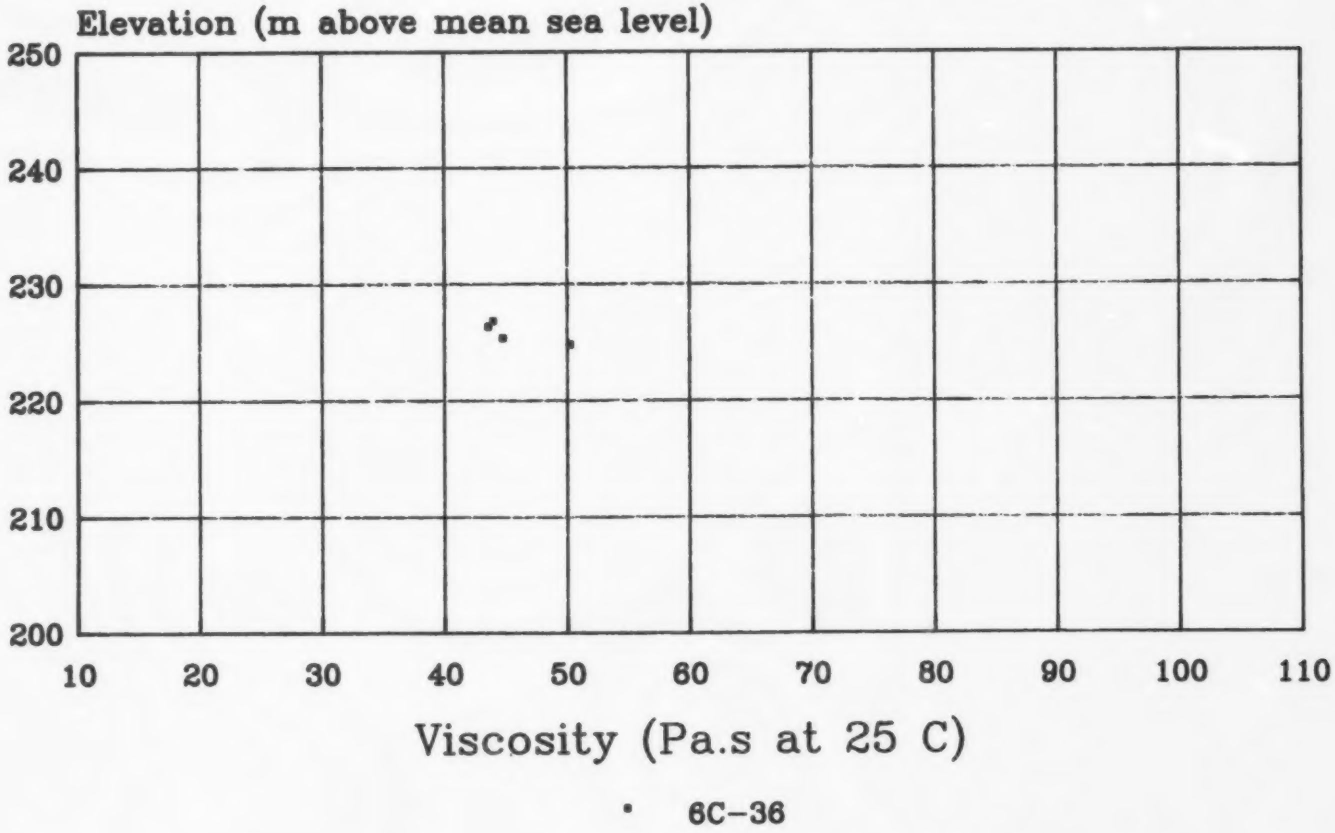

Figure 5
Caribou Lake Well 7C–20

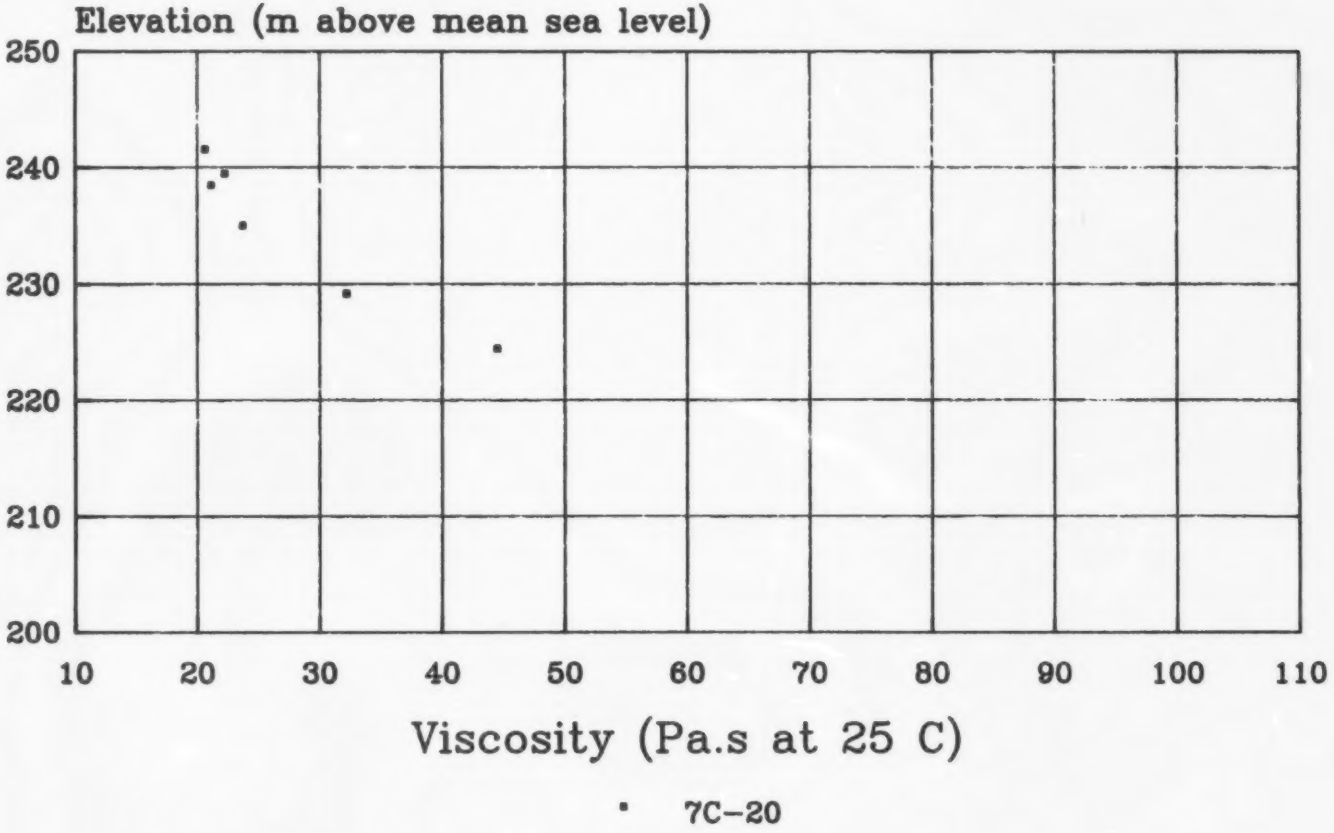

Figure 6
Caribou Lake Well 5D−9

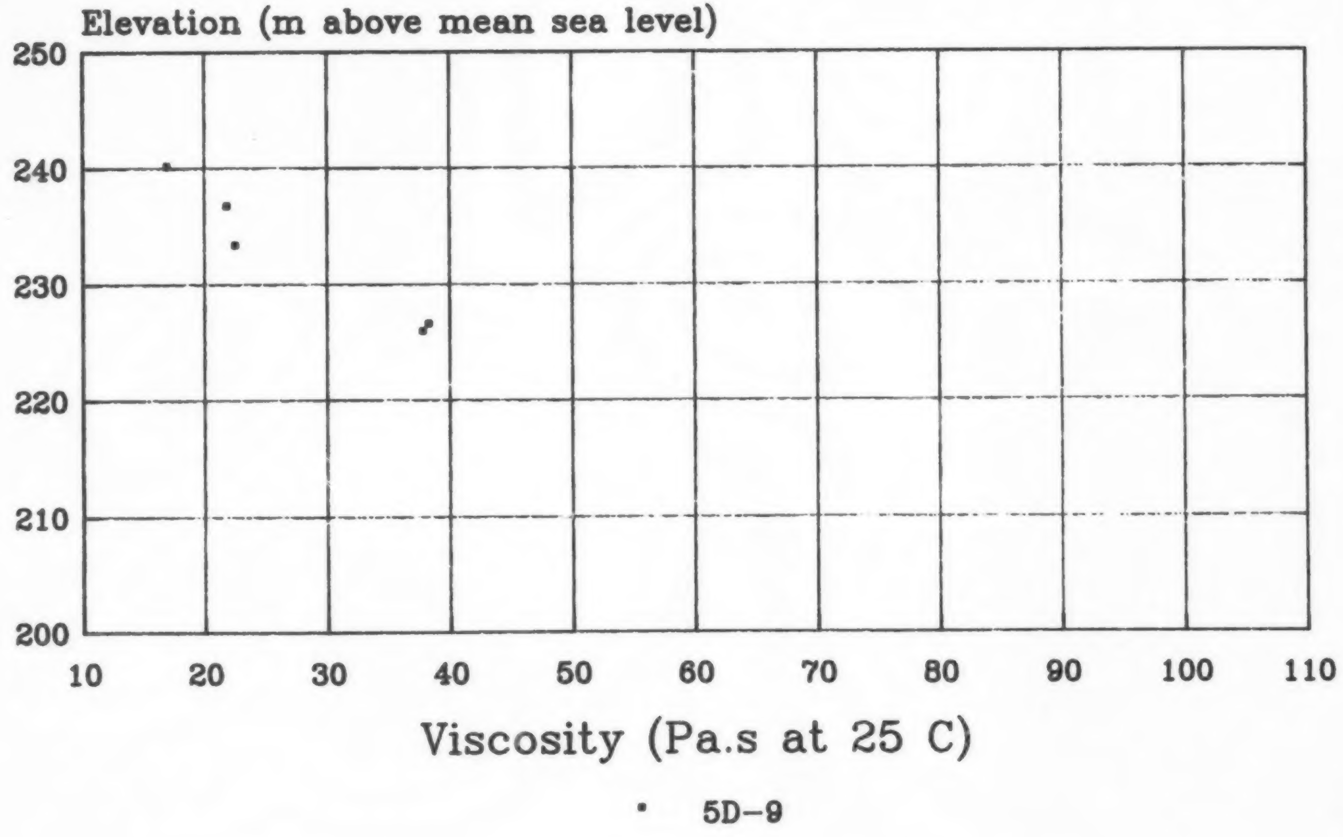

Figure 7
Caribou Lake Well 8C−9

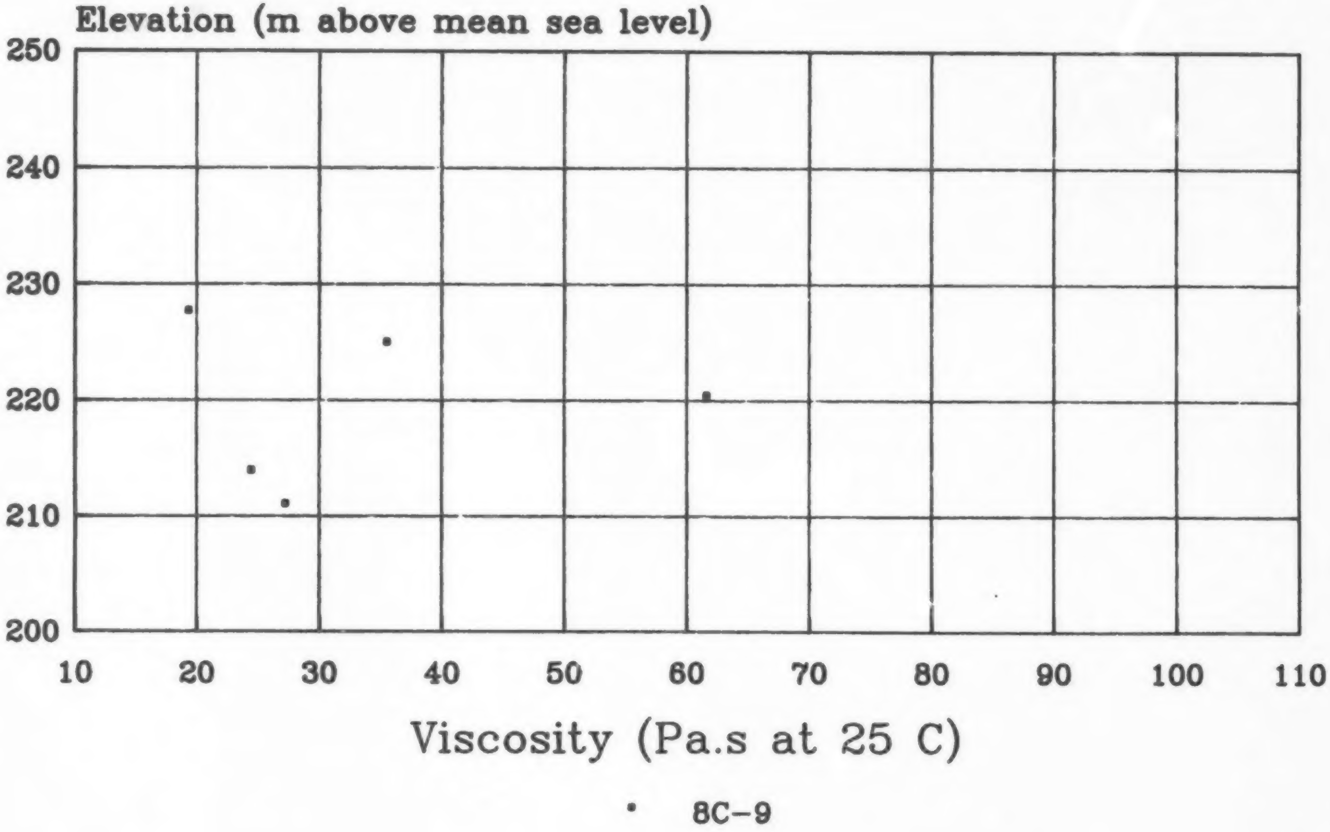

Figure 8
Caribou Lake Well 8C–27

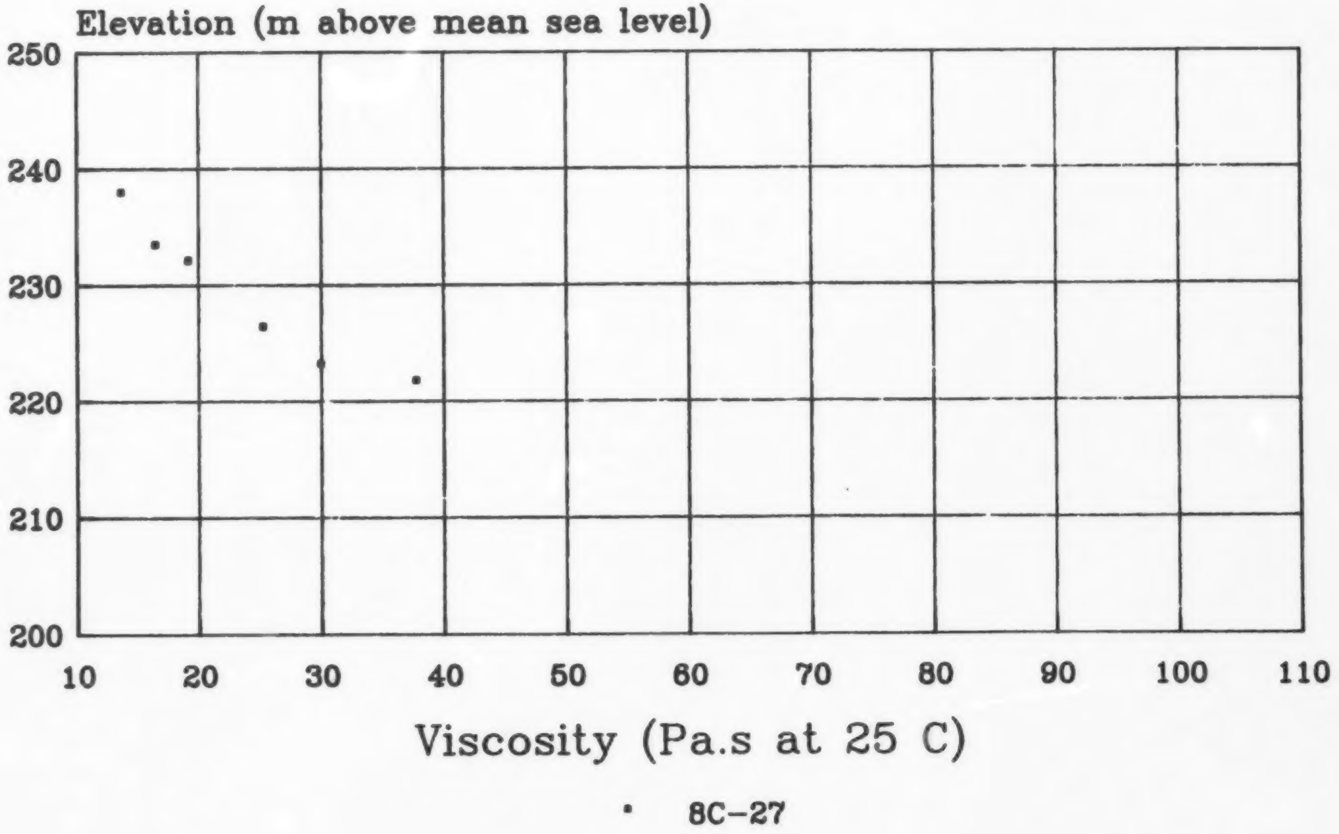

Figure 9
Caribou Lake Well 5C−14

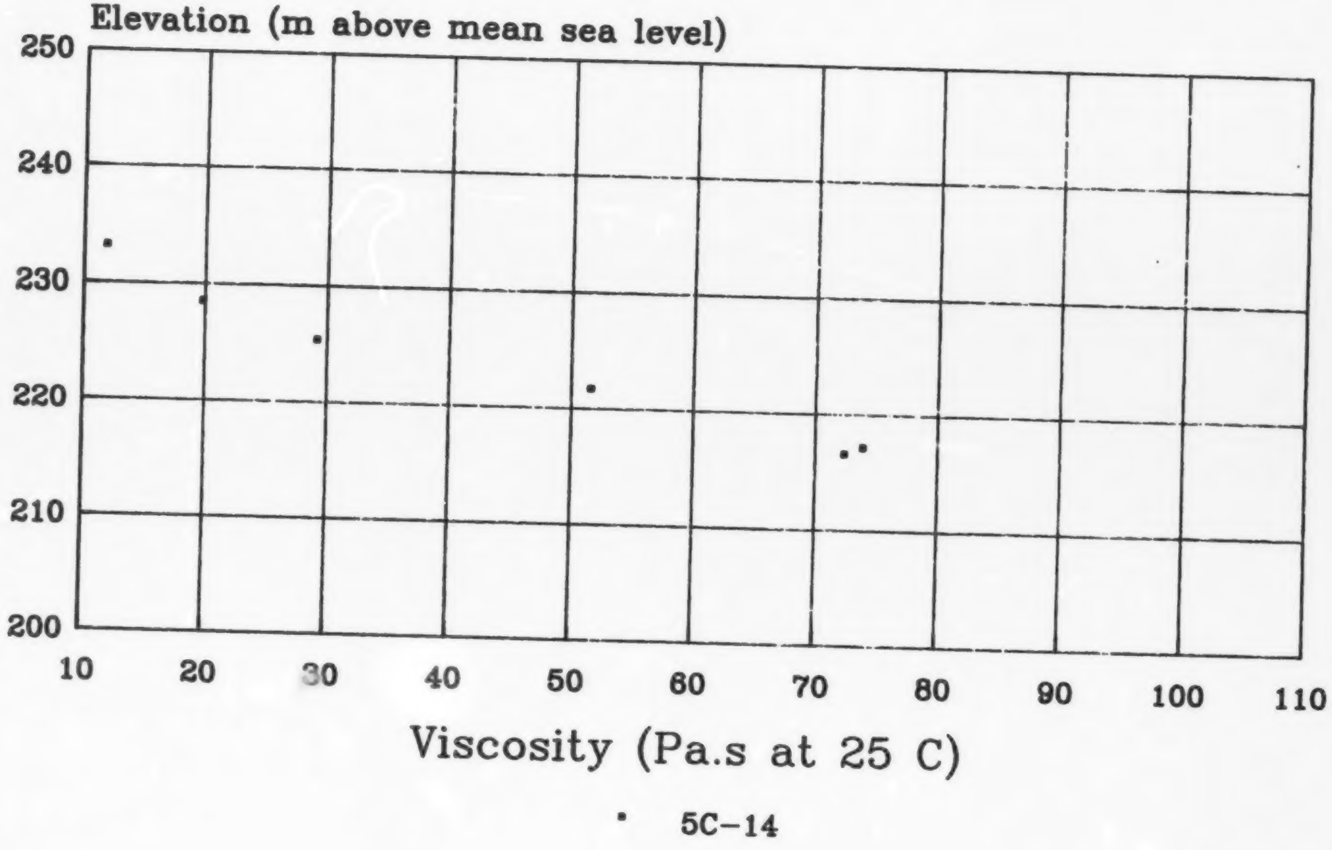

Figure 10
Caribou Lake Well 5D-24

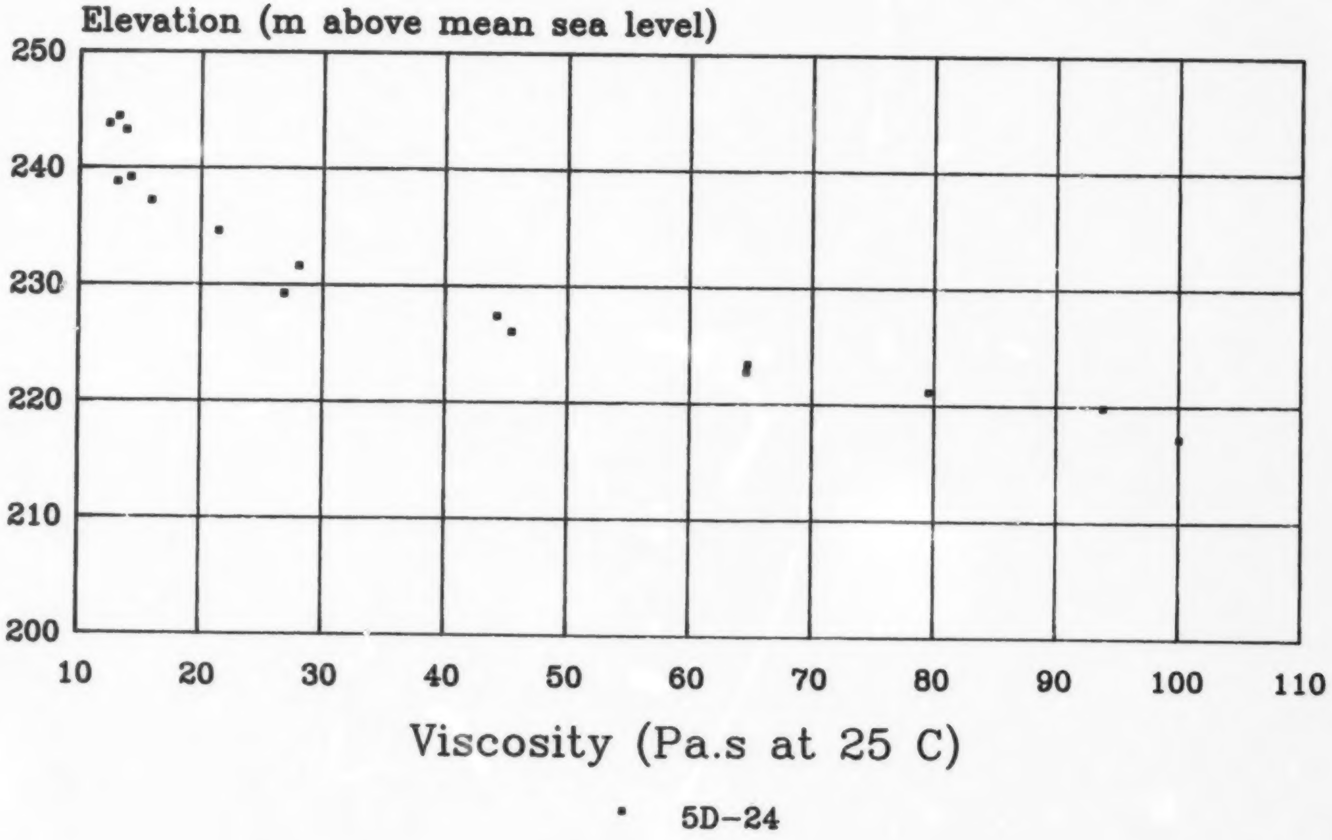

Figure 11
Caribou Lake Well 5C−13

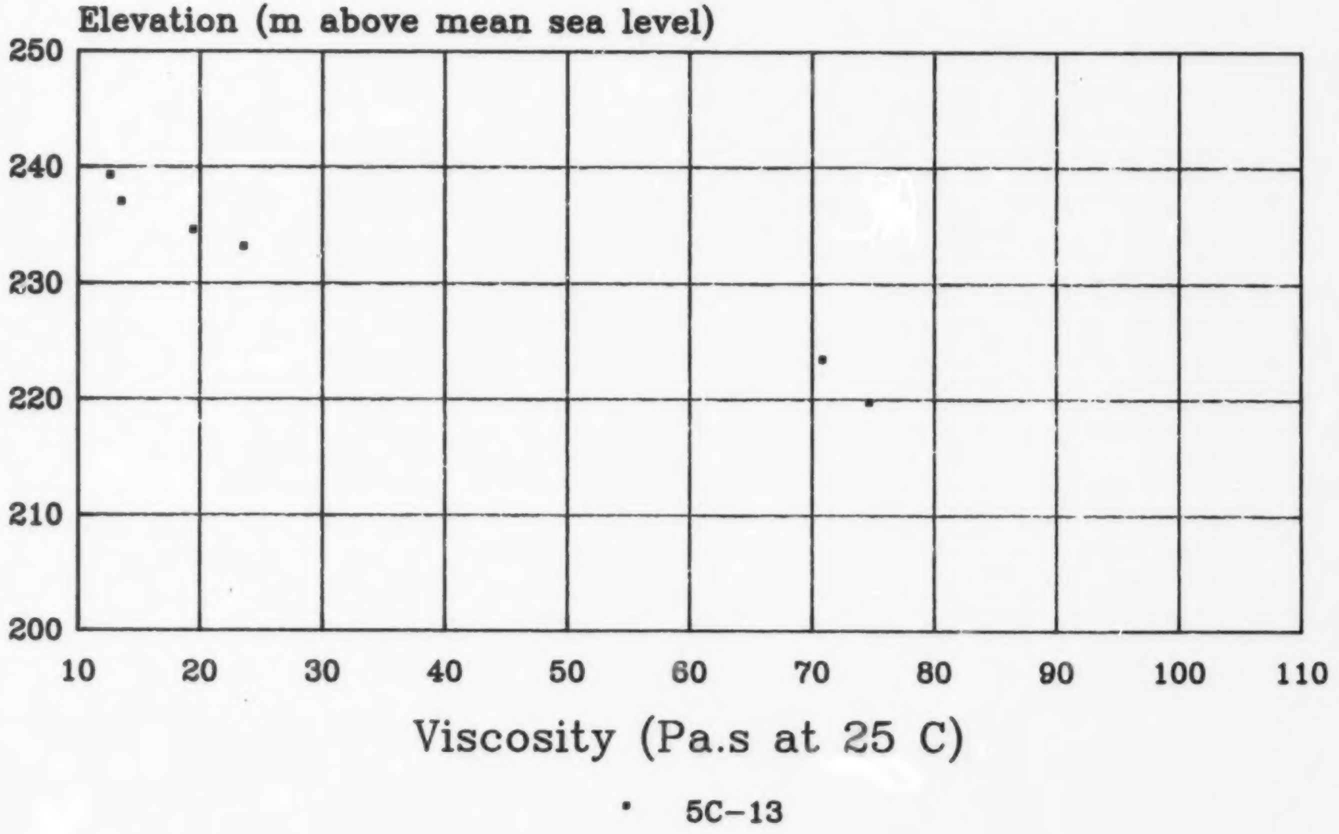

Figure 12
Caribou Lake Well 7C-12

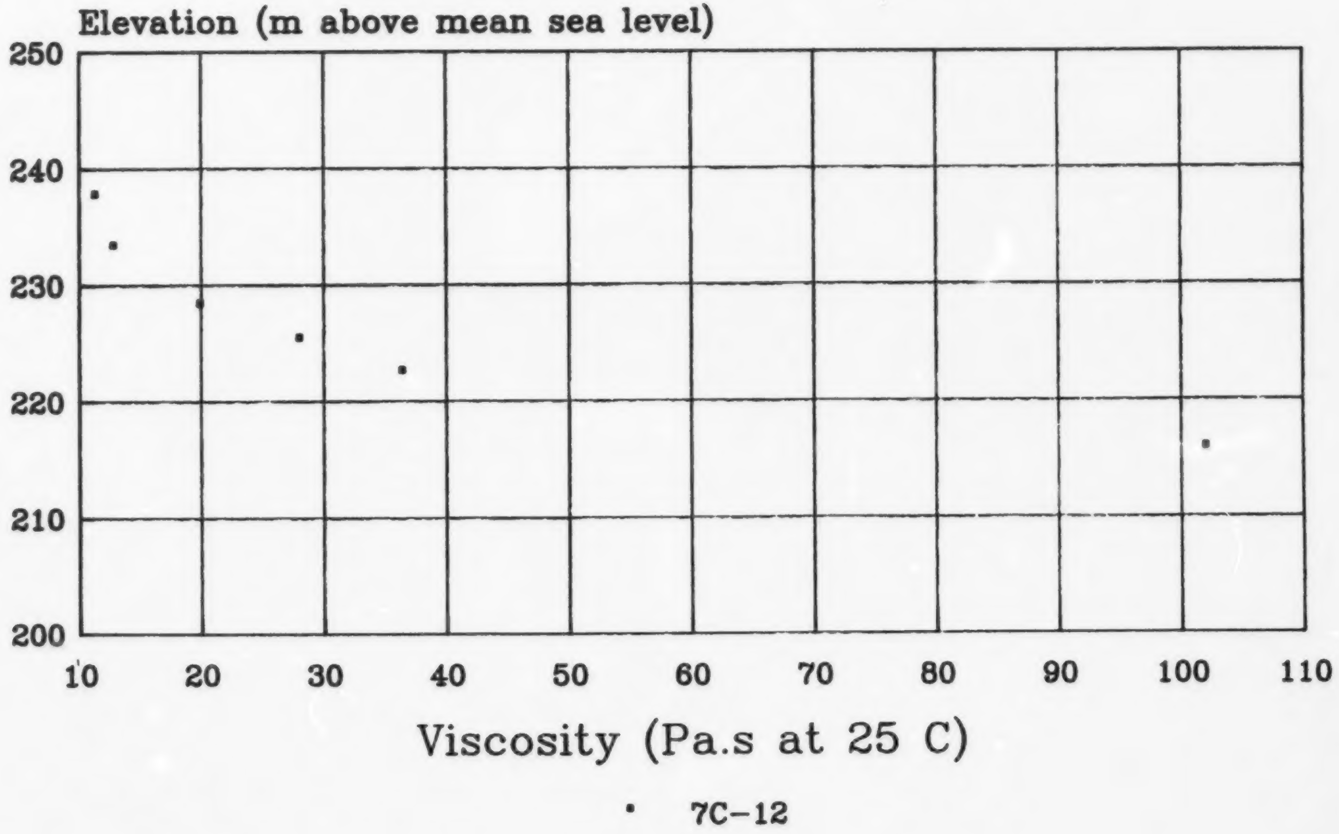

Figure 13
Caribou Lake Well 11C–6

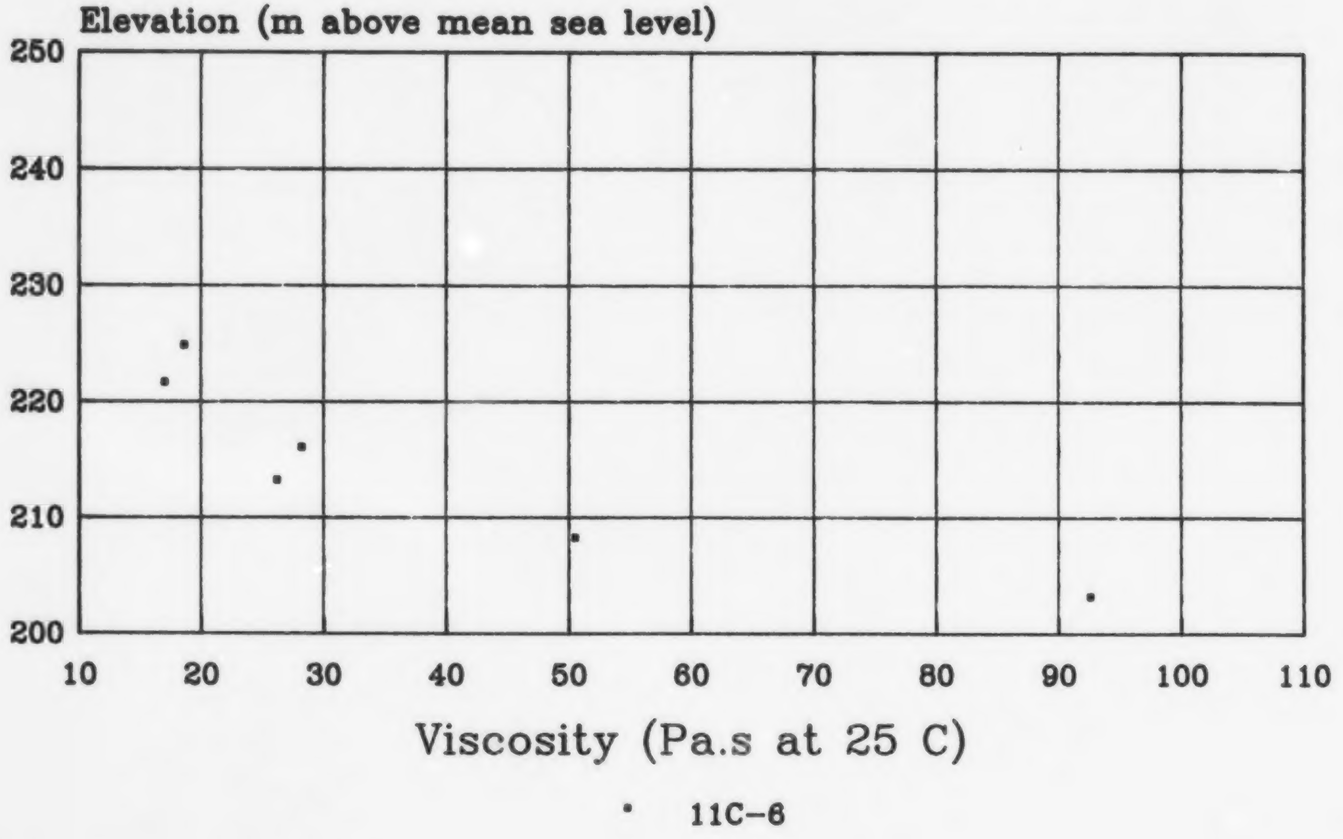

Figure 14
Caribou Lake Well 6C-32

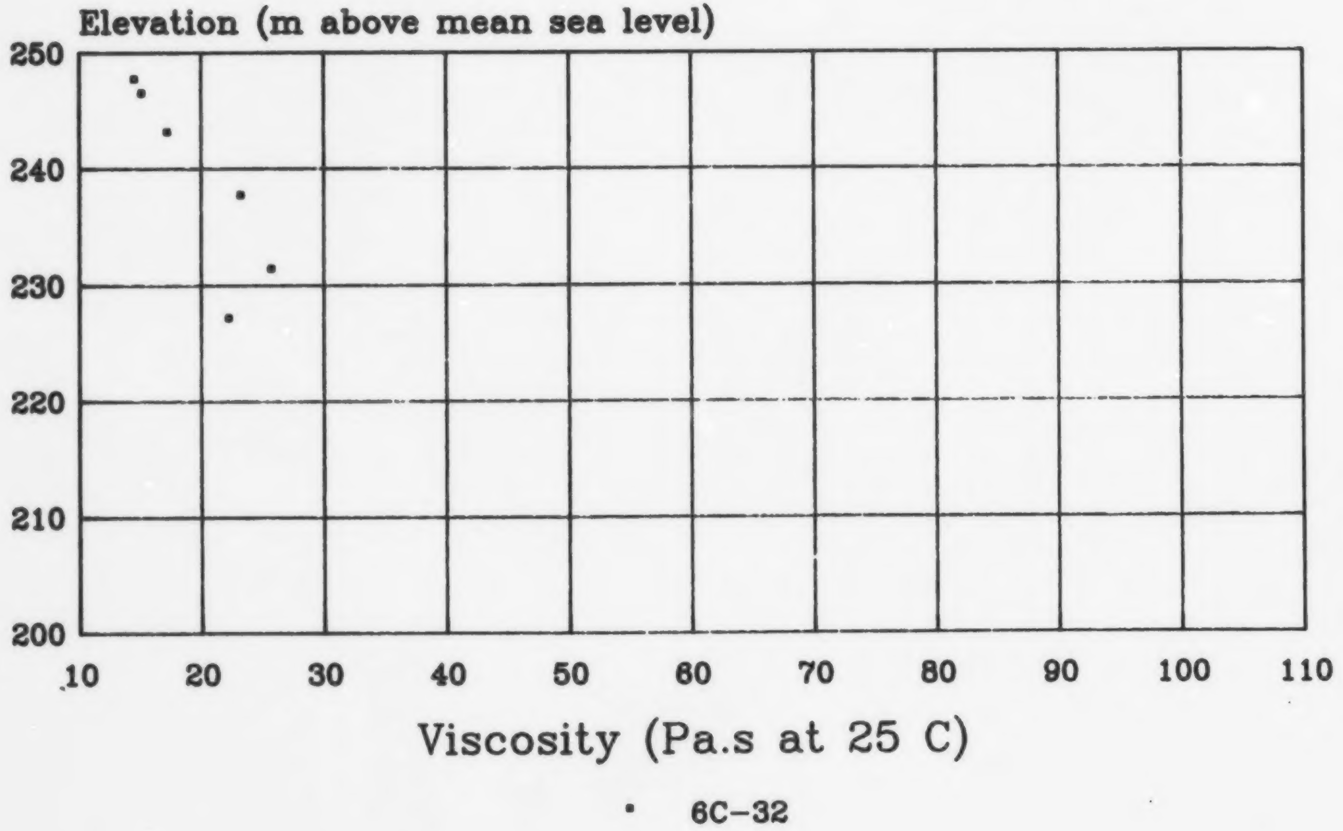

Figure 15
Caribou Lake Viscosity

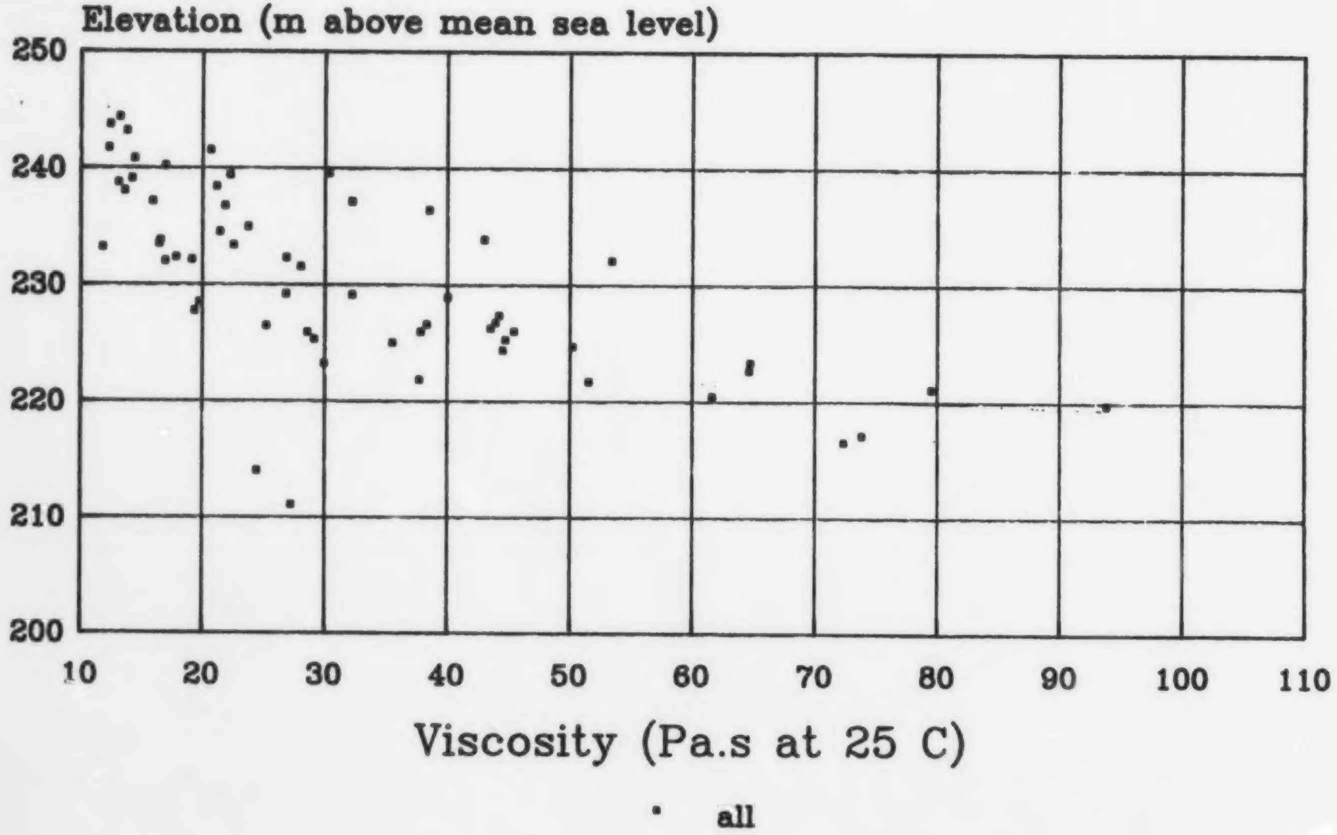

FIGURE 16

Distillation Curves for Oil from Well 5D-24

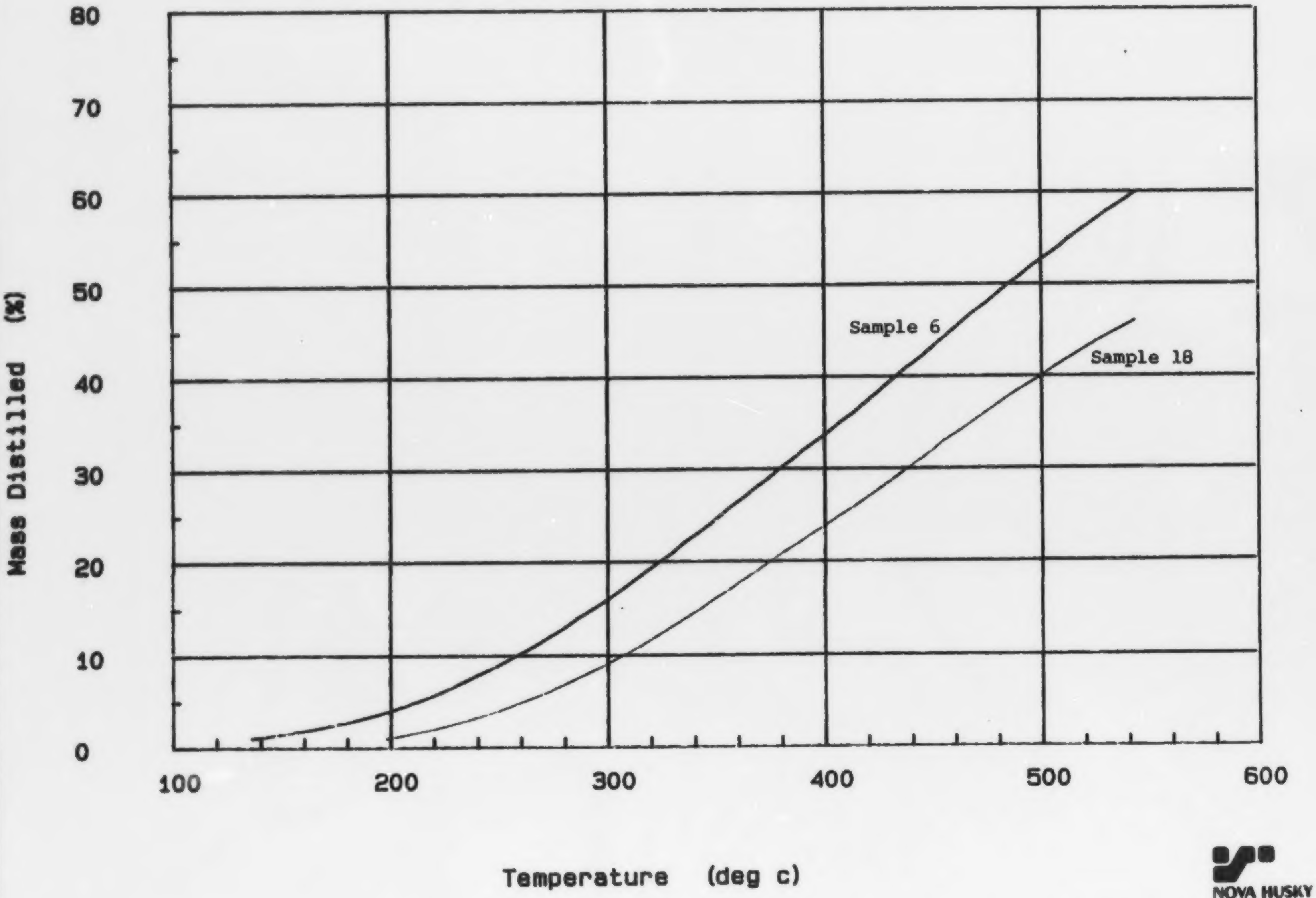

NOVA HUSKY
RESEARCH
CORPORATION

Figure 17: Distillation Curves for Oil from Well 5D-9

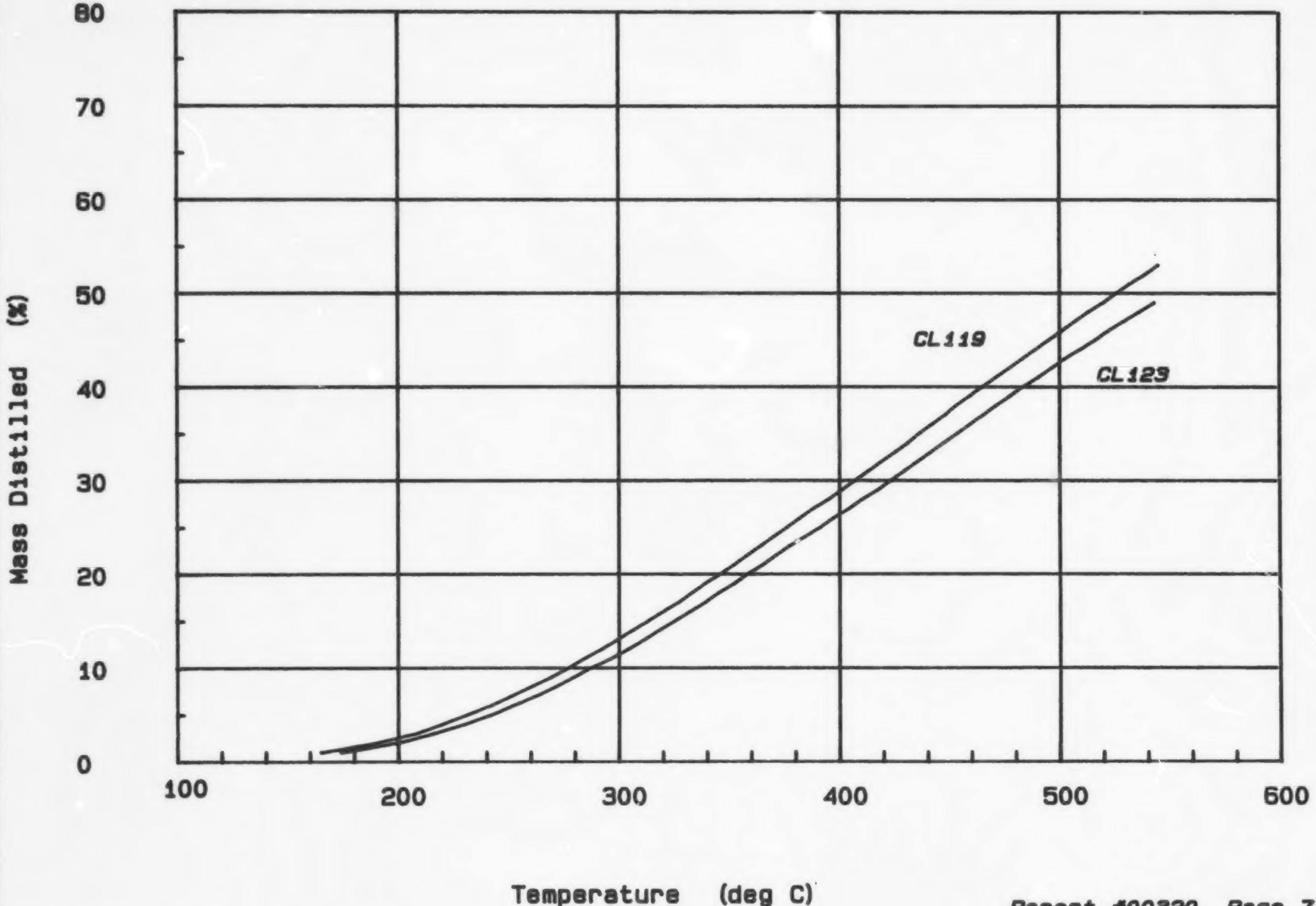

Figure 18: Distillation Curves for Oil from Well 5C-13

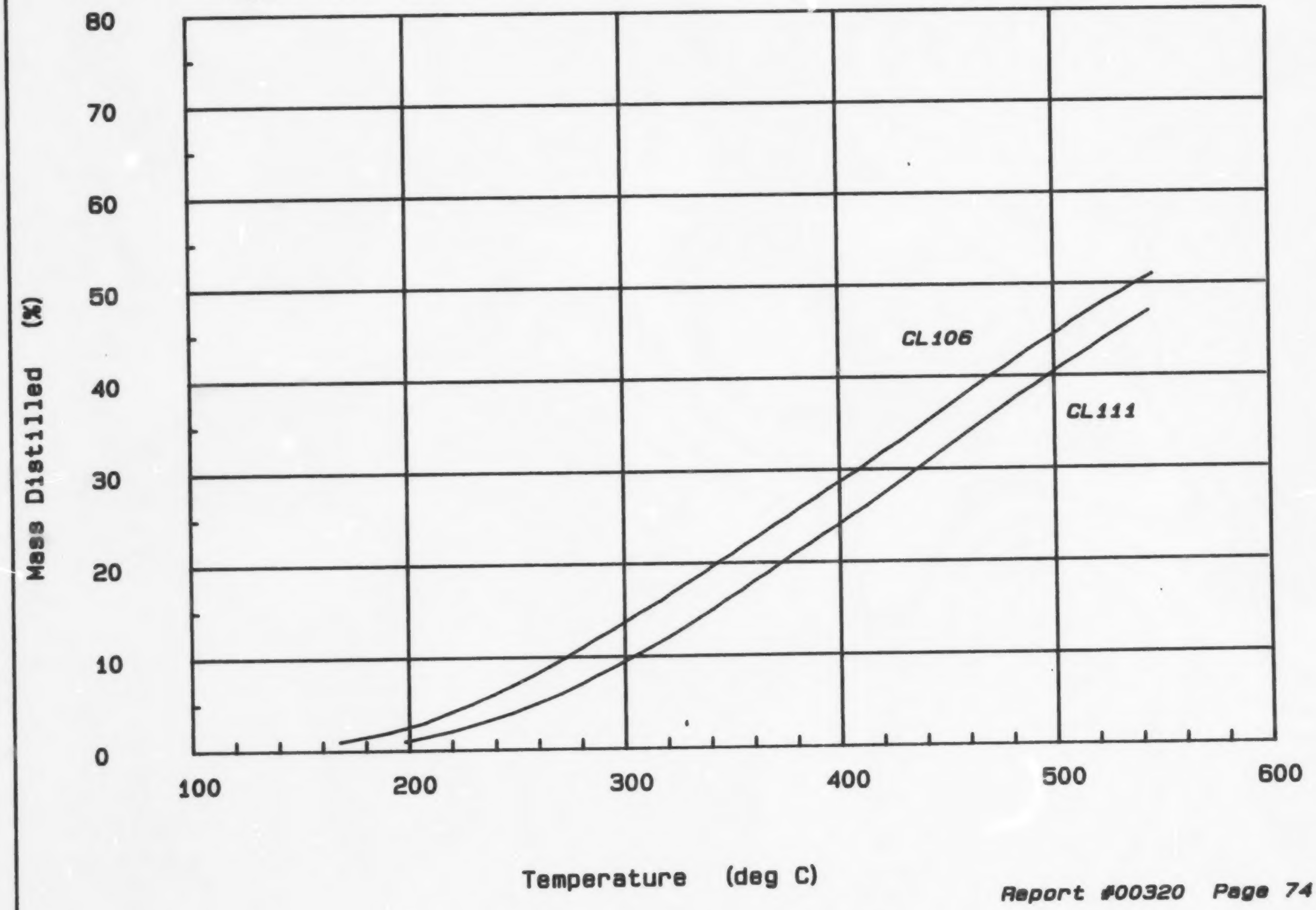

FIGURE 19

Distillation Curves for Oil from Well 8C-9

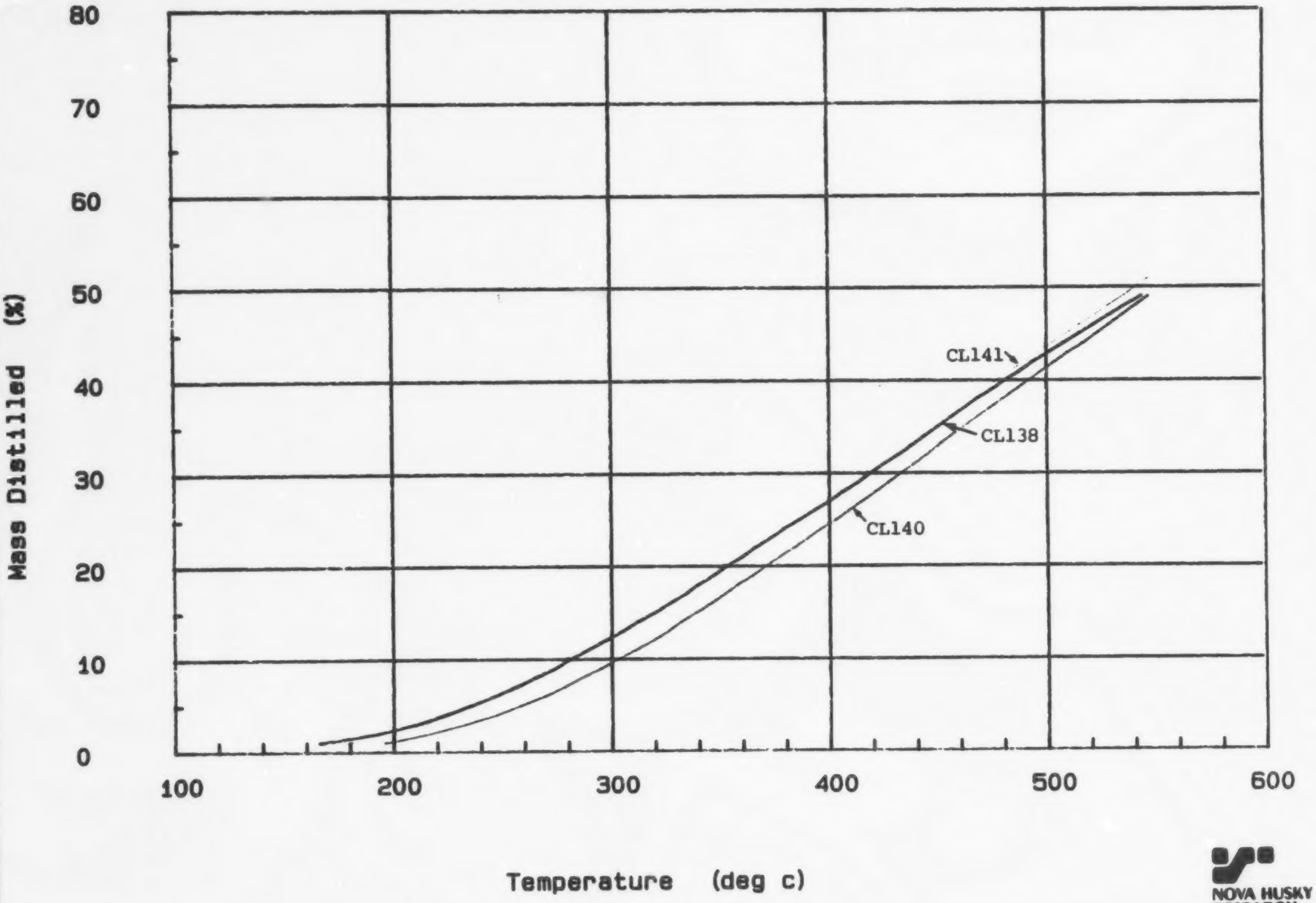

NOVA HUSKY RESEARCH CORPORATION

Figure 20: Distillation Curves for Oil from Well 7C-20

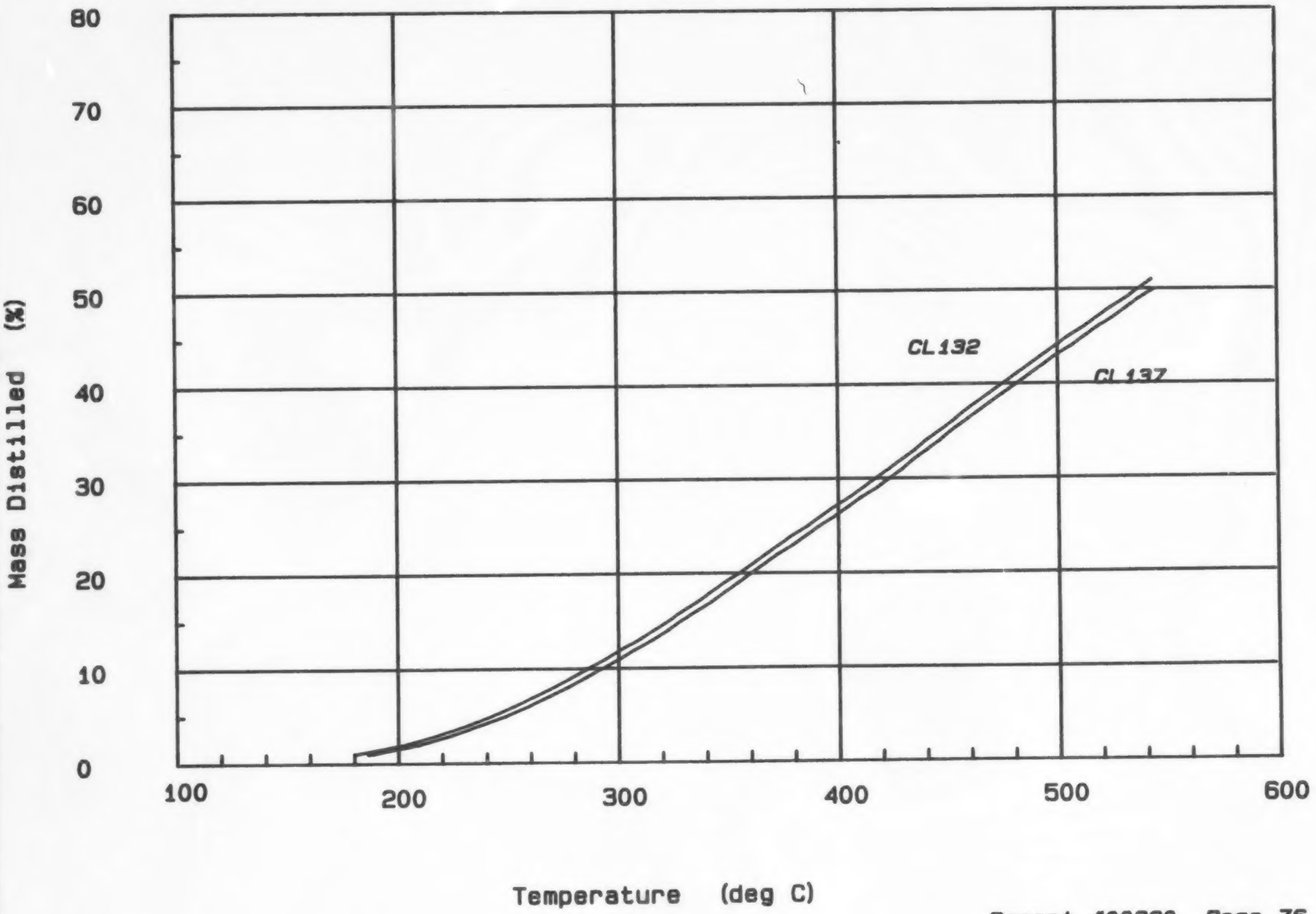

Figure 21: Distillation Curve for Oil from Well 6C-36

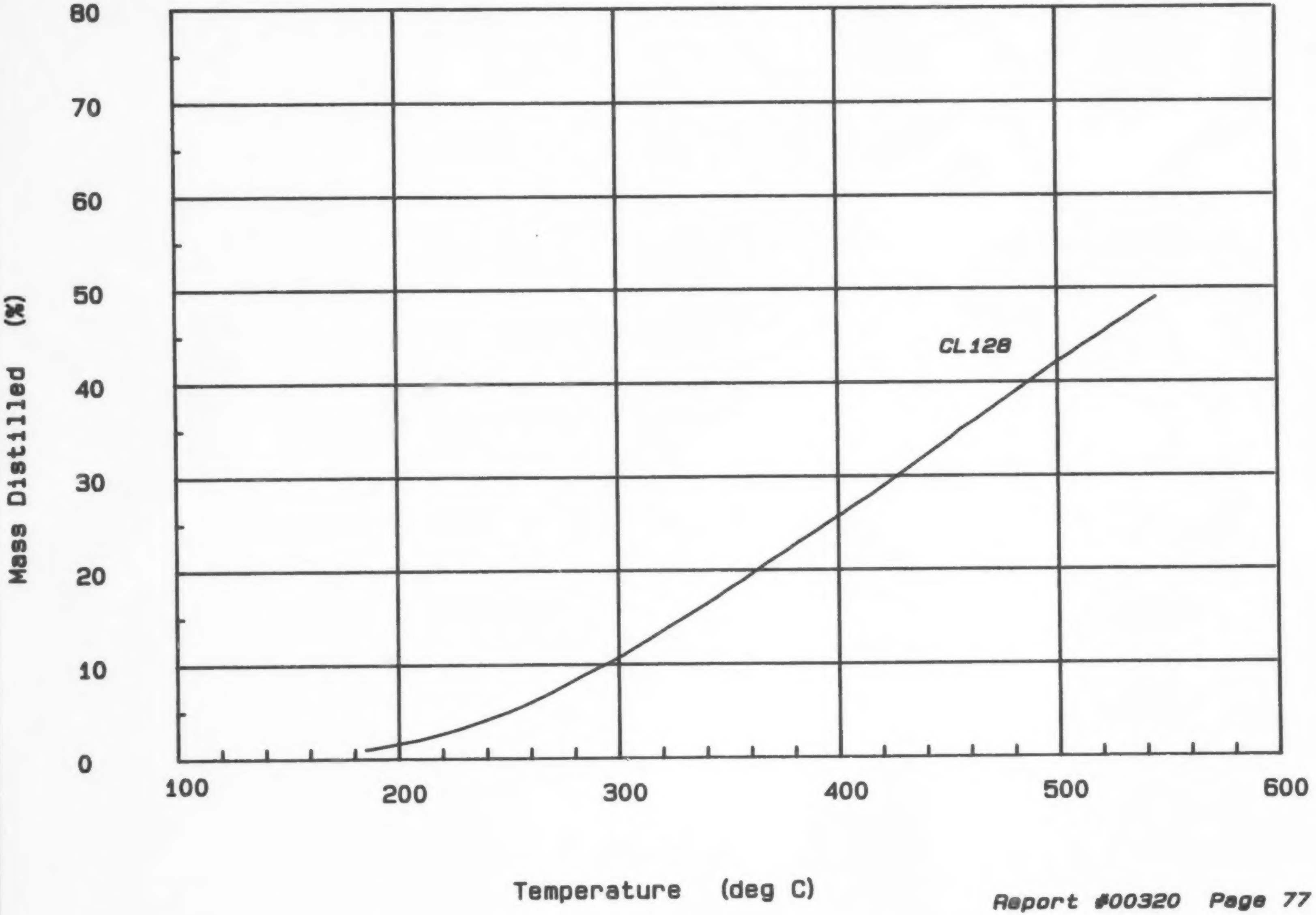

4.0 INVESTIGATION OF THE INFLUENCE OF ASPHALTENES ON OIL VISCOSITY (TASK 5)

4.1 Summary

Oil samples from two different Lloydminster reservoirs were separated into their respective asphaltene and maltene components. These componenets were then re-combined in different ratios to give oils of various asphaltene content. Preliminary work showed that re-constitution to the original asphaltene content gave an oil of similar viscosity to the native sample. This helped to establish the validity of the re-combination method.

Viscosity and density measurements were then made on two series of oil samples, ranging from 7 to 21% asphaltenes. Oil viscosity increases almost logarithmically with increasing asphaltene concentration. Although this behavior is not consistent with most theoretical predictions, it is similar to observations reported by others for analogous mixtures, and has been attributed to aggregation of the solid components in the solvent phase.

Density measurements indicate that "dissolution" of asphaltenes in maltenes is accompanied by a small negative "excess volume of mixing". In other words, the resulting mixtures are more compactly organized than the two components.

4.2 Introduction

In a study of fluids produced from fireflood wells, oil viscosity was observed to vary considerably even among samples taken over several months from the same well. More detailed comparisons indicated that the lower viscosity oil contained slightly less asphaltenes than the higher viscosity oil. These and other observations of viscosity variation raised the question of the relationship between viscosity and concentration of asphaltenes in a heavy oil.

Consistent with other work in this project, the oils chosen for this task are from producing heavy oil fields in the Lloydminster region. Work has been done on an oil sample from the Pike's Peak field, and on another from the Tangleflags field. Both of these fields are located east of Lloydminster in west central Saskatchewan.

4.3 Materials and Methods

4.3.1 Origin and Preparation of Oil Samples

The oil samples used in this work originated from wellhead emulsions taken from Husky Tangleflags well D11-13-51-25-W3, May 6, 1987 and Pikes Peak well 3B7-6-50-23, December 3, 1986. Water was removed by heated centrifugation using an L8-55 MP Beckman centrifuge. Samples were preheated, and then centrifuged for 90 minutes at 90°C, 14,000 rpm (approximately 30,000 X gravity). Residual water was $<1\%$. At 25°C, the Tangleflags oil viscosity was 5020 mPa.s; its density was 971.6 kg/m^3 at 25°C. The Pikes Peak oil viscosity was 11,500 mPa.s at 25°C and its density was 978.9 kg/m^3 at 25°C.

4.3.2 Determination of the Water Content, Density and Viscosity of Oil Samples

Residual water in the clean oil was quantified using a coulometric Karl Fischer instrument (Aquatest IV, Photovolt Corp.) with Hydranal reagents. Oil samples were diluted in a 60/40 toluene/ isopropanol solution prior to analysis.

Density of the oil samples was determined at 25°C using a PAAR PMA 46 oscillating tube density meter with internal temperature control.

Viscosity was measured with a Wells-Brookfield cone and plate microviscometer (Model RVT DCP, CP-51 spindle 1.565° cone). 0.5 g samples were measured over a shear rate range of 1.92 to 384 sec^{-1} at 25° and 60°C, using a Julabo circulating bath for temperature control.

4.3.3 Preparation of Asphaltenes and Maltenes

The asphaltenes were precipitated from the whole oil using excess n-pentane. About 15-20 g of oil were weighed into a 1 L erlenmeyer flask. About 600 mL (at least 30 x weight of sample) of reagent grade n-pentane were added at the rate of 20 mL every 3 minutes while stirring (magnetically) at room temperature. After mixing, the solution was stored overnight (16-22 hours) in darkness. The asphaltenes were then separated by vacuum filtration on a filter consisting of a glass fibre pad (GF/A) and a cellulose (Whatman #1, Qualitative) paper in a Buchner funnel. The asphaltenes were washed with n-pentane until the filtrate was colorless. They were then dried for one hour in a fumehood and for one hour in an 80°C oven, cooled, and weighed. Small amounts of residue remaining in the flask used for the precipitation were assumed to be only asphaltenes and were therefore included as part of the total mass of asphaltenes. The pentane was removed from the maltenes by rotary evaporation. The evaporation flask containing the sample was heated to approximately 40°C; a water aspirator was used for vacuum. Residual pentane was measured by GC as described in Section 4.3.5.

4.3.4 Recombination of Asphaltenes and Maltenes

The asphaltenes were dissolved in 50-80 mL of HPLC grade dichloromethane and then recombined with the maltenes in a 250 mL rotary evaporation flask. The solution was stirred for one minute on a vortex mixer and then swirled by hand for at least 30 minutes. After mixing, the dichloromethane was removed by rotary evaporation under the same conditions used to remove the pentane from the maltenes.

In an initial attempt to prepare oils without adding a solvent, asphaltenes were added directly to maltenes in a scintillation vial and mixed by hand with a spatula. As this was not sufficient to dissolve the asphaltenes, the sample was placed in a sonic bath for 3.5 hours. This also did not give a homogeneous sample. The last variation was to heat the sample to 80°C, and then place in the sonic bath for 6 hours. The asphaltenes remained in the bottom of the vial, mostly undissolved.

4.3.5 GC Fingerprint and Residual Solvent Determination

Both the GC fingerprint and residual solvent content of the oil samples were determined using a Perkin-Elmer Sigma 2000 gas chromatograph equipped with an SPB-1 capillary column.

For the GC fingerprint, samples were diluted with carbon disulfide prior to injection. The chromatograph settings are included with the results in Appendix A. For residual solvent (pentane, dichloromethane) analysis, samples were diluted with toluene and quantified using an internal standard method.

4.3.6 Determination of Asphaltene Content (micro method)

This method is almost the same as one reported by Pearson *et al* (2.6.3[8]). Approximately 0.2 g of oil were weighed (to 0.1 mg) into a 20 ml scintillation vial and 15 mls of reagent grade n-pentane were added to precipitate the asphaltenes. The sample was shaken and then stored in darkness overnight (16-20 hours).

A Millex SR 0.5 mm PTFE membrane filter was heated at 80^{o}C for 1 hour, cooled in a dessicator, and weighed. The sample was then filtered using a 20 ml glass syringe (filter attached with Luerlok fitting) and water aspirator vacuum. After filtering, the sample was washed with three 10 mL aliquots of n-pentane. The filter, now containing the asphaltenes, was then dried at 80^{o}C for 1 hour, dessicated to cool, and reweighed to determine the asphaltene content of the oil.

4.3.7 Pycnometric Determination of the Density of Asphaltenes

Ten millilitre volumetric flasks with ground glass stoppers were used as pycnometers. Methanol was used as the diluting liquid, as asphaltenes float in water and dissolve in other solvents.

A Julabo HC water-filled circulating bath maintained the samples at 25°C. The temperature was checked with an NBS calibrated thermometer. All weighings were done to 0.1 mg on an analytical balance. Two density determinations were made, each using a separate portion of asphaltenes. Initially, the flasks were immersed in the water bath, removed and wiped dry with Kimwipe towels and weighed. They were then filled with distilled water and allowed to come to temperature equilibration in the bath for 15 minutes. The volume was periodically adjusted with water to the calibration mark. After wiping dry, the flask was reweighed. From these masses, and the known density of water at 25°C, the exact volume of the flask at 25°C was calculated.

The same procedure was followed using HPLC grade methanol, and then the methanol density was calculated using the previously obtained volume.

After drying the flasks, approximately 500 mg of asphaltenes were weighed into each one, and each flask was filled to the mark with methanol. The flasks were then placed in an ultrasonic bath, one for 1 hour, and the other for 6 hours to remove air. The samples were warmed to

25°C as before, their volumes were adjusted, and then they were reweighed. Combining the weight with the measured density of the methanol and the calculated volume of the flask gave the density of the asphaltenes. Values from the two determinations agreed within 0.3%.

4.4 Results

Throughout this report, the term *asphaltenes* will designate the fraction of the whole oil which is insoluble in excess n-pentane, and the term *maltenes* will be used to designate the asphaltene-free fraction of the whole oil. Resins are defined as the fraction of the maltenes which adsorb on silica. The oil which has had both asphaltenes and resins removed will be referred to as *petrolenes*.

It was recognized from the beginning that the critical step in this work was to develop a procedure for combining asphaltenes with maltenes which gives a whole oil similar in behavior and composition to the original native oil sample. If this could not be achieved, then there would be little point in continuing the study.

The simplest approach to recombination is to add solid asphaltenes into maltenes in the desired ratio, and mix in some defined fashion. Efforts to use this procedure, with mixing variations as detailed in the Methods Section, were not successful, because some undissolved asphaltenes were always observed at the end of the mixing step.

The second approach involved dissolving the asphaltenes in a solvent, mixing the asphaltene solution with maltenes in the desired ratio, and then removing the solvent by vacuum distillation. Dichloromethane was chosen because it is a good solvent for asphaltenes, has a relatively low boiling point (40°C), and is somewhat less hazardous than some other possible choices such as benzene. (Benzene was used in some similar work reviewed earlier in this report.)

Measurements indicated that the Tangleflags native oil sample prepared for this study contained 14.1% (by mass) asphaltenes. This is in good agreement with values averaging 13.9% obtained in previous work with another sample of oil from the same well. A first sample reconstituted to 12.9% asphaltenes had a viscosity of 4970 mPa.s at 25°C, nearly the same as the native oil. While the difference in asphaltene concentrations makes the comparison less than ideal, these preliminary results were considered sufficient to indicate that the combination procedure using dichloromethane would be satisfactory.

Three sets of 5 reconstituted oil mixtures were prepared, the first and the second sets derived from the Tangleflags oil, and the third set using the oil sample from a well at the Pike's Peak Steam Project. The Tangleflags data are collected in Table 1, and the Pike's Peak data are in Table 2. All samples were measured at 25°C, and in addition, the first set of Tangleflags oils was also measured at 60°C.

A plot of the data in Tables 1 and 2 (Figure 1) shows that viscosity increases in a smooth but non-linear way with increasing asphaltene concentration. The viscosities of the reconstituted samples having similar asphaltene content to the native oils appear to be somewhat higher than they should be, but the smoothness of the curves suggests that all of the samples in each set are self-consistent.

The small, but real discrepancies between the native oil viscosities and those of reconstituted samples of similar composition highlights the difficulty in selectively removing all of the added solvents from the blend after mixing. For the collection of the first two data sets, mass balance was initially used to decide when to end the evaporation. Measurements at this point indicated that 1-2% dichloromethane was still present, implying that some light components of the maltenes had been removed before all of the dichloromethane. Further evaporation was required to achieve the <0.5% solvent chosen as the target.

For the third set of samples, additional measurements were made to provide an assessment of the loss of light compounds during rotary evaporation. Capillary gas chromatography was used to obtain compositional fingerprints of several samples before and after evaporation. Two typical chromatograms are shown in Figure 2; the rest are given in Appendix A.

Examination of Figure 2 shows that many small peaks near the beginning of the chromatogram of the solvent diluted oil (TFF-4) are absent or less significant in the chromatogram of the same sample after removal of most of the solvent (TFF-6). This confirms that at least some light components of the oil are lost during removal of the solvents.

An estimate of the extent of loss of light compoinents was made using peak area data from the chromatograms. Results of this analysis are summarized in Table 3. Removals of the n-pentane from the maltenes (going from sample TFF2 to TFF3) was accompanied by a loss of 69% of the components smaller than C8(C8-) and 28% of the compounds between C8 and C10.

Similar comparison of the chromatograms of re-constituted oils at different stages in the removal of dichloromethane shows that reduction to 2.9% CH_2Cl_2 is accompanied by loss of 38% of C8- compounds.

Reducing CH_2Cl_2 below 1% removes essentially all of the C8- and 2/3 of C8-C10 components.

An alternative which does not require complete solvent removal was attempted for the collection of the third data set. By stopping the evaporation at an earlier point, loss of light components can be minimized. The viscosity of the oil diluted with a small amount of dichloromethane could be measured, and then corrected to account for the solvent using a separately determined curve of viscosity versus solvent concentration. This approach was attempted for the second set of Tangleflags oils, but unfortunately only 2 of the 5 samples ended up having measured residual solvent values of >0.5%. The data and approach required to correct for the effect of residual solvent are given in Appendix B. Viscosities obtained using this correction for samples 2-1 and 2-3 are given in brackets in Table 1. The corrected values are not very consistent with the rest of the data, perhaps because at 1% dichloromethane, the solvent effect is compensated by loss of light components. The uncorrected values were therefore used in further analysis of the data.

The plot in Figure 3 separates the effect of asphaltenes from maltenes on oil viscosity. The relative viscosity, which is the ratio of oil viscosity to maltenes viscosity, is a measure of the viscosity increasing effectiveness of the asphaltenes. The Pike's Peak and Tangleflags data at 25°C appear to follow a single curve. The curve of the analogous values at 60°C tracks below the 25°C data, as expected, and is distinctly non-parallel, indicating that the viscosifying power of asphaltenes is less at 60°C.

It is clear from earlier discussion that some of the scatter in Figure 3 results from the difficulties in selectively removing the solvents or in correcting for the presence of residual solvent. However, another potential source of error is the asphaltene concentration. The values given in Tables 1 and 2 were calculated on the assumption that the asphaltene and maltene fractions obtained in the original separations are unambiguously unique. If, for example, some resins ended up in the asphaltenes, a common occurrence discussed by other workers, then on remixing with maltenes on a mass basis, the actual asphaltene concentration may be lower than calculated.

This source of error in the data was assessed by separately determining the asphaltene concentration in some of the reconstituted samples. Comparison of the values in Table 1 shows that the measured values are generally larger than the calculated ones, but in most samples the difference is less than 10% relative.

As noted in the review section, several theoretical equations encountered in the literature relate viscosity to the volume fraction of asphaltenes. In order to test the applicability of these equations to our data, it is necessary to know the relationship between mass and volume fraction. This relationship is derived in Appendix C, with the following result.

$$F_a = \frac{d_o X_a}{d_a} \qquad (1)$$

where F_a and X_a are respectively, the volume, and mass fractions of asphaltenes, and d_o and d_a refer to the densities of the oil and the asphaltenes, respectively.

Although the oil density is also a function of X_a, thus making the relationship potentially complex, it is conceivable that over a small range of X_a, d_o/d_a may be essentially constant, in which case F_a is simply proportional to X_a.

To test this, the densities of one set of reconstituted oils, and of the maltenes and asphaltenes used to make them, were measured as described in the Methods Section, with results shown in Table 4. Densities of the oils all lie between the values for maltenes and asphaltenes, and increase in a consistent fashion with increasing asphaltene concentration. As suspected, the ratio d_o/d_a is approximately constant over the range of X_a of the oils. (see Table 4).

The density data were also collected for a more subtle reason. The density of an oil can be expressed as

$$d_o = \frac{m_a + m_m}{V_a + V_m + V_e} \qquad (2)$$

where m = mass, V = volume and subscripts o, a, and m refer to oil, asphaltenes, and maltenes, respectively. The term V_e is introduced to account for non-additivity of the volumes (i.e., if addition of asphaltenes to maltenes is not volumetrically additive, V_e will have a non-zero value). Manipulation of equation 2 (details in Appendix D) gives

$$\frac{1}{d_o} = \frac{(d_m - d_a)X_a}{d_a d_m} + \frac{1}{d_m} + V^* \qquad (3)$$

where X_a refers to mass fraction of asphaltenes, and $V^* = V_e/m_o$

If $V^* = 0$, Equation (3) predicts that a plot of $1/d_o$ versus X_a should be linear with a slope of $(d_m-d_a)/d_a d_m$ and an intercept of $1/d_m$. Alternatively, if $V^* <> 0$, but is constant, the intercept will change to $1/d_m + V^*$.

The data in Table 4 are plotted as suggested by Equation 3 in Figure 4. The solid line results from calculations of d_o, using the measured values of d_a and d_m in Equation 3, assuming $V^* = 0$. Note that the measured values all lie below the predicted line. The dotted line was obtained by assuming the measured values fit a line of the same slope with a lower intercept. A value of $V^* = -6.6 \times 10^{-6}$ m^3/kg is calculated from the lower intercept. This negative "mixing volume" means that when asphaltenes are added to maltenes, there is a net loss of 6.6 mL/g of oil. A negative volume change implies that the molecular packing of the oil is more efficient than expected by simply adding the separated components. Such a change is consistent with the view that the resins associate with the asphaltenes. Redistribution of the polar resins into asphaltene aggregates may allow the remaining non-polar petrolenes to organize in a more compact manner.

Spearot (2.6.3[4]) noted that the theoretically derived equation of Brinkman has been successfully used to predict viscosity of suspensions of up to 40% solids. Values calculated from the Brinkman expression (equation 4) are also plotted in Figure 3.

$$\log(\mu_o/\mu_m) = 2.5 \log(1-X_a) \tag{4}$$

Here μ_o and μ_m refer to the viscosities of the suspension and of the solvent respectively and X_a refers to the mass fraction of solids.

Comparison shows that the actual effect of asphaltenes on oil viscosity is considerably greater than that predicted by the Brinkman equation. This result is consistent with some of the data reported by Mack for reconstituted asphalts (2.6.3[3]), with the data on solutions of asphaltenes in solvents [2.6.3[1]), and with the results obtained on oxidized engine oils (2.6.3[4]). In all of these previous reports, the lack of agreement with theory has been attributed to aggregation of the asphaltenes.

Michaels and Bolger (2.6.3[5]) presented a theory to explain the rheology of aqueous suspensions of kaolinite, which takes account of the effect of aggregation of the particles into "flocs". More recently, Spearot applied this theory to his data for oxidized engine oils, and also to data from a study of asphalt emulsions (2.6.3[4]).

Spearot used a simplified version of the theory of Michaels and Bolger which leads to equation 5.

$$\mu_r = \frac{\mu_o}{\mu_m} = (1 - fX_a)^{-2.5} \qquad (5)$$

where μ_o = oil viscosity
μ_m = maltenes viscosity
and f = constant to account for aggregation

Assuming that the fraction of asphaltenes in aggregates is proportional to the mass fraction of asphaltenes, equation 5 rearranges to give

$$10^{\left(\frac{\log \mu_r}{-2.5}\right)} = 1 - fX_a \qquad (6)$$

This predicts that a plot of the left hand side versus mass fraction asphaltenes should give a straight line. The plots in Figure 5 confirm the linear relationship.
Spearot also derived an equation which relates the extent of aggregation α, to *f*, as follows:

$$f = 1 - \left[\frac{d_s}{\alpha d_o} - \left(\frac{d_s}{d_o} - 1\right)\right] X_s \qquad (7)$$

where d_s and d_o refer to the densities of the solids and the oil respectively, alpha is the fraction aggregated, and X_s is the mass fraction of solids.
Since d_s/d_o = 1.18 as determined from data in Table 3, the value of 3.95 for *f* obtained from the slope in Figure 5 corresponds to about 0.26 for alpha. This implies that 26% of the asphaltenes in the reconstituted oils are present as aggregates.

Using this analysis, one concludes that the fraction of asphaltenes aggregated does not vary substantially as the concentration of asphaltenes is increased over the range of concentrations studied.

4.5 Conclusions

1. The viscosity of two Lloydminster oils increases almost logarithmically with increasing asphaltene content. This result is similar to that observed in some other kinds of mixtures, but can only be accounted for theoretically by assuming that the asphaltenes are partially aggregated.

2. Density measurements of mixtures of asphaltenes and maltenes indicate that mixing is non-ideal. When asphaltenes "dissolve" in maltenes, there is a small shrinkage volume, implying that the mixture is more efficiently packed than the two separate components.

3. The method used in this work to re-constitute oils involved removal of almost all of the added solvents using vacuum evaporation. Although the solvents used were much more volatile than the lightest components in the oil, considerable losses of oil components were nevertheless observed. In spite of this deficiency, the results obtained appear to be consistent.

4.6 Tables

1. VISCOSITY OF RECONSTITUTED TANGLEFLAGS OILS
2. VISCOSITY OF RECONSTITUTED PIKE'S PEAK OILS
3. LOSS OF LIGHT COMPONENTS DURING SOLVENT REMOVAL
4. DENSITY OF TANGLEFLAGS OILS AND FRACTIONS

TABLE 1: VISCOSITY OF RECONSTITUTED TANGLEFLAGS OILS [a]

SAMPLE	ASPHALTENES (mass %) Calculated	ASPHALTENES (mass %) Measured	VISCOSITY (mPa.s at 25°C)	VISCOSITY (mPa.s at 60°C)
1-1	0	-	593	81.4
2-1	7.0	8.03	1300	135
1-2	9.1	9.89	2480	--
2-2	10.0	10.7	2980	231
1-3	10.8	11.2	3000	--
1-4	13.8	14.3	6410	--
Original oil	-	14.0	5020,4940	341
1-5	15.3	15.8	8790	--
1-6	16.9	16.9	12800	--
2-3	18.0	18.6	22600	854
2-4	21.0	22.1	54700	1560

a) All samples contained <0.05% n-pentane and <0.5% dichloromethane except 2-3 (0.7%) and 2-1 (1%).

TABLE 2: VISCOSITY OF RECONSTITUTED PIKE'S PEAK OILS

SAMPLE	ASPHALTENES (mass %)	VISCOSITY (mPa.s @ 25°C)
1	0	1220
2	11.0	5730
3	13.0	8750
4	15.3	14400
5	15.3	13100
Original	15.3	11500
6	17.0	23800
7	19.0	34600

TABLE 3: LOSS OF LIGHT COMPONENTS DURING SOLVENT REMOVAL

SAMPLE	SOLVENT	CONCENTRATION %	LOSS OF C8- %	LOSS OF C8-C10 %
TFF2	n-pentane	35	-	-
TFF3	n-pentane	9.1	69	28
TFF4	$CH_2C\ell_2$	25	-	-
TFF5	$CH_2C\ell_2$	2.9	38	8.6
TFF6	$CH_2C\ell_2$	<1	96	66

TABLE 4: DENSITY OF TANGLEFLAGS OILS AND FRACTIONS

SAMPLE	ASPHALTENES (mass %)	DENSITY (kg/m^3 @ 25°C)	d_o/d_a
Maltenes	0	941.1	0.83
	7.0	963.5	0.85
1-2	9.1	965.2	0.85
1-3	10.8	967.9	0.85
Original	14.0	971.6	0.85
1-4	13.8	973.8	0.86
1-5	15.3	976.6	0.86
1-6	16.9	978.9	0.86
	21.0	987.7	0.87
Asphaltenes	100	1137.6	1.0

4.7 Figures

1. VISCOSITY CORRELATION WITH % ASPHALTENES
2. COMPARISON OF GC FINGERPRINTS
3. RELATIVE VISCOSITY CORRELATION WITH ASPHALTENES
4. DENSITY CORRELATION FOR TANGLEFLAGS OILS

Figure 1 : Viscosity
Correlation with % Asphaltenes

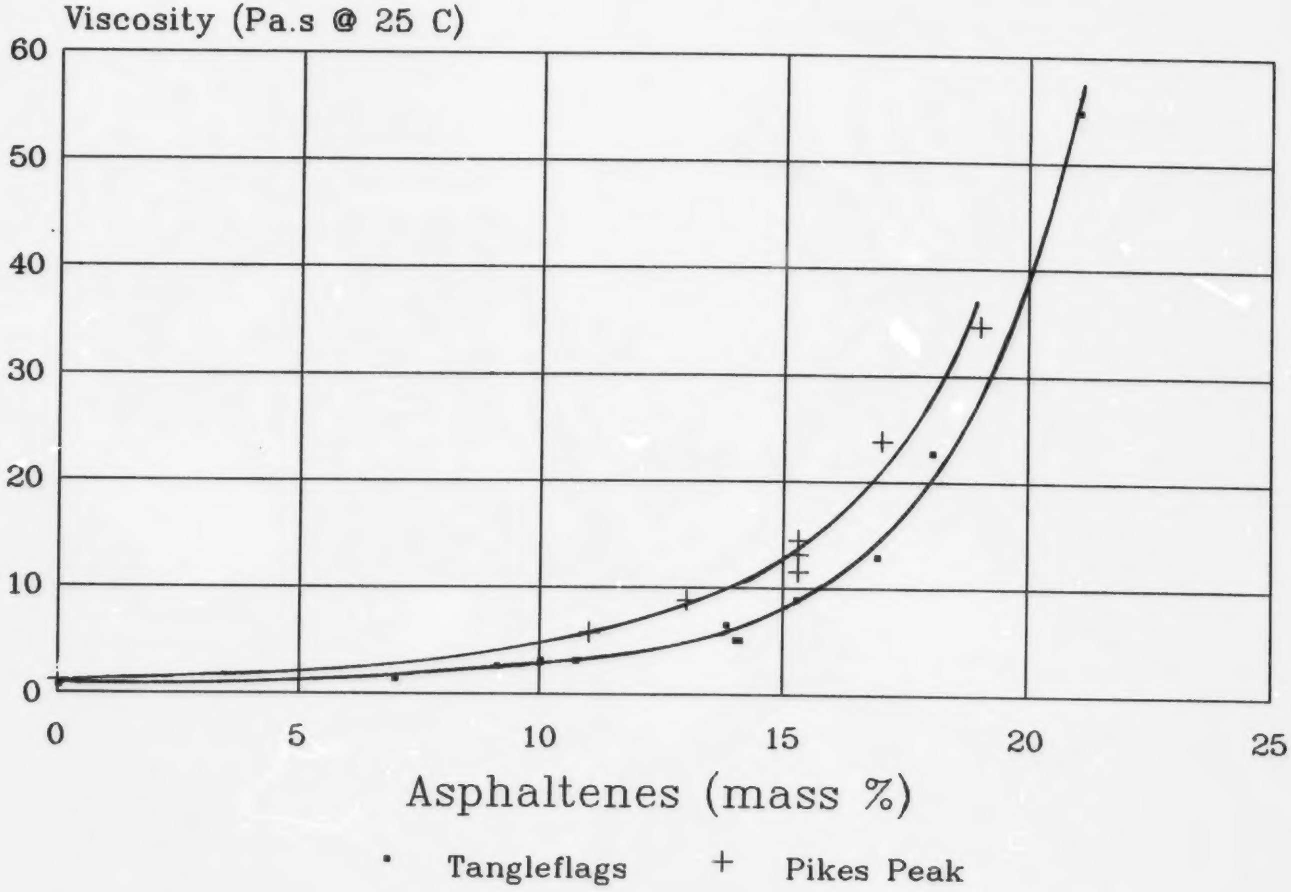

NOVA HUSKY
RESEARCH
CORPORATION

FIGURE 2: COMPARISON OF GC FINGERPRINTS
TFF5 Oil plus 2% CH_2Cl_2
TFF6 Oil after CH_2Cl_2 removal

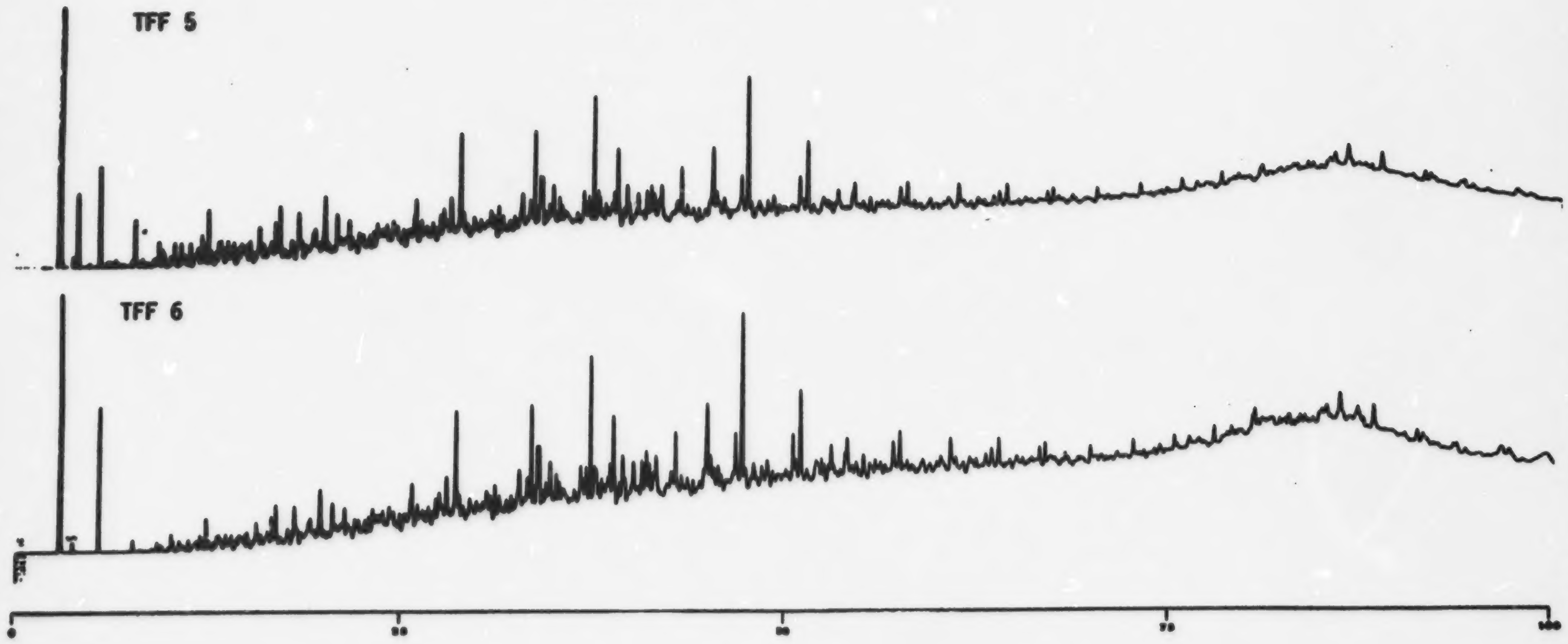

Figure 3: Relative Viscosity Correlation with Asphaltenes

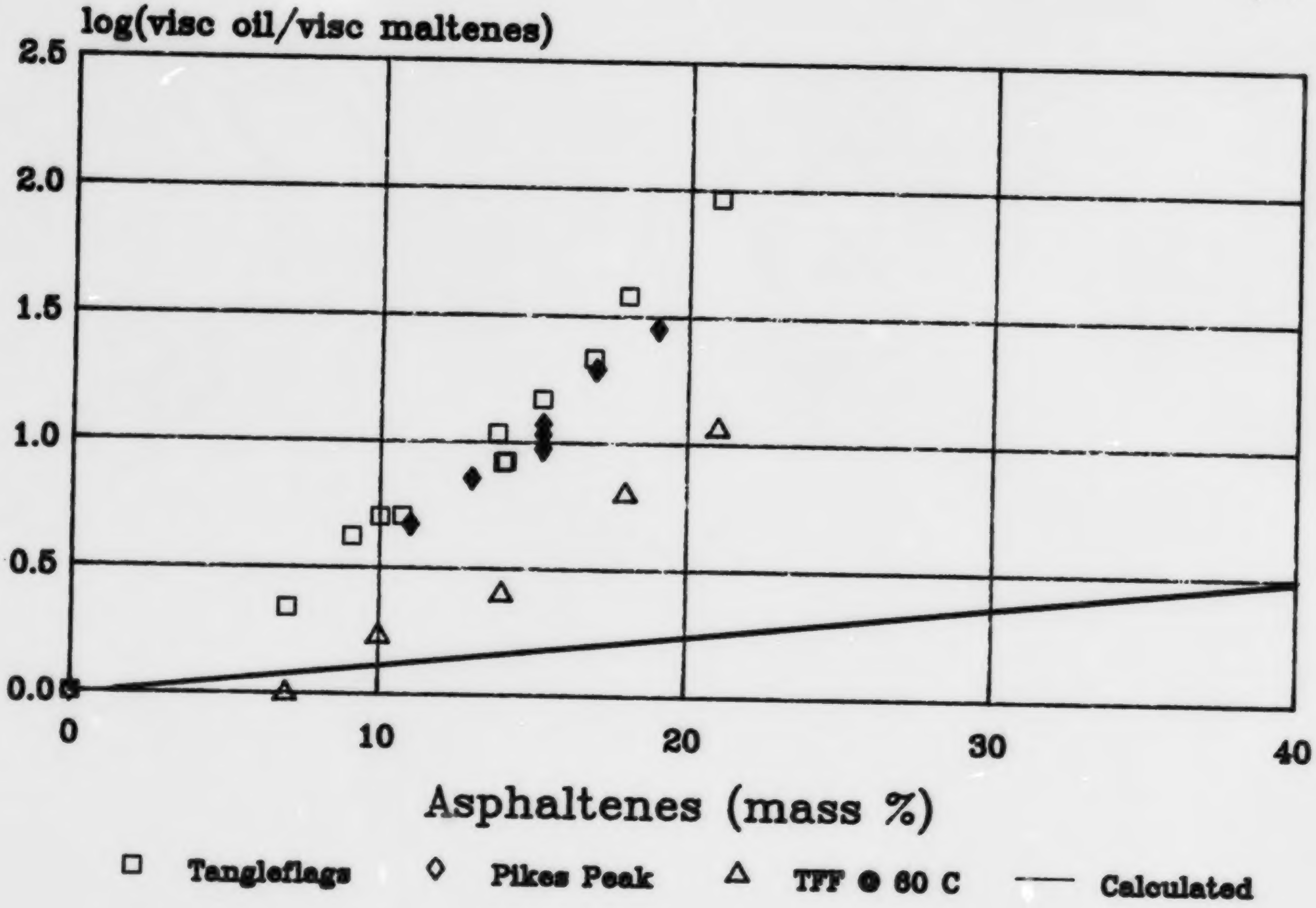

Figure 4 Density Correlation for Tangleflags Oils

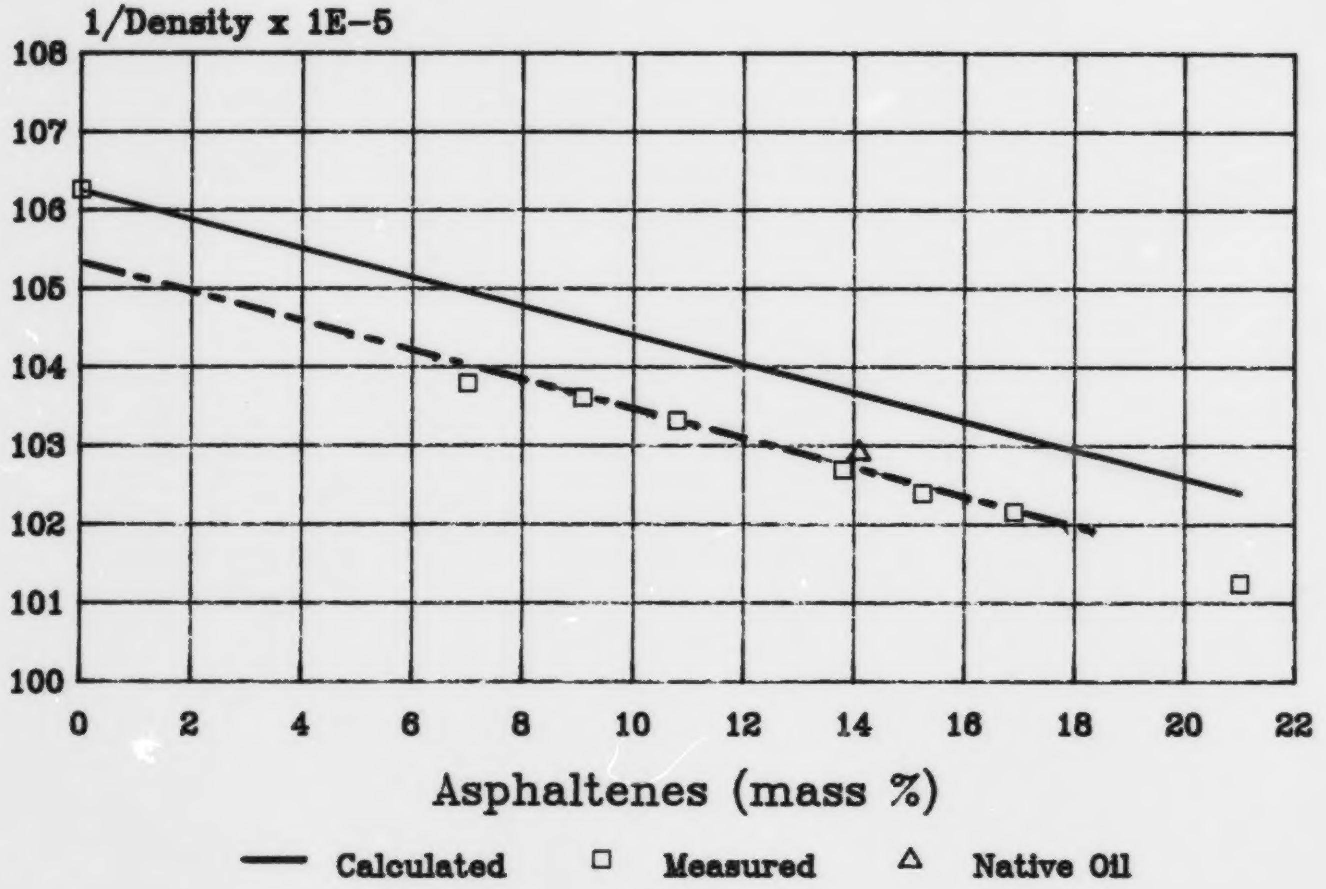

NOVA HUSKY RESEARCH CORPORATION

Figure 5: Plot suggested by Equation 6

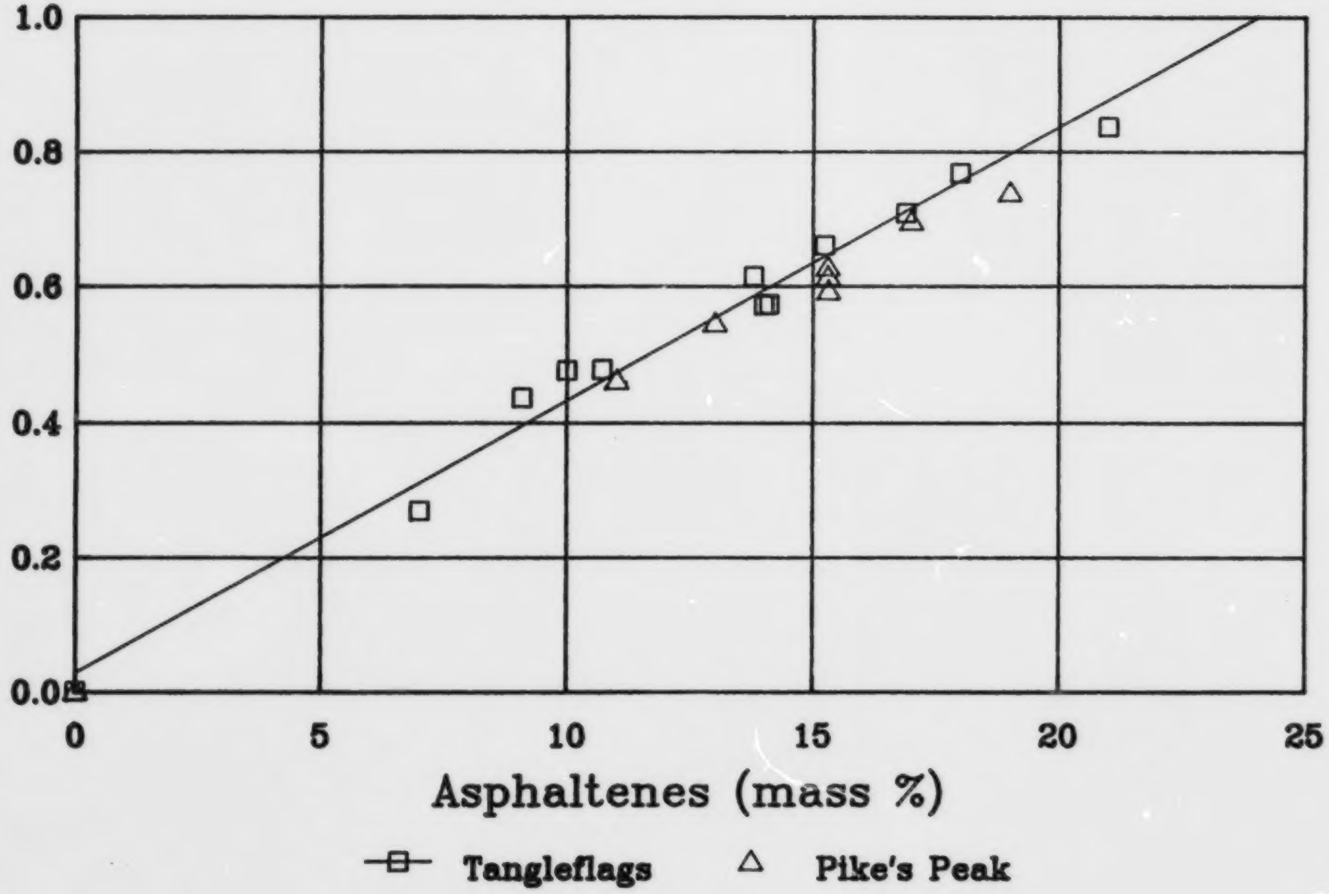

NOVA HUSKY
RESEARCH
CORPORATION

4.8 Appendices

APPENDIX A

LOSSES OF LIGHT ENDS FROM TANGLEFLAGS OIL DURING REMOVAL OF SOLVENT

Light end losses were assessed from differences in gas chromatograms of oil samples taken at different points during removal of the methylene chloride by rotary evaporation. The chromatograms obtained from each of the 5 samples described in Table 3 (Section 4.0) are shown in the following figures.

GAS CHROMATOGRAMS ANALYSIS CONDITIONS

A. Gas Chromatograph Conditions

Gas Chromatograph: Perkin Elmer Sigma 2000
Column: 30 metre, 0.32 mm ID SPB-1 capillary
Carrier Gas/Flow: UMP Helium, 0.9 mL/minute
Column Head Pressure: 40 kPa
Split Vent Flow: 50 mL/minute
Septum Purge Flow: 3 mL/minute
Oven Temperature Program: 50°C for 2 minutes
50 - 300° at 3°C/minute
300° for 20 minutes
Detector: Flame Ionization
Injector/Detector Temperature: 300°C

B. Integration Paramters

Range: 1
Zero: 5% FS
Attenuation: 16
Chart Speed: 0.4 cm/minute
Peak Width: 0.04
Threshold: 2
Area Rejection: 10,000

FIGURE 1 CAPILLARY CHROMATOGRAMS OF SAMPLES:

1) TFF2
2) TFF3
3) TFF4
4) TFF5
5) TFF6
6) Methylene Chloride (80 mL concentrated)

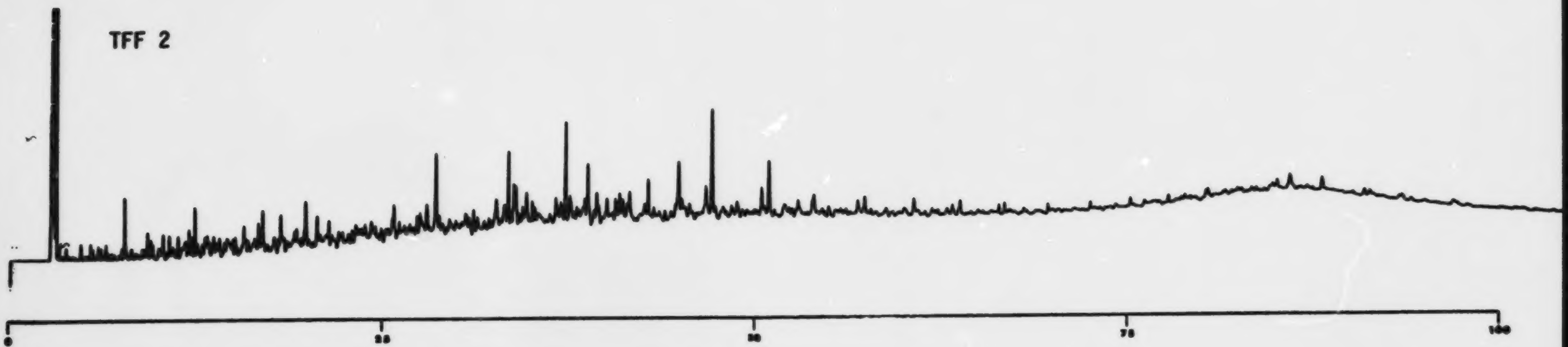

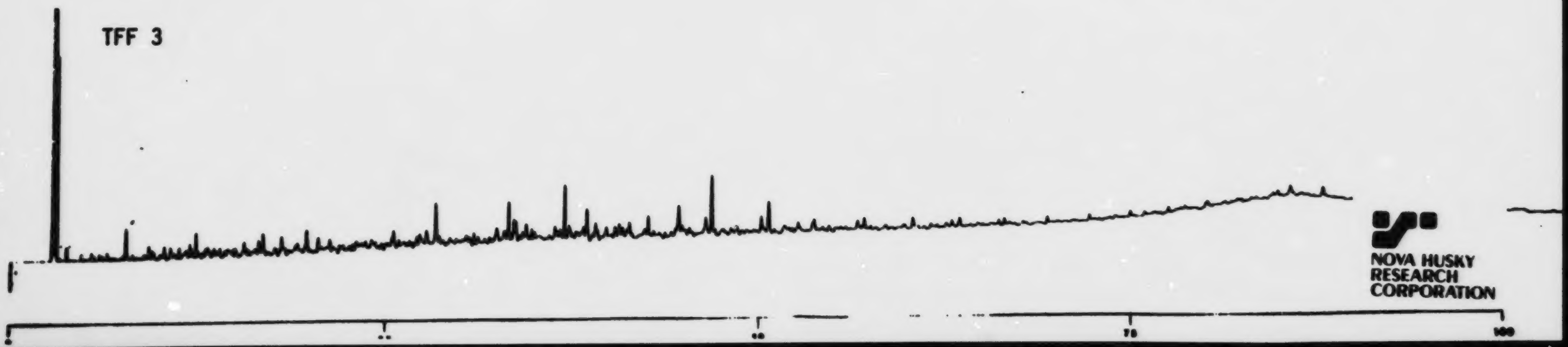

NOVA HUSKY
RESEARCH
CORPORATION

TFF 4

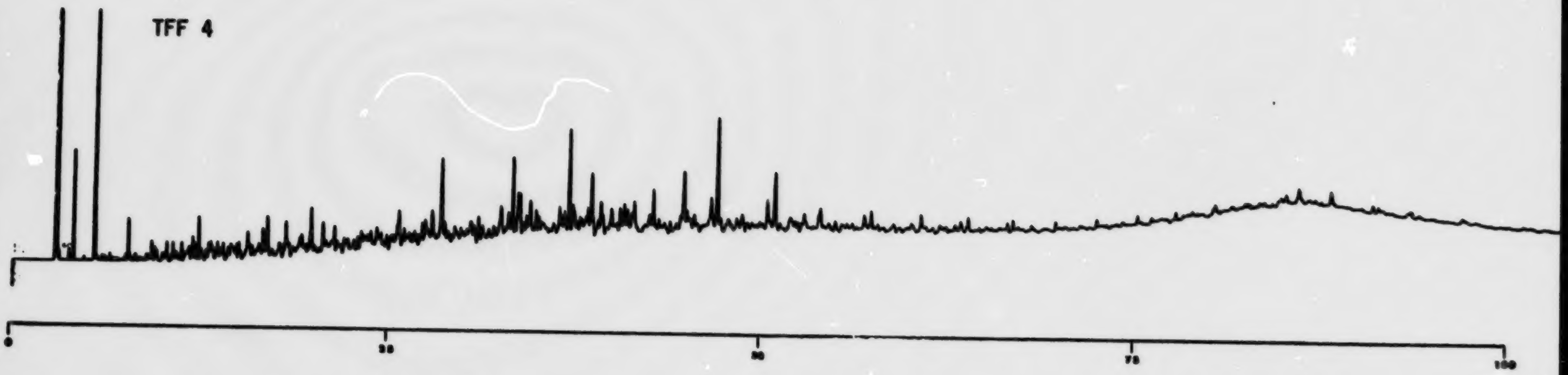

TFF 5

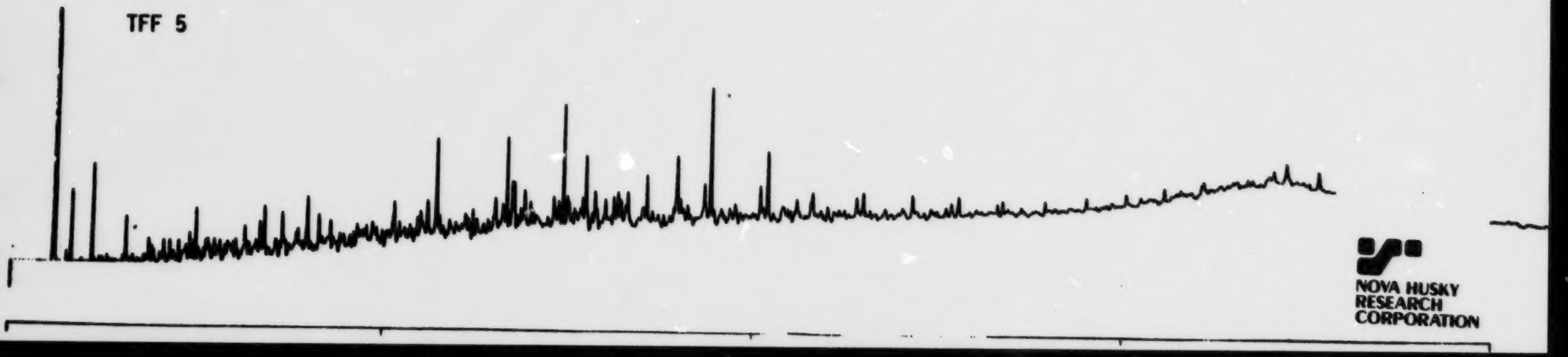

NOVA HUSKY
RESEARCH
CORPORATION

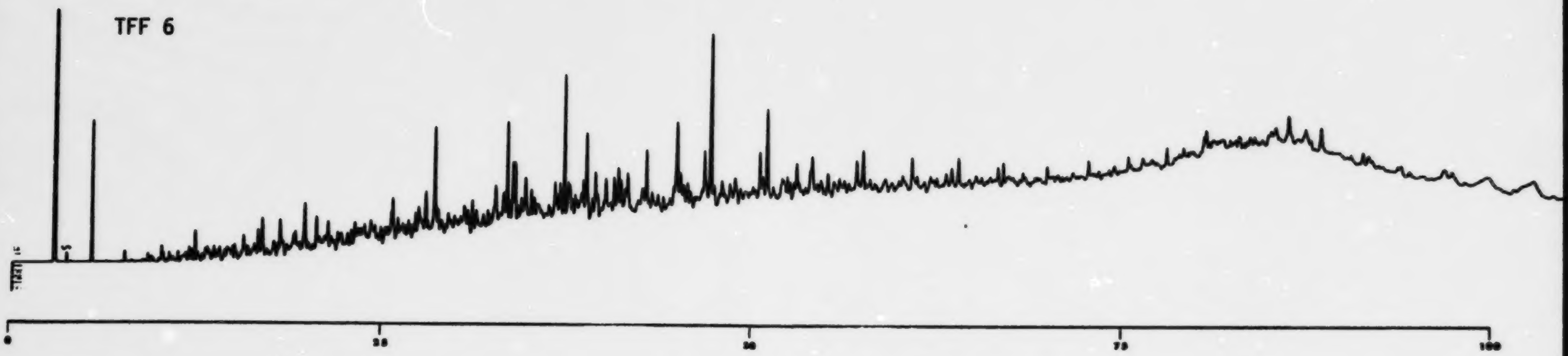

TFF 6

MeCl$_2$ Blank

NOVA HUSKY
RESEARCH
CORPORATION

FIGURE 5 CHROMATOGRAMS OF 1) Needle blank
2) Seven Component Aliphatic Standard

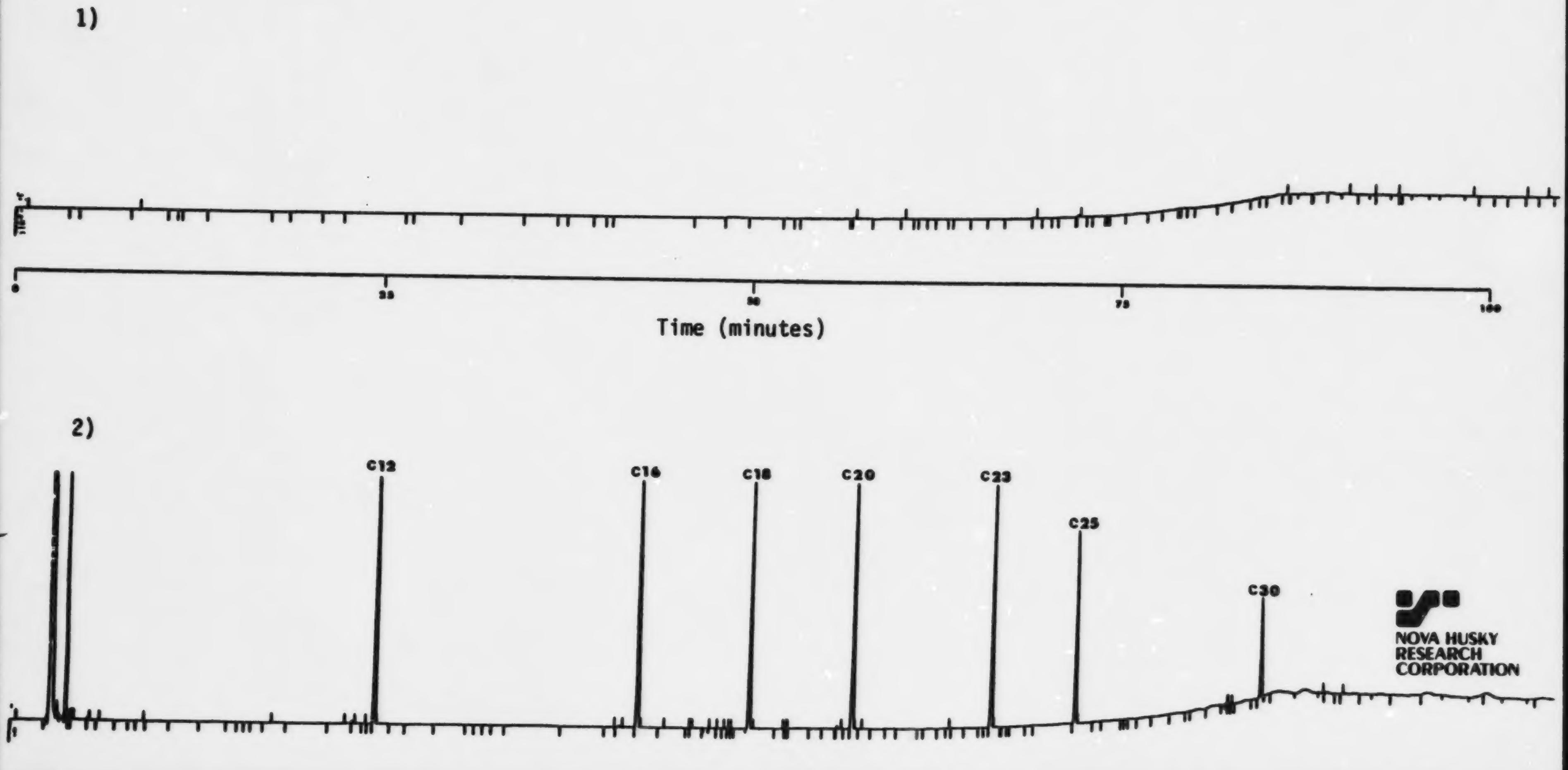

NOVA HUSKY
RESEARCH
CORPORATION

APPENDIX B

CORRECTION OF OIL VISCOSITY TO ACCOUNT FOR RESIDUAL SOLVENT

Methylene chloride at various concentrations was mixed with portions of native Tangleflags oil and the viscosity and density of each mixture were measured. Results are given in Table B-1 and are polotted in Figures B-1 and B-2. Note that the viscosity decreases smoothly with increasing solvent concentration. At concentrations up to 2%, the viscosity decrease can be approximated by a straight line. The viscosities of reconstituted oils of different asphaltene concentrations were corrected using this slope and extrapolating to 0% CH_2Cl_2.

TABLE B-1

VISCOSITY AND DENSITY OF TANGLEFLAGS OIL DILUTED WITH DICHLOROMETHANE

DICHLOROMETHANE (mass %)	VISCOSITY (mPa.s) @ 25°C	VISCOSITY (mPa.s) @60°C	DENSITY (kg/m^3 @ 25°C)
0.46	4840	333	966.5
1.14	3970	296	973.8
2.10	3120	255	976.0
4.45	1610	178	982.3
8.30	760	120	990.9

Figure B–1
Viscosity of Solvent Diluted Oils

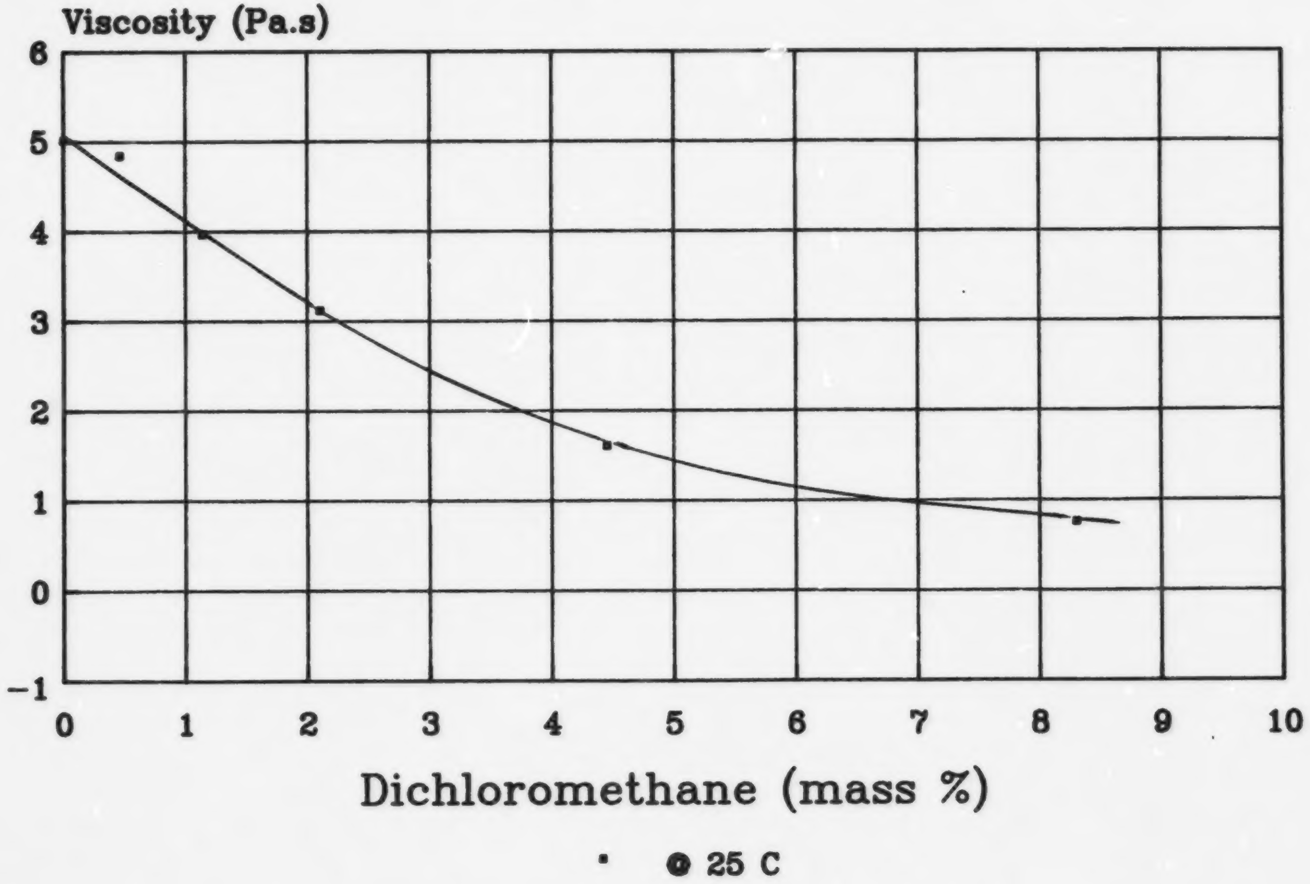

Figure B–2
Viscosity of Solvent Diluted Oils

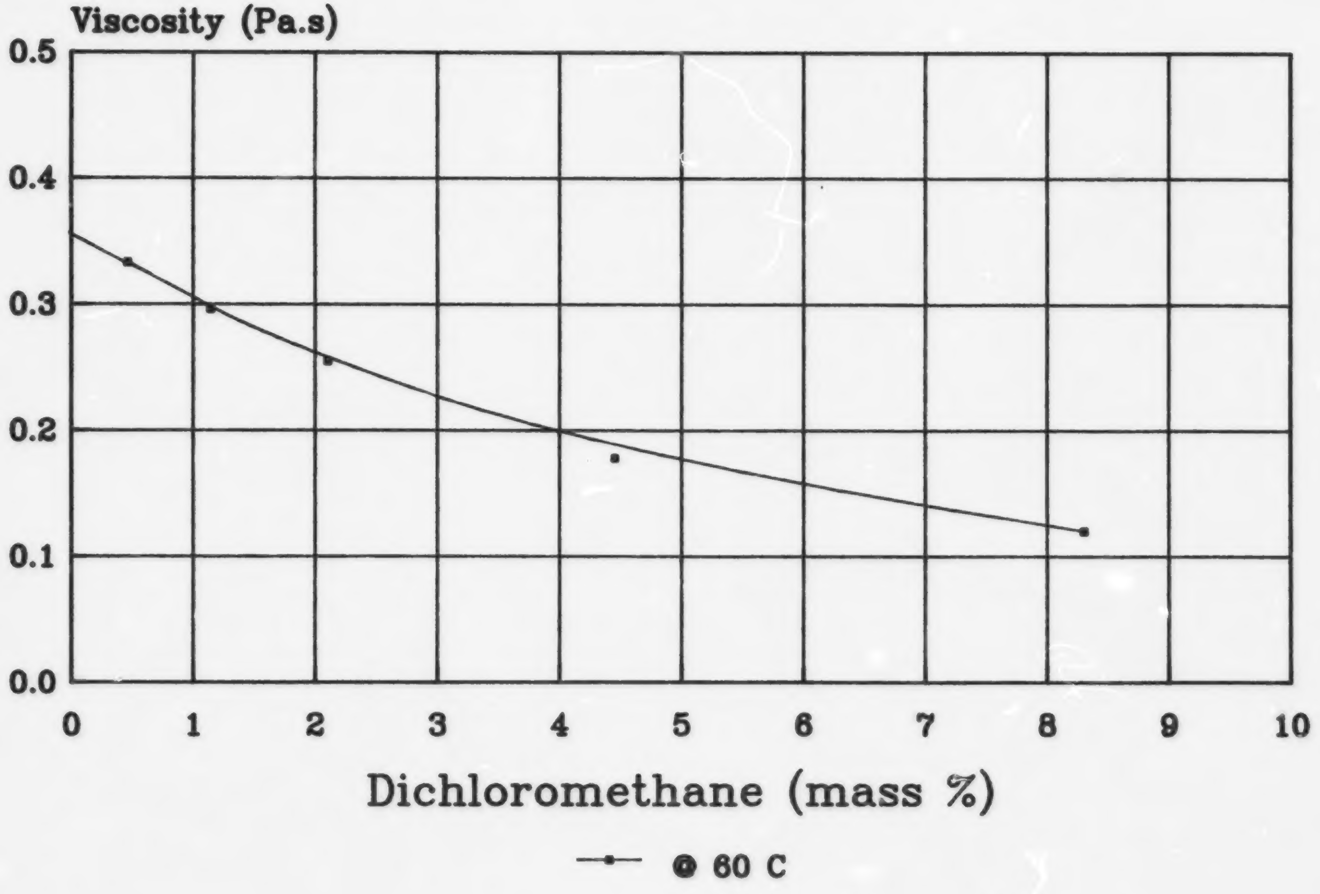

APPENDIX C

RELATIONSHIP BETWEEN MASS FRACTION AND VOLUME FRACTION

By definition,

$$F_a = \frac{V_a}{V_o} \qquad (1)$$

$$X_a = \frac{m_a}{m_o} \qquad (2)$$

$$d_a = \frac{m_a}{V_a} \qquad (3)$$

$$d_o = \frac{m_o}{V_o} \qquad (4)$$

where F = volume fraction
X = mass fraction
V = volume
m = mass
d = density

and subscripts a = asphaltenes
o = oil

Substituting for V_a and V_o in (1) using (3) and (4), gives

$$F_a = \frac{\frac{m_a}{d_a}}{\frac{m_o}{d_o}} = \frac{m_a \quad d_o}{m_o \quad d_a} \qquad (5)$$

and replacement using (2), results in

$$d_a = \frac{d_o}{d_a} \quad X_a \qquad (6)$$

APPENDIX D

DERIVATION OF RELATIONSHIP BETWEEN DENSITIES OF OIL AND ITS COMPONENTS

Mass balance requires that

$$m_a + m_m = m_o \tag{1}$$

and volume balance,

$$V_a + V_m + V_e = V_o \tag{2}$$

where
m = mass
V = volume

and subscripts
a = asphaltenes
m = maltenes
o = oil
e = excess

V_e refers to the "excess" volume associated with mixing. If mixing is ideal, $V_e = 0$.

By definition,

$$d_o = \frac{m_o}{V_o} \tag{3}$$

Combination of (1) and (2) and (3) gives

$$d_o = \frac{m_a + m_m}{V_a + V_m + V_e} = \frac{m_a}{V_a + V_m + V_e} + \frac{m_m}{V_a + V_m + V_e} \tag{4}$$

Also by definition

$$V_a = \frac{m_a}{d_a}, \qquad V_m = \frac{m_m}{d_m} \tag{5}$$

Substitution of (5) into (4)

$$d_o = \frac{m_a}{\frac{m_a}{d_a} + \frac{m_m}{d_m} + V_e} + \frac{m_m}{\frac{m_a}{d_a} + \frac{m_m}{d_m} + V_e} \tag{6}$$

Multiplication of (6) by (m_o/m_o), and defining

$$X_a = \frac{m_a}{m_o}, \qquad X_m = \frac{m_m}{m_o} \tag{7}$$

gives

$$d_o = \frac{\frac{m_a}{m_o}}{\frac{m_a}{m_o d_a} + \frac{m_m}{m_o d_m} + \frac{V_e}{m_o}} + \frac{\frac{m_m}{m_o}}{\frac{m_a}{m_o d_a} + \frac{m_m}{m_o d_m} + \frac{V_e}{m_o}}$$

$$= \frac{X_a}{\frac{X_a}{d_a} + \frac{X_m}{d_m} + \frac{V_e}{m_o}} + \frac{X_m}{\frac{X_a}{d_a} + \frac{X_m}{d_m} + \frac{V_e}{m_o}} \tag{8}$$

Defining $V^* = V_e/m_o$, and since $X_a + X_m = 1$,

$$d_o = \frac{1}{\frac{X_a}{d_a} + \frac{X_m}{d_m} + V^*} \tag{9}$$

Rearranging of (9) gives

$$d_o = \frac{d_a d_m}{X_a d_m + X_m d_a + V^* d_a d_m} \tag{10}$$

Substitution of $X_m = 1 - X_a$ in the denominator, results in

$$d_o = \frac{d_a d_m}{X_a(d_m - d_a) + d_a + V^* d_a d_m} \tag{11}$$

To obtain a linear plot, invert both sides to get

$$\frac{1}{d_o} = \frac{(d_m - d_a)X_a + d_a + V{*}d_a d_m}{d_a d_m} \qquad (12)$$

or

$$\frac{1}{d_o} = \frac{(d_m - d_a)X_a}{d_a d_m} + \frac{1}{d_m} + V{*} \qquad (13)$$

Equation (13) predicts that a plot of $1/d_o$ versus X_a should be linear with a slope of $(d_m - d_a)/d_a d_m$ and an intercept of $(1/d_m + V{*})$.

5.0 STEAM DISTILLATION STUDIES (TASK 7)

5.1 Summary

Linear coreflooding experiments were carried out to assess the contribution of steam distillation to thermal recovery of two similar Lloydminster oils. Ten experiments were completed in all, three of which were hot waterfloods. The others used combinations of water, steam and gas as the oil displacing fluid.

Although significant quantities of less viscous oil were produced in some experiments, and this oil was confirmed to have resulted from evaporative fractionation of the original oil, the recovery data do not conclusively show any contribution to overall recovery by this process. Recoveries ranged from 62 to 84 % OOIP under the various conditions used in the experiments.

5.2 Introduction

The experiments described in this section were designed to assess the role of steam distillation during thermal recovery of Lloydminster heavy oil. In both steam and combustion processes, conditions created in some parts of the reservoir are likely to enhance the evaporation of the lighter components of the oil. This volatile fraction would move forward with the steam phase, until it condenses or dissolves into cooler oil. Recovery enhancement might be expected to result from the reduced viscosity of the oil-light ends mixture.

Steam distillation might also impact on recovery by reducing the mobility of oil left in the zone partially swept by steam. This residual material might keep the permeability to steam lower than that of fully swept sand, and thus enhance steam over-ride. In addition, residual oil at the interface between steam and underlying water-swept zone might retard the downward movement of steam, and thus impede efficient recovery of oil from lower portions of a reservoir sand.

These ideas were motivated by results of some previous in-house studies. Oil from some wells in a fireflood project had much lower viscosity than the "native" reservoir oil. This lighter oil could have resulted from mixing of steam distillate formed near the combustion front with cooler native oil. In a study of post-steam core, residual oil taken from the steam-swept zone was found to be much less volatile than native reservoir oil. From a comparison of distillation curves, it was concluded that the residual oil had resulted from the loss of the lowest-boiling components of the native oil . Temperatures and pressures measured in the post-steam well from which the core was taken indicated that steam was present in the reservoir at that location.

5.3 Experimental

5.3.1 Materials

Reservoir sand from two different sources was used for these experiments. Sand for the Pike's Peak runs was obtained from core from well 4A11-1 at the Pike's Peak Steam Project. The reservoir inverval is the Waseca sand. The core sample was extracted with boiling toluene in a large extractor (Core Labs), and dried at 110 C. To restore water wettability, it was washed with acetone and air-dried at 22 C in a fume hood. In preliminary work, packs of this whole sand were found to decrease significantly in permeability with flow. To minimize this problem, most of the finest portion of the sand was removed by wet-sieving through a 200 mesh sieve. The sand was rinsed with acetone and dried at 22 C as before. Sieve analysis of a portion of the sample is given in Table 1. The sand is > 99 % quartz.

Sand from the Tangleflags reservoir was obtained from the desand pump outlet at the Tangleflags Battery. It This sand was co-produced with oil and water from wells, and settled to the bottom of the treater. The desand pump periodically washes this sand out of the treater into a pit. The production interval in the Tangleflags field is the General Petroleum. The wet oily sand was extracted with boiling toluene in a large extractor (Core Labs), wet sieved to remove material finer than 200 mesh (75 um) washed with acetone and dried at 22 C in a fume hood. Sieve analysis results in Table 1 show that the Tangleflags sand is finer-grained than the Pike's Peak sand.

Oil for the Pike's Peak runs was obtained Dec. 3, 1987 from the wellhead at 3B7-6, a cyclic well at the Pike's Peak Steam Project near the end of its first production cycle. Wellhead temperature for 2 weeks before and after sampling was about 45 ± 5 C. The emulsion as received contained about 30 % water. The oil was cleaned by centrifugation at 90 C,

~30,000 x gravity, for 60 minutes, using a Beckman L8/M heated ultracentrifuge. The original viscosity, density, and residual water content of the cleaned oil are given in Table 2. Also, since previous work at NHRC had indicated that oil viscosity increases gradually in samples stored at 22 C, the viscosity was measured periodically, with results as shown in Table 2.

For the Tangleflags experiments, a wellhead sample was obtained from D11-13, a well offsetting the fireflood patterns at the Tangleflags Fireflood Project. Previous studies had indicated that oil from this well had not as yet been affected by the fireflood process. The sample was taken June 3,1986; wellhead temperature was 10 C. Elevated wellhead temperatures have never been observed over the 3 years of operation of this Project . Clean oil was separated from the produced emulsion by heated centrifugation (same conditions as noted above), resulting in an oil sample with properties as listed in Table 2. Viscosity was re-measured periodically throughout the course of the experiments with values as shown in Table 2.

Synthetic brines were used for the initial saturation of the sandpack. The brines were made up by dissolving reagent grade salts in freshly distilled water , in the amounts shown in Table 3 .

5.3.2 Methods

5.3.2.1 Vapour Pressure Measurements

Two Monel cylinders (each 250 mL) were mounted vertically in an oven. Each one was connected via 1/8" SS tubing to a Shaevitz pressure transducer (0-517 kPa) mounted outside the oven. The tranducers were calibrated by comparison to a 30 cm Heise gauge. About 50 g of oil were added to each cylinder , and the temperature was increased to 150 C. The temperature was increased every few hours by about 50 C, to a maximum of 286 C, and then decreased incrementally. Pressures were monitored continuously on a strip chart recorder. Three sets of two experiments were conducted. The first 2 sets consisted of a sample of Tangleflags and a sample of Pike's Peak oil. In both of these runs, connections to the cylinder containing the Pike's Peak sample began to leak at the point in the experiment where the temperature was decreased. The third set included a Pike's Peak sample, and a blank containing only air.

5.3.2.2 Sandpack Flood Experiments

- Apparatus

A schematic drawing of the apparatus used in these experiments is given in Figure 1. It consists of reservoirs for holding fluids prior to injection, a high pressure syringe pump (ISCO LC-5000), a high pressure, high temperature "core holder", in which the sandpack was mounted, an oven to heat the fluids and sandpack, a back-pressure regulator, a fraction collector to receive the produced fluid, pressure tranducers and thermocouples, and necessary valves and piping.

The core holder was purchased from the Petroleum Recovery Institute in Calgary; a schematic is shown in Figure 2. It includes an internal copper sleeve, to contain the core or sand, surrounded by an outer steel body. The copper sleeve is radially pressurized with water, and axially stressed by tightening one end of the holder. This is intended to simulate the triaxial overburden stress experienced by sand in a oil reservoir. The ends of the holder are designed specifically to distribute injected fluids evenly at the injection end, and to hold the sand in place at both ends by means of 400 mesh SS screens mounted on top of the distributor plate.

The copper sleeve is machined to dimensions of 1.50 inches internal diameter by 9.00 inches length, and holds about 200 g of sand. Packing of the copper sleeve was carried out from the injection end, with the sleeve mounted in the holder. Dry sand was poured into the water-filled sleeve, while the outside of the holder was tapped to cause tighter packing. Water was drained slowly from the bottom (production end) as the holder was filled with sand. The process was completed in 3 - 4 "pours".

- Sandpack Preparation

Preparation of the sandpack for an experiment followed a fixed protocol throughout the work. When packing was complete, the injection end cap was installed, the holder was mounted on a rack in the oven, and pipes were connected for injection, production, and pressure measurement. Lines to the pressure transducers were filled with water and isolated by valves from the sandpack. Pressure on the outside of the copper sleeve was increased to 500 psig, and monitored to check for leaks. When starting with a fresh sandpack, about 200 mL of methanol was first pumped through the sandpack, after which nitrogen was blown through to remove the methanol. If the sandpack contained residual oil from a previous run, toluene was flowed through the sandpack until the effluent was colorless. The sandpack was then evacuated with a vacuum pump for a period of at least 15 hours. The oven was turned on at 30C, the lowest temperature at which it can control. Brine was then pumped into the sandpack and connecting pipes with the ISCO pump, until the pressure reached 2000 kPa. The water remaining in the pump cylinder at this point was purged and weighed. Since the cylinder holds 505.4 g of water when full, measurement of the amount remaining allowed calculation of the mass of water pumped. The volume of brine (measured at 22 C) in the sandpack was then calculated by subtracting the "dead volume". The dead volume is the volume of fluid in the connecting pipes, and held in the end caps of the core holder. Both flowing and non-flowing dead volumes must be included in calculating the volume of brine in the sandpack (the pore volume). Flowing dead volume is that portion which is flushed during flow through the sandpack, and includes mainly the end cap volumes. Non-flowing dead volume is not flushed during flow, but is evacuated and thus filled with brine when the sandpack is being filled. It includes the portion of the pipes leading to the pressure tranducers up to the valves, and the small reservoirs in the coreholder endcaps intended to minimize plugging of the pressure pipes (see Figure 2).

After the pore volume determination, the rest of the piping is filled with brine, and the overburden pressure is increased to 800 psig. The permeability of the sandpack to brine was determined from the pressure drop across the sandpack during flow at 75, 150 and 200 cm^3/hr.

Oil saturation was then initiated by pumping water to displace heavy oil from its reservoir into the sandpack. The water was pumped at 4 cm^3/hr (@ 22 C). Saturation was considered complete when the pressure drop across the pack remained constant for several hours; this usually occurred after about 40 hours of pumping, or about 1.6 pore volumes of oil injected. The total mass of oil in the sandpack and flowing dead volume was determined from the mass of oil injected and by measuring the mass of oil produced. The latter measurement required dilution of the production with toluene, and subtraction of the mass of brine produced from the total fluid produced. From these data the initial oil and water saturation of the sandpack were calculated.

- Hot Water Flood

All but one of the flood experiments were initiated by turning up the oven to 200 C, and collecting the oil which was produced as a result of expansion during heat-up. The back-pressure of 2000 kPa was sufficiently above saturated steam pressure at 200 C to ensure that no steam phase was formed. For the hot waterfloods, water was pumped at 10cm^3/hr (@ 22 C) into the pre-heat coil and from there into the sandpack. Production was collected in 30 mL vials mounted in a fraction collector. The mass of oil produced at each time was determined from the mass of the vial and oil after removal of the water.

- Steam Flood

Four different ways of introducing steam to the sandpack were tried. In Run PP29, after heat-up to 200 C, the back-pressure was lowered to 1400 kPa, initiating further production. After this "blowdown" was complete, water was pumped in at 10 cm^3/hr. This steaming phase was continued until the oil production rate was negligible.

In Run PP30, steaming was begun after heat-up, by increasing the oven temperature to 220 C, and simultaneously flowing water in at 10 cm^3/hr. The third approach, which was considered the least ambiguous was used in Runs PP32 and TFF34. The sandpack was first waterflooded at 200 C, 2000 kPa until the oil production rate was very low. The temperature was then increased to 220 C, resulting in steam flooding of the sandpack. For Run TFF35, an attempt was made to steam into a cold sandpack, using a small steam generator. While this is the approach that most closely simulates steam injection in the field, heat losses in the configuration we used were so large that little heat reached the sandpack, and thus the run was essentially a warm waterflood.

- Hot Gas Flood

Two attempts were made to perform a gas flood in which no steam was involved. In Run PP31, the sandpack was flooded with oil rather than brine directly after evacuation. The sandpack was then heated to 200 C, and allowed to produce against the 2000 kPa backpressure as usual. Nitrogen was then flowed into the sandpack at 825 cm^3/hr (measured at 22 C and 2000 kPa), using a Brooks Model 5850E mass flow controller. Production was collected in vials as in previous runs. Although there was initially no water in the sandpack or flowing dead volume, water was produced. This discrepancy was resolved, when checks after the run was over found gas in the lines to the differential pressure transducer. Apparently the gas had displaced water originally in these lines. In a later experiment, Run TFF36, the sandpack was again saturated completely with oil. The lines to the differential pressure transducer were disconnected and the ports plugged, to exclude this source of water. In spite of this change, water was again produced. In this case the water was found to have come from the small cylinder used to transmit pressure to the backpressure regulator.

- Residual Oil in Sandpack

At the end of each run, the sandpack was cooled, and any oil remaining in the sandpack was flushed out by flowing toluene. The toluene-oil mixture was rotovapped to remove the toluene, and the mass of residual oil measured. As toluene removal was often incomplete, toluene remaining in the rotovapped oil was determined using simulated distillation, and the mass of residual oil was corrected for the toluene.

5.4 Results and Discussion

5.4.1 Vapour Pressure Measurements

Vapor pressures of Tangleflags and Pike's Peak oils over the temperature range 150 to 290 C are listed in Table 4 and are plotted in Figure 3. The pressures were generally stable within 2 hours of changing the oven temperature. Readings were usually taken at a point just prior to changing the temperature, or at a time when the value had remained stable for several hours. Although there is considerable variation among the readings made at the same temperature at different points in the experiments, and among separate experiments with the same oil, the variation does not correlate with either the length of time at a particular temperature or with the direction of the last temperature change (heating or cooling). The vapor pressures of both oils increase with temperature as expected, and follow fairly smooth curves.

Pike's Peak oil has a higher vapor pressure than Tangleflags oil at all four temperatures. This is a rather surprising result, since the Pike's Peak oil has the higher density and viscosity. However, there is no fundamental reason why vapor pressure should correlate with density and viscosity. The vapor pressure is primarily determined by the low molecular weight oil components, whereas the viscosity and density are sensitive to both low and high molecular weight compounds. Recalling results from Section 4.0, the Pike's Peak oil has a higher asphaltene content than the Tangleflags oil. The effect of the asphaltenes in increasing viscosity apparently outweighs the viscosity reducing effect of a higher concentration of low molecular weight components.

5.4.2 Flood Experiments

Three different kinds of experiments were carried out. To begin with, oil-saturated sand was flooded with water at 200 C and 2000 kPa. Under these conditions no steam phase is formed, and recovery is due to displacement by hot water. Experiments were also performed in which a steam phase was purposely created, in one run by lowering the back-pressure and in others by increasing the temperature. In the third kind of experiment, the sandpack was flooded with nitrogen gas at 200 C.

5.4.2.1 Initial Sandpack Characteristics

The permeability, porosity and initial saturations of the sandpack prior to each run are given in Table 5.
For the Pike's Peak experiments the sandpack was changed between Runs PP24 and PP28. A single sandpack was used for all of the Tangleflag runs. Difficulties in maintaining a constant sandpack permeability were experienced throughout both series of experiments.

Pore volumes, and the porosities derived from them, correlate fairly well with permeability for the Pike's Peak sand, except for Run PP31 where the permeability appears to be too low. The less permeable Tangleflags sandpacks do not show this correlation, and have higher porosities (except TFF34) than the Pike's Peak sands.

Displacement of reservoir brine by oil gives oil saturations varying from 89 to 95 % in both Pike's Peak and Tangleflags sandpacks. These values are based on the measurement of the oil injected, corrected to account for the oil which goes into the connecting pipes (flowing dead volume). Brine saturations at the end of the oil injection are also given, as calculated from the amount of brine produced from the sandpack. In almost all cases, the amount of brine recovered appears to be too low compared to the amount of oil retained. Thus calculated brine saturations of 15 to 20 % are obtained for most runs, which are not consistent with the oil saturation data. An assessment of uncertainties in the data leads us to conclude that the injected oil measurements are the most accurate, and thus the initial oil saturations are used in calculations of recoveries. Initial brine saturations obtained by difference are given in parentheses in Table 5.

5.4.2.3 Heat-up to 200 C

As explained in detail in the experimental section, prior to beginning each flood, the oil-saturated sandpack was heated to 200 C, and production due to expansion was measured. Heat-up followed directly after oil saturation, so the pipes connected to the injection and production ends of the core holder, as well as the distributor plates at each end of the sandpack,(i.e the flowing dead volumes) were oil-filled. Since most of this volume was within the oven, the production during heat-up is due to expansion of both brine and oil within the sandpack and in the connecting pipes.

5.4.2.4 Hot Waterfloods

The first experiment in the series was a hot waterflood, Run PP24. Although production was directed to vials, and thus data was collected throughout the flood, there were significant discrepancies in the oil values derived. Several attempts to eliminate the discrepancies gave unacceptable results, and thus the production data for this run have not been included. Total oil recovery was calculated from the residual oil saturation.

In the second experiment, PP28, production was directed to a measurement cell instead of to the fraction collector. Production entered the top of the gas-filled cell, displacing the gas also out the top to the backpressure regulator. Details of the configuration are given in the methods section. The heights of the gas-oil and water-oil interfaces were recorded, which together with calibration data for the cell allowed calculation of produced oil and water volumes. Only a few data points were collected, because the interfaces, particularly the water-oil one, became more and more ambiguous as the flood proceeded. This confirmed observations made in earlier experiments, using a similar measurement approach, and convinced us to return to the alternate method of measuring production using glass vials. In Run PP28, total oil produced into the cell was measured by removing the oil and water mixture at the end of the run, diluting with toluene, and measuring the separated water.

The last run in the set, PP32, began with a hot waterflood performed in a similar manner to PP24. Oil production data from this waterflood are given in Table 6, and the net cumulative oil is plotted as a function of time in Figure 4. Note the apparent delay of about one hour in net oil, which results from deducting the flowing dead volume from the initial production (i.e. correcting for oil not in the sandpack). The sharp inflection at about 5 hours in the production curve (Figure 4) corresponds to breakthrough of water, at about 0.5 pore volume water injected. Oil production continues at a slower but steady rate for the rest of the flood.

In the second set of experiments, the first two runs (TFF33, TFF34) began with hot waterfloods. Production data are given in Tables 7 and 8, and net cumulative oil is plotted against time in Figures 5 and 6. The production curves are quite similar, except that water breakthrough was sharper in Run TFF34, and oil production lags somewhat. The oil production rate at the end of both runs (4.5 pore volumes) was steady and non-zero, at a final water/oil ratio of about 40.

5.4.2.5 Steam and Gas Floods

In Run PP29, after heating the sandpack to 200 C, the backpressure was dropped to cause steam to be the dominant phase. Oil production began soon after lowering the pressure, and continued for several hours. Only after this "blowdown" had stopped, was injection initiated. The total oil produced prior to injection was measured. Incremental production from the start of injection was recorded with time in the usual manner, giving the data in Table 9. The production during the blowdown stage, minus the flowing dead volume, has been included as the initial value. In this case, the time is relative to the beginning of injection. As seen in Figure 7, the oil production rate with steam is much lower than was observed in the waterfloods.

Run PP30 was also a steamflood, initiated after equilibration at 200 C, by increasing the oven temperature and simultaneously beginning water injection. Production data are listed in Table 10 and plotted in Figure 8. Total production is similar to that obtained in PP29, although the shapes of the production curves are quite different. Note, however, that the rate at the end of Run PP30 is also very low, unlike the waterfloods, and similar to PP29.

In Run PP31, we attempted to isolate the gasflood effects from those due to steam distillation. Water was excluded from the sandpack by saturating with oil directly after evacuation. In spite of this, some water was produced anyway, and we deduced after the run that it had come from the pipes which lead to the pressure transducers (see Figure 1). Until the water was produced, therefore, hot water, steam and gas were flowing simultaneously.

Oil production data from PP31 are listed in Table 11 and plotted in Figure 9. The very high value measured between 8 and 9 hours (in brackets in Table 11) is believed to be in error, and a value of 1 g was chosen as more reasonable. Even after this reduction, the amount of oil produced during this run was higher than any of the others.

Only total oil production was measured for the other steamflood and gasflood experiments; this data is discussed in the next section.

5.4.2.6 Comparison of Production Data

Results of all 10 floods are collected in Table 12. Examination of the last two columns shows that the values for oil produced based on direct measurement (Total produced) are often not in good agreement with the values calculated as the difference between original and residual saturation in the sandpack (i.e. by mass balance (MB)). In fact, in 6 out of the 9 data sets, the discrepancy is greater than 5 % OOIP. The discrepancy is most evident in data for Runs PP31, PP32, and TFF34, and in all of these cases the value based on total oil produced is unacceptably large. For this reason, the more reasonable values derived by mass balance are considered more reliable. Reasons for the discrepancies will be discussed later in this section.

The results from Runs PP24 and PP28 indicate that waterflooding of Pikes Peak oil at 200 C produces about 73 % of the oil in place, of which 15 % is due to expansion on heating from 30 to 200 C, and another 58 % results from the waterflood.

Results from the first two steamfloods (PP29 and PP30) suggest that steam is no more productive than hot water. In contrast, the last run in this set, PP32, produced 81 % OOIP, at least 8 % OOIP more than waterflood. In Run PP30, steamflooding was initiated directly after heat-up to 200 C by increasing the temperature and beginning water injection. In PP32, steamflooding followed after hot waterflood. This latter approach appears to be more effective.

Even with an unwanted contribution from water and steam, (see previous discussion) recovery from gasflood Run PP31 was less than that obtained by waterflood.

Hot waterflood of a sandpack of less viscous Tangleflags oil recovered 84 % OOIP (Run TFF33). Following the waterflood with steam was no more effective, according to the mass balance results from Run TFF34. In Run TFF35, in an effort to better simulate the reservoir situation, steam was injected into the sandpack without any other heating. Injection was begun at the usual 40 g/hr, but heat losses at this flow rate reduced the steam to about 60 C hot water before it even reached the sand. Later in the flood, the injection rate was raised in steps to 500 g/hr, and the temperatures at injection and production ends were monitored. Even at this highest flow rate, the temperature at the injection end was never high enough to maintain a steam phase, and thus Run TFF35 was effectively a non-isothermal hot water flood.

Run TFF36 was another attempt to determine the recovery by hot gasflood under dry conditions, so that no steam distillation occurred. The differential pressure (dP) reservoirs were initially oil filled, and the connecting lines were plugged off to prevent flashing of any water. The recovery of 68 % is much lower than obtained by hot waterflood.

Consider now the recovery data based on measured production. Produced oil from the waterflood TFF33 is in close agreement with the mass balance value. A similar produced oil value was obtained from the waterflood in Run TFF34, which lends credibility to the waterflood values. Good agreement between produced oil and mass balance values was also achieved in Runs PP29 and TFF35; recoveries from these two steamfloods were also similar.

Impossibly high produced oil values were obtained from experiments in which the steamflood followed hot waterflood (PP32,TFF34), and from the run in which steam and gas were begun directly after heat-up (PP31). No consistent explanation has been found to account for the very high measured values of produced oil. As described in the Experimental section, in all of these runs the produced fluids were collected in small glass vials. The amount of oil in each vial was determined from mass measurements made before and after removal of the water. Over-estimation of oil could result from incomplete removal of the water, and since such errors would cumulate, the total value could be significantly too large. However, if this is the reason for the discrepancy, it is difficult to understand the inconsistency from one run to the next.

A closer look at the produced oil data in Table 12 indicates that the waterflood in PP32 was unusually efficient. Recovery from heat-up and waterflood alone is already greater than the total recovery based on mass balance. A similar discrepancy is noted in the results from TFF34.

5.4.2.6 Evidence of Steam Distillation

From the discussion above, it is clear that the recovery data in Table 12 offer no unambiguous conclusion about the significance of steam distillation as a recovery mechanism. Evidence that steam distillation was occurring in some of the runs was obtained, mostly by visual observation of the produced oil. Significantly less viscous oil was produced in the later stages of Runs PP31, PP32, TFF34 and TFF36. In Run PP32, a sufficient quantity of lighter oil was recovered to characterize it by simulated distillation. Figure 10 shows a comparison of the distillation behavior of the original Pike's Peak oil placed in the sandpack, oil produced in the later stages of the steamflood phase of the experiment, and residual oil extracted from the sand at the end of the run. The curves clearly confirm the separation of the original oil into a more volatile produced oil and a less volatile residual oil, as expected to result from steam distillation.

5.4.2.7 Comparisons with Earlier Work

A review of the literature on steam distillation and its effect on thermal recovery was given in Section 2.4 of this report. Although the waterflood recoveries found in our experiments are similar to those reported by Willman et.al. (2.6.4 [1]) for oil of similar viscosity, neither steamflood alone or steamflood after hot waterflood gave a consistently higher recovery as reported by Willman. However, most of our experiments were done at constant temperature, and thus the solvent extraction effect discussed by Willman et.al. could not occur. Also, since no steam condensation could occur in our experiments, the full effect of the adverse steam-oil mobility ratio would be seen. In experiments where steam is injected into a cold sandpack, the condensed water at the steam front acts as a mobility buffer between steam and oil, with probable good effects on displacement.

Based on the work of Wu and Elder (2.6.4 [3,4]), one would predict that steam distillation yields of Tangleflags and Pike's Peak oils would be in the range of 10 - 15 %. From the correlation of Duerksen and Hsueh (2.6.4 [5]), steam distillation yields as high as 25 % would be predicted. The difficulty with using these yield predictions is that the correlations they are based upon include no Canadian heavy oils. In addition, the actual contribution of steam distillation depends not only on the steam distillation yield, but also on the "efficiency factor ". The latter factor is difficult to assess even in a laboratory coreflood.

5.5 Conclusions

1. Displacement of Lloydminster oils from reservoir sandpacks by hot water at 200 C is highly efficient. Recoveries of 73 and 84 % OOIP were obtained with Pike's Peak and Tangleflags oils respectively.

2. Gasfloods and steamfloods without a condensing front apparently are less efficient than hot waterflood.

3. Evidence that steam distillation has a significant effect on oil produced by steamflood was obtained, but the recovery data are too inconsistent to quantify the contribution of steam distillation to total oil recovery.

4. Vapor pressures of Lloydminster heavy oils range from 200 to 400 kPa over the temperature range 150 to 300 C. Pike's Peak oil has a higher vapor pressure than Tangleflags oil. These values confirm that under conditions where a gas phase is present (e.g. steam zone), evaporation and steam distillation of the lighter components of these oils will occur.

5.6 Tables

1. PARTICLE SIZE DISTRIBUTION OF SAND SAMPLES
2. PROPERTIES OF OIL SAMPLES
3. COMPOSITION OF SYNTHETIC RESERVOIR BRINES
4. VAPOUR PRESSURE OF LLOYDMINSTER OILS
5. INITIAL SANDPACK CONDITIONS
6. OIL PRODUCTION FROM HOT WATERFLOOD, PP32
7. OIL PRODUCTION FROM HOT WATERFLOOD, TFF33
8. OIL PRODUCTION FROM HOT WATERFLOOD, TFF34
9. OIL PRODUCTION FROM HOT WATERFLOOD, PP29
10. OIL PRODUCTION FROM HOT WATERFLOOD, PP30
11. OIL PRODUCTION FROM HOT WATERFLOOD, PP31
12. TOTAL OIL PRODUCTION FROM FLOOD EXPERIMENTS

TABLE 1

PARTICLE SIZE DISTRIBUTION OF SAND SAMPLES[a]

Sieve Size		Pike's Peak		Tangleflags	
US mesh	mm	Mass Retained %	Cumulative Mass Retained, %	Mass Retained, %	Cumulative Mass Retained, %
35	0.500	0.6	0.6	2.9	2.9
60	0.250	36.2	36.8	2.7	5.6
80	0.177	52.8	89.6	12.6	18.2
120	0.125	5.3	94.8	36.6	54.7
170	0.0884	1.2	96.0	25.3	80.0
230	0.0625	0.1	96.1	10.9	90.9
325	0.0442	0.0	96.1	1.7	92.6
<325	<0.0442	3.9	100.0	7.4	100.0
Median Grain Size,mm		0.2298		0.1305	
Mean Grain Size, mm		0.2418		0.1230	

a) Fine fraction was partially removed by wet sieving, as described in the Experimental Section.

TABLE 2
PROPERTIES OF OIL SAMPLES

Oil Source	Viscosity, mPa @ 25°C 87-01-29	 87-03-05	 87-08-26	Density kg/m^3 @ 30C	Residual Water, %
Pike's Peak	10200	11400	11500	975.9	<0.5
Tangleflags	4640	--	5020	968.2	0.6

TABLE 3

COMPOSITION OF SYNTHETIC RESERVOIR BRINES[a]

	Pike's Peak	Tangleflags
NaCl	49.79	58.5
$CaCl_2$	8.324	5.55
$MgCl_2.H_2O$	6.71	3.91
KCl	1.12	0.67
Na_2SO_4	0.710	-
$NaHCO_3$	0.671	-

a) Values expressed in grams of the specified salt per liter of solution.

TABLE 4

VAPOUR PRESSURE OF LLOYDMINSTER OILS

		Temperature (°C)	Total Pressure (kPa abs)	Net Vapour Pressure[a] (kPa, abs)
Tangleflags				
	1 -1	154.6	278	
	2 -3	154.6	261	
	1 -7	154.6	327	
	1 -4	154.6	314	175
	2 -6	154.6	292	
	2 -1	154.6	246	
	1 -2	204.8	355	213
	2 -2	204.8	304	
	2 -5	246.6	398	
	1 -5	246.6	442	289
	2 -4	286.0	452	361
	1 -6	286.0	527	
Pike's Peak				
	1 -1	154.6	299	
	1 -4	154.6	330	
	3 -1	154.6	313	224
	3 -7	154.6	371	
	1 -2	204.8	377	290
	3 -2	204.8	398	

Table 4 cont.

		Temperature (°C)	Total Pressure (kPa abs)	Net Vapour Pressure[a] (kPa, abs)
	3 -6	204.8	442	290
	3 -5	246.6	506	419
	3 -3	246.6	477	
	3 -4	286.0	562	449
	3 -8	286.0	595	
Blank				
	3-1	154.6	115	
	3-7	154.6	107	
	3-2	204.8	118	
	3-6	204.8	123	
	3-5	246.6	133	
	3-3	246.6	130	
	3-4	246.6	142	
	3-8	286.0	122	

a) Difference between average total pressure and average blank value at each temperature.

TABLE 5

INITIAL SANDPACK CONDITIONS

Run #	Permeability to Brine (Da)	Pore Volume (cm^3)	Porosity (%)	Oil Injected (cm^3)	Brine Recovered (cm^3)	Saturation[b]	
						Oil	Water
PP24	23.4	103.7	38.0	101.8	102.0	89.1	10.7 (10.9)
PP28	10.3	95.7	35.1	95.9	94.2	93.1	8.7 (6.9)
PP29	17.6	101.0	37.0	100.5	90.0	92.1	18.3 (7.9)
PP30	14.8	99.5	36.5	101.8	92.0	94.6	15.3 (5.4)
PP31	11.2[a]	95.4	35.0	106.5	0	100	0
PP32	10.3	96.4	35.3	93.5	87.0	89.0	17.7 (11.0)
TFF33	1.5	108.9	39.9	109.5	95.0	93.5	19.8 (5.5)
TFF34	2.0	96.7	35.4	97.2	90.0	92.5	14.9 (7.5)
TFF35	2.2	103.2	37.8	100.4	92.0	91.9	16.2 (8.1)
TFF36	-	101.7	37.3	112.8	0	100	0

a) Permeability to oil
b) Oil and water saturations were determined from independent data. The oil saturation values are considered more reliable. Water saturations derived from oil saturations are given in brackets.

TABLE 6

OIL PRODUCTION FROM HOT WATERFLOOD PP32

Time (hrs)	Oil (g)	Net Cumulative Oil (g)
1.0	7.7	0.0
2.0	6.7	6.7
3.0	10.3	17.0
4.0	10.0	27.0
5.0	10.4	37.3
6.0	3.1	40.5
7.0	1.0	41.5
8.0	1.2	42.7
9.0	0.9	43.6
10.0	1.6	45.2
11.0	0.0	45.2
12.0	0.8	46.0
13.0	0.6	46.6
14.0	0.7	47.3
15.0	0.4	47.7
16.0	0.6	48.3
17.0	0.4	48.7
18.0	0.5	49.2
19.0	0.5	49.8
20.0	0.7	50.4
21.0	0.4	50.8
22.0	0.7	51.5
23.0	0.4	51.8
24.0	0.5	52.4
25.0	0.4	52.8
26.0	0.7	53.4
27.0	0.5	53.9
28.0	0.3	54.3
29.0	0.4	54.6
30.0	0.5	55.1
31.0	0.4	55.5
32.0	0.3	55.8
33.0	0.3	56.1
34.0	0.3	56.4
35.0	0.3	56.6
36.0	0.2	56.8
37.0	0.4	57.3
38.0	0.5	57.8
39.0	0.4	58.2
40.0	0.6	58.8
41.0	0.4	59.2
42.0	0.3	59.5
43.0	0.4	59.9
44.0	0.4	60.3
45.0	0.3	60.7
46.0	0.2	60.9

TABLE 7

OIL PRODUCTION FROM HOT WATERFLOOD TFF33

Time (hrs)	Oil (g)	Net Cumulative Oil (g)
1.0	9.6	1.9
2.0	6.6	8.5
3.0	10.0	18.6
4.0	10.2	28.8
5.0	8.9	37.7
6.0	8.1	45.8
7.0	2.6	48.3
8.0	1.6	50.0
9.0	1.4	51.4
10.0	1.1	52.4
11.0	1.2	53.7
12.0	1.2	54.9
13.0	1.0	55.8
14.0	0.8	56.6
15.0	0.8	57.4
16.0	0.6	58.0
17.0	0.7	58.7
18.0	0.6	59.2
19.0	0.6	59.9
20.0	0.5	60.4
21.0	0.6	60.9
22.0	0.5	61.4
23.0	0.6	62.0
24.0	0.5	62.5
25.0	0.5	63.0
26.0	0.5	63.5
27.0	0.4	63.9
28.0	0.4	64.4
29.0	0.5	64.8
30.0	0.5	65.3
31.0	0.5	65.8
32.0	0.4	66.2
33.0	0.4	66.6
34.0	0.5	67.1
35.0	0.4	67.6
36.0	0.4	68.0
37.0	0.5	68.5
38.0	0.3	68.8
39.0	0.9	69.7
40.0	0.6	70.3
41.0	0.6	70.9
42.0	0.4	71.2
43.0	0.4	71.6
44.0	0.5	72.1
45.0	0.4	72.5

TABLE 8

OIL PRODUCTION FROM WATERFLOOD TFF34

Time (hrs)	Oil (g)	Net Cumulative Oil (g)
1.0	8.7	1.0
2.0	6.7	7.7
3.0	10.1	17.8
4.0	10.1	27.8
5.0	10.2	38.0
6.0	7.2	45.2
7.0	2.3	47.5
8.0	0.3	47.9
9.0	0.3	48.1
10.0	0.4	48.5
11.0	0.5	49.0
12.0	0.8	49.8
13.0	0.4	50.2
14.0	0.5	50.7
15.0	0.8	51.5
16.0	0.5	52.0
17.0	0.4	52.4
18.0	0.5	53.0
19.0	0.4	53.4
20.0	0.7	54.1
21.0	0.9	55.0
22.0	0.4	55.3
23.0	0.7	56.1
24.0	0.9	56.9
25.0	0.8	57.7
26.0	0.5	58.2
27.0	0.3	58.5
28.0	0.5	59.0
29.0	0.6	59.5
30.0	0.3	59.9
31.0	0.3	60.2
32.0	0.3	60.4
33.0	0.4	60.9
34.0	0.7	61.5
35.0	0.3	61.8
36.0	0.0	61.8
37.0	0.5	62.3
38.0	0.4	62.7
39.0	0.4	63.1
40.0	0.4	63.5
41.0	0.5	64.0
42.0	0.5	64.5
43.0	0.4	65.0
44.0	0.4	65.3
45.0	0.3	65.6

TABLE 9

OIL PRODUCTION FROM RUN PP29

Time (hrs)	Oil (g)	Net Cumulative Oil (g)
1.0	3.5	46.6
2.0	2.7	49.2
3.0	1.9	51.1
4.0	1.6	52.7
5.0	0.4	53.1
6.0	-0.0	53.1
7.0	0.2	53.3
8.0	0.8	54.1
9.0	0.2	54.3
10.0	0.9	55.2
11.0	0.6	55.8
12.0	0.5	56.3
13.0	0.0	56.4
14.0	-0.1	56.3
15.0	0.3	56.6
16.0	0.1	56.7
17.0	-0.1	56.5
18.0	-0.1	56.5
19.0	0.0	56.5
20.0	0.0	56.5
21.0	0.0	56.5
22.0	-0.1	56.5
23.0	0.1	56.5
24.0	-0.2	56.3
25.0	-0.2	56.2
26.0	-0.2	55.9
27.0	-0.0	55.9
28.0	0.0	55.9
29.0	-0.2	55.7
30.0	0.0	55.8
31.0	0.3	56.1
32.0	-0.2	55.9
33.0	-0.2	55.7
34.0	0.1	55.8
35.0	-0.1	55.6
36.0	-0.0	55.6
37.0	-0.2	55.4
38.0	-0.3	55.1
39.0	-0.1	55.0
40.0	0.1	55.1
41.0	-0.1	55.0
42.0	-0.0	54.9
43.0	-0.0	54.9
44.0	-0.1	54.8
45.0	-0.1	54.8

Table 9 continued..

46.0	0.1	54.8
47.0	-0.1	54.8
48.0	-0.1	54.7
49.0	-0.2	54.4
50.0	0.4	54.9
51.0	-0.2	54.7
52.0	-0.2	54.5
53.0	-0.1	54.5
54.0	-0.1	54.4
55.0	0.1	54.5

TABLE 10

OIL PRODUCTION FROM STEAMFLOOD PP30

Time (hrs)	Oil (g)	Net Cumulative Oil (g)
0.6	1.3	-6.4
1.6	9.8	3.5
2.6	4.3	7.8
3.6	2.4	10.2
4.6	7.5	17.7
5.6	11.2	28.9
6.6	1.3	30.1
7.6	1.2	31.3
8.6	1.3	32.6
9.6	0.7	33.3
10.6	0.5	33.8
11.6	0.4	34.2
12.6	0.5	34.6
13.6	0.6	35.2
14.6	0.5	35.7
15.6	0.4	36.1
16.6	0.4	36.5
17.6	0.3	36.8
18.6	0.4	37.2
19.6	0.4	37.6
20.6	0.3	37.9
21.6	0.3	38.2
22.6	0.6	38.9
23.6	0.4	39.3
24.6	0.5	39.8
25.6	0.5	40.3
26.6	0.5	40.8
27.6	0.5	41.3
28.6	0.5	41.8
29.6	0.5	42.3
30.6	0.5	42.8
31.6	0.5	43.4
32.6	0.5	43.9
33.6	0.5	44.4
34.6	0.6	45.0
35.6	0.1	45.2
36.6	0.2	45.3
37.6	0.2	45.5
38.6	0.2	45.7
39.6	0.2	45.9
40.6	0.3	46.2
41.6	0.2	46.4

Table 10 continued..

42.6	0.2	46.6
43.6	0.2	46.8
44.6	0.2	46.9
45.6	0.2	47.1
46.6	0.1	47.2

TABLE 11

OIL PRODUCTION FROM GASFLOOD PP31

Time (hrs)	Oil (g)	Net Cumulative Oil (g)
1.0	-2.6	-1.5
2.0	16.3	14.8
3.0	12.9	27.7
4.0	21.7	49.4
5.0	7.8	57.1
6.0	3.1	60.3
7.0	0.9	61.2
8.0	0.8	62.0
9.0	1.0 (14.1)	63.0
10.0	1.6	64.7
11.0	2.0	66.7
12.0	1.4	68.1
13.0	1.0	69.2
14.0	0.8	70.0
15.0	0.6	70.6
16.0	0.5	71.1
17.0	0.5	71.6
18.0	0.7	72.3
19.0	0.4	72.7
20.0	0.3	73.0
21.0	0.3	73.3
22.0	0.3	73.5
23.0	0.2	73.8
24.0	0.2	74.0
25.0	0.2	74.2
26.0	0.2	74.4
27.0	0.2	74.6
28.0	0.2	74.8
29.0	0.2	75.0
30.0	0.1	75.1
31.0	0.2	75.3
32.0	0.1	75.4
33.0	0.1	75.5
34.0	0.1	75.6
35.0	0.1	75.7
36.0	0.1	75.8
37.0	0.1	75.9
38.0	0.1	76.0
39.0	0.1	76.1
40.0	0.1	76.2
41.0	0.1	76.3
42.0	0.1	76.4
43.0	0.1	76.5
44.0	0.1	76.5
45.0	0.1	76.6
46.0	0.1	76.7

Table 11 continued..

47.0	0.1	76.8
48.0	0.1	76.9
49.0	0.1	76.9
50.0	0.1	77.0
51.0	0.1	77.1
52.0	0.1	77.2
53.0	0.1	77.2
54.0	0.1	77.3
55.0	0.1	77.4
56.0	0.0	77.4
57.0	0.1	77.5
58.0	0.1	77.5
59.0	0.1	77.6
60.0	0.1	77.6
61.0	0.1	77.7
62.0	0.1	77.8
63.0	0.1	77.8
64.0	0.0	77.9
65.0	0.0	77.9
66.0	0.0	77.9
67.0	0.1	78.0
68.0	0.1	78.0
69.0	0.0	78.1
70.0	0.0	78.1
71.0	0.1	78.2
72.0	0.0	78.2

TABLE 12

SUMMARY OF PRODUCTION DATA[a]

	Oil Produced, g[b]			Residual	Recovery, % 00IP			TOTAL		
Run #	HU	WF	SF/GF	Oil, g	HU	WF	SF/GF	Produced	MB	DESCRIPTION
PP24	16	-	-	26.9	16	-	-	-	74	Waterflood
PP28	14	58	-	26.1	14	58	-	72	73	Waterflood
PP29	14	-	62	37.6	14	-	59	73	63	Steamflood
PP30	14	-	54	25.4	14	-	50	64	74	Steamflood
PP31	13	-	80	36.3	12	-	82	94	62	Gasflood
PP32	13	69	13	18.3	14	71	15	100	81	Waterflood/Steamflood
TFF33	15	80	-	17.8	14	71	-	85	84	Waterflood
TFF34	14	73	18	16.5	15	73	21	109	83	Waterflood/Steamflood
TFF35	-	38	23	39.4	-	34	25	59	62	Steamflood (Cold)
TFF36	26	-	50	32.5	23	-	33	56	68	Gasflood

a) HU = Heat-up to 200C; WF = Waterflood at 200C; SF/GF = Steamflood and/or Gasflood; MB = calculated from mass balance.

b) Includes flowing dead volume

5.7 Figures

1. CORE FLOODING APPARATUS
2. CORE HOLDER
3. VAPOR PRESSURE OF LLOYDMINSTER OILS
4. OIL PRODUCTION FROM RUN PP32
5. OIL PRODUCTION FROM RUN TFF33
6. OIL PRODUCTION FROM RUN TFF34
7. OIL PRODUCTION FROM RUN PP29
8. OIL PRODUCTION FROM RUN PP30
9. OIL PRODUCTION FROM RUN TFF31
10. OIL PRODUCTION FROM RUN TFF34
11. COMPARISON OF STEAMFLOOD PRODUCED OIL WITH ORIGINAL AND RESIDUAL OILS

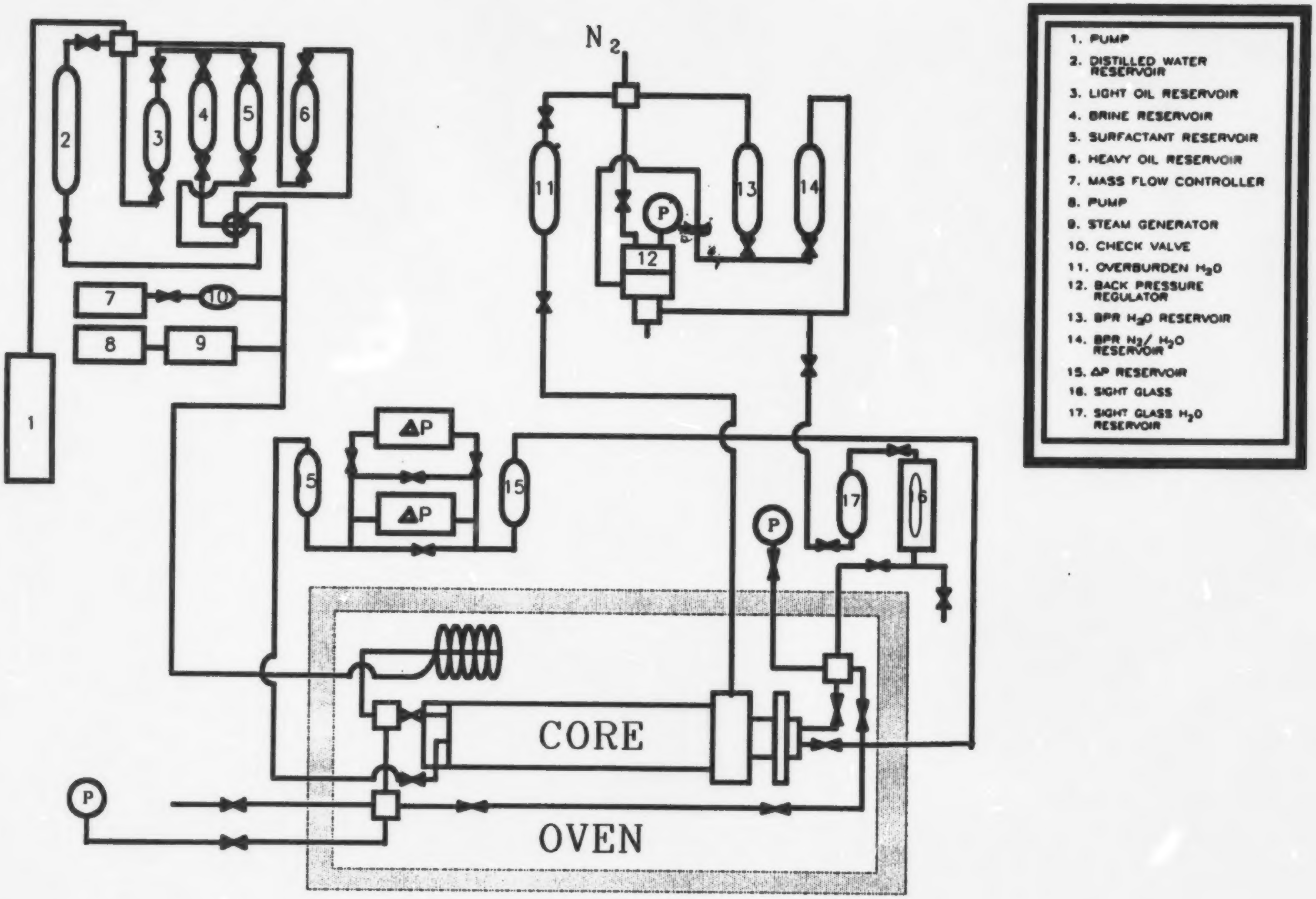
N2
1
2
3
4
5
6
7
8
9
10
11
12
13
14
15
15
16
17
P
P
P
ΔP
ΔP
CORE
OVEN
1. PUMP
2. DISTILLED WATER RESERVOIR
3. LIGHT OIL RESERVOIR
4. BRINE RESERVOIR
5. SURFACTANT RESERVOIR
6. HEAVY OIL RESERVOIR
7. MASS FLOW CONTROLLER
8. PUMP
9. STEAM GENERATOR
10. CHECK VALVE
11. OVERBURDEN H2O
12. BACK PRESSURE REGULATOR
13. BPR H2O RESERVOIR
14. BPR N2/H2O RESERVOIR
15. ΔP RESERVOIR
16. SIGHT GLASS
17. SIGHT GLASS H2O RESERVOIR

Figure 1: COREFLOODING APPARATUS

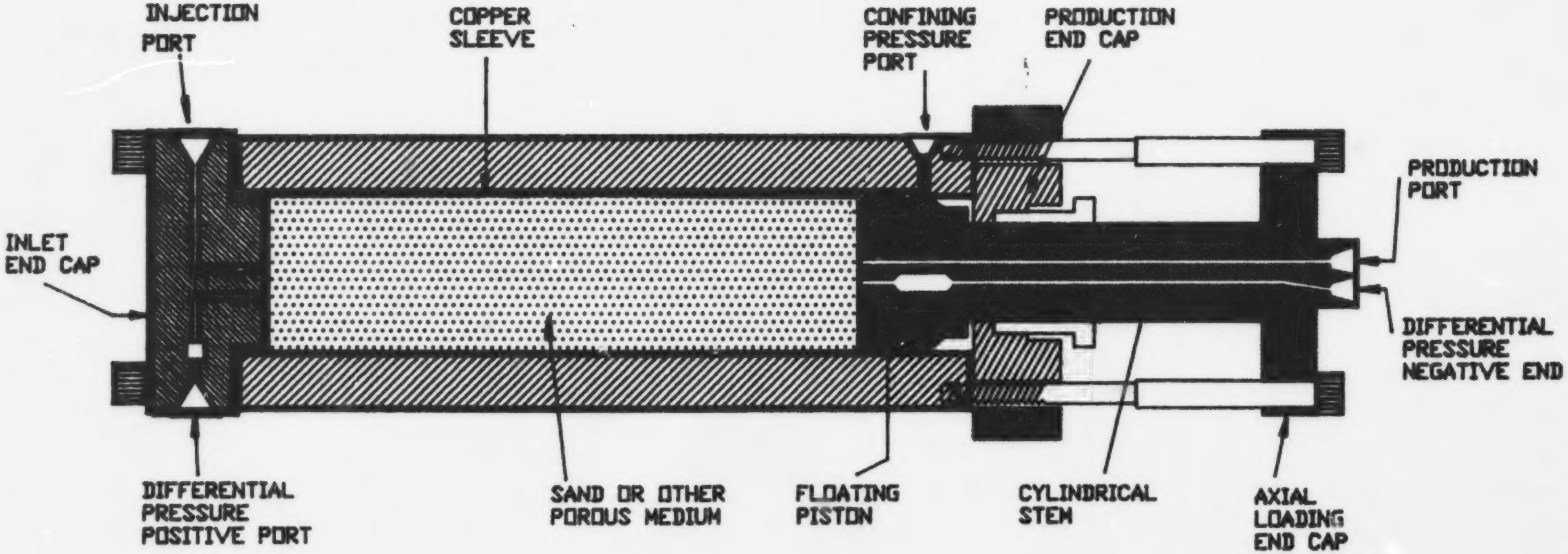
INJECTION PORT
COPPER SLEEVE
CONFINING PRESSURE PORT
PRODUCTION END CAP
PRODUCTION PORT
INLET END CAP
DIFFERENTIAL PRESSURE NEGATIVE END
DIFFERENTIAL PRESSURE POSITIVE PORT
SAND OR OTHER POROUS MEDIUM
FLOATING PISTON
CYLINDRICAL STEM
AXIAL LOADING END CAP

Figure 2: CORE HOLDER

Figure 3: Vapor Pressure of Lloydminster Oils

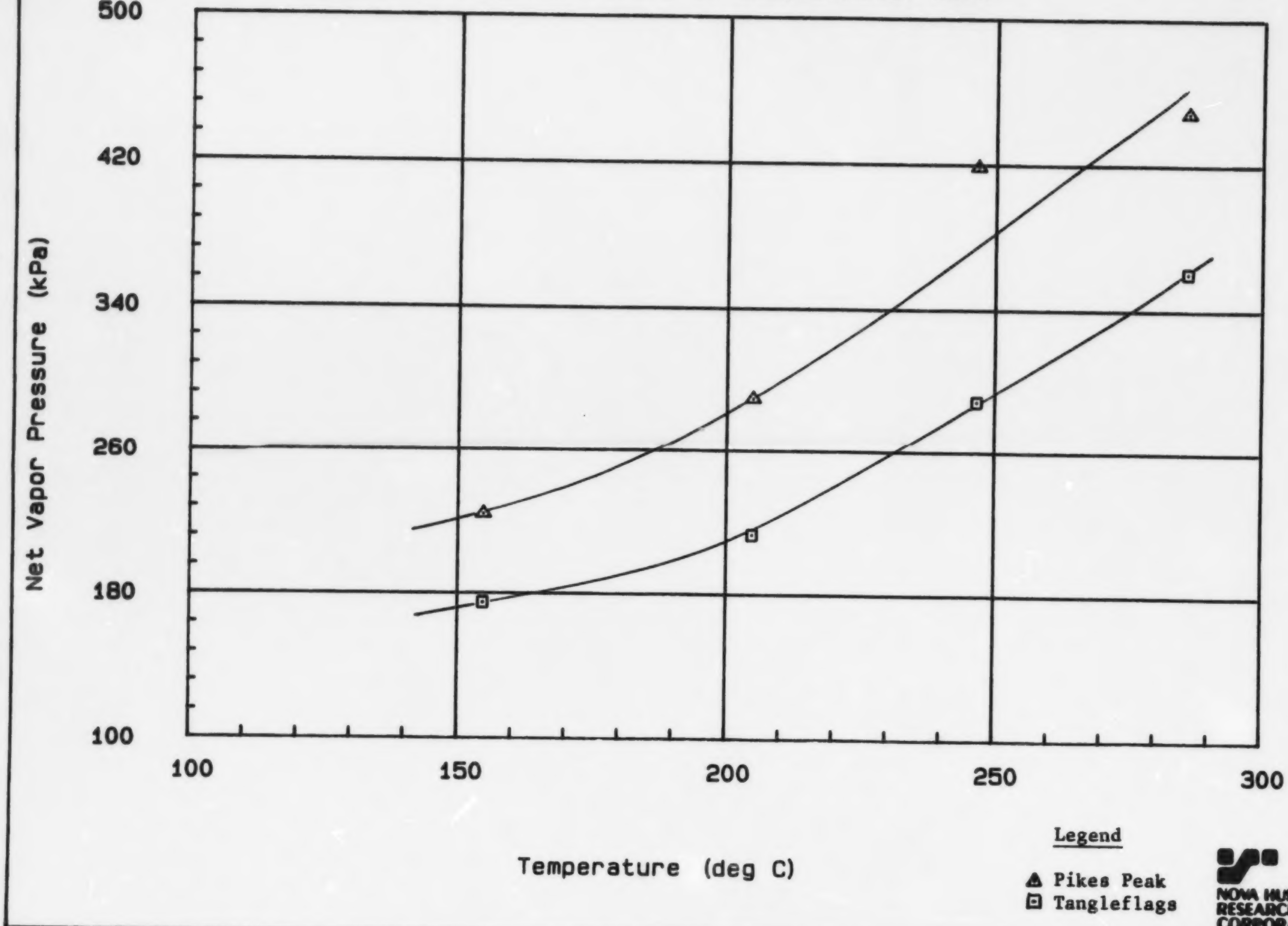

NOVA HUSKY RESEARCH CORPORATION

Figure 4: Oil Production from Run PP32

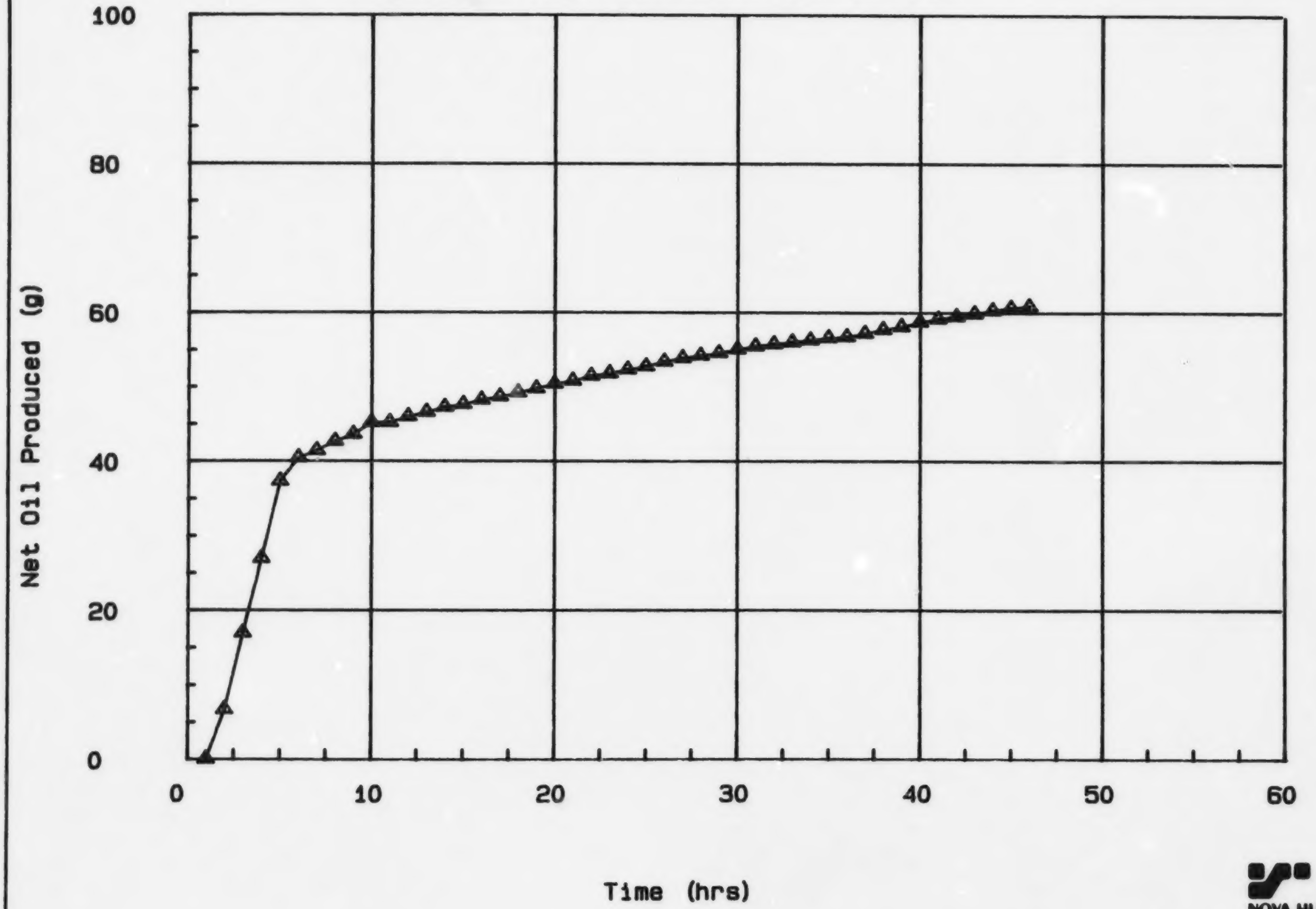

NOVA HUSKY
RESEARCH
CORPORATION

Figure 5: Oil Production from Run TFF33

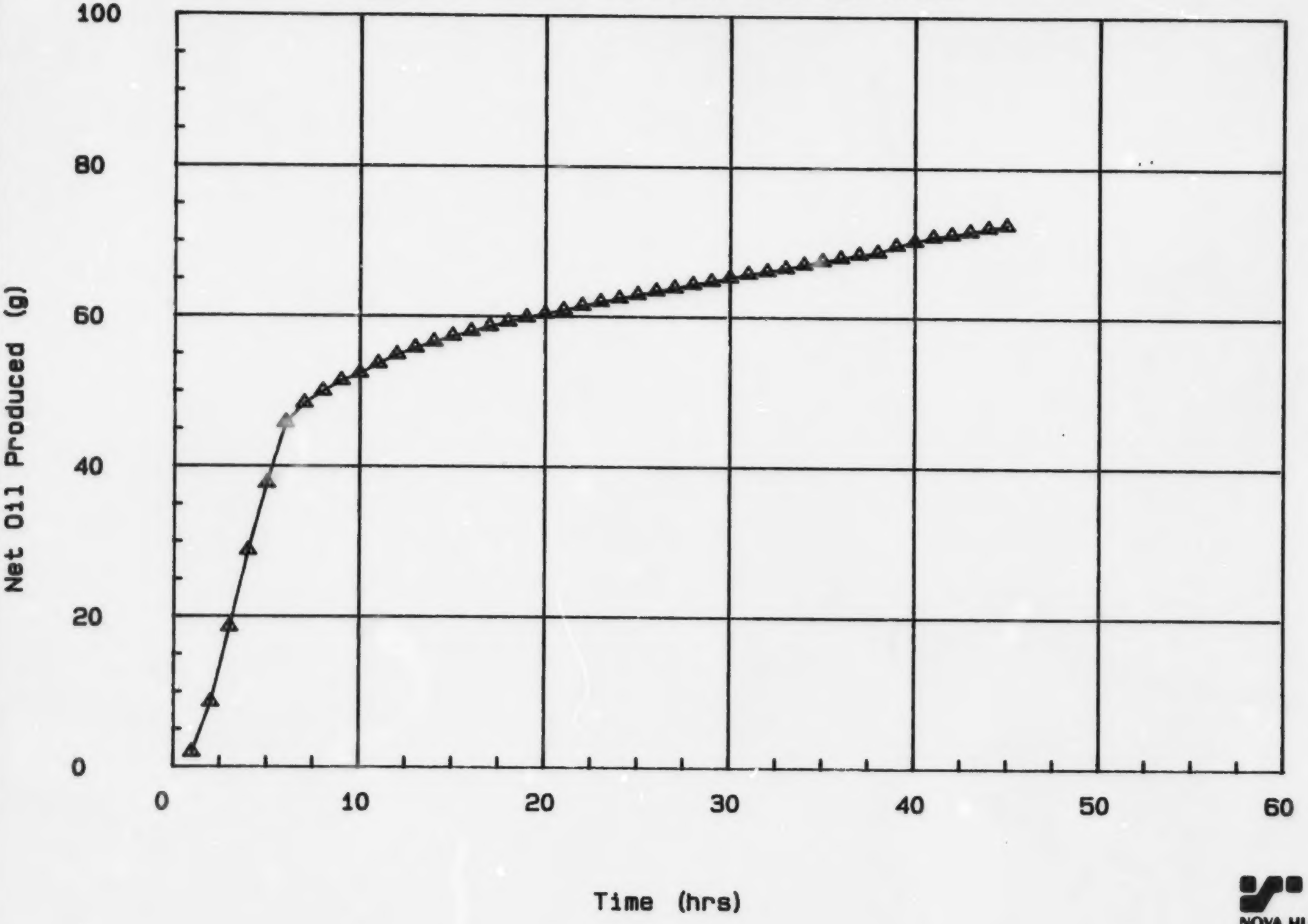

NOVA HUSKY
RESEARCH
CORPORATION

Figure 6: Oil Production from Run TFF34

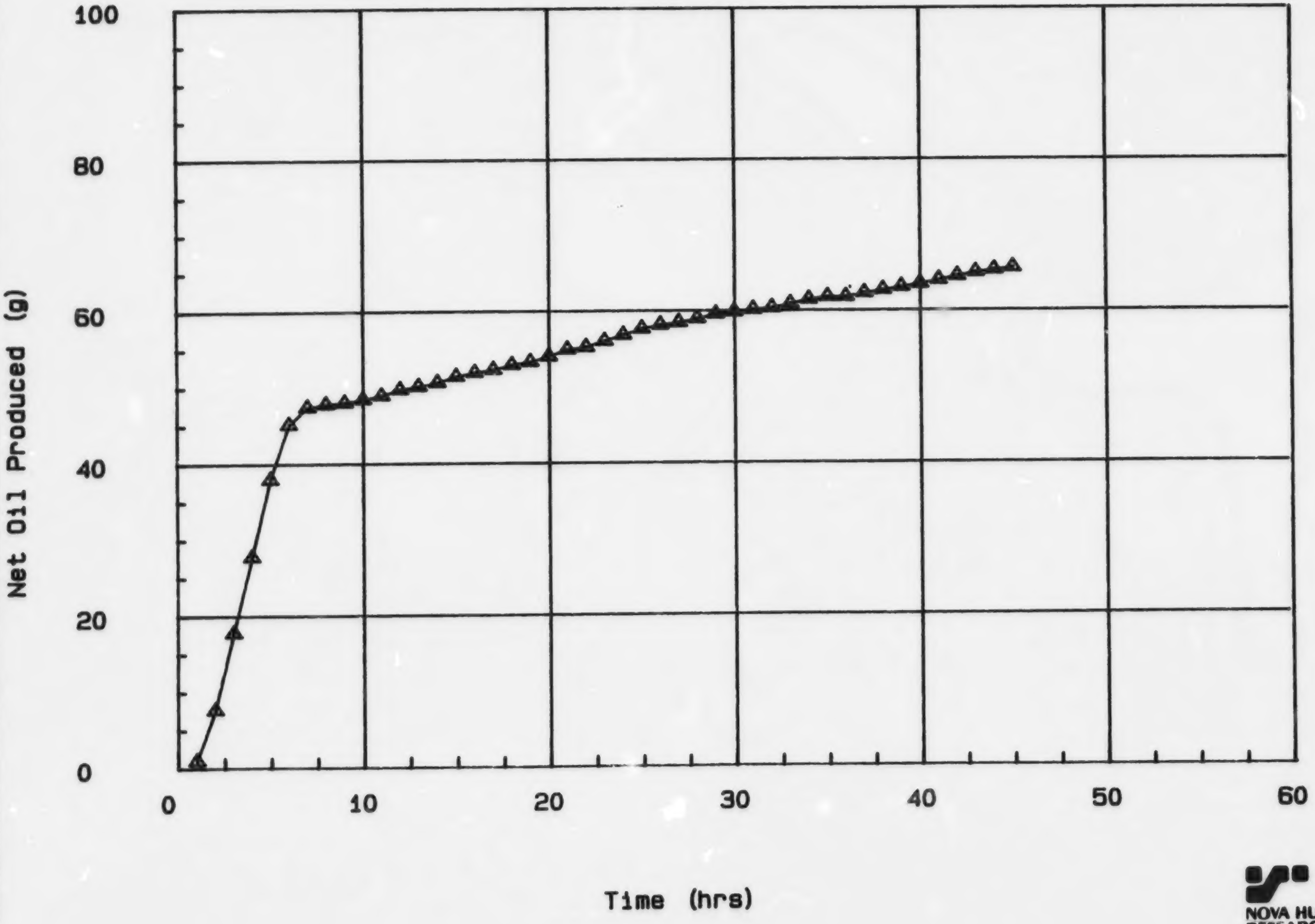

NOVA HUSKY
RESEARCH
CORPORATION

Figure 7: Oil Production from Run PP29

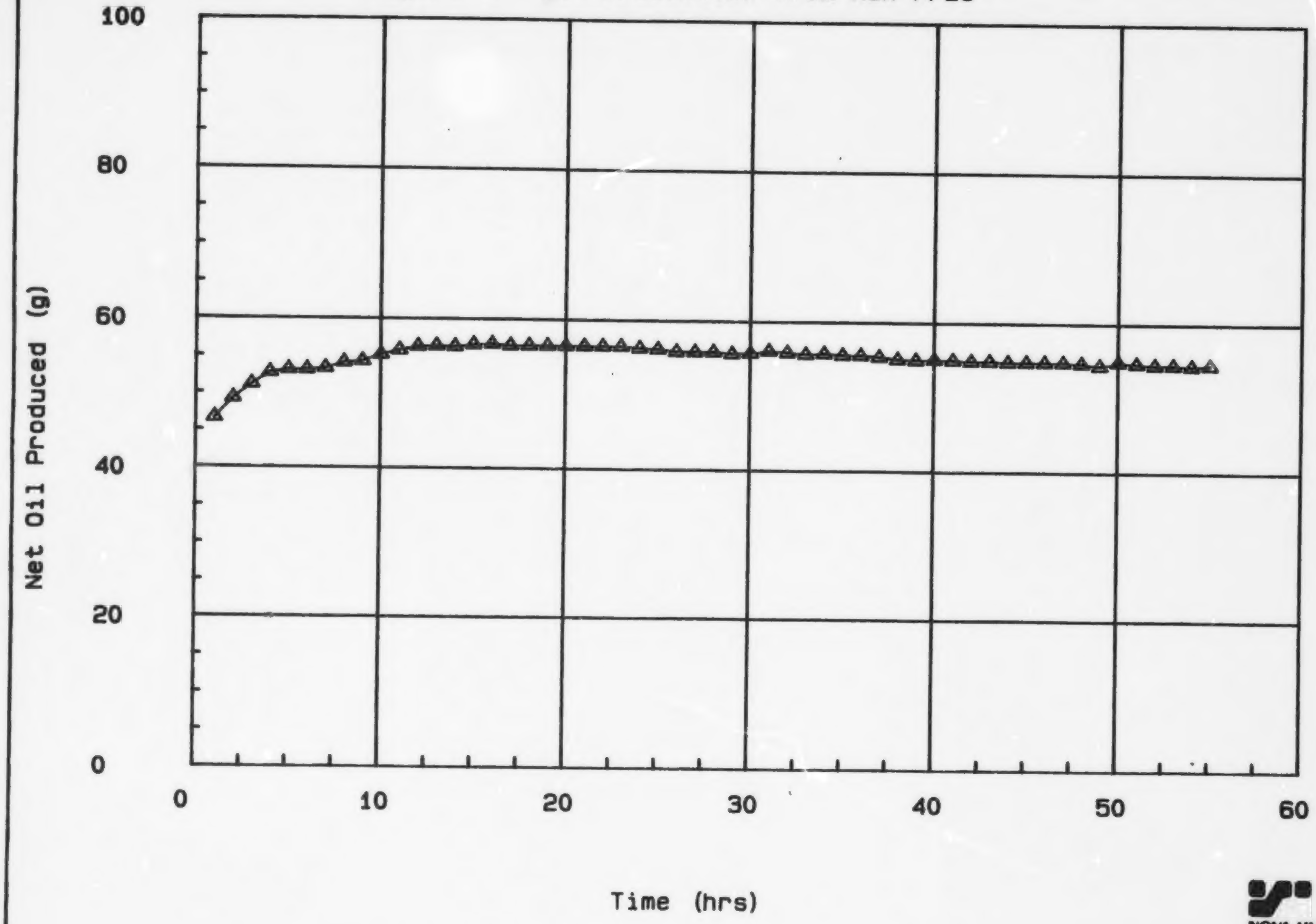

NOVA HUSKY
RESEARCH
CORPORATION

Figure 8: Oil Production from Run PP30

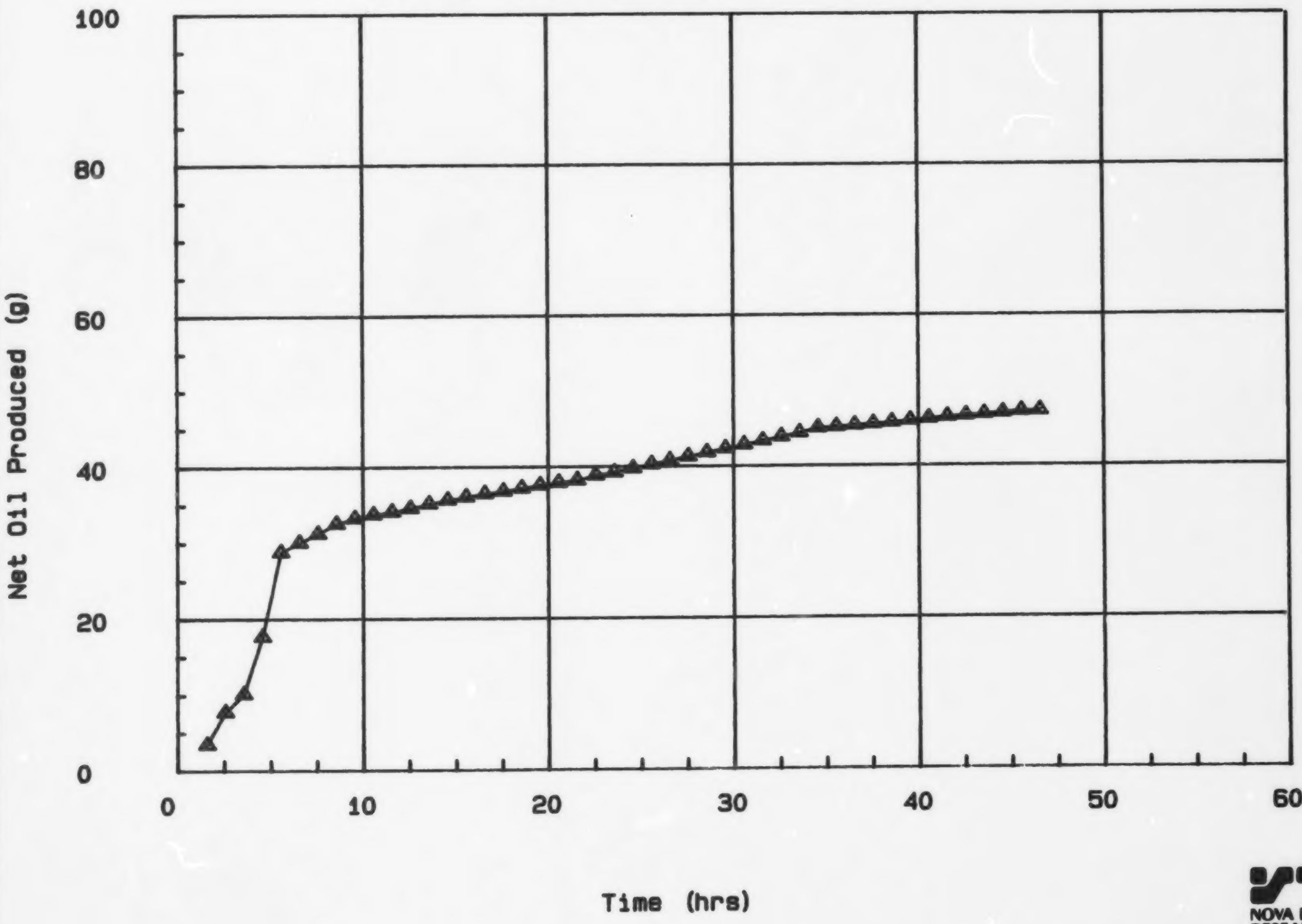

NOVA HUSKY
RESEARCH
CORPORATION

Figure 9: Oil Production from Run PP31

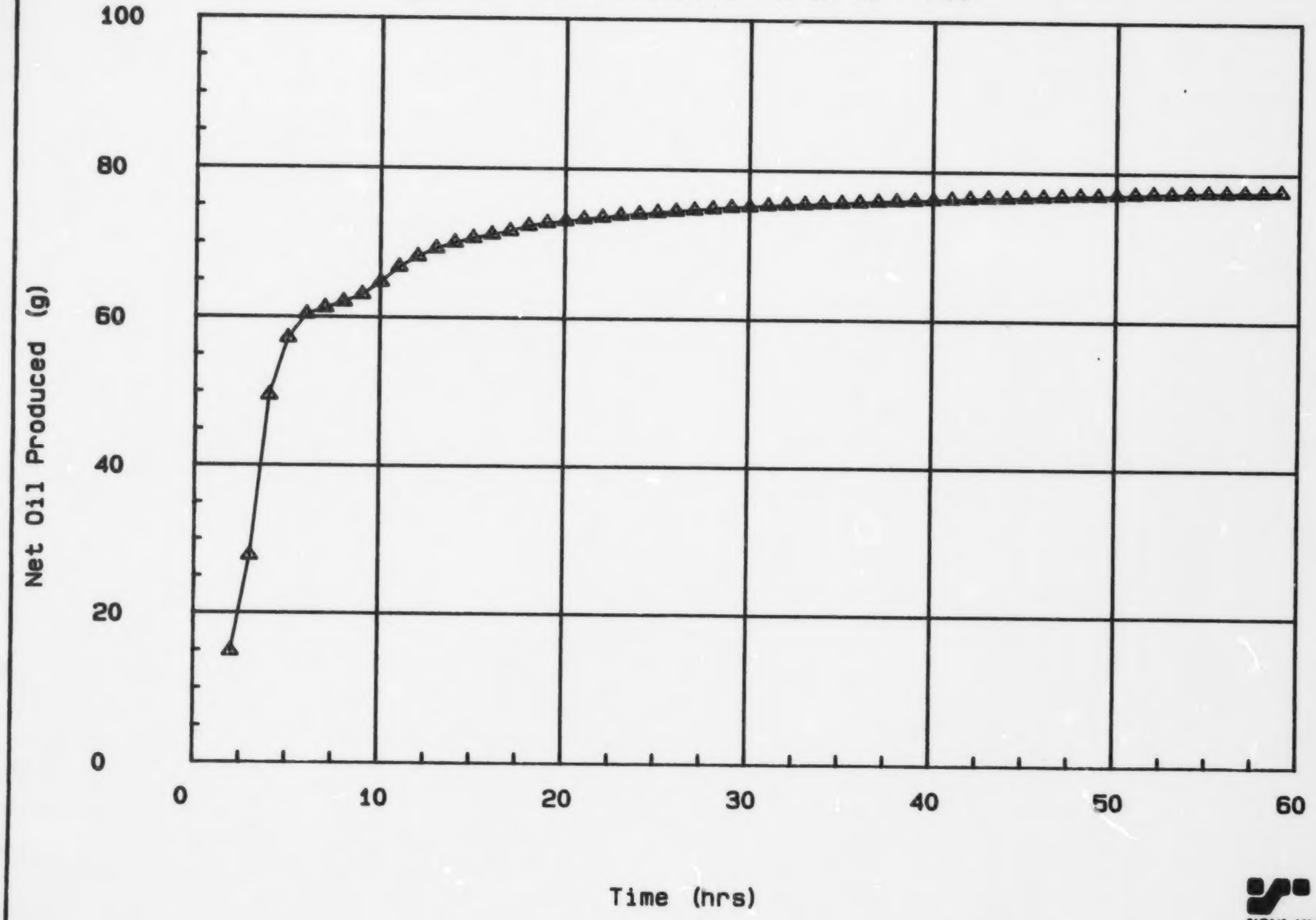

NOVA HUSKY
RESEARCH
CORPORATION

Fig 10: Comparison of steamflood produced oil with original and residual oils

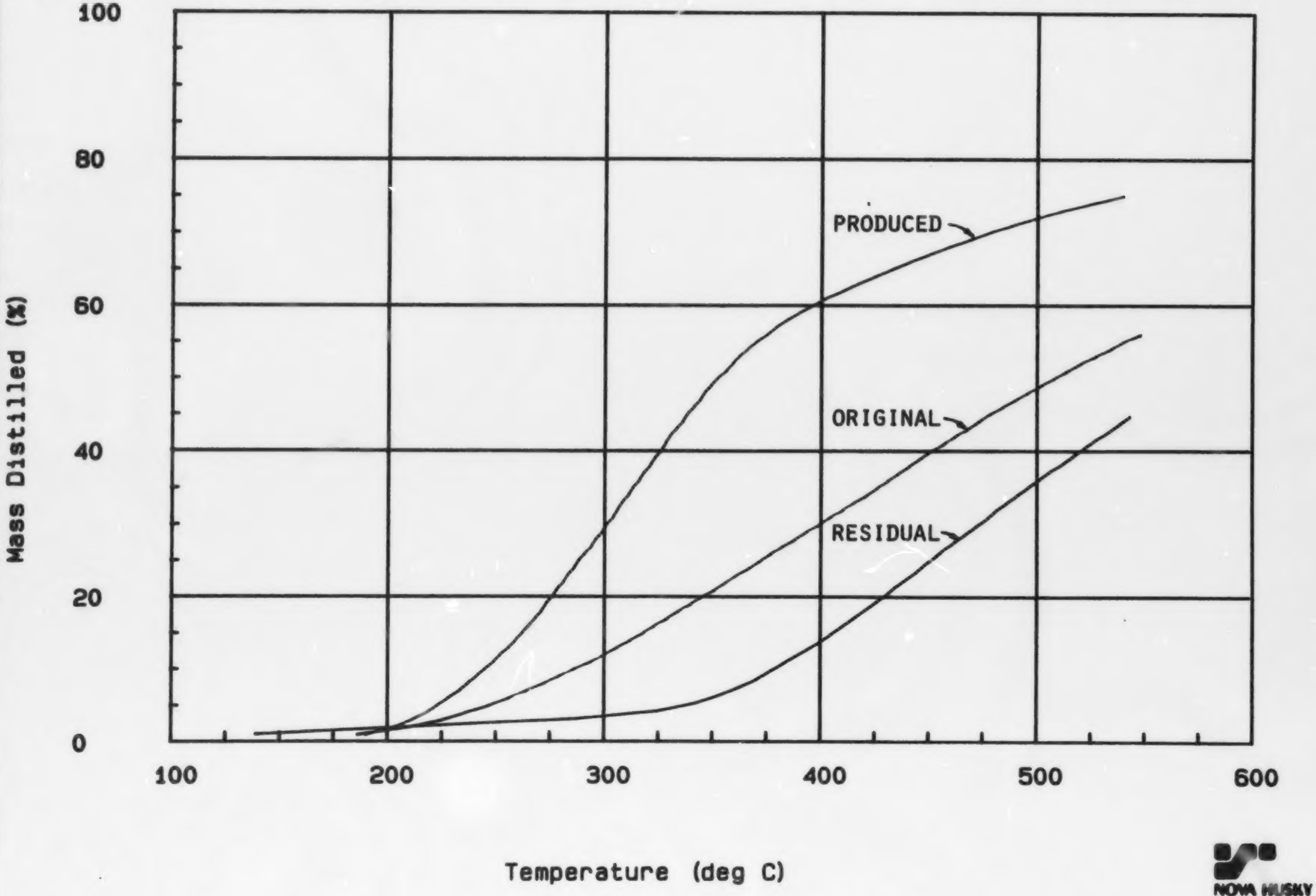

NOVA HUSKY
RESEARCH
CORPORATION

CLASSIFICATION: NHRC, NOVA, HUSKY
and Subsidiaries
REPORT NUMBER: 00423

THERMAL RECOVERY MECHANISMS

TASKS 3 & 4 -
THERMAL ALTERATION OF HEAVY OIL

February 1989

Authors

Patricio Herrera
Charles Tsang

DEPARTMENT:	Chemical Sciences
PROJECT NO:	688-048
PREPARED FOR:	Albert George - Energy, Mines & Resources
KEYWORDS:	experiment, thermal, viscosity, distillation, oxidized, cracking

This report contains the valuable proprietary and confidential information of the NOVA HUSKY RESEARCH CORPORATION LTD., and may not be used, disclosed or reproduced without permission in writing from NOVA HUSKY RESEARCH CORPORATION LTD.

(C) 1989 NOVA HUSKY RESEARCH CORPORATION LTD.

38 pp

MICROMEDIA

DISTRIBUTION LIST

	Copies
ENERGY, MINES & RESOURCES, Ottawa	
A. George	10
NOVA HUSKY RESEARCH CORPORATION:	
C. Tsang	1
P. Herrera	1
T. Jack	1
B. Erno	1
HUSKY OIL OPERATIONS LTD.:	
J. Peggs	1
P. Tsang	1
NHRC Library	2
Husky Library	1
Files	2
	--
TOTAL NUMBER OF COPIES	**21**

TABLE OF CONTENTS

Page

1.0 SUMMARY....1

2.0 OBJECTIVES....2

3.0 INTRODUCTION....2

4.0 EQUIPMENT DESIGN....4

4.1 Experimental Set Up....4
4.2 Reactor Design and Accessories Description....4

4.2.1 Reactor and Feed System....4
4.2.2 Accessories....5
4.2.3 Gas Supply System....5
4.2.4 Product Oil Collection System....5
4.2.5 Gas Products Collection System....6

4.3 Process Conditions....6
4.4 Operation Procedure....6

5.0 RESULTS....9

5.1 Summary of Results....9
5.2 Detailed Results....10

5.2.1 Effects of Cracking Temperatures and Residence Time....10
5.2.2 Effects of Cracking Oxidized Oil....14
5.2.3 Effects of Water....15
5.2.4 Effects of Sand....16

6.0 REFERENCES....17

7.0 TABLES....19

8.0 FIGURES....29

1.0 SUMMARY

The experimental results on thermal alteration of Tangleflags and Pikes Peak oils are presented in this report. Temperatures ranging from 270° C to 500° C were studied. Heat treatment periods ranged from 8 minutes at 500° C to 21 days at 270° C. The effects of other variables, including pre-oxidized oil, presence of steam and sand, were also studied.

An apparatus consisting of three reactors operated in parallel was constructed. Batches of oil samples were heat treated in closed reactors for different lengths of time. The products (oil, gas and coke) were quantified. The viscosity and distillation behavior of the liquid product were measured.

This study has provided a preliminary database for the two Lloydminster heavy oils under various thermal conditions. The study found that thermal cracking reactions became dominant between 300 and 330° C for both oils. At temperatures below 300° C, the viscosity of Tangleflags oil (all viscosities were measured at 25° C) increased with heating time. However, at 330° C and above, the viscosity dropped with increasing heating time. For the Pikes Peak oil at 300° and 270° C, the oil viscosity dropped in the first 2 hours of heating, then increased steadily steadily with increasing heating time. At temperatures above 300° C, the viscosity dropped with time.

The coke and gas yields were very small in experiments operated below 350° C; typically less than 2% of the total product, even for extended runs up to 21 days. However, the yields for these products increased rapidly with increasing temperature.

The coke yields of Tangleflags oil at temperatures between 400° C and 500° C were only about one half of those observed in Athabasca bitumen under similar conditions. Since only low temperature (below 350° C) experiments were done on Pikes Peak oil, no direct comparison could be made.

Tangleflags oil which has previously been oxidized generated significantly more coke than the same oil which has not been oxidized.

The presence of steam during thermal cracking appeared to slow down the conversion of oil to lighter fractions. In comparing with oil products from experiments conducted in the absence of steam, the steam experiments gave slightly heavier oil products in terms of viscosity and distillation behavior.

The experiments with sand presented some major difficulties in getting reasonable hydrocarbon balance. The difficulties were related to measuring the amount of product oil that wetted the surface of the sand, and the amount of coke deposited on the sand. The distillation behavior of the product oil appeared to be similar to the experiments with oil alone.

2.0 OBJECTIVES

To study the reactivity of Tangleflags and Pikes Peak heavy oil to thermal alteration under various conditions. The variables include: temperature, heating time, pre-oxidized oil, the presence of steam and indigenous minerals.

3.0 INTRODUCTION

There are about twenty published reports (see the report on literature review) on thermal cracking experiments designed to provide data on the behavior of oil during thermal recovery. It is well established that oils from different origins behave differently when heated. The trends are similar, but the magnitude of the changes in oil properties are different. There is a relatively large amount of information on the reactivity of Athabasca bitumen and Cold Lake heavy oil, but little was known about oil from the Lloydminster region. Since the Lloydminster area has a large reserve of heavy oil, there is a definite need to fill this information gap.

In the laboratory, there are two main approaches to study thermal cracking under controlled conditions: closed versus open reactor design. Both methods are often used by researchers in this field. The closed reactor method involves placing a known amount of oil in the reactor, followed by blanketing the oil with an inert gas at a selected pressure. The reactor is subsequently closed. As thermal reactions proceed and light components are evolved, the pressure of the reactor would increase with time. At the end of the reaction period, the system is cooled to room temperature. The chief advantage of the method is all the hydrocarbon components are heated at the same temperature for the defined reaction period. The disadvantage is the uncontrolled pressure change as the run proceeds.

In the open reactor design, the procedures are similar to those mentioned above except the pressure of the reactor is controlled at a fixed level. This is most commonly done by installing a pressure regulator which allows a controlled release of vapor components to a receiver. To avoid condensation due to pressure drop in the regulator, and thus malfunctioning of the latter, a condenser is installed between the reactor and the regulator. A variation of the open reactor design involves purging the reactor continuously during an experiment with an inert gas and sweep the vapor product from the reaction zone.

The obvious advantage of the open reactor scheme is the possibility to control pressure. The main disadvantage is the migration of lighter products during the experiment to a cool zone where thermal reactions are arrested. The amount of light products carry-over varies depending on many factors such as the temperature of the condenser, pressure setting of the reactor, flow rate of the purge gas, temperature of the transfer tubing between the reactor and condenser, and geometry of the reaction system.

The results of open experiments are far less reproducible among different research groups. Also, the results are very difficult to analyse because the product has been subjected to a complex thermal history with different components experiencing different time-temperature profiles.

Another important issue in conducting these experiments is the definition of reaction residence time, particularly when high temperature experiments exceeding 400° C are performed. All the previous work that we have reviewed involved placing oil sample into the reactor at room temperature. The reactor was then heated to the target temperature, followed by soaking at a constant temperature. At the end of the reaction period, the reactor was cooled by a variety of methods such as forced convection , immersing reactor into a cold bath etc.

The choice of time zero was arbitrary. It could be the time at which the target temperature was reached. It could also be a certain time or temperature interval before the target temperature was reached. The end-of-run time was usually defined as the time when the heaters were turned off or when the reactor was immersed into a cold bath. Depending on how these de-limiters are chosen, as well as the rates of initial heating and final cooling, the thermal history of the oil may vary significantly.

The original design of our apparatus was one with pressure control. We later found that there were substantial amounts of products collected in the condenser (in the range of 20 to 30 %) during the runs at 400° C. This was unacceptable because kinetic analysis cannot be done on this data. We subsequently made many attempts to modify the system to reduce hold-up of condensate and yet be able to control pressure; but none of those attempts was successful.

We finally changed the system to a closed-reactor design in order to obtain useful results. To improve upon the techniques used by others, we inject the oil sample into a pre-heated reactor. By doing this, it only took 2 to 3 minutes for the oil to arrive at target reaction temperature. Time zero was considered as the moment at which injection of oil was complete. At the end of a run, the contents of the reactor (liquid and vapor phases) were withdrawn by a dip-tube and sent to a cold receiver to stop any further thermal reaction. The receiver was immersed in a bath of dry ice and isopropanol.

The following sections describe the design of the apparatus and the experimental results.

4.0 EQUIPMENT DESIGN

4.1 Experimental Set Up

A schematic diagram of the experimental setup used in this research is shown in Figure 1. The bench-scale unit was made up of three reactor lines operated in parallel. This arrangement allowed us to run a maximum of three separate experiments simultaneously. The major component of each reactor line was the stainless steel reactor, designed in-house to withstand a maximum pressure of 2000 psi at 560° C. The top part of the reactor had connections for the heavy oil feed line, vent line, thermocouple and a dip-tube . The hot product oil was transferred for product removal using differential pressure from the reactor to the liquid product receiver, which was immersed in a dry ice bath. The non-condensable gases produced during the reaction period were withdrawn from the liquid product receiver and sent to a previously evacuated plastic bag where they were held temporarily before being directed to an evacuated tank of known volume.

Each reactor line was equipped with the following supporting instruments: pressure and vacuum measuring devices (gauges and transmitters); thermocouples; safety head assemblies with a rupture disc; heating units connected to temperature controllers; on-line filters and check valves and connections for sampling liquid and gas products. The reaction conditions were continuously monitored and recorded using a multipoint recorder and several temperature and pressure read outs.

4.2 Reactor Design and Accessories Description

4.2.1 Reactor and Feed System

All three reactors are identical in design: they all have bolted-closures type of reactor heads. The internal capacity was 390 cm^3 and each reactor was rated (maximum allowable working pressure) to 5250 psi at 370° C. All the connections to the vessel were located at the top cover and comprised one

1/4" feed charging port, a 1/4" product transfer and sample tube connection, a 1/8" thermocouple connection and a 1/8" port to connect the vent tube and safety head assembly.

A flexible cable heater (220V, 1500W) was placed on the outside wall of the reactor and it was controlled by a Barber Coleman temperature controller. A type K thermo-couple which monitored the outside skin temperature of the reactor was also connected to the same temperature controller. The reactor and heater were thermally insulated using 2 inch thick Fiberbrax Durablanket 2500. In order to facilitate the handling of materials and cleaning of the reactor, a SS316 thin-walled liner was placed inside the reactor. The feed system, for all the experiments carried out above 350° C, had a heated feed vessel (capacity = $300 cm^3$) and an arrangement of valves to purge through the vessel itself and connecting lines. The feed was charged into the reactor after the reactor was heated to a target temperature which was slightly above the reaction temperature. For lower temperature experiments, the heavy oil feed was placed inside the reactor before the reactor was heated.

4.2.2 Accessories

External accessories to the reactor

The reactor pressure was monitored and recorded using a 2.50" diameter stainless steel pressure gauge, 0-3,000 psi, a Rosemount gauge pressure transmitter provided with an on line indicator and a Molytek model 2701 multipoint recorder. A safety head assembly with rupture disc complemented the pressure measuring and controlling system. The temperature inside the reactor was measured using a 1/8" thermocouple, type K, Inconel shield, also connected to the Molytek recorder.

4.2.3 Gas Supply System

Helium was used to purge the reactor and connecting lines. The gas, of pre-purified quality, was injected to the unit through a system of tubes, valves and fittings heated by wrapping heating tape around it.

4.2.4 Product Oil Collection System

At the end of the reaction period, the hot liquid product was transferred from the reactor to the liquid product receiver using a 1/4" tube. A high temperature, high pressure 1/4" valve located close to the reactor separated the reactor from the product receiver. The capacity of the product receiver was 500

cm^3 and it was immersed in a dry ice bath which provided the low temperature required to stop the thermal reactions.

4.2.5 Gas Products Collection System

The non-condensable gas stream was transferred from the liquid product vessel to a TEDLAR (Du Pont proprietary plastic) gas sampling bag of 125 litre capacity. Initially, the bag was evacuated and as soon as it was filled with gaseous products, its content was sent to a gas tank that had also been evacuated. Gas samples were taken from this tank for GC analysis. The pressure of this section was measured using a Rosemount Absolute Pressure transmitter provided with an on-line indicator.

4.3 Process Conditions

A wide range of conditions were studied and heavy oil from two fields in Saskatchewan were used: Tangleflags and Pikes Peak. The properties of these two oils are given in Table 1.

The Tangleflags heavy oil was processed in the range of temperature between 270 and 500° C. The initial pressure for all these experiments was kept in at about 200 psig, which is typical of a Tangleflags area.

The Pikes Peak heavy oil was processed at a temperature range of 270 - 300° C. The starting pressure for this set of experiments was around 500 psi.

The detailed experimental program carried out with these two heavy oils is shown in Table 2.

4.4 Operation Procedure

The following procedure was followed before running an experiment.

- The weights of the following components of the system were recorded before their installation: liner, feed tank, heavy oil injection line, oil transfer line, liquid product vessel.
- The liner was installed into the reactor and the reactor was bolted up and connected to the setup.
- The entire reaction system was then pressure tested and purged with Helium several times.

- A slight positive pressure of Helium was left in the reaction system. The reactor heater and line heaters were then turned on.

- The multipoint recorder was activated and speeded up to monitor the reactor temperature during the heating up period.

- The liquid product vessel, TEDLAR gas bag, gas tank and connecting lines were fully evacuated and isolated from the reactor system. The liquid product vessel was immersed in a cooling bath made from a mixture of isopropanol and dry ice.

- For those experiments using a direct heavy oil injection to the reactor (reaction temperature above 350° C,) a charge of approximately 100 g of oil was put into the feed tank. Its weight was recorded and then the tank was installed above the reaction unit.

- The feed tank was then purged with Helium and heated up to 90° C. At that temperature its head pressure was adjusted with Helium to 100 psi.

- For the experiments having a reaction temperature below 350° C, the heavy oil was put in the liner before it was put into the reactor. The weights of the clean liner and the liner plus oil were recorded.

- The reactor temperature, when using direct heavy oil injection, was set 30° C above target reaction temperature and was left at that level for several minutes in order to stabilize it.

The following sequential procedure was taken when making a run:

- The temperature of the controller was set back by 30° C.

- The reactor pressure was adjusted with Helium to 50 psi.

- The heavy oil was then charged to reactor by controlling valve located at the bottom part of feed tank. The time required to complete feeding was recorded.

- After pressure in feed tank and reactor were equalized, the feed tank was thoroughly purged with Helium.

- The reactor was then isolated from the system, its pressure adjusted to 10 psi below target and its temperature fine tuned after stabilization. Depending on the amount of oil injected and the target temperature, it took 10 to 15 minutes to reach the reaction temperature level.

- The weight of the empty feed tank was then recorded.

- For those experiments having a reaction temperature below 350° C, the heating up of the reactor and the oil charged into it took place within approximately 40 minutes since the heater was turned on.

At the end of the reaction period, the following procedure took place:

- Heaters were turned off (including heat trace).

- Hot oil was transferred from reactor to liquid product tank by opening of valves located at the top of reactor and at the inlet of tank. The differential pressure existing between these two sections of the system was enough to transfer more than 80% of the material charged into the reactor in less than one minute.

- The oil was left cooling down for a few minutes in the liquid product tank, and meanwhile, the reactor was taken from the system and it was put inside a cooling pot.

- The time required to cool down the reactor to 300° C and 270° C was recorded.

- The non-condensable gas remaining in the oil product vessel was transferred then to the TEDLAR gas bag and from there to the gas tank. The vacuum reading of the gas tank was recorded.

- The liquid product vessel was left stabilizing at room temperature and any extra gas released was transferred to the gas bag and gas tank.

- After the reactor was cooled down, it was opened and the liner taken out and weighed.

- The liquid product vessel was then removed from the set up and its weight recorded.

- To complete the mass balance, all the weights for the transferring lines were also registered.

- A gas sample was taken from the gas tank for GC analysis.
- The contents of the liner and liquid product vessel were then analyzed and characterized.

5.0 RESULTS

This study was focused on heavy oils produced from two fields in Saskatchewan: Tangleflags and Pikes Peak; where fireflood and steam stimulation respectively have been operated.

For the Pikes Peak oil, the study covered a temperature range of 270° C to 330° C. The initial reactor pressure was set at about 500° psig to simulate the field condition. Since the reactor was closed during the reaction period, the pressure increased as gaseous products evolved. The final pressure recorded at the end of the reaction period varied depending on the amount of heavy oil feed used, the reaction temperature and the residence time.

To simulate the temperature regime of a fireflood operation, the experiments with Tangleflags oil involved a broader temperature range (270° C to 500° C) and higher temperatures. The reactor was set at about 200 psig at the beginning of the reaction period to simulate reservoir condition. Again, this pressure increased during the run due to production of gases caused by thermal cracking.

Additional experiments were conducted with the Tangleflags oil to study the effects of thermal cracking on oxidized oil, and cracking oil in the presence of steam and indigenous minerals found in the reservoir. The results of all these experiments are described in this section. A listing of all the various types of experiments are presented in Table 2.

5.1 Summary of Results

Before getting into a more detailed discussion, the more important observations of this experimental program are summarized as follows:

1. For both oils, thermal cracking reactions became dominant in the temperature range of 300° to 330° C. This was demonstrated by the rapid decrease in oil viscosity and increase in gas production.

2. At and below 300° C, the viscosity of the heat-treated oil, measured at 25° C, increased as the heat treatment period was extended. Polymerization of reactive species was suspected to be the cause of this behaviour. It may be inferred from this observation that thermal recovery methods involving lower temperatures covered by these experiments (270° C to 300° C), would have a negative impact on the permanent viscosity of the oil.

3. The presence of water or steam during thermal cracking of heavy oil appeared to suppress the cracking reactions. As a result, less light products were formed in the product oil. The suppression of cracking reactions was, according to a previous research group, attributed to the increase in the overall pressure of the system in the presence of steam.

4. Pre-oxidized oil produced significantly more coke during thermal cracking. The gas yield and product oil quality were similar to those generated by non-oxidized oil. However, the oil yield was lower due to the increase in coke make.

This observation implies that the use hot flue gas, which normally contains some excess oxygen, in the initial heat-up of a fireflood reservoir may produce more coke once ignition is started due to low temperature oxidation in the preheat stage. The use of steam during the preheat would reduce low temperature oxidation. However, the presence of steam may suppress the production of light oil products in the cracking zone, which in turn, has an impact on the mobility of the product oil.

Also, once the fireflood is established, any air that bypasses the fire-front and channels towards the producer may also cause low temperature oxidation.

5.2 Detailed Results

5.2.1 Effects of Cracking Temperature and Residence Time

For reaction temperatures above 400° C, the residence time of the oil in the reactor was extremely crucial in determining product yield structure. In these experiments, heavy oil feed was injected into a preheated reactor at time zero, and it usually took **8 to 10 minutes** for the entire system to stabilize at the target reaction temperature. At the end of the reaction period, the product oil was quickly removed from the hot reactor and chilled to stop any thermal reactions. The whole operation of liquid withdrawal and chilling took approximately **2 to 3 minutes.**

For experiments operated at temperatures below 350° C, the residence time issue was less important; therefore, for the sake of convenience, the heavy oil feed was placed inside the reactor at room temperature. The reaction system was subsequently heated to the target reaction temperature; and the residence time was counted after the reaction temperature was reached. At the end of the reaction period, the product oil was immediately withdrawn and chilled.

TANGLEFLAGS OIL

Most of the experiments involved two residence time periods: 1 hour and 2 hours. However, for the lower temperature (270° C and 300° C) experiments, longer residence times were also studied. The large amounts of gas produced in the high temperature (450° C and 500° C) experiments limited the residence time to minutes in order to avoid exceeding the upper pressure limit of the system.

DISTILLATION BEHAVIOR OF LIQUID PRODUCT

For temperatures below 300° C, 99% of the heavy oil remained in liquid phase after the heat treatment. The oil became even slightly heavier than the original feed, as shown by the simulated distillation results (Table 3).

The one-hour and two-hours experiments conducted at 350° C showed that the heavy oil was slightly upgraded (Table 3). At this temperature, the total coke and gas yields were still small (less than two percent of total hydrocarbons).

At higher temperatures (400° C to 500° C), the oil yield became progressively smaller with increasing temperature and residence time (Table 3). Also, the oil became considerably lighter. Figure 3 illustrates the impact of temperature and residence time on the distillation behavior of the oil product.

VISCOSITY OF LIQUID PRODUCT

Viscosity is a very sensitive parameter. Although it can be useful to indicate small changes in the oil composition, it is also very sensitive to minor variations in experimental procedure.

In designing our experiments, extreme care was taken to ensure consistency in all phase separation steps and to avoid the use of solvent. In spite of that, we still observed some inconsistencies in the viscosity results from several experiments, particularly in experiments involving long residence times (those lasted for days). In those runs, any small leak in the system would lead to the loss of light ends and thus unreliable viscosity data. Viscosity data for the runs with Tangleflags oil are shown in Table 3. The data obtained from the longer runs at low temperatures are of suspect.

In order to get consistent results on viscosity, we performed several experiments again; but this time the experiments were not stopped when liquid samples were withdrawn. In one batch of oil, five samples were taken at different times (1hr, 2hr, 24h, 48hr, 72hr). Precautions were taken to ensure sample uniformity and that the samples were not taken from the dead volume in the sample line. These data are presented in Table 4 and Figure 4.

Figure 4 shows that the product oil viscosity (measured at 25° C) increased with residence time in the lower temperature experiments: 270° C and 300° C. Since only the liquid phase was sampled from a heated reactor, one may suspect vaporization of light ends from the original feed inside the reactor may account for the observed increase in liquid viscosity. However, the data shows that the viscosity increase was more significant at 270° C than at 300° C. This indicates that distillation inside the reactor was not the only reason for the observed viscosity increase.

Also, the above data is fully consistent with simulated distillation data shown earlier, which indicated that the oil got heavier at these temperatures.

J. Hyne and co-workers [1] also observed similar behavior with Athabasca bitumen at 200° C and 240° C. However, he found that the viscosity of bitumen decline with residence time at 300° C. Venkatesan et al [2] found that the asphaltene contents of Celtic oil at 300° C and Cold Lake crude at 285° C went through a maximum with increasing heating time. But they observed that the viscosities of these crudes decline progressively with increasing heating time.

J. Hyne et al proposed that the increase in viscosity at low temperatures was caused by the polymerization of reactive organic species to form large molecules which have an impact on the asphaltene content as well as the observed viscosity. At temperatures where cracking reactions are weak, such effects are more noticeable. The different nature of the crudes worked on by the different research groups may well explain the variations of results.

Figure 4 also shows that at 330° C, the product oil viscosity decreased with heating time. One may infer from these data that thermal cracking reactions became prominent in the temperature range of 300° C and 330° C.

COKE AND GAS PRODUCTION

The coke and gas production at temperatures lower than 350° C were very small (Table 3). The coke yields were hardly measurable at these temperatures except for the run at 350° C and 2 hours, where the coke yield was 0.6 %.

The gas yields at these temperatures were also small (less than 1%), but they were measurable. As expected, the gas and coke make increased as temperature went up and became significant at temperatures above 400° C. Figure 5 shows the changes in product yield as a function of temperature when residence time was fixed at 2 hours. Figure 6 shows the yield changes as a function of residence time when temperature was fixed at 400° C.

In comparing the coke yield of Tangleflags oil with crudes studied by other groups, we could only find data on Athabasca bitumen where direct comparison can be made. These data (Table 5) showed that Athabasca bitumen produces almost twice as much coke as Tangleflags oil under similar thermal conditions. Our own experience with coking Athabasca bitumen and Lloydminster crude also show the same trend; for example, coking bitumen at 510° C for 5 minutes (liquid residence time) gave about 14% coke; whereas coking Lloydminster crude under similar conditions gave only 8% coke.

PIKES PEAK OIL

Since steam stimulation is the main method of interest in the Pikes Peak field, the maximum temperature expected for that particular area is around 330° C. All the experiments on Pikes Peak oil were focused on three temperatures: 270° C, 300° C and 330° C. Since reaction rates are very low at these temperatures, the experiments had to be run longer (days instead of hours) in order to see changes in the oil properties.

DISTILLATION BEHAVIOR OF PRODUCT OIL

Trends that were similar to the Tangleflags oil were observed. The distillation data (Table 6) showed that the oil became heavier after heating at 270° C and 300° C. However, when the oil was heated at 330° C, it turned lighter. This again indicates that thermal cracking became prominent in the temperature range of 300° C and 330° C.

VISCOSITY OF PRODUCT OIL

The viscosity data is shown in Table 6 and plotted in Figure 7. These data shows that viscosity decreased rapidly in the first two hours of heating. After this period, the viscosity went up in the 270° C and 300° C runs; and went down in the 330° C run. The latter parts of the experiments were similar to those of the Tangleflags experiments. But the initial viscosity decline was not observed in the Tangleflags runs. The reason for this behavior is still unclear.

COKE AND GAS PRODUCTION

The coke and gas make (Table 6) were also small at these temperatures. Since the coke yield is near the detection limit of our analytical method, a comparison with the Tangleflags data would not be useful.

5.2.2 Effects of Cracking Oxidized Oil

The purpose of these experiments was to determine the impact of low temperature oxidation on the product yield structure of Tangleflags oil. Pre-oxidized Tangleflags oil was used in two experiments, both operated at 400° C. One experiment had one hour of residence time, and the other had two hours. The procedures used in oxidizing the feed oil is described in NHRC Report #00395. Since only a small batch of oil could be oxidized at a time; therefore several batches were needed to provide enough material for one thermal cracking experiment.

The results on product yield and oil quality are shown in Table 7. These results are compared with the baseline experiments in which regular Tangleflags feed was used. The most significant difference between these two sets of experiments is the higher coke yield in the oxidized oil runs. There was a nine-fold increase in the one-hour experiment and a four-fold increase in the two-hour experiment. The two experiments used different batches of oxidized oil. We found that the procedures for preparing the oxidized oil were not very repeatable; which may explain the smaller increase in coke yield in the two-hour experiment.

The gas yields of the two sets of experiments were similar. The oil yields of the oxidized oil runs were lower than the baseline because of the higher coke yield in the former. The distillation behavior of the liquid product from the oxidized oil experiments were similar to those from the baseline runs.

It appears that the main impact of low temperature oxidation is a higher coke yield coupled with a proportionately lower oil yield. The impact on gas yield and product oil quality appears to be minimal.

5.2.3 Effects of Water

To explore the effects of water on thermal cracking, these experiments were conducted at 400° C for periods of one and two hours. The feed contained 5% distilled water and the balance was Tangleflags oil.

Since the reaction temperature exceeded the critical temperature of water, all the water added to the system was expected to be vaporized. To avoid over-pressuring the reactor, smaller amounts of feed were used (about 50 grams of oil instead of 100 grams). The final pressure of the two experiments were about 80 psi higher than the baseline runs in which no water was used.

The results of these water-addition experiments are compared with the baseline experiments in Table 8. The coke yields of the two types of experiments were small and near the detection limit of the analytical method; therefore, no significant difference was observed. The gas yields were slightly higher in the water-addition experiments; hence, the oil yields were proportionately lower. The viscosities and distillation curves of the oil products showed that the water-addition experiments gave slightly heavier oil products.

In the literature, there appears to be no consensus on the effects of water. Hesp et al [3] conducted closed-vessel thermal cracking experiments on Australian crude in the presence of water. They observed a reduction in gas yield. They attributed this behavior to the increase in overall pressure of the reaction system caused by the presence of steam. They also performed experiments in which pressure was exerted by Helium, similar reduction in gas yield was observed. They concluded that high pressure reduces the rate of thermal cracking reactions, regardless of whether it is developed by steam or other gases. Unfortunately, they did not report the response of liquid product quality to pressure. Their conclusions support our observations on the liquid properties, but there is a disagreement on the gas yield.

Henderson et al [4] and McNab et al [5] conducted experiments with Athabasca bitumen in the presence of steam and different pressures. They concluded that pressure and water had no appreciable effects on the conversion of heavy oil into lighter products.

5.2.4 Effects of Sand

These experiments were performed by adding equal amounts of Tangleflags oil and sand into the reactor. The sand came from a treater tank in the Tangleflags field. It was placed inside the reactor at room temperature, followed by heating the reactor to a target temperature. Once the reactor stabilized at the target temperature, the oil feed was injected into the hot sand bed inside the reactor and reaction time was counted.

At the end of the reaction period, approximately 80% of the product oil was withdrawn from the reactor, using a dip-tube, and transferred to a cold receiver to stop further reactions. The contents of the reactor, which included the coked sand moistened with oil, was cooled by forced convection of room air on the outside of the reactor. It took approximately 30 minutes to lower the temperature of the reactor from 400° C to 300° C.

The coke yield was measured by first washing the wet coke sand, followed by burning the coke in a muffle furnace. However, it was later found that clean sand also lost some weight in the muffle furnace and the weight loss was not repeatable. In some instances, the discrepancies in weight loss by different clean sand samples were large in comparison with the weight loss caused by coke combustion. Consequently, the coke yield results were erratic and unreliable.

We also found that the material balance of these experiments were not satisfactory; typically 3% of the sand was not accounted for. Since part of the oil yield was obtained by weight difference between samples containing sand and coke, unreliable sand and coke numbers also caused unreliable oil yield results.

The viscosities and distillation behavior of the oil products are shown in Table 9. The addition of sand did not appear to have any significant impact on the oil quality.

6.0 REFERENCES

[1] Hyne, J.B., Synopsis report no. 50, AOSTRA contracts no. 11, 103, Apr. 1986.

[2] Venkatesan, V.N. and Shu, W.R., Preprint no. 84-35-108, 35 Annual Tech. Mtg. CIM, 1984.

[3] Hesp, W. and Rigby, D., Erdol and Kohle - Erdgas - Petrochemie rereinigt mit Brennstoff - Chemie 26 (2), 70, 1973.

[4] Henderson, J.H. and Weber, L.,J. Can. Pet. Tech., 4, p. 206, 1965.

[5] McNab, J.G., Smith, P.V. and Bette, R.L., Ind. Eng. Chem., 44(11), p 2556, 1952.

[6] Millam, J.P., Moore, R.G., Bennion, D.W., Ursenbach, M.G., Gil, D.N., SPE 14226, Sept. 22-25, 1985.

7.0 TABLES

TABLE 1: HEAVY OILS PROPERTIES

	Tangleflags	Pikes Peak
Density at 15° C, Kg/m^3	968.2	975.9
Viscosity at 25° C, cp	5,734	15,872
Simulated Distillation (wt% off)		
200° C	2.6	2.9
350° C	22.8	21.0
520° C	50.7	51.1

© 1988

TABLE 2: EXPERIMENTAL PROGRAM FOR TANGLEFLAGS HEAVY OIL

Temperature, °C	270	300	350	400	400	400	400	400	450	500
Reaction time, hrs (minutes)	66 240	1-2 24-48 96	1 2	1-2 4	1 2	1 2	1 2	1 2	(14) (28)	(8)
Additive	-	-	-	-	Steam	Sand	Sand + Steam	Oxidized Oil	-	-

EXPERIMENTAL PROGRAM FOR PIKES PEAK HEAVY OIL

Temperature, °C	270	300	330
Reaction time, hrs	66 288 504	24 48 120	24 48

TABLE 3: TANGLEFLAGS OIL : EFFECTS OF TEMPERATURE AND TIME

RUN CONDITIONS	RUN #	NORMALISED YIELD, WT % OIL,%	GAS,%	COKE,%	MASS BALANCE TOTAL,%	VISCOSITY CP	SIMULATED DISTILLATN WT % OFF 200C	350C	520C
270 C, 2.75 DAY	53	99.79	.18	.03	98.96	11400	2.30	19.80	45.50
270 C, 2.75 DAY	63	99.02	.92	.06	99.74	10300	2.20	20.10	45.40
270 C, 10 DAY	52	99.09	.85	.06	99.84	6600	2.80	21.90	48
300 C, 1 HOUR	55	99.49	.18	.33	98.94		2.30	18.80	47.20
300 C, 2 HOUR	54	99.73	.19	.08	98.56	7980	2.30	19.80	46.10
300 C, 1 DAY	56	99.74	.18	.08	98.74	12400	2.30	19	45.30
300 C, 2 DAY	57	99.76	.18	.06	99.26	6200	2.30	20.30	46.30
350 C, 1 HOUR	51	99.76	.15	.09	99.17	4120	2.90	23.30	51
350 C, 2 HOUR	50	98.80	.58	.62	97.92	3810	2.80	23.50	51.90
400 C, 1 HOUR	35	98.05	1.41	.54	97.89	289	7	36	69
400 C, 2 HOUR	31	97.81	1.86	.32	96.35	26.70	13.80	46.40	73.90
400 C, 2 HOUR	32	95.62	2.76	1.62	96.68	30.90	14.30	48.20	77.30
AVG. RUN(31,32)		96.72	2.31	.97	96.52	28.80	14	47.30	75.60
400 C, 4 HOUR	33	89.11	3.25	7.64	94.82	9.99	24	66	94
450C,14M	66	88.35	4.15	7.50	95.19	4.20	35	77.20	97.40
450C,28M	65	80.63	5.15	14.22	94.65	3.20	37	77.60	95.60
500C,8M	64	87.76	5.20	7.04	92.51	5.90	31	67.60	90.50

TABLE 4 : TANGLEFLAGS AND PIKES PEAK
VISCOSITY CHANGE AS FUCTIONS OF TIME & TEMPERATURE
(viscosities measured at 25 C, in cp)

TANGLEFLAGS

TIME	270 C	300 C	330 C
0 HOUR	5734	5734	5734
1 HOUR	5837	5591	5427
2 HOUR	6308	5939	4710
24 HOUR	10854	8192	1966
48 HOUR	18432	12493	1116
72 HOUR	28518	14438	727

PIKES PEAK

TIME	270 C	300 C	330 C
0 HOUR	15872	15872	15872
1 HOUR	14848	12390	10394
2 HOUR	13312	12032	9134
24 HOUR	14643	20634	5632
48 HOUR	18586	29953	3379
72 HOUR	23706	42394	2273

TABLE 5 : COMPARISON OF COKE YIELDS BETWEEN TANGLEFLAGS OIL AND ATHABASCA BITUMEN

	COKE YIELD, WT %	
CONDITIONS	TANGLEFLAGS	ATHABASCA[6]
400 C, 1 HOUR	.50	2.60
400 C, 4 HOUR	7.60	15.30

TABLE 6: PIKES PEAK OIL : EFFECTS OF TEMPERATURE AND TIME

RUN CONDITIONS	RUN #	NORMALISED YIELD, WT % OIL,%	GAS,%	COKE,%	MASS BALANCE TOTAL,%	VISCOSITY CP	SIMULATED DISTILLATION WT % OFF 200C	350C	520C
270 C, 2.75 DAYS	46	96.95	2.36	.69	100.97	31800	2	17.80	44.50
270 C, 12 DAYS	48	99.63	.29	.08	96.72	20900	1.50	18.70	46
270 C, 21 DAYS	49	99.60	.25	.14	99.31	68100	1.90	17	39.80
300 C, 1 DAY	37	96.27	3.72	.01	102.13	16900	1.70	17.60	47
300 C, 2 DAYS	34	96.80	2.94	.25	101.32	24400	2.10	16.70	44.20
300 C, 5 DAYS	45	95.69	3.78	.52	102.51	12000	2.20	18.70	46.70
330 C, 1 DAY	44	96.04	3.83	.13	103.17	6480	3	19.60	48.20
330 C, 2 DAYS	39	96.19	3.77	.04	98.71	4510	3.60	22.30	51

TABLE 7: TANGLEFLAGS OIL : EFFECTS OF OXIDIZED OIL

REACTION TEMPERATURE = 400 C

RUN CONDITIONS	RUN #	NORMALISED YIELD, WT % OIL,%	GAS,%	COKE,%	MASS BALANCE TOTAL,%	VISCOSITY CP	SIMULATED DISTILLATION WT % OFF 200C	350C	520C
ONE HOUR EXPT.:									
BASELINE OIL	35	98.05	1.41	.54	97.89	289	7	36	69
OXIDIZED OIL	41	93.58	1.95	4.48	97.10	121	7.50	37	69
TWO HOUR EXPT.:									
BASELINE OIL	31,32	96.72	2.31	.97	96.52	28.80	14	47.30	75.60
OXIDIZED OIL	43	93.43	2.29	4.27	97.04	30.20	13	45	73.60

TABLE 8: TANGLEFLAGS OIL : EFFECTS OF WATER ADDITION

REACTION TEMPERATURE = 400 C

RUN CONDITIONS	RUN #	NORMALISED YIELD, WT % OIL,%	GAS,%	COKE,%	MASS BALANCE TOTAL,%	VISCOSITY CP	SIMULATED DISTILLATN WT % OFF 200C	350C	520C
ONE HOUR EXPT.:									
BASELINE OIL	35	98.05	1.41	.54	97.89	289	7	36	69
OIL WITH 4.5% H2O	36	97.29	2.22	.48	98.06	234	7.60	36	66.30
TWO HOUR EXPT.:									
BASELINE OIL	31,32	96.72	2.31	.97	96.52	28.80	14	47.30	75.60
OIL WITH 5% H2O	40	94.32	2.89	2.79	94.98	66.50	12	45	74

TABLE 9: TANGLEFLAGS OIL : EFFECTS OF SAND AND WATER

REACTION TEMPERATURE = 400 C

		VISCOSITY	SIMULATED DISTILLATN WT % OFF		
RUN CONDITIONS	RUN #	CP	200C	350C	520C
ONE HOUR EXPT.:					
BASELINE OIL	35	289	7	36	69
88gm oil,90gm sand	47	185	7	38.30	69.60
68gm oil,3.6gm H20,70gm sand	59	235	5.90	32.40	57.80
81gm oil,4.3gm H20,85gm sand	61		7.60	34.70	61.10
TWO HOUR EXPT.:					
BASELINE OIL	31,32	28.80	14	47.30	75.60
85gm oil,90gm sand	60	70.30	11	46	76
57gm oil,3gm H20,60gm sand	62	14.90	16	59	84.50

8.0 FIGURES

© 1988

FIGURE 1: EQUIPMENT DIAGRAM

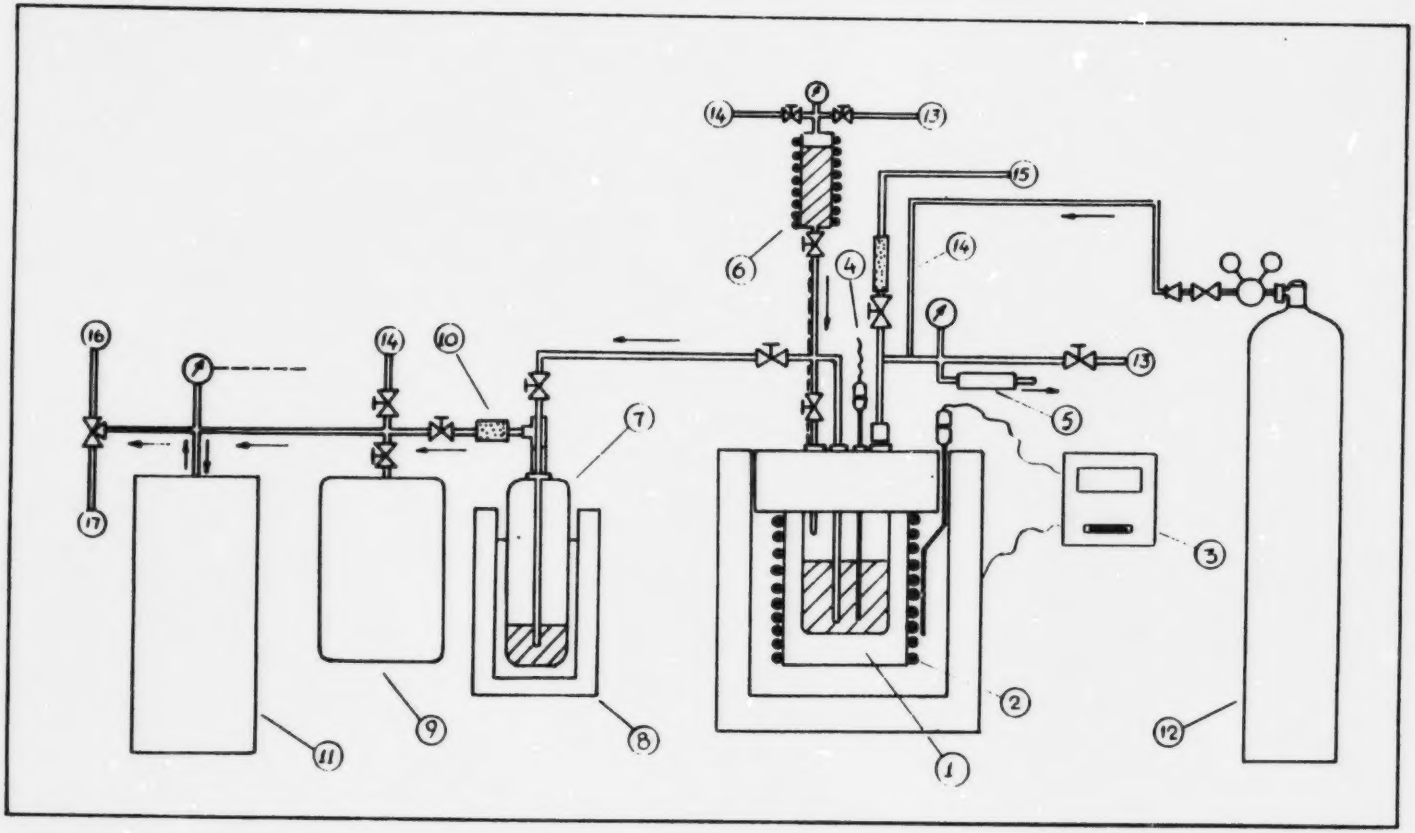

1	Reactor
2	Heating units
3	Temperature controller
4	Thermocouple
5	Safety head
6	Feed vessel
7	Liquid product vessel
8	Cooling bath
9	Gas sampling bag
10	Filter
11	Vacuum tank
12	Helium cylinder
13	Vent
14	Helium purge
15	To pressure transmitter
16	Vacuum
17	Gas sampling line

FIGURE 2: DETAILS OF REACTOR AND SAMPLING SYSTEM.

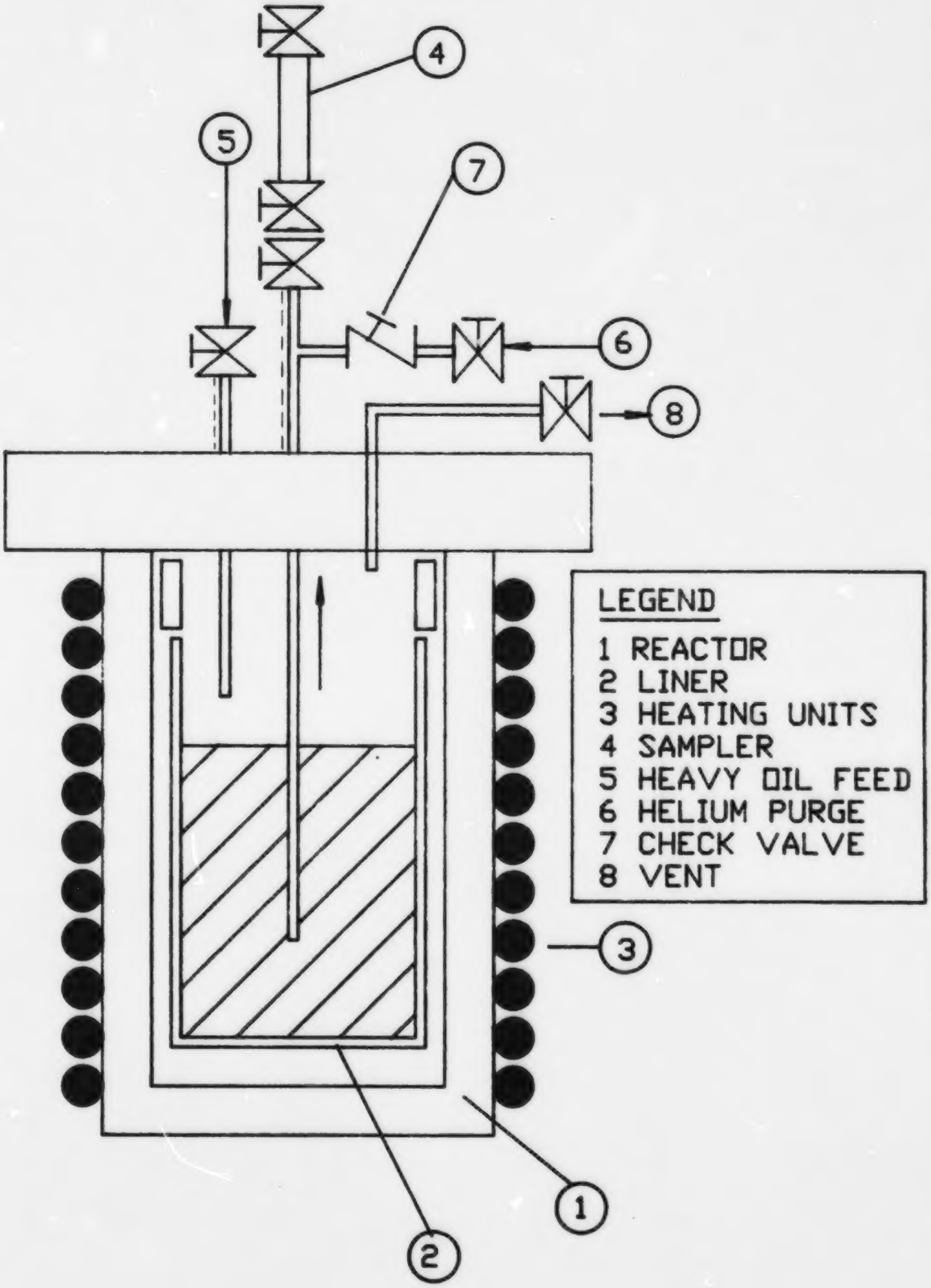
4
5
7
6
8
3
1
2
LEGEND
1 REACTOR
2 LINER
3 HEATING UNITS
4 SAMPLER
5 HEAVY OIL FEED
6 HELIUM PURGE
7 CHECK VALVE
8 VENT

FIGURE 3: EFFECTS OF TEMPERATURE AND TIME ON SIMULATED DISTILLATION OF TANGLEFLAGS OIL

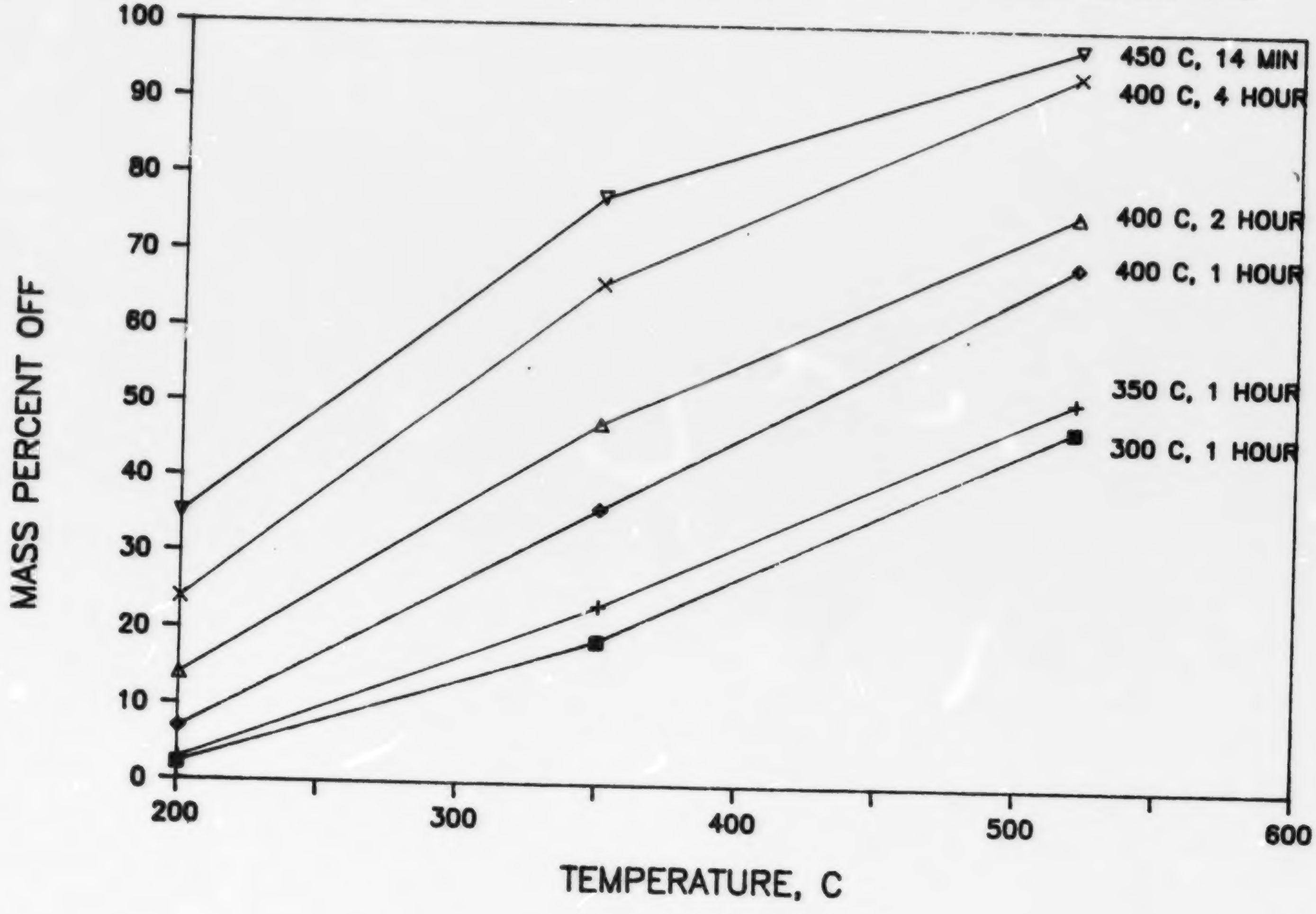

FIGURE 4: TANGLEFLAGS OIL: CHANGES IN VISCOSITY AS FUNCTION OF HEATING TIME

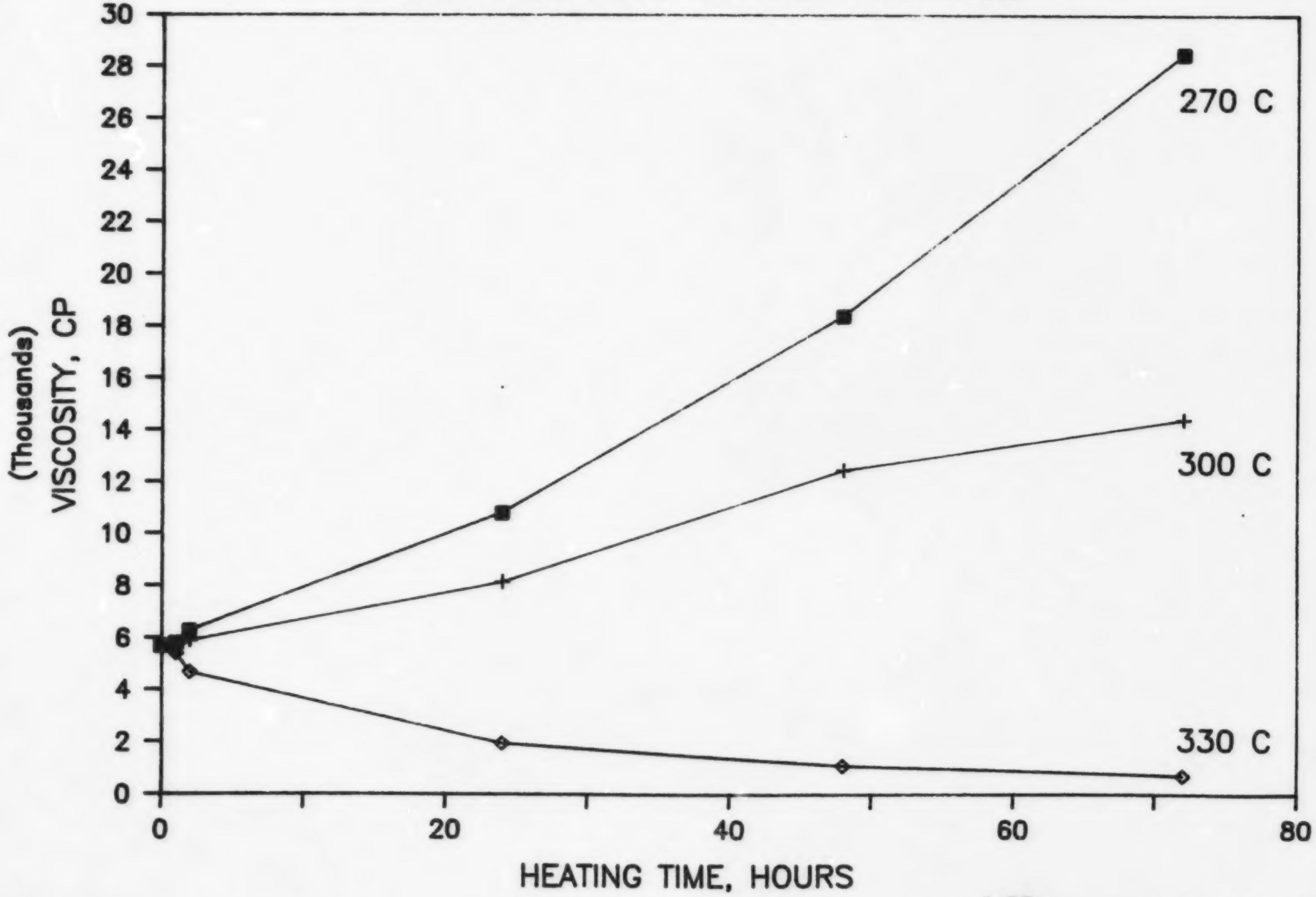

FIGURE 5: EFFECTS OF TEMPERATURE ON YIELD
REACTION TIME = 2 HOURS

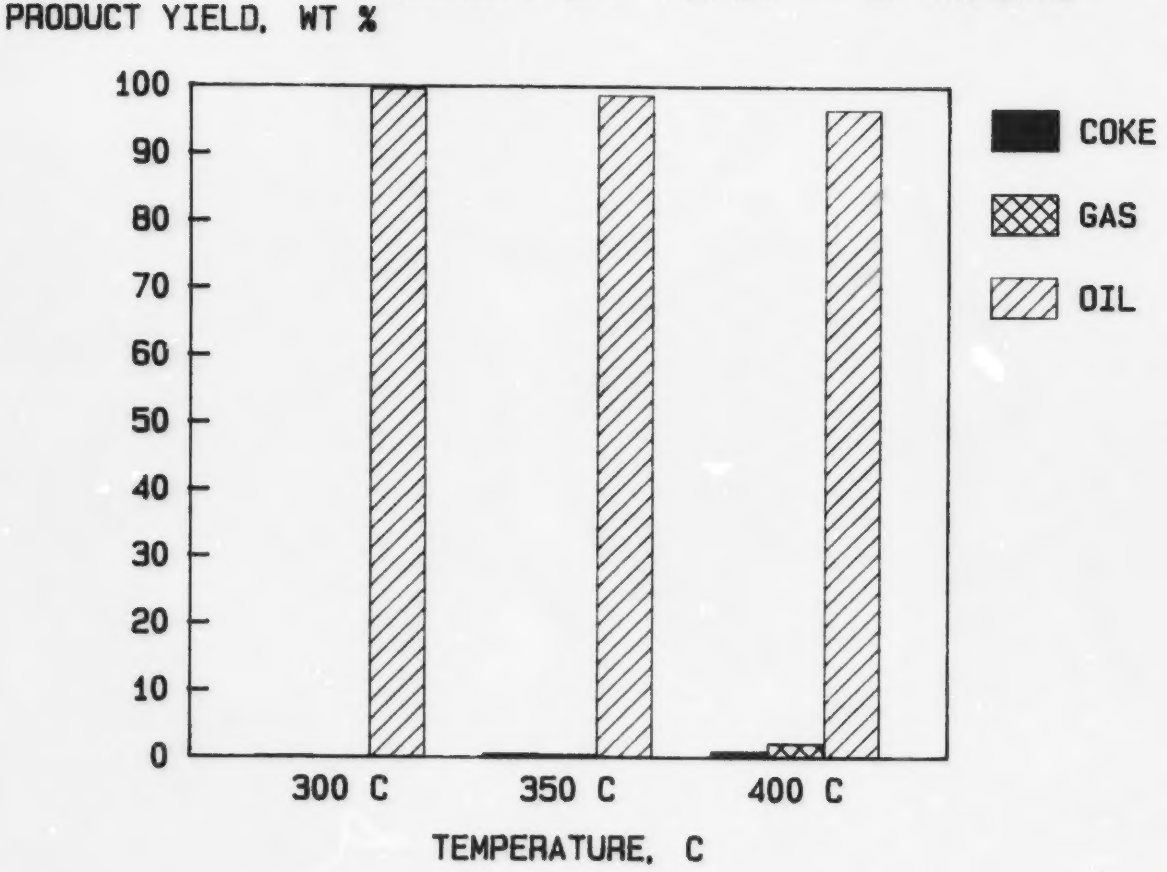

# FIGURE 6: EFFECTS OF REACTION TIME ON YIELD
TEMPERATURE = 400 C

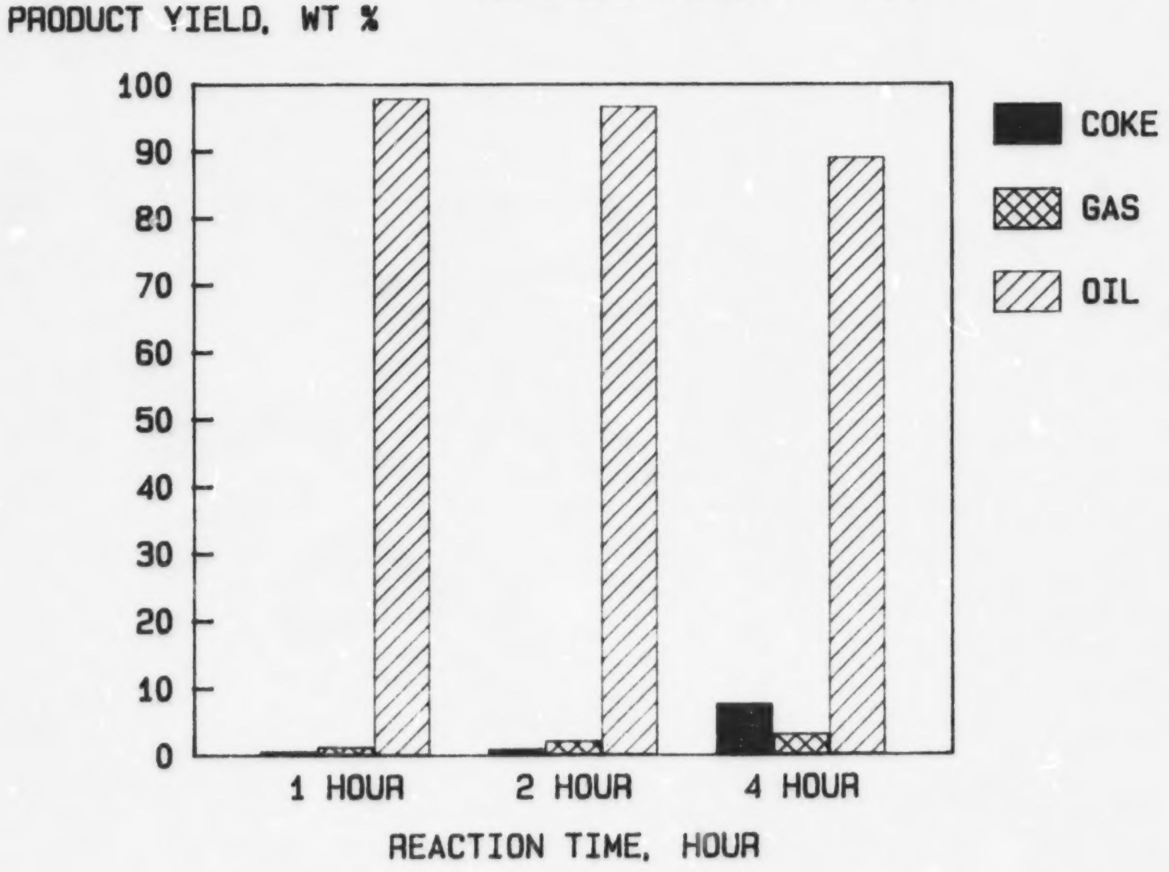

FIGURE 7: PIKES PEAK OIL: CHANGES IN VISCOSITY AS FUNCTION OF HEATING TIME

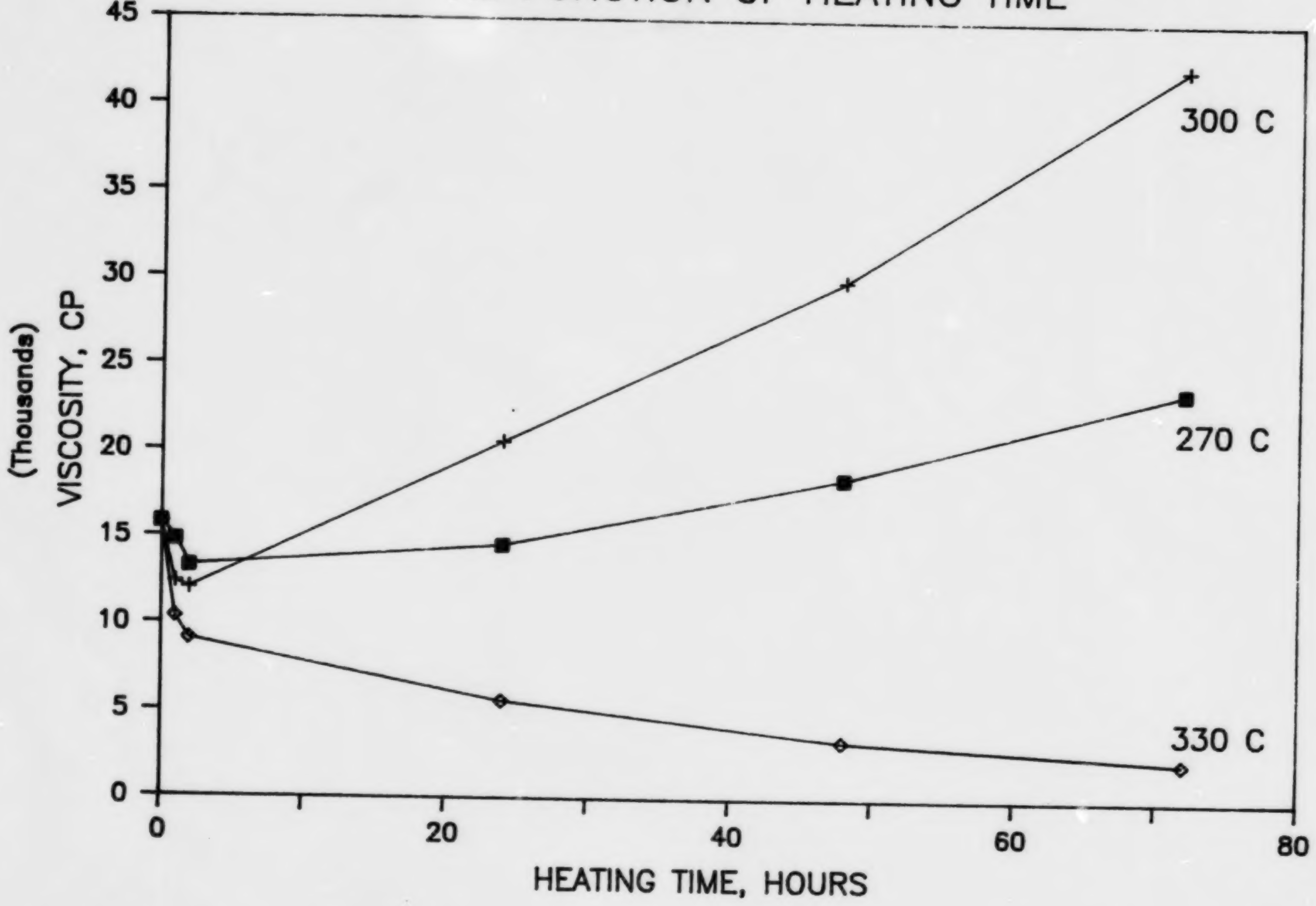

CLASSIFICATION: NHRC, NOVA, HUSKY
and Subsidiaries
REPORT NUMBER: 00395

THERMAL RECOVERY MECHANISMS
TASK 6 FLOW STUDIES

November 1988

Authors

Brian Erno
Dwayne Davis

Reviewed by

Apostolos Kantzas

DEPARTMENT: Applied Science (Resource Recovery)
PROJECT NO: 688-048
PREPARED FOR: Albert George - Energy, Mines & Resources
KEYWORDS: coreflood, waterflood, permeability, Tangleflags, oil, recovery, viscosity

This report contains the valuable proprietary and confidential information of the NOVA HUSKY RESEARCH CORPORATION LTD., and may not be used, disclosed or reproduced without permission in writing from NOVA HUSKY RESEARCH CORPORATION LTD.

51 pp

MICROMEDIA

DISTRIBUTION LIST

	Copies
ENERGY, MINES & RESOURCES, Ottawa	
A. George	10
NOVA HUSKY RESEARCH CORPORATION:	
T. Jack	1
B. Erno	1
D. Davis	1
HUSKY OIL OPERATIONS LTD.:	
J. Peggs	1
P. Tsang	1
NHRC Library	2
Husky Library	1
Files	2
	--
TOTAL NUMBER OF COPIES	**20**

TABLE OF CONTENTS

Page

1.0 SUMMARY 1

2.0 INTRODUCTION 1

2.1 Background 1
2.2 Literature Review 2

3.0 EXPERIMENTAL 3

3.1 Materials 3
3.2 Procedures 4
3.2.1 Description of coreflood equipment 4
3.2.2 Preparation of the sand pack 4
3.3.3 Oil-flow experiments 6

4.0 RESULTS AND DISCUSSION 7

4.1 Initial Sandpack Conditions 7
4.2 Oil Flow Experiments 8
4.3 Displacement Experiments 9

5.0 CONCLUSIONS 13

6.0 REFERENCES 13

7.0 TABLES 15-35

8.0 FIGURES 37-48

1.0 SUMMARY

The experiments described in this section were designed to explore the potential impact of thermal alterations in the oil on flow behavior through a sandpack. Flowing Tangleflags oil through a sandpack containing residual water at elevated temperature and pressure, had no effect on sand permeability over periods of 8 hours, and the produced oil had a constant viscosity. These results give no indication of asphaltene destabilization or other thermal changes to the oil. A second experiment in which water, steam and oil were flowed simultaneously at elevated temperature also showed no changes in sand permeability, although some changes were observed in oil viscosity.

The second set of experiments examined the effects of abrupt changes in fluid viscosity on oil recovery from a sandpack. Injection of a slug of oil of increased viscosity (achieved by partial oxidation of the native oil) resulted in a small decrease in recovery during a subsequent waterflood at 200 C. A similar experiment using a low viscosity slug showed no significant change in waterflood recovery. Gasflooding at 200 C was less effective than waterflooding, and injection of a low viscosity oil slug prior to a gasflood did not improve recovery.

2.0 INTRODUCTION

2.1 Background

In the in-situ combustion recovery process, a region of the reservoir ahead of the high temperature oxidation front is swept with fluids at an elevated temperature controlled by saturated steam properties at or near reservoir pressure. In a typical Lloydminster sand, reservoir pressure after some depletion due to primary recovery is about 2000 kPa, and thus one can expect a heated region of about 200 C to exist downstream of the combustion front. Flow through this region will consist of water and steam, produced from combustion and flashed from the reservoir, combustion and volatile hydrocarbon gases, and hot oil. The flowing oil may have lower viscosity than reservoir oil, due to cracking reactions occurring in the region immediately downstream from the combustion front, or higher viscosity, caused by partial oxidation at or ahead of the combustion front. Mixing in of this altered oil may change the displacement behavior of the native oil, and thus affect recovery. Flow of hot, altered oil may affect sand permeability, and/or the miscible interface between native and altered oil may change the geometry of the displacement front. The work described in this section was initiated to explore these aspects of thermal recovery.

2.2 Literature Review

The oil flow experiments described in this report were derived from similar experiments reported by Waxman et.al.(1) They flowed Peace River bitumen and brine, at a constant ratio of 5:2, through Bullhead reservoir sand (as core plugs), at 195 C and 2758 kPa, and observed a continually increasing differential pressure across the core. The absence of a pressure build-up across 15 and 7 μm filters in the bitumen supply line upstream of the core argued against plugging of the core with fines in the bitumen. They also found lower asphaltene content in the bitumen produced from the sand, and from post-analysis, noted that bitumen extracted from the injection half of the core was enhanced in asphaltenes relative to the original sample. Experiments conducted with various core samples, and with two different bitumen samples (one extracted from core and the other cold- bailed from a well prior to steaming), gave similar results.

When these experiments were repeated using thermally produced oil, the permeability initially decreased but eventually levelled, at a value significantly higher than in experiments with oil which was not thermally altered.

The authors suggest that the observed flow behavior is due to gel structures in the bitumen, due to interacting asphaltene micelles or aggregates. Under the low shear rates generated by flow, these gel structures may control bitumen flow rather than the sand permeability. Based on evidence from an earlier report, they suggest that the asphaltenes in thermally produced bitumen interact less strongly with the solvent maltenes, producing weaker gel structures and thus less flow restriction than the native bitumen.

Although much work has been reported on asphaltene precipitation from light oils (2), and several models have been developed to predict the tendency for asphaltene precipitation (3), few studies of the solubility characteristics of asphaltenes in heavy oils appear to have been done. Current theories picture the asphaltenes existing as aggregates within the maltene portion of the oil. These aggregates are solubilized (or kept dispersed) within the oil by layers of resins adsorbed on the surfaces of the aggregates. Any changes in the stability of these resin-asphaltene aggregates affect the solubility of the asphaltenes in the oil. For example, compositional changes which increase resin solubility in the oil, such as addition of some solvents, lead to an increase in the size of asphaltene aggregates, resulting in reduced asphaltene solubility. Pressure changes are particularly significant for "live" oils, since pressure reduction causes both expansion and compositional change of the liquid phase. These opposing effects give rise to a minimum in asphaltene solubility at the bubble point of the oil. Temperature effects are the least studied, and other than the work by Waxman *et al.* discussed above, no studies of asphaltene solubility at temperatures of 100 - 300 C have been found. Work at lower temperatures, with light oils, indicates that solubility is reduced with increasing temperature.

Adding to the apparent complexity and interdependence of the effects of temperature and pressure on the stability of two phase heavy crude oil/solution gas samples, there is increasing evidence that significant compositional changes occur as a result of thermal recovery. For example, in a comparison of cold-bailed and steam produced Cold Lake bitumen samples, Gould (4) found significant differences in the asphaltene fractions, which he attributed to exposure of the oil to temperatures up to 300 C. No comments were made on the effect of these changes on asphaltene aggregation or flow behavior in the reservoir. Changes in asphaltenes exposed to steam have been attributed by Hyne *et al.* to reactions with water, and such reactions are significant at temperatures as low as 240 C. These changes are more fully discussed in the thermal cracking section of this work. The effects of these changes in the asphaltenes, and possibly in the resins, are likely to affect asphaltene aggregation and solubility.

3.0 EXPERIMENTAL

3.1 Materials

Sand for these experiments was produced from wells at the Tangleflags Fireflood Project, and was obtained from the treater de-sand system. The perforated zone is the General Petroleum. Oil and water were removed by hot toluene extraction (Core Labs), and then the sand was dried at 110 C. Most of the finest fraction was removed from the sand by washing it through a 200 mesh (75 um) sieve, then rinsing with methanol and drying at 22 C. Results of a sieve analysis are shown in Table 1.

Oil produced from well D11-13 at the Tangleflags Fireflood Project was de-watered by heated centrifugation, to give a sample with <0.5 % residual water. Oil from this offset well showed no effects of the combustion process, and is thus considered representative of native reservoir oil. It was sampled on June 3, 1986; wellhead temperature was 10 C. After cleaning, the oil was stored in a freezer until needed. The brine used for initial saturation of the sandpack was prepared from reagent grade salts dissolved in freshly distilled water, with amounts as shown in Table 2.

The oxidized oil sample was prepared by sealing about 100 g of Tangleflags oil in a zirconium pressure vessel (400 mL) and pressurizing to 5270 kPa with air. The vessel was then heated to 214 C in an oven for 24 hr. The pressure increased to 8432 kPa, and then gradually decreased as oxygen was removed. After cooling to 20 C, the pressure was 3400 kPa. The oil sample was drained through a coarse screen, which removed several lumps formed at the air-oil interface. The remaining oil was mixed to homogenize it, and subsamples were taken for characterization.

The data in Table 3 show that the oxidized oil is more than 10 times as viscous as native Tangleflags oil, has nearly 4 times as much oxygen, and 6 mass % more asphaltenes. Infrared spectra compared in Figure 1 also show the effects of oxidation, specifically by the presence of a C=O peak at 1693 cm^{-1} in the spectrum of the oxidized oil.

Oil of reduced viscosity was prepared by adding 7 mass % toluene to a sample of the native Tangleflags oil. This reduced its viscosity about 8 fold, as shown in Table 3.

3.2 Procedures

3.2.1 Description of Coreflood Equipment

A schematic drawing of the apparatus used in these experiments is given in Figure 2. It consists of reservoirs for holding fluids prior to injection, a high pressure syringe pump (ISCO LC-5000), a high pressure, high temperature "core holder", in which the sandpack was mounted, an oven to heat the fluids and sandpack, a back-pressure regulator, a fraction collector to receive the produced fluid, pressure tranducers and thermocouples, and necessary valves and piping.

The core holder was purchased from the Petroleum Recovery Institute in Calgary. It includes an internal copper sleeve, to contain the core or sand, surrounded by an outer steel body. The copper sleeve is radially pressurized with water, and axially stressed by tightening one end of the holder. This is intended to simulate the triaxial overburden stress experienced by sand in a oil reservoir. The ends of the holder are designed specifically to distribute injected fluids evenly at the injection end, and to hold the sand in place at both ends by means of 400 mesh SS screens mounted on top of the distributor plate.

3.2.2 Preparation of the sand pack

Preparation of the sandpack for an experiment followed a fixed protocol throughout the work. Packing of the copper sleeve was carried out from the injection end, with the sleeve mounted in the holder. The copper sleeve has dimensions of 1.50 inches internal diameter by 9.00 inches length, and holds about 200 g of sand. Dry sand was poured into the water-filled sleeve, while the outside of the holder was tapped to cause tighter packing. Water was drained slowly from the bottom (production end) as the holder was filled with sand. The process was completed in 3 - 4 "pours".

When packing was complete, the injection end cap was installed, the holder was mounted on a rack in the oven, and pipes were connected for injection, production, and pressure measurement. Lines to the pressure transducers were filled with water and isolated by valves from the sandpack. Pressure on the outside of the copper sleeve was increased to 500 psig, and monitored to check for leaks. When starting with a fresh sandpack, about 200 mL of methanol was first pumped through the sandpack, after which nitrogen was blown through to remove the methanol. If the sandpack contained residual oil from a previous run, toluene was flowed through the sandpack until the effluent was colorless. The sandpack was then evacuated with a vacuum pump for a period of at least 15 hours. The oven was turned on at 30C, the lowest temperature at which it can control. Brine was then pumped into the sandpack and connecting pipes with the ISCO pump, until the pressure reached 2000 kPa. The water remaining in the pump cylinder at this point was purged and weighed. Since the cylinder holds 505.4 g of water when full, measurement of the amount remaining allowed calculation of the mass of water pumped. The volume of brine (measured at 22 C) in the sandpack was then calculated by subtracting the "dead volume". The dead volume is the volume of fluid in the connecting pipes, and held in the end caps of the core holder. Both flowing and non-flowing dead volumes must be included in calculating the volume of brine in the sandpack (the pore volume). Flowing dead volume is that portion which is flushed during flow through the sandpack, and includes mainly the end cap volumes. Non-flowing dead volume is not flushed during flow, but is evacuated and thus filled with brine when the sandpack is being filled. It includes the portion of the pipes leading to the pressure tranducers up to the valves, and the small reservoirs in the coreholder endcaps intended to minimize plugging of the pressure pipes.

After the pore volume determination, the rest of the piping is filled with brine, and the overburden pressure is increased to 800 psig. The permeability of the sandpack to brine was determined from the pressure drop across the sandpack during flow at 75, 150 and 200 cm^3/hr.

Oil saturation was then initiated by pumping water to displace heavy oil from its reservoir into the sandpack. The water was pumped at 4 cm^3/hr (@ 22 C). Saturation was considered complete when the pressure drop across the pack remained constant for several hours; this usually occurred after about 40 hours of pumping, or about 1.6 pore volumes of oil injected. The total mass of oil in the sandpack and flowing dead volume was determined from the mass of oil injected and by measuring the mass of oil produced. The latter measurement required dilution of the production with toluene, and subtraction of the mass of brine produced from the total fluid produced. From these data the initial oil and water saturation of the sandpack were calculated.

3.2.3 Oil-flow experiments

Following oil saturation at 30 C, and heat-up of the saturated sandpack to the desired temperature, oil or oil plus water were pumped at constant rates for a number of hours. Samples of the production were collected in glass vials at fixed intervals using an autosampler.

4.0 RESULTS AND DISCUSSION

4.1 Initial Sandpack Conditions

The properties and initial saturation conditions of the sandpacks used in these experiments are gathered in Table 4. The sandpack used in Run TFF37 was the one originally prepared for Run TFF33 of Task 7. Its permeability to brine after cleaning was 1.0 Da, about half the average value obtained prior to the previous four floods. Despite the lower permeability, it appeared stable at several flow rates, and was considered adequate for further runs. At the end of Run TFF37, it was cleaned of residual oil, dried,evacuated, and brine saturated in the usual manner (see details in Experimental section) to prepare for another run. However, this time the permeability had dropped to a very low value, and it was decided to prepare a fresh pack. The initial brine permeability of this new pack was identical to the pre-run value of the previous pack, although the porosity was higher. Run TFF38 was an unsuccessful experiment, but the sandpack was again cleaned and prepared for the next run. Permeability increased slightly to 1.3 Da for Run TFF39, but following this run, after clean-up, the permeability once again had deteriorated to a lower and unstable value.

These re-occurring and unpredictable variations in sandpack permeability are attributed to the movement of fine particles, probably partially plugging the screen at the outlet end of the pack. Such plugging phenomena may or may not be relevant to the native reservoir sand, since the "natural" arrangement of grains may be quite different than the arrangement achieved by our packing procedure. The cleaning procedure, which uses organic solvents, may also amplify the fines movement. Such problems are a result of using reservoir sand which still contains a significant amount of fine-grained particles. Up to this point, the advantages of using a more realistic sand for the experiments were considered to outweigh the problems created by permeability variations. This decision was reconsidered, and a more thorough removal of fine particles was performed prior to preparation of the sandpack used for Run TFF43. Other experiments were performed for another project between Runs TFF39 and TFF43, and in addition, NHRC moved to its new facilities, and the coreflooding apparatus was rebuilt.

As seen from data in Table 4 , the re-worked sand gave a much more permeable pack, initially at 10 Da for TFF43, changing to 16 prior to Run TFF44, and dropping back to 10 and 9.0 for subsequent runs. Porosity values measured for this last pack are higher than those obtained for the previous packs, but individual values among the last four measurements correlate poorly with permeability.

The initial oil saturations reported in Table 4 vary from 89 to 98 %, while the separately determined initial brine saturations range from 8 to 17 %. Since the pairs of oil and water values sum to greater than 100%, it is evident that one or the other of them has a consistent positive error. The source of this error has not been identified, and attempts to reduce it by changing the procedures have failed. Consideration of the procedures suggests that oil saturations are determined more directly, and are thus more reliable.

4.2 Oil Flow Experiments

Relevant information was obtained from flow experiments under three different sets of conditions: oil flow at 30 C, oil flow at elevated temperature, and oil-water flow at elevated temperature.

The injection pressure history was collected during oil saturation, as oil displaced brine from the sand at 30 C. Plots of this data for several runs (Figures 3-5) show an increasing injection pressure as the oil saturation in the sand increases, followed by a period of relatively constant pressure at the end of the flood when only oil is flowing. The constancy of the pressure at the end of each flood suggests that neither the sand nor the oil are being affected during the flow at 30 C.

Although the final differential pressure (ΔP) across the sandpack at the end of each of these oil saturation floods was beyond the range of our transducers, and thus could not be measured directly, values were estimated from the injection pressure curves in Figures 3-5. These (ΔP) values were combined with the known flow rate, sandpack dimensions, and oil viscosity to give the effective permeabilities to oil at irreducible brine, koi, shown in brackets in Table 4. The values for Runs 37 and 38 are essentially the same as the brine values, consistent with the high oil saturations (k_{ro} close to 1) and confirming that oil saturation has not changed the permeability. The lower effective permeability for Run 39 may indicate some permeability loss during oil saturation.

Oil was also flowed through the sand at elevated temperatures, with a back pressure sufficient to maintain single phase flow. In Run TFF44, following oil saturation and heat-up, oil was flowed for an additional 8 hr at 226 C. The plot of the differential pressure across the sandpack (ΔP) during this flow (Figure 6) shows very little fluctuation, with an average value of about 5.9 kPa. This indicates that the permeability of the sandpack is not affected by oil flow at elevated temperature.

Viscosities of samples of the oil exiting the sand are given in Table 5 . The constancy of the viscosity confirms that the oil is unchanged by flow through the sand at elevated temperature and pressure.

In Run TFF43, upon completion of oil saturation and heatup to 243 C, both oil and brine were flowed simultaneously through the sandpack, at rates of 4.0 and 1.0 cm^3/hr respectively. As shown in Figure 7, the (ΔP) increases from under 6 kPa initially to level at about 8.5 after 25 hr of flow (1.25 pore volumes, PV). The (ΔP) remained constant for a further 16 hr of two component flow. The brine was then stopped, and only oil was flowed for an additional 8 hr. The gradual increase in (ΔP) over the first 25 hr most likely results from small changes in the saturations in the sand to match the 4:1 oil water ratio being injected. These saturation changes alter the relative permeabilities to oil and brine, and thus affect the (ΔP). However, after injection of 1.25 PV, the (ΔP) became constant reflecting attainment of steady-state saturations. When brine flow was stopped, saturations again adjusted, and the changes in (ΔP) reflect the combination of relative permeability adjustment and lower total flow rate. There is no indication that the fluid flow is altering the absolute permeability of the sandpack.

Viscosity data are plotted in Figure 8(Table 6), for samples of the oil produced during Run TFF43. The viscosity was low in the first sample, jumped to a high value in the second, and gradually decreased to a value lower than that of the original oil within the first 18 hr. The viscosity then remained relatively constant for the remainder of the experiment.

The low viscosity of the first sample was due to an enhancement in light components in this sample, resulting from a small amount of flashing and steam distillation which occurred during heatup. The back pressure was unintentionally left at 2000 kPa during heatup to 243 C, and this caused most of the water remaining in the sandpack and also in the pipes leading to pressure transducers to flash, driving out much more oil than normally obtained due to thermal expansion. The back pressure was then increased, and oil was pumped into the sand to replace that produced. The low viscosity of the first sample produced after beginning to flow oil and water still shows the effects of the flashing during the heatup. The higher viscosity oil produced after the first sample is oil which was depleted slightly in light components, but also may have contained some emulsified water further increasing its viscosity. The lower than expected values from samples produced in the latter part of the experiment were a surprise, for which we have no consistent explanation.

4.3 Displacement Experiments

Four different kinds of flood experiments were carried out. The first experiment, TFF37, was a waterflood at 200 C, with the back-pressure sufficient to prevent steam formation. Oil and water production data throughout the flood are listed in Table 7, and the net oil production history is plotted in Figure 9. The change of slope in the oil production curve after injection of 0.6 pore volumes (PV) of water indicates water breakthrough. Production continued at a slowly declining but still significant rate for the remaining 4.5 PV of flooding.

In Run TFF45, a small slug of oxidized oil with a viscosity nearly 10 fold higher than the native oil, was injected into the oil saturated sandpack prior to waterflooding it at 200 C. The production data presented in Table 8 and plotted in Figure 10 are similar to those from Run TFF37. Direct comparison shows that the change of slope occurs earlier in TFF37 than in TFF45, and the latter curve levels more quickly than the former.

Run TFF46 was also a hot waterflood, but in this case, a slug of lower viscosity oil was injected onto the sand prior to beginning the waterflood. Production data are listed in Table 9. The plot of oil production during the flood (Figure 11) is again very similar to the other two runs, and direct comparison between TFF46 and TFF37 shows the latter had a slightly earlier water breakthrough, but otherwise the two curves are identical.

The fourth experiment, Run TFF39, was analogous to TFF46, but the reduced viscosity slug introduced to the sand was followed by flooding with nitrogen gas rather than water. Since the production was only gas and oil, it was collected in a vessel on a balance, giving oil production directly. The data are given in Table 10 and are plotted in Figure 12. Comparison with the waterfloods shows that considerably less oil was produced by gas before breakthrough, but the rate of production after breakthrough is similar to the rate observed in the waterflood experiment (TFF37).

A summary of all of the recovery data is given in Table 11. Recovery due to expansion on heat-up from 30 to 200 C varied from 13 to 16 % of the original oil in place (OOIP), with the higher values from the higher porosity more permeable sandpack used for Runs TFF45 and TFF46. Recovery on heat-up does not correlate consistently with the amount of oil originally in the sandpack.

Two values for the total recovery are given in Table 11, one obtained directly from the measurements of the oil produced during the flood, and the other derived from measurements of the residual oil left in the sandpack at the end of the flood. While in theory these two values should agree, it is apparent that the recoveries obtained from production measurements are consistently higher than those obtained from residual oil determination. For Run TFF39, the two values are within 3 % OOIP, not unreasonable considering the number and type of measurements involved. The other 3 sets of values differ from 9 to 13 % OOIP. It is evident that there is a significant source of non-random error in these latter 3 runs.

Note that the production data from Run TFF39 were obtained directly from real-time mass measurements. In contrast, production data from the other runs were derived from post-run measurements of the amounts of water or oil collected during the run in a number of small tubes. The latter approach is clearly more complex, and the larger discrepancies between these values and their analogous residual oil derived numbers suggests that the tube data consistently over estimates oil production. Note also that data from TFF37 and TFF46 disagree to about the same extent, despite the change from quantifying oil in the former and water in the latter (see details in Experimental section). Similar discrepancies were observed and discussed in the Steam Distillation experiments (Task 7) reported separately. While the reasons for this discrepancy have not been conclusively identified, the procedure for quantifying the amount of oil produced into a vial has several potential sources of error. During removal of oil from the top of the vials, it is difficult to avoid also removing a small amount of water, either through wetting of the swab used to collect the oil, or emulsified within the oil. Tests confirmed that the swabs used absorb up to 0.2 g of water. Considering that 40-50 vials containing mostly water were collected in each run, an over-estimation of 8-10 grams oil could have occurred.

Comparison of total recoveries from Runs TFF37 and TFF45, (production derived values) suggests that the higher viscosity slug reduced recovery efficiency somewhat. The values from residual oil determinations are less convincing, but support the same conclusion. As noted from comparison of the plots of the production data, recovery due to waterflood was nearly the same for Runs TFF37 and TFF46. The data in Table 11 suggest that the low viscosity slug may have caused a slight increase in recovery.

When a low viscosity slug was followed by gas, recovery was much lower than in the analogous experiment with water, consistent with results obtained in Task 7 experiments. A gasflood without an initial slug in those previous runs recovered 56 % OOIP (see Table 12, Task 7 results). Although some of the conditions in this previous flood were different than in Run TFF39, it appears that recovery was reduced by the slug of lower viscosity oil.

These displacement experiments were intended to examine the sensitivity of recovery under thermal conditions to the introduction of variations in oil viscosity in the region of the displacement front. It was reasoned that introduction of oil of reduced viscosity, analogous to that produced by thermal cracking just downstream of a combustion front, would reduce the mobility ratio (M_w/M_o) at the displacement front, and that this would increase the displacement efficiency. An alternate mechanism might be important, in which the low viscosity oil would actually allow faster fingering through of the water or gas, resulting in poorer recovery. The results showed that a slug of oil of reduced viscosity, placed in the region just downstream of a water-oil or gas-oil displacement front, gave only a very small difference in the flood behavior. Altering the mobility ratio in the opposite way, by introducing a slug of higher viscosity oil, produced a noticeable decrease in the recovery curve. Although the differences among the three waterflood experiments are small, the shifts in the time required for water breakthrough, the differences in the slopes of the curves, and the changes in total recovery all present a consistent picture. Introducing a high viscosity slug changes the mobility ratio (displaced to displacing fluid) at the front sufficiently to increase fingering of the water, which results in faster water breakthrough. After breakthrough, the mobility ratio remains less favorable to displacement, and the rate of recovery (slope of production curve) is thus lower than in the waterflood case. The low viscosity slug has the opposite effect, slowing breakthrough, but the improved mobility ratio is either too short-lived or too small in magnitude to have a noticeable effect on the recovery rate after breakthrough.

In the gasflood experiment, the mobility ratio is probably an order of magnitude less favorable, and thus the change resulting from a slug of low viscosity oil is overwhelmed by other effects. There are actually relatively few reports in the literature of waterfloods of heavy oils at elevated temperatures. The work of Willman *et al.* (5) has already been thoroughly discussed in the Literature Review section, in Volume I of this Report. These workers flooded cold, oil saturated cores with water and steam under a variety of temperature and pressure conditions. The most relevant experiments were those using a crude oil having a viscosity of 6500 mPa.s at room temperature. Injection of water at 166 C (pressure above saturated steam value) recovered 60 % OOIP, and subsequent steamflood increased recovery to 71 %. Other runs with the same crude oil gave steam recoveries of 74 and 77 % OOIP. These values are quite similar to those in Table 11 obtained under isothermal waterflood conditions. The similarity between these results under apparently different experimental conditions may not be coincidental, since the actual fluid at the displacing front in the non-isothermal steamfloods is likely mostly hot water.

Edmondson (6) reported on a number of isothermal hot water floods of consolidated cores saturated with several different oils. Results with crude oil "B" , which had a viscosity of several thousand mPa.s at 25 C, show 48 % PV recovery from waterflood at 149 C after 6 pore volumes of injection. Noting that the initial oil saturation was 78 % PV, the recovery corresponds to 61 % OOIP. Adding another 10 % contribution from thermal expansion during heat-up to 149 C, which was explicitly excluded by Edmondson, brings the total recovery to 71%, quite similar to the 75-80 % values reported in Table 11.

5.0 CONCLUSIONS

1. Flowing native Tangleflags oil at low rate through reservoir sand had no effect on either the permeability of the sand or on the viscosity of the oil, at temperatures of 30 and 226 C and pressures sufficient to prevent steam formation.

2. Simultaneous flow of Tangleflags oil and water, both at fixed rates, through a sandpack at 243 C, also had no effect on the absolute permeability of the sand, but the viscosity of the oil produced showed some small unexplained variations.

3. In a hot waterflood of a Tangleflags sandpack, injection of a slug of high viscosity oxidized oil ahead of the water gave a slight reduction in recovery efficiency. A slug of low viscosity oil injected ahead of water gave a small improvement in oil recovery. Recovery with nitrogen at 200 C was reduced by introducing a low viscosity slug prior to beginning the gas flood.

6.0 REFERENCES

1. Waxman, M.H., Closmann, P.J., and Deeds, C.T. "Peace River Tar Flow Experiments under *in situ* Conditions". SPE 9511, 1980.

2. Mansoori, G.A. and Jiang, T.S. "Asphaltene Deposition and its Role in EOR Miscible Gas Flooding", 3rd AGIP *et al.* Improved Oil Recovery, Europ. Mtg., Proc. Vol. 2, p. 75, 1985.

3. Hirschberg, A., *et al.*, "Influence of Temperature and Pressure on Asphaltene Flocculation", SPEJ 24(3), 283, 1984.

4. Gould, K.A., "Influence of Thermal Processing on the Properties of Cold Lake Asphaltenes. 2. Effect of steam treatment during oil recovery", Fuel 62, 370, 1982.

5. Willman, B.T., *et al.*, "Laboratory Studies of Oil Recovery by Steam Injection", J. Petr. Tech. July 1961, p. 681.

6. Edmondson, T.A., "Effect of Temperature on Waterflooding", J.C.P.T. Oct.-Dec. 1965, p. 236.

7.0 TABLES

Table 1: Particle Size Distribution of Tangleflags Sand Sample

Sieve Size		Mass Retained %	Cumulative Mass Retained, %
US Mesh	mm		
35	0.500	2.9	2.9
60	0.250	2.7	5.6
80	0.177	12.6	18.2
120	0.125	36.6	54.7
170	0.0884	25.3	80.0
230	0.0625	10.9	90.9
325	0.0442	1.7	92.6
<325	<0.0442	7.4	100.0

Median Grain Size, mm	0.1305
Mean Grain Size, mm	0.1230

Table 2: Composition of Native Tangleflags Brine[a]

NaCl	58.5
$CaCl_2$	5.55
$MgCl_2 \cdot H_2O$	3.91
KCl	0.67

a) Amounts are given in grams of the specified salt per liter of solution

Table 3: Comparison of Native and Oxidized Oil Samples

	Native	Oxidized	Diluted[a]
Viscosity (mPa.s)			
@ 25C	5500	51800	730
@ 30C	3600		-
Oxygen Content (mass %)	0.42	1.58	-
Pentane Insolubles (mass %)	13.8	19.7	-

a) Sample of native oil with 7 mass % toluene added.

Table 4: Initial Sandpack Conditions

Run #	Sandpack #	Permeability[a] (Da)	Pore Volume (cm^3)	Porosity (Volume %)	Oil Injected (cm^3)	Brine Recovered (cm^3)	Saturation[b] Oil	Saturation[b] Water
TFF37	1	1.0 (0.9)	96.5	35.3	97.5	93.5	93.0	7 (11)
TFF38	2	1.0 (1.0)	101.7	37.3	98.5	95.0	89.0	11 (14)
TFF39	2	1.3 (0.7)	98.7	36.1	104.5	92.0	98.0	2 (14)
TFF43	3	10	109.9	40.3	na	na	na	na
TFF44	3	16	105.6	38.7	112.8	105.0	98.0	2 (8)
TFF45	3	10	107.0	39.2	103.9	97.0	89.0	11 (17)
TFF46	3	9	104.2	38.2	103.1	95.0	91.0	9 (17)

a) Values determined from differential pressure measurements at 3 different fixed flow rates of brine. Values in brackets calculated from ΔP measurements at the end of oil saturation.

b) Oil saturations in volume %, determined from oil mass balance, water values by difference. Bracketted water values determined from brine produced during oil saturation.

Table 5: Viscosities of Oil Samples Produced from Sandpack at 226 C

Sample[a]	Viscosity Pa.s @ 25 C
Original	5.50
1	5.72
2	5.53
3	5.76
4	5.55
5	5.66
6	5.75
7	5.67

a) Measurements made on a small portion of the 10 cm^3 of oil collected over a 1 hour period from Run TFF44.

Table 6: Viscosity of Oil Produced from Run TFF 43

Time (hr)	Viscosity @25C (Pa.s)
1.5	2.87
3.0	8.96
4.5	7.56
6.0	7.61
7.5	7.66
9.0	7.61
10.5	7.48
12.0	7.27
13.5	6.67
15.0	5.83
16.5	5.10
18.0	4.81
19.5	4.71
21.0	4.70
22.5	4.87
24.0	5.10
25.5	5.04
27.0	4.97
28.5	4.90
30.0	4.92
31.5	4.89

Table 6 continued...

Time (hr)	Viscosity @25C (Pa.s)
33.0	4.94
34.5	4.93
36.0	4.94
37.5	4.86
39.0	4.86
40.5	4.89
42.0	4.89
43.5	4.85
45.0	4.86
46.5	5.04
48.0	4.95
49.5	4.90
51.0	4.86
52.5	4.93
54.0	5.04

Table 7: Oil Production During Waterflood - Run TFF 37

Time (hr)	Volume Injected (PV)	Incremental Oil (g)	Net Cum Oil (g)	Net Oil (%OIP)
1.0	0.1	10.2	2.5	17.0
2.0	0.2	6.7	9.2	24.4
3.0	0.3	11.1	20.3	36.8
4.0	0.4	10.2	30.5	48.2
5.0	0.5	9.9	40.4	59.2
6.0	0.6	3.5	44.0	63.2
7.0	0.7	1.6	45.5	64.9
8.0	0.8	1.2	46.8	66.3
9.0	0.9	1.1	47.9	67.5
10.0	1.0	1.0	48.9	68.7
11.0	1.1	0.9	49.7	69.5
12.0	1.2	1.1	50.9	70.9
13.0	1.3	0.9	51.7	71.8
14.0	1.5	0.9	52.6	72.8
15.0	1.6	0.8	53.4	73.7
16.0	1.7	0.7	54.0	74.3
17.0	1.8	0.7	54.8	75.2
18.0	1.9	0.8	55.5	76.0
19.0	2.0	0.7	56.2	76.8
20.0	2.1	0.7	56.9	77.6

Table 7 continued...

Time (hr)	Volume Injected (PV)	Incremental Oil (g)	Net Cum Oil (g)	Net Oil (%OIP)
21.0	2.2	0.7	57.6	78.3
22.0	2.3	0.5	58.2	79.0
23.0	2.4	0.6	58.7	80.2
25.0	2.6	0.2	59.5	79.6
24.0	2.5	0.5	59.3	80.5
27.0	2.8	0.4	60.4	81.5
28.0	2.9	0.6	61.0	82.1
29.0	3.0	0.3	61.4	82.6
30.0	3.1	0.4	61.8	83.5
32.0	3.3	0.3	62.5	83.0
31.0	3.2	0.4	62.2	83.8
33.0	3.4	0.4	62.8	84.1
34.0	3.5	0.4	63.2	84.6
35.0	3.6	0.2	63.5	84.9
36.0	3.7	0.4	63.9	85.4
37.0	3.8	0.4	64.3	85.8
38.0	3.9	0.3	64.6	86.1
39.0	4.0	0.3	64.9	86.5
40.0	4.1	0.8	65.7	87.4
41.0	4.2	0.2	65.9	87.6
42.0	4.4	0.3	66.2	87.9

Table 7 continued...

Time (hr)	Volume Injected (PV)	Incremental Oil (g)	Net Cum Oil (g)	Net Oil (%OIP)
43.0	4.5	0.3	66.4	88.1
45.0	4.7	0.2	66.9	88.7
44.0	4.6	0.2	66.7	88.5
46.0	4.8	0.4	67.3	89.1
47.0	4.9	0.2	67.6	89.5
48.0	5.0	0.2	67.8	89.7
49.0	5.1	0.3	68.1	90.0
50.0	5.2	0.2	68.3	90.3

Table 8: Oil Production during Waterflood Run TFF 45

Time (hr)	PV INJ.	Increm. Prod.	Net Cum Oil (g)	Net Oil (%OIP)
2.00	0.21	6.70	6.10	21.41
3.00	0.32	10.00	16.10	31.93
4.00	0.42	10.00	26.10	42.44
5.00	0.53	10.10	36.20	53.07
6.00	0.63	3.90	40.10	57.17
7.00	0.74	2.70	42.80	60.01
8.00	0.84	2.10	44.90	62.21
9.00	0.95	1.60	46.50	63.90
10.00	1.05	1.40	47.90	65.37
11.00	1.16	1.20	49.10	66.63
12.00	1.26	1.10	50.10	67.68
13.00	1.37	1.10	51.20	68.84
14.00	1.47	0.90	52.10	69.78
15.00	1.58	0.90	53.00	70.73
16.00	1.68	0.90	53.90	71.68
17.00	1.79	0.70	54.60	72.41
18.00	1.89	0.70	55.30	73.15
19.00	2.00	0.50	55.80	73.68
20.00	2.10	0.50	56.20	74.10
21.00	2.21	0.40	56.60	74.52
22.00	2.31	0.10	56.70	74.62

Table 8 continued...

Time (hr)	PV INJ.	Increm. Prod.	Net Cum Oil (g)	Net Oil (%OIP)
23.00	2.42	0.30	57.00	74.94
24.00	2.52	0.30	57.30	75.25
25.00	2.63	0.30	57.60	75.57
26.00	2.74	0.40	58.00	75.99
27.00	2.84	0.30	58.30	76.30
28.00	2.95	0.10	58.40	76.41
29.00	3.05	0.30	58.70	76.72
30.00	3.16	0.30	59.00	77.04
31.00	3.26	0.10	59.10	77.15
32.00	3.37	0.00	59.10	77.15
33.00	3.47	0.50	59.60	77.67
34.00	3.58	-0.30	59.60	77.67
35.00	3.68	0.60	60.10	78.20
36.00	3.79	-0.50	60.10	78.20
37.00	3.89	0.00	60.20	78.30
38.00	4.00	0.50	60.70	78.83
39.00	4.10	0.80	61.50	79.67
40.00	4.21	0.10	61.60	79.77
41.00	4.31	0.20	61.80	79.98
42.00	4.42	0.10	62.00	80.19

Table 8 continued...

Time (hr)	PV INJ.	Increm. Prod.	Net Cum Oil (g)	Net Oil (%OIP)
43.00	4.52	0.10	62.10	80.30
44.00	4.63	0.10	62.20	80.40
45.00	4.73	0.00	62.20	80.40
46.00	4.84	0.10	62.30	80.51
47.00	4.94	0.10	62.50	80.72
48.00	5.05	0.10	62.60	80.83
49.00	5.15	0.10	62.70	80.93
50.00	5.26	0.80	63.50	81.77
51.00	5.37	0.20	63.70	81.98
52.00	5.47	0.10	63.80	82.09
53.00	5.58	0.20	64.00	82.30
54.00	5.68	0.10	64.10	82.40
55.00	5.79	0.10	64.30	82.61
56.00	5.89	0.10	64.40	82.72
57.00	6.00	0.10	64.50	82.82
58.00	6.10	0.10	64.60	82.93
59.00	6.21	0.10	64.70	83.03
60.00	6.31	0.10	64.80	83.14
61.00	6.42	0.10	64.90	83.24
62.00	6.52	0.10	65.00	83.35
63.00	6.63	0.10	65.10	83.45

Table 8 continued...

Time (hr)	PV INJ.	Increm. Prod.	Net Cum Oil (g)	Net Oil (%OIP)
64.00	6.73	0.20	65.20	83.56
65.00	6.84	0.30	65.50	83.87
66.00	6.94	0.10	65.60	83.98
67.00	7.05	0.10	65.70	84.09
68.00	7.15	0.10	65.80	84.19
69.00	7.26	0.20	66.00	84.40
70.00	7.36	0.10	66.00	84.40

Table 9: Oil Production during Waterflood Run TFF 46

Time (hr)	PV INJ.	Increm. Prod.	Net Cum Oil (g)	Net Oil (%OIP)
1.00	0.11	9.30	0.50	16.83
2.00	0.21	6.70	7.20	23.94
3.00	0.32	10.00	17.20	34.54
4.00	0.42	9.60	26.80	44.72
5.00	0.53	9.40	36.20	54.69
6.00	0.64	4.90	41.10	59.88
7.00	0.74	3.50	44.60	63.60
8.00	0.85	2.50	47.10	66.25
9.00	0.95	2.00	49.10	68.37
10.00	1.06	2.00	51.10	70.49
11.00	1.17	1.70	52.80	72.29
12.00	1.27	1.10	53.90	73.46
13.00	1.38	1.30	55.30	74.94
14.00	1.48	0.80	56.10	75.79
15.00	1.59	0.60	56.70	76.43
16.00	1.70	0.60	57.40	77.17
17.00	1.80	0.70	58.10	77.91
18.00	1.91	0.70	58.80	78.65
19.00	2.01	0.40	59.20	79.08
20.00	2.12	0.20	59.50	79.40
21.00	2.23	0.50	60.00	79.93
22.00	2.33	0.50	60.50	80.46

Table 9 continued...

Time (hr)	PV INJ.	Increm. Prod.	Net Cum Oil (g)	Net Oil (%OIP)
23.00	2.44	0.30	60.80	80.78
24.00	2.54	0.60	61.40	81.41
25.00	2.65	0.30	61.70	81.73
26.00	2.76	0.40	62.10	82.15
27.00	2.86	0.40	62.50	82.58
28.00	2.97	0.40	62.90	83.00
29.00	3.07	0.40	63.30	83.43
30.00	3.18	0.50	63.80	83.96
31.00	3.29	0.50	64.30	84.49
32.00	3.39	0.40	64.70	84.91
33.00	3.50	0.40	65.10	85.33
34.00	3.60	0.50	65.70	85.97
35.00	3.71	0.40	66.10	86.40
36.00	3.82	0.50	66.50	86.82
37.00	3.92	0.40	66.90	87.24
38.00	4.03	0.70	67.60	87.99
39.00	4.13	0.20	67.80	88.20
40.00	4.24	0.40	68.20	88.62
41.00	4.35	0.30	68.50	88.94

Table 9 continued...

Time (hr)	PV INJ.	Increm. Prod.	Net Cum Oil (g)	Net Oil (%OIP)
42.00	4.45	0.50	68.90	89.36
43.00	4.56	0.40	69.30	89.79
44.00	4.66	0.20	69.50	90.00
45.00	4.77	0.50	69.90	90.43
46.00	4.88	0.00	69.90	90.43
47.00	4.98	0.40	70.30	90.85
48.00	5.09	0.00	70.30	90.85
49.00	5.19	0.00	70.30	90.85
50.00	5.30	0.00	70.30	90.85

Table 10: Oil Production during Gasflooding Run TFF 39

Time (hr)	PV INJ.	Increm. Prod.	Net Cum Oil (g)	Net Oil (%OIP)
0.00	0.0	25.70	-7.7	5.1
0.30	0.2	35.30	1.9	15.1
0.70	0.5	37.70	4.3	17.5
1.00	0.8	41.40	8.0	21.4
1.30	1.0	44.30	10.9	24.4
1.70	1.3	48.20	14.8	28.4
2.00	1.5	50.00	16.6	30.2
2.30	1.7	51.40	18.0	31.7
2.70	2.1	51.70	18.3	32.0
3.00	2.3	52.00	18.6	32.3
3.30	2.5	52.30	18.9	32.6
3.70	2.8	52.80	19.4	33.1
4.00	3.0	53.30	19.9	33.7
4.30	3.3	53.90	20.5	34.3
4.70	3.6	54.20	20.8	34.6
5.00	3.8	54.70	21.3	35.1
5.30	4.0	55.30	21.9	35.7
5.70	4.3	55.80	22.4	36.2
6.00	4.6	56.40	23.0	36.9
6.30	4.8	56.90	23.5	37.4
6.70	5.1	57.10	23.7	37.6
7.00	5.3	57.40	24.0	37.9

Table 10 continued...

Time (hr)	PV INJ.	Increm. Prod.	Net Cum Oil (g)	Net Oil (%OIP)
7.30	5.5	57.80	24.4	38.3
7.70	5.9	58.40	25.0	38.9
8.00	6.1	58.60	25.2	39.1
8.30	6.3	59.00	25.6	39.5
8.70	6.6	59.20	25.8	39.8
9.00	6.8	59.50	26.1	40.1
9.30	7.1	59.60	26.2	40.2
9.70	7.4	59.90	26.5	40.5
10.00	7.6	59.90	26.5	40.5
10.30	7.8	60.20	26.8	40.8
10.70	8.1	60.40	27.0	41.0
11.00	8.4	60.60	27.2	41.2
11.30	8.6	61.00	27.6	41.6
11.70	8.9	61.10	27.7	41.7
12.00	9.1	61.50	28.1	42.1
12.30	9.3	61.50	28.1	42.1
12.70	9.7	61.80	28.4	42.4
13.00	9.9	62.00	28.6	42.6
13.30	10.1	62.30	28.9	43.0
13.70	10.4	62.50	29.1	43.2
14.00	10.6	62.80	29.4	43.5

Table 10 continued...

Time (hr)	PV INJ.	Increm. Prod.	Net Cum Oil (g)	Net Oil (%OIP)
14.30	10.9	62.90	29.5	43.6
14.70	11.2	63.10	29.7	43.8
15.00	11.4	63.50	30.1	44.2
15.30	11.6	63.60	30.2	44.3
15.70	11.9	63.80	30.4	44.5
16.00	12.2	64.00	30.6	44.7
16.30	12.4	64.30	30.9	45.0
16.70	12.7	64.50	31.1	45.2
17.00	12.9	64.70	31.3	45.4
17.30	13.1	65.00	31.6	45.7
17.70	13.5	65.20	31.8	46.0
18.00	13.7	65.40	32.0	46.2
18.30	13.9	65.70	32.3	46.5
18.70	14.2	65.80	32.4	46.6
19.00	14.4	66.10	32.7	46.9
19.30	14.7	66.30	32.9	47.1
19.70	15.0	66.50	33.1	47.3
20.00	15.2	66.70	33.3	47.5
20.30	15.4	66.90	33.5	47.7

Table 11: Results of Displacement Experiments

Run #	Conditions[a]	OOIP (g)	Oil Produced (g)		FDV[c]	Recovery (% OOIP)				Residual Oil, % PV
								TOTAL PRODUCED		
			HU	WF/GF[b]		HU	WF/GF	Produced	Mass Balance	
TFF37	200C WF	89.8	13.8	76.0	7.7	14.2	76.1	90	77	21
TFF45	High viscosity Slug, 200C WF	95.1	15.6	74.8	8.8	15.0	69.4	84	75	22
TFF46	Low viscosity Slug, 200C WF	94.3	16.8	79.1	8.8	16.3	74.6	91	80	19
TFF39	Low viscosity Slug, 200C GF	96.8	13.7	41.4	7.7	13.1	34.8	48	45	54

a) WF = waterflood. GF = gasflood
b) Total production from waterflood or gasflood, including flowing dead volume
c) Flowing dead volume, cm^3

8.0 FIGURES

FIGURE 1

INFRARED SPECTRUM OF OXIDIZED TANGLEFLAGS OIL

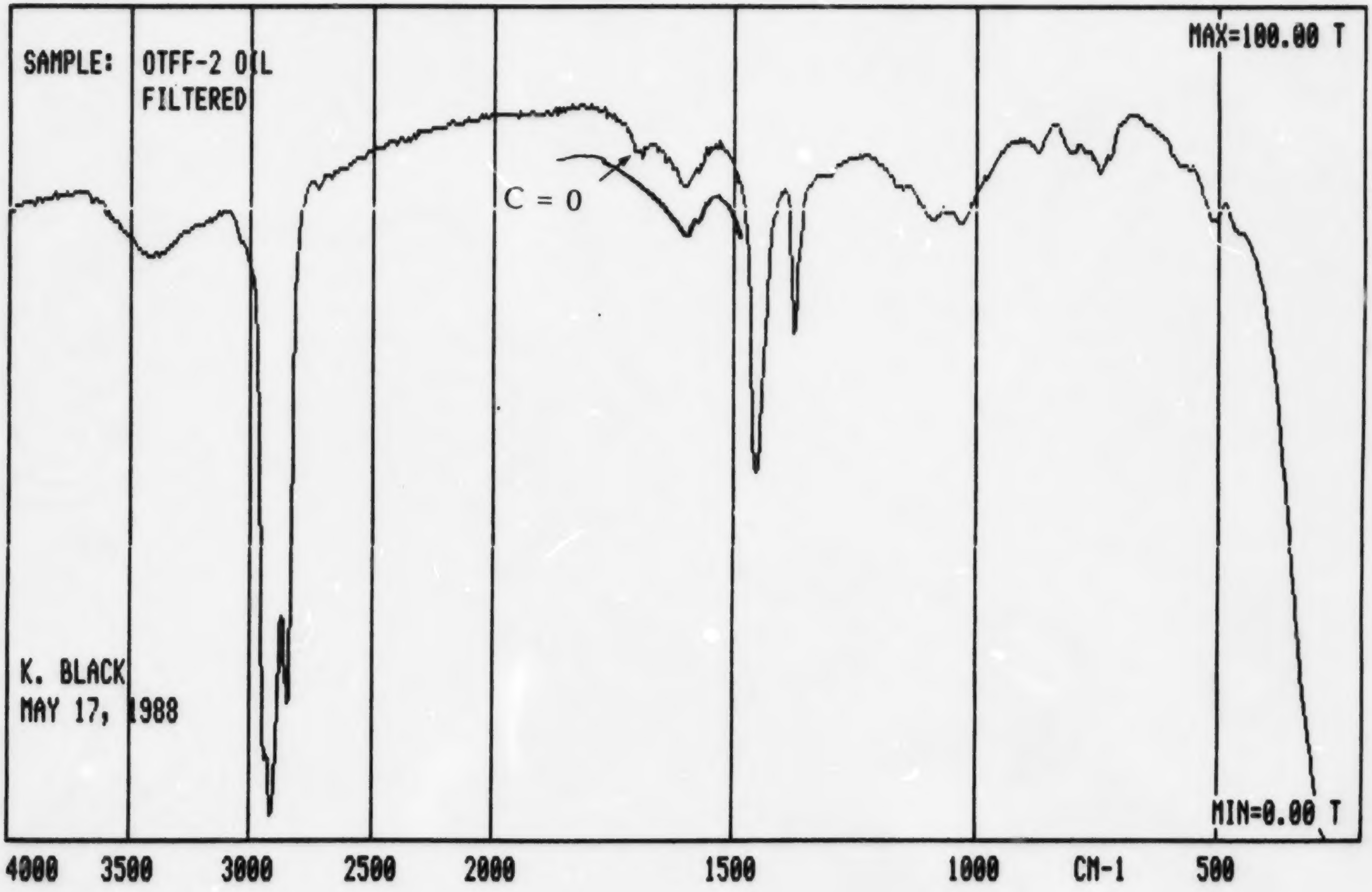

FIGURE 2

SCHEMATIC DIAGRAM OF COREFLOOD APPARATUS

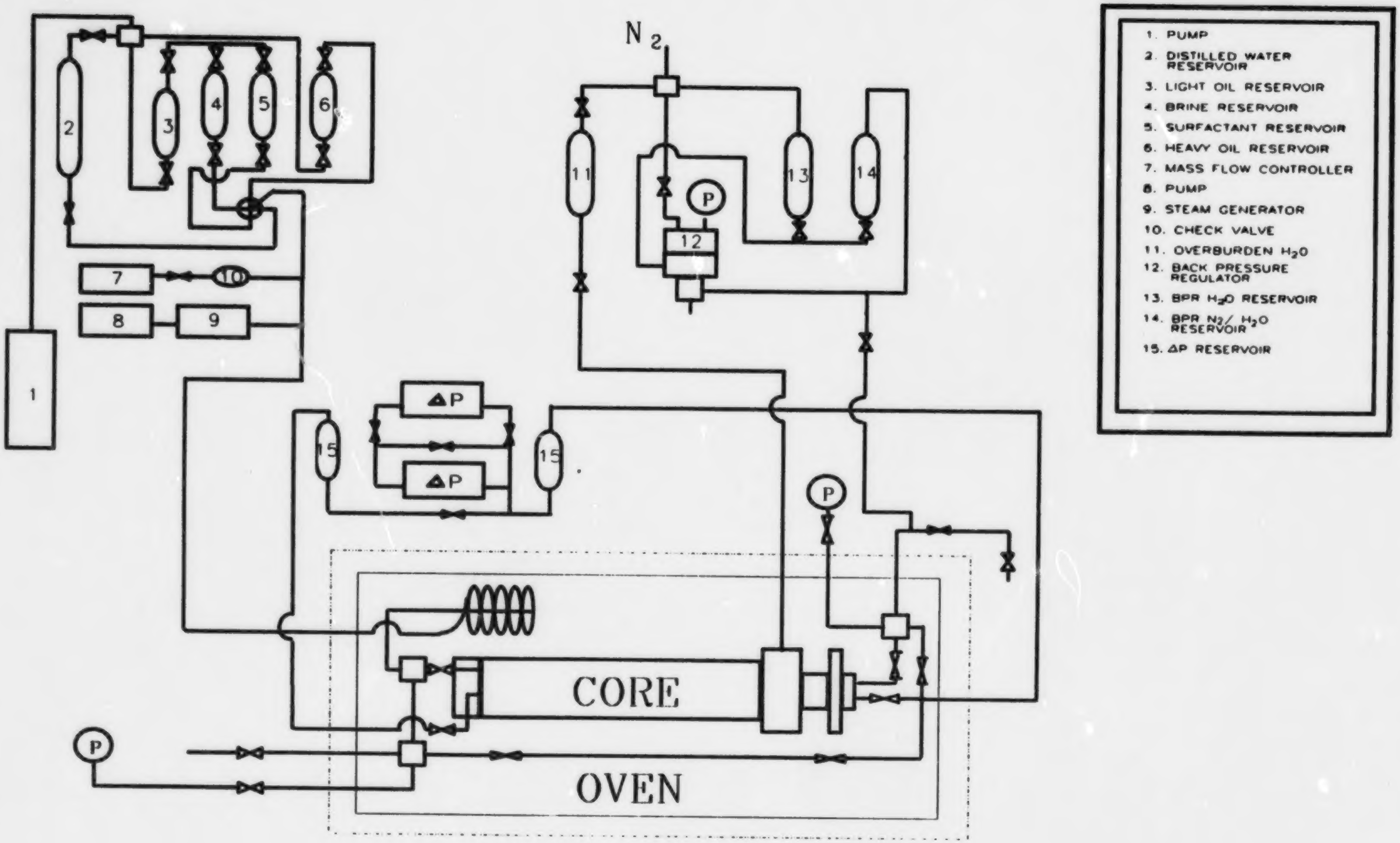
1. PUMP
2. DISTILLED WATER RESERVOIR
3. LIGHT OIL RESERVOIR
4. BRINE RESERVOIR
5. SURFACTANT RESERVOIR
6. HEAVY OIL RESERVOIR
7. MASS FLOW CONTROLLER
8. PUMP
9. STEAM GENERATOR
10. CHECK VALVE
11. OVERBURDEN H_2O
12. BACK PRESSURE REGULATOR
13. BPR H_2O RESERVOIR
14. BPR N_2/ H_2O RESERVOIR
15. ΔP RESERVOIR
N_2
P
ΔP
ΔP
CORE
OVEN

© 1988 NOVA HUSKY RESEARCH CORPORATION

Figure 3: Oil Saturation for TFF37

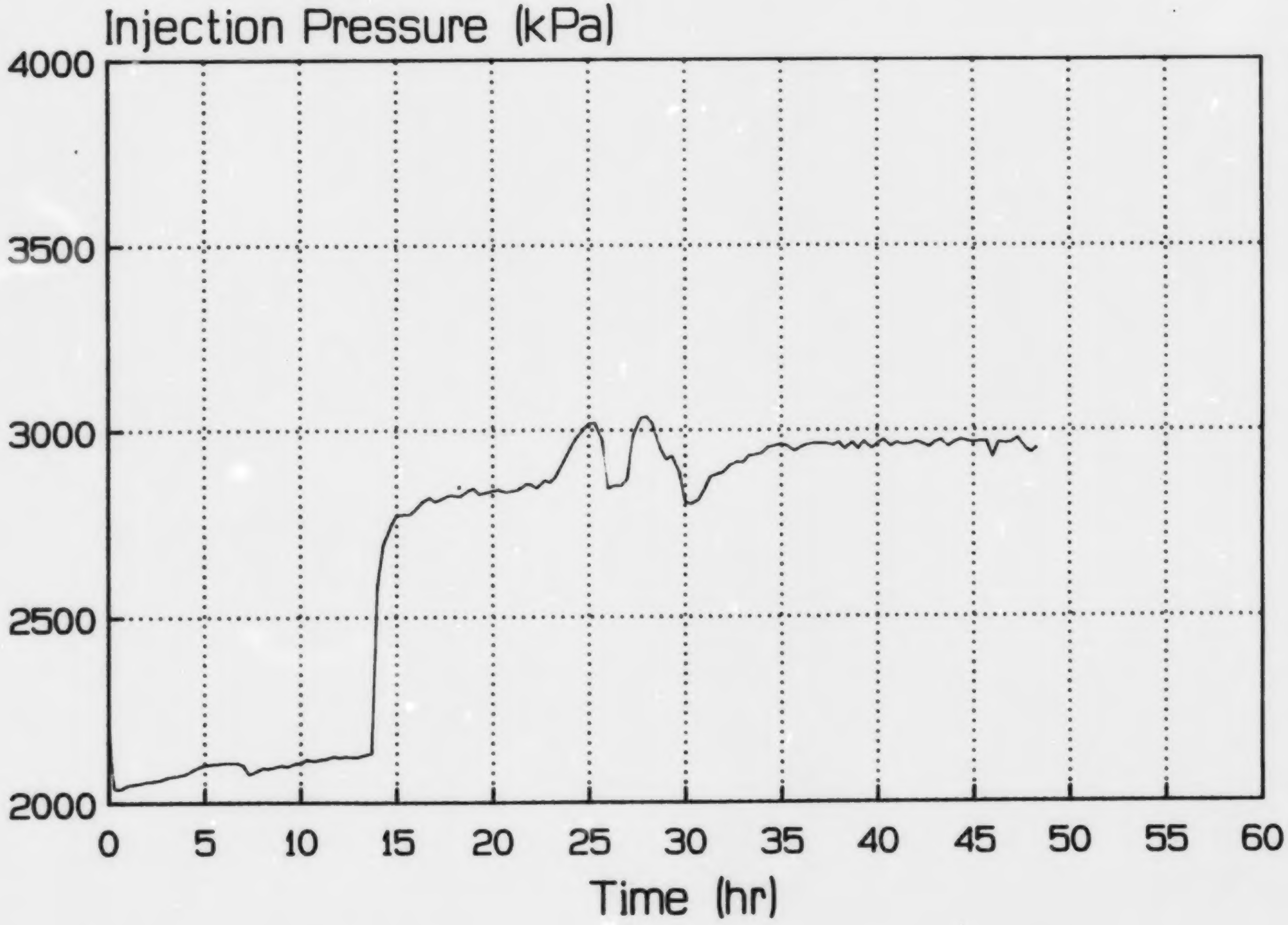

Figure 4: Oil Saturation for TFF38

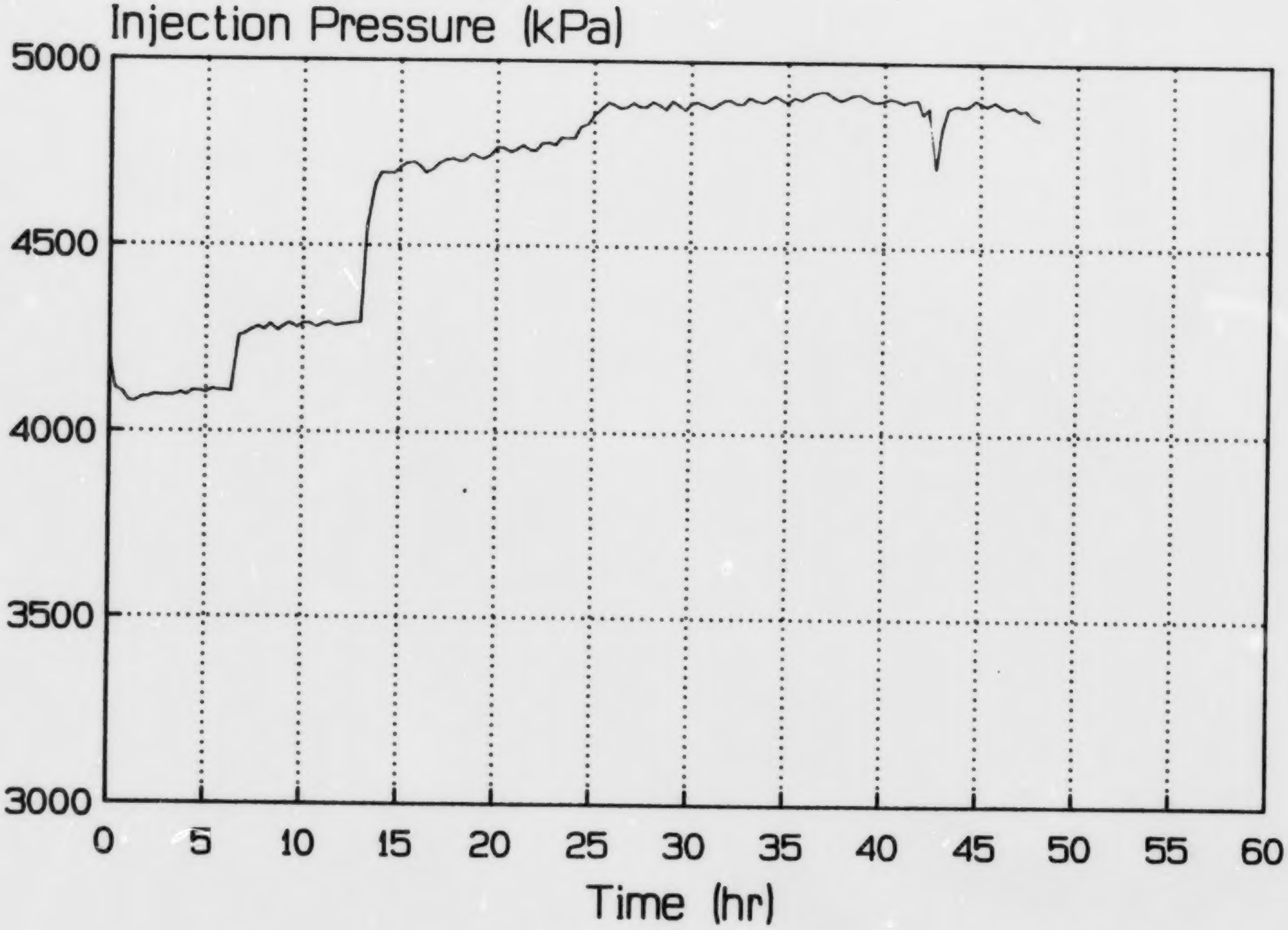

Figure 5: Oil Saturation for TFF39

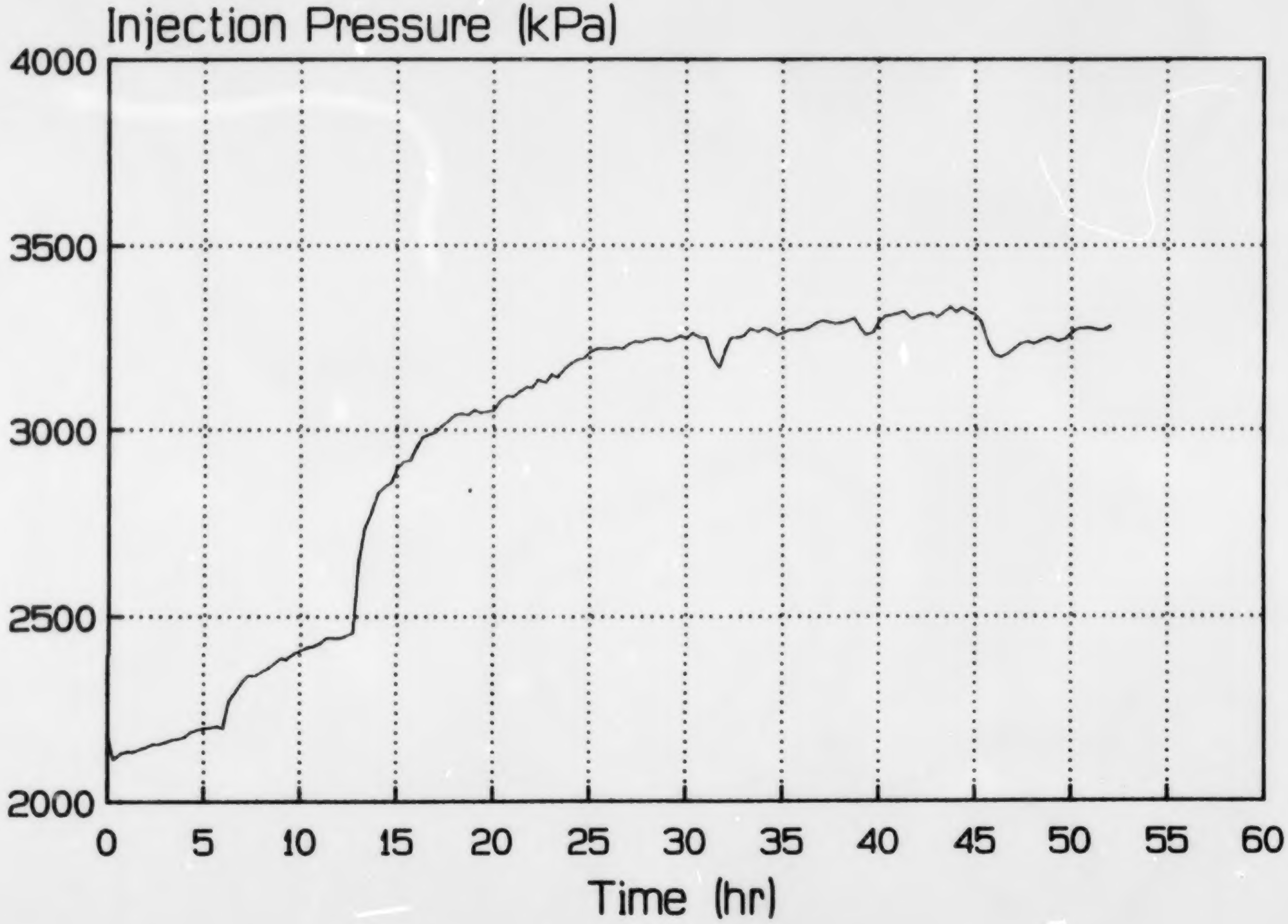

Figure 6: Oil Flood Run TFF44

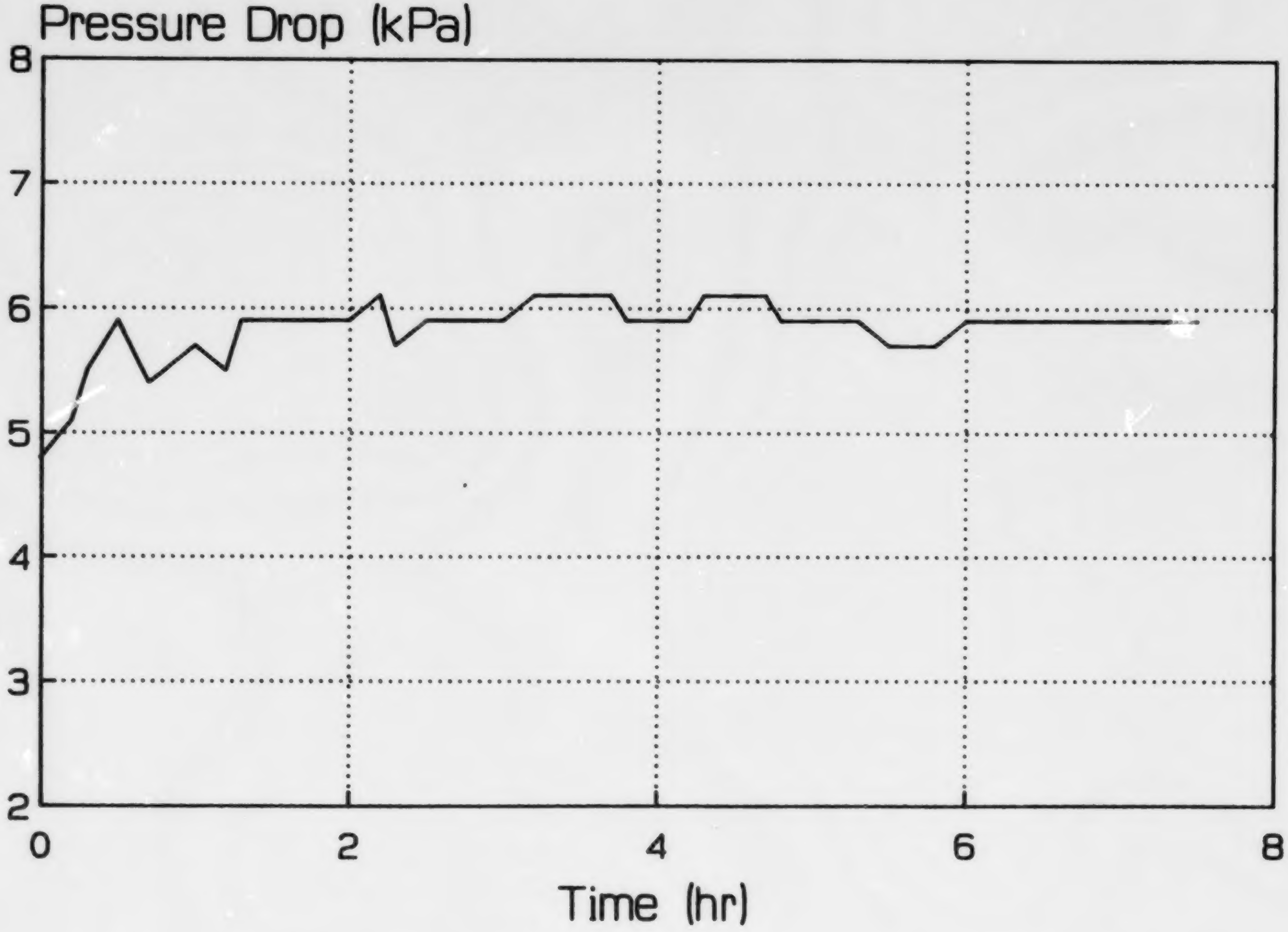

Figure 7: Oil/Water Flood Run TFF43

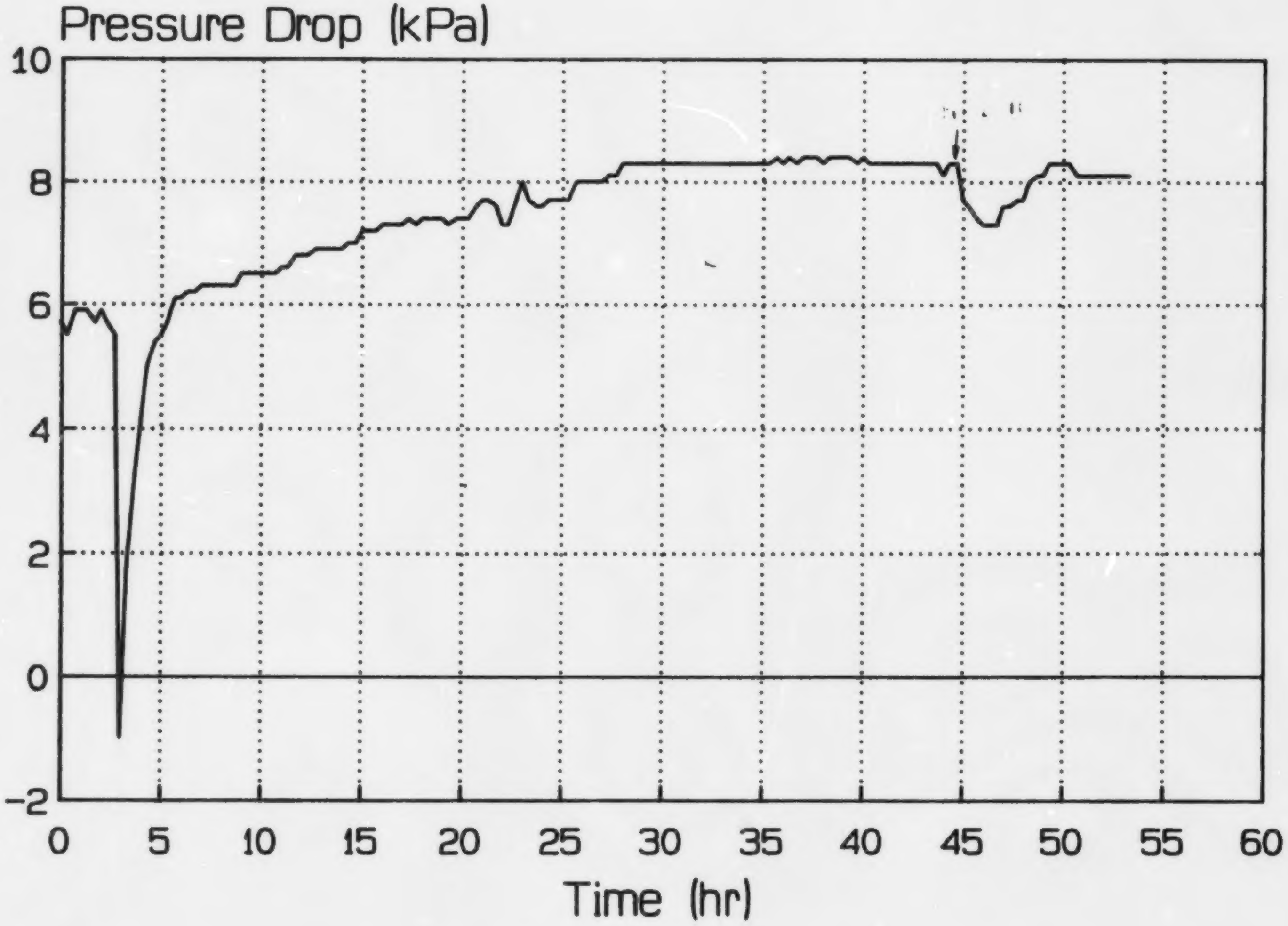

Figure 8: Viscosity of Produced Oil from Run TFF43

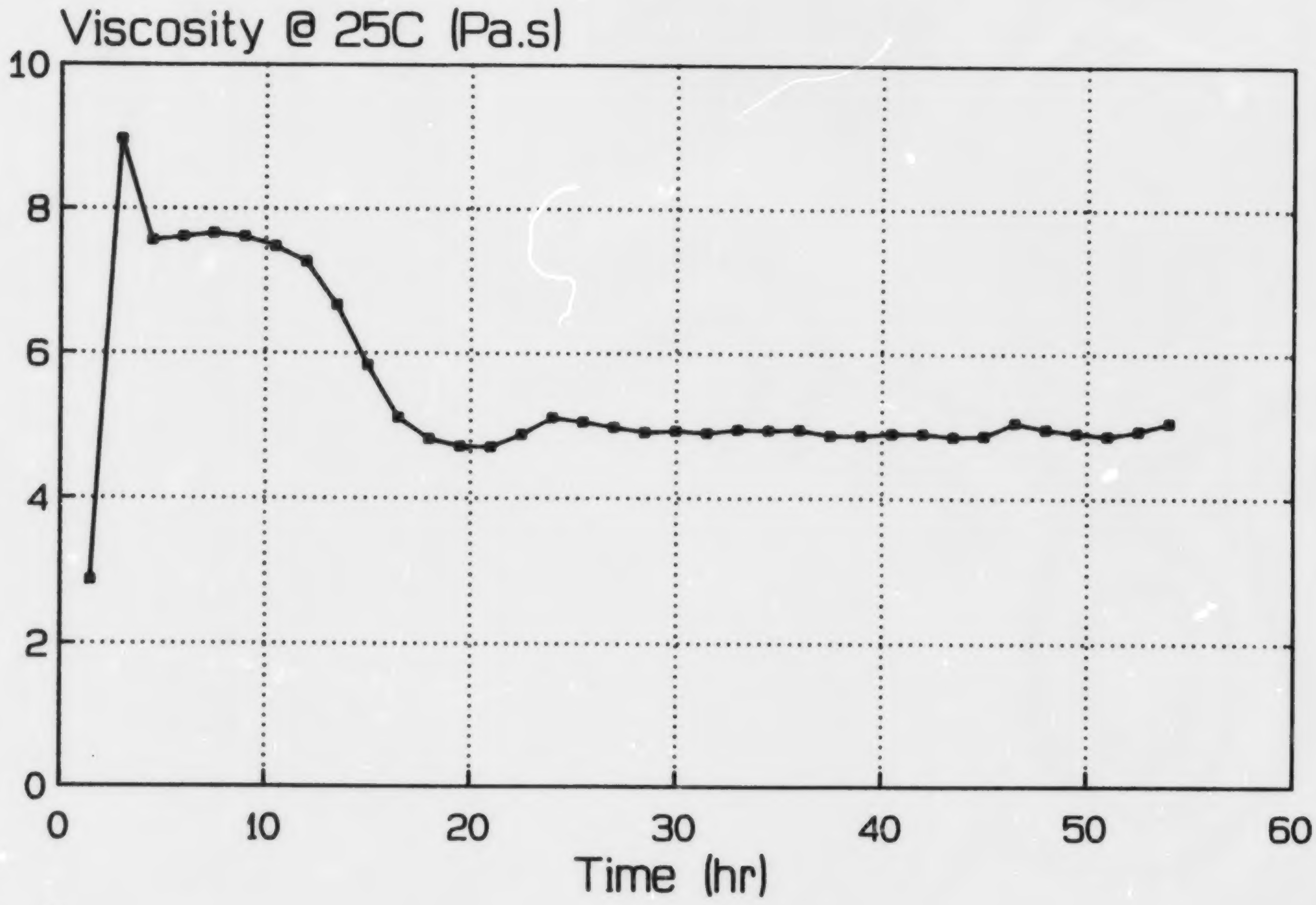

Figure 9: Oil Production during Waterflood Run TFF 37

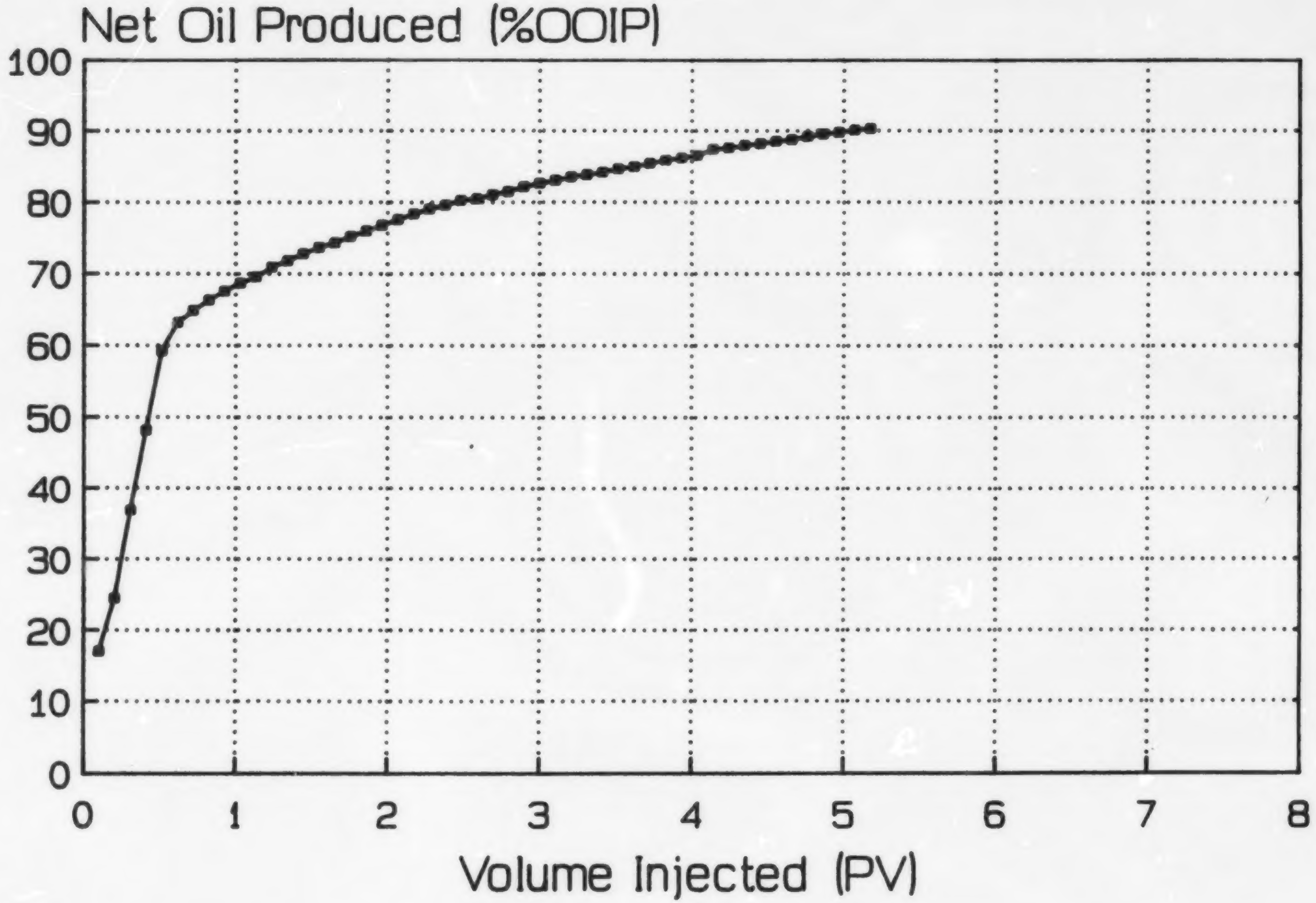

Figure 10: Oil Production during Waterflood Run TFF 45

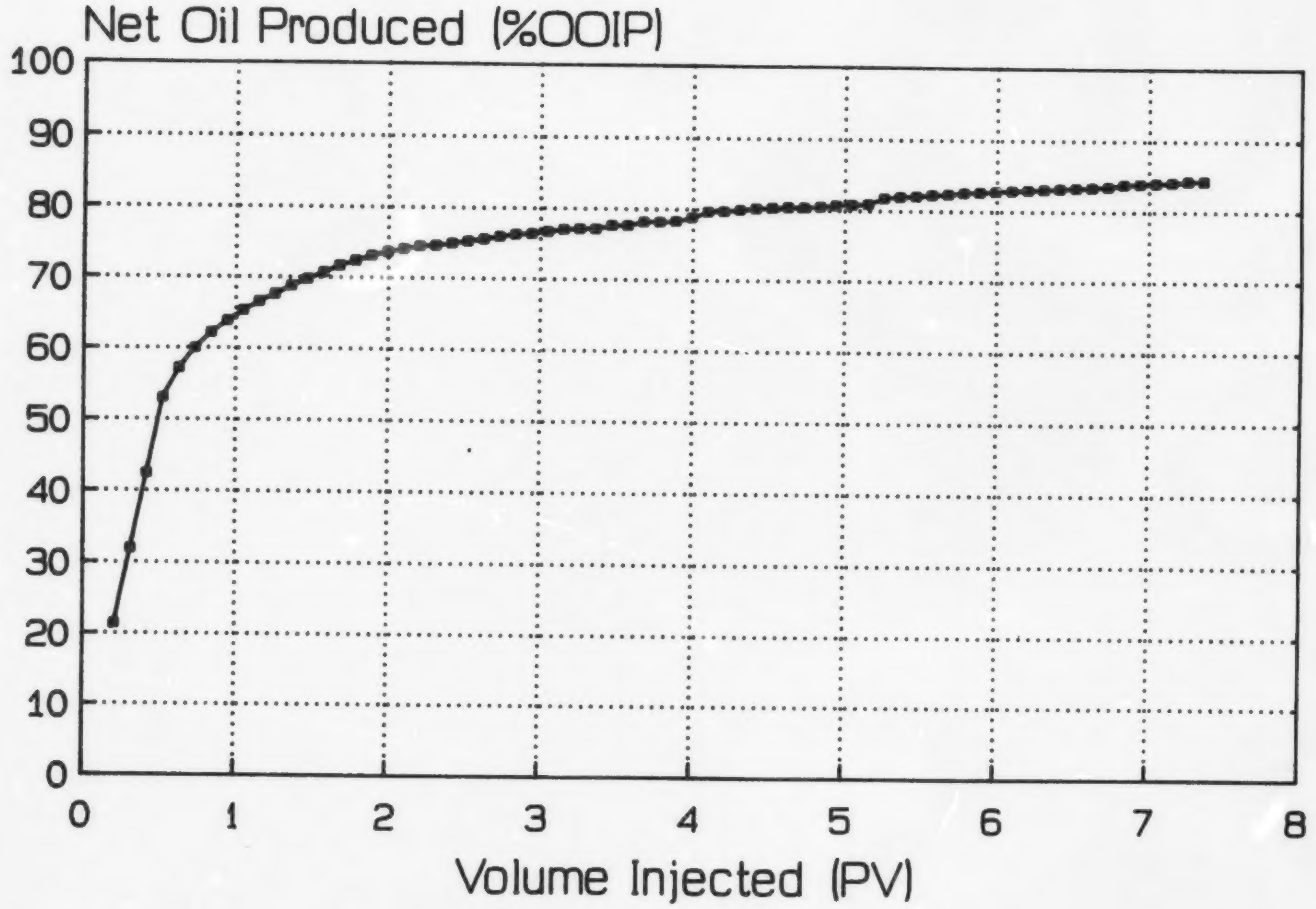

Figure 11: Oil Production during
Waterflood Run TFF 46

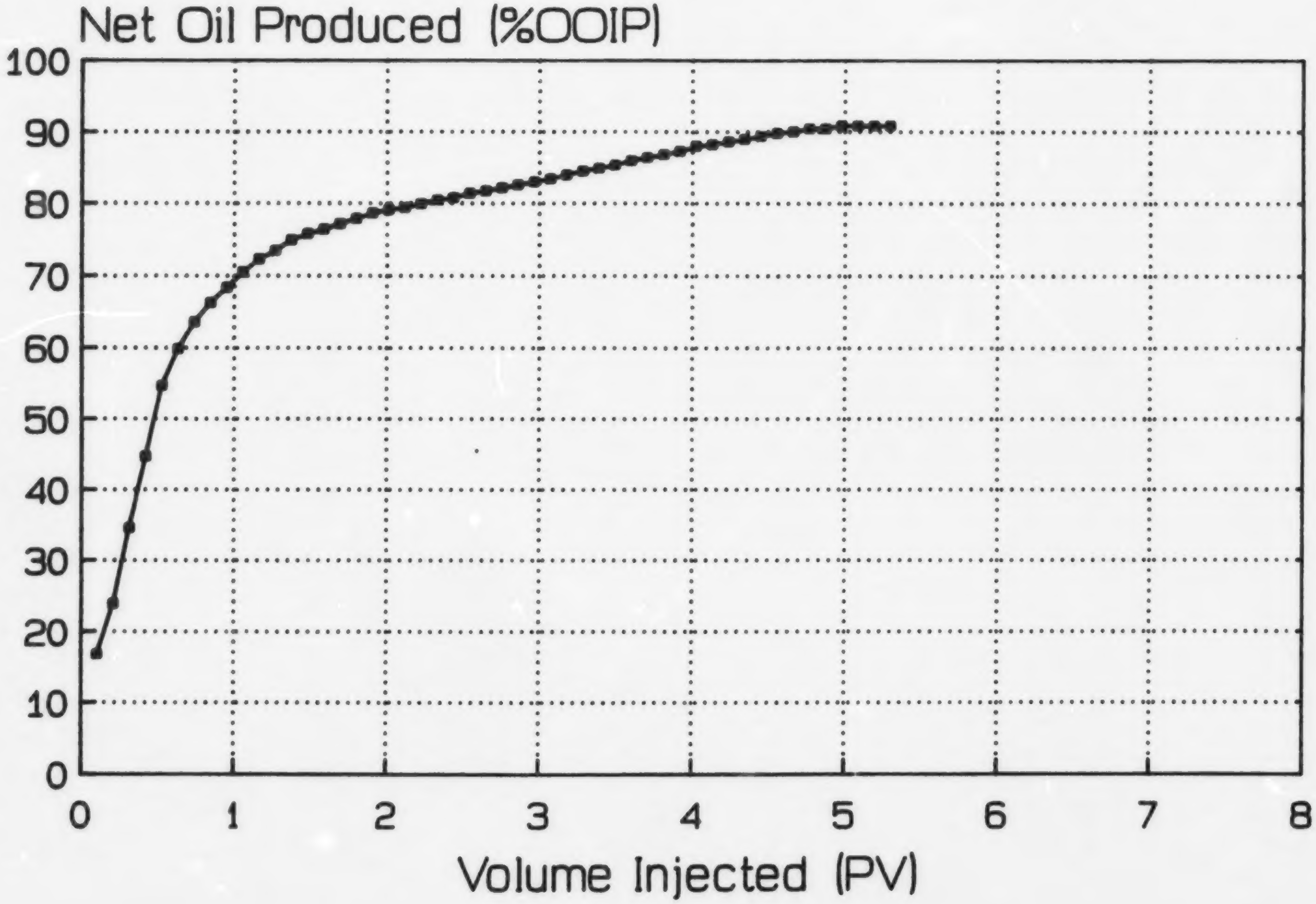

Figure 12: Oil Production during
Gasflood Run TFF 39

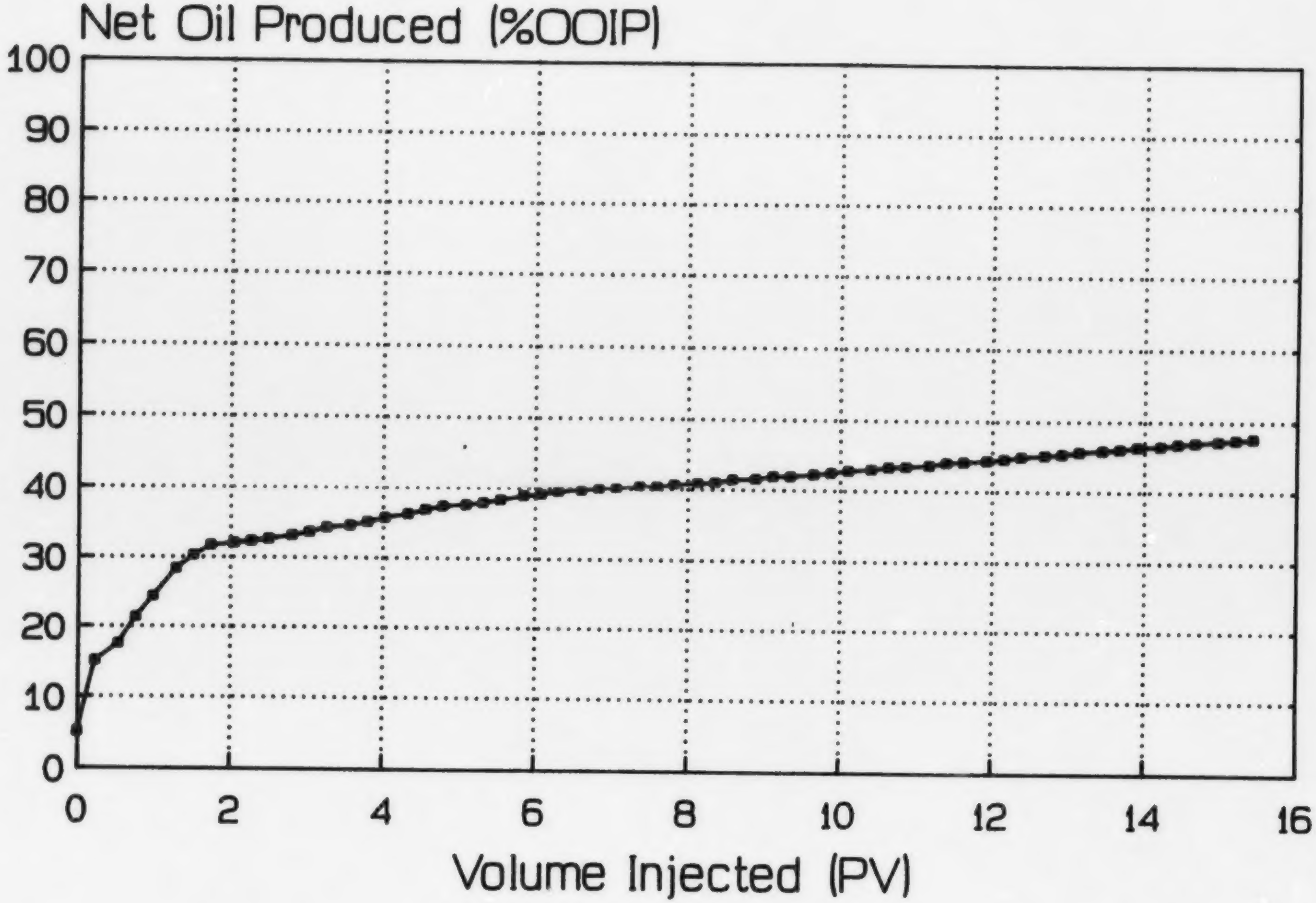

**CLASSIFICATION: NHRC, NOVA, Husky
and Affiliates
REPORT NUMBER: 00427**

THERMAL RECOVERY MECHANISMS
TASK 8
INSTRUMENTAL THERMAL ANALYSIS

March, 1989

Authors

**Rolf Saetre
Brian Erno**

DEPARTMENT: Analytical Services/Resource Recovery
PROJECT #: 687-048
PREPARED FOR: Albert George, Energy Mines and Resources
KEYWORDS: oil, Tangleflags, cracking, evaporation, combustion, oxidation, thermogravimetry, TG

This report contains the valuable proprietary and confidential information of the NOVA HUSKY RESEARCH CORPORATION, and may not be used, disclosed or reproduced without permission in writing from NOVA HUSKY RESEARCH CORPORATION.

110 AP

MICROMEDIA

DISTRIBUTION LIST

Albert George, EMR	10 copies
Peter Tsang, Husky Oil	1 copy
Jon Peggs, Husky Oil	1 copy
Rolf Saetre, NHRC	2 copies
Brian Erno, NHRC	1 copy
Charles Tsang, NHRC	1 copy
File	1 copy
NHRC Library	3 copies
TOTAL	**20 copies**

TABLE OF CONTENTS

Page

1.0 SUMMARY **1**

2.0 INTRODUCTION **2**

3.0 EXPERIMENTAL **3**

4.0 RESULTS AND DISCUSSION **4**
- 4.1 Repeatability 4
- 4.2 TG of Tangleflags Native Oil 5
  - 4.2.1 Thermal Behaviour of Nitrogen 5
  - 4.2.2 Thermal Behaviour of Air 6
  - 4.2.3 Effect of Sand 7
  - 4.2.4 Effect of Heating Rate 8
- 4.3 Comparison of Thermograms of Different Oils 10
  - 4.3.1 Samples from Other Tangleflags Wells 10
  - 4.3.2 Samples from Different Reservoirs 11
- 4.4 TG of Asphaltenes from Tangleflags Oil 12
- 4.5 Effect of LTO on Coke Production 12
- 4.6 Ignition 13

5.0 CONCLUSIONS AND RECOMMENDATIONS **14**

6.0 REFERENCES **15**

7.0 TABLES **16**

8.0 FIGURES **18**

9.0 APPENDIX **50**

1.0 SUMMARY

A number of thermal analysis experiments has been performed with the intent of exploring and evaluating some applications related to heavy oil recovery. The main focus of the study was the extent to which meaningful information can be extracted from thermograms of crude oils and the sensitivity of thermal analysis as a crude oil characterization technique.

Thermograms of a Tangleflags (Lloydminster, Alberta) oil with and without sand in nitrogen and air were successfully interpreted in a qualitative manner using well established mass loss (and gain) mechanisms such as evaporation, polymerization, thermal cracking, low temperature oxidation (LTO), and combustion. However, it was shown that heating rate strongly affects interpretation with regard to the relative importance of certain mechanisms as well as to the apparent onset temperatures of mechanisms such as thermal cracking, LTO, and combustion. For example, only at low heating rates did polymerization reactions manifest themselves, while apparent onset temperatures decreased with decreasing heating rates. The presence of reservoir sand was shown to catalyze LTO reactions, i.e., the apparent onset temperature was lowered.

Experiments with oils from different Tangleflags wells, while establishing a relationship between mass loss and viscosity, showed that thermal analysis cannot differentiate between oils with different thermal history. Samples from three different reservoirs showed that differences in thermograms of crude oils can be correlated with their simulated distillation curves as well as their viscosities.

By changing the atmosphere from air to nitrogen during some thermal analysis experiments, it was demonstrated that LTO dramatically increases coke production. Additional experiments with only asphaltenes showed that asphaltenes are not the only components in crude oils contributing towards coke production.

Attempts to use thermal analysis to determine an ignition temperature of Tangleflags oil were unsuccessful, despite claims to the opposite by other researchers. The thermograms showed no dramatic increase in mass loss rate at any temperature as would be expected if "ignition" of the sample had occurred. It thus appears that the process of initiating combustion in a reservoir is quite different from the familiar process of lighting a fire.

2.0 INTRODUCTION

Various thermal analysis techniques, including thermogravimetry (TG), differential thermal analysis (DTA), and differential scanning calorimetry (DSC), have been available for many years. These three common techniques all involve precise measurements of the mass and/or the temperature of a small sample while it is being heated, usually in a linear fashion with respect to time. In TG, the mass is recorded as a function of temperature (and time), whereas in DTA and DSC, differences in the temperature or heat content between the sample and a reference are monitored. Because there are mass and heat changes involved in almost all physical changes and chemical reactions, thermal analysis can be used in a very wide range of applications. On the other hand, because mass and heat changes are so universal, meaningful interpretation of thermal analysis data is only possible with supporting information regarding the processes causing the changes to occur.

As a result of its wide applicability, instrumental thermal analysis has been used in many different scientific disciplines (1,2) for both very specific tests and quite general kinds of experimental exploration. In the area of oil recovery, numerous reports have attempted to demonstrate the utility of thermal analysis methods for gaining both basic design data and fundamental understanding of thermal recovery processes. This literature has been thoroughly reviewed under Task 1 of this project. In spite of all these reports, which on closer examination have recently come from only a small group of researchers, information from thermal analysis has remained primarily qualitative in nature, and it appears to have been used mostly in an empirical rather than a fundamental manner to study thermal changes to oils.

The work carried out under this task was intended to explore and critically evaluate some of these applications related to heavy oil recovery.

3.0 EXPERIMENTAL

All experiments were performed with a Netzsch STP 429 high temperature thermal analyser connected through an HP 3421A control unit to an HP 86B computer for data acquisition. The recorded thermogravimetric (TG) and differential thermogravimetric (DTG) data were plotted and also stored on 3 1/2 inch disks.

The data were acquired without buoyancy correction in the combination mode (i.e both TG and DTA data were recorded for each sample). Amounts of oil used varied from 15 to 40 mg, weighed to the nearest 0.1 mg. High purity alumina crucibles (0.3 mL capacity) were used for sample and reference cups, and were typically reused. In the experiments using cleaned Tangleflags reservoir sand, equal amounts of sand were added to both cups. The sand to oil mass ratio in the sample cup was approximately 5:1.

The crude oil samples all originated from produced wellhead w/o emulsions. Oil with <0.5% water was separated by heated high speed centrifugation (90°C in sealed container, 60 min. at ~30,000 x gravity). The asphaltenes used in several experiments were separated by precipitation with a large excess of n-pentane.

Experimental conditions included gas flows of 70 mL/min through the sample compartment and 100 mL/min for blanketing the opening to the balance compartment. The gases used (air, nitrogen and oxygen) were "ultra high purity" grade supplied by Matheson. Heating rates were programmed between 0.2°C/min and 50°C/min from 20°C to 800°C. Rates of 10°C/min and 5°C/min were the most common. Because of the large thermal mass of the furnace, the actual heating rates lagged behind the programmed ones for a considerable portion of the experiments, especially at higher heating rates.

Additional details on individual experiments have been recorded both on the original plots of the thermograms (see Appendix A) and in NHRC Laboratory Notebook #03 (R. Saetre). All of the raw data collected during this work is stored on hard disks.

4.0 RESULTS AND DISCUSSION

This section presents and discusses the results collected in the form of thermograms. To facilitate the discussion, a number of the original thermograms plotted by the instrument have been re-drawn in a simpler format on common axes (Figures 1-31). However, since the additional information provided on the original plots may also be required, copies of the originals have been provided in Appendix A. In addition to the 31 originals of the figures, 26 other thermograms are given in Appendix A, many of which are replicates.

4.1 REPEATABILITY

In thermal analysis experiments, as in many other analyses, the behavior of a substance is deduced from measurements on a small sample of the substance. In such cases, the validity of the conclusions depends not only on the experiment themselves, but also on how representative the sample is of the whole. This was of particular concern in this work, because of the potential heterogeneity of the crude oils studied. To address this concern about representative subsampling, as well as the instrumental repeatability, many of the experiments were repeated several times.

Examination of the thermograms of oil and of oil plus sand (see Table 1), heated in nitrogen at 10°C/min, shows that repeatability is usually excellent under these conditions, with thermograms lying exactly on top of each other. When oil is heated in air, however, repeatability appears to be more erratic, especially in the region above about 400°C. Attempts to determine what causes the occasional loss of repeatability were not successful, although several changes in the details of the technique were tested. In addition to these examples in Table 1, a number of other replicate experiments were performed. Thermograms of these runs are given in Appendix A.

© 1988

4.2 TG OF TANGLEFLAGS NATIVE OIL

4.2.1 Thermal Behavior in Nitrogen

A thermogram obtained from heating Tangleflags oil at 10°C/min in flowing nitrogen is shown in Figure 1. After an initial period in which the sample mass appears to increase by 2-3%, the sample begins to lose mass, slowly at first, increasing to a fairly steady rate, then loses mass more rapidly up to about 480°C, and finally levels with about 17% of the sample remaining.

The initial apparent mass increase is due to the reduction in density of the air around the sample and reference crucibles, as the temperature increases. This density change decreases their buoyancy and thus increases their weight. The buoyancy effect can be seen more directly from a blank experiment, in which both sample and reference crucibles are left empty. As seen in Figure 2, the effect reaches a maximum of about 0.5 mg at about 100°C, and remains fairly constant thereafter. Note that the magnitude of the buoyancy effect may appear to vary in different thermograms. Most of this variation is a consequence of expressing the vertical axis as a percentage of initial sample mass.

By the time the sample reaches 130°C, mass loss is about equal to the buoyancy effect. From 130 to 400°C in Figure 1, the loss of mass is determined by evaporation of lighter components in the oil. It is apparent that the evaporation rate increases to a maximum, and then continues at that maximum rate until affected by another process.

Above 400°C, the rate of mass loss increases significantly, but by 470°C it begins to decrease, and mass loss beyond 500°C is very small. The increased mass loss rate above 400°C is attributed to the production of light components by thermal cracking. Evaporation of these components extends the mass loss from about 50% to greater than 80%. A GC simulated distillation curve for this oil shows that only 50% is distillable up to 525°C. Thus the additional 30% lost in the TG experiment is mostly a result of thermal cracking.

The constancy of the mass loss rate between 230°C and 400°C is consistent with a sample having a fairly continuous distribution of boiling points. The increase in mass loss rate above 400°C suggests formation of significant amounts of components of lower boiling point.

The evaporation rate of crude oil in a flowing nitogen stream in the TG apparatus is probably sensitive to many variables. The trend with viscosity noted above suggests that the evaporative mass loss rate is determined by vapour pressure. As the sample is heated, the vapour pressure increases, until evaporation begins at a measurable rate. In the early stages of heating, the vapour pressure increases, and mass loss rate also increases. As the temperature increases, however, the vapour pressure approaches an approximately constant value (as a result of the multicomponent nature of the sample), and thus the mass loss rate becomes constant. The more viscous the sample, the higher the temperature when it reaches the point of maximum mass loss rate.

Mass loss slows and then stops when cracking has proceeded to the stage that only coke is left.

4.2.2 Thermal Behavior in Air

When Tangleflags oil is heated at 10°C/min in air, the rate of mass loss increases up to about 250°C, then levels to a fairly constant value (Figure 3). Above 400°C, there is first a small deviation from linearity, and then a more significant decrease in mass loss rate between 470° and 500°C.
Above 500°C, mass loss resumes at close to the previous rate, until reaching 600°C, at which point very little sample mass remains in the crucible, and no further mass loss is seen.

Comparison of Figures 1 and 3 shows that changing the gas from nitrogen to air had no observable effect on the first part of the thermogram, (i.e. between 30° and 400°C). Evaporation of light components from the sample is not affected by the type of gas in the chamber. Above 400°C, however, the curves are very different. The increase in mass loss rate seen in nitrogen, which was attributed to evaporation of the light products of thermal cracking, is not observed. Instead, there is only a small change between 400° and 450°C, followed by a large decrease. It is deduced that oxidation reactions become dominant under these temperature-time conditions, particularly oxidation reactions which produce less volatile components. These reactions remove molecules which would have undergone cracking in the absence of oxygen. Above about 510°C, at this heating rate, high temperature oxidation (combustion) becomes dominant, and the remainder of the sample is converted to volatile carbon oxides and water. Although all of the sample mass is lost, the thermogram remains above the zero level because of the buoyancy effect (see Figure 2).

4.2.3 Effect of Sand

In a stream of flowing oxygen or air, the presence of reservoir sand has a significant effect on the thermal behavior of Tangleflags oil. The thermograms in Figures 4 and 5 show decreases in slope (i.e. mass loss rate) near 320°C and 350°C, respectively. In the absence of sand, such a slope change is not evident (Figure 3). The differences are attributed to incomplete oxidation reactions being more significant in the presence of sand. Also, an increase in partial pressure of oxygen lowers the "onset" temperature for these reactions. The uptake of oxygen reduces the amount of volatile material available for evaporation and thus reduces the mass loss rate between 320° and 400°C.

A second decrease in mass loss rate is seen at about 450°C in Figures 4 and 5. Although a similar feature is present in the curve in the absence of sand (Figure 3), the changes in the latter curve are more exaggerated.

Figure 6 is the thermogram resulting when Tangleflags oil and reservoir sand are heated at 10°C/min in flowing nitrogen. Comparison with Figure 1 shows that the sand has no observable effect on either the evaporation or cracking portions of the curve, but does lead to some additional mass loss above 500°C. This mass loss is attributed to a small amount of dehydration and decomposition of the sand, as confirmed by a separate experiment in which only the sand was heated.

In a stream of flowing air, the presence of reservoir sand has a significant effect on the thermal behavior of Tangleflags oil. The thermogram in Figure 6 shows an abrupt decrease in slope near 350°C, which is not evident in Figure 3 (no sand). A second decrease in mass loss rate is seen at about 450°C in Figure 6. Although a similar feature is present in the curve in the absence of sand (Figure 3), the changes in the latter curve are more exaggerated.

In the presence of sand, partial oxidation reactions are apparently more significant. These reactions reduce the amount of volatile material available for evaporation, and thus reduce the mass loss rate between 350° and 400°C. Combustion reactions become more significant by about 430°C, causing increased mass loss rate for a while, until only coke remains to be oxidized. The drop in rate at about 460°C in Figure 6 is attributed to the unavailability of combustible components other than coke. As the temperature increases further, the rate of coke combustion increases, and mass loss rate increases once again.

4.2.4 Effect of Heating Rate

Since thermal analyses are conducted under non-equilibrium thermodynamic conditions, heating rate is expected to significantly affect the shape and thus the interpretation of thermograms. Despite this, the effect of heating rate has been largely ignored in previously reported studies. The degree of the effect on thermograms of Tangleflags crude oil in the presence and absence of sand and in nitrogen as well as air is qualitatively discussed in the following section.

When heating a multicomponent, hydrocarbon mixture such as crude oil in a nitrogen atmosphere, the two most prominent mechanisms contributing to the mass loss profile, as discussed above, are expected to be evaporation of original components and evaporation/flashing of components produced by thermal cracking. Also possible are polymerization reactions in the region around 300°C. Such reactions have been associated with observed viscosity increases of oil after treating it at 250-300°C for several days in an inert atmosphere. Thus, a thermogram of crude oil heated under a flowing stream of nitrogen should show at least two distinct slope sections and possibly three.

Such thermograms obtained at heating rates of 10° and 4°C/min are shown in Figures 1 and 7. After the initial increase in the slope of the mass vs. temperature curve, the slope becomes approximately constant between 280° and 350°C for the 10°C/min run and between 220° and 370°C for the 4°C/min run. Just above 400°C, a significant increase in slope is noticed before a levelling off occurs between 480° and 500°C.

Both thermograms can be interpreted as evaporation of original components up to about 400°C, at which point the additional evaporation of thermal cracking products increases the rate of mass loss. The constant slope section can be accounted for by a constant vapour pressure due to evenly distributed boiling points of the sample components over a broad temperature range. A comparison of the two thermograms shows a horizontal shift which is related to the heating rate. Because of the non-equilibrium conditions of the experiments, a low heating rate will produce a greater mass loss at a given temperature than a higher rate. This will hold true until the heating rate becomes so slow that the additional mass loss at each temperature interval becomes too small to manifest itself.

Thus, without any additional experiments, thermal analysis of oil in an inert atmoshphere appears to show that only evaporation and thermal cracking contribute to the mass loss profile. Additional experiments, however, with heating rates down to 0.2°C/min, clearly show (Figures 8 to 10), in addition to a further horizontal displacement, a slight flattening (i.e. decrease in slope) of the thermogram between about 280° and 350°C. Since this is prior to the manifestation of thermal cracking, it has to be due to either a decrease in the evaporation rate or to the presence of a third mechanism. A decrease in evaporation rate with half the sample left can be explained only if the boiling point distribution of the components in the sample is nonsymmetrical, i.e. skewed heavily towards high boiling point components.

A somewhat more plausible explanation involves polymerization reactions at temperatures below 300°C. Such reactions consume components that otherwise would evaporate, and, as a result, the overall rate of mass loss decreases until thermal cracking becomes predominant. At high heating rates, this mechanism does not show up because of the much shorter dwell time at polymerization temperatures.

As can be seen from Figures 5 and 14, the presence of reservoir sand does not measurably alter the mass loss profile of Tangleflags oil. Also, its heating rate dependence is the same as without sand.

Although much more complex, a similar heating rate dependence is observed for the thermograms of Tangleflags oil in air. For the same reason as discussed earlier, the thermograms shift horizontally towards lower temperatures (Figures 3, 11, 12) with decreasing heating rates, i.e. various mechanisms appear to occur at lower temperatures. In addition to evaporation, polymerization, and thermal cracking, complex reactions involving oxygen (i.e. LTO, HTO, and combustion) now have to be included in the interpretation of the thermograms.

The first part of the three thermograms obtained at 10°, 5°, and 1°C/min is, as in nitrogen, governed only by evaporation. Depending on the heating rate, this mass loss mechanism appears to dominate up to anywhere between 280°C for 1°C/min and 400°C for 10°C/min. This evaporation region is followed by two distinct steps. The first step, which is barely visible just beyond 400°C at 10°C/min, becomes a very dominant feature between 300° and 350°C in the 1°C/min experiment. A comparison with the tests performed in nitrogen clearly shows that this step, i.e. decrease in mass loss rate, has to be related to reactions involving oxygen.

Hydrocarbons are known to incorporate oxygen at a measurable rate at temperatures below 300°C to form alcohols, ketones, aldehydes, and carboxylic acids. Such compounds will have higher boiling points than their parent compounds and will therefore temporarily be unavailable for evaporative mass loss. At low heating rate, this should manifest itself in a thermogram as a significant decrease in mass loss rate which is exactly what is observed (Figure 11). The subsequent, quite sudden (particularly at 1°C/min) increase in mass loss is possibly related to thermal cracking/evaporation (or distillation) of the produced oxygen compounds as well as unaltered hydrocarbons. If thermal cracking of the limited amount of oxygen-containing molecules is thermodynamically more favorable than the corresponding hydrocarbon cracking, the mass loss rate should slow down again as soon as the supply is exhausted to a rate similar to the one observed in the absence of oxygen (Figures 1, 7, 8). This is very much what is observed (Figures 3, 11, 13).

The last increase in mass loss rate is due to combustion which completely removes the remaining components. A comparison of Figures 3 and 12 clearly shows that the temperature at which combustion appears to be complete decreases from 600°C at 10°C/min to about 475°C at 1°C/min.

Addition of sand to the oil-in-air experiments produces some noticeable changes to the thermograms as seen in Figures 6, 13, and 14. The first step, which was barely noticeable around 400°C in the absence of sand at a heating rate of 10°C/min, has become very prominent (compare Figures 3 and 6). If the oxygen up-take explanation for this step is correct, then reservoir sand must act as a catalyst for this process. The result is a thermogram profile very similar to that of oil in the absence of sand at a 3-4 times slower heating rate.

With decreasing heating rate, the first step becomes more and more prominent, which agrees with the observed behaviour of the oil in the absence of sand. At a heating rate of 0.2°C/min (see Figure 14), the initial decrease in mass loss rate due to LTO is followed by a steady increase without any further steps until all the sample is completely oxidized at about 420°C. All that can be said about the latter region is that of all the described mechanisms no one mechanism is predominant at any point in time under the slow heating regime used. However, the lack of features and thus the apparent simplicity of the mass loss process illustrates how essential a knowledge of heating rate dependence is for a meaningful interpretation of thermograms of samples such as crude oils.

4.3 COMPARISON OF THERMOGRAMS OF DIFFERENT OILS

4.3.1 Samples from Other Tangleflags Wells

Samples of produced emulsion from seven wells at the Tangleflags Fireflood project were collected in August 1987, and portions of clean oil were separated from each as described in the experimental section. In late 1987, these wells were producing fluids of quite different characteristics. As discussed more fully elsewhere (3), several of these wells were believed to be producing oil which originated near the combustion front, while others were believed to be producing "native" reservoir oil. Thus these oil samples have very different kinds of thermal history.

TG curves for each of these samples, collected during heating in nitrogen at 5°C/min, are shown in Figures 16-22. Comparison shows that the curves are all very similar to each other, including oil from the Tangleflags well D11-13 which was used for most of the other experiments (Figure 22). Small differences can be seen on closer comparison, between the thermogram for oil from well 1A10 (Figure 16), that from well D3 (Figure 21) and that from well D7 (Figure 17). Thermograms for the samples from the other 3 wells (4C3,4C2 and 4B7) are all identical with that from well D7.

Table 2 compares the values of % mass remaining at two temperatures, with the viscosities of the oil samples at 25°C. While there is an apparent trend to less mass loss (higher mass remaining) with increasing oil viscosity, the magnitudes of the differences are similar to the repeatability.

4.3.2 Samples from Different Reservoirs

Thermograms from three different heavy oil reservoirs, Golden Lake (Sparky), Tangleflags (General Petroleum) and Caribou Lake (Clearwater B) are shown in Figures 22-24. The Golden Lake and Tangleflags reservoirs are both in the Lloydminster area, but the Golden Lake oil is about 40% more viscous and has a slightly higher density. The thermograms of these two reservoir oils are very similar, except that the Tangleflags sample appears to reach the constant evaporation mass loss rate slightly later than the Golden Lake oil, and then shows more rapid mass loss by cracking. The amounts of coke formed by Tangleflags and Golden Lake samples are almost identical.

The Caribou Lake lease is located in Alberta, north of Lloydminster near the Cold Lake heavy oil area. Oil from this reservoir is denser and seven times more viscous than the Tangleflags oil. Comparison of its TG curve (Figure 24) with the other two shows some significant differences. The Caribou Lake sample reaches the limiting evaporative mass loss rate more slowly than either of the Lloydminster oils, but catches up in the cracking region. The Caribou Lake oil gives the same amount of coke left at the end of the run as the other two oils.

The data in Table 2 for the Golden Lake and Caribou Lake oils confirm the trend within the Tangleflags samples. Within the part of the thermogram controlled by evaporation, oils of higher viscosity lose less mass on heating to the same temperature. Note also that the slopes of the thermograms throughout most of the evaporative region (200-400°C at 5°C/min) are very similar.

Since in this region, the temperature is directly proportional to time, the similar slopes indicate similar rates of mass loss. Thus the differences in the thermograms result not from different mass loss rates, but because it takes longer for less volatile (more viscous) samples to reach the constant mass loss rate. This is consistent with the explanation, developed in earlier sections of this report, that evaporation of a multicomponent mixture at a fixed linear heating rate reaches a limiting mass loss rate, governed by the vapour pressure in the cup above the sample.

4.4 TG OF ASPHALTENES FROM TANGLEFLAGS OIL

Figures 25 and 26 show thermograms of asphaltenes heated in nitrogen at two different heating rates. The deviation above 100% is due to the change in buoyancy effect; it looks larger than usual (compare Figure 2) because the sample size was very small (4 mg). Since asphaltenes contain very little volatile component, no mass loss is visible until thermal cracking becomes significant. At the slower heating rate, mass loss becomes visible about 250°C, whereas at the faster rate, it is not apparent before 350°C. This difference again demonstrates that the temperatures at which reactions become apparent in a TG experiment are determined by kinetics as well as thermodynamics. In the 300° to 400°C region, more reaction occurs between any two temperatures at the slower heating rate because of the longer time available for reaction. In both cases, cracking of asphaltenes to give more volatile components increases the mass loss rate, but eventually most of the components which can undergo cracking are used up, and the mass loss rate decreases rapidly.

It is interesting to note that mass loss does not stop completely, even above 600°C, as it does with samples of oil. It appears that the other high molecular weight components in oil (those remaining when cracking reactions become significant) affect the cracking of asphaltenes. About 50% of the asphaltenes are readily cracked, and the remainder is converted to coke. In the Tangleflags oil, coke remaining after heating in nitrogen is about 10% of the original oil. Tangleflags oil contains about 14% asphaltenes, so it is evident that in the presence of other oil components, either more asphaltene becomes coke, or the other components contribute significantly to the coke yield.

4.5 EFFECT OF LTO ON COKE PRODUCTION

There has been much discussion of the role of low temperature oxidation (LTO) reactions in contributing to the coke fuel left to sustain a combustion front. Figure 27 shows a thermogram of a sample of Tangleflags oil which had been previously exposed to air at elevated pressure and 214°C for 24 hours (details are given in Task 6 Report). Comparison of Figures 27 and 22 shows that the evaporation and cracking appear identical, but the oxidized oil sample produced several percent more coke. This is consistent with conclusions from other studies, indicated higher coke yield after LTO.

When the same sample of pre-oxidized oil was heated in air, the thermogram shown in Figure 28 was obtained. Comparison of this curve with that in Figure 11 for non-oxidized oil shows that significant deviation occurs only in the region between 350° and 400°C. The oxidized oil runs out of volatile components sooner than the native sample, but by the time they reach 425°C, cracking has become dominant in both samples, with no apparent difference due to different thermal history.

The thermogram in Figure 29 resulted from another approach to determine the effects of low temperature oxidation on cracking and coking reactions. Heating was begun in a flowing air stream, but when the temperature reached 430°C, the gas stream was changed to nitrogen. In this way, combustion of the coke was prevented, and the mass remaining at the end of the run gives a measure of the coke produced.

Comparison of Figures 29 and 23 shows that coke yield is more than doubled (26 versus 12%) when the oil sample is heated to 430°C in air rather than in nitrogen. Partial oxidation reactions occurring lower temperatures clearly affect the amount of coke produced.

4.6 IGNITION

One of the difficulties encountered in applying in-situ combustion to heavy oil reservoirs is that of initiating high temperature combustion. This often involves installing a downhole burner for a short period of time, after which air or oxygen injection begins. To simulate the rapid heating of oil in the reservoir near the well, during use of a downhole burner, several experiments were performed in which a very rapid heating rate in air was used. The thermogram in Figure 31 has much the same general shape as those at lower heating rates. Evaporation dominates up to about 400°C, when cracking and combustion begin to be evident. Surprisingly, there is no indication of excessive mass loss, as would be expected if "ignition" of the sample had occurred. It is evident that the process of initiating combustion in a reservoir is quite different from the familiar process of lighting a fire.

5.0 CONCLUSIONS AND RECOMMENDATIONS

The results of the work described in this report led us to the following conclusions:

1. Thermal analysis can be successfully used to establish the relative importance of thermal mechanisms contributing to in-situ combustion oil recovery.

2. Thermal analysis is a useful and simple means to determine the effect of LTO on coke production from crude oils.

3. Coke production from Tangleflags oil was found to be about 30% higher than the amount produced from its pentane asphaltenes.

4. The evaporative mass loss rate of crude oils, as determined by thermal analysis, correlated with their viscosities.

5. Known mass loss mechanisms have been successfully incorporated into a qualitative interpretation of crude oil thermograms. Thus, it ought to be possible to develop a mathematical model for most of the thermograms. As this would produce information which could be incorporated into numerical simulators of in-situ combustion oil recovery, additional work in this area is recommended.

6. Onset temperatures of processes such as thermal cracking, LTO, HTO, and ignition cannot be determined accurately by thermal analysis.

7. Based on the limited number of samples studied, thermal analysis does not appear to be sensitive enough to distinguish between crude oils with different thermal histories.

6.0 REFERENCES

1. Wendlandt, W.W.M., "Thermal Analysis", Revised Edition, Wiley and Sons, Toronto, 1986.

2. Mackenzie, R.C. (editor), "Differential Thermal Analysis", Volume 2, Applications, Academic Press, New York, 1972.

7.0 TABLES

TABLE 1
EXAMINATION OF EXPERIMENTAL REPEATABILITY

SAMPLE	ATMOSPHERE	HEATING RATE °C/min	THERMOGRAM [a]
Oil	N_2	10	A-1, A-2, A-3
	N_2	5	A-4, A-5, A-6
Oil	Air	10	A-12 to A-16
		5	A-17, A-18, A-19
Oil/Sand	N_2	10	A-22, A-23, A-24
Oil/Sand	Air	10	A-27, A-28

a) Refer to Appendix A

© 1988

TABLE 2

CORRELATION OF TG THERMOGRAMS WITH OIL VISCOSITY

RESERVOIR	WELL	MASS REMAINING (%)		VISCOSITY (Pa.s @ 25°C)
		200°C	300°C	
Tangleflags (General Petroleum)	4C2	90.0	70.0	2.4
	D3	90.5	71.0	2.4
	4C3	90.0	69.5	2.5
	D7	90.0	69.5	2.7
	4B7	89.7	70.0	3.0
	1A10	92.1	72.5	4.9
	D11	91.7	71.5	5.0
Golden Lake (Sparky)		93.0	74.2	7.0
Caribou Lake (Clearwater 'B')		94.0	76.4	30

8.0 FIGURES

FIGURES 1 THROUGH 31

© 1988

Figure 1: TG Thermogram of Tangleflags Oil in Nitrogen

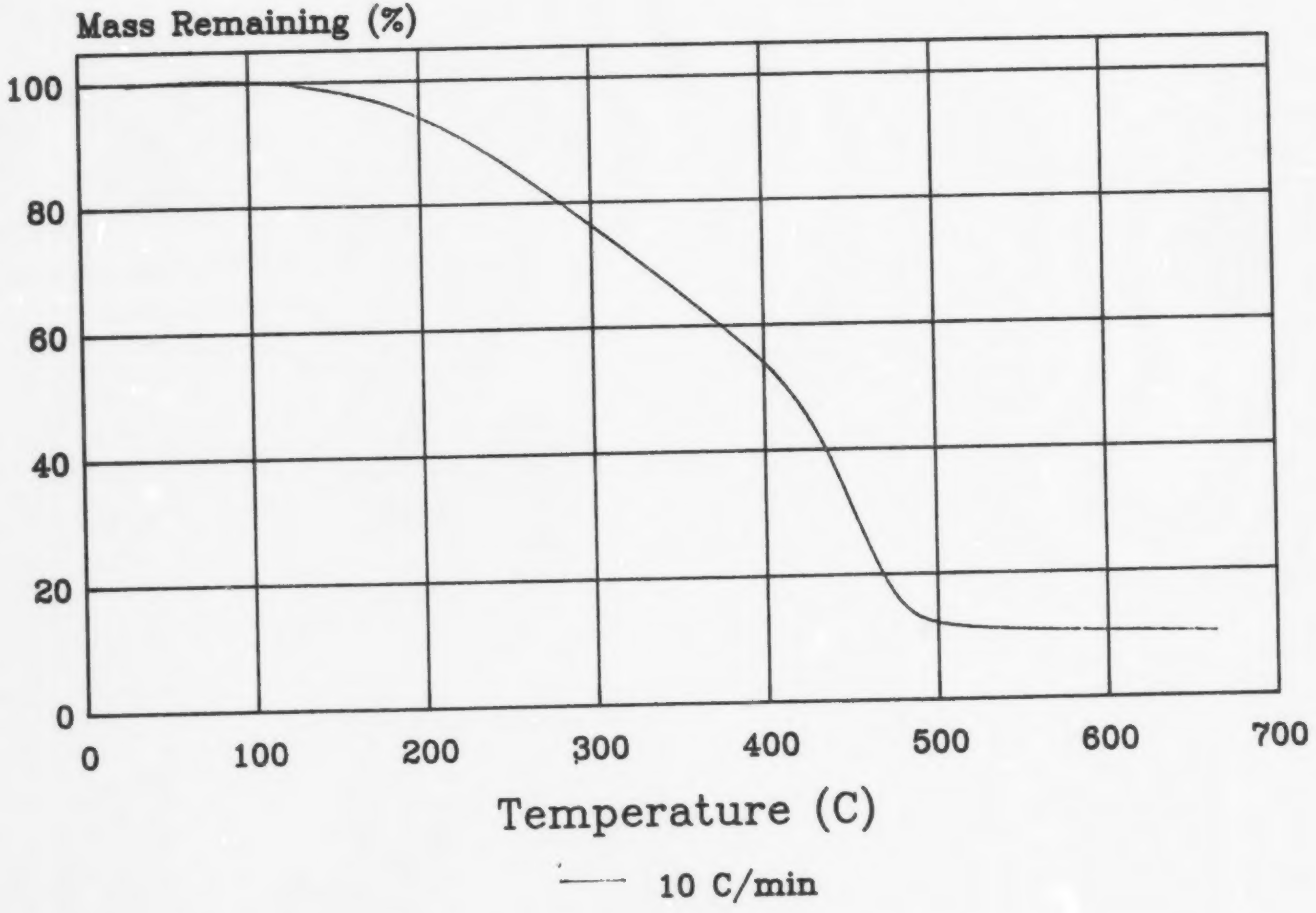

Figure 2 : TG Thermogram of Empty Alumina Crucible

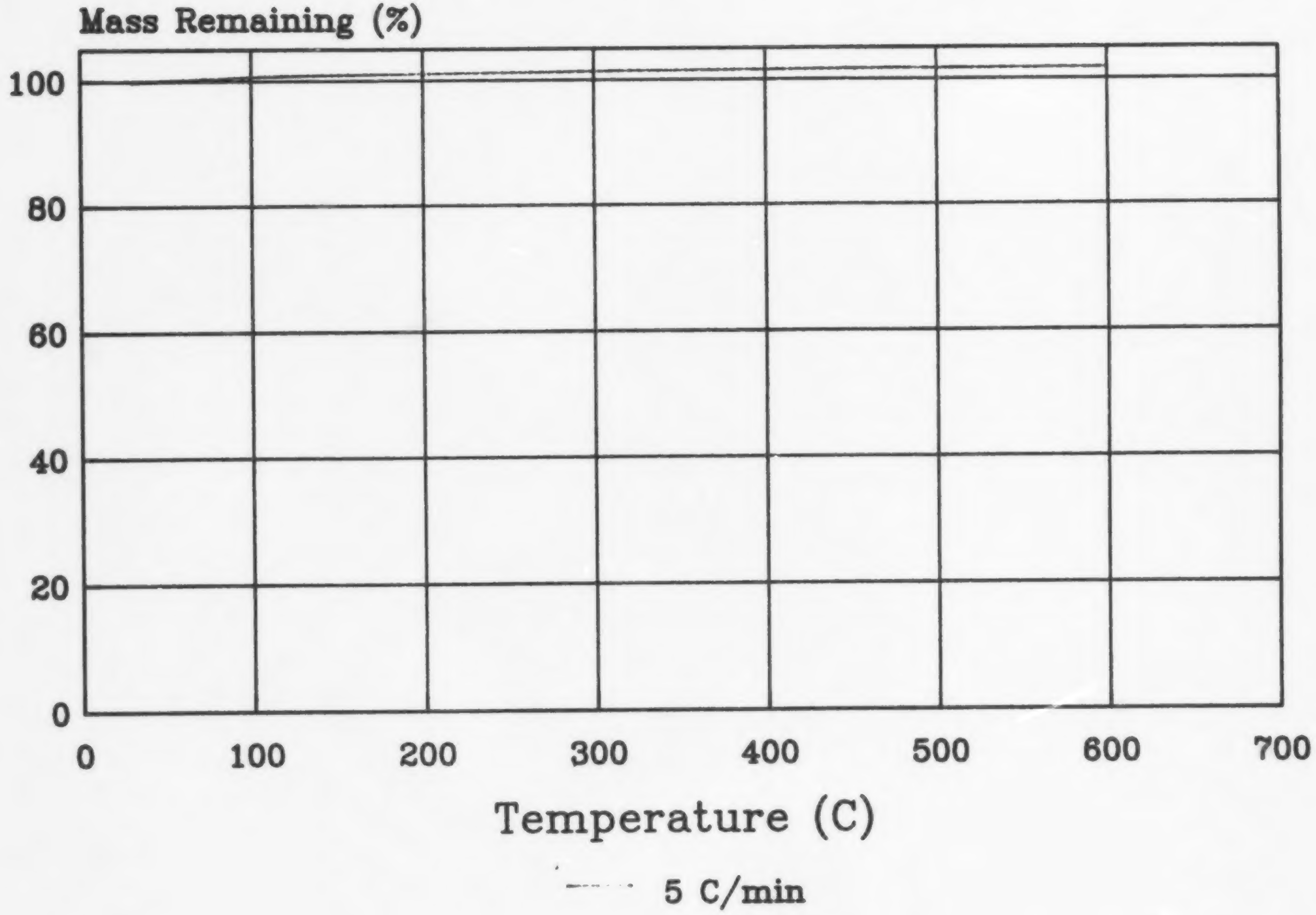

Figure 3 : TG Thermogram of Tangleflags
Oil in Air

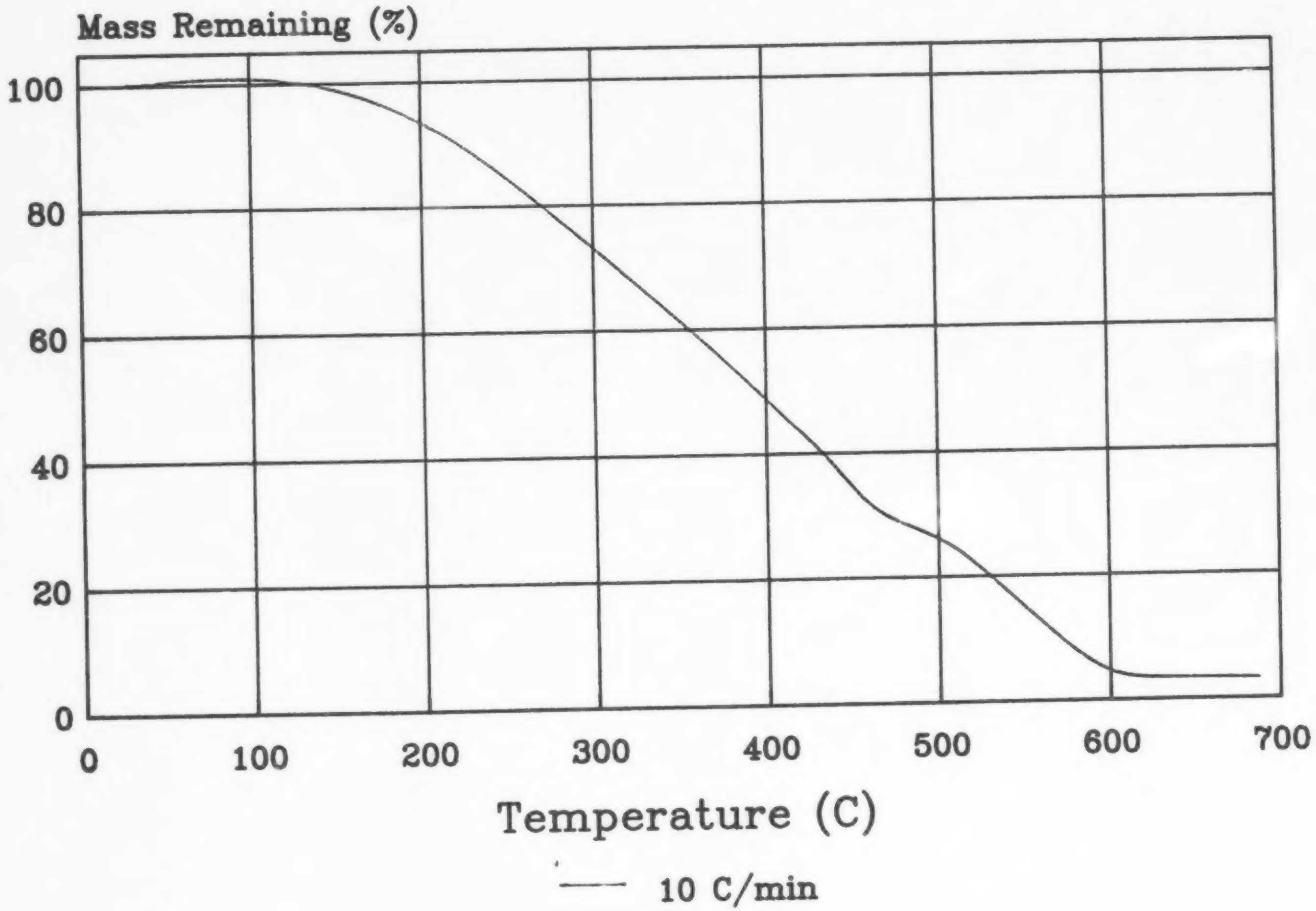

Figure 4 : TG Thermogram of Tangleflags Oil in Oxygen

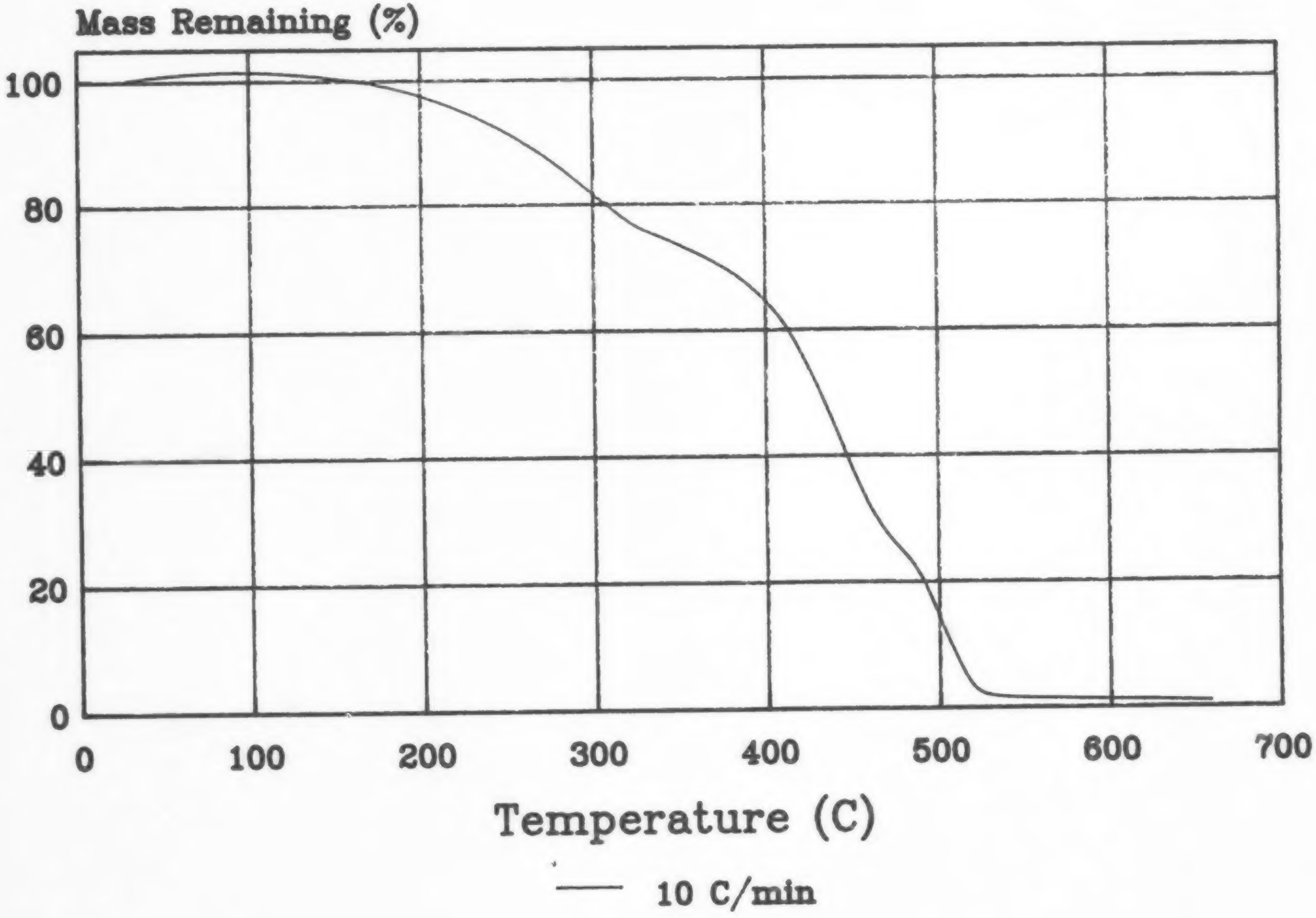

Figure 5: TG Thermogram of Tangleflags
Oil and Sand in Air

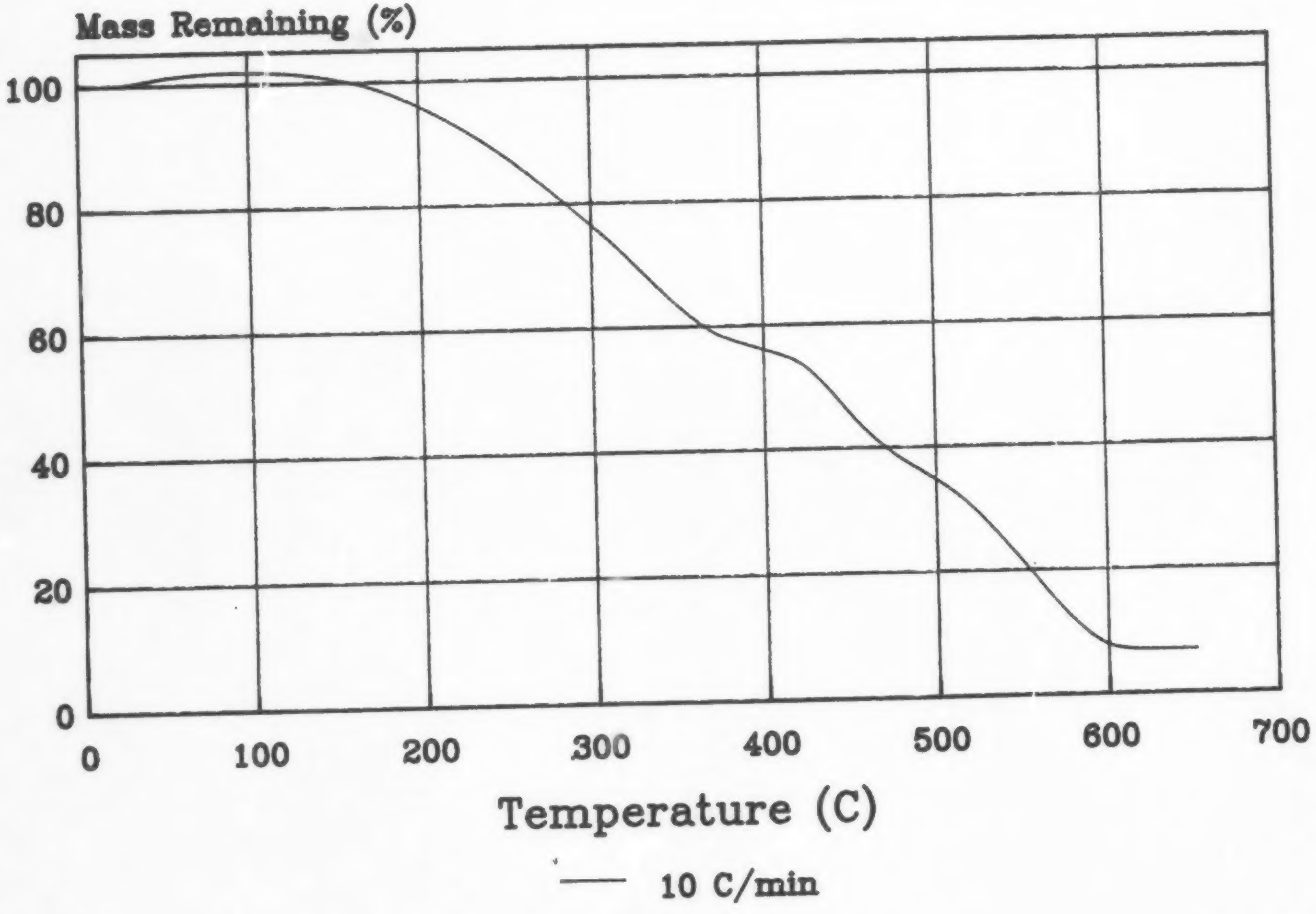

Figure 6 : TG Thermogram of Tangleflags Oil and Sand in Nitrogen

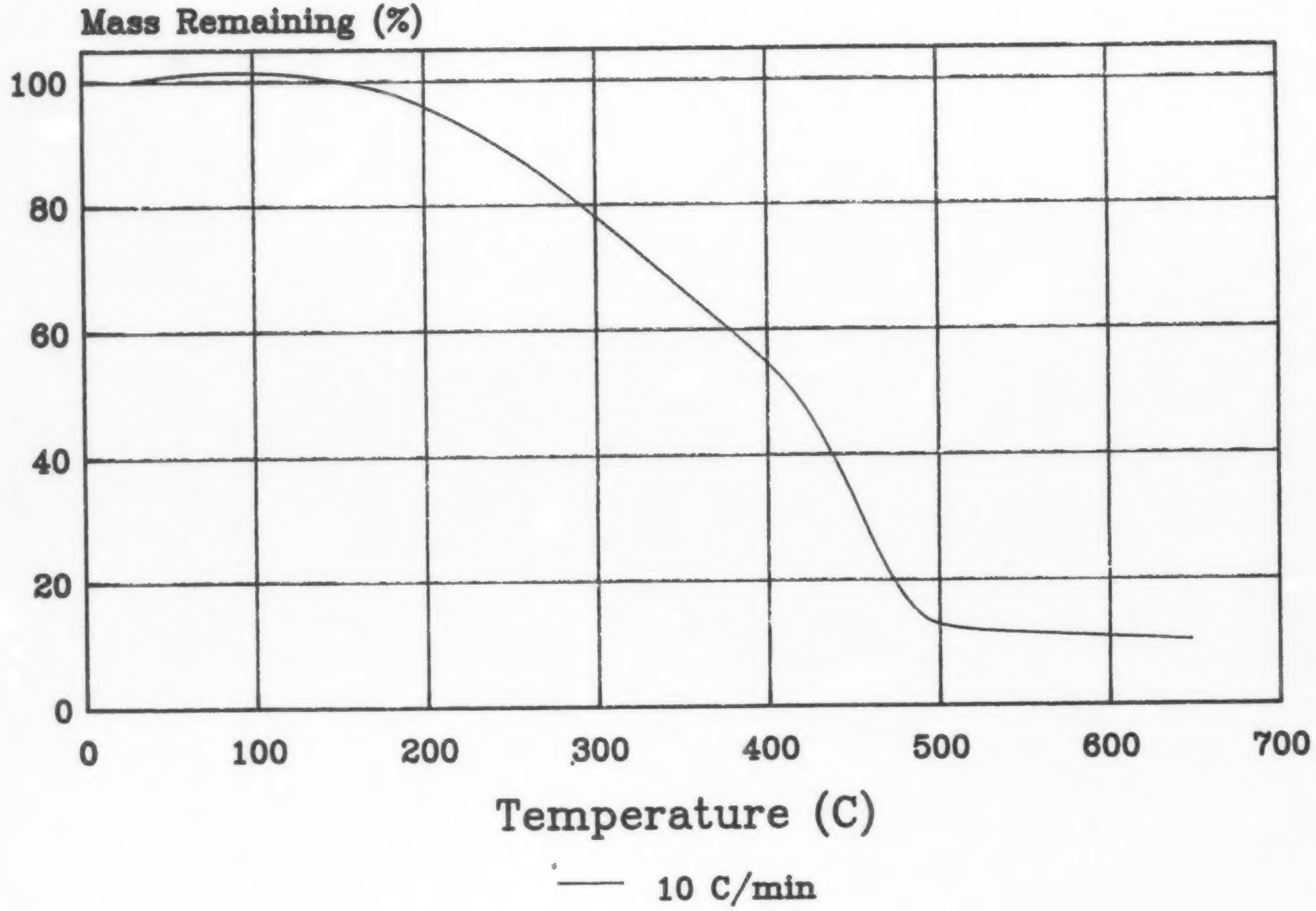

Figure 7 : TG Thermogram of Tangleflags Oil in Nitrogen

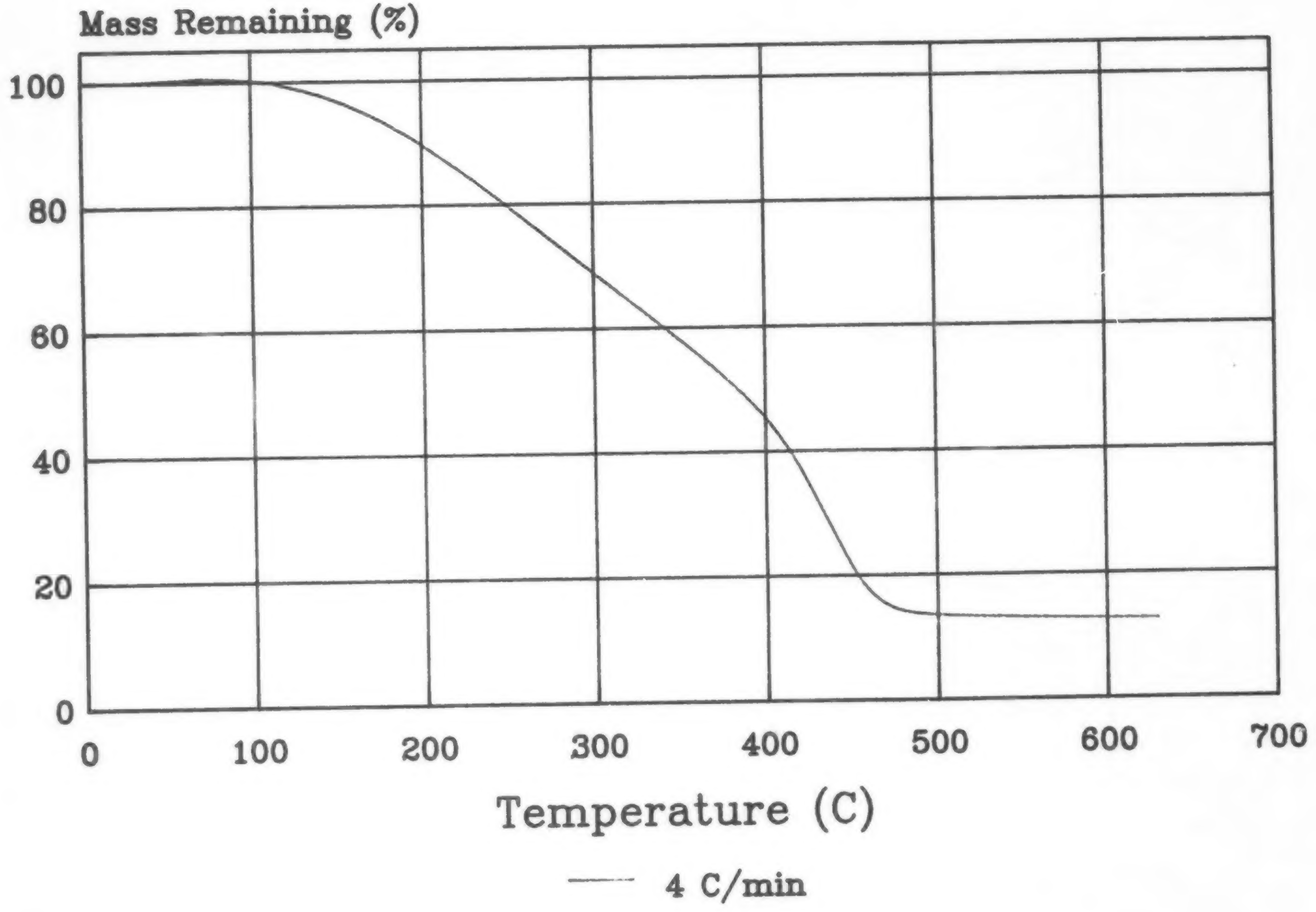

Figure 8 : TG Thermogram of Tangleflags
Oil in Nitrogen

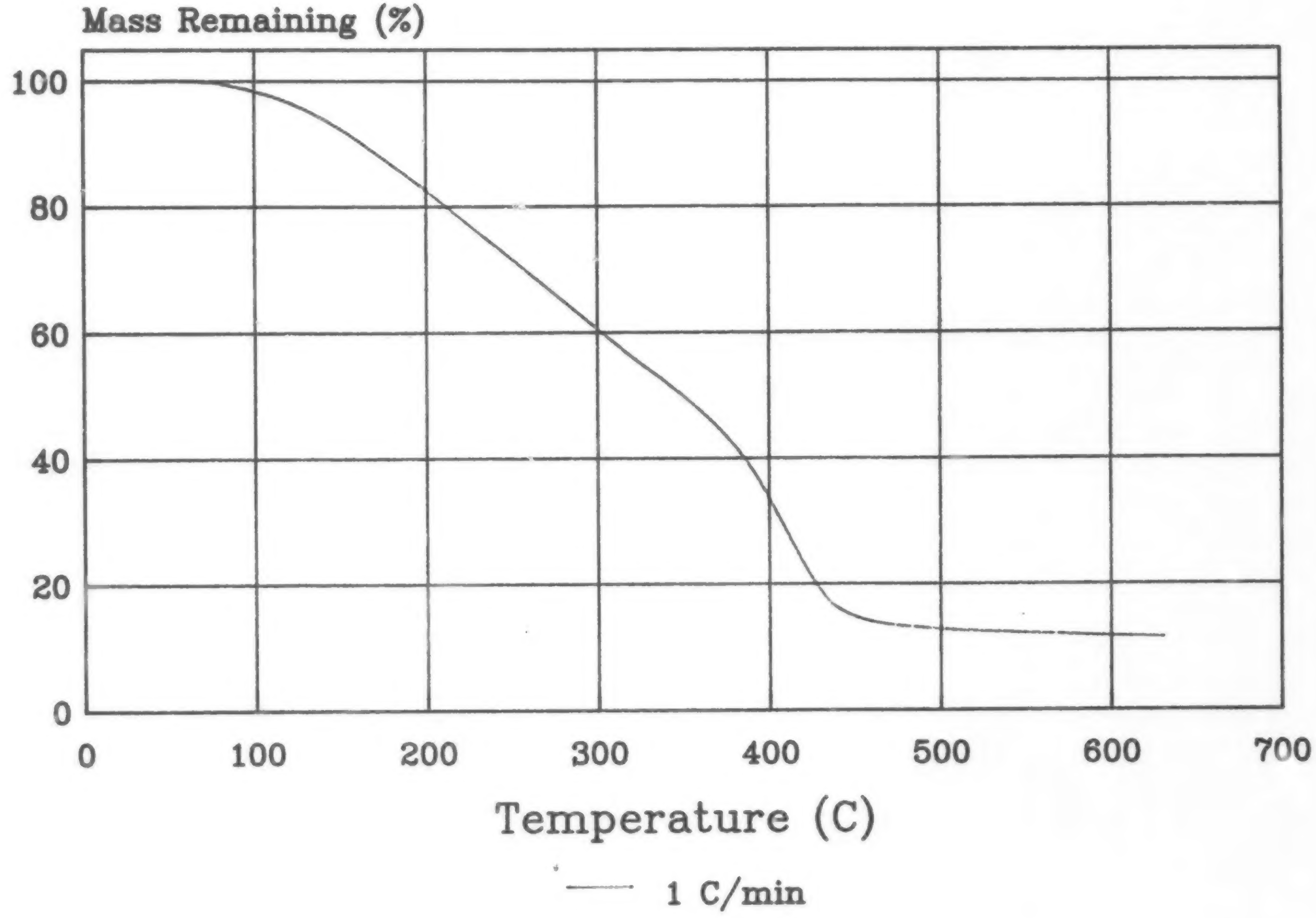

Figure 9 : TG Thermogram of Tangleflags
Oil in Nitrogen

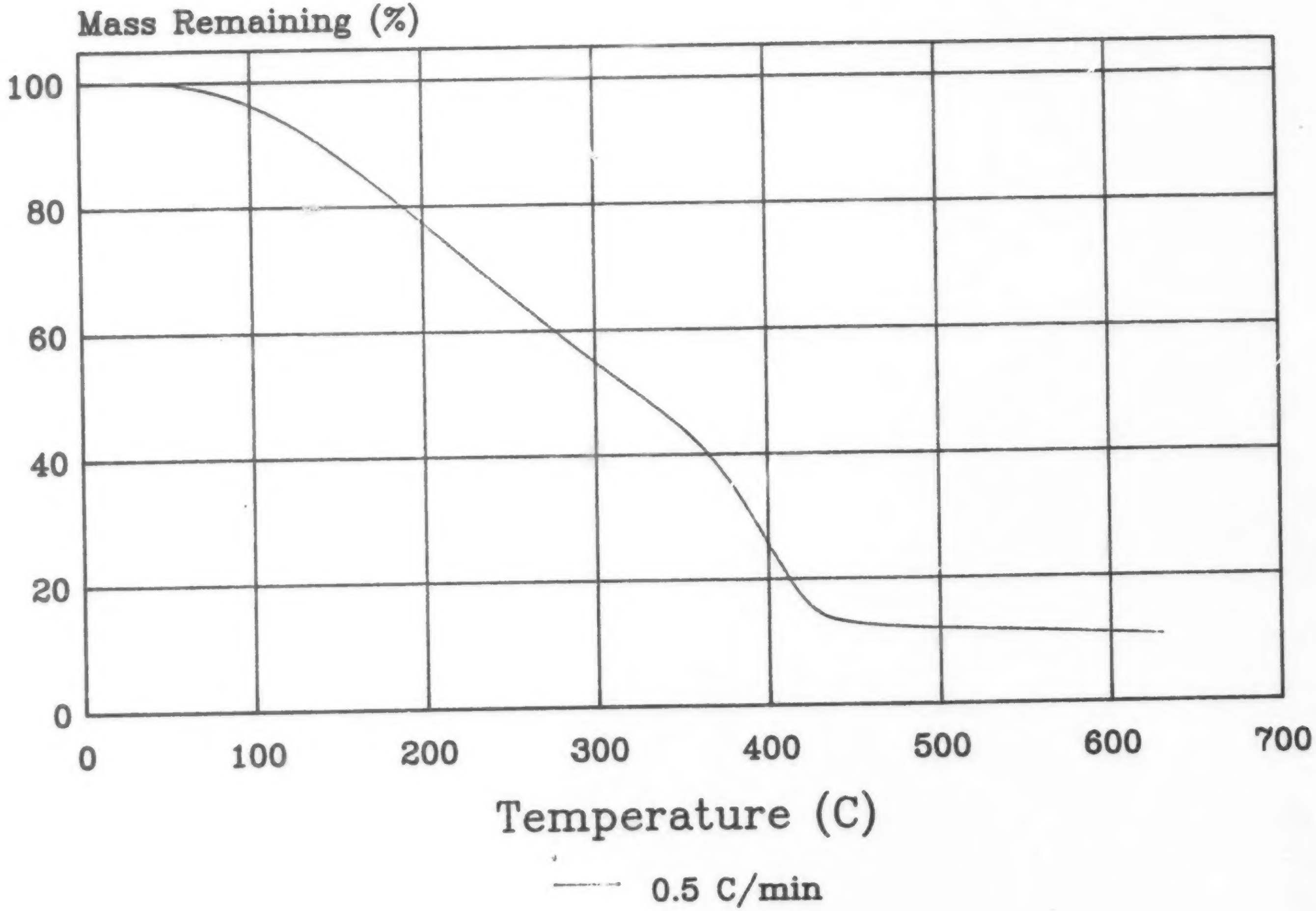

Figure 10: TG Thermogram of Tangleflags Oil in Nitrogen

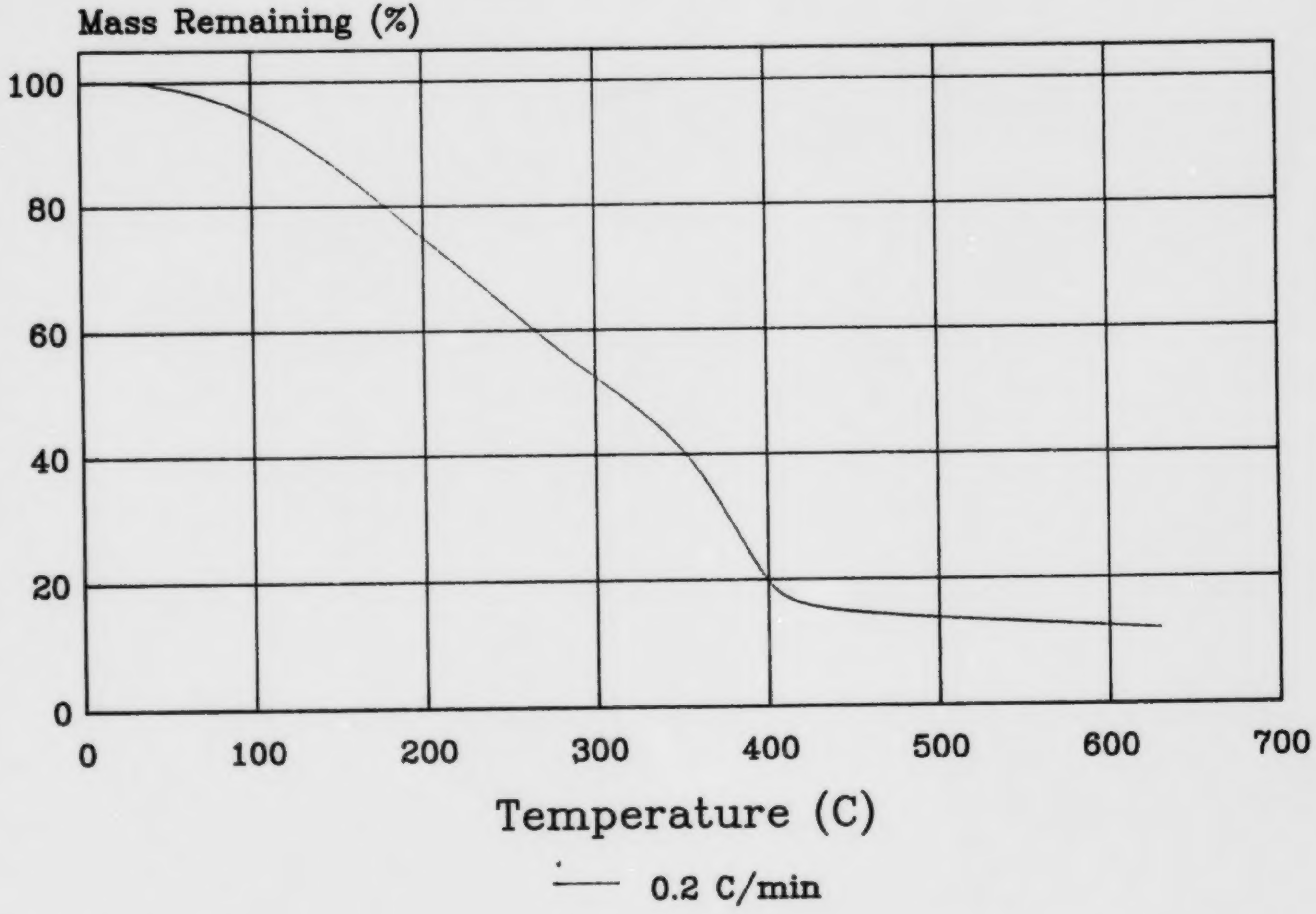

Figure 11: TG Thermogram of Tangleflags Oil in Air

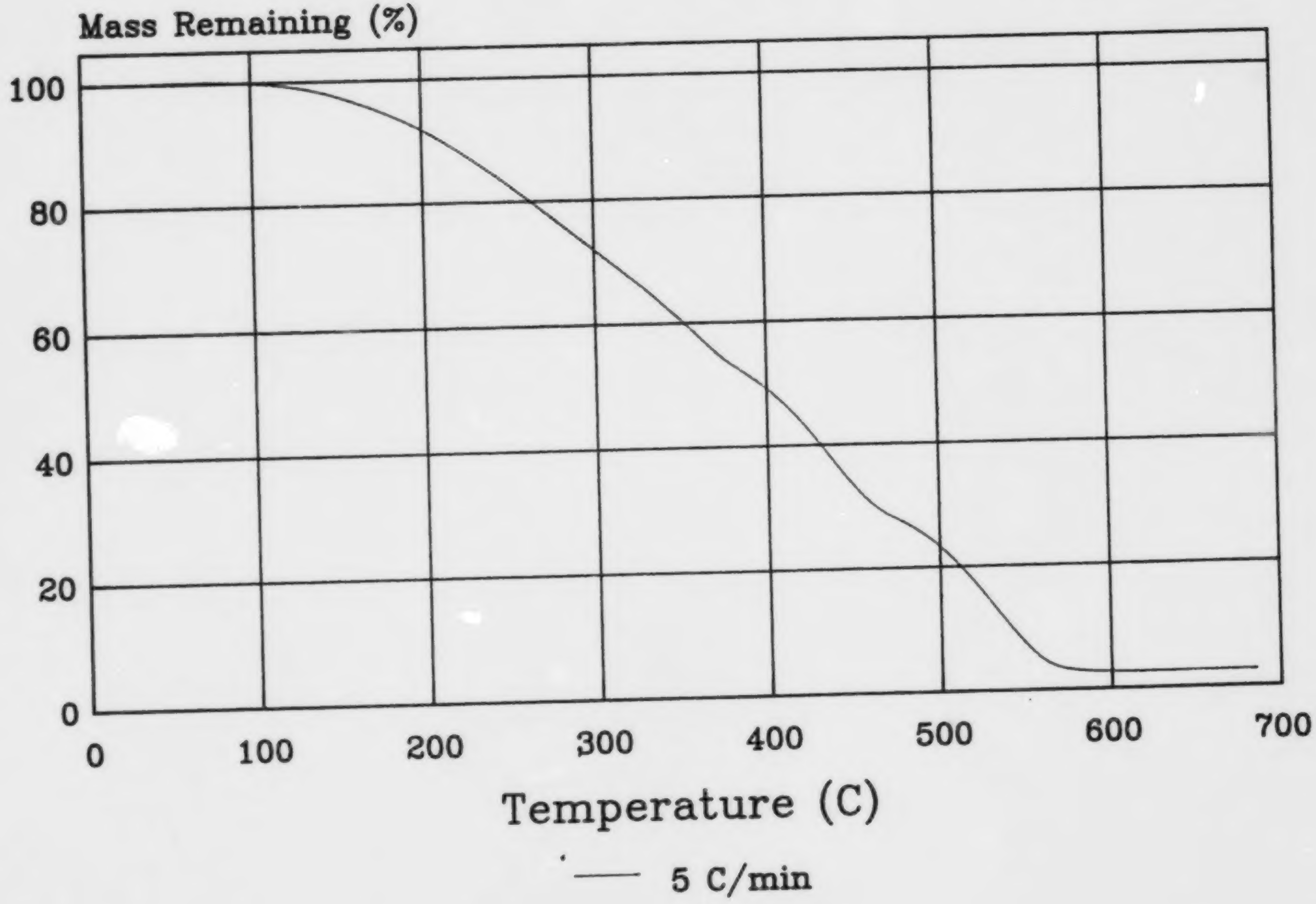

Figure 12: TG Thermogram of Tangleflags Oil in Air

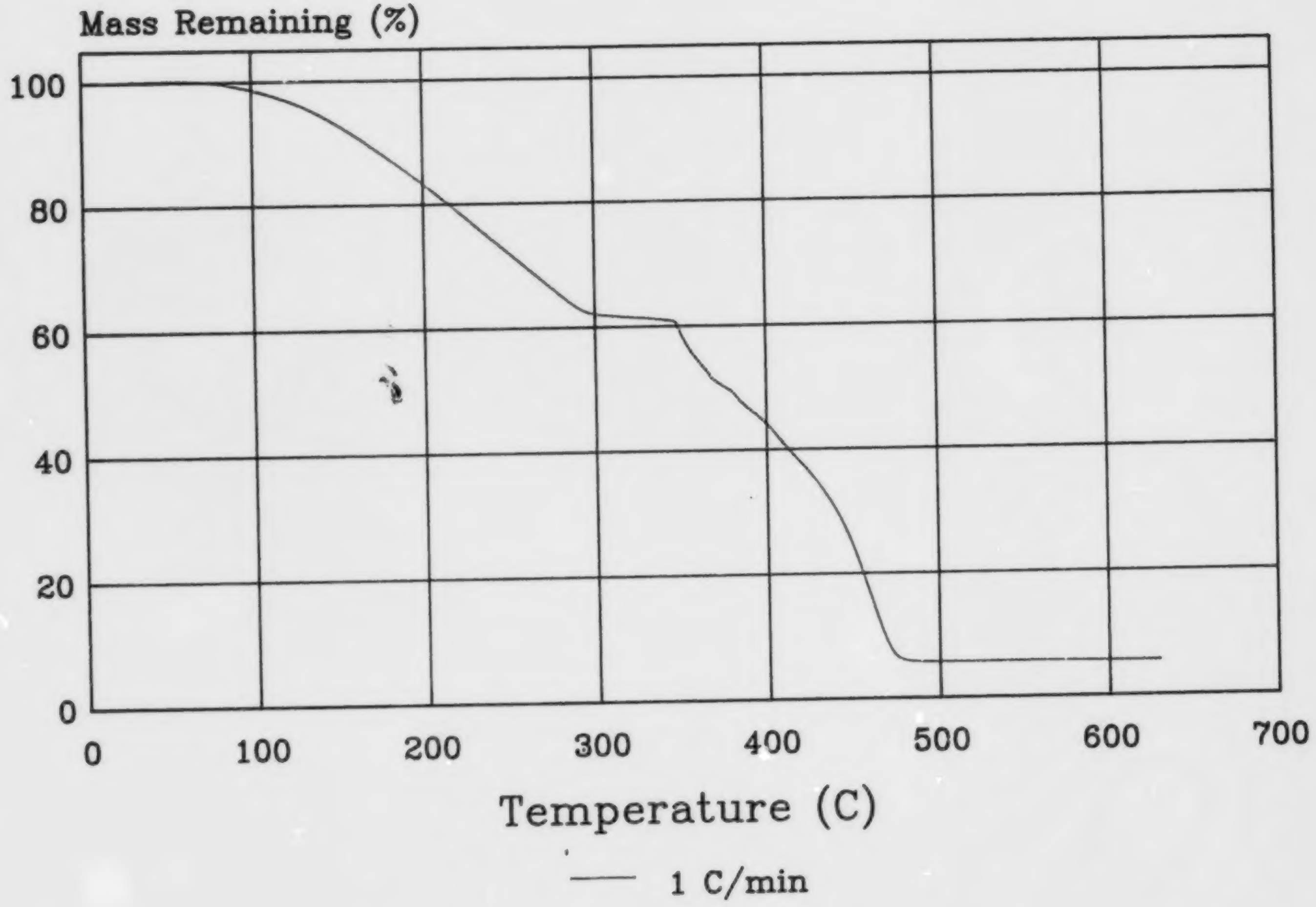

Figure 13: TG Thermogram of Tangleflags Oil and Sand in Air

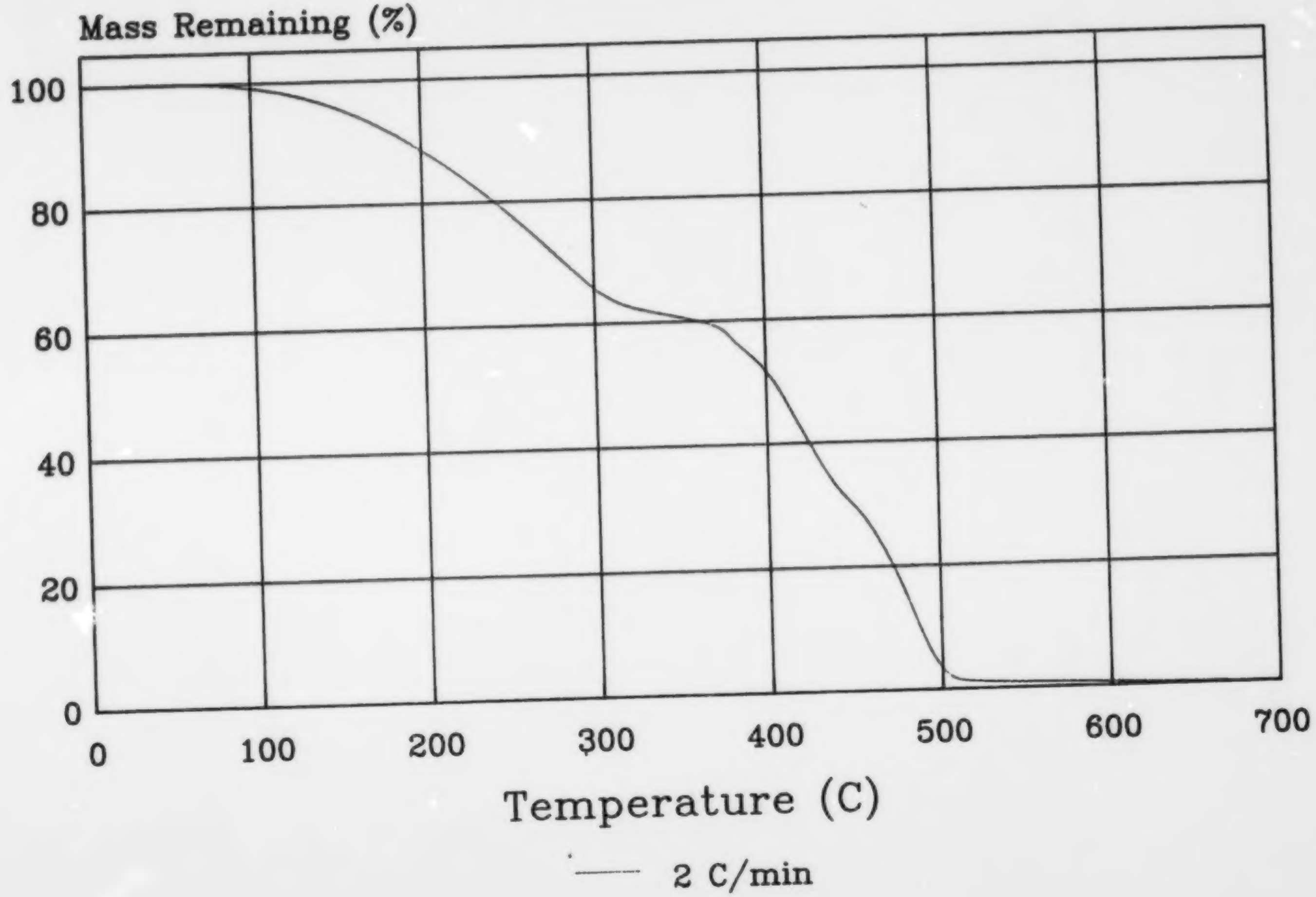

Figure 14: TG Thermogram of Tangleflags Oil and Sand in Air

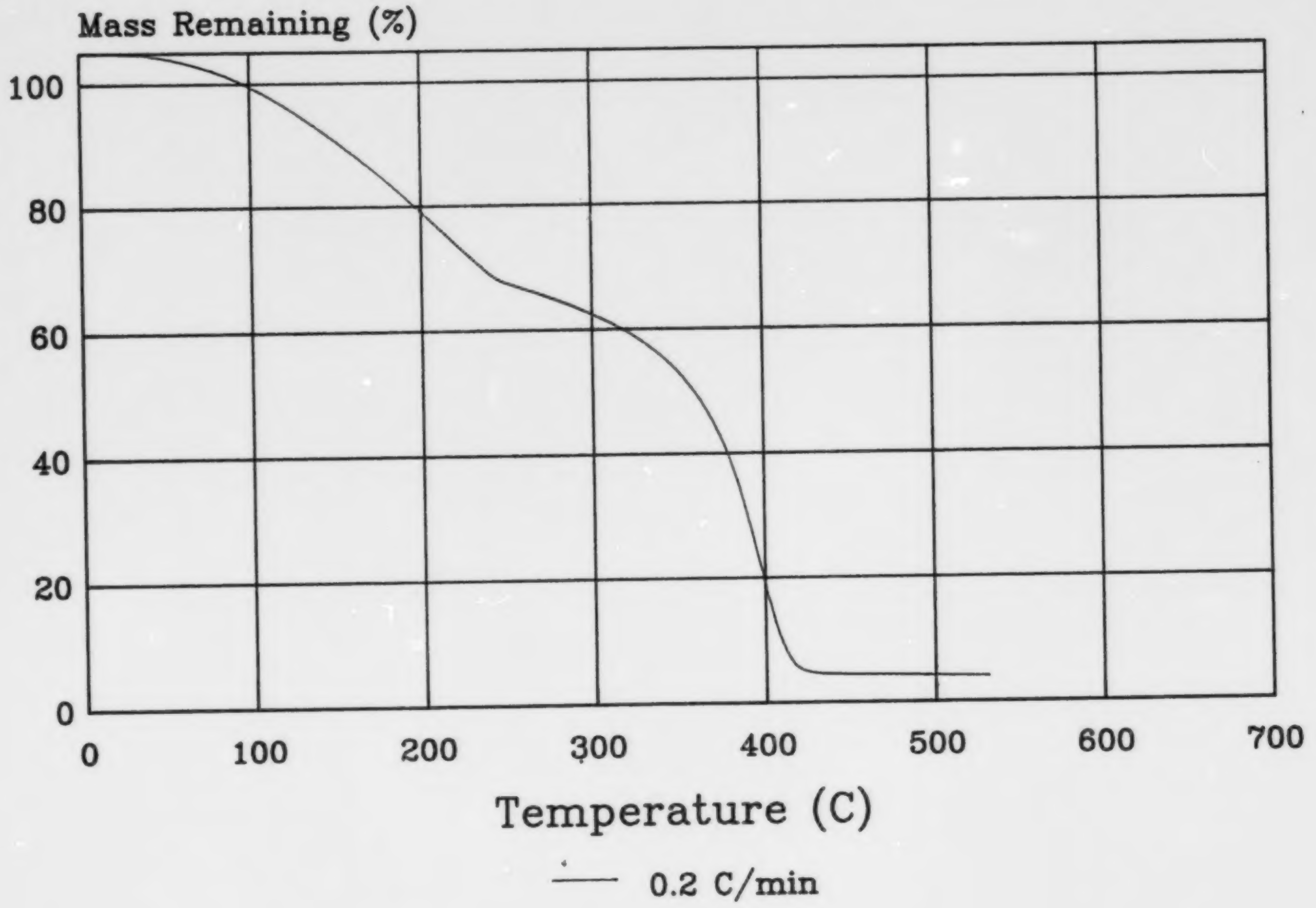

Figure 15: TG Thermogram of Tangleflags Oil and Sand in Nitrogen

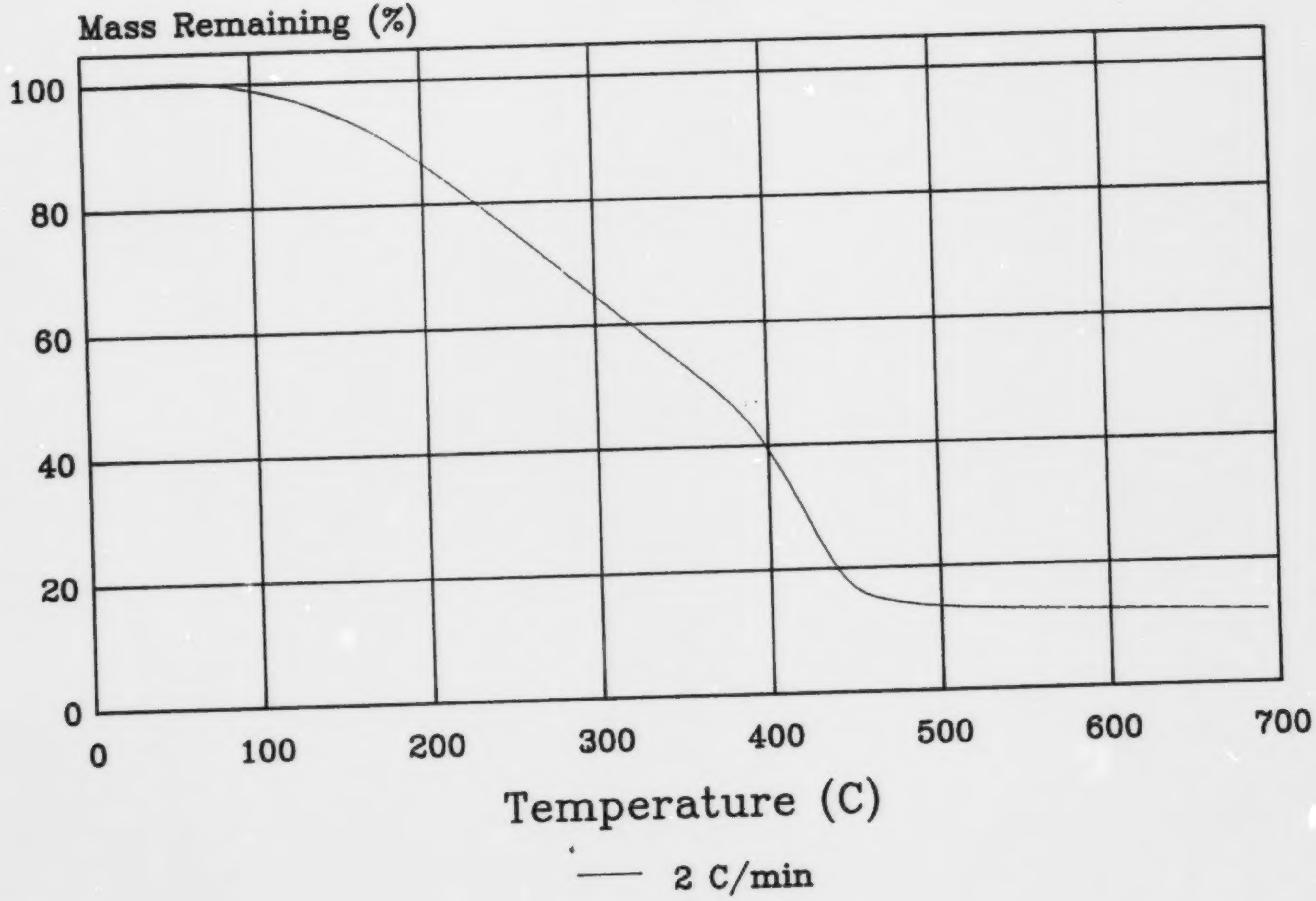

Figure 16 : TG Thermogram of Tangleflags Oil from Well 1A10 in Nitrogen

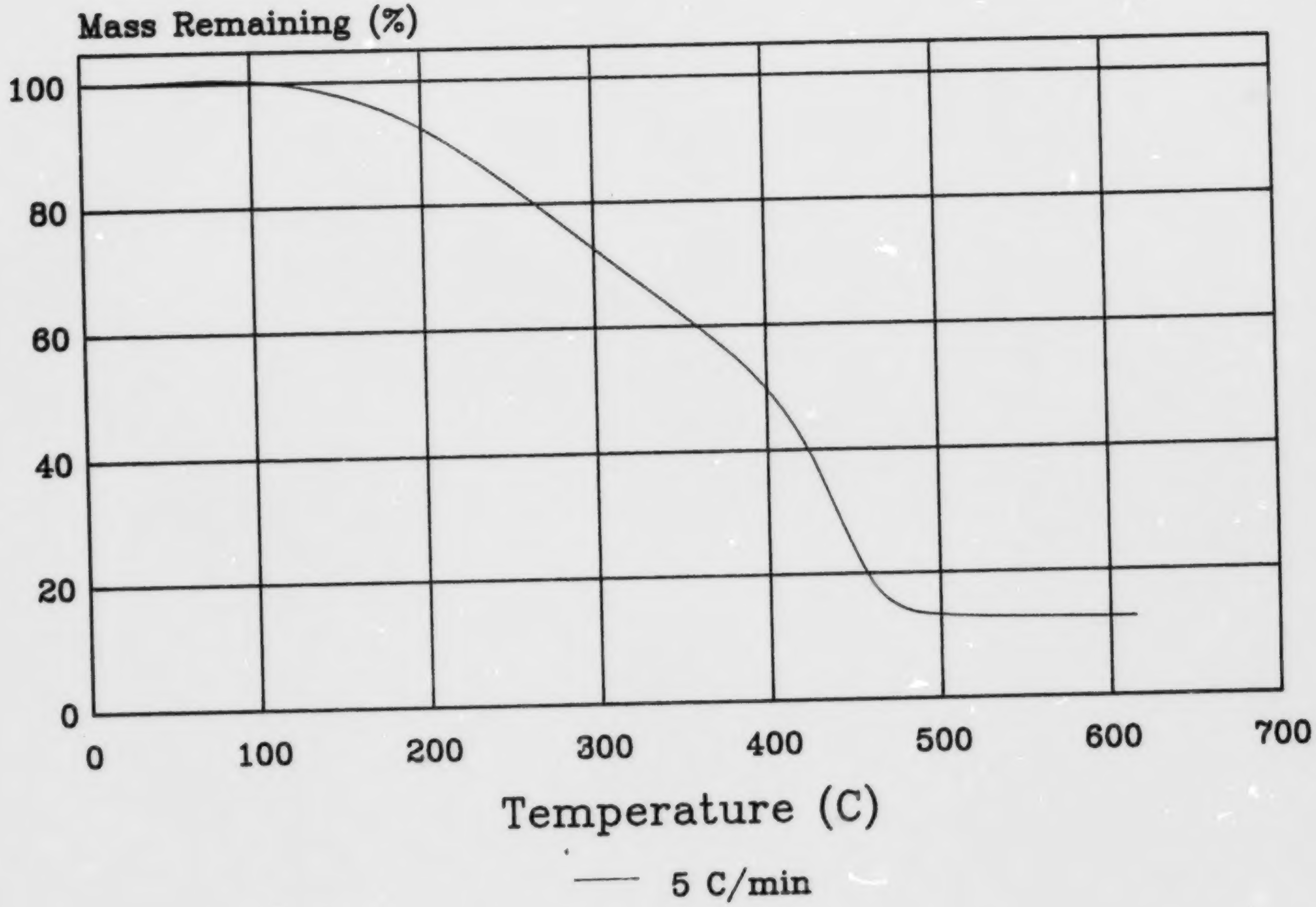

Figure 17 : TG Thermogram of Tangleflags Oil from Well D7 in Nitrogen

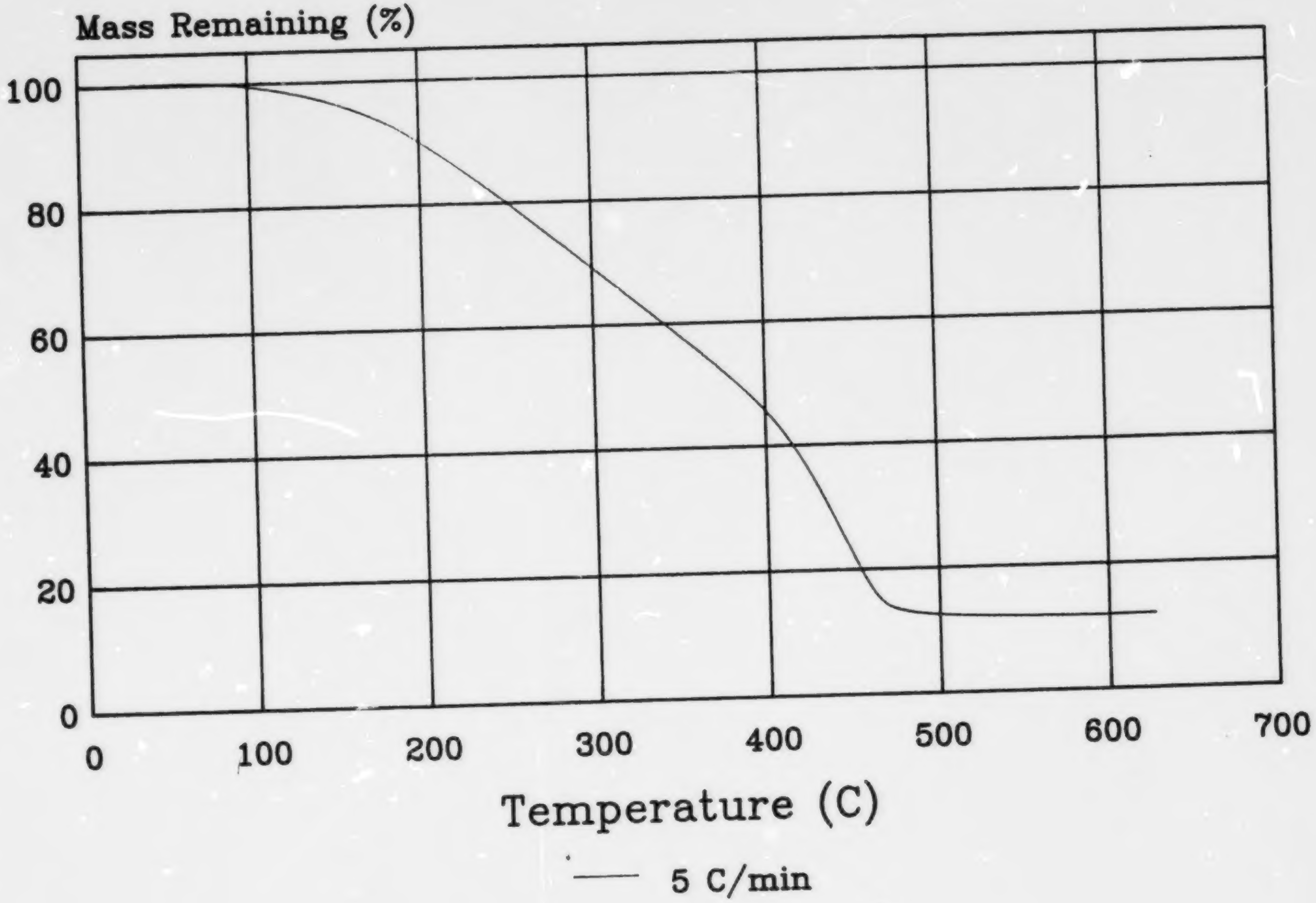

Figure 18 : TG Thermogram of Tangleflags
Oil from Well 4C3 in Nitrogen

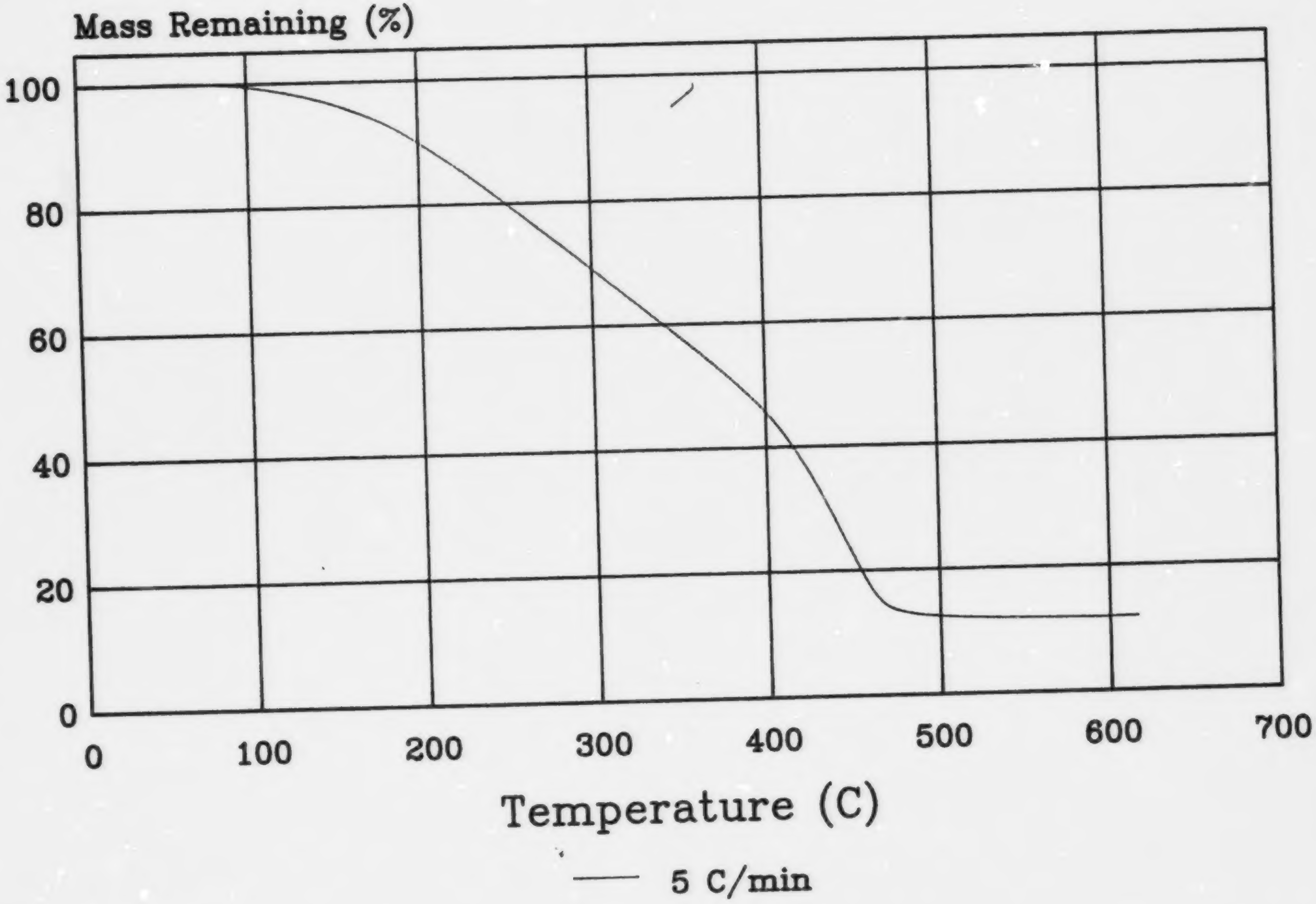

Figure 19 : TG Thermogram of Tangleflags Oil from Well 4B7 in Nitrogen

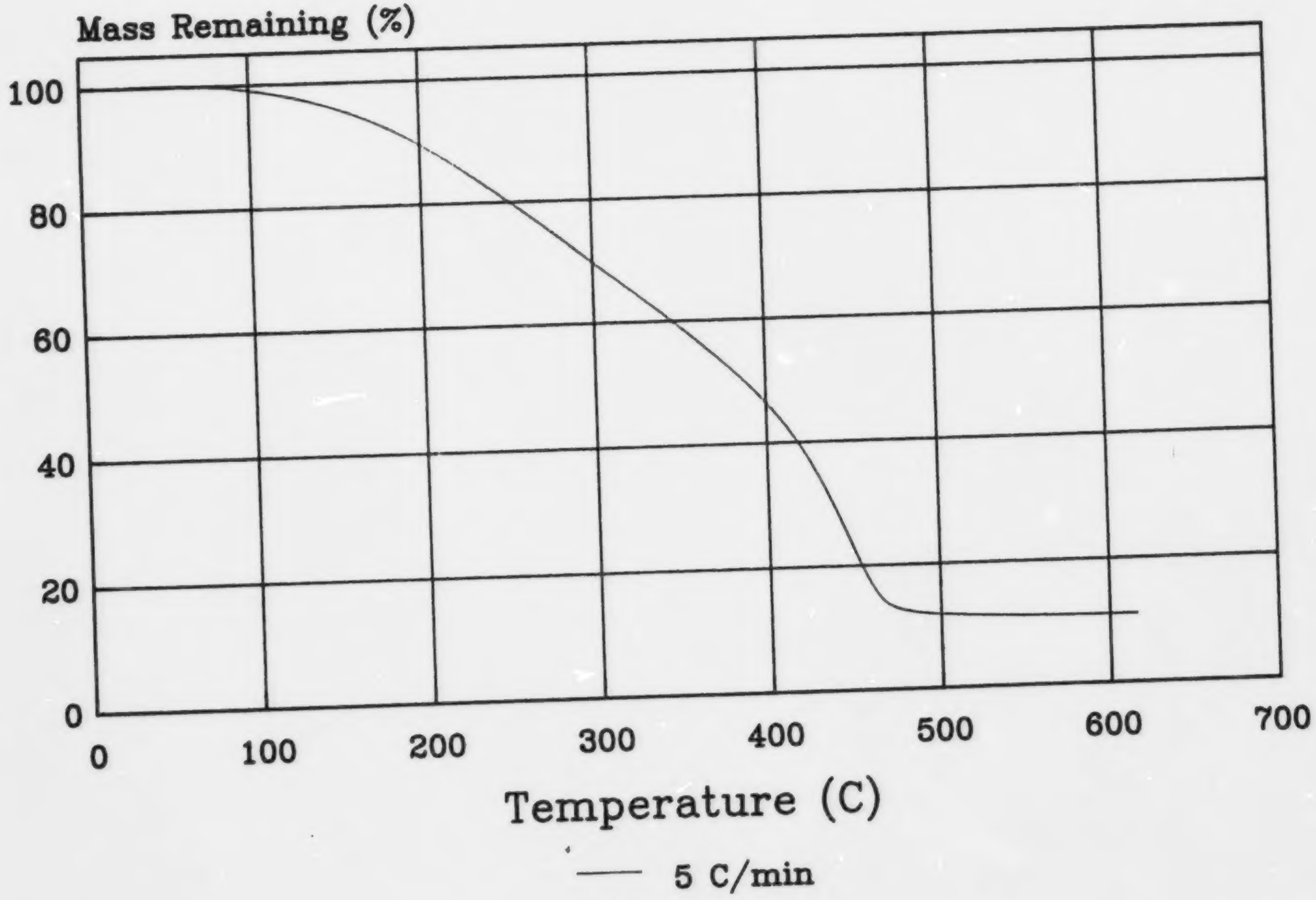

Figure 20 : TG Thermogram of Tangleflags Oil from Well 4C2 in Nitrogen

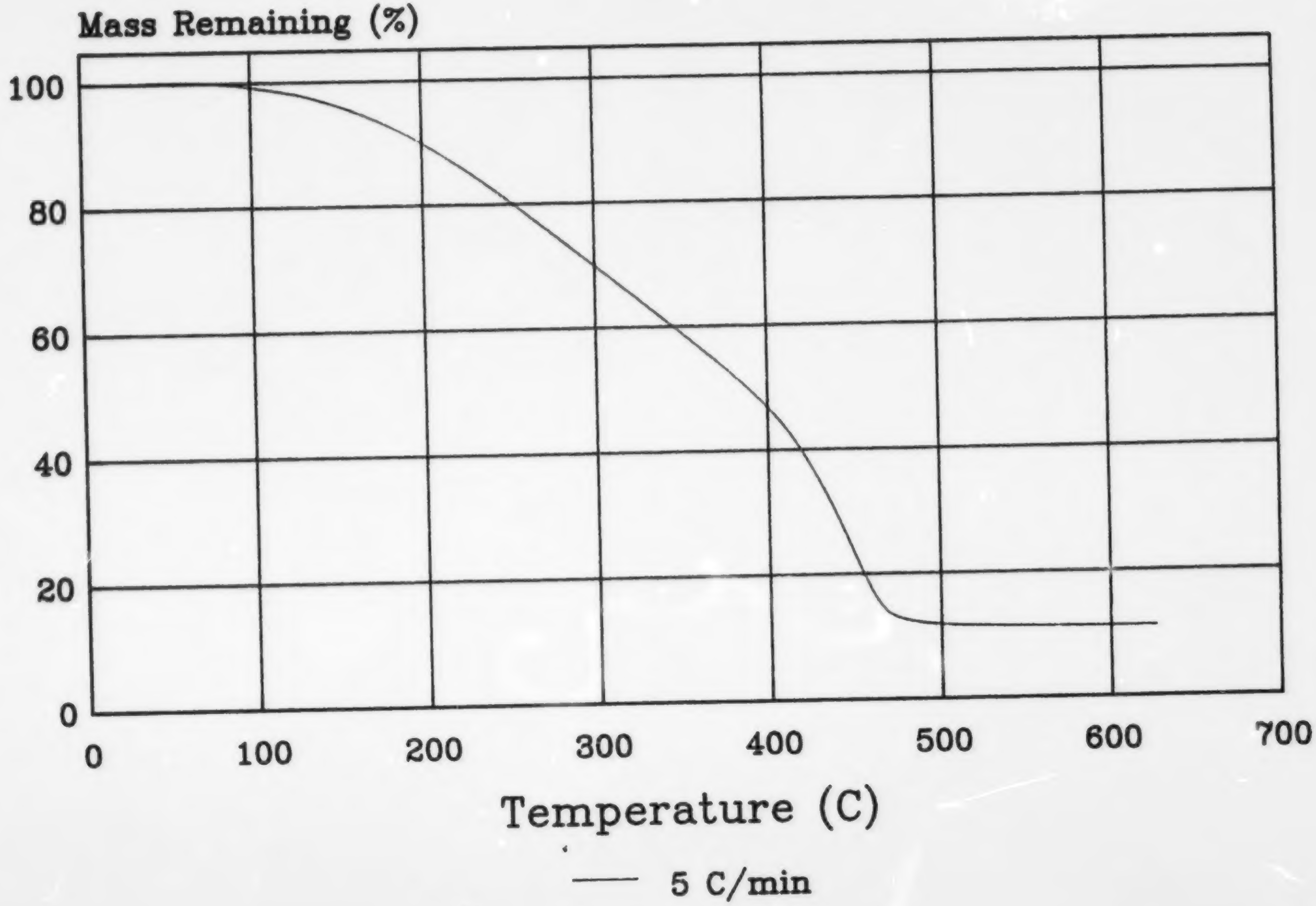

Figure 21 : TG Thermogram of Tangleflags Oil from Well D3 in Nitrogen

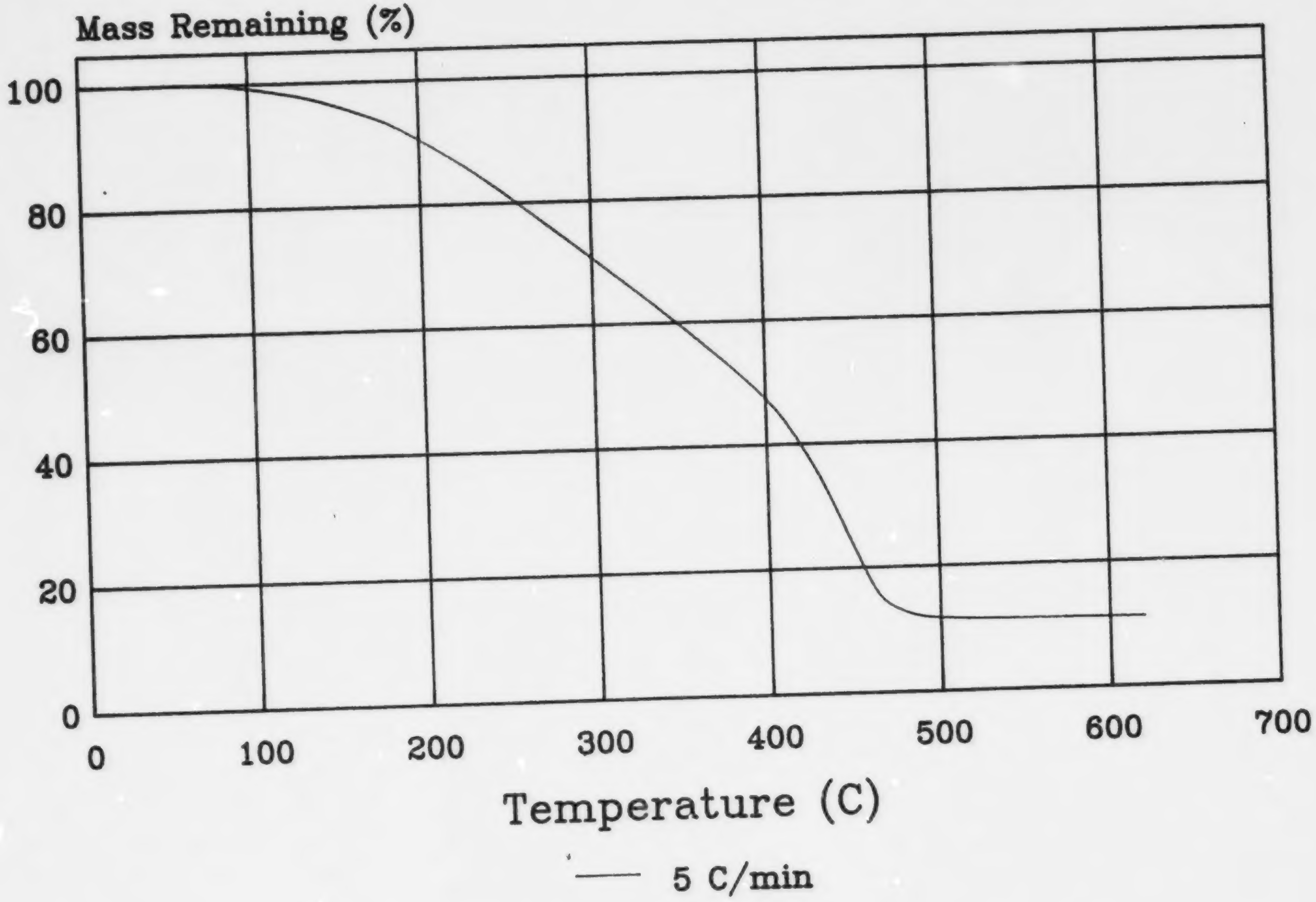

Figure 22: TG Thermogram of Tangleflags Oil from Well D11 in Nitrogen

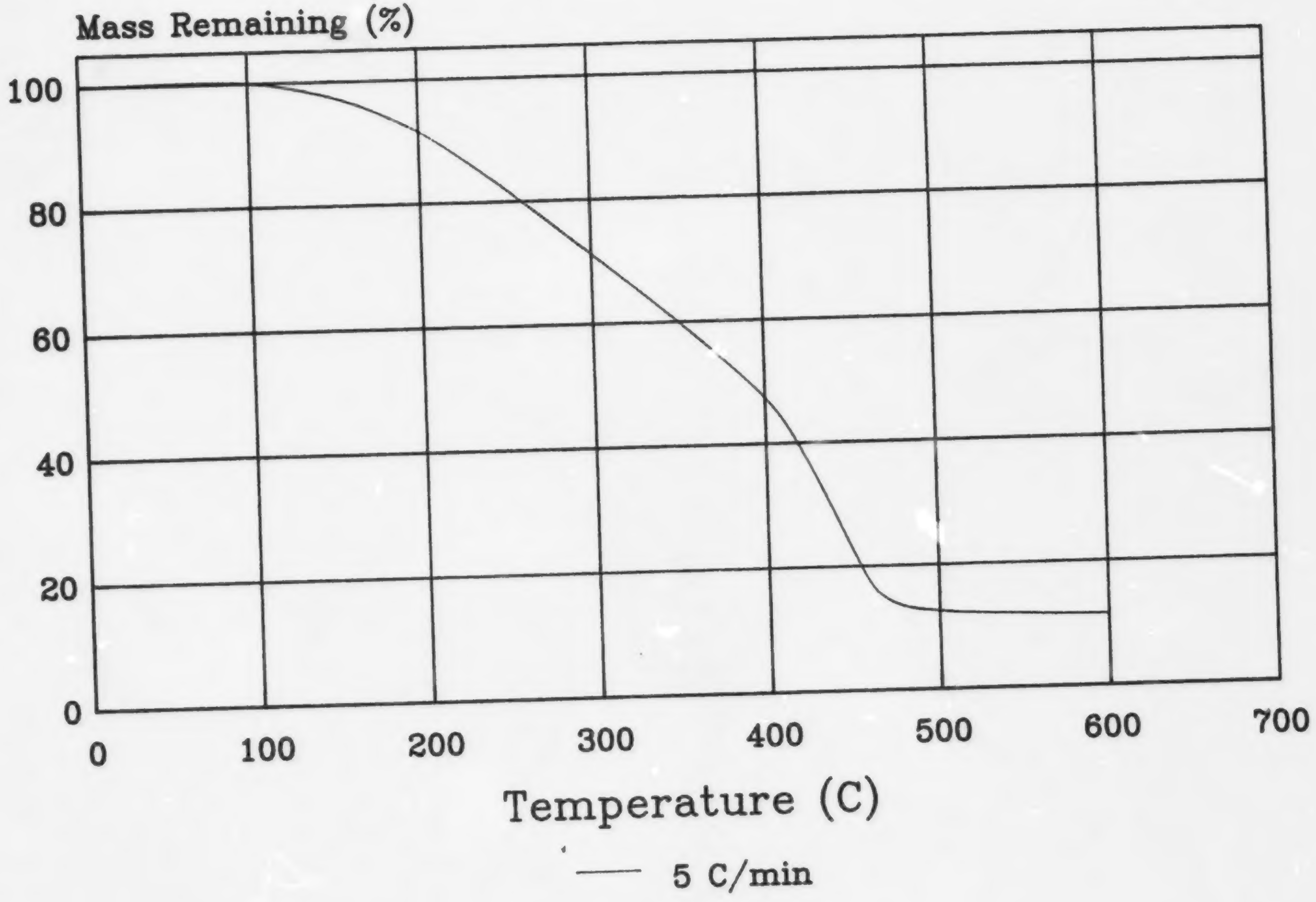

Figure 23: TG Thermogram of Golden Lake Oil in Nitrogen

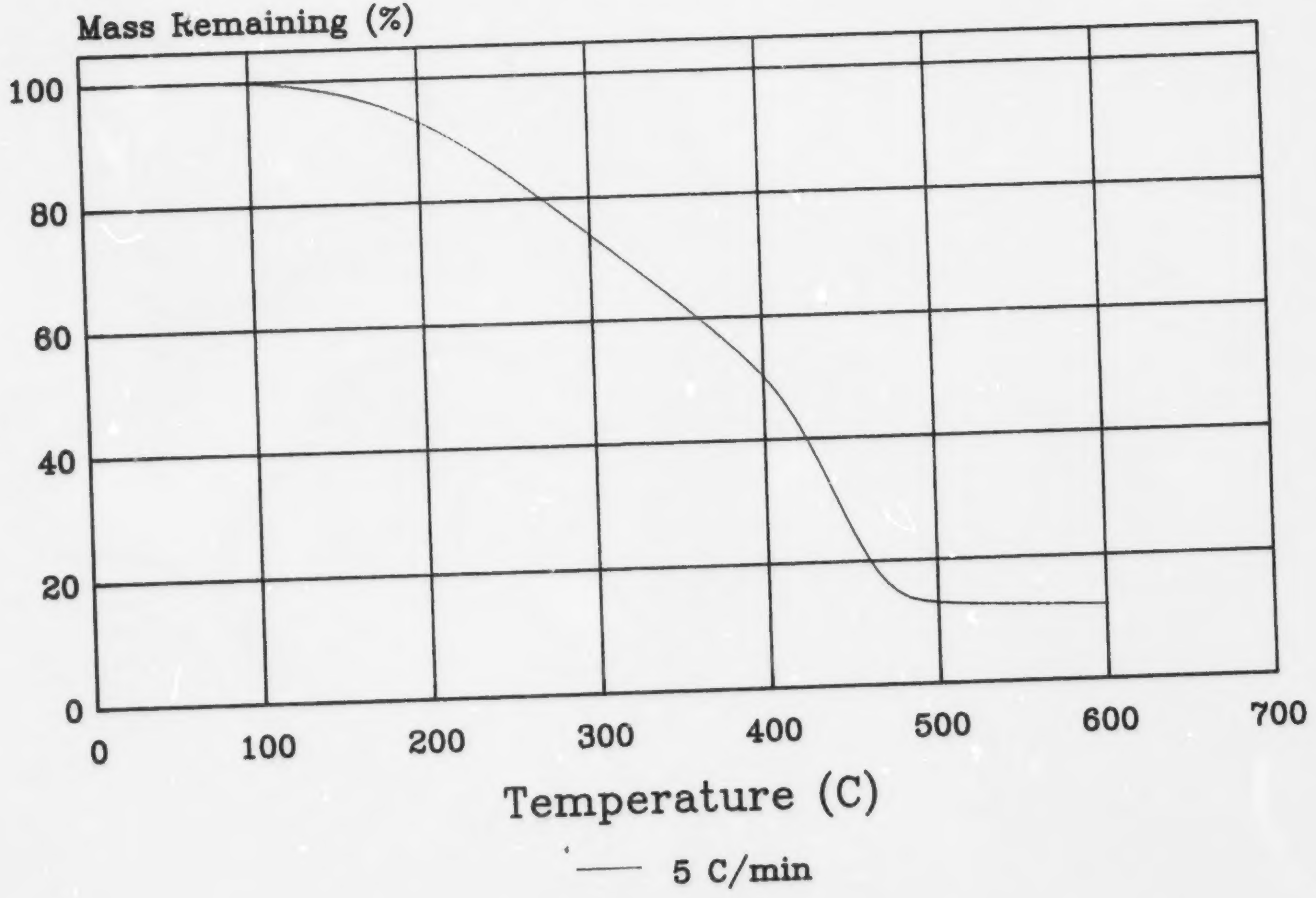

Figure 24 : TG Thermogram of Caribou Lake Oil in Nitrogen

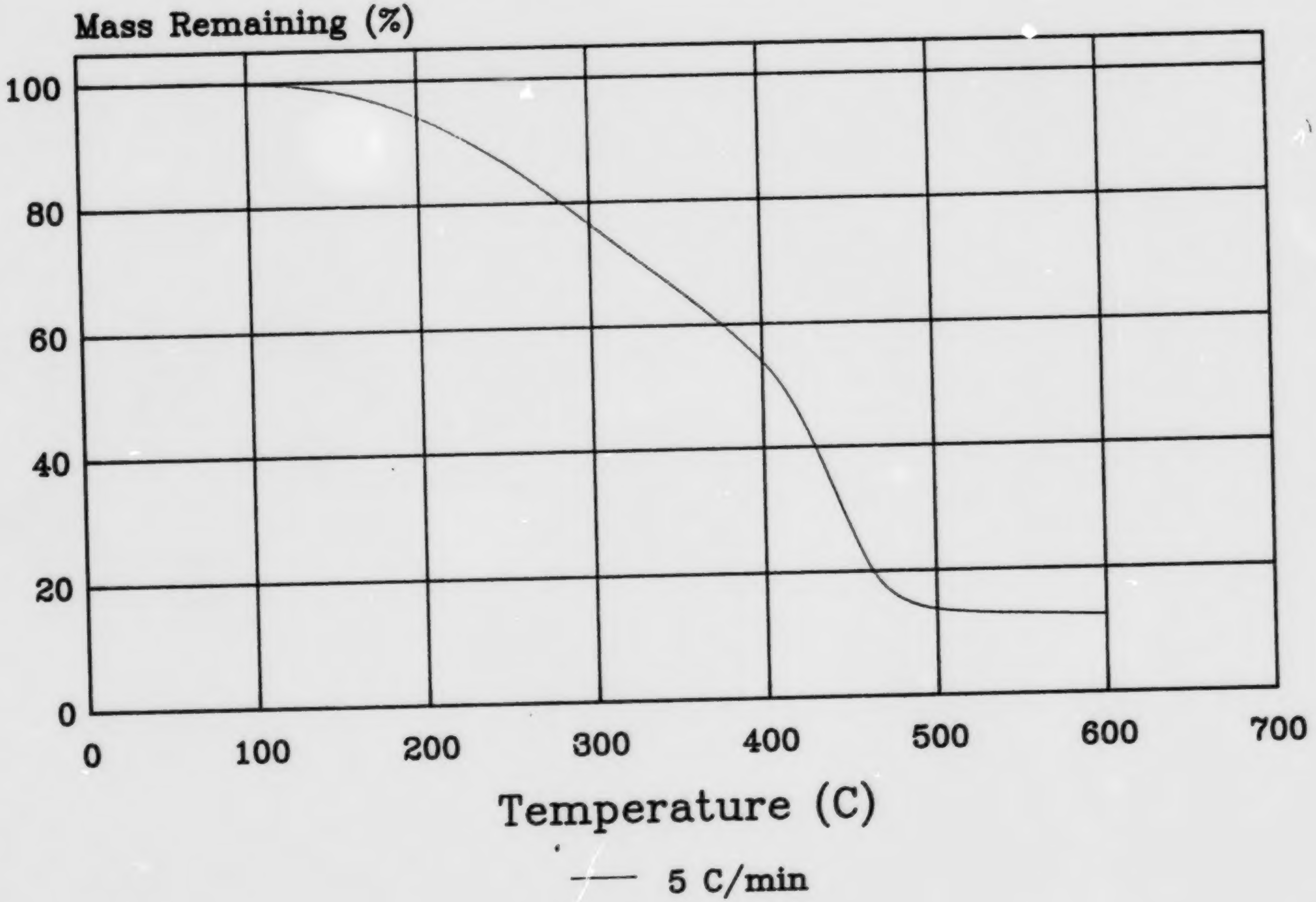

Figure 25: TG Thermogram of Tangleflags Asphaltenes in Nitrogen

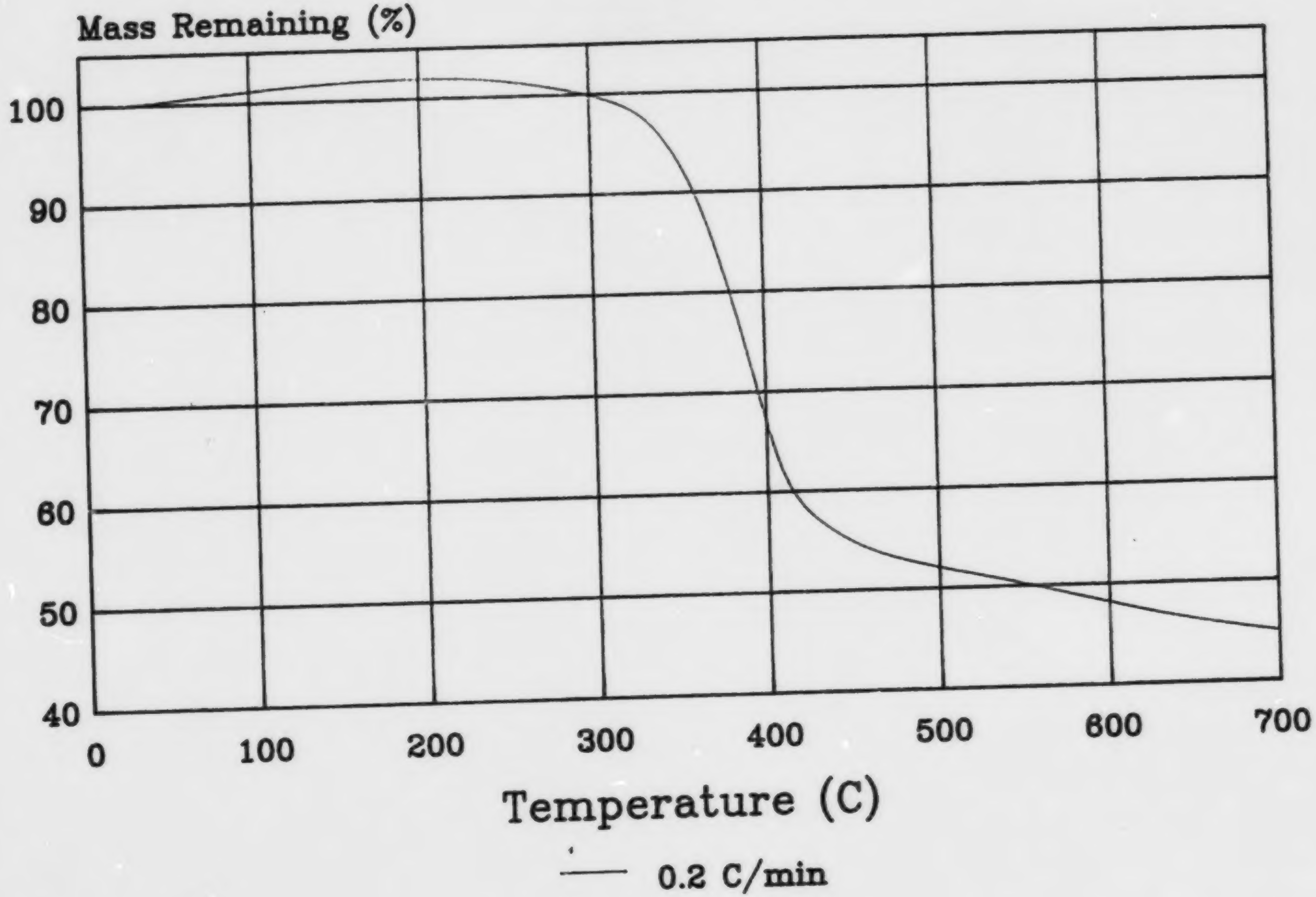

Figure 26: TG Thermogram of Tangleflags Asphaltenes in Nitrogen

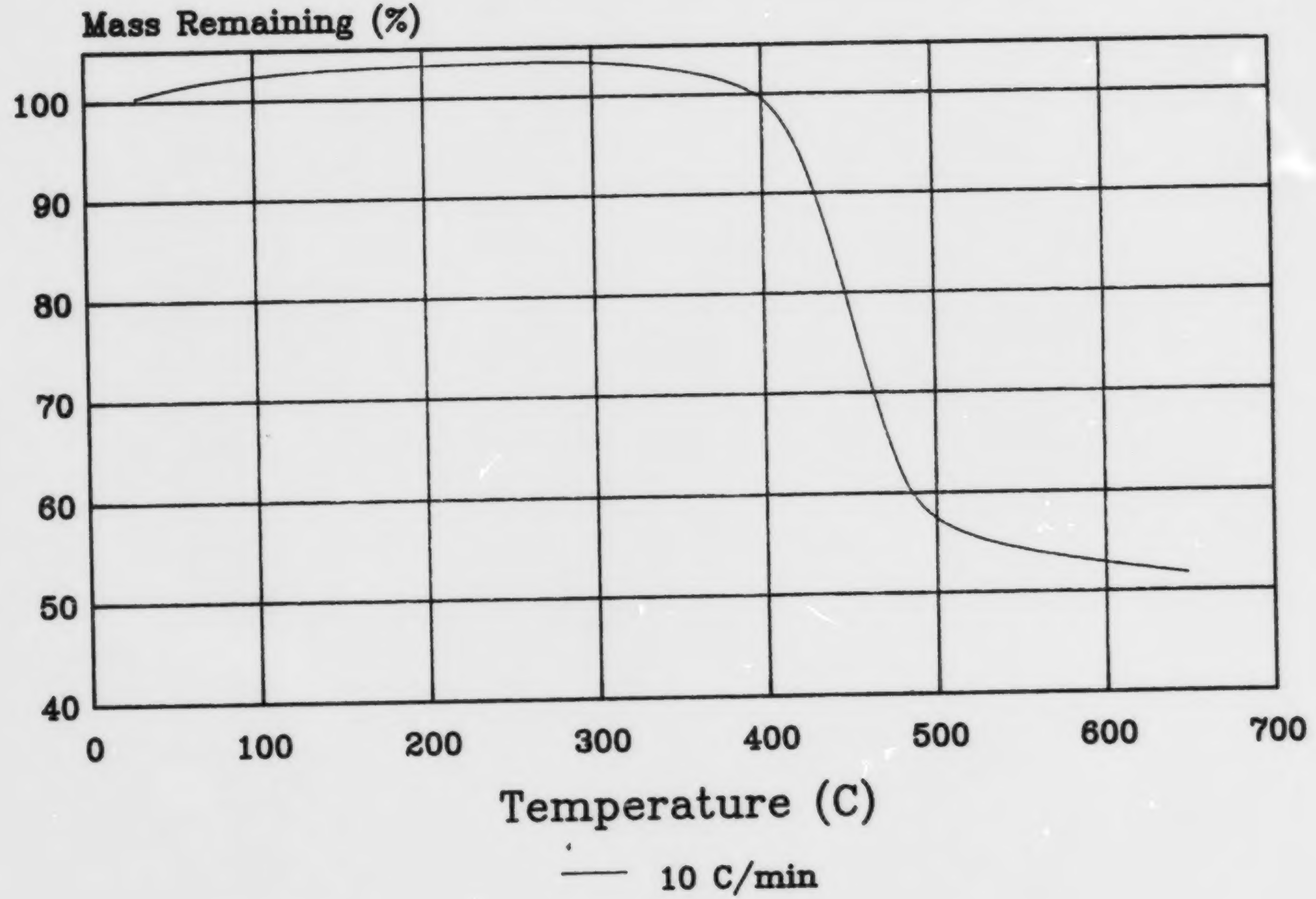

Figure 27: TG Thermogram of Oxidized Tangleflags Oil in Nitrogen

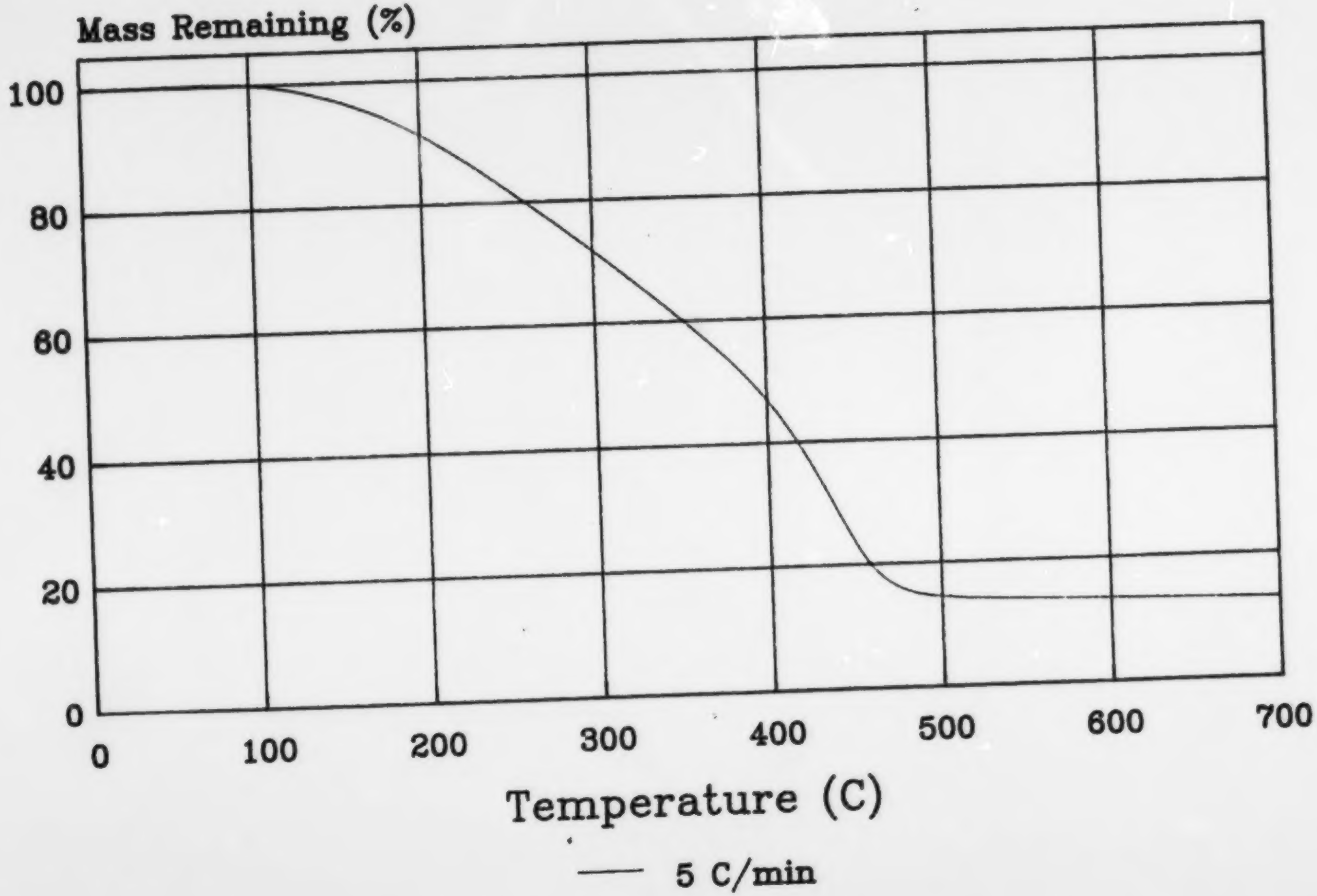

Figure 28: TG Thermogram of Oxidized Tangleflags Oil in Air

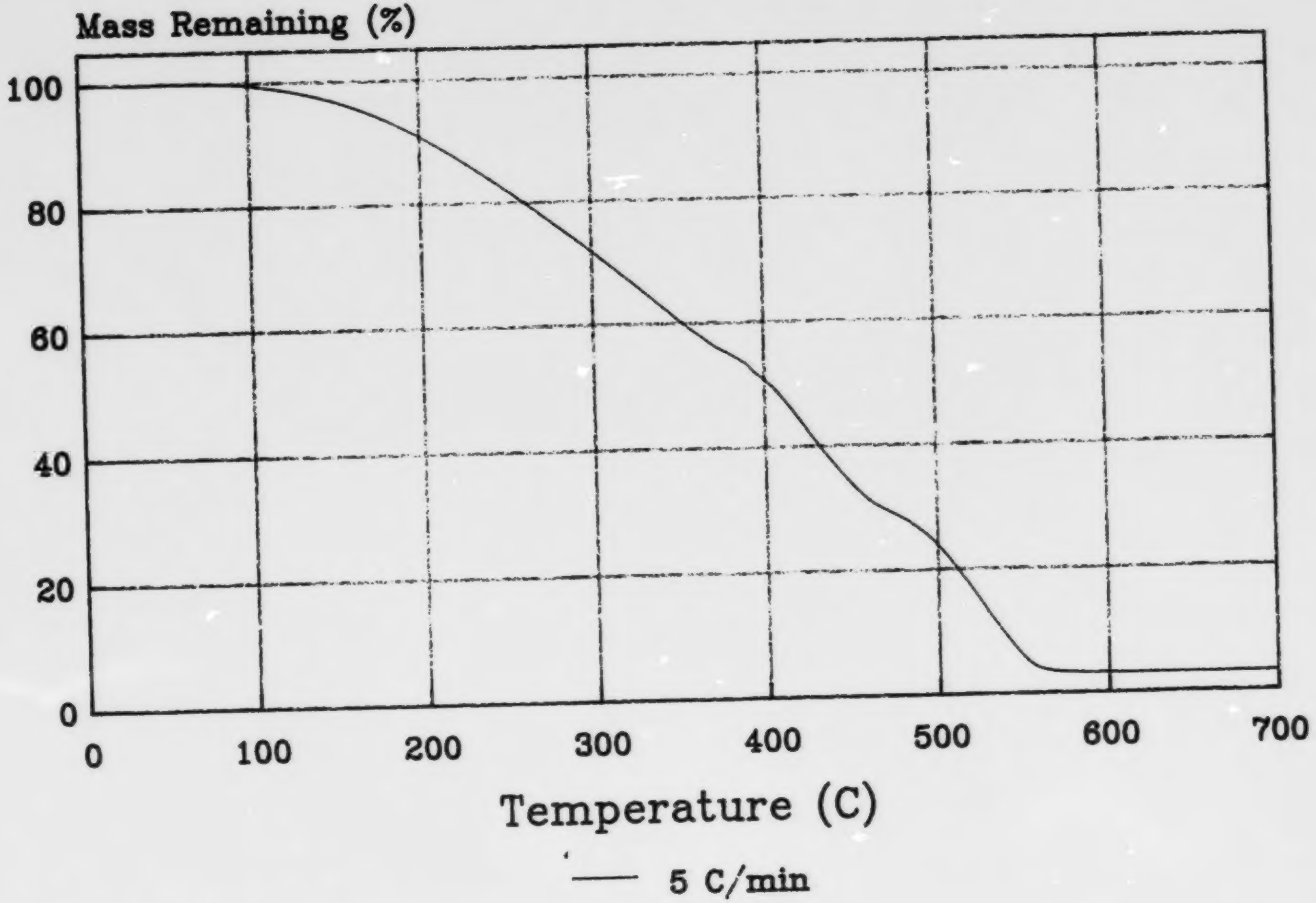

Figure 29: TG Thermogram of Tangleflags Oil in Air Followed by Nitrogen

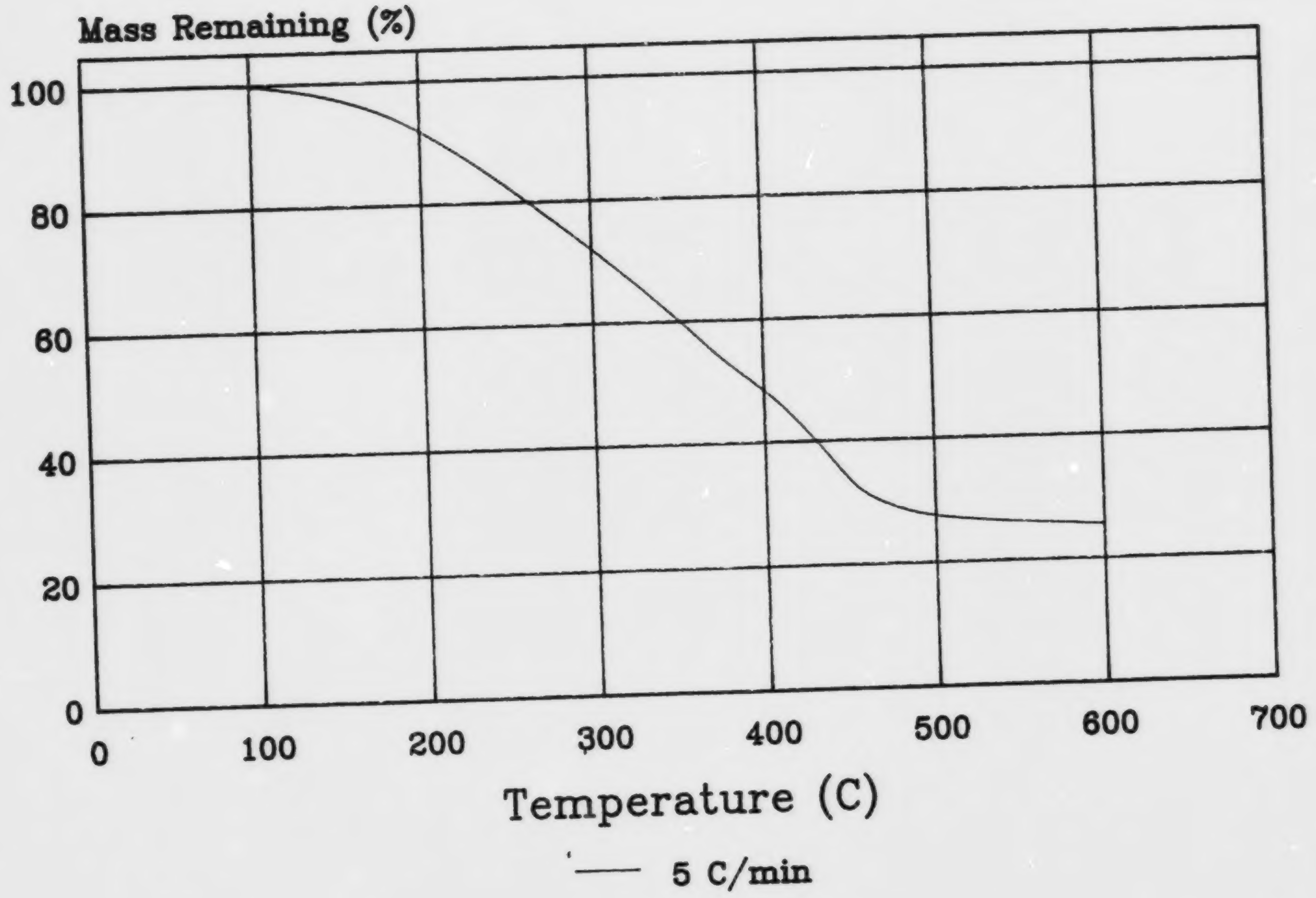

Figure 30: TG Thermogram of Tangleflags Oil in Air Followed by Nitrogen

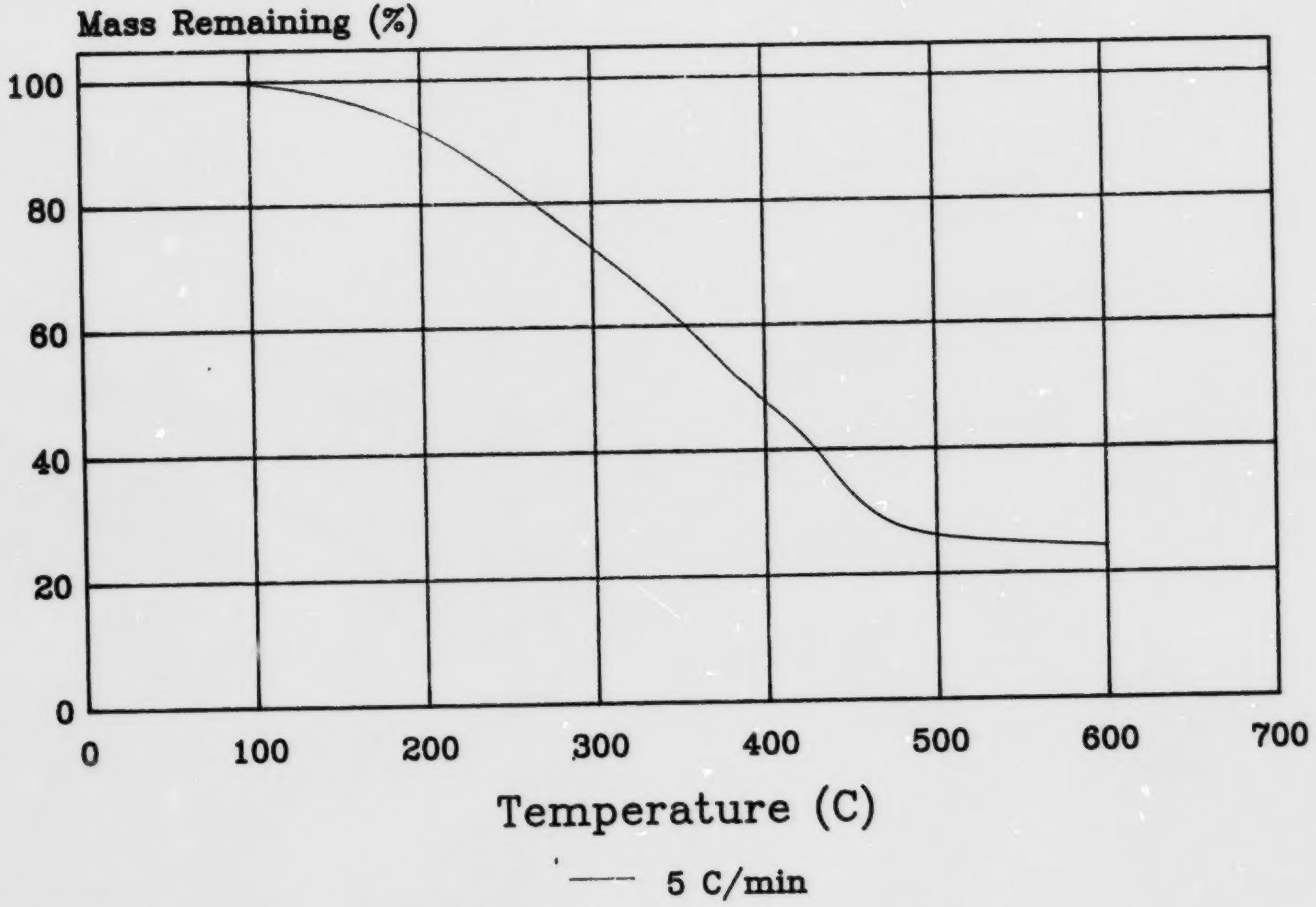

Figure 31: TG Thermogram of Tangleflags
Oil Heated Rapidly in Air

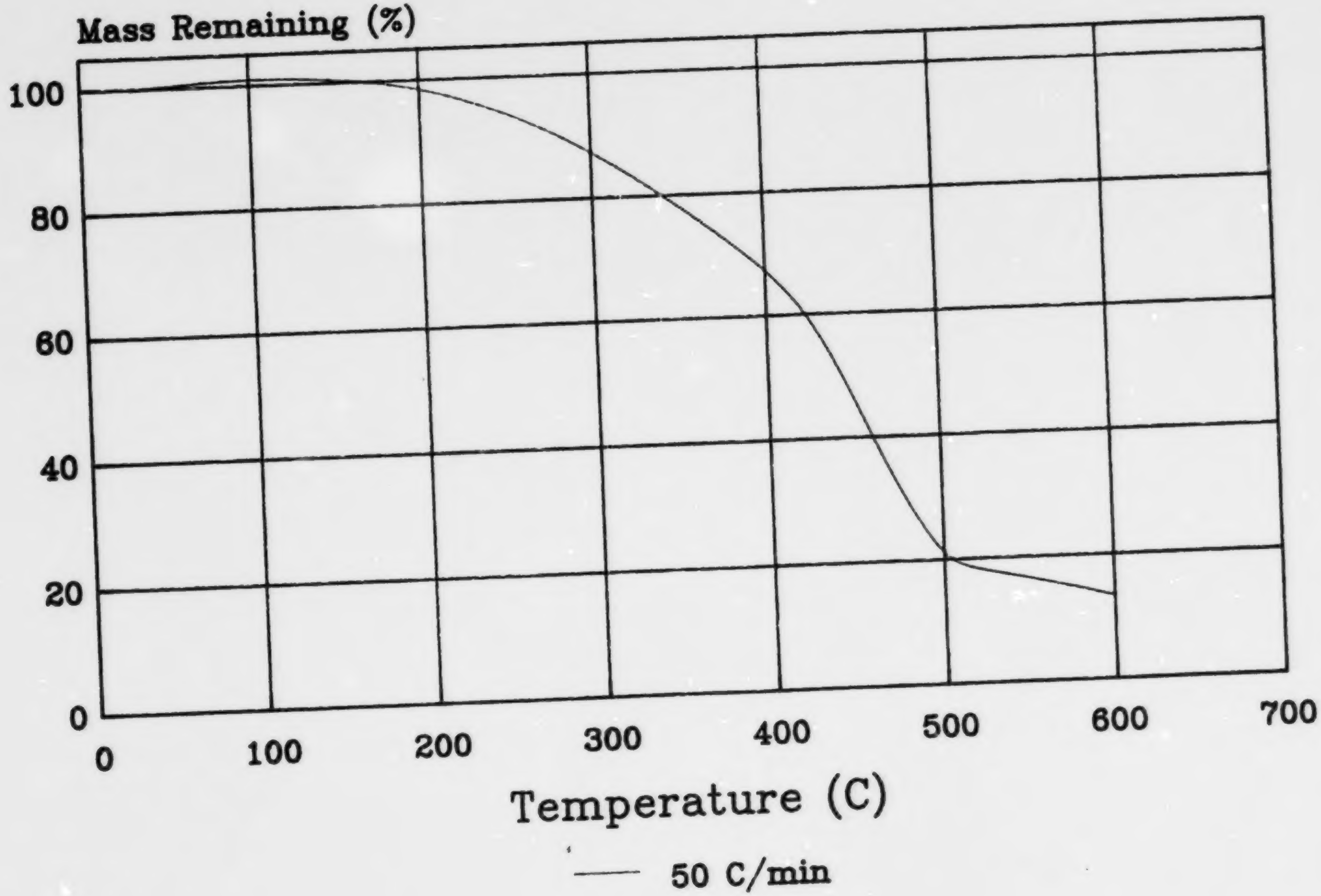

9.0 APPENDIX

OPERATOR: R.SAETRE
DATE: 03/04/87
RUN No. 1
TG Setting 50mg
DTA Setting 0.1mV

NETZSCH STA 429/409
REFERENCE : AL203
CRUCIBLE : AL203
FILE NAME : TOIL1
MATERIAL TOIL

ATM. NITROGEN
FLOW = 70 cc/min
HEAT RATE = 10 C/min
SAMPLE WT.= 32.4 mg
REF WEIGHT 0 mg

(Figure 1)

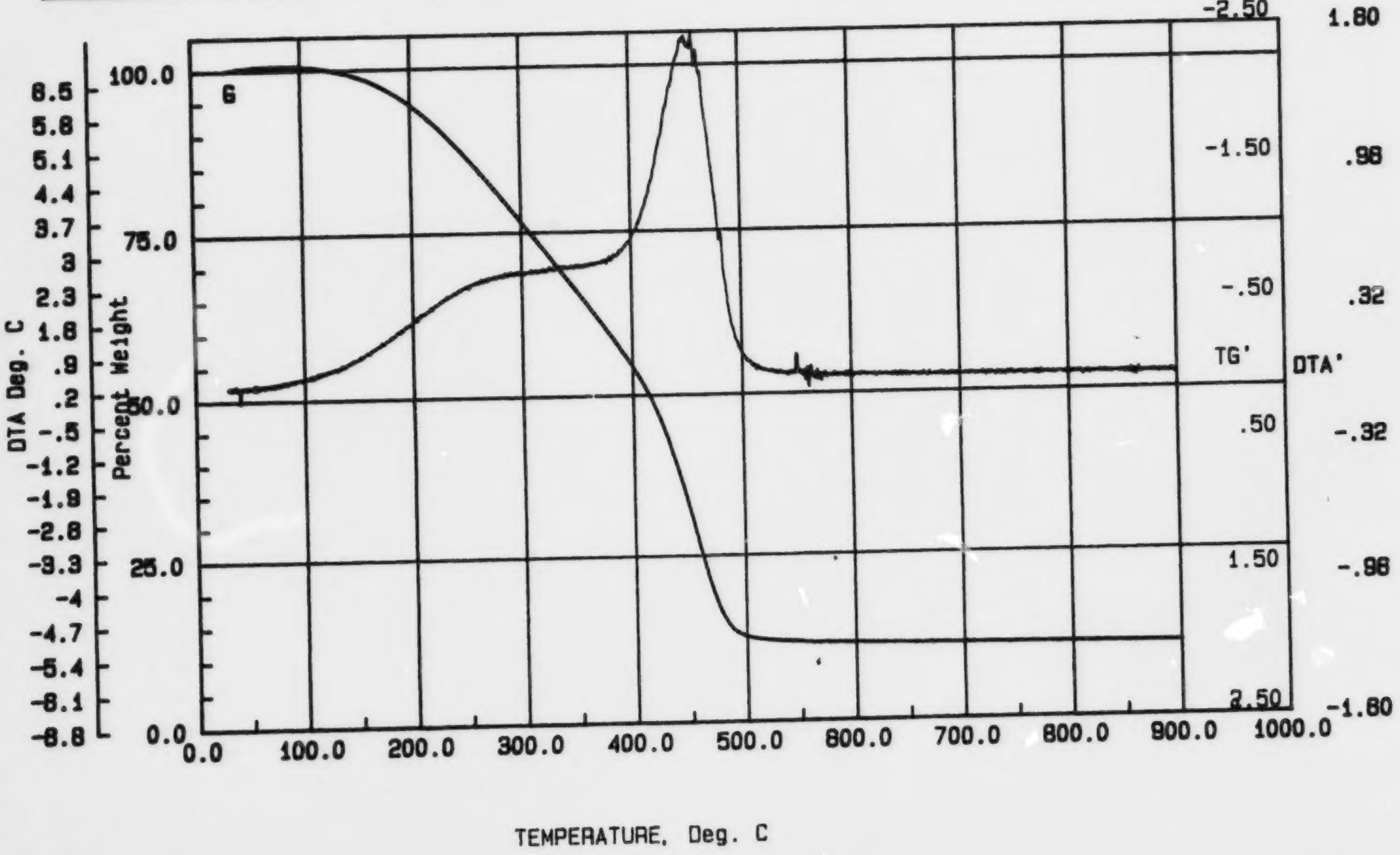

OPERATOR:	R.SAETRE	NETZSCH STA 429/409		ATM.	NITROGEN
DATE:	09/06/87	REFERENCE :	AL203	FLOW =	70 cc/min
RUN No.	3	CRUCIBLE :	AL203	HEAT RATE =	10 C/min
TG Setting	50mg	FILE NAME :	TOIL1B	SAMPLE WT.=	28.4 mg
DTA Setting	0.1mV	MATERIAL	TOIL2	REF WEIGHT	0 mg

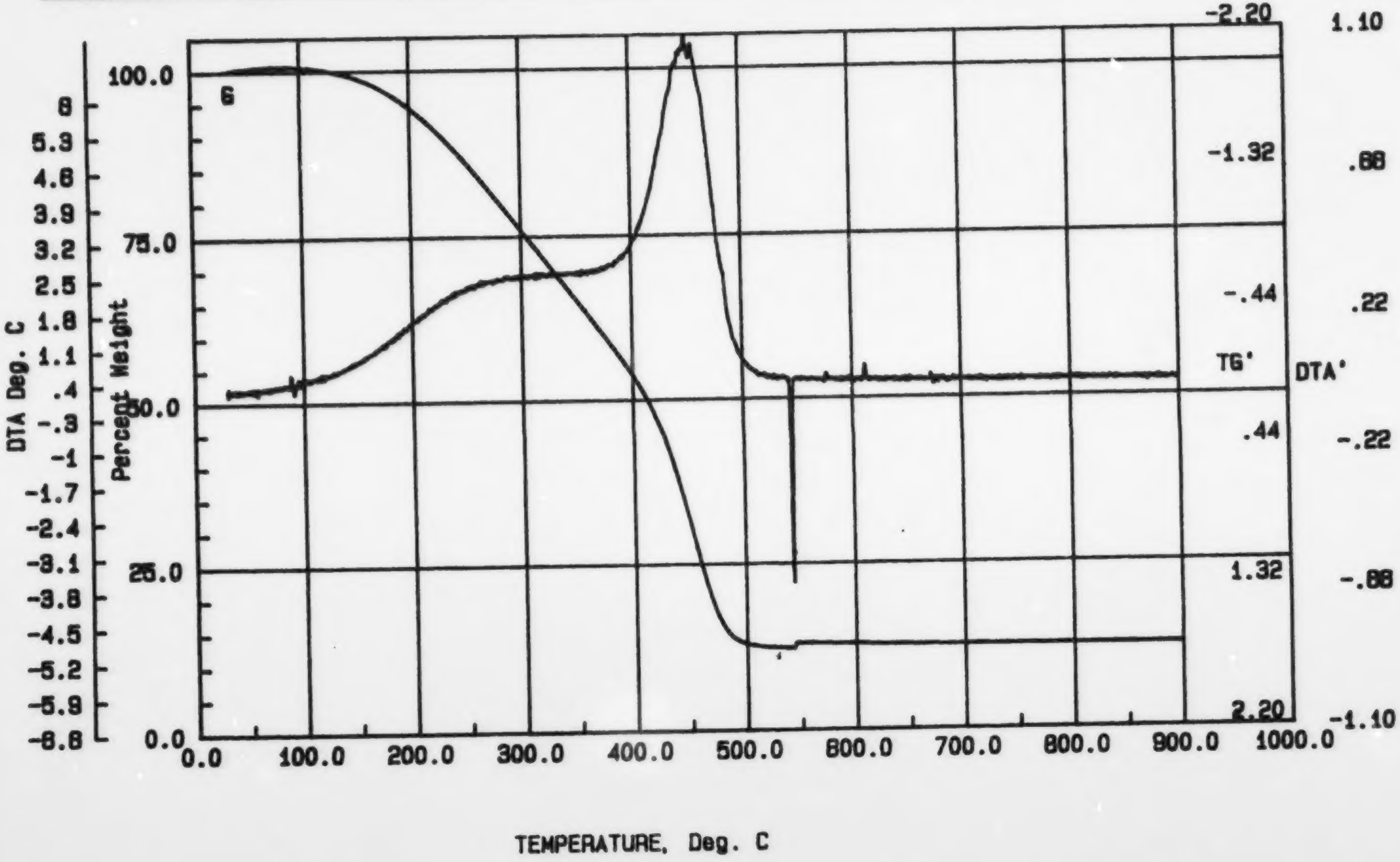

OPERATOR: R.SAETRE
DATE: 09/04/87
RUN No. 3
TG Setting 50mg
DTA Setting 0.1mV

NETZSCH STA 429/409
REFERENCE : AL203
CRUCIBLE : AL203
FILE NAME : TOILN3
MATERIAL TOILN3

ATM. NITROGEN
FLOW = 70 cc/min
HEAT RATE = 10 C/min
SAMPLE WT.= 14.8 mg
REF WEIGHT 0 mg

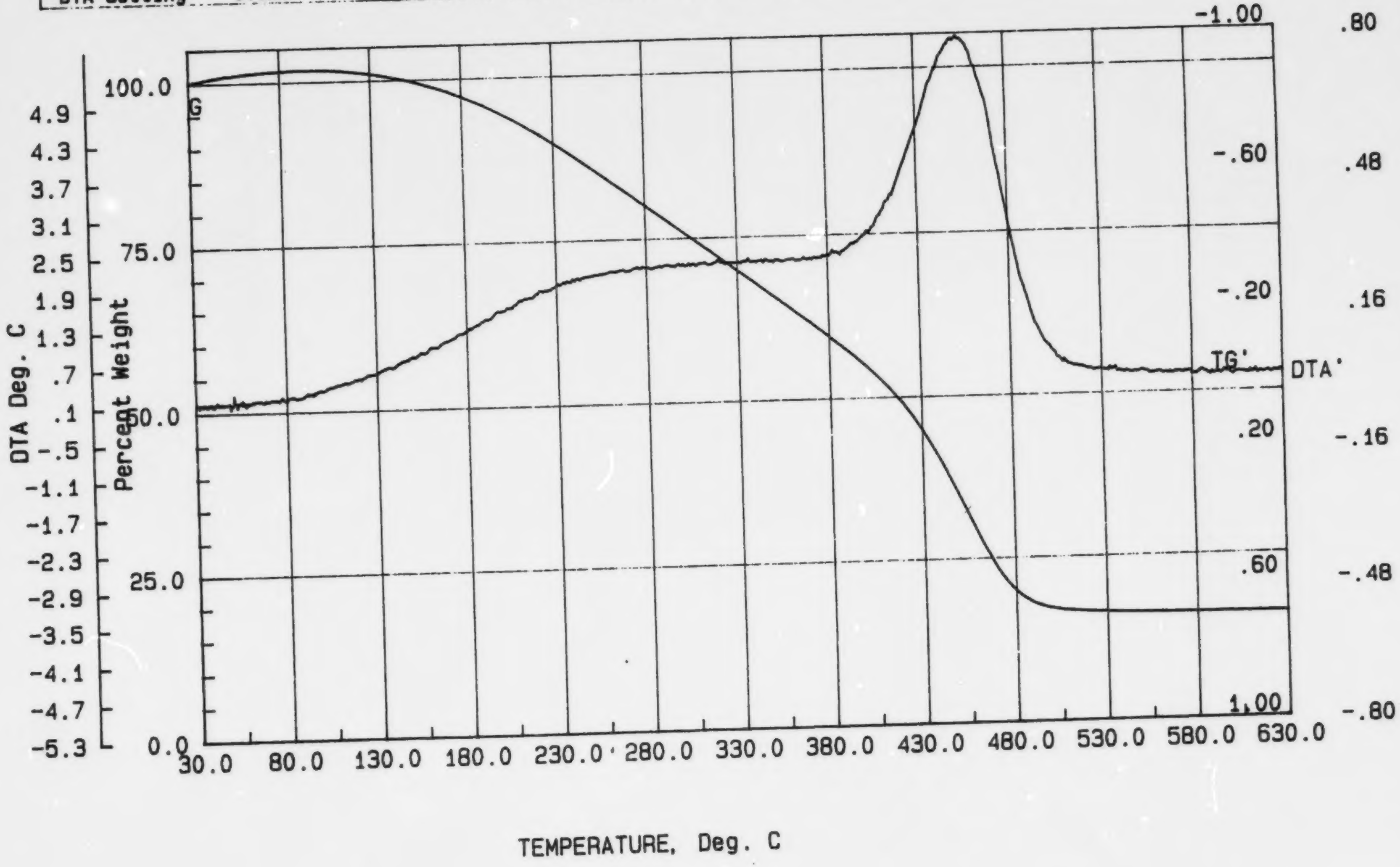

OPERATOR: R.SAETRE
DATE: 01/21/89
RUN No. 4
TG Setting 50mg
DTA Setting 0.1mV

NETZSCH STA 429/409
REFERENCE : AL203
CRUCIBLE : AL203
FILE NAME : TFFN22
MATERIAL TFFOIL

ATM. NITROGEN
FLOW = 70 cc/min
HEAT RATE = 5 C/min
SAMPLE WT.= 36.3 mg
REF WEIGHT 0 mg

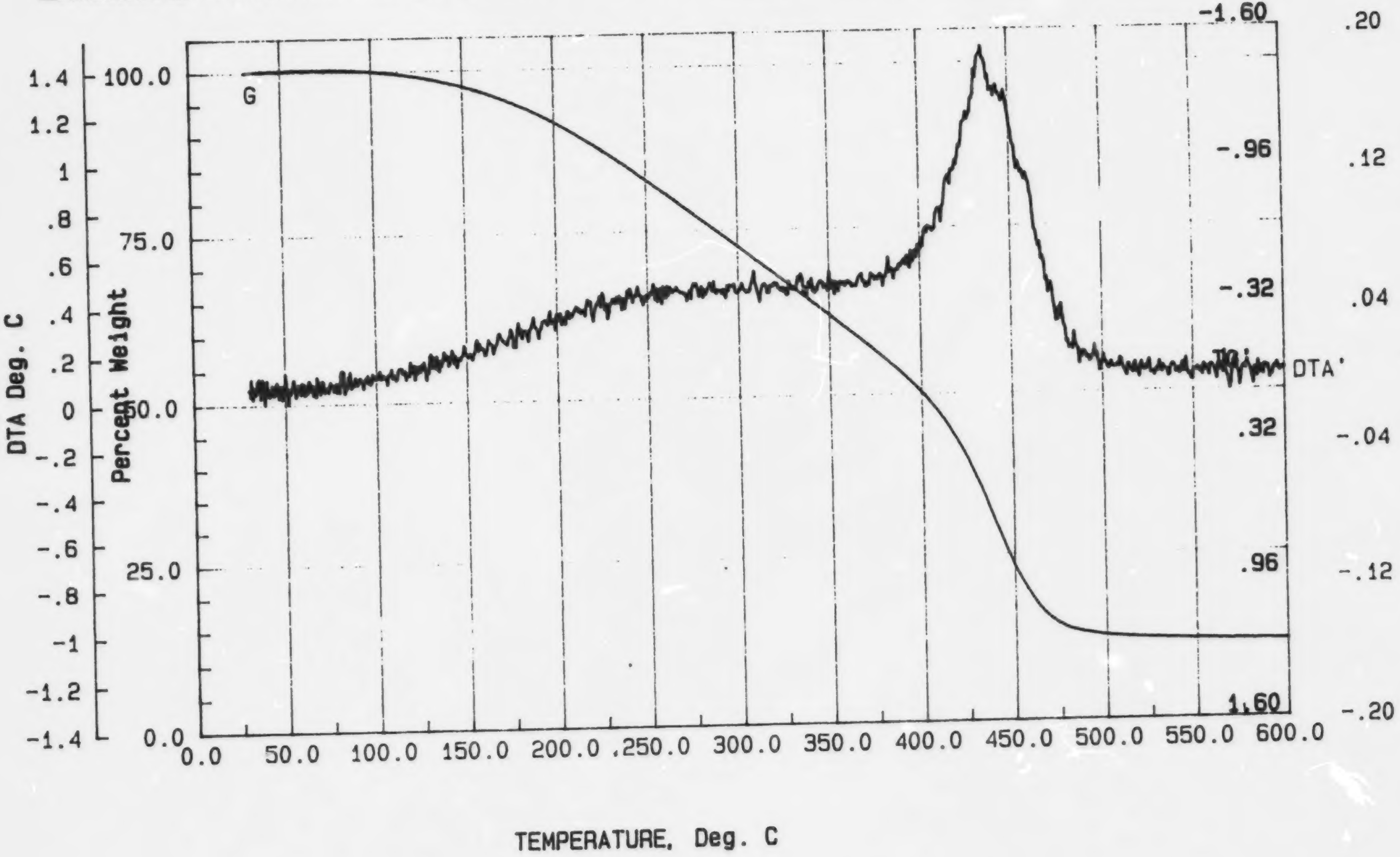

OPERATOR: R.SAETRE
DATE: 01/20/89
RUN No. 2
TG Setting 50mg
DTA Setting 0.1mV

NETZSCH STA 429/409
REFERENCE : AL203
CRUCIBLE : AL203
FILE NAME : TFFN21
MATERIAL TFF1

ATM. NITROGEN
FLOW = 70 cc/min
HEAT RATE = 5 C/min
SAMPLE WT.= 33.1 mg
REF WEIGHT 0 mg

(Figure 22)

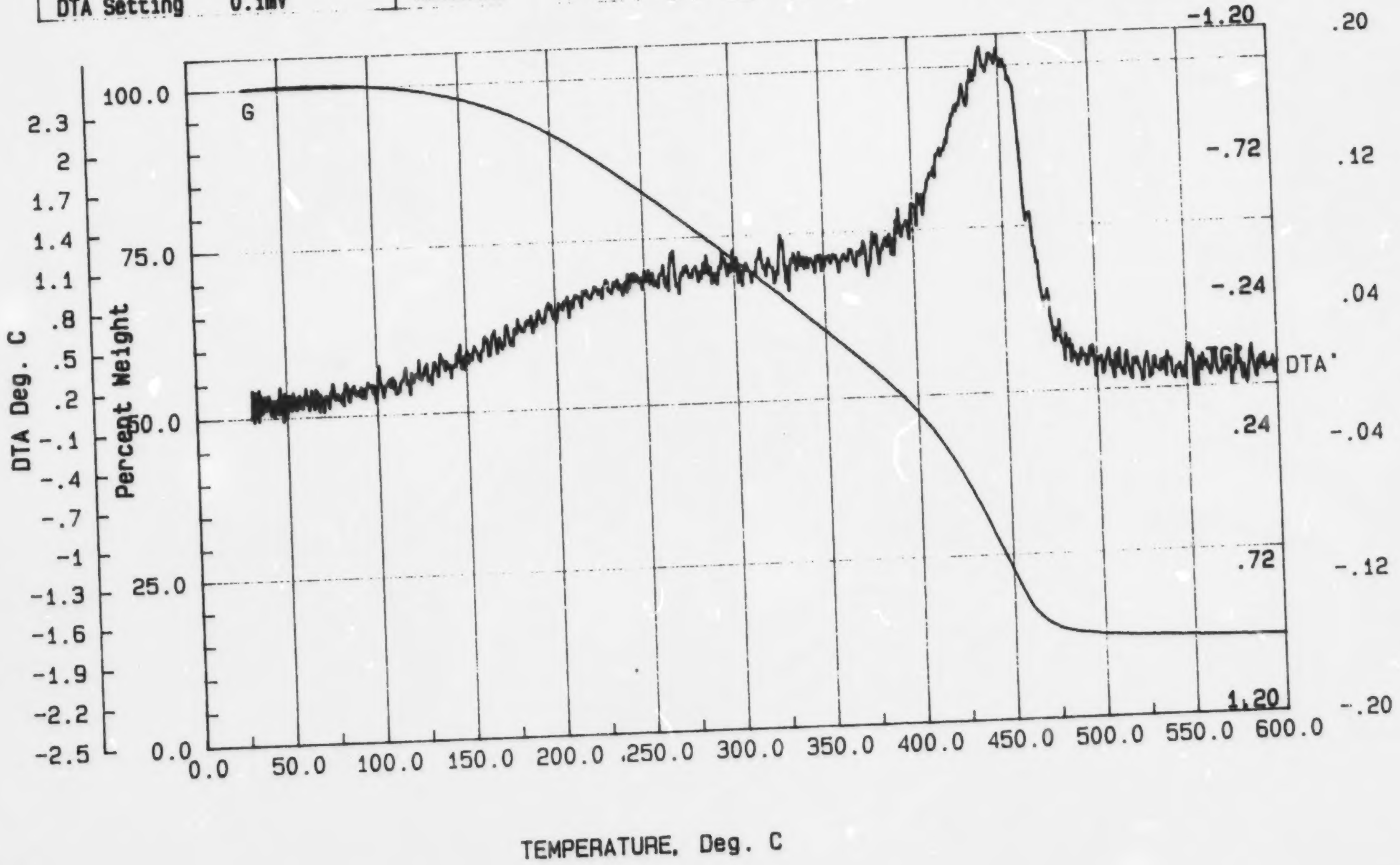

OPERATOR:	R.SAETRE	NETZSCH STA 429/409		ATM.	NITROGEN
DATE:	05/20/88	REFERENCE :	AL203	FLOW =	70 cc/min
RUN No.	2	CRUCIBLE :	AL203	HEAT RATE =	5 C/min
TG Setting	50mg	FILE NAME :	TFF1	SAMPLE WT.=	28.9 mg
DTA Setting	0.1mV	MATERIAL	TFOIL	REF WEIGHT	0 mg

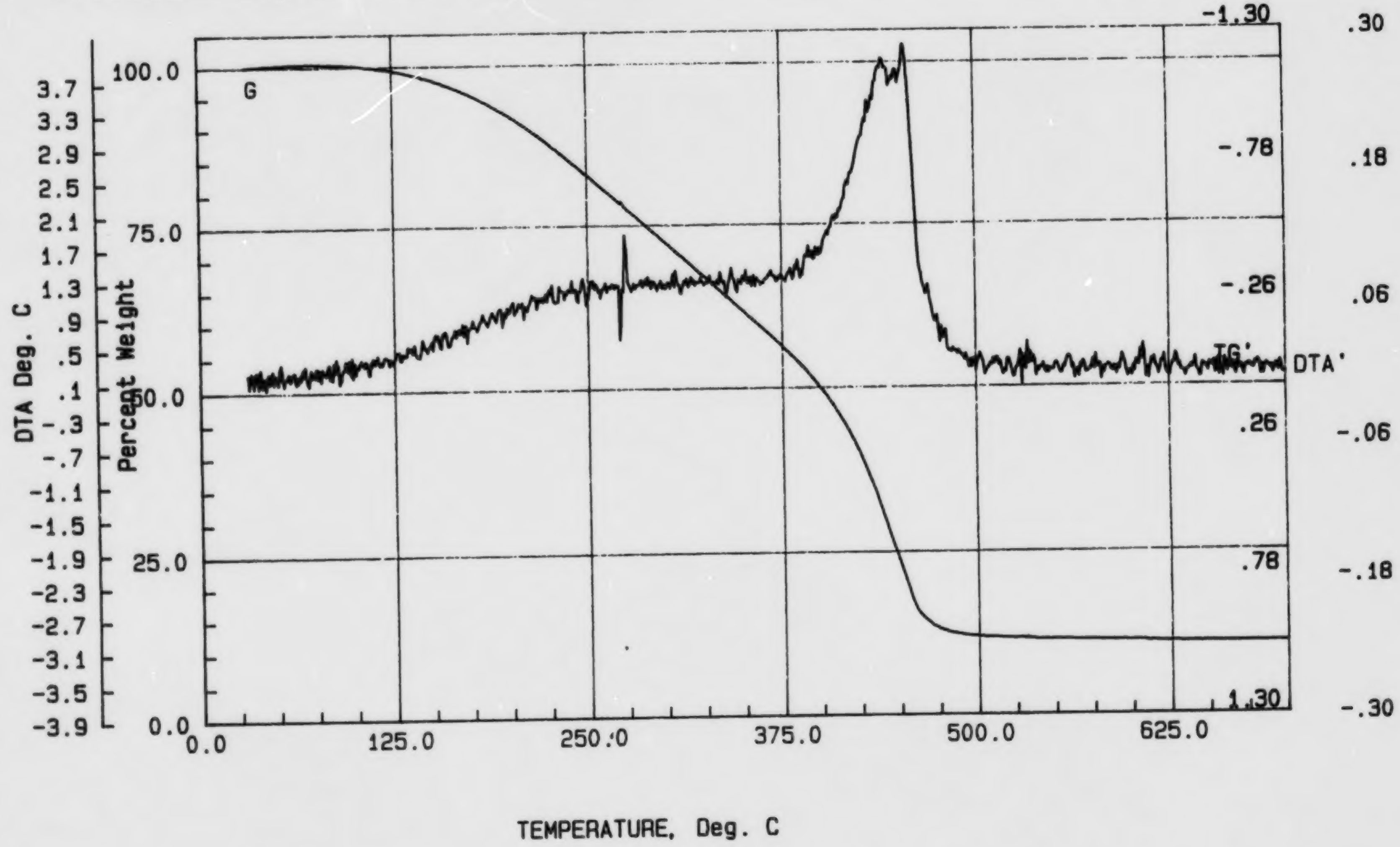

OPERATOR:	R.SAETRE	NETZSCH STA 429/409		ATM.	NITROGEN
DATE:	09/14/87	REFERENCE :	AL203	FLOW =	70 cc/min
RUN No.	9	CRUCIBLE :	AL203	HEAT RATE =	4 C/min
TG Setting	50mg	FILE NAME :	TOILN9	SAMPLE WT.=	20.3 mg
DTA Setting	0.1mV	MATERIAL	TOILN9	REF WEIGHT	0 mg

(Figure 7)

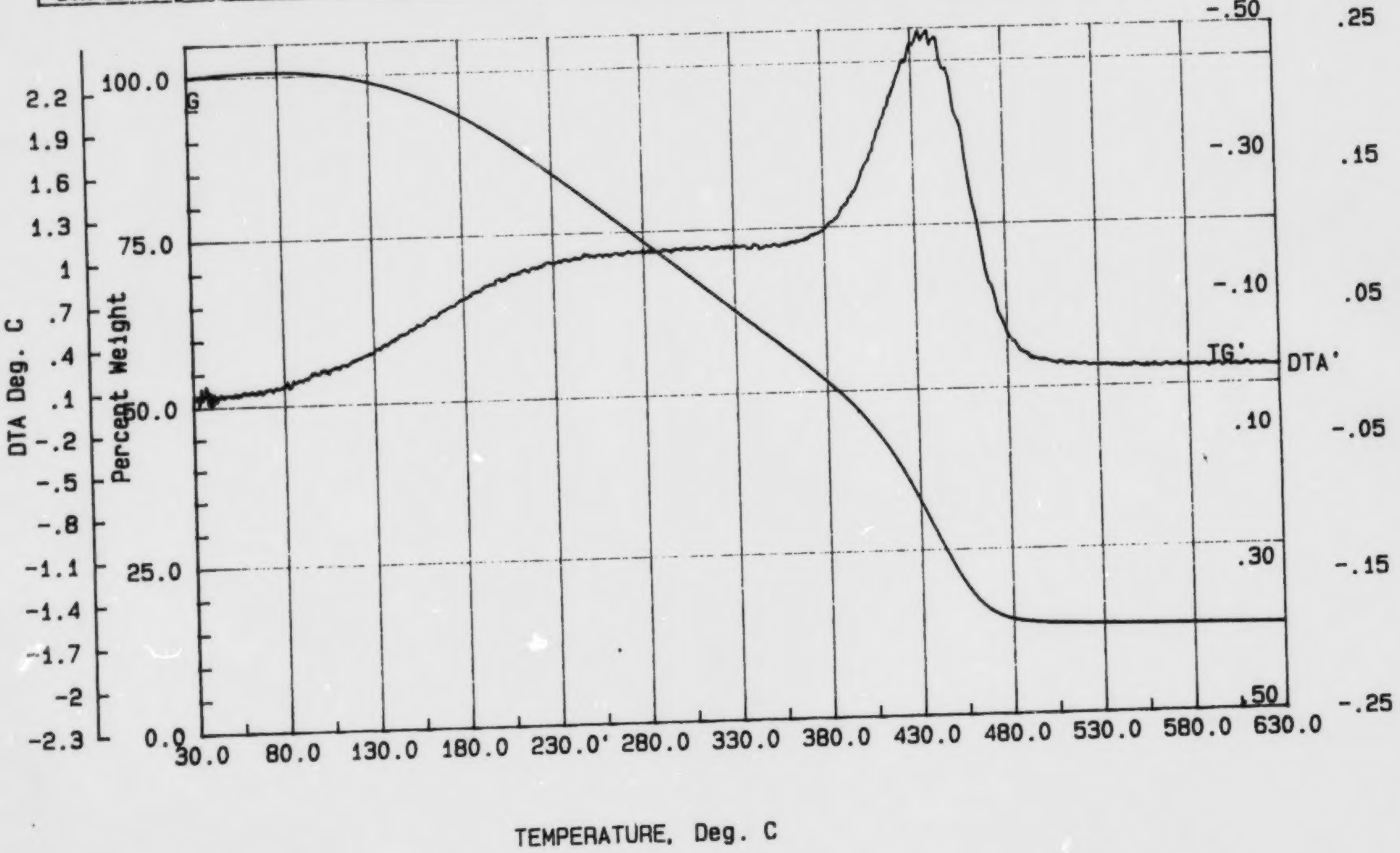

OPERATOR:	R.SAETRE	NETZSCH STA 429/409		ATM.	NITROGEN
DATE:	09/09/87	REFERENCE :	AL203	FLOW =	70 cc/min
RUN No.	6	CRUCIBLE :	AL203	HEAT RATE =	1 C/min
TG Setting	50mg	FILE NAME :	TOILN6	SAMPLE WT.=	18.9 mg
DTA Setting	0.1mV	MATERIAL	TOILN6	REF WEIGHT	0 mg

(Figure 8)

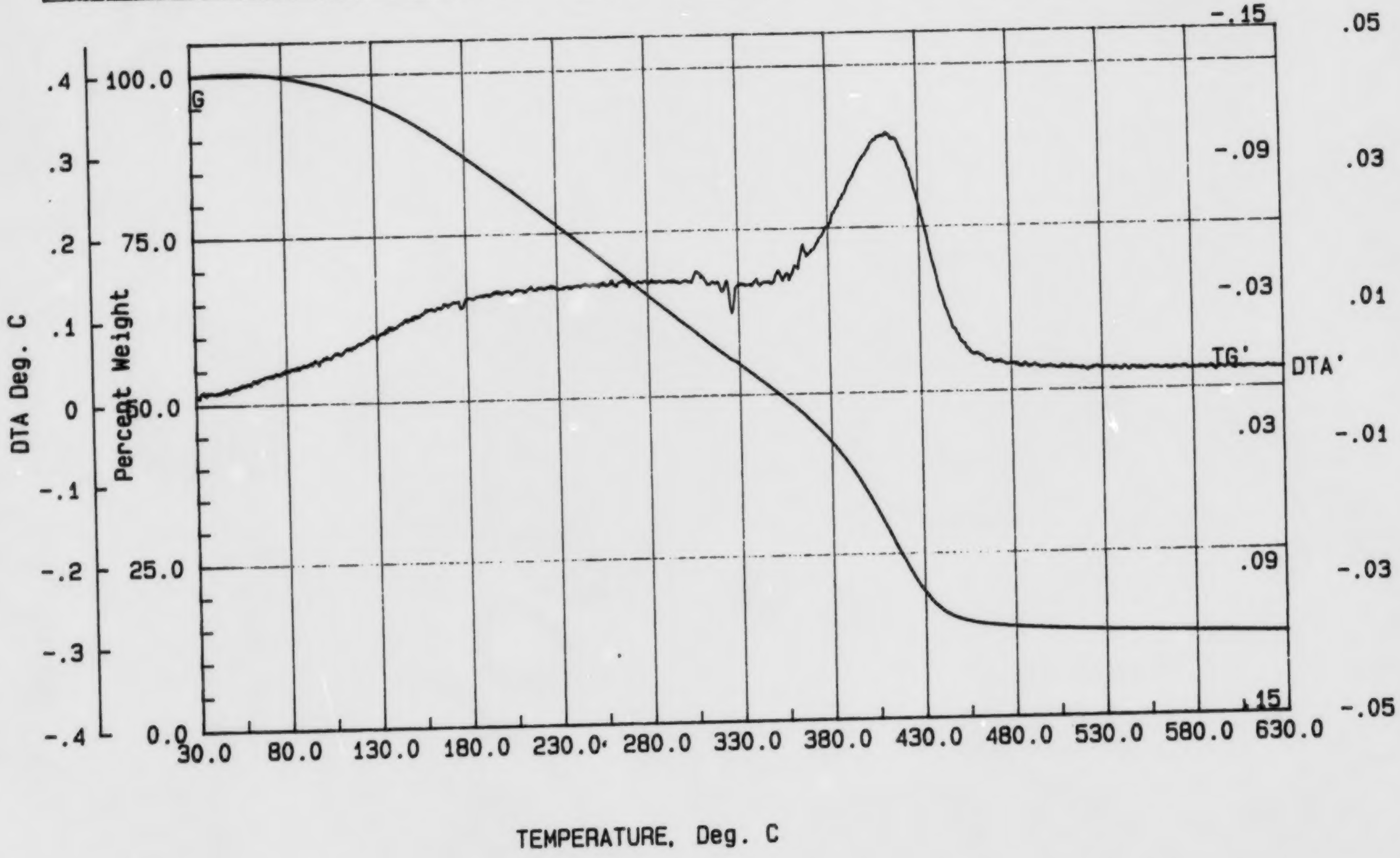

OPERATOR: R.SAETRE
DATE: 09/10/87
RUN No. 7
TG Setting 50mg
DTA Setting 0.1mV

NETZSCH STA 429/409
REFERENCE : AL203
CRUCIBLE : AL203
FILE NAME : TOILN7
MATERIAL TOILN7

ATM. NITROGEN
FLOW = 70 cc/min
HEAT RATE = .5 C/min
SAMPLE WT.= 15.9 mg
REF WEIGHT 0 mg

(Figure 9)

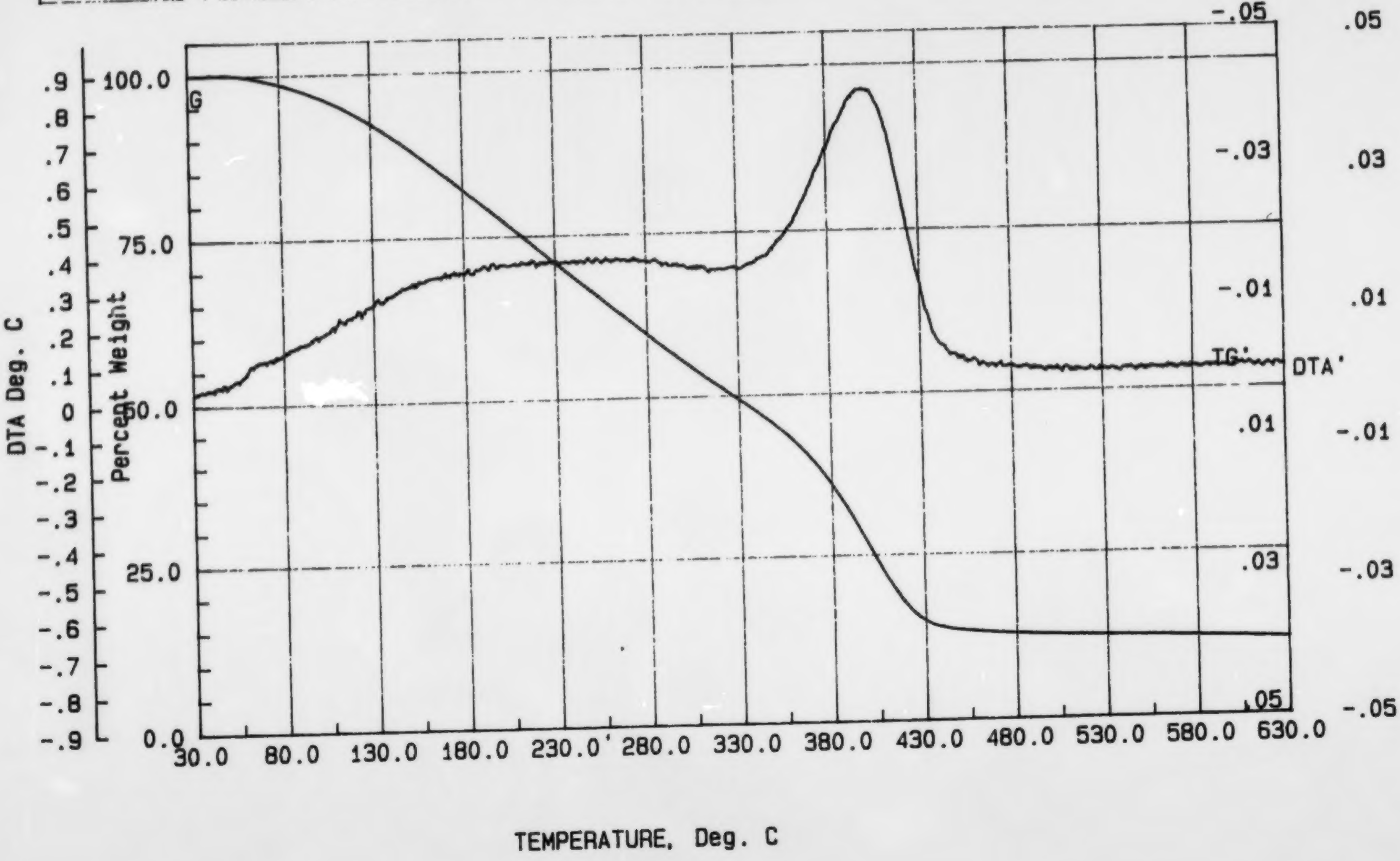

OPERATOR: R.SAETRE DATE: 09/11/87 RUN No. 8 TG Setting 50mg DTA Setting 0.1mV	NETZSCH STA 429/409 REFERENCE : AL203 CRUCIBLE : AL203 FILE NAME : TOILN8 MATERIAL TOILN8	ATM. NITROGEN FLOW = 70 cc/min HEAT RATE = .2 C/min SAMPLE WT.= 18.2 mg REF WEIGHT 0 mg	*Report #00427* *Page A-10* (Figure 10)

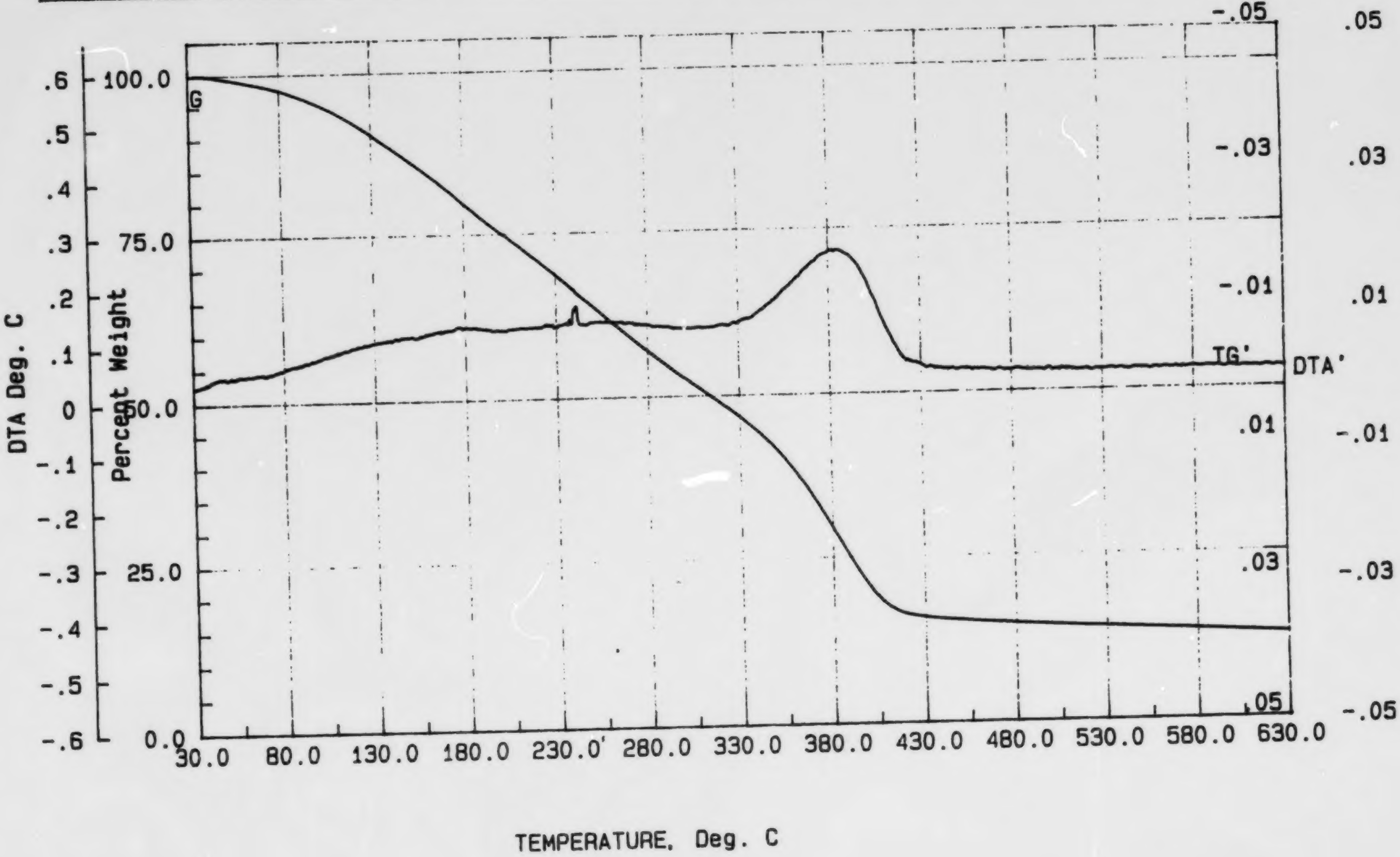

OPERATOR: R.SAETRE
DATE: 02/01/89
RUN No. 18
TG Setting 50mg
DTA Setting 0.1mV

NETZSCH STA 429/409
REFERENCE : AL203
CRUCIBLE : AL203
FILE NAME : BLANK1
MATERIAL BLANK

ATM. AIR
FLOW = 70 cc/min
HEAT RATE = 5 C/min
SAMPLE WT.= 35 mg
REF WEIGHT 0 mg

(Figure 2)

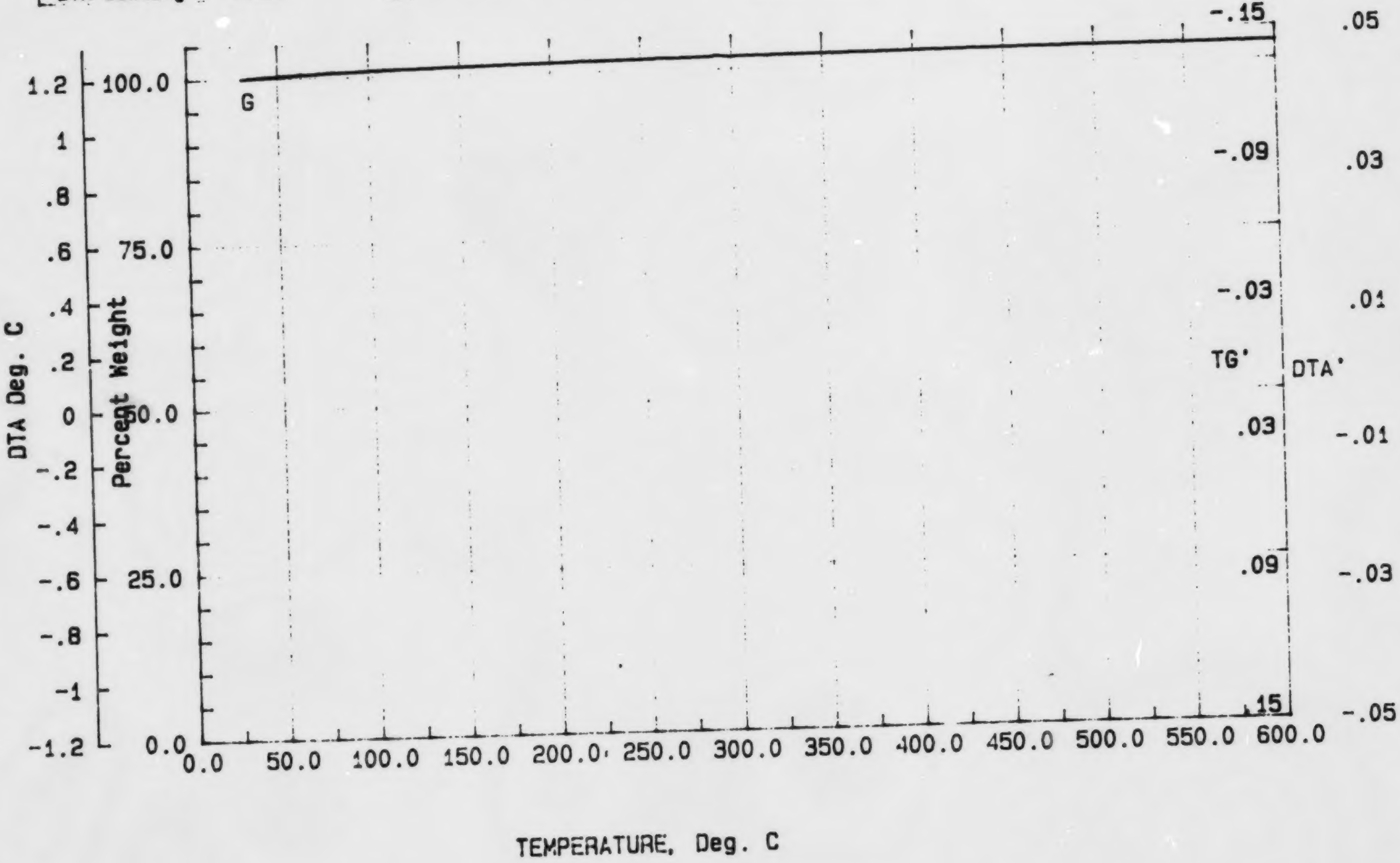

OPERATOR: R.SAETRE	NETZSCH STA 429/409	ATM. AIR	(Figure 3)
DATE: 03/19/87	REFERENCE : AL2O3	FLOW = 70 cc/min	
RUN No. 1	CRUCIBLE : AL2O3	HEAT RATE = 10 C/min	
TG Setting 50mg	FILE NAME : TOILAIR1	SAMPLE WT.= 22 mg	
DTA Setting 0.1mV	MATERIAL TAOIL	REF WEIGHT 0 mg	

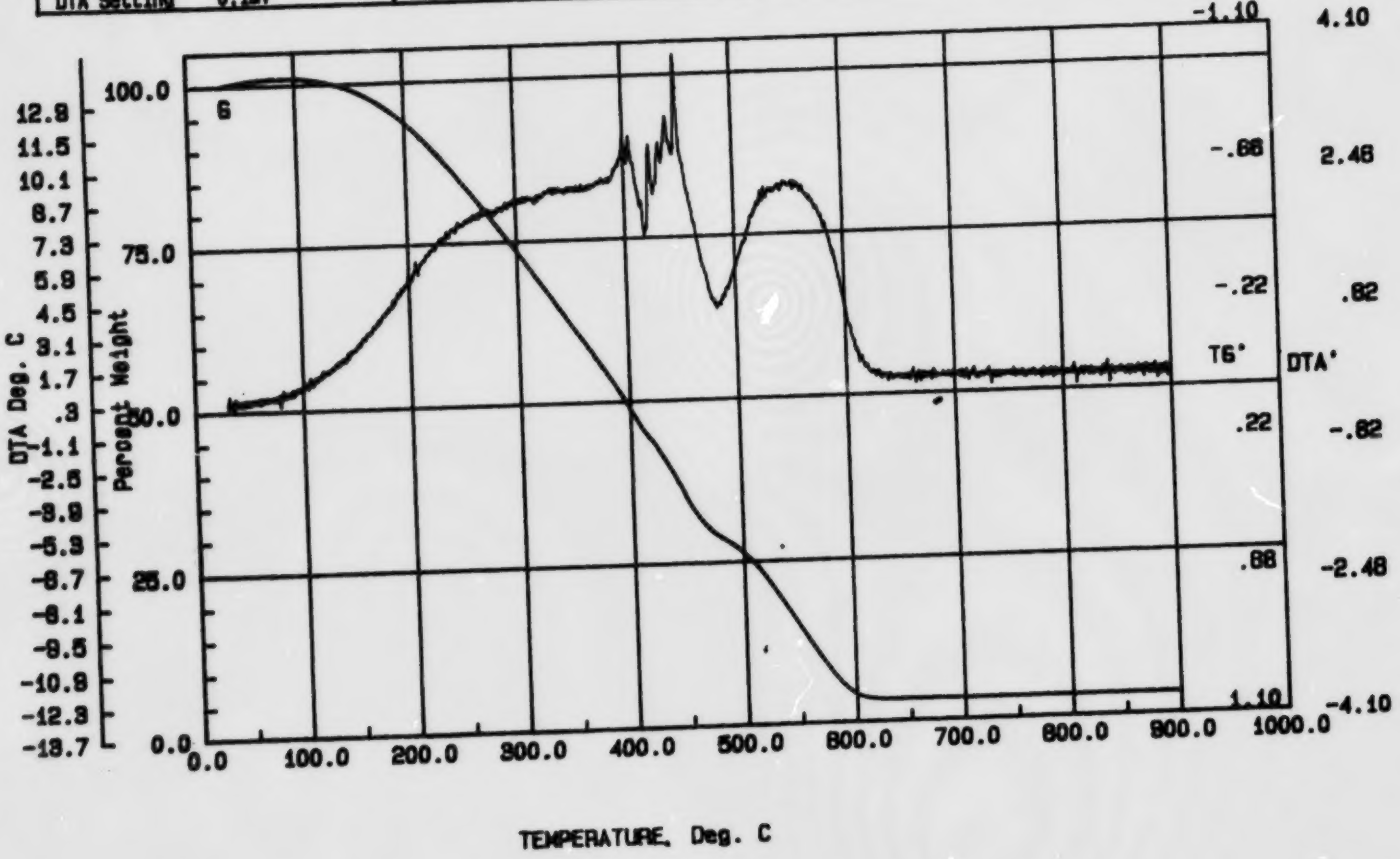

OPERATOR: R.SAETRE
DATE: 03/19/87
RUN No. 2
TG Setting 50mg
DTA Setting 0.1mV

NETZSCH STA 429/409
REFERENCE : AL203
CRUCIBLE : AL203
FILE NAME : TOILAIR2
MATERIAL TAOIL2

ATM. AIR
FLOW = 70 cc/min
HEAT RATE = 10 C/min
SAMPLE WT.= 15.2 mg
REF WEIGHT 0 mg

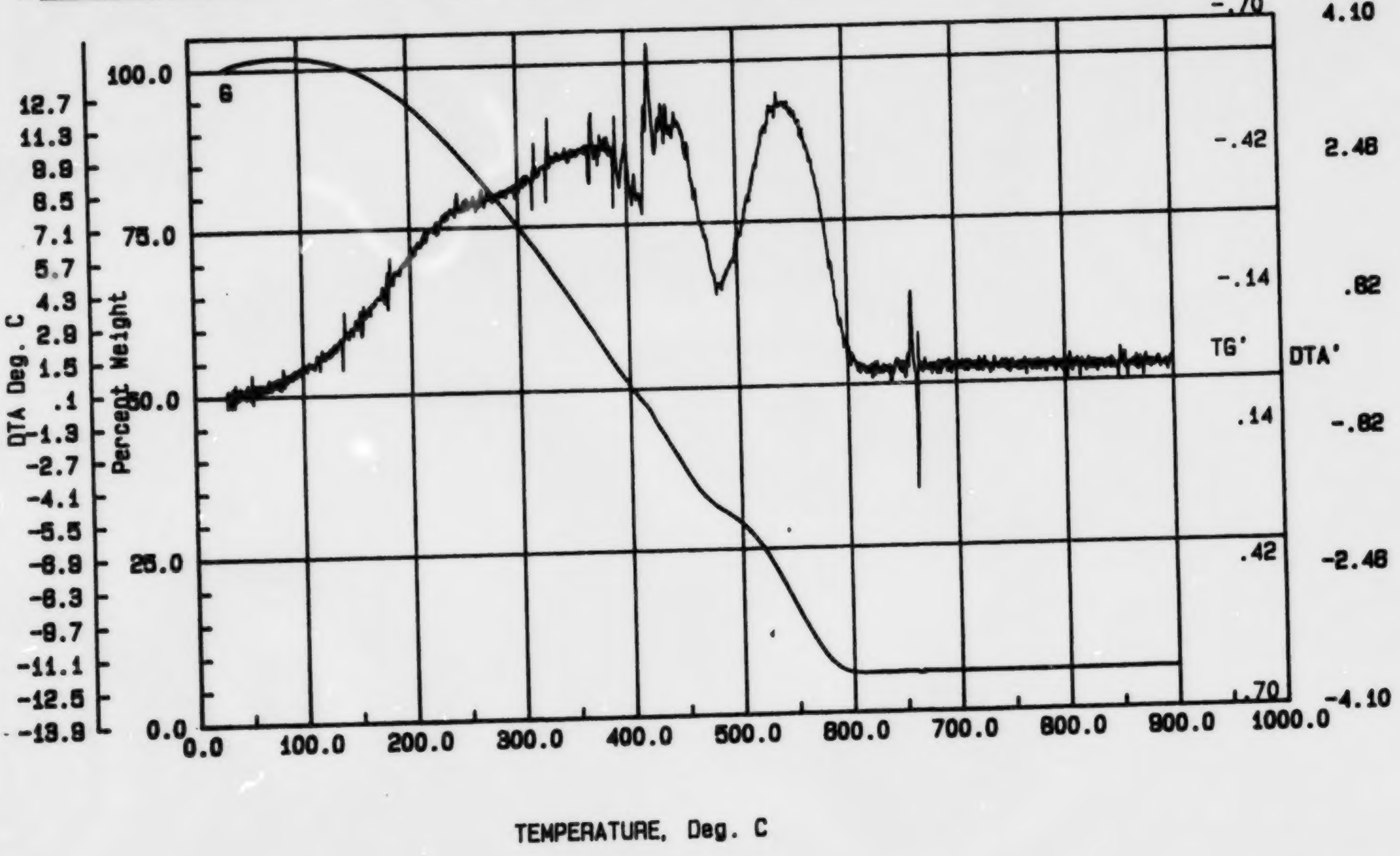

OPERATOR:	R.SAETRE	NETZSCH STA 429/409		ATM.	AIR
DATE:	03/23/87	REFERENCE :	AL203	FLOW =	70 cc/min
RUN No.	5	CRUCIBLE :	AL203	HEAT RATE =	10 C/min
TG Setting	50mg	FILE NAME :	TOILAIR3	SAMPLE WT.=	23.2 mg
DTA Setting	0.1mV	MATERIAL	TAOIL	REF WEIGHT	0 mg

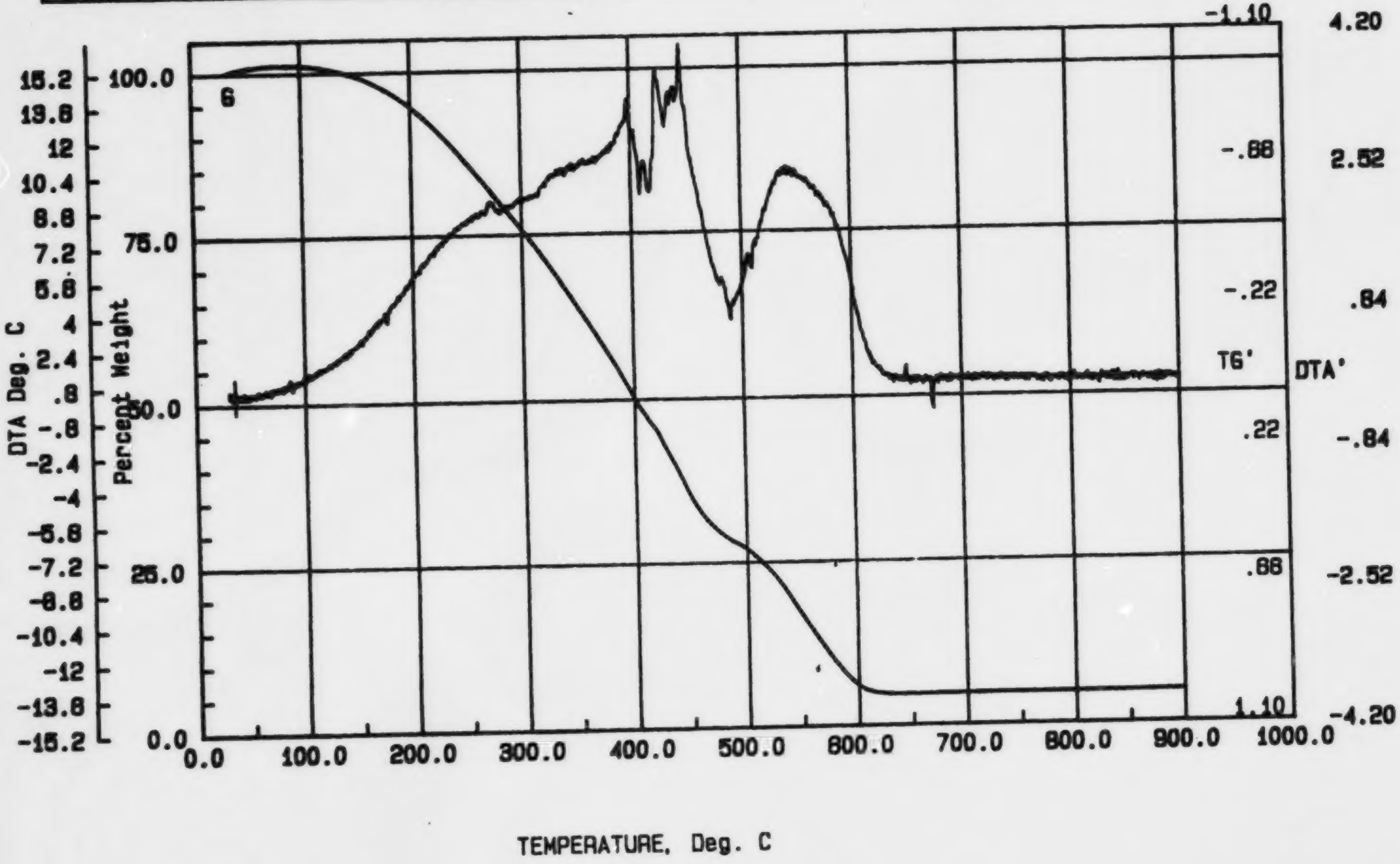

TEMPERATURE, Deg. C

OPERATOR:	R.SAETRE	NETZSCH STA 429/409		ATM.	AIR	Report #00427 Page A-15
DATE:	09/04/87	REFERENCE :	AL203	FLOW =	70 cc/min	
RUN No.	2	CRUCIBLE :	AL203	HEAT RATE =	10 C/min	
TG Setting	50mg	FILE NAME :	TOILN2	SAMPLE WT.=	18.4 mg	
DTA Setting	0.1mV	MATERIAL	TOILN2	REF WEIGHT	0 mg	

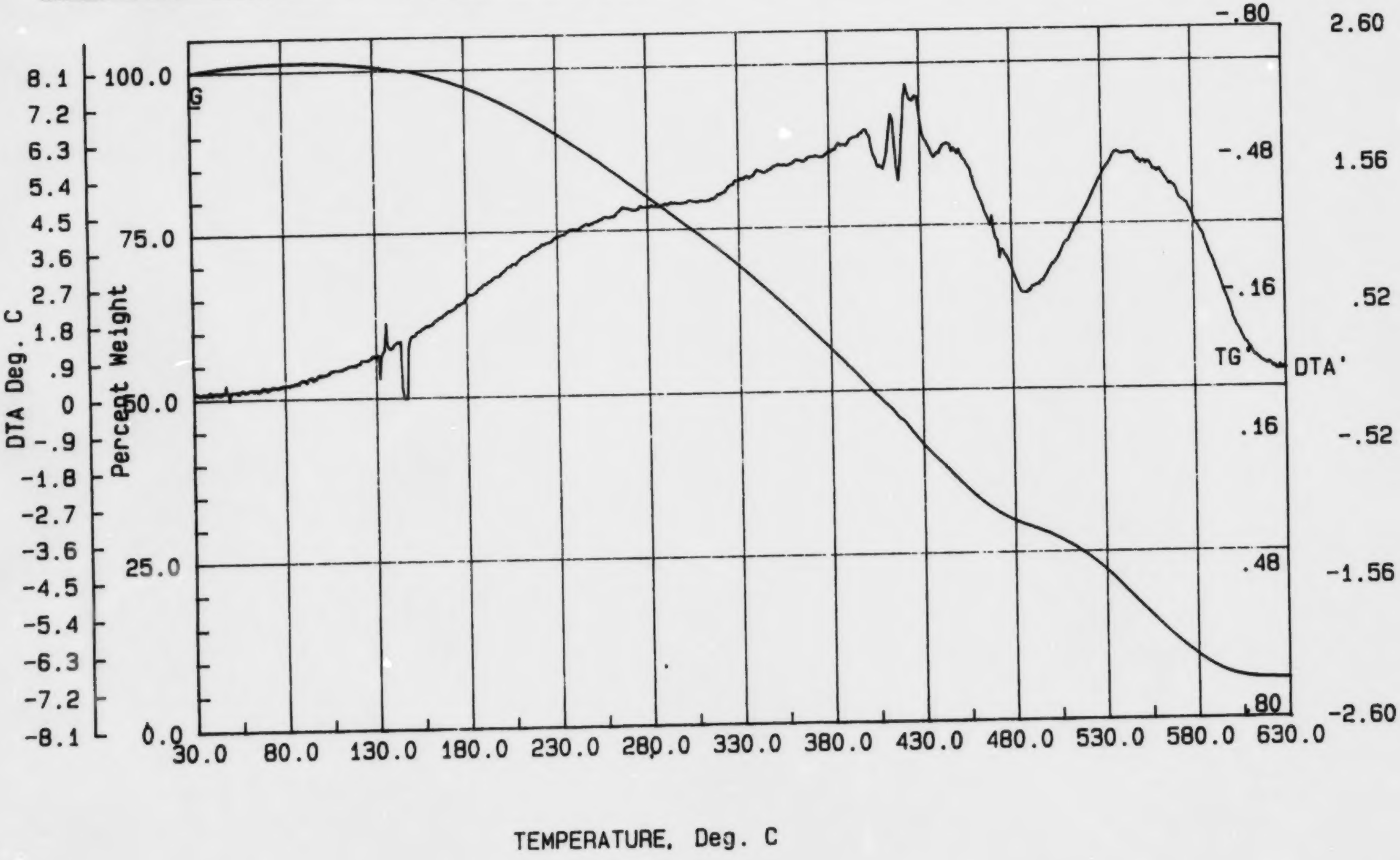

OPERATOR:	R.SAETRE	NETZSCH STA 429/409		ATM.	AIR	Report #00427 Page A-16
DATE:	09/08/87	REFERENCE :	AL203	FLOW =	70 cc/min	
RUN No.	4	CRUCIBLE :	AL203	HEAT RATE =	10 C/min	
TG Setting	50mg	FILE NAME :	TOILN4	SAMPLE WT.=	16.1 mg	
DTA Setting	0.1mV	MATERIAL	TOILN4	REF WEIGHT	0 mg	

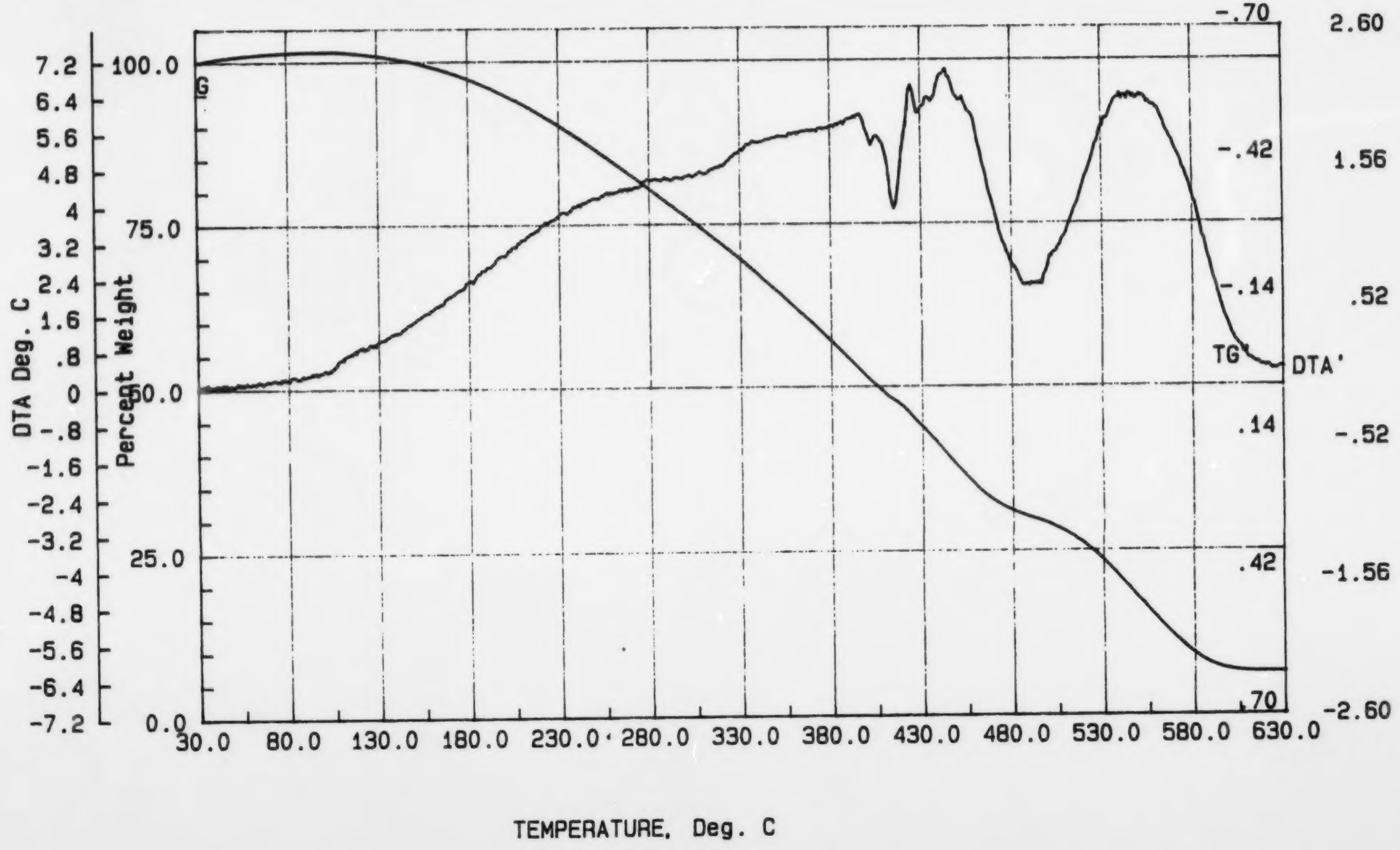

OPERATOR: R.SAETRE
DATE: 05/26/88
RUN No. 6
TG Setting 50mg
DTA Setting 0.1mV

NETZSCH STA 429/409
REFERENCE : AL203
CRUCIBLE : AL203
FILE NAME : TFF3
MATERIAL TFOIL

ATM. AIR
FLOW = 70 cc/min
HEAT RATE = 5 C/min
SAMPLE WT.= 35.6 mg
REF WEIGHT 0 mg

Report #00427
Page A-17

(Figure 11)

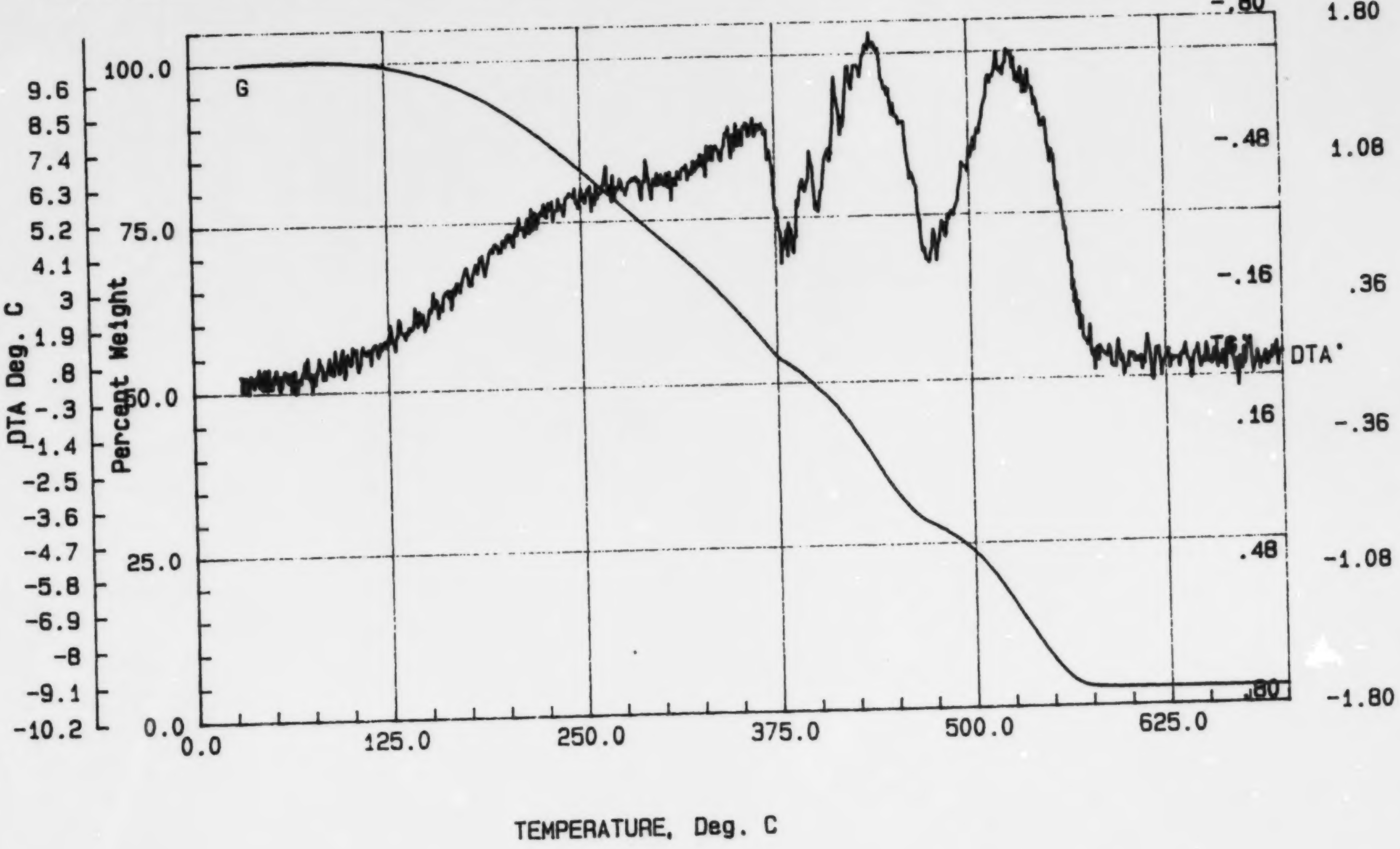

OPERATOR: R.SAETRE
DATE: 05/24/88
RUN No. 4
TG Setting 50mg
DTA Setting 0.1mV

NETZSCH STA 429/409
REFERENCE : AL203
CRUCIBLE : AL203
FILE NAME : TFF2
MATERIAL TFOIL

ATM. AIR
FLOW = 70 cc/min
HEAT RATE = 5 C/min
SAMPLE WT.= 34.2 mg
REF WEIGHT 0 mg

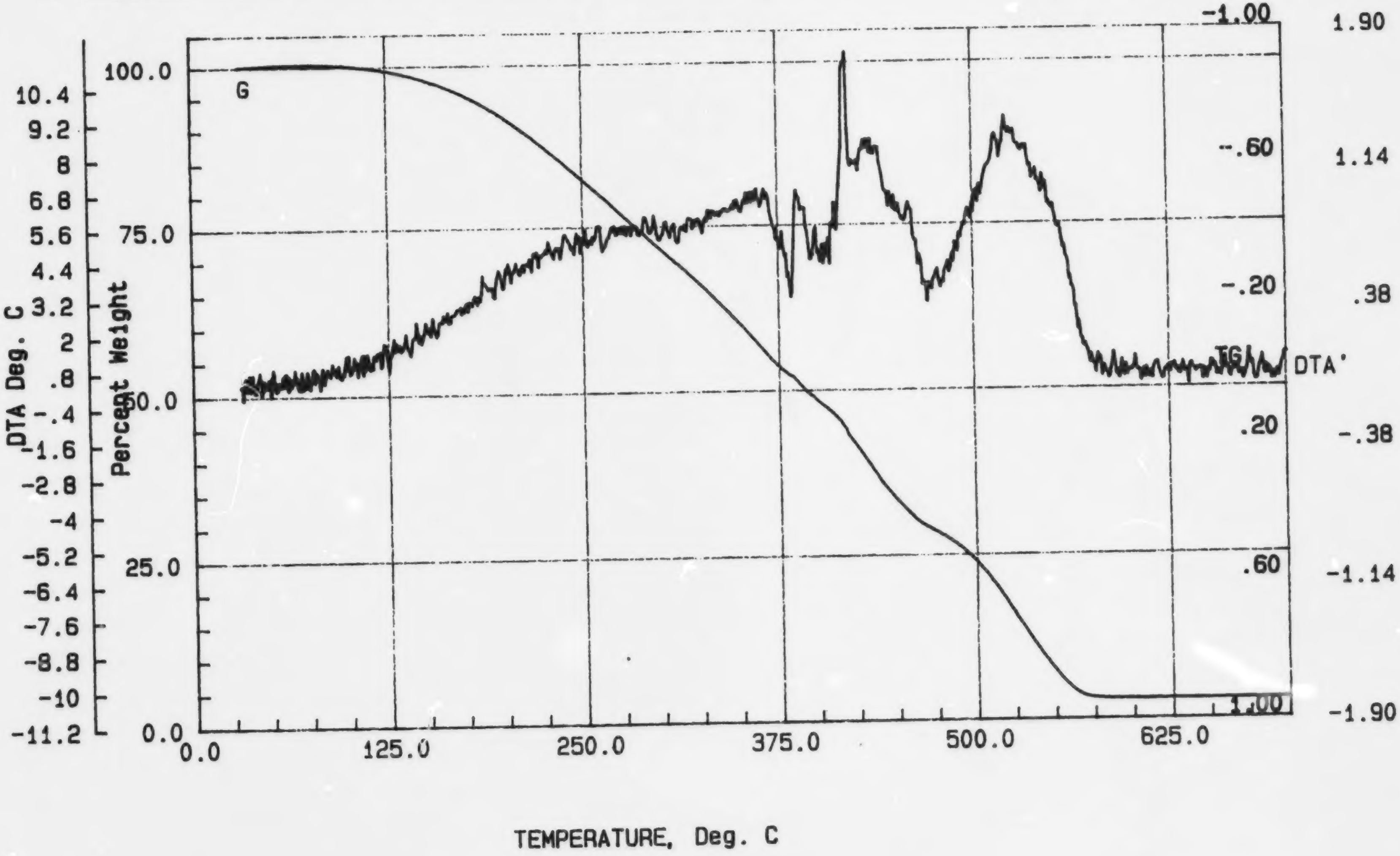

OPERATOR: R.SAETRE
DATE: 01/19/89
RUN No. 1
TG Setting 50mg
DTA Setting 0.1mV

NETZSCH STA 429/409
REFERENCE : AL203
CRUCIBLE : AL203
FILE NAME : TFFAIR1
MATERIAL TFF1

ATM. AIR
FLOW = 70 cc/min
HEAT RATE = 5 C/min
SAMPLE WT.= 38 mg
REF WEIGHT 0 mg

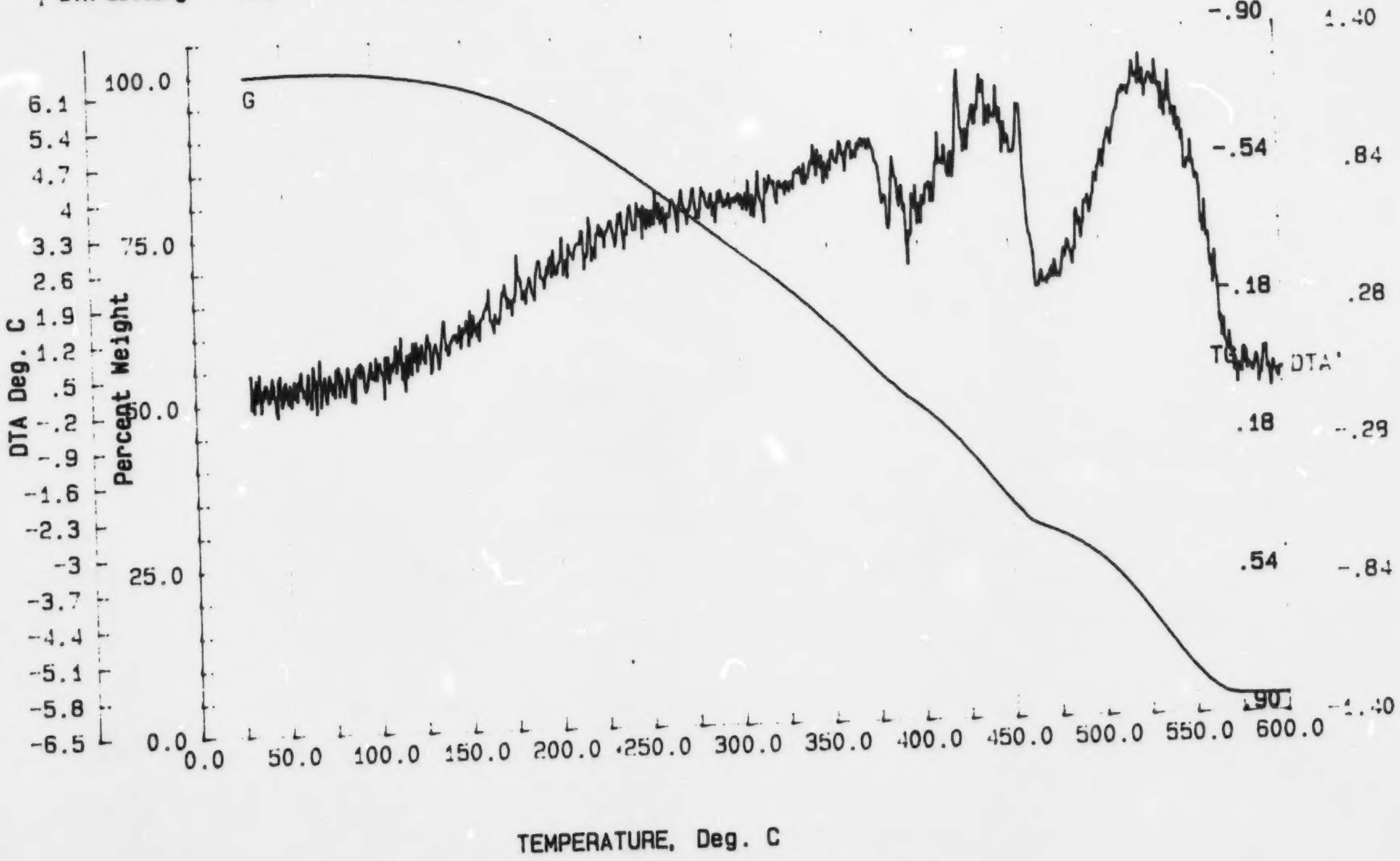

OPERATOR:	R.SAETRE	NETZSCH STA 429/409		ATM.	AIR	Report #00427
DATE:	09/03/87	REFERENCE :	AL203	FLOW =	70 cc/min	Page A-20
RUN No.	1	CRUCIBLE :	AL203	HEAT RATE =	1 C/min	(Figure 12)
TG Setting	50mg	FILE NAME :	TOILN1	SAMPLE WT.=	15.2 mg	
DTA Setting	0.1mV	MATERIAL	TOILAIR	REF WEIGHT	0 mg	

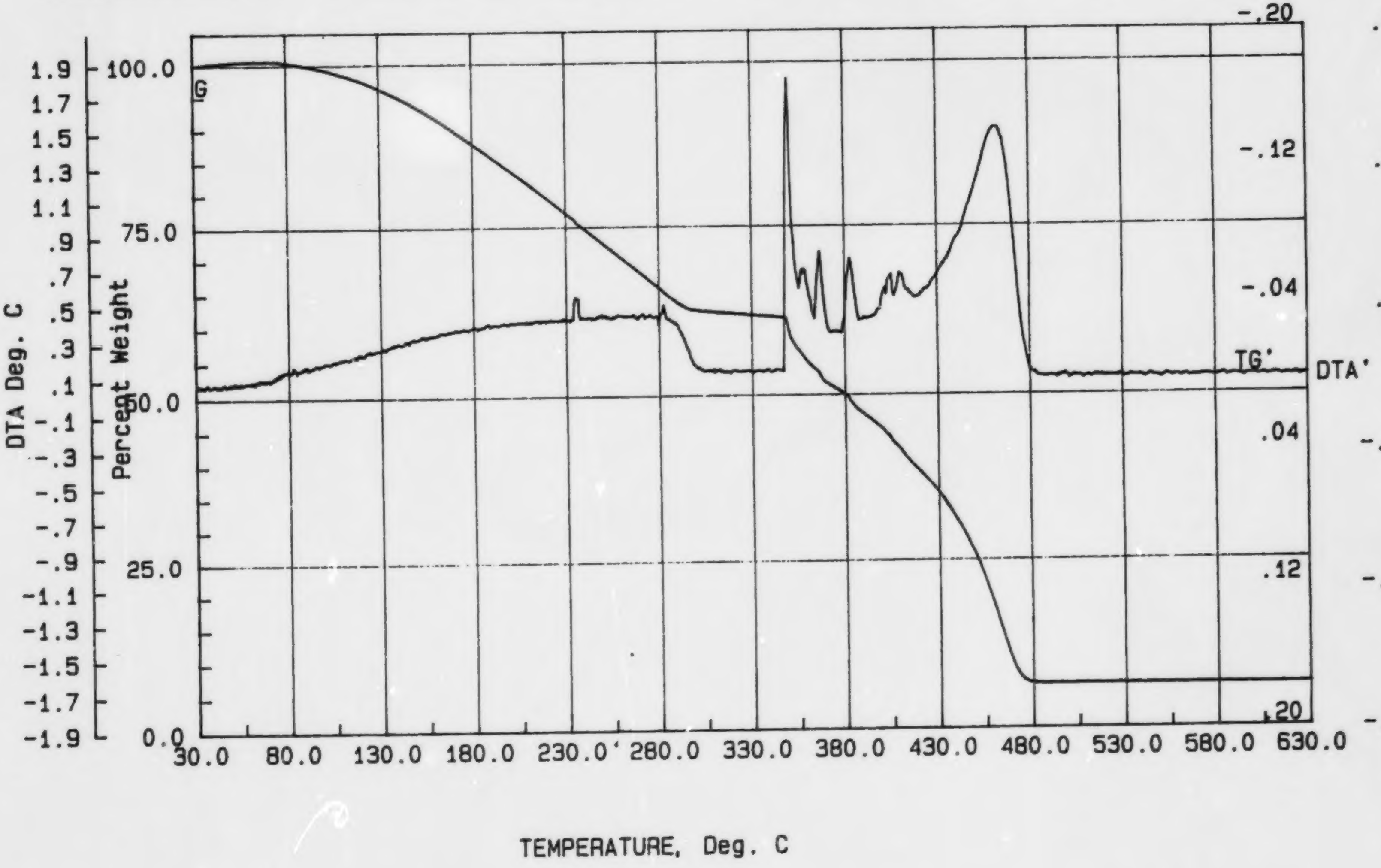

OPERATOR: R.SAETRE
DATE: 09/08/87
RUN No. 5
TG Setting 50mg
DTA Setting 0.1mV

NETZSCH STA 429/409
REFERENCE : AL203
CRUCIBLE : AL203
FILE NAME : TOILN5
MATERIAL TOILN5

ATM. AIR
FLOW = 70 cc/min
HEAT RATE = 1 C/min
SAMPLE WT.= 17.6 mg
REF WEIGHT 0 mg

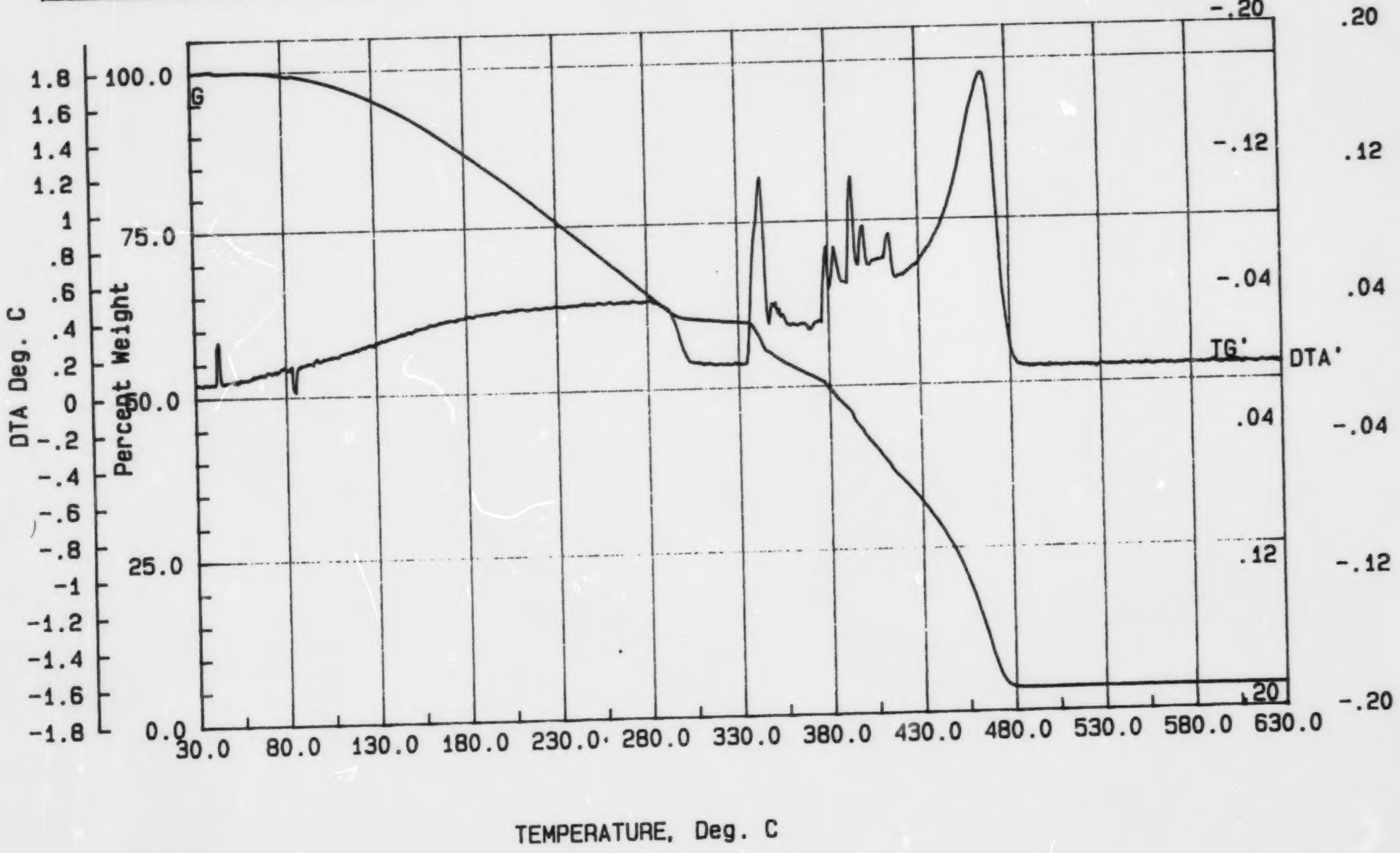

OPERATOR: R.SAETRE DATE: 03/05/87 RUN No. 2 TG Setting 50mg DTA Setting 0.1mV	NETZSCH STA 429/409 REFERENCE : SAND CRUCIBLE : AL203 FILE NAME : TOILS1 MATERIAL TOILS1B	ATM. NITROGEN FLOW = 70 cc/min HEAT RATE = 10 C/min SAMPLE WT.= 16.4 mg REF WEIGHT 0 mg	(Figure 6)

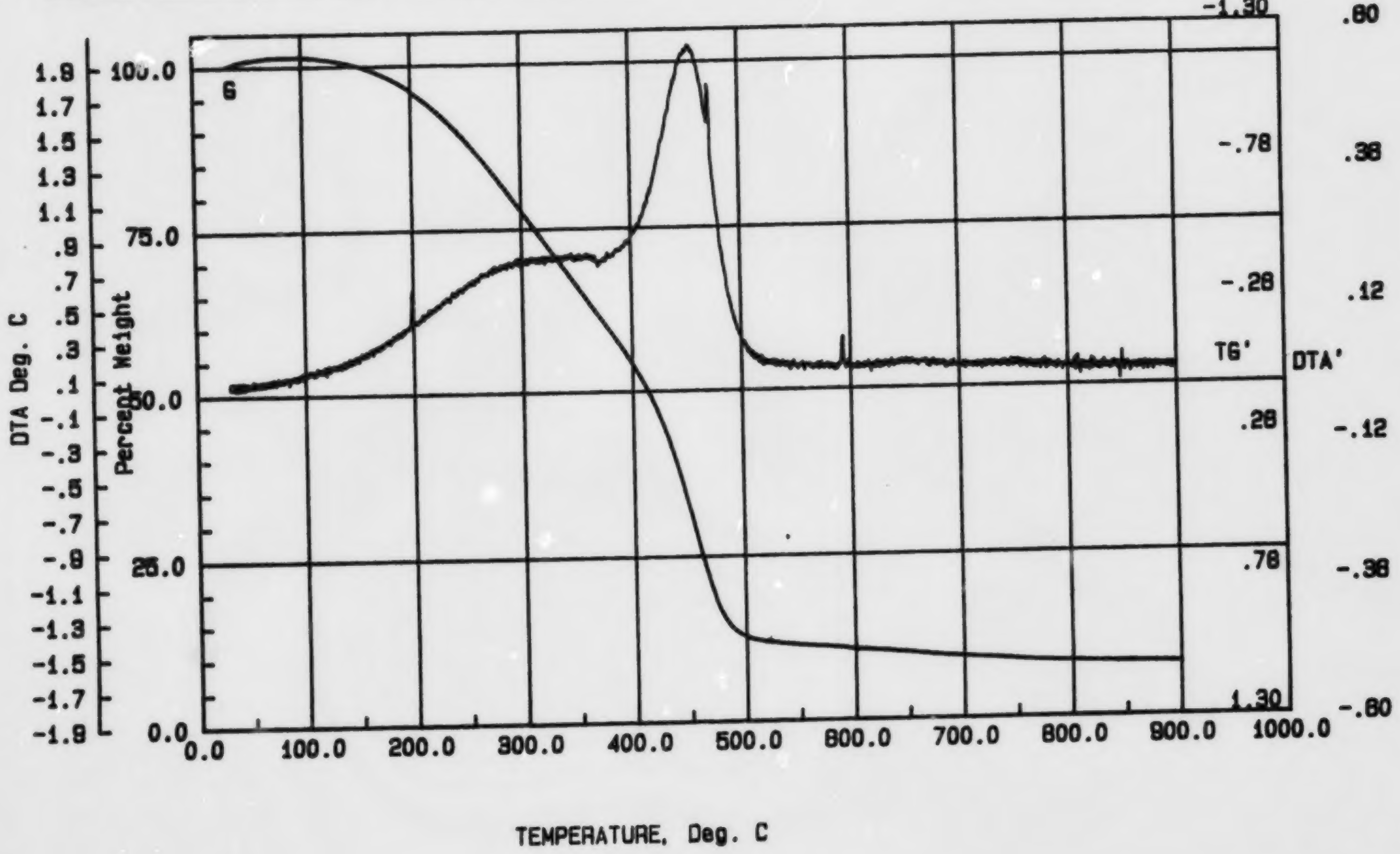

OPERATOR:	R.SAETRE	NETZSCH STA 429/409		ATM.	NITROGEN
DATE:	08/31/87	REFERENCE :	SAND	FLOW =	70 cc/min
RUN No.	2	CRUCIBLE :	AL203	HEAT RATE =	10 C/min
TG Setting	50mg	FILE NAME :	TOILS4	SAMPLE WT.=	16.3 mg
DTA Setting	0.1mV	MATERIAL	TOILS	REF WEIGHT	0 mg

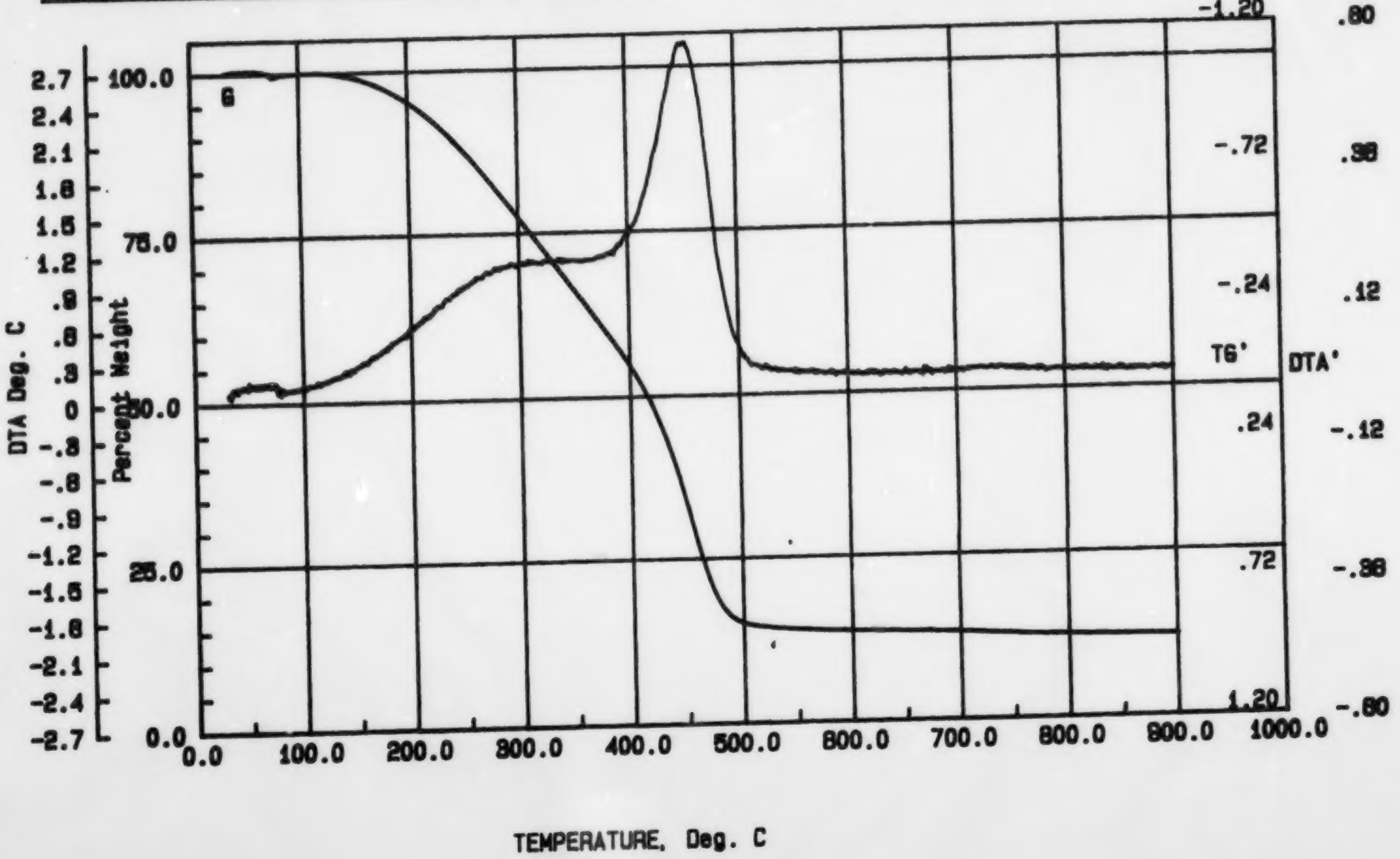

Not
Stored

OPERATOR: R.SAETRE		NETZSCH STA 429/409		ATM.	NITROGEN
DATE:	03/05/87	REFERENCE :	TSAND	FLOW =	70 cc/min
RUN No.	1	CRUCIBLE :	AL203	HEAT RATE =	10 C/min
TG Setting	50mg	FILE NAME :	TOILS1	SAMPLE WT.=	17.1 mg
DTA Setting	0.1mV	MATERIAL	TOILS1	REF WEIGHT	0 mg

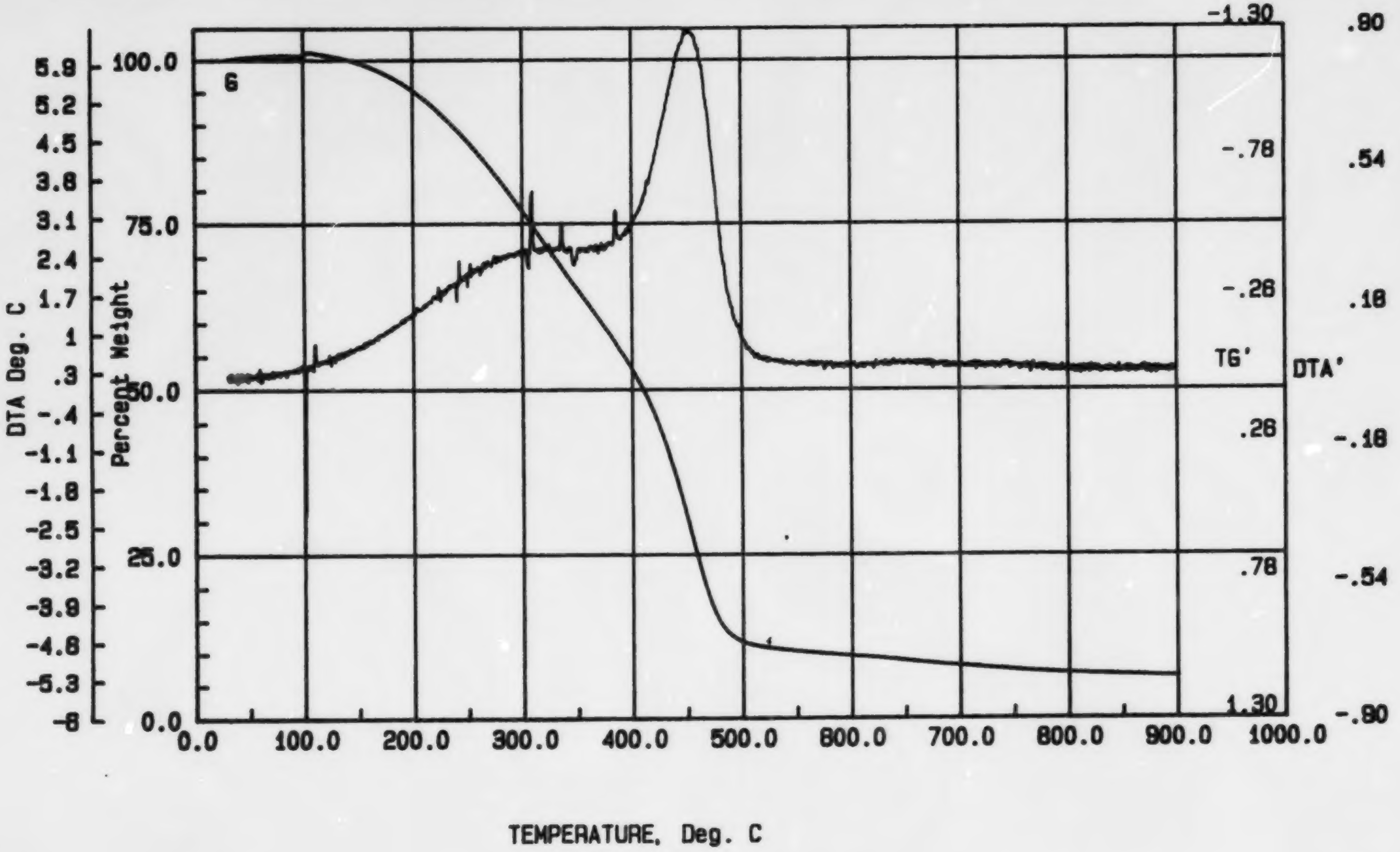

OPERATOR:	R.SAETRE	NETZSCH STA 429/409		ATM.	NITROGEN
DATE:	03/30/87	REFERENCE :	SAND	FLOW =	70 cc/min
RUN No.	1	CRUCIBLE :	AL203	HEAT RATE =	2 C/min
TG Setting	50mg	FILE NAME :	TOILS3	SAMPLE WT.=	18 mg
DTA Setting	0.1mV	MATERIAL	TOILS	REF WEIGHT	0 mg

(Figure 15)

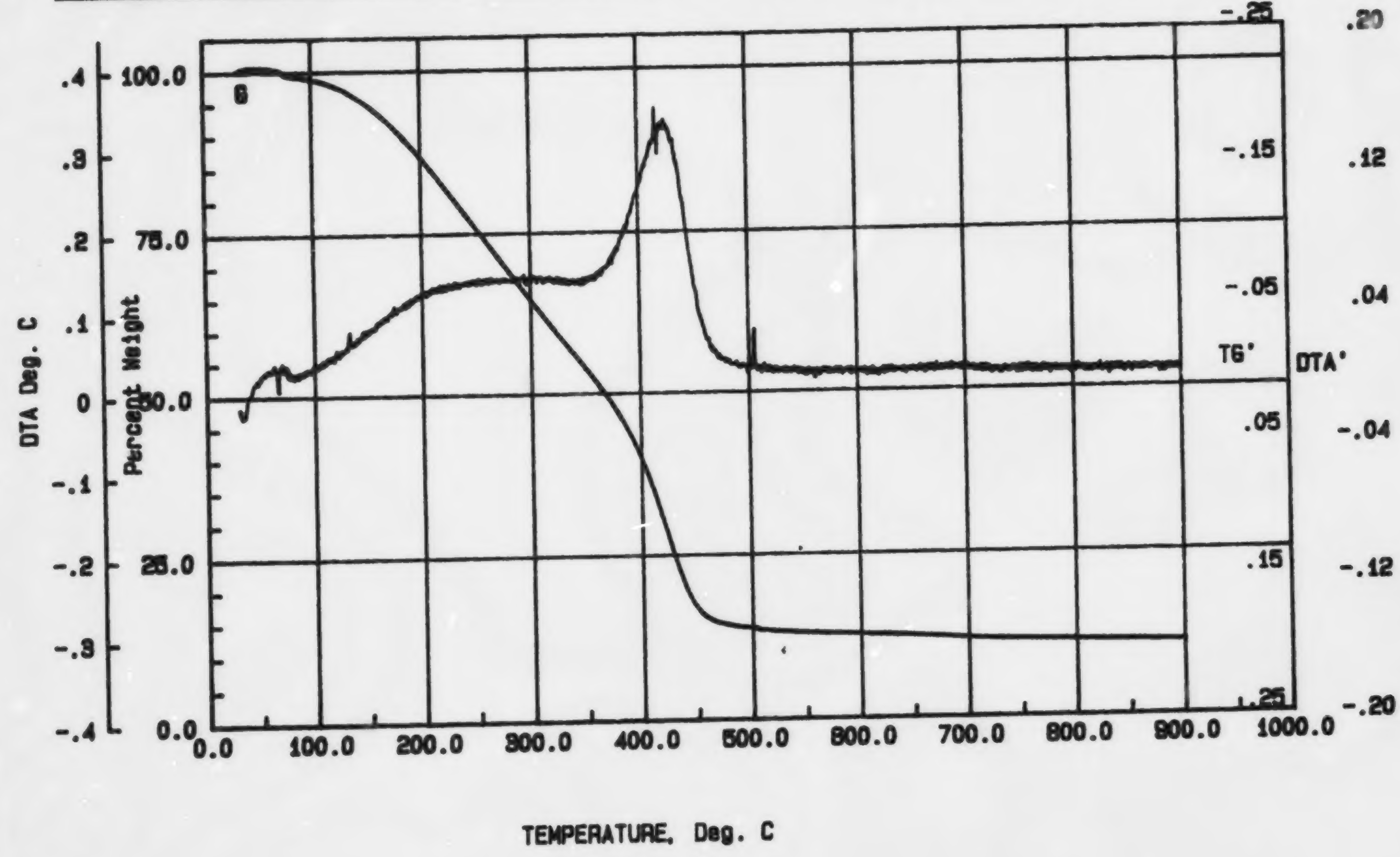

OPERATOR: R.SAETRE		NETZSCH STA 429/409		ATM.	NITROGEN	
DATE:	08/27/87	REFERENCE :	SAND	FLOW =	70 cc/min	
RUN No.	1	CRUCIBLE :	AL203	HEAT RATE =	.2 C/min	
TG Setting	50mg	FILE NAME :	TOILS2	SAMPLE WT.=	18.4 mg	
DTA Setting	0.1mV	MATERIAL	TOILS	REF WEIGHT	0 mg	

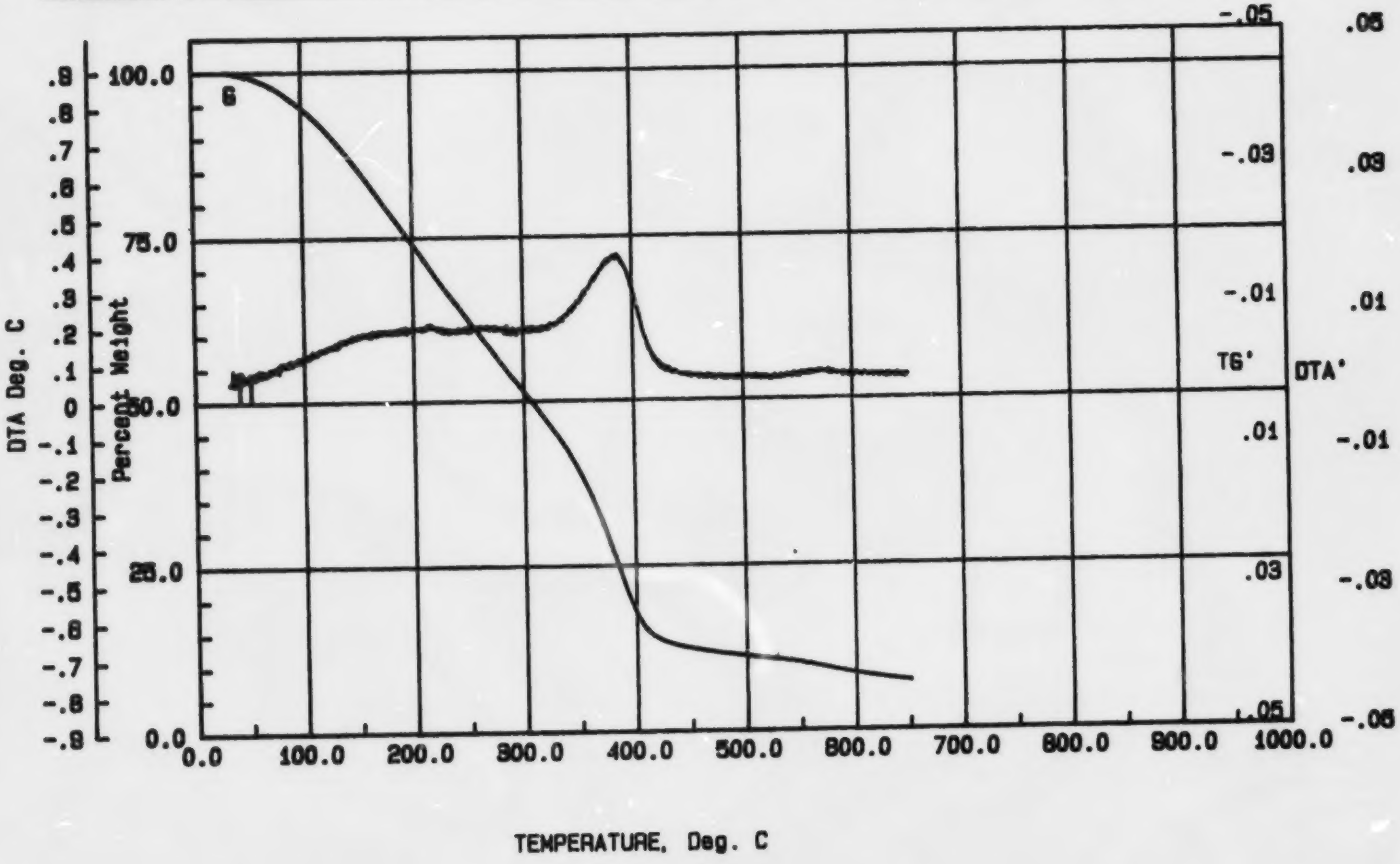

OPERATOR: R.SAETRE	NETZSCH STA 429/409	ATM. AIR
DATE: 03/20/87	REFERENCE : SAND	FLOW = 70 cc/min
RUN No. 3	CRUCIBLE : AL203	HEAT RATE = 10 C/min
TG Setting 50mg	FILE NAME : TOILAIS1	SAMPLE WT.= 15.2 mg
DTA Setting 0.1mV	MATERIAL TAOILS	REF WEIGHT 0 mg

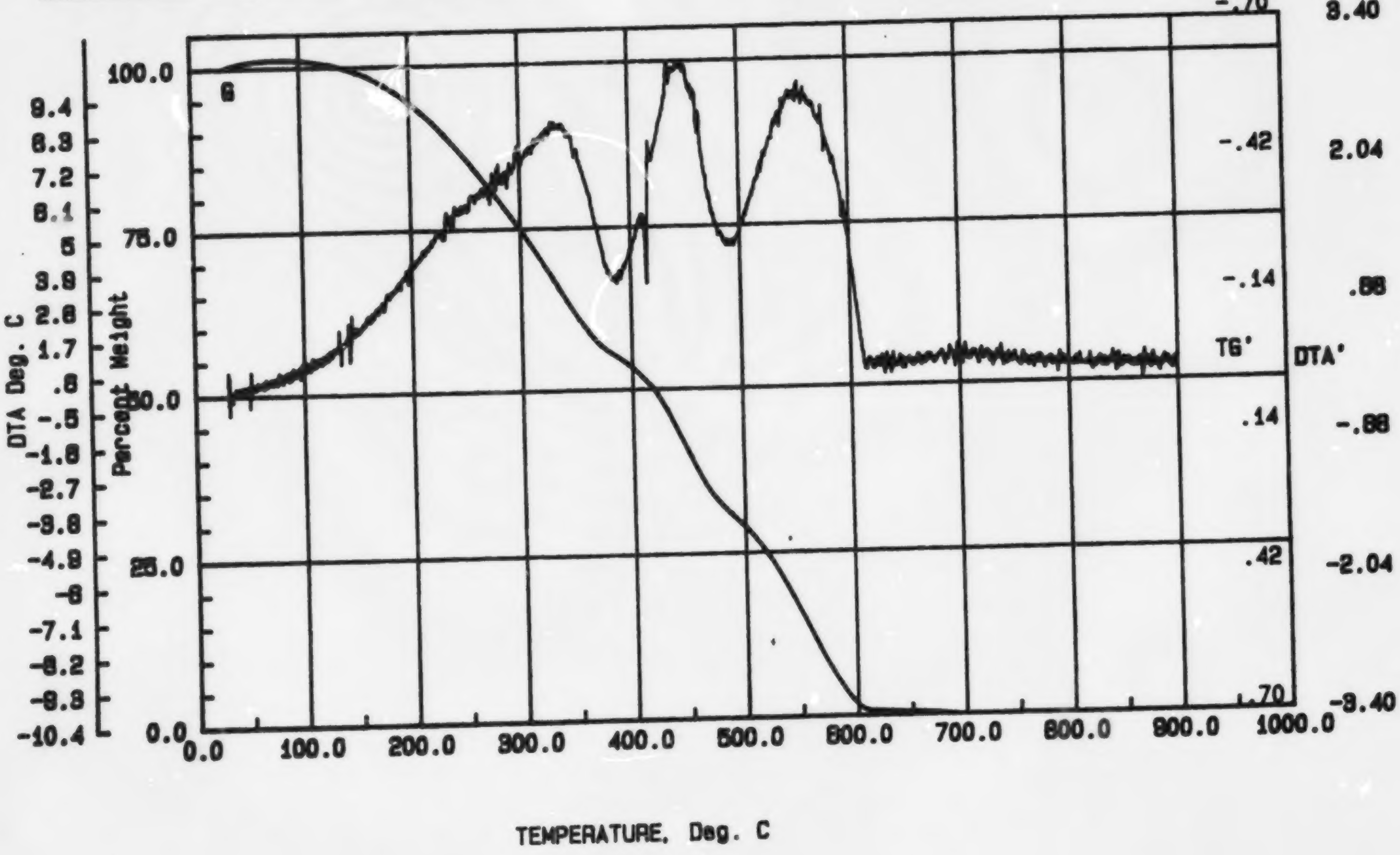

OPERATOR: R.SAETRE	NETZSCH STA 429/409	ATM. AIR	(Figure 5)
DATE: 09/20/87	REFERENCE : SAND	FLOW = 70 cc/min	
RUN No. 4	CRUCIBLE : AL203	HEAT RATE = 10 C/min	
TG Setting 50mg	FILE NAME : TOILAIS2	SAMPLE WT.= 14.4 mg	
DTA Setting 0.1mV	MATERIAL TAOILS	REF WEIGHT 0 mg	

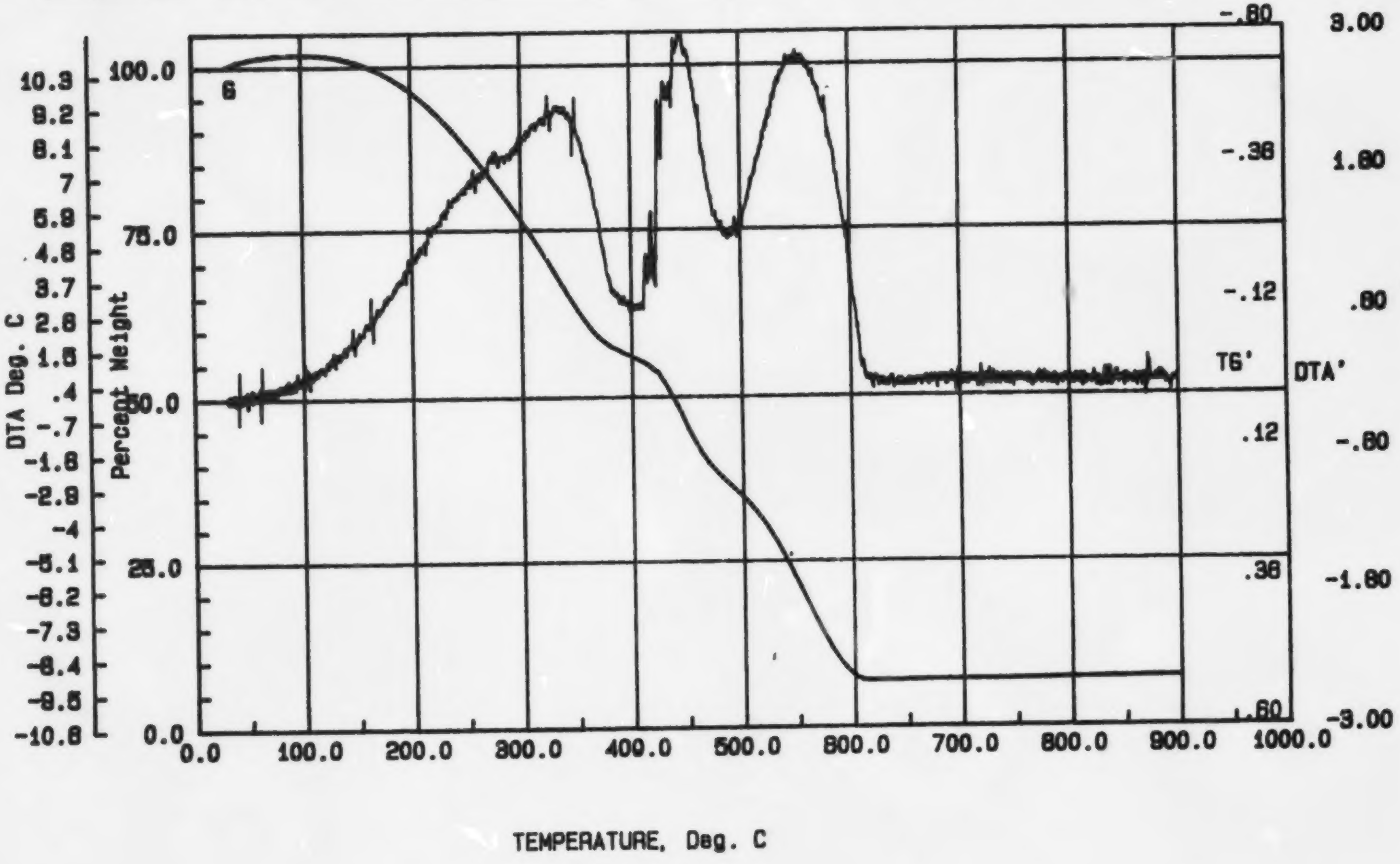

OPERATOR:	R.SAETRE	NETZSCH STA 429/409		ATM.	AIR	(Figure 13)
DATE:	09/24/87	REFERENCE :	SAND	FLOW =	70 cc/min	
RUN No.	6	CRUCIBLE :	AL203	HEAT RATE =	2 C/min	
TG Setting	50mg	FILE NAME :	TOILAIS3	SAMPLE WT.=	23 mg	
DTA Setting	0.1mV	MATERIAL	TOILS	REF WEIGHT	0 mg	

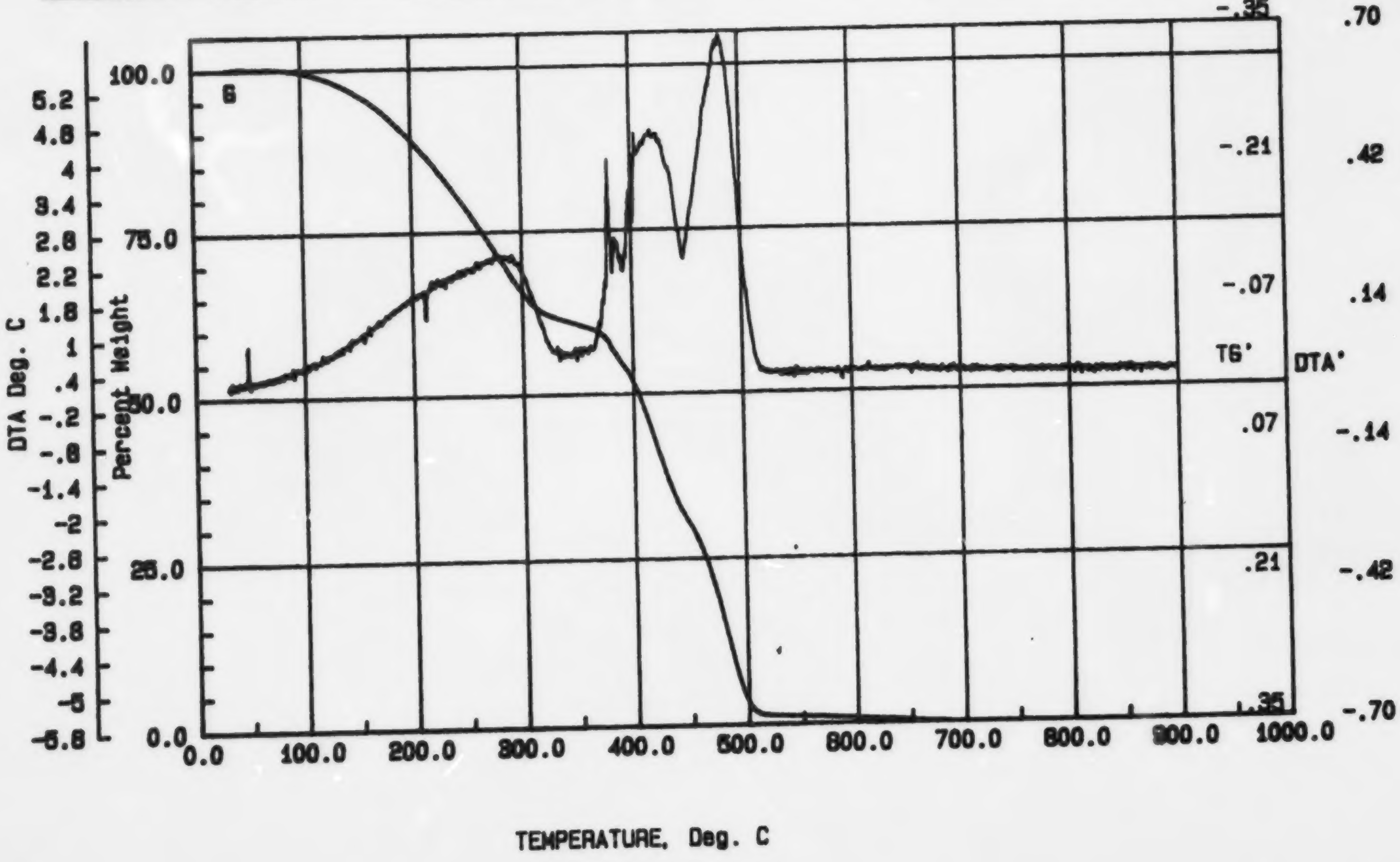

OPERATOR: R.SAETRE DATE: 09/25/87 RUN No. 6 TG Setting 50mg DTA Setting 0.1mV	NETZSCH STA 429/409 REFERENCE : SAND CRUCIBLE : AL203 FILE NAME : TOILAIS4 MATERIAL TOILS	ATM. AIR FLOW = 70 cc/min HEAT RATE = .2 C/min SAMPLE WT.= 19.3 mg REF WEIGHT 0 mg	(Figure 14)

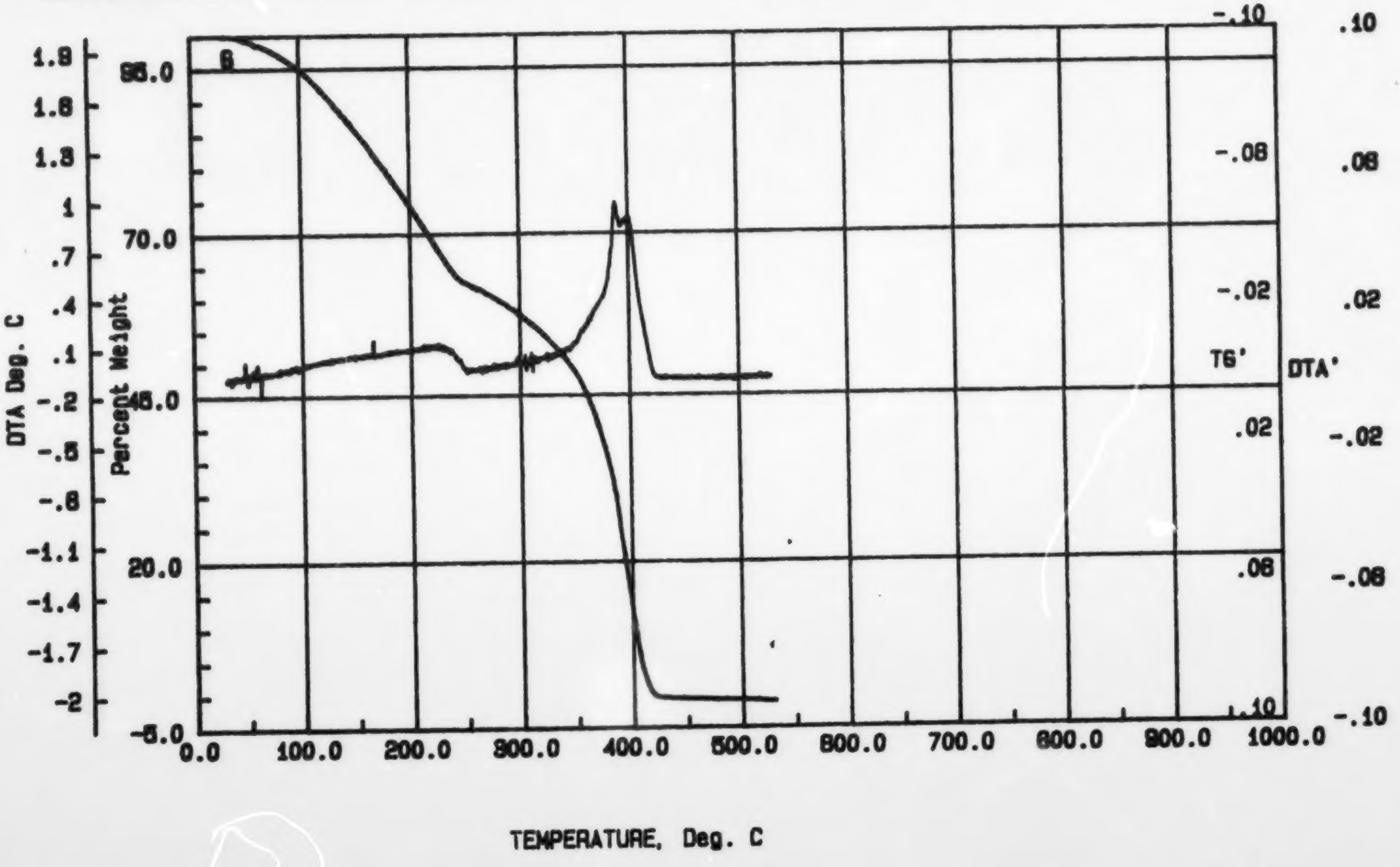

OPERATOR:	R.SAETRE	NETZSCH STA 429/409		ATM.	OXYGEN
DATE:	03/30/87	REFERENCE :	SAND	FLOW =	70 cc/min
RUN No.	1	CRUCIBLE :	AL2O3	HEAT RATE =	10 C/min
TG Setting	50mg	FILE NAME :	TOILOXS1	SAMPLE WT.=	21.7 mg
DTA Setting	0.1mV	MATERIAL	TOILS	REF WEIGHT	0 mg

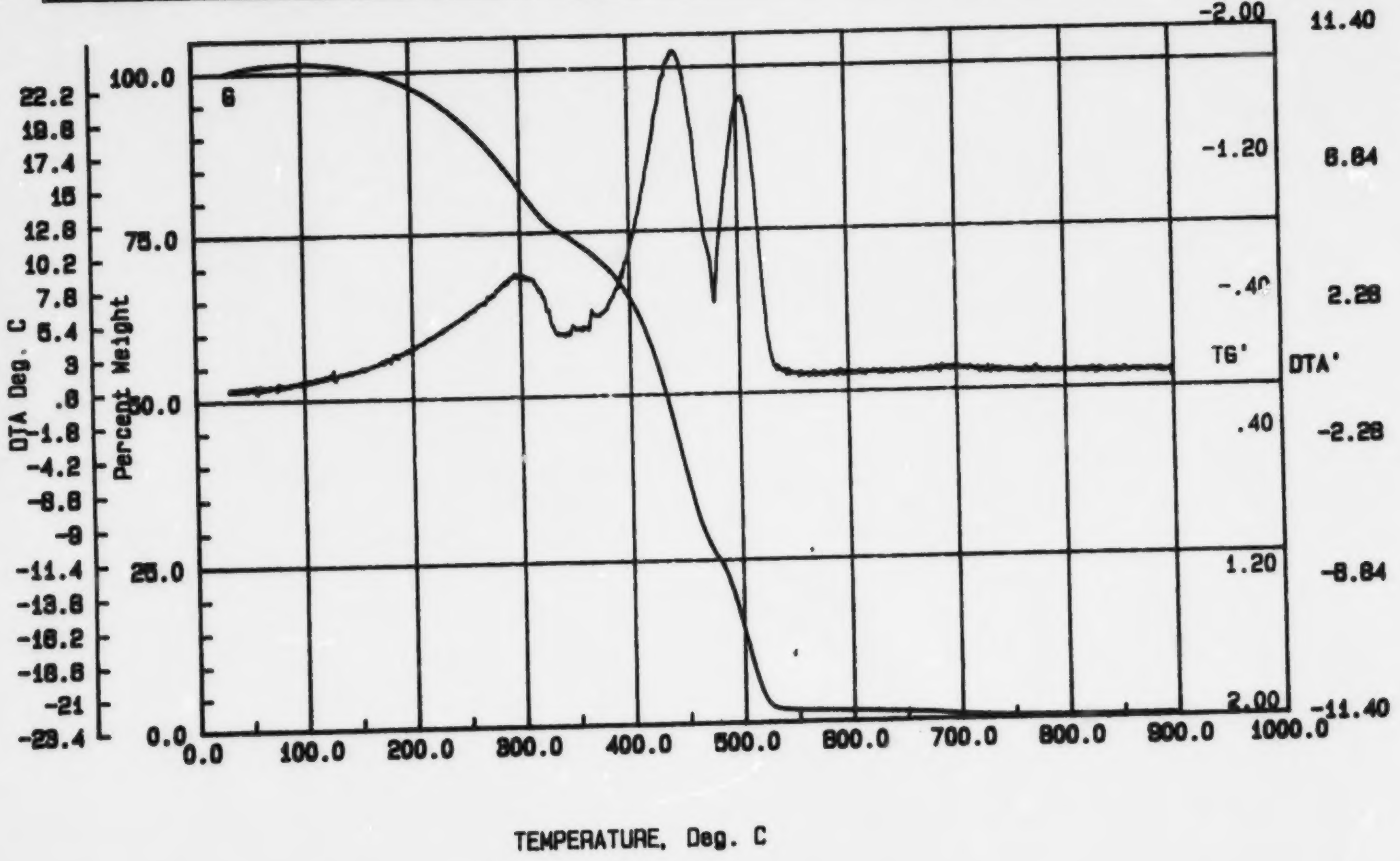

OPERATOR: R.SAETRE
DATE: 09/15/87
RUN No. 1
TG Setting 50mg
DTA Setting 0.1mV

NETZSCH STA 429/409
REFERENCE : AL203
CRUCIBLE : AL203
FILE NAME : TOIL1A10
MATERIAL TOIL1A10

ATM. NITROGEN
FLOW = 70 cc/min
HEAT RATE = 5 C/min
SAMPLE WT.= 30.4 mg
REF WEIGHT 0 mg

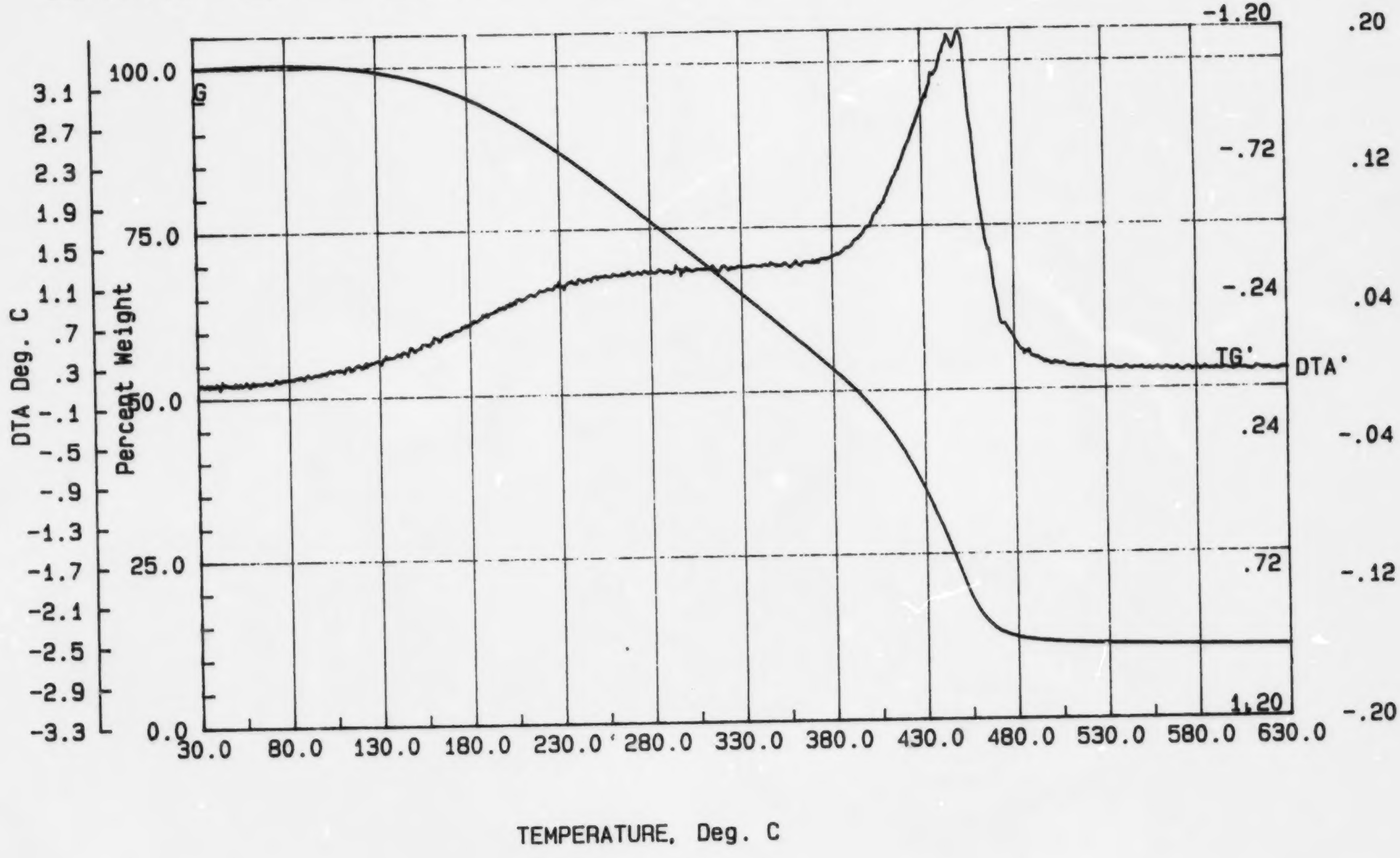

OPERATOR:	R.SAETRE
DATE:	09/21/87
RUN No.	8
TG Setting	50mg
DTA Setting	0.1mV

NETZSCH STA 429/409

REFERENCE :	AL203
CRUCIBLE :	AL203
FILE NAME :	TOI1A10A
MATERIAL	TOI1A10A

ATM.	NITROGEN
FLOW =	70 cc/min
HEAT RATE =	5 C/min
SAMPLE WT.=	29.2 mg
REF WEIGHT	0 mg

Report #00427
Page A-33

(Figure 16)

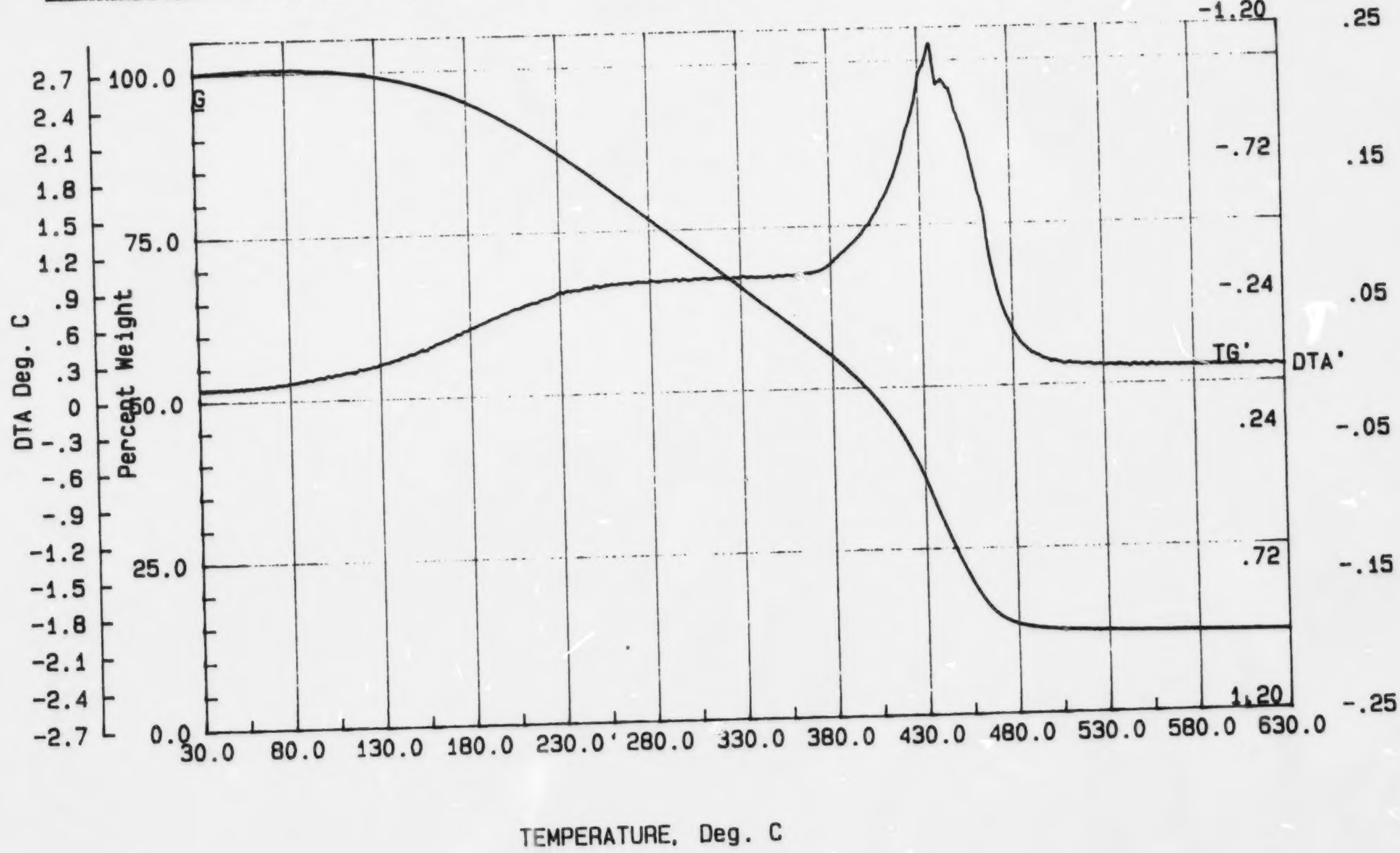

OPERATOR: R.SAETRE
DATE: 09/18/87
RUN No. 6
TG Setting 50mg
DTA Setting 0.1mV

NETZSCH STA 429/409
REFERENCE : AL203
CRUCIBLE : AL203
FILE NAME : TOILD7
MATERIAL TOILD7

ATM. NITROGEN
FLOW = 70 cc/min
HEAT RATE = 5 C/min
SAMPLE WT.= 32.8 mg
REF WEIGHT 0 mg

Report #00427
Page A-34
(Figure 17)

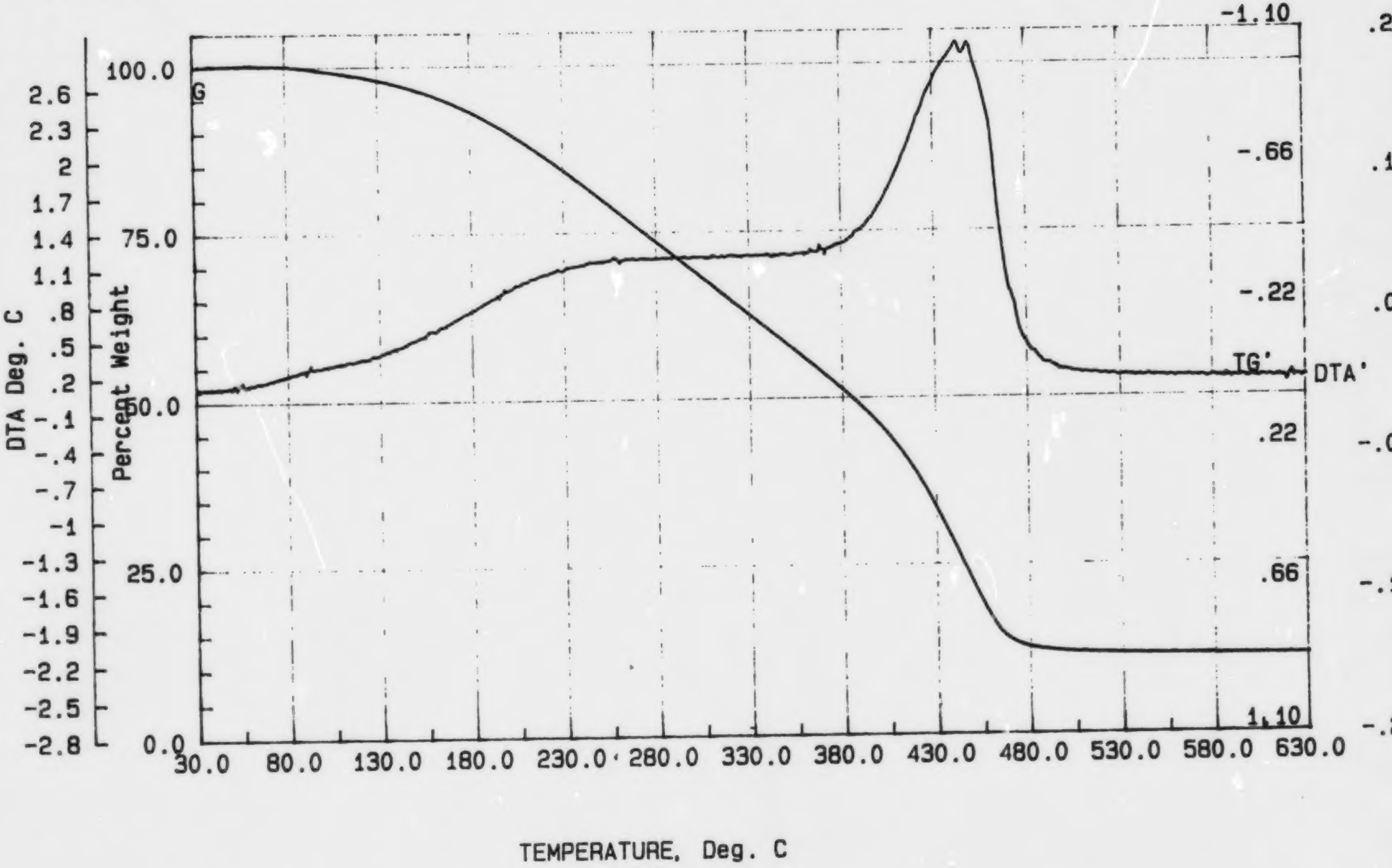

OPERATOR: R.SAETRE
DATE: 09/16/87
RUN No. 4
TG Setting 50mg
DTA Setting 0.1mV

NETZSCH STA 429/409
REFERENCE : AL203
CRUCIBLE : AL203
FILE NAME : TOIL4C3
MATERIAL TOIL4C3

ATM. NITROGEN
FLOW = 70 cc/min
HEAT RATE = 5 C/min
SAMPLE WT.= 27.8 mg
REF WEIGHT 0 mg

(Figure 18)

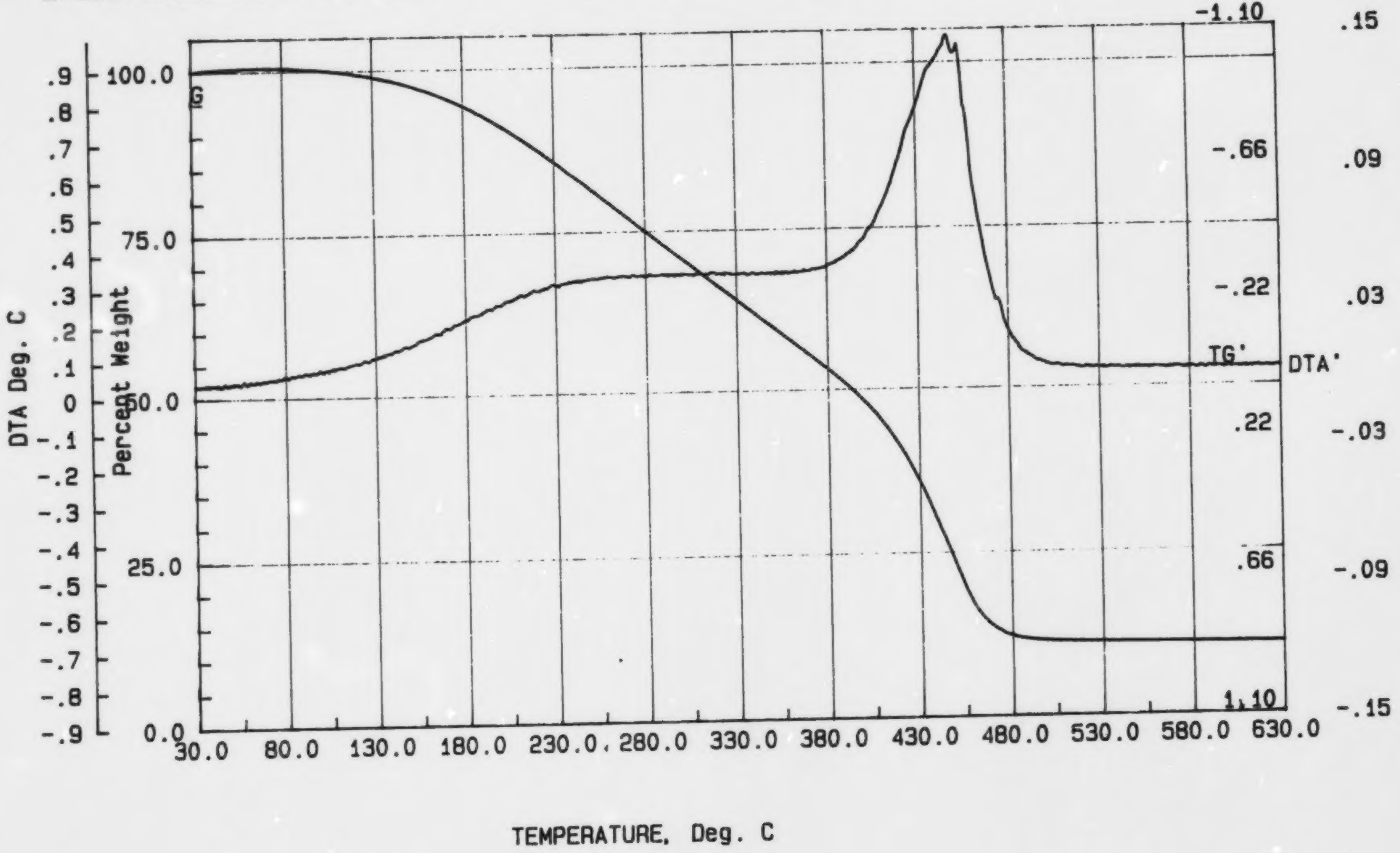

NOVA/Husky Research Corporation Ltd.

OPERATOR:	R.SAETRE	NETZSCH STA 429/409		ATM.	NITROGEN	Report #00427 Page A-36
DATE:	09/21/87	REFERENCE :	AL203	FLOW =	70 cc/min	
RUN No.	7	CRUCIBLE :	AL203	HEAT RATE =	5 C/min	(Figure 19)
TG Setting	50mg	FILE NAME :	TOIL4B7A	SAMPLE WT.=	31.2 mg	
DTA Setting	0.1mV	MATERIAL	TOIL4B7	REF WEIGHT	0 mg	

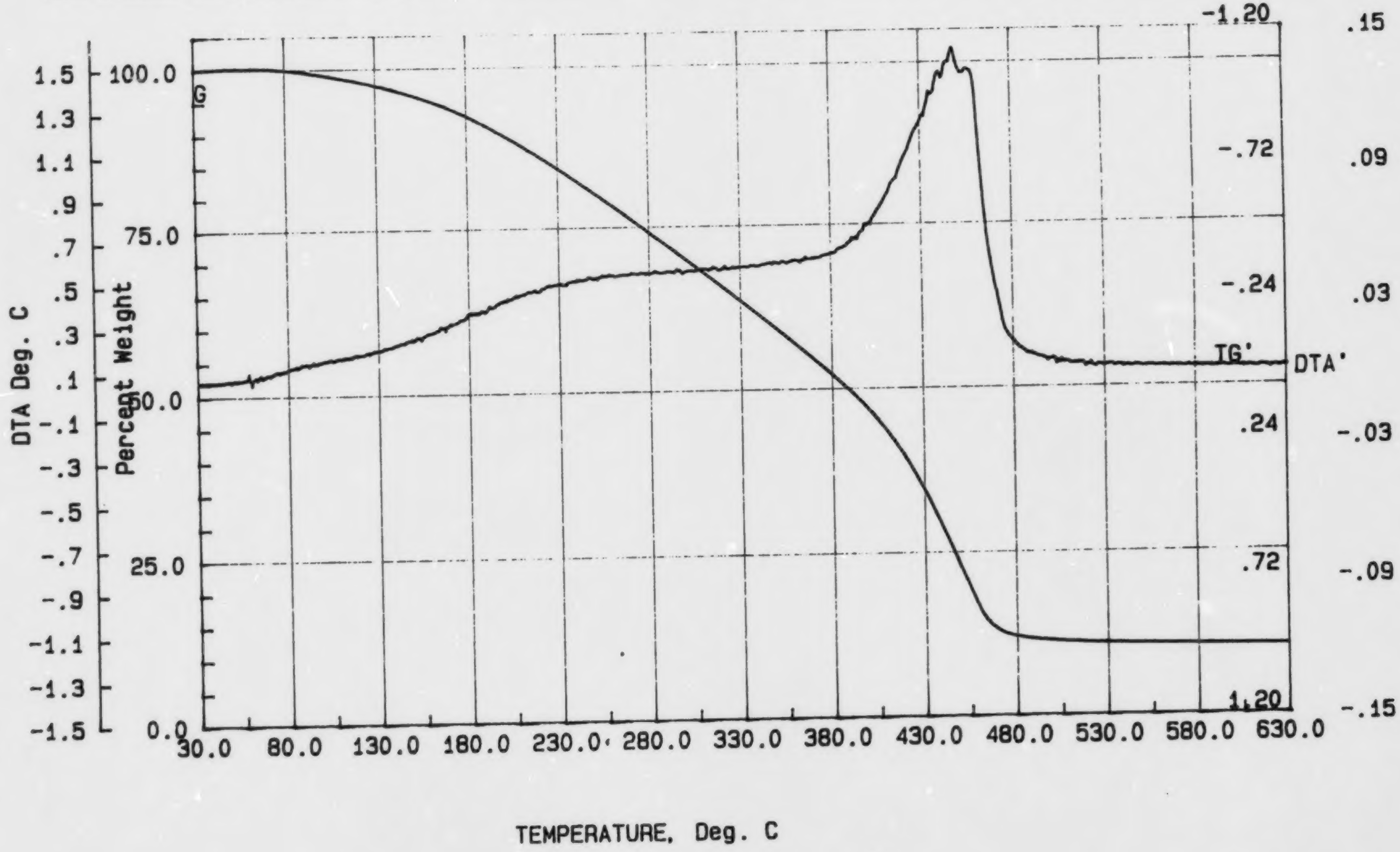

OPERATOR:	R.SAETRE	NETZSCH STA 429/409		ATM.	NITROGEN	Report #00427 Page A-37	
DATE:	09/15/87	REFERENCE :	AL203	FLOW =	70 cc/min		
RUN No.	2	CRUCIBLE :	AL203	HEAT RATE =	5 C/min		
TG Setting	50mg	FILE NAME :	TOIL4B7	SAMPLE WT.=	31.7 mg		
DTA Setting	0.1mV	MATERIAL	TOIL4B7	REF WEIGHT	0 mg		

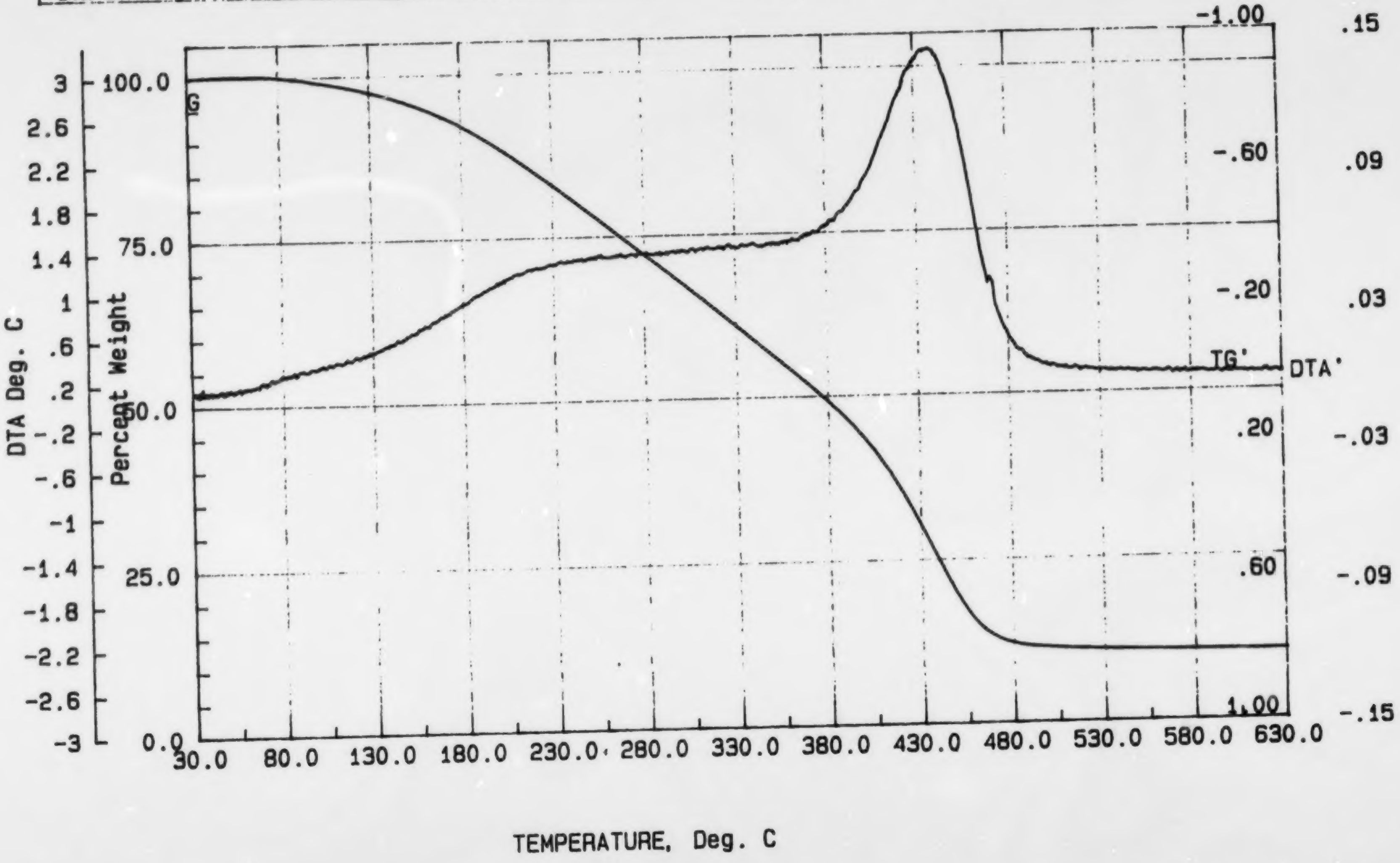

NOVA/Husky Research Corporation Ltd.

OPERATOR: R.SAETRE
DATE: 09/16/87
RUN No. 3
TG Setting 50mg
DTA Setting 0.1mV

NETZSCH STA 429/409
REFERENCE : AL203
CRUCIBLE : AL203
FILE NAME : TOIL4C2
MATERIAL TOIL4C2

ATM. NITROGEN
FLOW = 70 cc/min
HEAT RATE = 5 ~~10~~ C/min
SAMPLE WT.= 33 mg
REF WEIGHT 0 mg

Report #00427
Page A-38
(Figure 20)

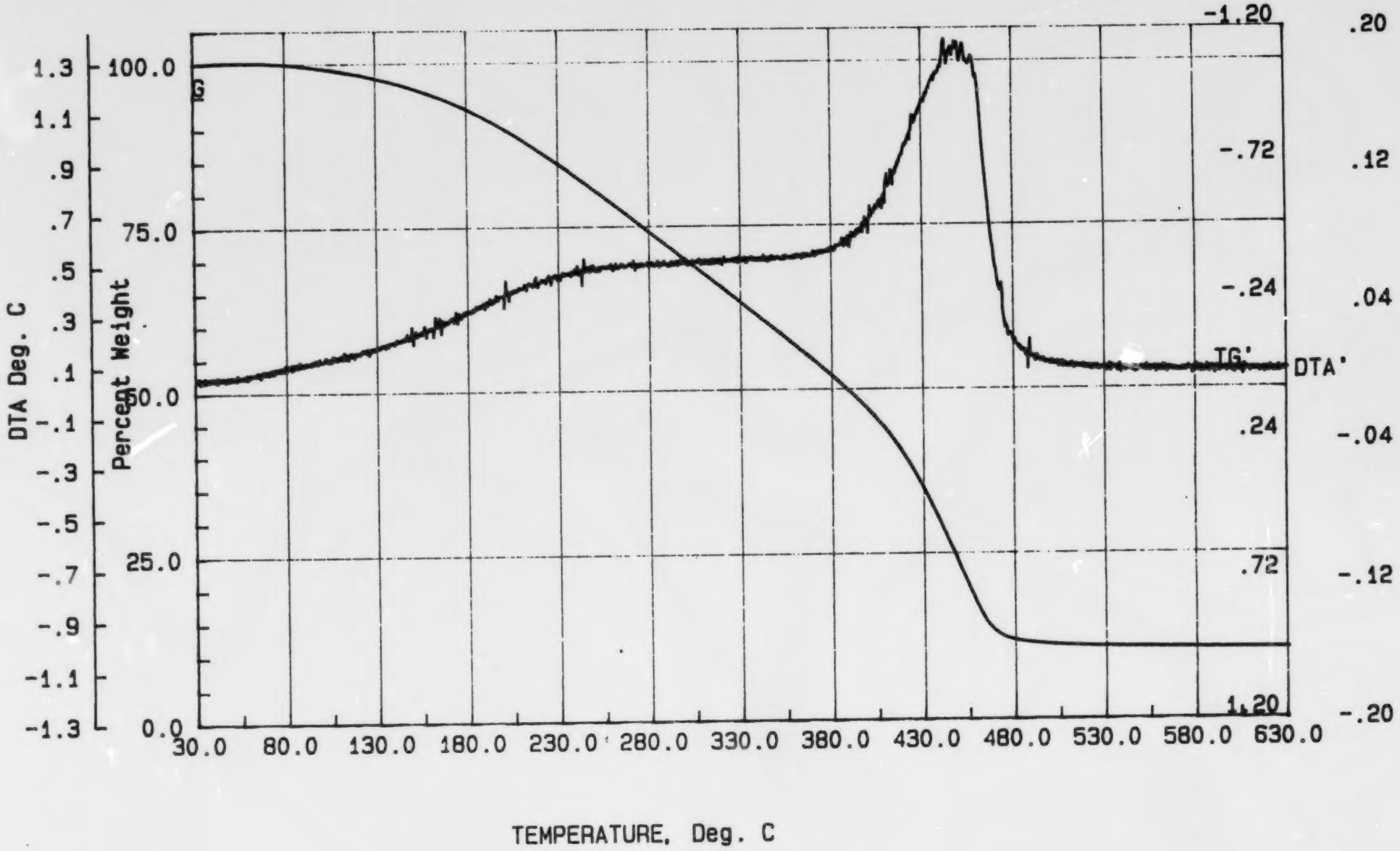

OPERATOR: R.SAETRE
DATE: 09/17/87
RUN No. 5
TG Setting 50mg
DTA Setting 0.1mV

NETZSCH STA 429/409
REFERENCE : AL203
CRUCIBLE : AL203
FILE NAME : TOILD3
MATERIAL TOILD3

ATM. NITROGEN
FLOW = 70 cc/min
HEAT RATE = 5 C/min
SAMPLE WT.= 31.5 mg
REF WEIGHT 0 mg

Report #00427
Page A-39

(Figure 21)

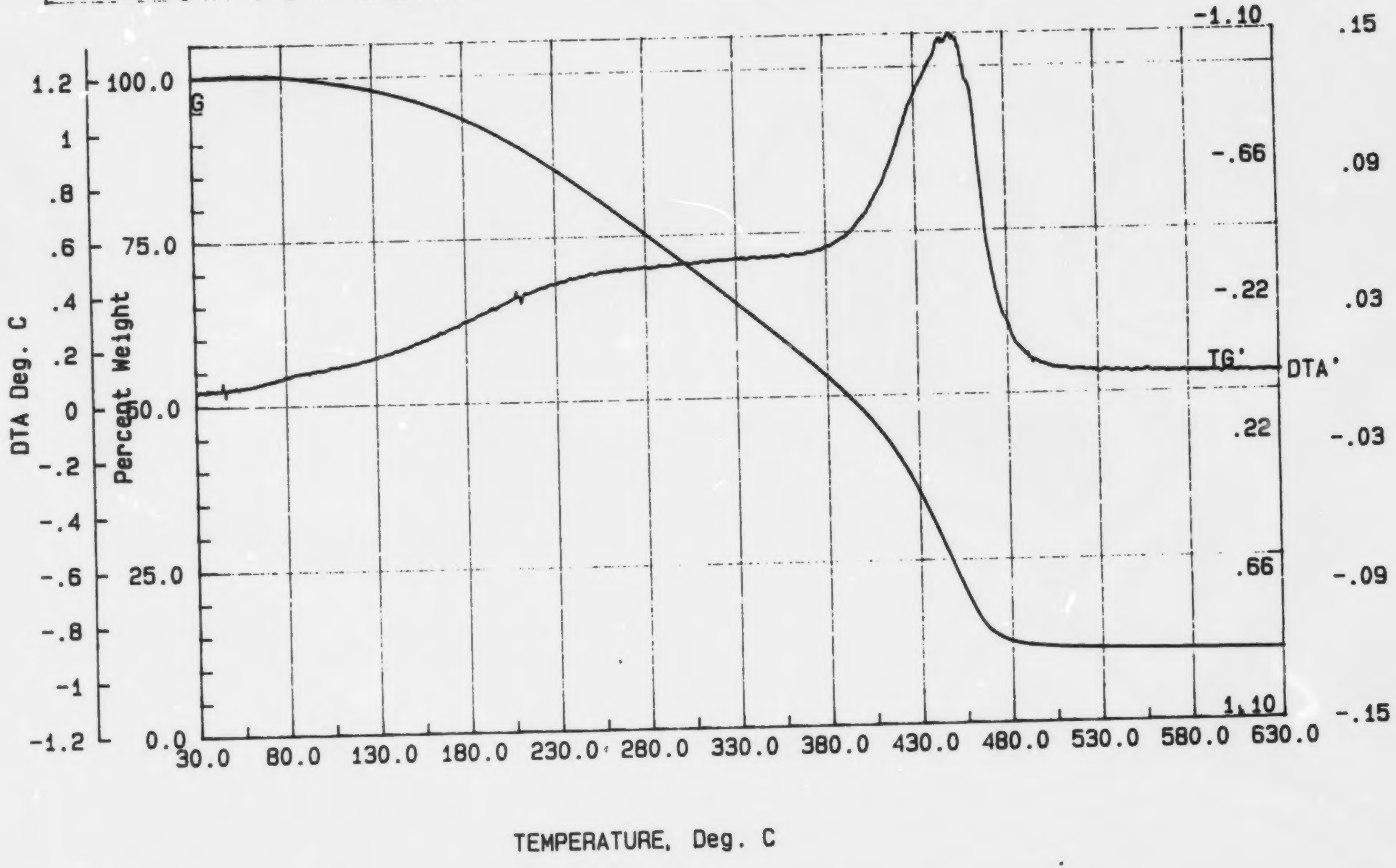

OPERATOR:	R.SAETRE	NETZSCH STA 429/409		ATM.	NITROGEN
DATE:	01/25/89	REFERENCE :	AL203	FLOW =	70 cc/min
RUN No.	8	CRUCIBLE :	AL203	HEAT RATE =	5 C/min
TG Setting	50mg	FILE NAME :	GLN21	SAMPLE WT.=	35.5 mg
DTA Setting	0.1mV	MATERIAL	GOLDLAKE	REF WEIGHT	0 mg

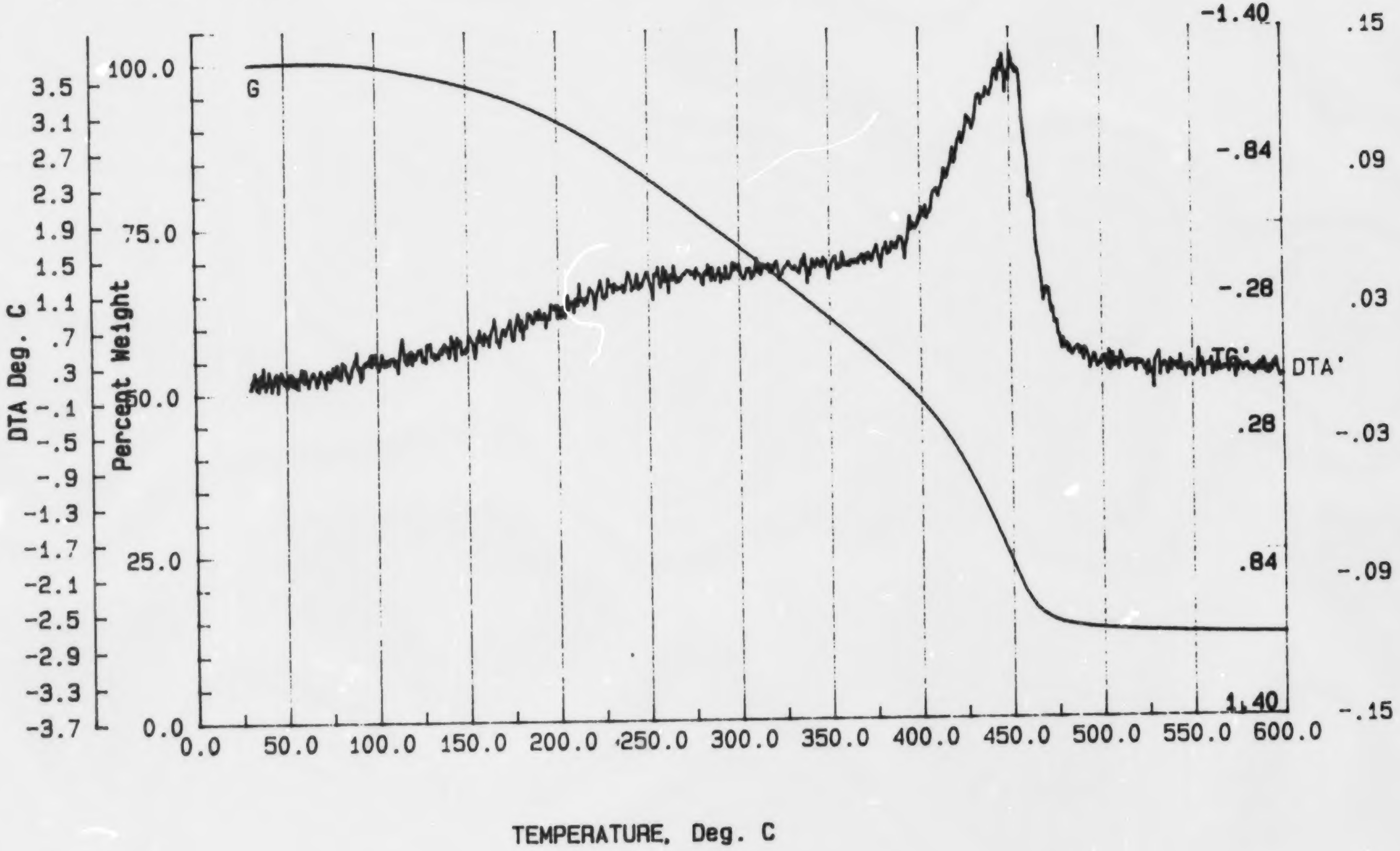

(Figure 23)

OPERATOR: R.SAETRE
DATE: 01/27/89
RUN No. 11
TG Setting 50mg
DTA Setting 0.1mV

NETZSCH STA 429/409
REFERENCE : AL203
CRUCIBLE : AL203
FILE NAME : 6LN22
MATERIAL GOLDLAKEB

ATM. NITROGEN
FLOW = 70 cc/min
HEAT RATE = 5 C/min
SAMPLE WT.= 31.9 mg
REF WEIGHT 0 mg

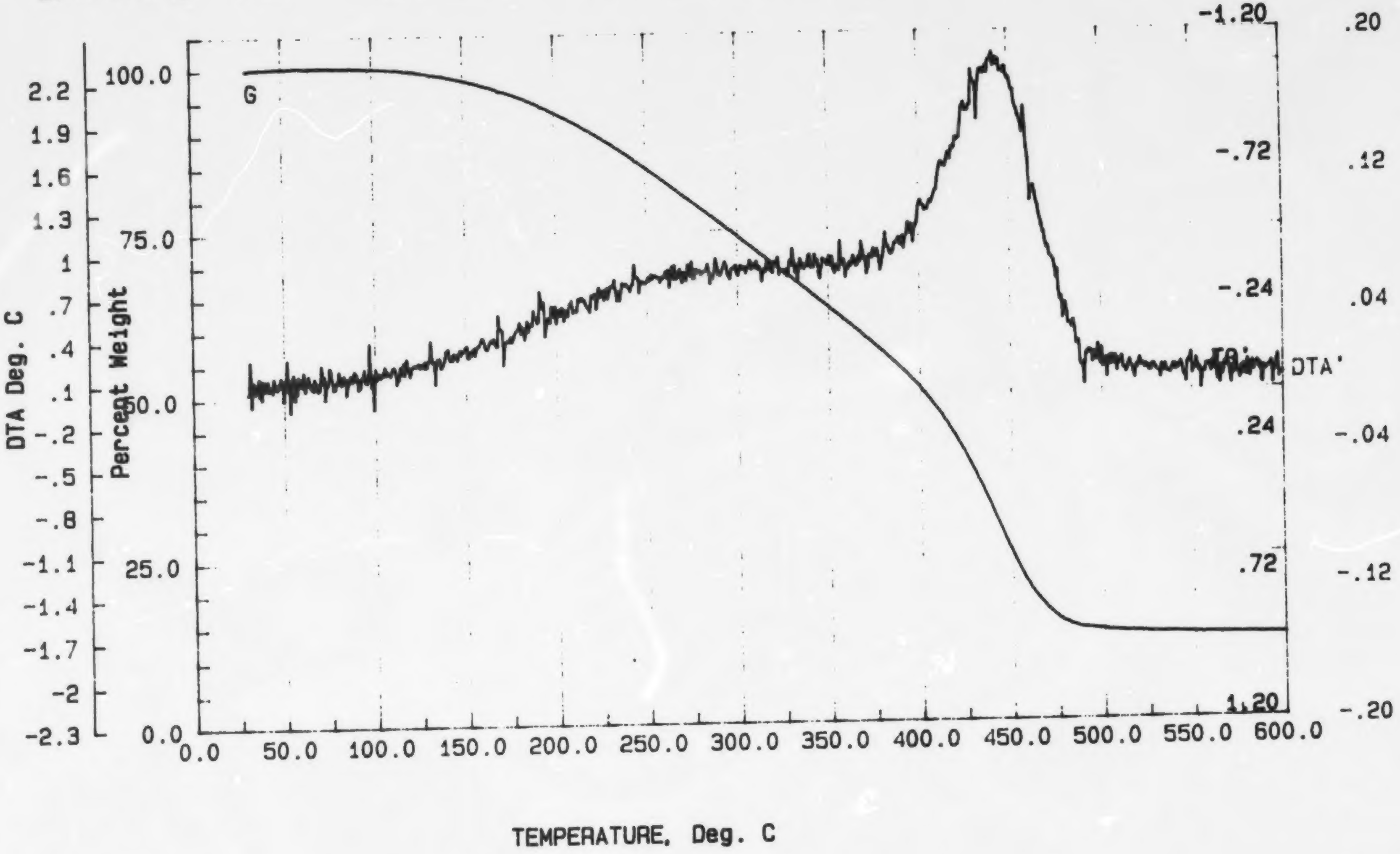

OPERATOR: R.SAETRE
DATE: 01/24/89
RUN No. 7
TG Setting 50mg
DTA Setting 0.1mV

NETZSCH STA 429/409
REFERENCE : AL203
CRUCIBLE : AL203
FILE NAME : GLAIR1
MATERIAL GOLDLAKE

ATM. AIR
FLOW = 70 cc/min
HEAT RATE = 5 C/min
SAMPLE WT.= 33.3 mg
REF WEIGHT 0 mg

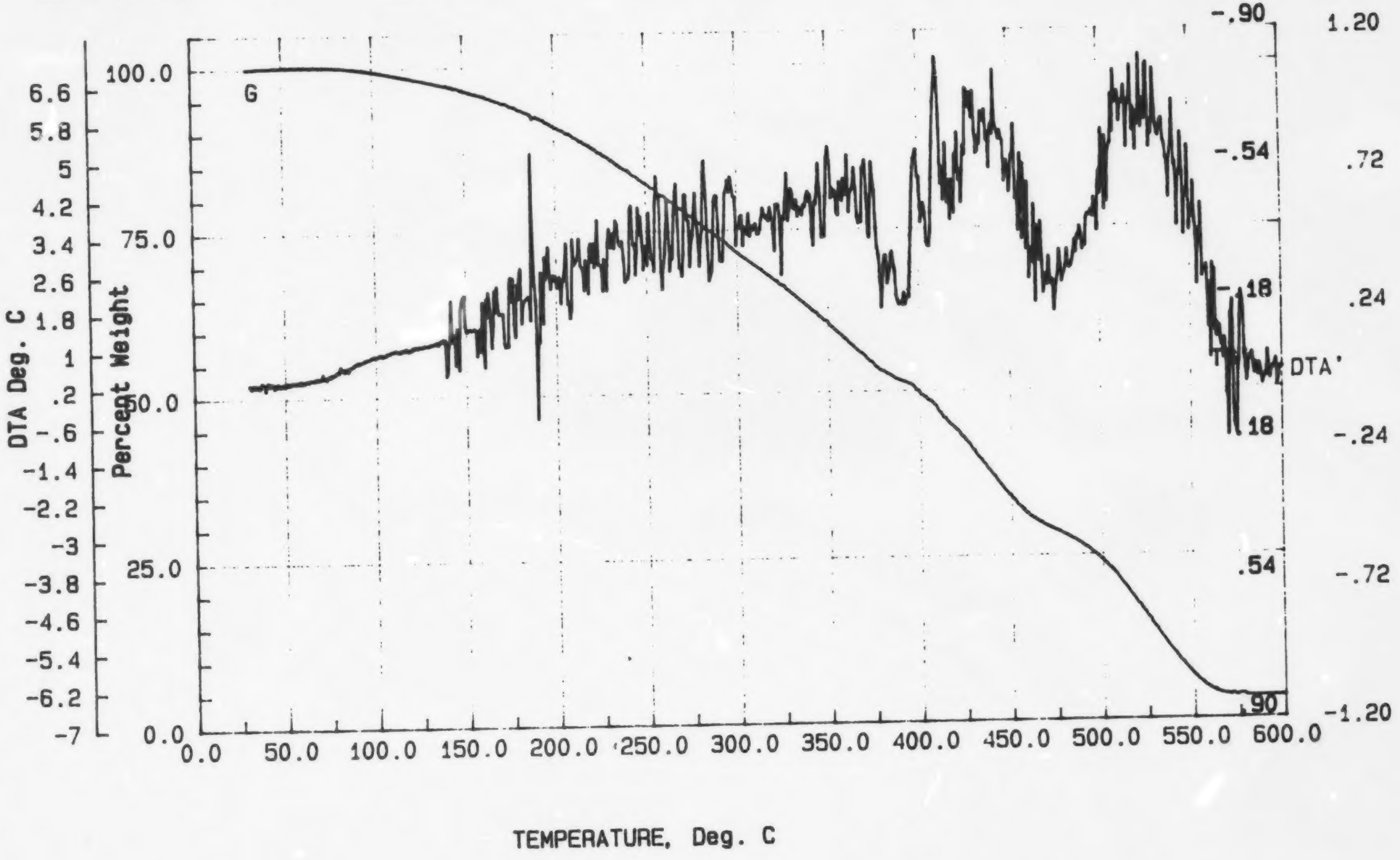

OPERATOR:	R.SAETRE
DATE:	01/26/89
RUN No.	9
TG Setting	50mg
DTA Setting	0.1mV

NETZSCH STA 429/409	
REFERENCE :	AL203
CRUCIBLE :	AL203
FILE NAME :	GLAIR2
MATERIAL	GOLDLAKEB

ATM.	AIR
FLOW =	70 cc/min
HEAT RATE =	5 C/min
SAMPLE WT.=	37.2 mg
REF WEIGHT	0 mg

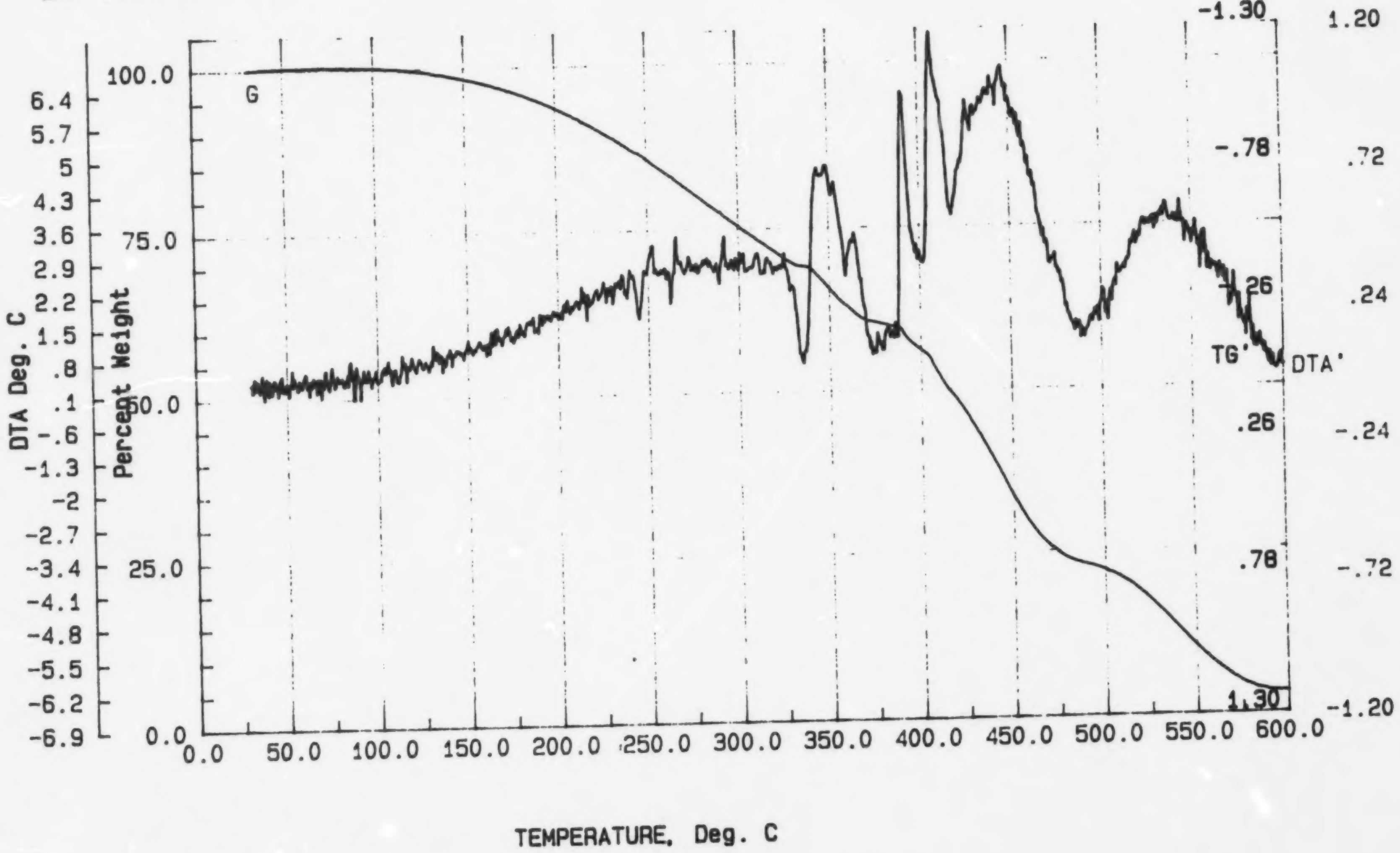

OPERATOR: R.SAETRE
DATE: 01/26/89
RUN No. 10
TG Setting 50mg
DTA Setting 0.1mV

NETZSCH STA 429/409
REFERENCE : AL203
CRUCIBLE : AL203
FILE NAME : GLAIR2B
MATERIAL GOLDLAKEB

ATM. AIR
FLOW = 70 cc/min
HEAT RATE = 5 C/min
SAMPLE WT.= 35.3 mg
REF WEIGHT 0 mg

Report #00427
Page A-44

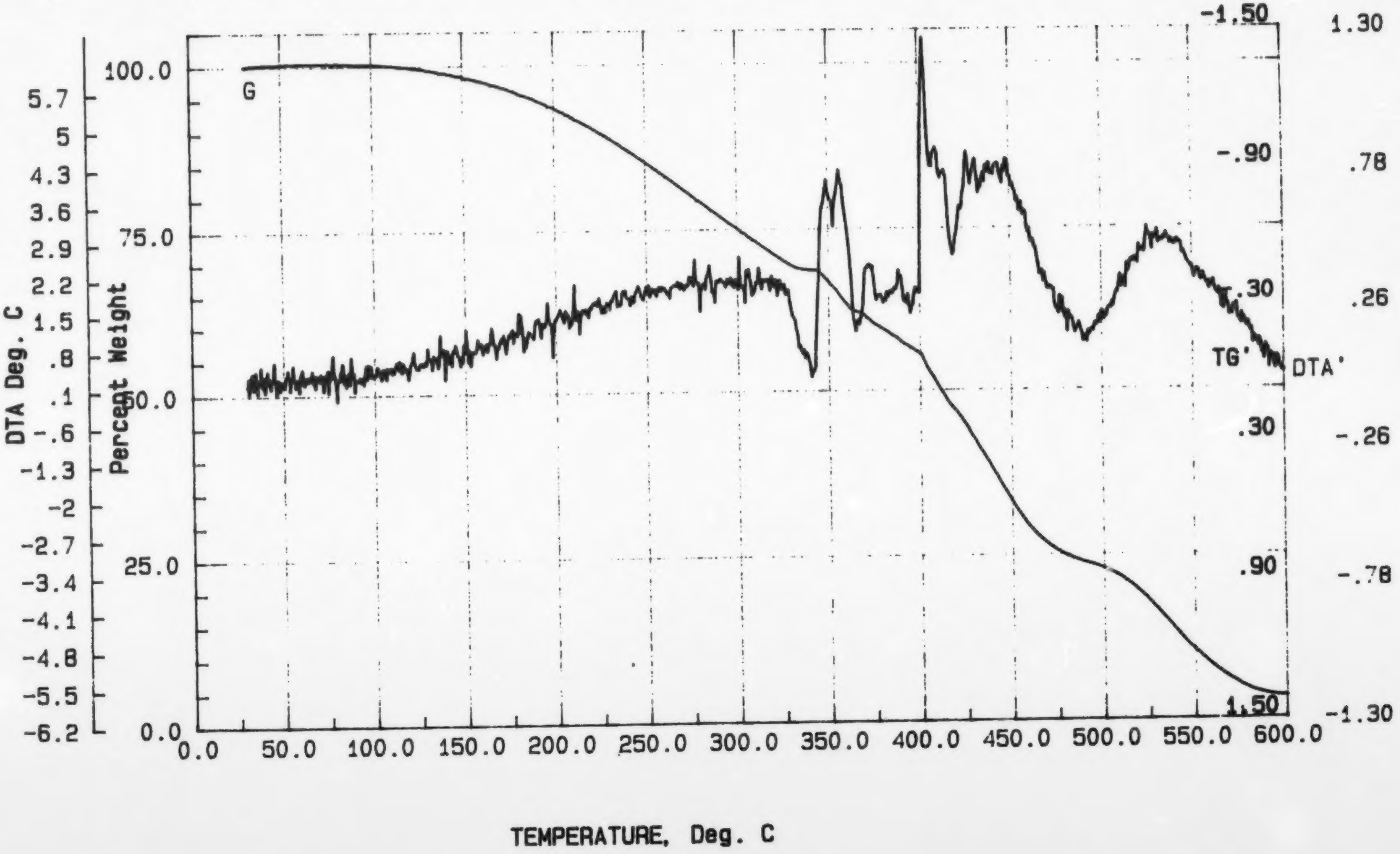

OPERATOR: R.SAETRE
DATE: 01/20/89
RUN No. 3
TG Setting 50mg
DTA Setting 0.1mV

NETZSCH STA 429/409
REFERENCE : AL203
CRUCIBLE : AL203
FILE NAME : CLN21
MATERIAL CARLAKE

ATM. NITROGEN
FLOW = 70 cc/min
HEAT RATE = 5 C/min
SAMPLE WT.= 33.6 mg
REF WEIGHT 0 mg

(Figure 24)

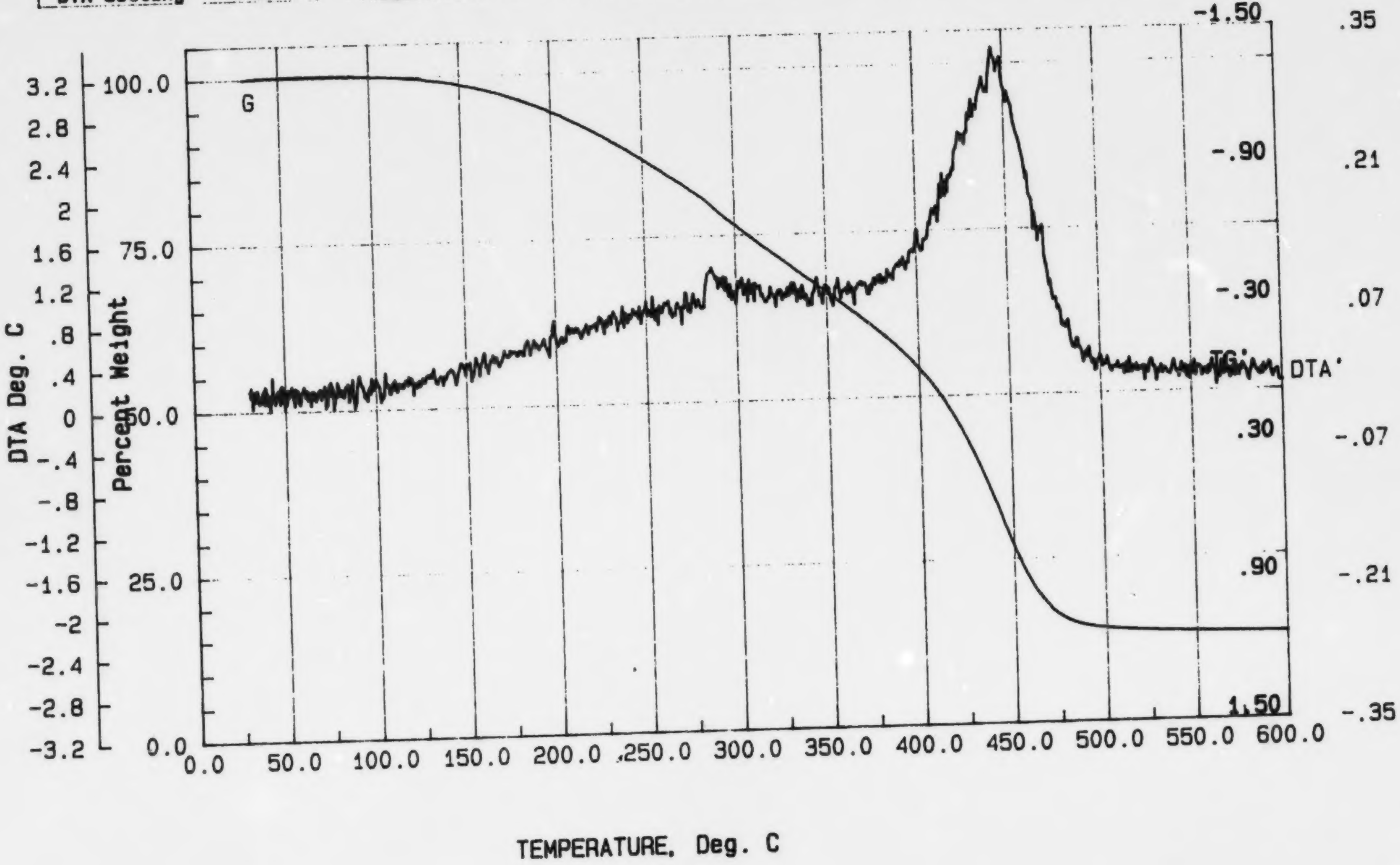

OPERATOR: R.SAETRE
DATE: 01/23/89
RUN No. 6
TG Setting 50mg
DTA Setting 0.1mV

NETZSCH STA 429/409
REFERENCE : AL203
CRUCIBLE : AL203
FILE NAME : CLN22
MATERIAL CARLAKE

ATM. NITROGEN
FLOW = 70 cc/min
HEAT RATE = 5 C/min
SAMPLE WT.= 37.4 mg
REF WEIGHT 0 mg

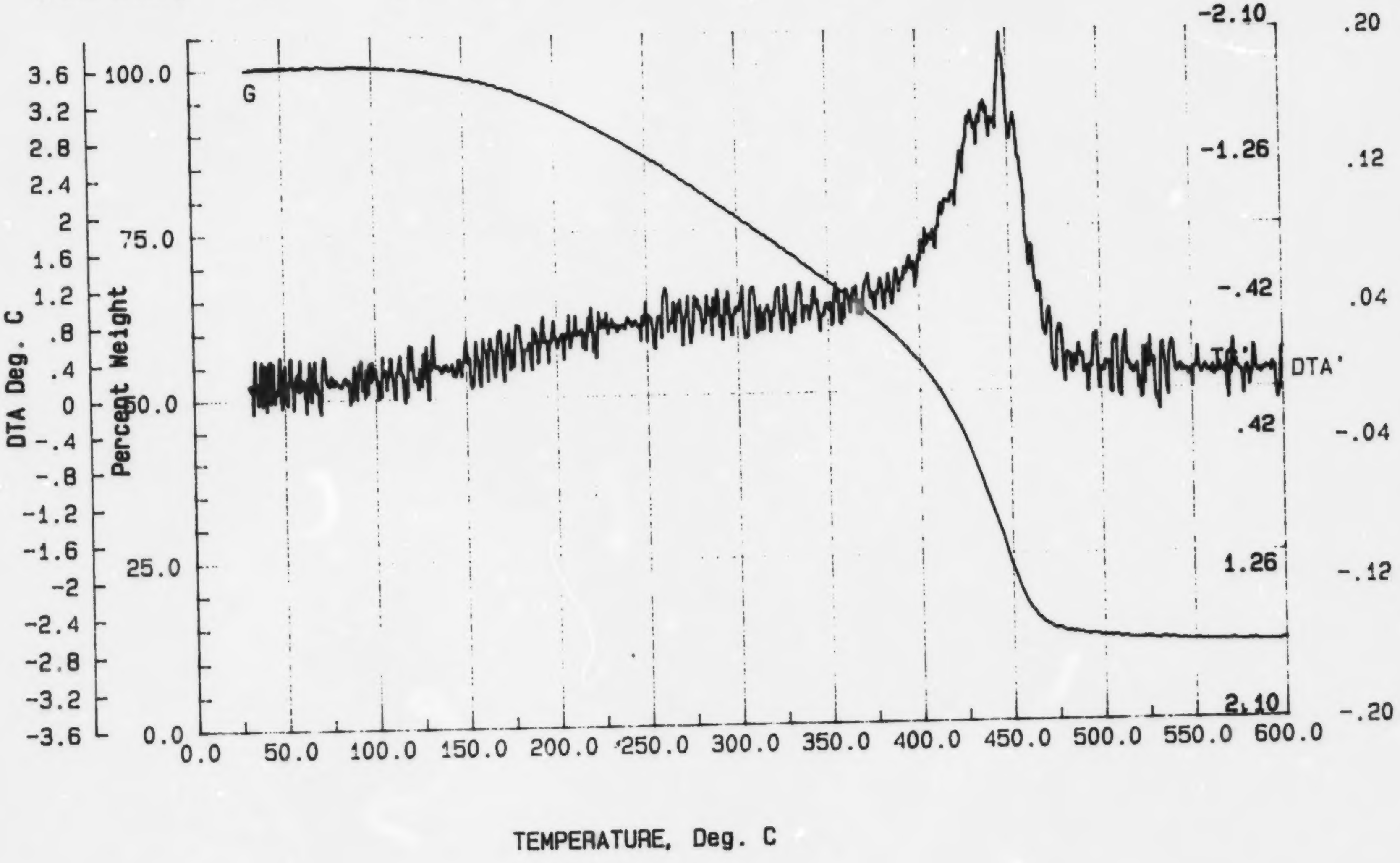

OPERATOR:	R.SAETRE	NETZSCH STA 429/409		ATM.	AIR
DATE:	01/23/89	REFERENCE :	AL203	FLOW =	70 cc/min
RUN No.	5	CRUCIBLE :	AL203	HEAT RATE =	5 C/min
TG Setting	50mg	FILE NAME :	CLAIR1	SAMPLE WT.=	34.5 mg
DTA Setting	0.1mV	MATERIAL	CARLAKE	REF WEIGHT	0 mg

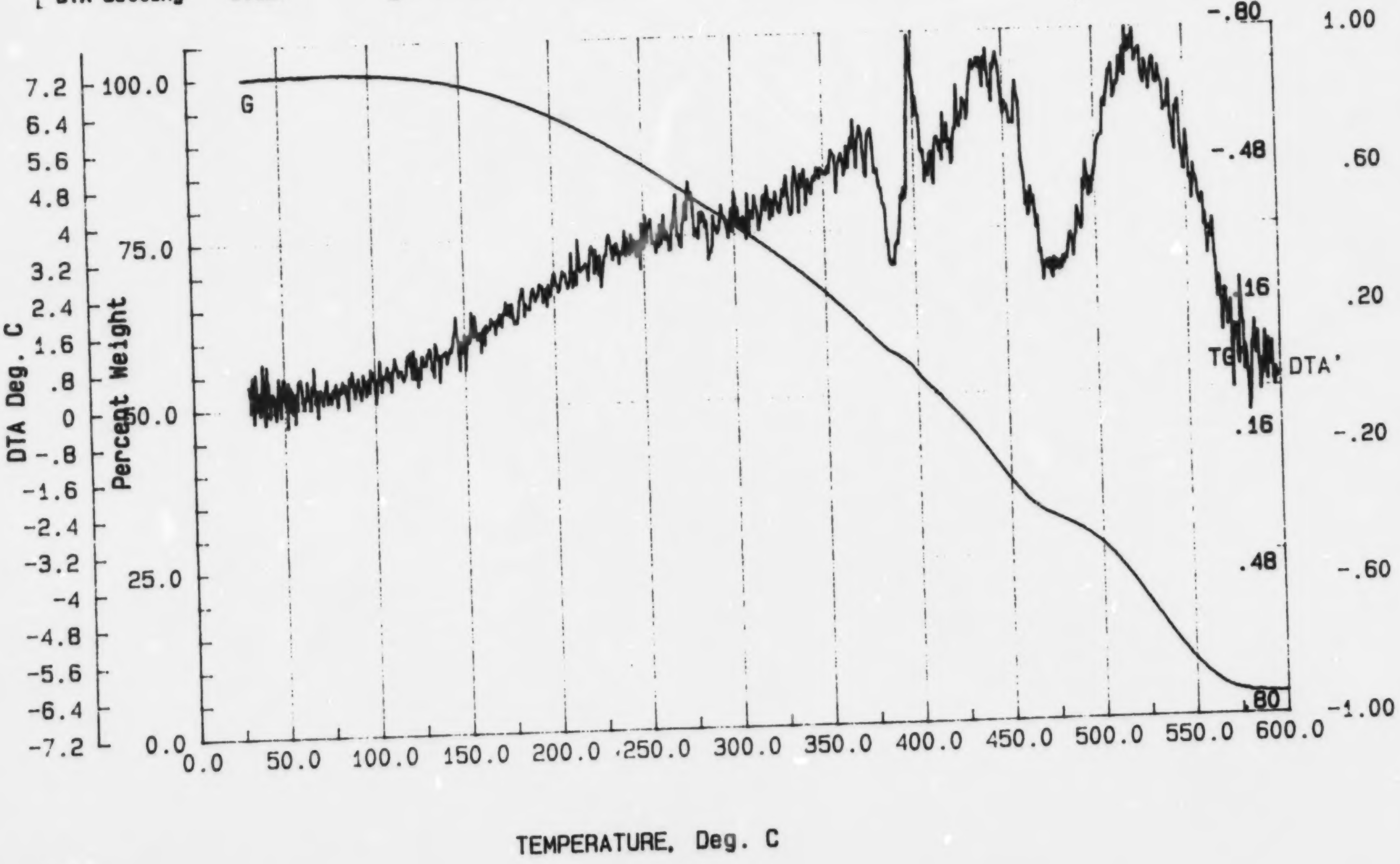

OPERATOR: A.SAETRE	NETZSCH STA 429/409	ATM. NITROGEN
DATE: 04/08/87	REFERENCE : AL203	FLOW = 70 cc/min
RUN No. 1	CRUCIBLE : AL203	HEAT RATE = 10 C/min
TG Setting 50mg	FILE NAME : ASPH1	SAMPLE WT.= 19.8 mg
DTA Setting 0.1mV	MATERIAL GLASPH	REF WEIGHT 0 mg

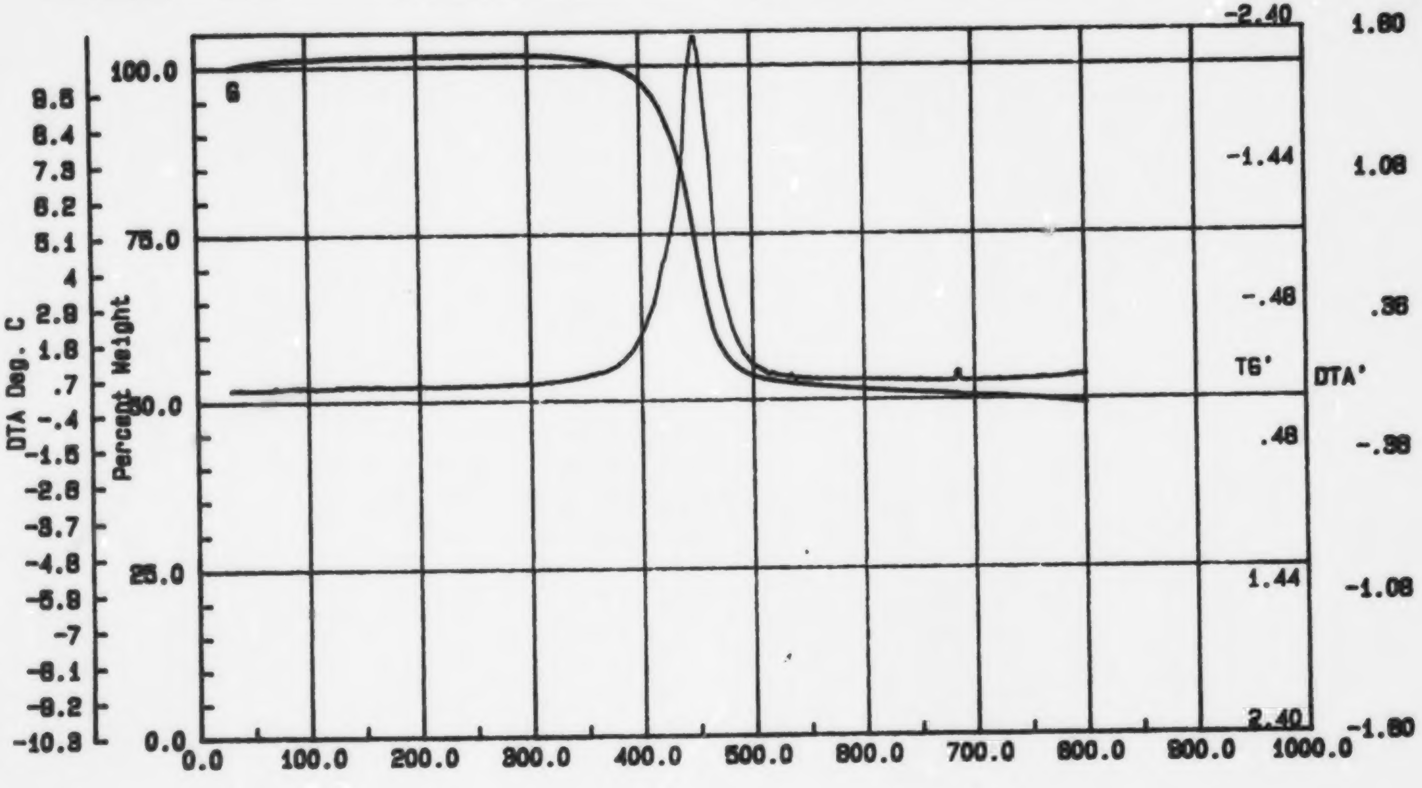

TEMPERATURE, Deg. C

OPERATOR: R.SAETRE DATE: 04/08/87 RUN No. 2 TG Setting 50mg DTA Setting 0.1mV	NETZSCH STA 429/409 REFERENCE : SAND CRUCIBLE : AL203 FILE NAME : ASPH2 MATERIAL ASPH	ATM. NITROGEN FLOW = 70 cc/min HEAT RATE = 10 C/min SAMPLE WT.= 12.1 mg REF WEIGHT 0 mg	(Figure 26)

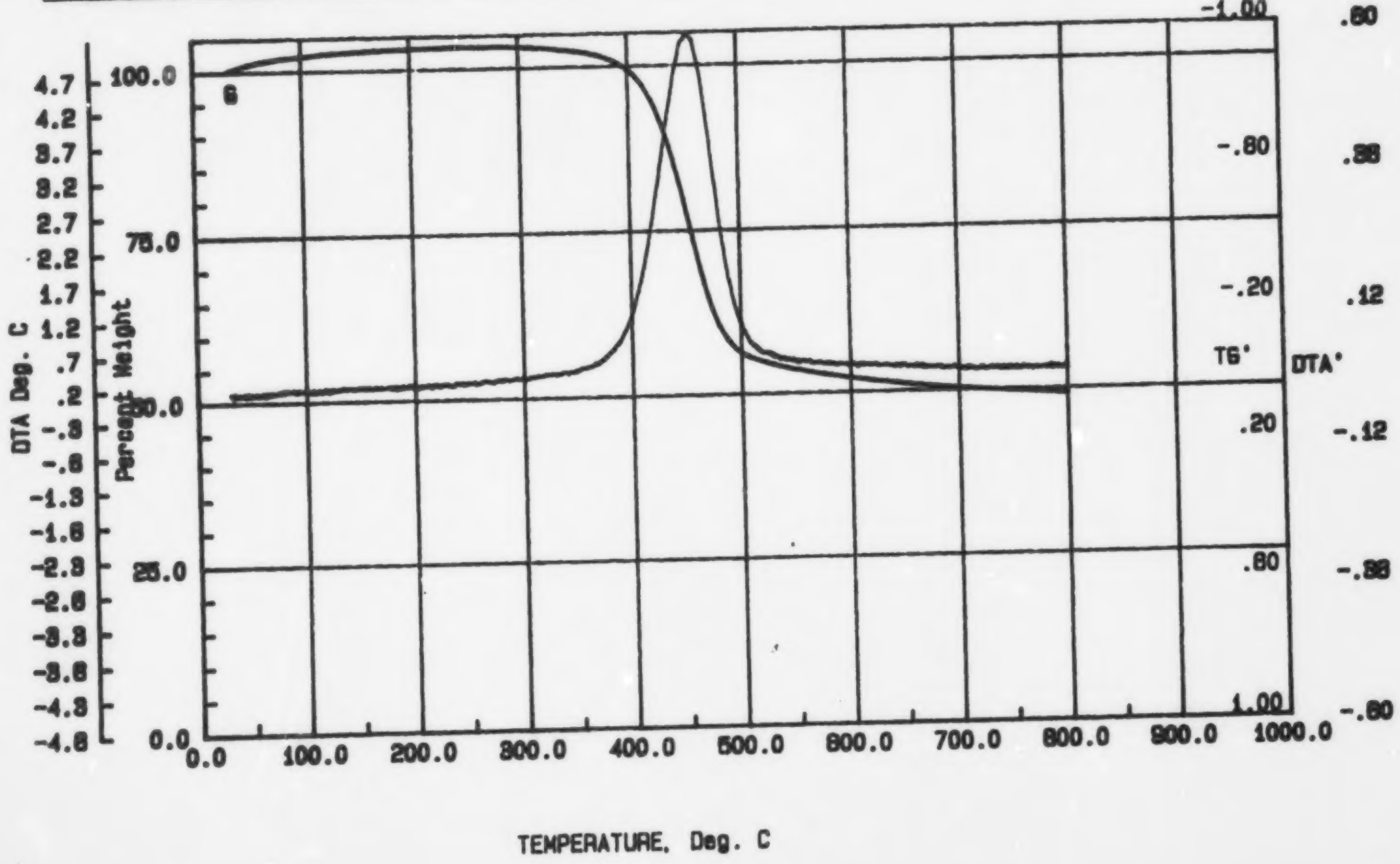

OPERATOR: R.SAETRE DATE: 04/07/87 RUN No. 3 TG Setting 50mg DTA Setting 0.1mV	NETZSCH STA 429/409 REFERENCE : SAND CRUCIBLE : AL203 FILE NAME : ASPH3 MATERIAL ASPH	ATM. NITROGEN FLOW = 70 cc/min HEAT RATE = .2 C/min SAMPLE WT.= 10.7 mg REF WEIGHT 0 mg	(Figure 25)

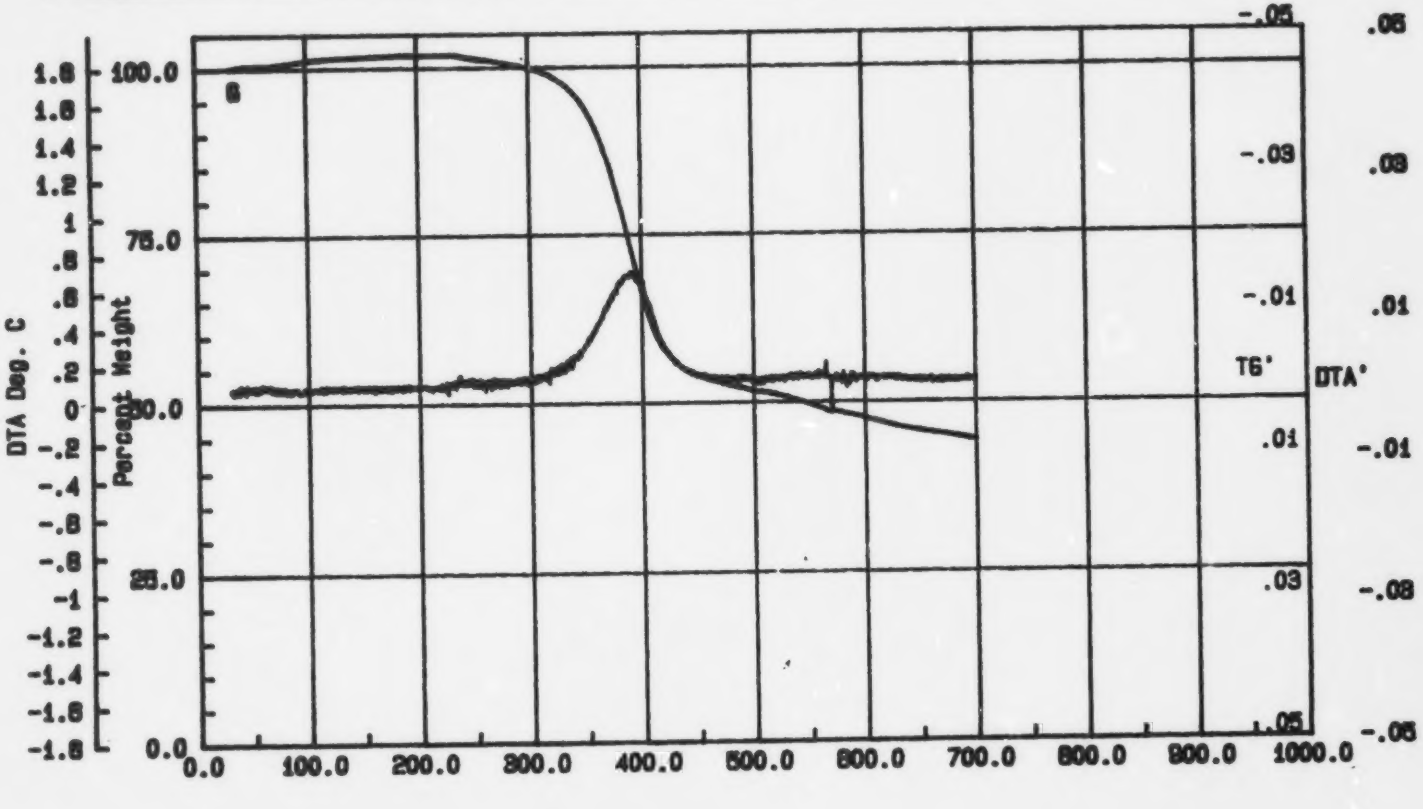

TEMPERATURE, Deg. C

OPERATOR:	R.SAETRE	NETZSCH STA 429/409		ATM.	NITROGEN	
DATE:	04/10/87	REFERENCE :	SAND	FLOW =	70 cc/min	
RUN No.	4	CRUCIBLE :	AL2O3	HEAT RATE =	.1 C/min	
TG Setting	50mg	FILE NAME :	ASPH4	SAMPLE WT.=	10.4 mg	
DTA Setting	0.1mV	MATERIAL	ASPH	REF WEIGHT	0 mg	

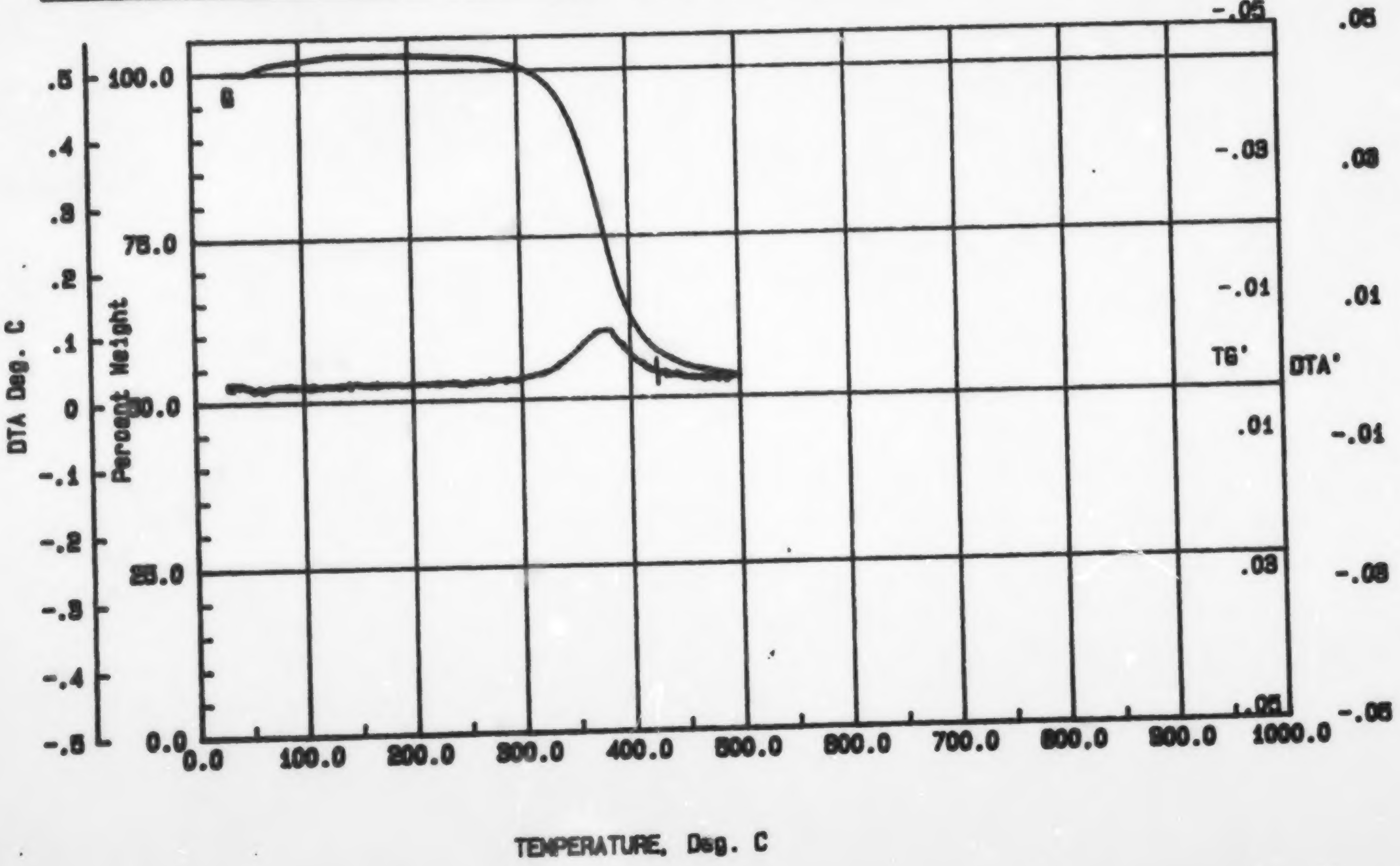

OPERATOR:	R.SAETRE	NETZSCH STA 429/409		ATM.	NITROGEN
DATE:	05/18/88	REFERENCE :	AL203	FLOW =	70 cc/min
RUN No.	1	CRUCIBLE :	AL203	HEAT RATE =	5 C/min
TG Setting	50mg	FILE NAME :	OTFF1	SAMPLE WT.=	31.5 mg
DTA Setting	0.1mV	MATERIAL	OXTFOIL	REF WEIGHT	0 mg

Report #00427
Page A-52

(Figure 27)

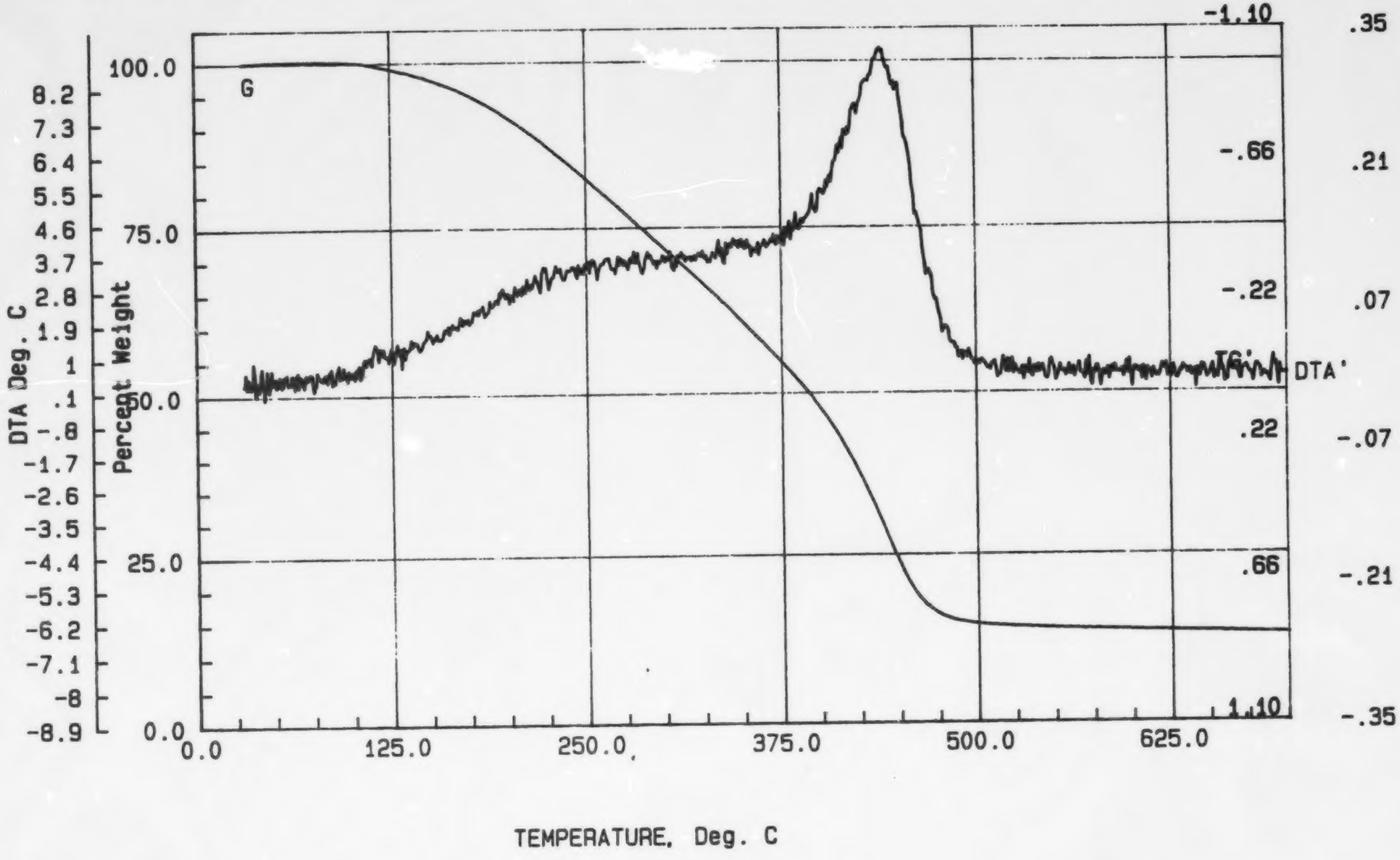

OPERATOR: R.SAETRE
DATE: 05/20/88
RUN No. 2
TG Setting 50mg
DTA Setting 0.1mV

NETZSCH STA 429/409
REFERENCE : AL203
CRUCIBLE : AL203
FILE NAME : TFF1
MATERIAL TFOIL

ATM. NITROGEN
FLOW = 70 cc/min
HEAT RATE = 5 C/min
SAMPLE WT.= 28.9 mg
REF WEIGHT 0 mg

Report #00427
Page A-53

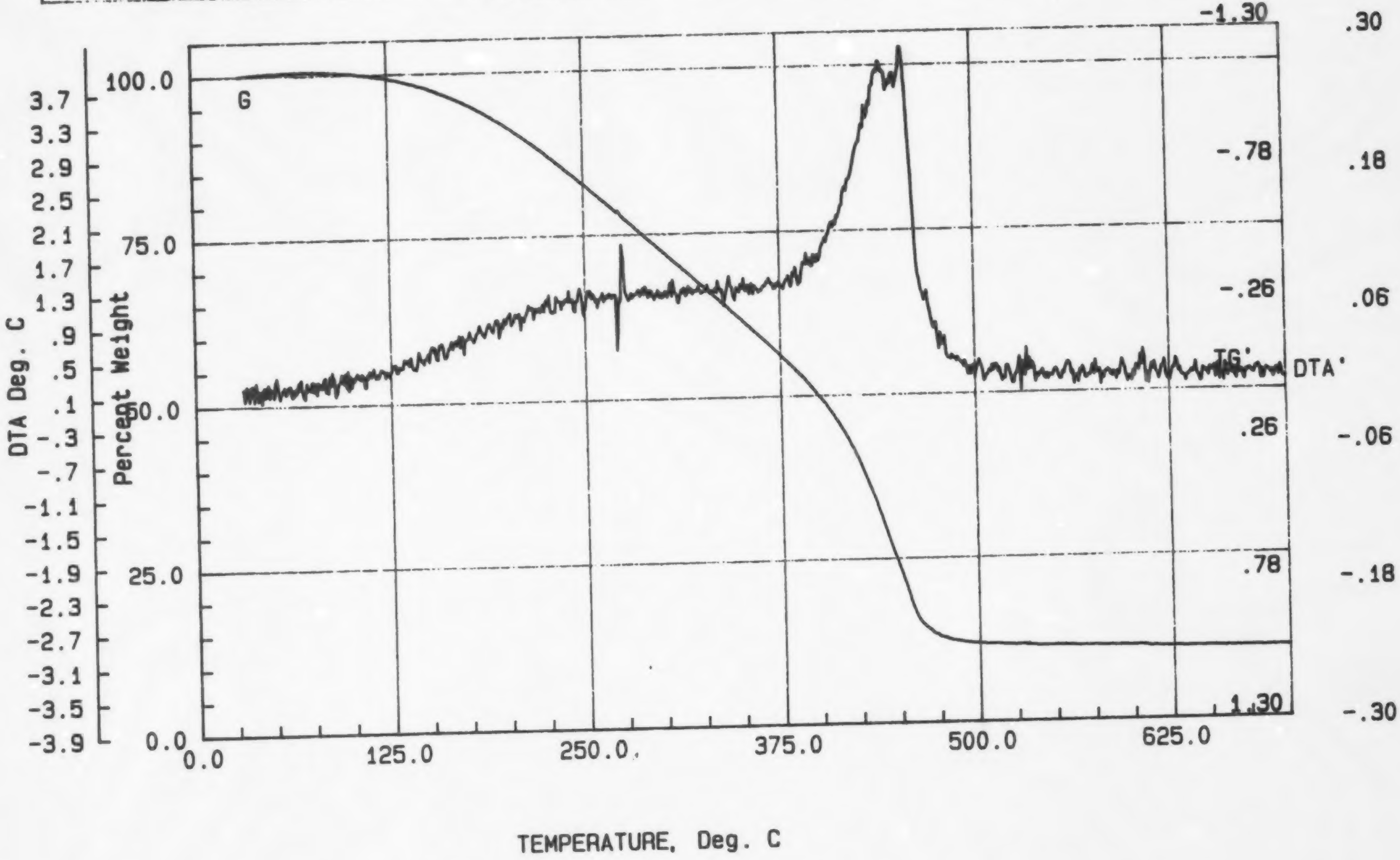

OPERATOR: R.SAETRE DATE: 05/24/88 RUN No. 4 TG Setting 50mg DTA Setting 0.1mV	NETZSCH STA 429/409 REFERENCE : AL203 CRUCIBLE : AL203 FILE NAME : TFF2 MATERIAL TFOIL	ATM. AIR FLOW = 70 cc/min HEAT RATE = 5 C/min SAMPLE WT. = 34.2 mg REF WEIGHT 0 mg	Report #00427 Page A-54

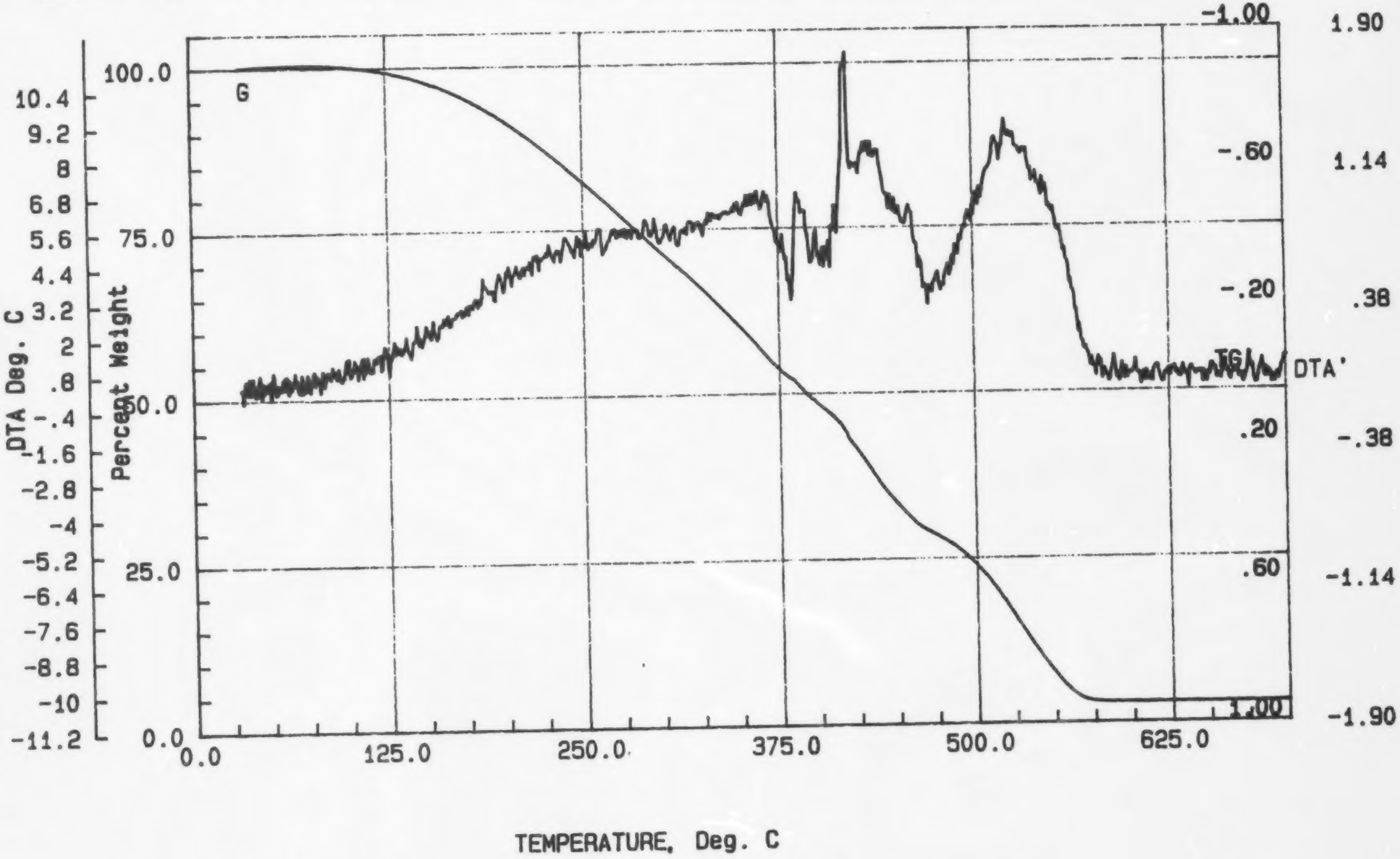

OPERATOR:	R.SAETRE	NETZSCH STA 429/409		ATM.	AIR	Report #00427 Page A-55
DATE:	05/25/88	REFERENCE :	AL203	FLOW =	70 cc/min	
RUN No.	5	CRUCIBLE :	AL203	HEAT RATE =	5 C/min	
TG Setting	50mg	FILE NAME :	OTFF3	SAMPLE WT.=	34.3 mg	
DTA Setting	0.1mV	MATERIAL	OXTFOIL	REF WEIGHT	0 mg	

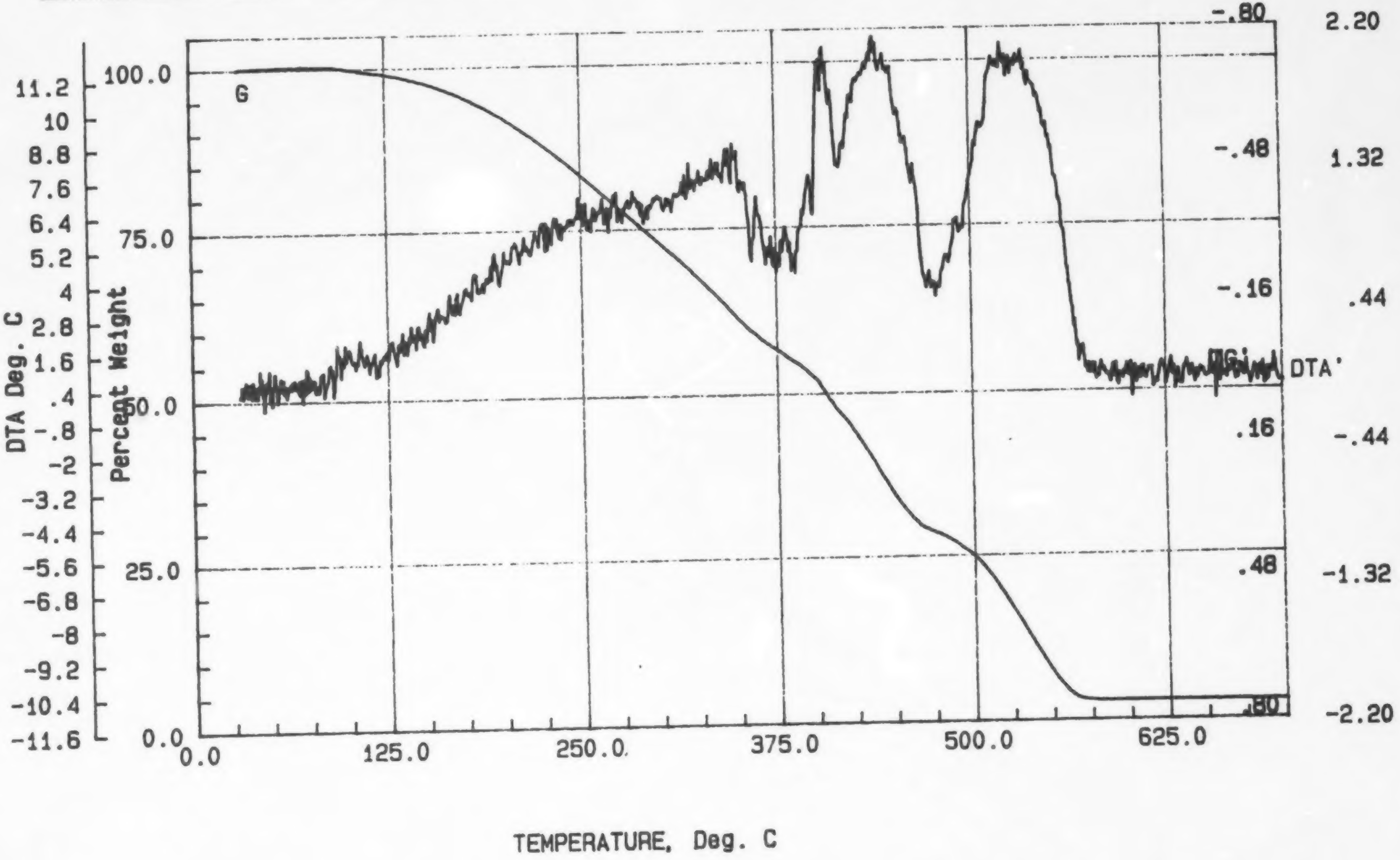

© 1988 NOVA HUSKY RESEARCH CORPORATION

OPERATOR:	R.SAETRE	NETZSCH STA 429/409		ATM.	AIR	Report #00427 Page A-56 (Figure 28)
DATE:	05/23/88	REFERENCE :	AL203	FLOW =	70 cc/min	
RUN No.	3	CRUCIBLE :	AL203	HEAT RATE =	5 C/min	
TG Setting	50mg	FILE NAME :	OTFF2	SAMPLE WT.=	31.6 mg	
DTA Setting	0.1mV	MATERIAL	OXTFOIL	REF WEIGHT	0 mg	

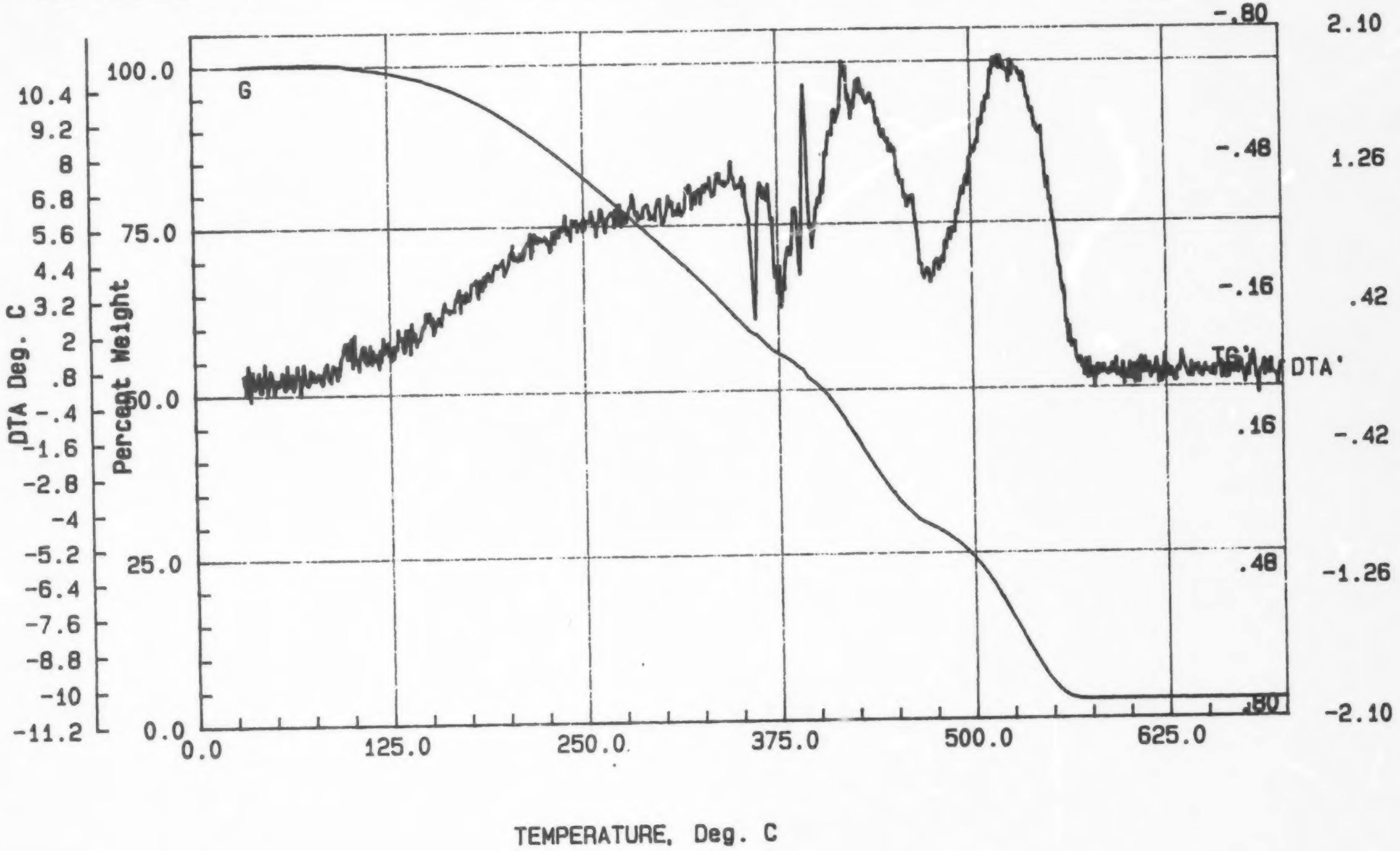

(Figure 29)

OPERATOR: R.SAETRE
DATE: 01/27/89
RUN No. 13
TG Setting 50mg
DTA Setting 0.1mV

NETZSCH STA 429/409
REFERENCE : AL203
CRUCIBLE : AL203
FILE NAME : TFFAN1
MATERIAL TFFOIL

ATM. AIR/N2
FLOW = 70 cc/min
HEAT RATE = 5 C/min
SAMPLE WT.= 35.1 mg
REF WEIGHT 0 mg

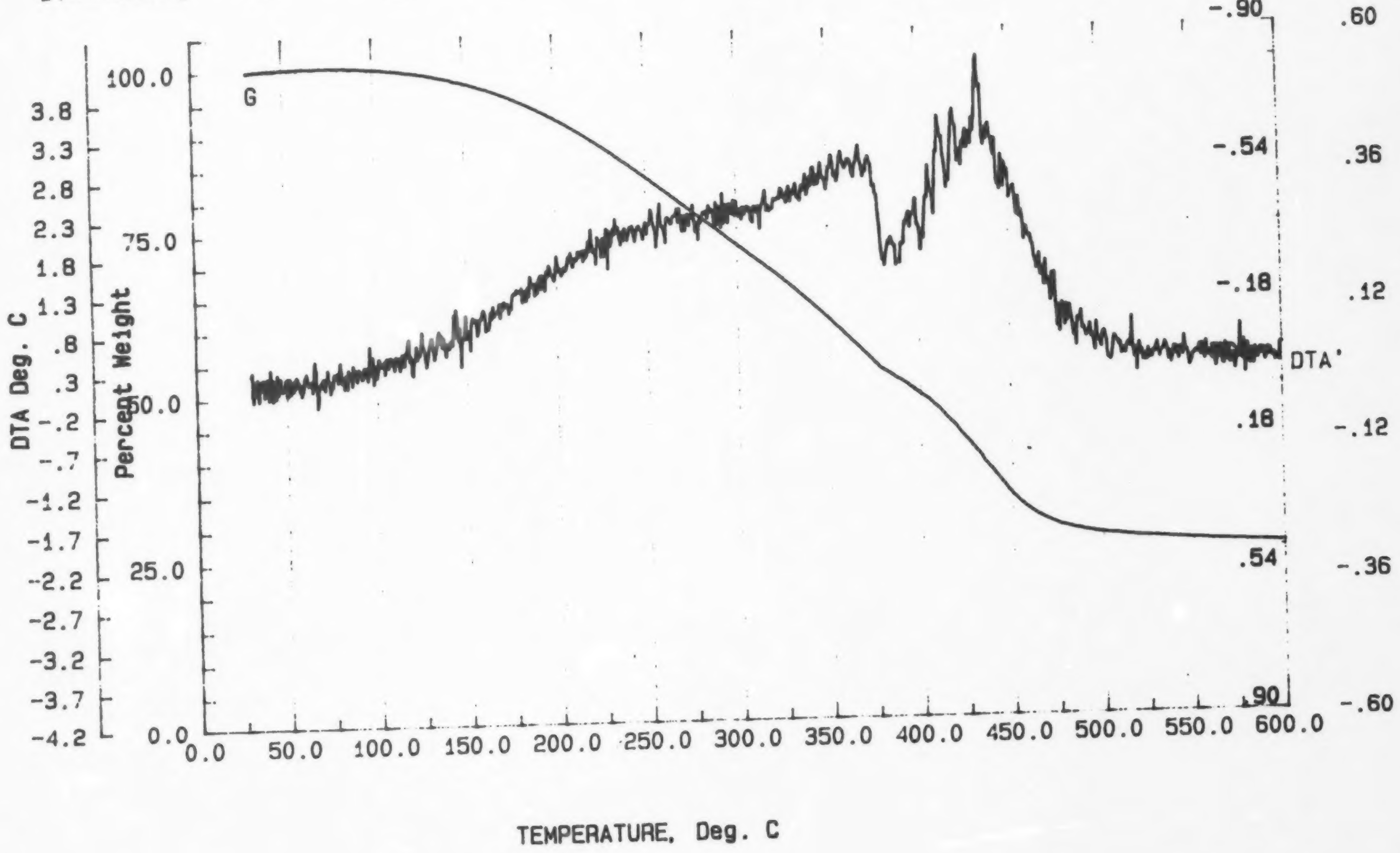

(Figure 30)

OPERATOR: R.SAETRE
DATE: 01/29/89
RUN No. 14
TG Setting 50mg
DTA Setting 0.1mV

NETZSCH STA 429/409
REFERENCE : AL203
CRUCIBLE : AL203
FILE NAME : TFFAN2
MATERIAL TFFOIL

ATM. AIR/N2
FLOW = 70 cc/min
HEAT RATE = 5 C/min
SAMPLE WT.= 36.2 mg
REF WEIGHT 0 mg

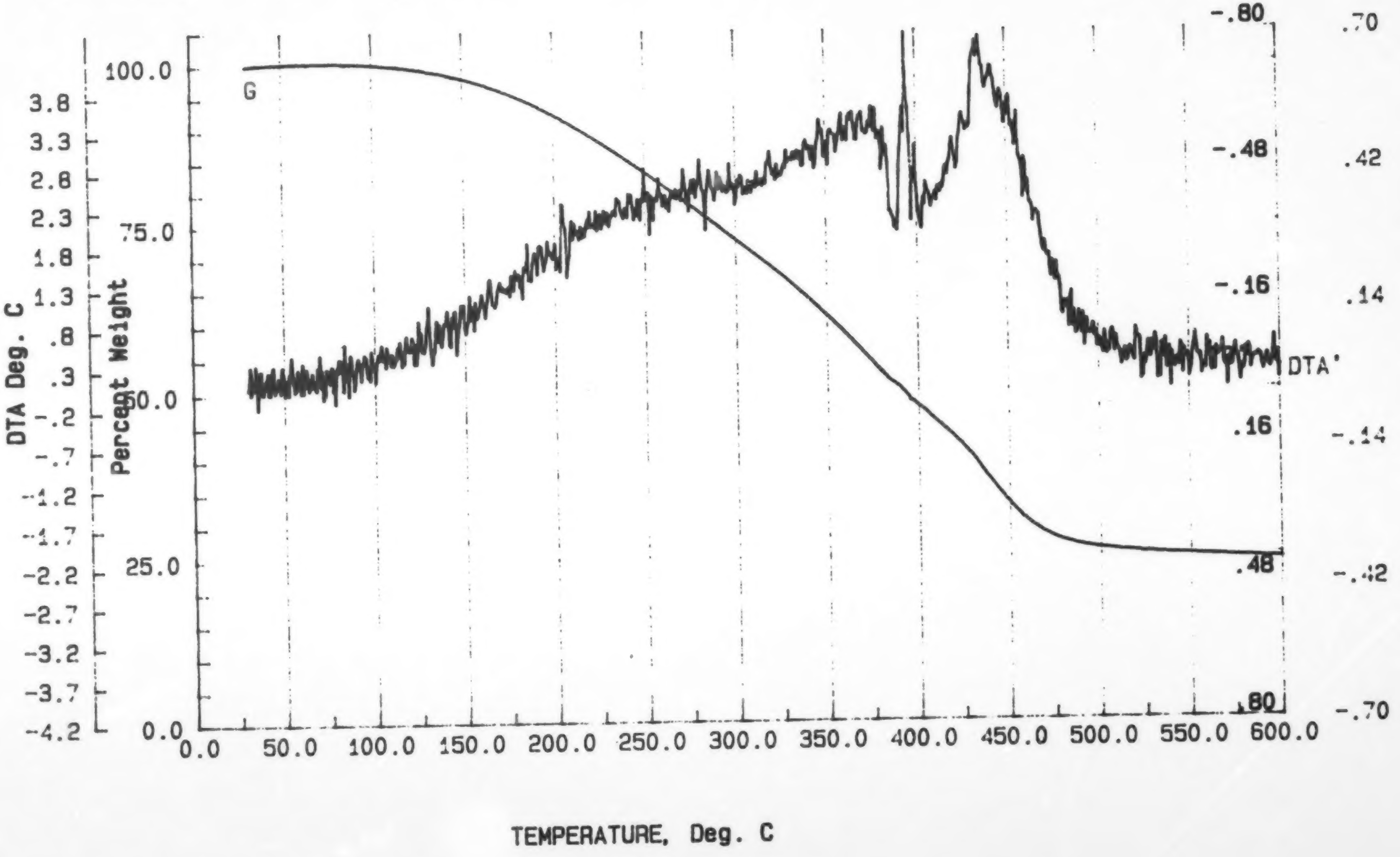

CLASSIFICATION: NHRC, NOVA, HUSKY
and Subsidiaries
REPORT NUMBER: 00419

THERMAL RECOVERY MECHANISMS TASK 9 - SIGNIFICANCE TO NUMERICAL MODELLING

February 1989

Authors

M.R. Islam

Reviewed by

Tom Jack

DEPARTMENT: Applied Science (Resource Recovery)
PROJECT NO: 688-048
PREPARED FOR: Albert George - Energy, Mines & Resources
KEYWORDS: in situ combustion, numerical simulation, kinetic models

This report contains the valuable proprietary and confidential information of the NOVA HUSKY RESEARCH CORPORATION LTD., and may not be used, disclosed or reproduced without permission in writing from NOVA HUSKY RESEARCH CORPORATION LTD.

(C) 1989 NOVA HUSKY RESEARCH CORPORATION LTD.

MICROMEDIA

57 pp

DISTRIBUTION LIST

	Copies
ENERGY, MINES & RESOURCES, Ottawa	
A. George	10
NOVA HUSKY RESEARCH CORPORATION:	
T. Jack	1
B. Erno	1
R. Islam	1
HUSKY OIL OPERATIONS LTD.:	
J. Peggs	1
P. Tsang	1
NHRC Library	2
Husky Library	1
Files	2
	--
TOTAL NUMBER OF COPIES	**20**

© 1988

TABLE OF CONTENTS

Page

EXECUTIVE SUMMARY iii

1.0 INTRODUCTION 1

2.0 AN IDEAL IN SITU COMBUSTION MODEL 1

FIGURE 1 2

FIGURE 2 4

TABLE 1 5

3.0 USEFULNESS OF THE PRESENT STUDY 6

4.0 RECOMMENDATIONS 6

5.0 CONCLUSIONS 8

APPENDIX A

EXECUTIVE SUMMARY

In situ combustion continues to be an important oil recovery process. The applicability of *in situ* combustion to a wide range of reservoirs, and the recent advances, show that this process has unique advantages (as well as disadvantages). This report analyzes existing numerical models developed in recent years. Also reviewed is the state-of-the-art of *in situ* combustion from the point of experimental modeling. The contribution of the research conducted at the NOVA HUSKY RESEARCH CORPORATION is analyzed in the light of providing data for mathematical modeling.

A comparative evaluation of existing *in situ* combustion numerical models helped identify shortcomings of each model and detect missing links. This helped in developing new ideals and drew attention to areas which have been largely ignored in past numerical simulation studies. A complete *in situ* combustion model description is presented and difficulties in implementing such a model are pointed out.

Finally, guidelines are provided for experiments to be conducted in order to provide data for an ideal *in situ* combustion simulator. Such data are required to be able to keep pace with increasingly sophisticated numerical models.

1.0 INTRODUCTION

Thermal recovery processes account for over 80% of oil production by enhanced oil recovery (EOR) methods. *In situ* combustion constitutes a part of thermal recovery processes. *In situ* combustion can be dry or wet. In most cases forward combustion is employed; however, reverse combustion is also of interest in oil recovery as well as in the underground gasification of coal.

Numerical modeling of thermal methods is much more complex than conventional black oil or compositional (isothermal) simulation. The complexity in modeling thermal processes is at first because temperature becomes an additional variable. Moreover, temperature influences many rock and fluid properties, such as viscosity, density, K-values, permeability, porosity, relative permeability, capillary pressures, wettability, etc. In addition, changes in phenomena, such as silica dissolution and precipitation, clay swelling, emulsion formation and flow regime may become significant as a result of thermal changes. Besides, for *in situ* combustion problems, severe changes may occur in chemical kinetics and invoke additional phenomena which are extremely difficult to model rigorously. Only recently have some of these phenomena begun to be incorporated in numerical simulators. Figure 1 shows a schematic of the main mechanisms encompassed by *in situ* combustion. It can be seen in this figure that *in situ* combustion includes most other EOR processes.

Appendix A provides detailed background of numerical simulators as well as of kinetic models developed in the last few decades. One limitation of the available simulators is the incomplete mathematical description of the process mechanisms, often due to the fact that the mechanisms are not completely understood. An effort has been made in the present study to isolate various problems and propose an ideal in-situ combustion model. This model is idealistic based on knowledge available to date.

2.0 AN IDEAL IN-SITU COMBUSTION MODEL

In situ combustion involves the initiation and propagation of an oxidation zone in the formation as a result of air and/or oxygen injection. Water is often injected along with air to improve thermal efficiency by heat transport. The high temperature generated by combustion creates a 'piston like' front which displaces and consumes fluids ahead of it. The formation water as well as any injected water is evaporated, and the steam thus formed passes through the reservoir, and condenses in the cold formation ahead, thus providing a **steam drive**.

FIGURE 1: Process· Mechanisms Involved in In Situ Combustion

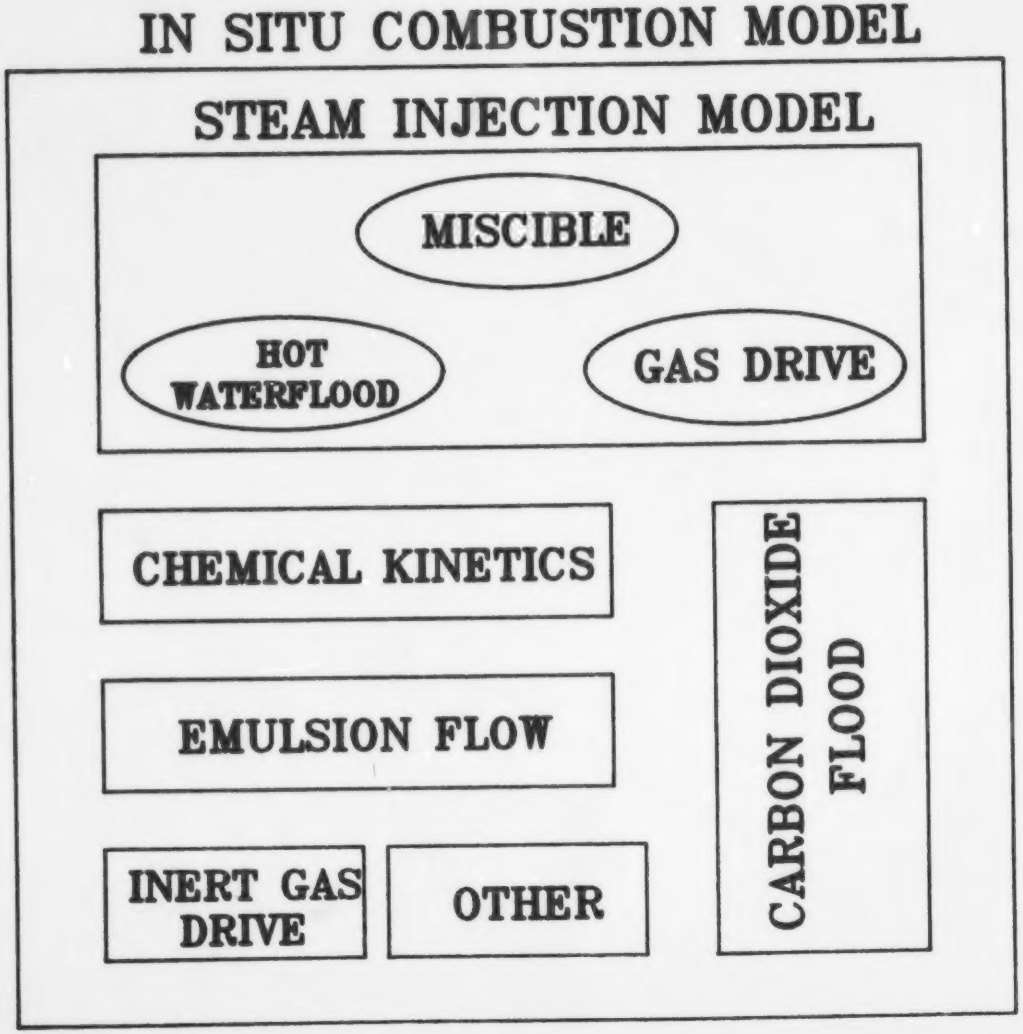
IN SITU COMBUSTION MODEL
STEAM INJECTION MODEL
MISCIBLE
HOT WATERFLOOD
GAS DRIVE
CHEMICAL KINETICS
EMULSION FLOW
INERT GAS DRIVE
OTHER
CARBON DIOXIDE FLOOD

The combustion gases produce a **gas drive/immiscible carbon dioxide drive** effect in the reservoir. This picture could be slightly different for very high reservoir pressure for which miscible displacement may take place. The oil immediately ahead of the combustion zone is subjected to very high temperatures, leading to the deposition of heavy fractions, which serve as the 'fuel' for supporting combustion, and distillation of light fractions, which may provide a miscible drive in the cooler portions of the reservoir. The mechanistic picture is further complicated by the channeling of oxygen past the combustion zone, which may occur for a variety of reasons, causing the low temperature oxidation of oil. Gravity overlay of the combustion zone, and separation of the air and water are other important effects to consider. All these mechanisms call for a very complicated chemical picture which is depicted in Figure 2. This figure indicates that the number of reactions needed to represent an *in situ* combustion process is very large. The primary reactions are: a high temperature oxidation (HTO) reaction, a low temperature oxidation (LTO) reaction, and a cracking reaction to represent fuel deposition. However, a rigorous treatment should include reaction kinetic adjustment for each component. Besides, reactions involving the products of LTO with the in-place crude oil, leading to the precipitation of 'sludge like' solids may be important especially due to the fact that they may plug up the production wells. Similarly, the rock could neutralize a certain portion of the acid formed. The catalytic action of some of the reservoir materials may be incorporated. Consideration of all these phenomena will increase the number of reactions involved dramatically.

One of the most difficult aspects of developing an ideal mathematical model for in-situ combustion is the problem related to obtaining proper data. As the mathematical model becomes more sophisticated the physical input data become more difficult to obtain. This can be seen in Table 1 in which major numerical simulators are listed historically along with their required data. Even though it is fairly easy to increase the number of reactions in a numerical simulator with the advent of fast and large computers, the major constraints appear to be the availability of input data. Reaction parameters are extremely difficult to obtain even for simple two pseudo-component systems. The mechanisms involved in emulsification, rock wettability alteration, catalytic effects of various rock materials are yet to be understood and useful physical parameters will be available only after a considerable research effort in this direction.

FIGURE 2: Chemical Reactions and Processes Involved in a Combustion Front

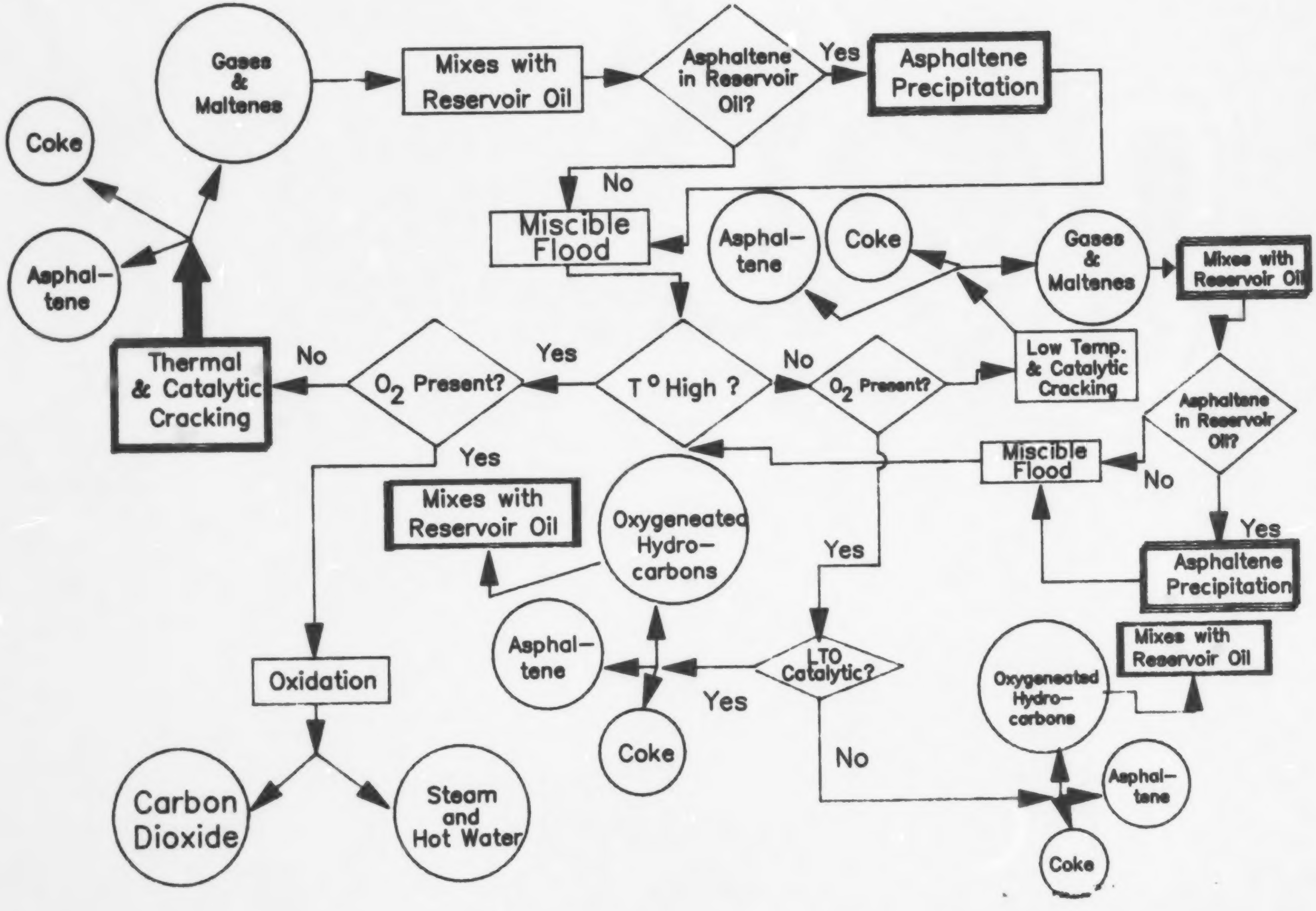
Gases & Maltenes
Mixes with Reservoir Oil
Asphaltene in Reservoir Oil?
Yes
Asphaltene Precipitation
Coke
Asphal-tene
No
Miscible Flood
Asphal-tene
Coke
Gases & Maltenes
Mixes with Reservoir Oil
Thermal & Catalytic Cracking
No
O_2 Present?
Yes
T ° High ?
No
O_2 Present?
Low Temp. & Catalytic Cracking
Asphaltene in Reservoir Oil?
Yes
Miscible Flood
No
Mixes with Reservoir Oil
Oxygeneated Hydro-carbons
Yes
Yes
Asphaltene Precipitation
Asphal-tene
LTO Catalytic?
Mixes with Reservoir Oil
Oxidation
Yes
Coke
No
Oxygeneated Hydro-carbons
Asphal-tene
Carbon Dioxide
Steam and Hot Water
Coke

TABLE I

Authors	Phases	Oil Component	Dimensions	Chemical Reactions	Thermal Parameters Used
Gottfried (1965)	Gas, Water, Oil	1	1	1	Arrhenius eqn.
Smith & Farouq Ali (1971)	Gas	N.A.	2	1	Total burn
Adler (1975)	Gas, Water, Oil	2	1	8	Arrhenius eqn. Reaction terms for each reaction
Farouq Ali (1977)	Gas, Water, Oil	1	2	1	Modified Arrhenius equation
Crookston et al. (1979)	Gas, Water, Oil, Coke	2	2	4	Reaction rates for coke oxidation light oil oxidation heavy oil oxidation heavy oil cracking Heat of reaction for light oil oxidation heavy oil oxidation coke oxidation coke formation
Grabowski et al. (1979) Coats (1980)	Gas, Water, Oil, Coke	Variable	3	Variable (LTO included)	Parameters used same as above due to lack of data
Youngeren (1980)	Gas, Water, Oil	3	3	3	Reaction rates for light oil oxidation heavy oil oxidation heavy oil cracking Heat of reaction for light oil oxidation heavy oil oxidation coke oxidation coke formation
Hwang et al. (1982)	same as Youngeren (1980)	with special front tracking technique			

3.0 USEFULNESS OF THE PRESENT STUDY

The present work was devoted to understanding mechanisms of various reactions involved in an in-situ combustion process. Initial effort was to obtain proper fluid characterization. In common numerical simulation, the oil phase composition is considered to be homogeneous throughout the reservoir. Even though there have been several instances of oil viscosity variability with depth, very little has been done to modify a numerical simulation approach. The work reported in Task 2 of the present study determined viscosity variation as a function of depth in a heavy oil reservoir in Alberta. This constitutes a valuable initial condition for reservoir simulation studies.

Figure 2 shows various reactions which take place in *in situ* combustion. One of the most important phenomena which was ignored in previous numerical studies is the reaction of precipitated asphaltene with in-situ oil. Mobility of oil is decreased drastically with addition of asphaltene beyond some threshold value (shown in previous literature). This aspect was investigated in this study. An explanation in terms of asphaltene agglomeration helped understanding of the physical mechanisms involved and the viscosity data can be used effectively to determine compositional dependence of oil viscosity.

The areas of contribution of the present study are highlighted in bold lines in Figure 2 and include thermal cracking data as well as asphaltene effects. An additional task was conducted to obtain steam distillation data in a sand-packed core. They constitute valuable information as outlined in Figure 1. These data can be used by a numerical simulator with two pseudocomponents and steam distillation options.

4.0 RECOMMENDATIONS

Appendix A details the shortcomings of existing numerical simulators. In order to overcome some of the shortcomings, a simulator capable of using a front-tracking technique for the combustion front is required. Also required are capability of modeling channelling, dispersion, diffusion, non-equilibrium in carbon dioxide flooding, and emulsion generation and propagation. Also, the problem of multiple solutions to thermal problems needs to be addressed.

While problems in mathematical modeling appear to be plenty, problems related to experimental modeling are also numerous. Only the phenomenon of high temperature oxidation appears to be understood. In order to generate significant data in thermal cracking future experiments should consider dividing the oil phase into several components. Initially, it could be divided into maltene and asphaltene, but a more rigorous approach should involve further division into groups of similar boiling point or solubility. Thermal cracking data should then be obtained under various temperatures. Thermal cracking data thus obtained could be used to develop better kinetic models.

The area of low-temperature oxidation (LTO) should be thoroughly investigated. Initial investigation should involve positive identification of LTO products. Virgin heavy oil could be used for these experiments. After this initial stage, convenient ways should be found to classify various components. These groups could, therefore, be used to obtain more detailed LTO data. Mathematical models generated from these experiments would be very valuable for numerical simulation.

As indicated in Appendix A, catalytic effects may be important in all the reactions taking place in contact with the reservoir matrix. Initial experiments should identify catalytic minerals present in the reservoir matrix and investigate the effect of these minerals on various reaction parameters obtained in previous experiments in the absence of such catalytic material.

Scaled model studies have gained popularity in recent years. Such a model eliminates some of the shortcomings of linear combustion tube experiments and experimental results are supposedly correlatable to those of the field. Scaled model experiments are complementary to numerical models and often used for validation of numerical simulators. These experiments, however, are cumbersome and very expensive to perform.

The existence of multiple solutions in thermal problems, as discussed in Appendix A, should be studied in a controlled laboratory environment. Initial experiments should use only one phase in order to isolate the problem. Once, multiple solutions and hysteresis are positively identified in single phase, research may be extended to multiphase situations.

5.0 CONCLUSIONS

A state-of-the-art review of *in situ* combustion modeling is undertaken. On the basis of this review, an ideal *in situ* combustion simulator is proposed. Difficulties in implementing such a model are pointed out. The main difficulty in using such a simulator is identified as the lack of experimental data. With current knowledge, a guideline is provided for systematic experimental and numerical modeling of *in situ* combustion.

APPENDIX A

REVIEW OF EXISTING IN SITU COMBUSTION SIMULATORS

1.0 REVIEW OF IN SITU COMBUSTION PROCESS

1.1 Introduction

The oil recovery process known as *in situ* combustion or fireflooding has been a source of interest, effort and considerable frustration for at least 30 years. The concept of enhancing the recovery of oil from a reservoir by burning a portion of the oil is technically and economically attractive, particularly since the portion burned is likely to be the least valuable. This attractiveness has stimulated extensive laboratory study and led to at least forty field projects (Chu and Crawford, 1983). Unfortunately, in practice, *in-situ* combustion has many complications, and, in contrast to steam injection processes, few *in-situ* combustion field projects have achieved commercial status or economic success. Various reasons have been advanced for the failure of *in-situ* combustion to achieve greater success as a recovery technique. Operational problems, and the frustration and expense these have caused, are perhaps the most well-known cause of failure of *in-situ* combustion projects. A more subtle reason arises from the selection of reservoirs for *in-situ* combustion application. Screening criteria have been advanced for *in-situ* combustion, but the limited number and varied nature of the successful projects, together with the growing recognition of the complexity of the *in-situ* combustion process, raises questions about the validity of the criteria. More specifically, *in-situ* combustion has often been selected after all other techniques have been considered and eliminated. Perhaps the greatest hindrance to improving *in-situ* combustion has been the lack of a sufficiently reliable numerical model for predicting field performance. This lack is a consequence of the complexity of the *in-situ* combustion process. Although there has been extensive laboratory study of most aspects of *in-situ* combustion, there remain several areas which are poorly understood. It is the objective of this paper to review what has been done previously, and to identify those areas where understanding and modeling could be improved.

1.2 Types of In-Situ Combustion

Several different operating strategies have been used into initiate and maintain combustion in a reservoir. In all cases, an oxygen containing gas (most commonly air) is injected into the reservoir to achieve combustion. Forward combustion, in which the combustion front moves from the injection well to one or more producing wells, has been the most commonly used. In an alternate approach, reverse combustion, the reservoir is ignited at the producing wells and burns towards the injection wells. In both forward and reverse combustion, the process is termed "dry" if no water is injected with the gas, or "wet" if small amounts of water are injected. Addition of water is considered beneficial, because it enhances the production of steam. Steam moves heat forward much more effectively than combustion gases alone, and also improves displacement efficiency in several ways. A further variation is known as "super-wet" combustion. This is achieved by increasing the ratio of water to gas injected, such that significant quenching of the combustion occurs. Under super-wet conditions, distinct differences are observed in the composition of produced oil and gases, and in recovery performance (Moore *et al.*, 1988). Other variations in strategy involve varying the pressure in the reservoir, either through changes to the rate of gas injection, selective use of back-pressure on producing wells, or both. These strategies are an attempt to reduce the competition between oil and gas in the producing wells.

1.3 Mechanisms of In-Situ Combustion

In the forward combustion process, ignition takes place near the injection well and the burning front moves towards the producing wells. Once the process has proceeded for sometime, a number of zones are established in the reservoir between the injector and producers, which are distinguished as follows. The burnt zone is the region of the reservoir through which the burning front has already passed. If the combustion has been efficient, the burnt zone will contain no residual oil, but will be saturated with the injected gas (air or oxygen) and water. The combustion zone is a narrow region where high temperature oxidation takes place, to produce primarily water and carbon dioxide, and liberate heat. The fuel is predominantly a coke formed by thermal decomposition and polymerization of the non-volatile portion of the reservoir oil. The coke is formed in the thermal cracking zone just downstream of the combustion front. In addition to coke, considerable amounts of volatile hydrocarbons are produced by thermal cracking in this zone. These volatile products are carried with the combustion gas and steam downstream, to eventually condense or dissolve in oil in a cooler zone. Adjacent to the cracking zone is the steam zone, in which condensing steam displaces oil, and steam distillation and evaporation further lower oil saturation. Temperature of this zone is controlled by the fluid pressure, as determined by saturated steam. Reactions between oil and water (aquathermolysis), reservoir minerals and water, and some oil components will also be most significant in this zone. This zone will be extended if additional water is injected, or if water can flow into the reservoir from adjacent formations. Depending on the efficiency of the steam displacement processes, a zone of enhanced oil saturation will be formed ahead of the condensing steam and hot water. The oil in this zone may have increased mobility as a result of increased temperature and also because of dissolution of lighter components into it. Downstream of the oil zone is a region of reservoir which has seen minimum effects of the combustion process, other than a possible increase in gas saturation or dissolved gas.

1.4 Coke Formation During Thermal Cracking

It is widely believed that coke is formed as a result of reactions between the cracked products, not directly from the feed stock itself. For example, coke formation during thermal cracking of bitumen results from condensation and dehydrogenation of the large unsaturated systems primarily consisting of the asphaltenes and the heavy aromatic oil fractions. According to Sukhanov and Tilichev (1928), coke formation during thermal cracking of paraffins is preceded by complete decomposition of the paraffins. Similarly, Medorskii (1967) noted that there is no coke formation during thermal cracking of polyolefins when the reaction products are removed quickly from the reaction zone. In fact a new generation of coke free, high temperature, cracking reactors, such as the Advanced Cracking Reactor (ACR), which Hosoi and Keister (1975) have been developed in recent years, are based on the concept of a short reaction time (few milliseconds), and rapid withdrawal of the reactants from the reaction chamber followed by rapid quenching.

The above discussion on coke formation has important implications with regards to *in situ* combustion. In the *in situ* combustion situation, the light components formed due to evaporation, distillation, visbreaking etc., may be removed from the combustion zone along with the flowing combustion gases. Therefore, coke formation under such circumstances might be less than what one would normally obtain in closed laboratory reactors. Therefore, a numerical simulator must be able to predict the formation as well as movement of the lighter fractions away from the combustion front in order to be able to predict the coke formation quantitatively.

1.5 Kinetic Modeling of Thermal Cracking

Thermal cracking is defined as the change in composition of an oil when it is heated in the absence of oxygen (Moore *et al.*, 1988). When cracking is carried out in the presence of steam or catalysts, the respective processes are known as steam cracking and catalytic cracking. Thermal cracking has been extensively used in the petroleum refining industry for converting naphtha into light olefins and also for viscosity reduction of heavy oils. Such earlier thermal cracking kinetic models were derived from petroleum refining experience.

The reactions involved in thermal cracking are complex and usually involve a number of reactions even for a simple compound. Thermal cracking usually is initiated by a carbon-carbon bond scissions at a location from the carbon atom with an unpaired electron. This is then followed by a hydrogen abstraction reaction. The free radicals generated as a result of carbon-carbon bond scission and hydrogen abstraction reactions may recombine to form heavier molecules eventually leading to the formation of "coke". The relative rates of hydrogen abstraction can be predicted from the theory of Rice and co-workers (Rice, 1933; Rice and Teller, 1939; Kossiakoff and Rice, 1943) for paraffinic hydrocarbons. The relative rates of thermal cracking of straight and branched chain paraffins can also be predicted from this theory, if the hydrogen abstraction rate is slow (Gates *et al.*, 1979). Product distribution of cracking products arising from thermal cracking of n-nonane (Kunzru *et. al* ., 1972) and n-octane, iso-octane and cyclohexane (Illes *et al.* 1973) could be predicted within 20% of the experimental results by using the free radical theory of Kossiakoff and Rice (1943). Unfortunately, petroleum is composed of of numerous individual compounds, and therefore, petroleum cracking reactions can not be precisely described. As such either an overall reaction scheme based on the feed or a pseudo component approach based on a number of pseudo components has to be employed in describing the reactions and deriving appropriate rate parameters.

Although numerous studies have been reported on the cracking of light hydrocarbons, only a few studies have been reported on the cracking of heavier hydrocarbons. Miller (1963) has studied the cracking of α-olefins in the gaseous phase and was able to describe the reaction mechanism by a molecular type scission. Giraud-horvalleur and Blouri (1977) found the gas phase cracking of 1 and 2-tetradecene to take place via the molecular as well as the radical route. Blouri *et al.* (1984) carried out liquid phase cracking of high molecular weight hydrocarbons including C_{21} - C_{27} paraffins under relatively mild temperature conditions (350 - 440°C) and found cracking to occur according to the molecular mechanism. However, the kinetic parameters were found to be the same as those of a radical type cracking. Overall hydrocarbon thermal cracking reaction has traditionally been modeled by a first order, Arrhenius type rate expression (Rosen, 1941; Fabuss *et al.* 1964). First order kinetics have also been applied to the pyrolysis of gas oil (Geniesse and Reuter, 1932) and crude oils (McNabb *et al.*, 1952; Crawford and Cunningham, 1956; Madwick *et al.*, 1959; Henderson and Weber, 1965). In most of these studies oil was considered to be a single component. Only Henderson and Weber (1965) divided the crude into two pseudo components.

Moore and co-workers at the University of Calgary have undertaken extensive research work on the kinetics of *in situ* combustion and have made significant contributions in this field. They were the first ones (Hayashitani *et al.* 1979) to derive kinetic data and formulate kinetic models by dividing the oil into five or six pseudo-components, namely, coke, asphaltenes, heavy oils, distillable oils and gas. They derived the appropriate rate parameters such as the activation energy and the frequency factors by matching the reaction product concentrations. Their work was based on cracking of Athabasca bitumen in the absence of any core material or water. They observed an initial delay in coke formation during the experiments carried out at 360°C and 397°C which could not be explained and the models proposed did not take this into account. These temperature levels are considered to be in the lower range of typical cracking temperatures used in petroleum upgrading. Recent experimental work on hydrocracking of individual components derived from heavy oils (Chornet, 1988) suggest that at these temperature levels, conversion of asphaltenes to maltenes is favored over their conversion to coke.

All the reactions considered in the models discussed above were assumed to follow first order kinetics. However, the overall reaction order in a multicomponent feed system such as the crude oil, is known to be greater than unity because of compositional changes with temperature (Weekman, 1968; Kemp and Wojciechowski, 1974). Lin *et al.* (1984) introduced a correction factor to take the compositional effect into account and proposed two kinetic models with two and three pseudo-components respectively. They also allowed coke to be formed from intermediate compounds as well. This factor which had been recognized for quite some time (Appelby *et al.*, 1962; Nace *et al.* 1971) and was supported by recent experimental work at the University of Sherbrooke, Quebec, Canada (Chornet, 1988) where the polyaromatic and polar fractions of maltenes were also found to form coke like the asphaltenes, although, their reactivity was somewhat lower than that of the asphaltenes. Therefore, it is very likely that the delay time in coke formation as observed by Hayashitani *et al*. (1979), was caused by the conversion of a large fraction of asphaltenes into maltenes.

Millour *et al*. (1985) extended the work of Hayashitani *et al*. (1979) to bitumens containing core material and water (Millour *et al*. 1985) in which the authors accounted for the initial time delay observed in coke production by introducing an "incubation time" during which coke formation was considered to be zero. They have correlated the coke "incubation time" as a function of temperature in the form of an Arrhenius type equation. The higher the temperature the lower the "incubation time" and vice versa. This approach, quite understandably gave a better match of the coke concentration data. They have included this "incubation time" in the calculation of the maltene concentration. For times less than the "incubation time", they assumed the maltenes to increase linearly versus time from the original bitumen concentration to their maximum value which is reached at the "incubation time". They justified the rather simplistic linear assumption due to lack of experimental data and the difficulty in obtaining experimental data as the time required for heating the reactor becomes significant as compared to the actual reaction time. However, there are reactors which can be heated up to the desired reaction temperature in less than 2 minutes time (Chakma *et al*. 1988) which might be used to obtain reliable data in this region.

All the above stated models were based on batch reactor data. Abu-Khamsin *et al*. (1988) recently reported experiments conducted cracking experiments in a packed bed of sand/oil mixture heated under nitrogen flow conditions in an effort to simulate actual reservoir conditions. The difficulty with such flow system is that both axial and radial temperature gradients exist in the packed bed and therefore the kinetic data obtained may not truly represent the temperature dependence of the kinetic parameters. In fact, the data obtained in such experiments have the temperature and hydrodynamics effect lumped in them, therefore, the kinetic parameters derived can not be applied if the hydrodynamic conditions are not similar. Furthermore, the authors did not analyze the reactants issuing out of the reaction chamber directly, and subjected them to further oxidation in a secondary chamber and analyzed the flue gases issuing out of the oxidizer for the convenience of analysis. This approach is highly questionable for the evaluation of reaction kinetics of a multicomponent system. It would have been desirable to analyze the reactor effluent directly, as is done in most other situations, and then extract kinetic data from the effluent concentration changes.

1.6 Coke Combustion

Fuel combustion in *in situ* combustion, where oxygen and fuel must react under flow conditions in a porous media, is essentially a heterogeneous flow reaction involving gas, liquid and solid phases. The fuel to be burnt would normally be solid, i.e. coke, if the combustion temperature is sufficiently high (above 400°C). However, there might still be some heavier liquid fuel available for combustion. Furthermore, some of the fuel may have been deposited inside the pores of the reservoir rock. Therefore, a series of transport phenomena comes into play before the combustion reaction can proceed. The oxygen first must be transferred from the bulk gas phase to the fuel interface, possibly through the rock pores and then diffuse into the fuel. The reactions can then proceed. The reaction products desorb and finally diffuse into the bulk gas stream. The overall process will be controlled by the slowest step. In general chemical reactions proceed at a much faster rate than the diffusional transport processes. The issue of whether the combustion reaction is kinetically limited or diffusion controlled is rather controversial. However, it is generally accepted that the overall process is chemical reaction controlled (Bousaid and Ramey, 1968; Burger and Sahuquet, 1972; Fassihi *et al.*, 1984, Hughes *et al.*, 1987) and the combustion rate, Rc, of crude oil in a porous medium can be described by the following rate equation:

$$Rc = -\frac{dC}{dt} = k\,C^m\,P^n_{O_2}$$

where

C = instantaneous concentration of fuel,
k = rate constant
P_{O_2} = oxygen partial pressure
m,n = reaction orders.

Dabbous *et al.* (1974) found that the combustion reaction was diffusion controlled. Lin *et al.* (1987) in their work with medium and heavy crudes found oxygen concentration to drop virtually to zero level at the combustion front and therefore concluded oxygen diffusion to be limiting step. Greaves *et al.* (1988) in their combustion tube experiments found oxygen diffusion to be an important controlling parameter for wet combustion. The laboratory tests for *in situ* combustion mostly use loosely packed cores with high porosity and initial gas saturation (Ito and Chow, 1988). Furthermore, laboratory experiments do not allow for free unreacted oxygen to pass through the combustion front. In many field cases oxygen breakthrough was found to occur at the time when as much as 90% of original oil in place remained in the reservoir indicating oxygen channeling (Ito and Chow, 1988). Farouq Ali (1972) has pointed out that channeling is the cause of failure for several *in situ* combustion projects. Therefore, in laboratory experiments conducted under such ideal situations the interfacial mass transfer rate for oxygen transfer may be quite high and mass transfer limitations may not be evident from such experimental work.

Most of the numerical simulators (Crookston *et al.*, 1979; Youngren, 1980; Hwang *et al.*, 1982; Coats, 1983) fail to take the channeling effect and the possibility of mass transfer limitation effects into account. Only very recently Ito and Chow (1988) have attempted to account for the channeling effects by introducing a molecular diffusivity based formula in a numerical simulator.

Contrary to the widely held view that the overall process is reaction rate limited, we believe that diffusion plays important role in field situations. Therefore, we strongly recommend further experimental work in this area.

Greaves *et al.* (1988) have recently published experimental work on the kinetics of *in situ* combustion of Maya crude of 22.8° API gravity. They found the reaction order with respect to carbon concentration to be unity. The reaction order with respect to oxygen partial pressure was found to be unity for dry combustion and less than 0.5 for wet combustion.

1.7 Low Temperature Oxidation

When channelling of oxygen occurs in *in situ* combustion, oxygen can bypass the combustion front and react with crude oil in the formation ahead of the combustion front at temperature levels relatively lower than the combustion temperatures, in the vicinity of 200°C, low temperature oxidation (LTO) takes place. According to Moore *et al.* (1986), in superwet combustion thermal cracking reactions do not occur to any appreciable extent and coke deposition is mainly dominated by the low temperature oxidation of the residual oil left by the steam bank.

While carbon oxides and water are the primary reaction products in combustion, LTO produces oxygenated hydrocarbons as its reaction products. These oxygenated compounds are usually more viscous, less volatile and denser than the original crude oils from which they are formed (Severin *et al.*, 1983; Babu and Cormack, 1984). LTO has been found to increase the asphaltene content of crude oils (Moschopedis and Speight, 1975; Meyers *et al.*, 1986; Adegbesan *et al.*, 1987). This leads to higher viscosity of the oxygenated products, thus LTO affecting the performance of *in situ* combustion processes (Burger and Sahuquet, 1972; Dabbous and Fulton, 1974; Adegbesan *et al.*, 1987).

Low temperature oxidation reactions are highly complex and not well understood. However, it is believed that LTO reactions consist of condensation of lower molecular weight components to higher molecular weight products. The resins and the aromatic fractions are preferentially oxidized faster than other components of the oil.

While most of the LTO kinetics models only predict overall rates of oxygen consumption (Dabbous and Fulton, 1974; Fassihi *et al.*, 1984), the model of Adegbesan *et al.* (1987) describes reaction kinetics of pseudo components in the liquid phase as well.

1.8 Effect of Sand Matrix

The nature and composition of the reservoir rock influences *in situ* combustion process by affecting the rate of fuel deposition. Hardy *et al.* (1972) as well as Vossoughi *et al.* (1982) in their laboratory investigations encountered difficulty in sustaining combustion when clean sand packs rather than reservoir rocks were used. They concluded that the fuel deposition in clean sand packs was low due to a number of factors including lower rate of fuel adsorption on to the sand surface. Bardon and Gadelle (1977) examined the effects of the matrix on the oxidation reaction of a French crude oil by using sands of different grain sizes as well as the original matrix. They found the activation energy obtained with the original reservoir matrix to be lower than that of the sand packs in all experiments. They attribute this to the presence of 5% kaolinite in the original reservoir matrix which exerted some catalytic effects on the the combustion reaction. Bousaid and Ramey (1969) also noted the catalytic effect of clays present in reservoir rocks and observed a 10% reduction in the activation energy with the addition of 20% clay to the sand matrix. Fassihi and Brigham (1982) also found the activation energies with the original reservoir rock matrix to be lower than that with sand with crude oils from Jobo (Venezuela) and Lynch Canyon (California) fields. They also found the molar ratio of CO_2/CO in the combustion gases to be lower in the original matrix than in the sand. Phillips *et al.* (1985) thermally cracked bitumen and bitumen derived products with and without sand. They separated the products into six pseudo components following the approach of Hayashitani *et al.* (1979). They found the presence of sand to result in higher coke and gas yields, and also to affect the yield of other pseudo components. The asphaltene yield was found to be higher due to the presence of sand. They proposed two kinetic models and found the activation energy to be lower for the bitumen-sand mixture than for bitumen alone. This led them to conclude that sand was playing a catalytic role in the thermal cracking of bitumen.

Vossoughi *et al.* (1982, 1985) have found the surface area of the sand grain to affect the combustion process as well by using sand grains of different specific surface area. The found that only the experiments with sand grains of higher specific area produced self-sustained combustion fronts.

Lin *et al.* (1984) carried out numerical simulation of dry forward combustion tube experiments in order to study the effects of reaction kinetics on the combustion process. For a 26.5^o API gravity crude oil, they found coke to account for only 21% of the fuel burned and the fuel deposition to be insensitive to the reaction kinetics,when non catalytic reaction parameters were used in the simulation. However, when catalytic reaction parameters were used the fuel deposition was found to depend on the reaction kinetics and stoichiometry and coke accounted for almost 100% of the fuel consumed. The latter approach reflects the conventional wisdom that most of the fuel in *in situ* combustion is burned in the form of coke. For a heavier crude of 13^o API gravity, fuel deposition was always dependent on reaction kinetics and coke accounted for 100% of the fuel consumed regardless of the extent of the catalytic effect. This shows that the catalytic effects of the reservoir rocks must be taken into account in the modelling of *in situ* combustion processes.

Monin and Audibert (1985) studied the effect of reservoir minerals on thermal cracking of different crude oils by carrying out cracking reactions in the presence of different minerals including calcite, kaolinite, montmorillonite, silica and illite. They found that the cracking reactions are affected by the specific area of the minerals as well as the characteristics of the matrix. In a second paper (1987) these same authors conclude that all the minerals tested promote cracking reactions.

The catalytic activity of minerals such as clays, quartz, and feldspars, etc. is due to their acidic nature and depends on the acid site density and strength. The catalytic activity increases with increasing acidity and the activation energy decreases with it (Tanabe, 1970). Considerable experience gained in the catalytic cracking of hydrocarbons suggests that increased catalytic site density and acid strength enhances the coke formation rate (Venuto and Habib, 1979).

Although these catalytic effects have been recognized, to date, no kinetic model incorporating these catalytic effects, exists in the open literature and for that matter we know of no systematic experimental research program to quantify these effects.

2.0 AN IDEAL IN-SITU COMBUSTION SIMULATOR

2.1 Introduction

In-situ combustion continues to be important oil recovery processes. The applicability of *in situ* combustion to a wide range of reservoirs, and the recent advances, show that this process has unique advantages. A good field project usually depends on laboratory experiments as well as numerical simulation studies. Laboratory studies of *in situ* combustion have been hampered by the lack of suitable scaling criteria for the design of experiments. Recently Islam and Farouq Ali (1988) have proposed a complete set of scaling criteria and various scaling approaches, but these experiments are very labour-intensive and costly. Reservoir simulators using numerical models, with the help of the basic data obtained from laboratory experiments, can remedy this problem in scaled model studies and make predictions of field performance under combustion. However, numerical models have problems of their own. Mathematical models lack the microscopic simulation of the recovery process and may be marred by fine grid size requirement, and the problem of stability and numerical dispersion. Also, mathematical models for combination process, such as steam-emulsion flow, etc. are yet to be developed. In order to propose a complete numerical simulator for *in situ* combustion, one has to understand the physical consequences of the processes involved and look into mathematical models that tackle the problem.

2.2 Historical Background

Earlier researchers developed mathematical models which considered only certain aspects of the *in situ* combustion process, such as, heat transfer (Bailey and Larkin, 1959, 1960; Baker, 1962; Couch, 1962; Chu,1963; Ramey, 1959; Thomas, 1963), heat transfer with phase change(Chu, 1964), heat transfer with chemical reaction (Cooperman,1959) or three-phase flow (Wilsonet al., 1958). Even though these models helped understanding different mechanisms involved in the process, there was a need to include all these phenomena in a single mathematical model.

Gottfried (1965) was the first researcher to develop a general theory which included all these phenomena. His mathematical model included conduction-convection heat transfer with convective external heat loss, chemical reaction between air and oil, aqueous phase change, and the hydrodynamics of three phase flow. His model was essentially a black-oil type model with two additional equations for oxygen and steam transport. He used an Arrhenius-type expression for the combustion rate. He used a linear model to predict laboratory-scale *in situ* combustion performance, from which he reported optimum grid and time step size of 3 cm and 36 sec respectively. Most of the input data were not obtained from experimental studies. However, sensitivity studies showed that reaction rates depended largely on the oil content of the reservoir rather than on the oxygen concentration. Limitations of Gottfried's approach were

- gravity and capillary effects were not accounted for
- oil was considered to be the only fuel source with no allowance for coke formation and oxidation
- water and steam were not considered to be in equilibrium
- no oil vaporization was allowed.

Couch and Rodriguez (1970) used essentially the same model as Gottfried's for a study on the effect of permeability and porosity on fuel content. Smith and Farouq Ali (1971) developed a mathematical model of *in situ* combustion in a two-dimensional reservoir, with conductive heat transfer in the third dimension. They considered single-phase gas flow for a constant fuel content. They considered heat transfer by conduction and convection in the reservoir, heat losses by conduction to adjacent formations, and different permeability to gas on either side of the combustion zone. This simulator was designed for predicting sweep efficiencies in confined well patterns.

One of the phenomena largely overlooked by earlier researchers is the occurrence of low-temperature oxidation (LTO). If oxygen is used completely at the combustion front, the question of LTO does not occur. However, this is not likely to happen in *in situ* combustion and oxygen is often available at the leading front in contact with cooler residual oil. Burger and Sahuquet (1972) were the first group to show the utility of low-temperature oxidation kinetic data in the predictions of reverse combustion by numerical models. However, their model considered only heat transfer. In this same aspect, Dabbous and Fulton (1974) elaborated more on the importance of LTO in *in situ* combustion.

They showed that LTO was undesirable due to adverse effects of the reaction products on the viscosity and distillation characteristics of the crude.

Grabowski and Aziz (1977) proposed a comprehensive one dimensional *in situ* combustion model. Farouq Ali (1977) developed a two-dimensional, four-component (one oil component) IMPES combustion model. He included the effects of solubility of hydrocarbon gases in the liquids, water vaporization and condensation under equilibrium conditions, and solubility of oxygen and nitrogen, and carbon dioxide mixtures in the oil phase. He also included capillary pressure effects in the simulator. Even though his model was more complete than previous models, he did not include the effects of coke formation and oxidation. Also, material balance reported was relatively high (5% or more). Crookston *et al.* (1979) presented a mathematical formulation without some of the restrictions discussed so far. They developed a simulator which included two-dimensional flow of three-phases including gravity and capillary effects. They also included heat transfer by conduction and convection in the reservoir and heat losses to the surrounding rocks by conduction. Vaporization and condensation of both oil and water were considered by vapor-liquid equilibria. They divided oil into two pseudo components and used four chemical reactions to represent the formation of coke from the heavy pseudo component of the oil, and the oxidation of coke, heavy pseudocomponent and light pseudo component. Therefore, this was the first consistent model to have considered coke formation as well as oxidation. Essentially the same model was extended to three dimensions and solved in fully implicit form by Grabowski *et al.*(1979). The first field-scale reservoir simulation results for *in situ* combustion were reported by Youngeren (1980). He used a mixture of explicit and implicit formulation to include three phases, five components, gravity and capillary forces, heat transfer by convection and conduction within the reservoir and conductive heat loss to adjacent strata in three dimensions. However, he treated the combustion reaction by assuming that the combustion rate was limited by oxygen flux only. Consequently, this simulator could not model partially quenched wet combustion or low temperature, spontaneous ignition. The five components considered were water, non volatile (dead) oil, oxygen, and two arbitrary volatile components that partitioned between oil and gas phases. Coke formation, oxidation, and thermal cracking were left out of the formulation. Consequently, fuel laydown could not be predicted from this approach. Nevertheless, he obtained excellent agreement with experimental *in situ* combustion data. A rather comprehensive model was proposed by Coats (1980) who developed an *in situ* combustion simulator capable of handling any number of components, any number of chemical reactions, with reactants, products, and stoichiometry specified through input data. Gravity and capillary forces were incorporated along with vaporization/condensation phenomena allowing for any components to be distributed in any or all of the four phases. The solid phase used was coke and the formation permeability was allowed to vary with changing coke concentration. The numerical simulation results were obtained by neglecting thermal cracking of heavy oils. However, he obtained excellent agreement with previously published experimental data.

Rubin and Vinsome (1980) reported numerical simulation results for *in situ* combustion in one dimension using a very similar numerical technique to that reported by Coats (1980). However, they treated coke concentration following the approach reported by Crookston *et al.* (1979). Also, they incorporated a very heavy pseudocomponent of oil so that no residual oil could be present in the combustion zone. They reported comparison of numerical results with combustion tube experimental results.

In order to investigate the mechanism of fuel deposition and to identify the key kinetic parameters affecting the performance of a dry, forward combustion process, Lin *et al.* (1984) used the simulator developed previously by Crookston *et al.* (1979). They reported on the necessity to further split the light-oil components into two or more components due to sensitivity of the simulation results to the phase equilibrium K-values. They observed no sensitivity of the simulation results to reaction rates of oxidation. However, the influence of cracking reactions and stoichiometry depended mainly on the crude oil type and on whether or not the reaction was catalytic. This work, which focused on the mechanisms involved in *in situ* combustion, brought valuable insight into the incompleteness of the existing formulation of the *in situ* combustion problem.

In order to overcome some of the problems related to grid block size and dimensionality, Anis *et al.* (1983) suggested the use of pseudo functions for relative permeability and kinetic parameters as outlined previously by Camey and Emanuel (1977) in the context of CO_2 flooding. Ito and Chow (1984) introduced a pseudokinetic scheme for field-scale simulation in order to tackle grid size problem.

Rubin and Buchannan (1985) developed a fully implicit four-phase(oil, water, gas, solid fuel) numerical reservoir model for simulating *in situ* combustion (as well as hot water injection and steam injection) in multidimensional (Cartesian, radial, or curvilinear geometry) form. They used a fully implicit well model among other implicitness. They also allowed for variation in relative permeability (through end-point values) and capillary pressure (through interfacial tension) with temperature. The model was tested against laboratory experiment results. However, no field data were reported in the case of *in situ* combustion. No mention of low temperature oxidation or grid sensitivity analysis was done in this work.

Vaughn (1987) developed a one dimensional multi-component, three-phase *in situ* combustion model. In this work, essentially the same equations as Crookston *et al.* were used except that a Newton Raphson scheme with variable time step was used. Novelty of this work came from the observation that inert gas had to be replaced by four components (CO_2, CO, H_2, and N_2) along with modification of the reaction modules. In addition to the combustion and cracking reactions, four other reactions were suggested. They are:

- the secondary coke pyrolysis reaction
- the steam coke reaction
- the water-gas shift reaction
- the carbonate decomposition reaction

Thiez and Lemonnier (1988) developed a numerical simulator for modelling *in situ* combustion using four components (water, oil,oxygen and inert gas) and one reaction for fuel combustion. In representing the combustion front with only one reaction of fuel combustion, they used a new formulation using a heat release curve which improved numerical stability and gave accurate temperature distribution with large grid block sizes. They gave results of sensitivity analysis of grid sizes up to 2 meters.

2.3 Mathematical Formulations:

The generalized continuity equation for the component i may be written as:

$$\frac{\partial}{\partial t}\left[\phi \sum_{j=1}^{N_p} \rho_j S_j x_{ji}\right] = -\nabla\left(\sum_{j=1}^{N_p} \rho_j u_j x_{ji} + \mathbb{D}_{ji}\right) + \sum_{j=1}^{N_p} \rho_j u_j x_{ji}$$

$$\sum_{j=1}^{N_p} \rho_j q_j x_{ji} + \sum_{l=1}^{N_p} G_{li} + \sum_{j=1}^{N_p} N_{jri}$$

$$+\sum_{j=1}^{N_p} \sum_{\substack{k=1 \\ k \neq j}}^{N_p} N_{ijk}$$

where x_{ji} is the mole fraction of the ith component in the jth phase, $\mathbb{D}_{ji}$ is the rate of diffusion of the ith component in the jth phase and G_{li} is the rate of generation of the ith component in the *l*th chemical reaction. A total of N_r independent chemical reactions are assumed to take place between different components. N_{rai} represents chemical loss of the ith component into the rock surface through the aqueous phase. It is, therefore, assumed that the rock is water wet. N_{ijk} represents non-equilibrium mass transfer of the ith component to and from i and j phases. There is extensive evidence (Lozada and Farouq Ali, 1987, 1988) that for the most important combustion product product (CO_2), mass transfer into and from different phases does not reach equilibrium in the short time available. Consequently, these terms may be important for CO_2 propagation.

The generalized Darcy's law for each phase is given by:

$$u_j = -k \frac{k_{rj}}{\mu_j}\left(\nabla p_j - \rho_j \nabla z\right)$$

Each chemical reaction can be represented by a stoichiometric equation of the form

$$\sum_{j=1}^{N_p} S_{li} A_i = 0 \qquad (l = 1,2, \ldots ,N_r)$$

where A_i's are the different chemical components of the system and S_{li}'s are the stoichiometric coefficients of the ith component in the *l*th reaction These coefficients are positive for the products, negative for the reactants and zeros for the components not participating in the reaction.

The kinetic reaction rate (moles per unit time per unit volume) may be given by the Arrhenius equation

$$r_l = \rho_l \; \sigma_r \; (1-\phi) \; F_l \; f_l \; (C_{ji}) \; \exp \left(\frac{\Delta E_l}{RT}\right)$$

$$\text{with} \quad f_l \; (C) = \prod_{i=1}^{N_c} C_{li}^{\,bli}$$

where b_{li} is the order of the *l*th reaction with respect to the ith component, C_{li} is the molar concentration of the ith component in the phase participating in the *l*th reaction, ΔE is the activation energy, F is the frequency coefficient, ρ_s is the density and σ_s is the specific surface area of the rock.

The rate of generation of the ith component from the *l*th reaction is given by

$$G_{li} = S_{li} \; r_l$$

The total rate of generation of the ith component from all the N_r reactions is given by

$$G_{i\ \mathrm{total}} = \sum_{l=1}^{N_r} G_{li} = \sum_{l=1}^{N_r} S_{li}\, r_l$$

Diffusion in porous media is often expressed in terms of binary diffusion by lumping all components except one into one pseudo component. In terms of mole fraction, the rate of diffusion of the ith component in the jth phase may be expressed as:

$$\mathbf{D}_{ji} = - D_{ji}\, \nabla\, (\rho_j\, x_{ji})$$

In D_{ji} both dispersion and diffusion may be incoporated.

The energy balance for the system is expressed using the internal energy and the enthalpy. The energy equation may be written as:

$$\frac{\partial}{\partial t} \left[(1-\phi)\, \rho_r\, U_r + \phi \left(\sum_{j=1}^{N_p} \rho_j\, S_j \sum_{i=1}^{N_c} x_{ji}\, h_{ji} \right) + \right.$$

$$\left. + \frac{1}{2Jg_c} \left(\sum_{j=1}^{N_p} \rho_j\, u_j^2 \right) \right] = \nabla\, (K_r\, \nabla T) - \nabla \left(\sum_{j=1}^{N_p} \rho_j\, v_j \sum_{i=1}^{N_c} x_{ji}\, h_{ji} \right)$$

$$- \nabla \left(\sum_{j=1}^{N_p} \sum_{i=1}^{N_c} G_{ji}\, h_{ji} \right)$$

$$- \nabla \left(\sum_{j=1}^{N_p} \rho_j\, q_j^{*} \sum_{i=1}^{N_c} x_{ji}\, h_{ji} \right)$$

$$- \frac{K_r}{\Delta z} \frac{\partial T^{*}}{\partial z} \bigg|_{\mathrm{boundary}} - \frac{1}{2Jg_c} \nabla \left[\sum_{j=1}^{N_p} \rho_j\, \bar{u}_j\, u_j^2 \right]$$

$$- \nabla \left(\sum_{j=1}^{N_p} \tau_j\, u_j \right)$$

where T^* is the temperature in the surrounding formations, obtained by the solution of the heat balance

$$\nabla [K_r^* \nabla T^*] = \frac{\partial}{\partial t} [\rho_r^* C_{pr}^* T^*]$$

where * signifies formations surrounding the producing layer.

The phase saturations and composition constraints may be written as:

$$\sum_{j=1}^{N_p} S_j = 1 \quad \text{and} \quad \sum_{i=1}^{N_c} x_{ji} \qquad (j = 1,2,\ldots,N_p)$$

The thermal equilibrium condition requires the equality of temperature in all phases at the same point. The mechanical equilibrium requires that the pressure in different contiguous phases be different by the capillary pressure which is given as:

$$p_k - p_j = p_{ckj} \; (S_1, S_2, \ldots, S_{N_p}) \qquad (k,j = 1,2,\ldots,N_p, \; k \neq j)$$

Finally, the phase equilibrium requires for each component that the partial fugacities of a component be the same in all the phases in which that component is present. That is,

$$\frac{x_{ji}}{x_{ki}} = K_{jki} \qquad \begin{array}{l} (j,k = 1,2, \ldots,N_p, \; j \neq k) \\ (i = 1,2,\ldots,N_c) \end{array}$$

where K_{jki} is the distribution coefficient of the ith component between the jth and kth phases.

In case of an immobile phase, one or more components may be allowed to adsorb on the solid surface of the rock matrix. The saturation of the adsorbed phase is related to the surface concentration of the adsorbed component so that

$$S_{ad_i} = \frac{\rho_r \, \sigma_r \, (1-\phi)}{\rho_{ad_i} \, \phi} \, \delta_i \, C_{si}$$

where δ_i is the thickness of the adsorbed film of the ith component.

2.4 Common Assumptions:

In numerical simulators developed for modelling *in situ* combustion processes, the following assumptions have been taken frequently,

1. Water and oil phases are mutually insoluble, i.e.,

$$x_{ow} = 0, \quad x_{wi} = 0, \quad i = 1,2, \ldots, N_c$$

2. The contribution of kinetic energy and the work done by viscous forces are frequently neglected, i.e., J and τ terms are not considered in the energy equation.

3. Thermal equilibrium is considered to be spontaneous.

4. Phase equilibrium is considered to be spontaneous, that is, N_{ijk} terms are neglected in the flow equations.

5. No adsorption of any component is allowed, that is, N_{ari} is neglected in the flow equations.

6. Mass transfer between oil and gas phases is described by the two-phase equilibrium. The mass transfer of water between aqueous and gaseous phases is given by Dalton and Raoult's law:

$$x_{gw} = \frac{P_{sat}}{P_g} \quad \text{since } x_{aw} = 1$$

7. Diffusional and dispersional forces are neglected. That is, the D_{ji} term in the flow equation is omitted.

8. Heat losses through lateral reservoir boundaries are ignored.

9. All fluids are considered Newtonian.

3.0 PROBLEMS RELATED TO IN-SITU COMBUSTION MODELLING

3.1 Problems Related to Grid Size:

There are some serious problems in representing the combustion front zone with grid blocks which are usually larger in size than the burning zone. This problem leads to inaccurate distributions of pressure, temperature, and other reservoir state variables. The degree of inaccuracy depends on the grid size used in numerical simulation. The impact of inaccurate temperature distribution would be the greatest because this leads to incorrect estimation of reaction as well as convection effects on mass and energy transfer which are key factors in determining reservoir performance.

In a field situation, the combustion front, where most drastic chemical and thermal changes occur, extends only a few feet (Chu, 1980). Consequently, in order to obtain representative reaction and convection effects, ideally one has to use a grid size of a few centimeters. If this grid size has to be maintained throughout the reservoir, the simulation time will be excessive even with the fastest and most powerful computer. Hwang *et al*. (1982) *et al*. (1983) were the first groups to have focused on this problem of numerical simulation of *in situ* combustion. They specified an amount of oil to be burned per unit bulk volume of formation. The burning zone was considered to be a moving interface. For the combustion block, an infinite reaction rate was assumed. Their technique was a somewhat modified form of the technique previously suggested by Prats *et al*. (1968) and Dietz and Weijdema (1968).

Anis *et al*. (1983) investigated the effects of grid size and dimensionality on numerical simulation of *in situ* combustion processes. For the 2D case, they observed that oxygen consumption decreased as the number of blocks increased leading to increased injection pressure and lower oil recovery for higher number of grid blocks. Comparisons were also made between the results of 1D (40x1x1) and 2D (10x1x4) runs and2D (10x1x4) and 3D (5x3x4) runs. The results were considerably different. For instance, at 6000 days, cumulative production was 84% of the initial oil in place (IOIP) for the 1D run as compared to 6 % IOIP for the 2D run. Oxygen break through took only half as much time for the 2D run as that of the 1D run. Consequently, gas-oil ratio (GOR) and water-oil ratio (WOR) were significantly higher for the 2D case. Injection pressure consistently decreased as the dimension was increased from 1D to 3D. Oxygen consumption was much lower for the 3D case for which the drop in temperature was so severe that combustion could not be sustained for long. In order to overcome some of the problems related to grid block size and dimensionality, they suggested the use of pseudo functions for relative permeability and kinetic parameters as outlined previously by Camey and Emanuel (1977) in the context of CO_2 flooding.

Ito and Chow (1984) introduced a pseudokinetic scheme for field-scale simulation in order to tackle the grid size problem. They defined the reaction rate by a formula taking into account the grid block temperature and specified values of maximum reaction rate and minimum and maximum reaction temperature.

Coats (1983) introduced the concept of activation temperature to ensure that the fire would be sustained by an increase in the reaction rate when the block temperature is below the activation temperature.

Chu (1980) calculated overall relative reaction rate as a function of grid block size (varying from 0.25 to 2.5 ft). He showed that the relative reaction rate with 2.5 ft could be three orders of magnitude different from the actual reaction rate (assumed to be the one with grid size of 0.25 ft). He also showed that the calculated reaction rate may be higher or lower than the true reaction rate depending on whether a block includes a high temperature region behind the combustion front or a low temperature region in front of the combustion zone. He concluded that a block size of 10-25 ft for field simulation is totally unacceptable since the combustion zone is likely to be around only 5 ft. He suggested two possible techniques in order to solve the grid size problem. They are:

- the use of a compressional wave-type grid where a region of refined grids is concentrated in order to enclose the combustion zone and is allowed to propagate along the combustion front.
- the use of a front tracking technique, similar to that of Hwang *et al.* (1983) with the exception that the Arrhenius equation be used to describe the finite reaction rates rather than using infinite reaction rates.

Even though fixed refinement of grids in numerical simulation of petroleum related problems has been well known for a number of years, only recently (Heinemann *et al.*, 1984) dynamic grid refinement technique has been proposed. Heinnemann *et al.* (1984) introduced automatic or free formulation selection and automatic or free selection per block and time step of the implicitly computed variables. Consequently, grid refinement could be done as a function of time. Han *et al.* (1987) presented methods for ordering and solving for unknowns using dynamic local grid refinement which could also be used in the fixed refinement case.

More recently, Ewing (1986) developed data structures using local refinement and unrefinement as a function of time and space. Later on, Ewing and Lazarov (1988) developed a preconditioning technique in order to allow grid refinement in existing codes without disrupting the basic solution process. The preconditioner was used to solve separate matrix systems for the local refinements and the matrix system for the quasi uniform grid on the original domain. The quasi uniform grids overlap the local refinement region leaving corresponding matrix problems invariant when local refinement is dynamically added or removed. They presented three strategies in order to approximate flow rates across irregular faces. They are:

- point-centered grid with local refinement
- cell-centered grid with local refinement
- cell-centered grid with local refinement in a polar coordinate system

We recommend the use of this technique in numerical simulation of *in situ* combustion. In order to apply this technique in *in situ* combustion problems, grid refinement has to be matched with the propagation of the combustion front so that the sharp combustion front encounters constant dynamic refinement.

3.2 Emulsification

Although it is strongly suspected that emulsions (both oil-in-water and water-in-oil) are formed in reservoirs undergoing thermal recovery, and that these emulsion affect fluid flow, these effects have not been incorporated into numerical simulators. This is mainly due to the lack of numerical models which are capable of properly describing emulsion flow through porous media. Recently, Abou-Kassem and Farouq Ali (1988) have developed an emulsion flow model. However, this model is not applicable to a multi-phase system. More recently, Islam and Farouq Ali (1988, 1989) have shown that emulsion flow can be effectively modelled by introducing permeability reduction as a function of emulsion throughput. Their model (Islam and Farouq Ali, 1989) also incorporated emulsion breaking and reformation. Although they cited examples of only isothermal problems, their model can be easily extended for thermal applications. In this regard, more experimental work is needed in order to have a quantitative picture of surfactant generation in an *in situ* combustion process. A chemical-diffusion based kinetic model incorporated with the semi-empirical model proposed by Islam and Farouq Ali (1989) should be a start in right direction.

3.3 Choosing Proper Reactions

In studying the effect of number of reactions, there is no consensus reported by the researchers. Even though, recent researchers have attempted to increase the number of reactions considered in numerical simulation of *in situ* combustion, often the numerical results have been marred by the lack of consistent reaction data. There has been very little quantitative work done in describing one of the most important factors, namely low temperature oxidation. Due to extreme difficulty in obtaining experimental data, very little is known in most of these reactions. However, qualitatively it is known that phenomena, such as the precipitation of asphaltene may be of dual counteracting interest. For instance, asphaltene precipitation may cause significant damage to the process by creating plugging. However, the same could contribute in increasing fuel laydown in case of partial plugging. These aspects can be studied by a numerical simulator by allowing plugging due to asphaltene precipitation. A semi-empirical model is desirable in this regard.

Besides, mixing of reservoir oil (ahead of the combustion front) with the productions of low-temperature oxidation may generate other products which are not yet completely known. This phenomenon is perhaps the most ignored in present numerical simulation approaches.

3.4 Implementing Various Components In The Gas Phase:

In the existing numerical models, gases other than oxygen are lumped under 'inert gas phase'. However, the role of various gases are different. Consequently, with existing numerical models, the gas phase components are not matched with that produced in the field. By introducing this option of multi-component gas phase, the gas phase production data of the field can be matched. This will also identify the role of different gaseous components and simulate the gas-drive ahead of the combustion zone. The existence of this process has been known for some time and has been quantified recently (Islam, 1989). However, no previous work has incorporated this feature in the model to match gas production data of the field.

3.5 Channelling Phenomena

The fact that in many field situations, oxygen breakthrough occurs when more than 90% of oil remains in place suggests that channelling plays an important role in *in situ* combustion processes (Farouq Ali, 1972; Ito and Chow, 1988). In order to model channelling phenomena, Ito and Chow (1988) used the following expression for overall chemical reaction rate constant:

$$\frac{1}{r_{overall}} = \frac{1}{r} + \frac{1}{\eta}$$

where r is the chemical reaction constant and η is the diffusivity of oxygen. They rendered η dependent on flow rate, temperature, and degree of combustion, hence, treating it as a 'fudge factor' to represent the contact efficiency of the reactants in a simulator. Even though, this approach was the first effort to break away from simulation of idealistic burn situation, considering the complexity of the process, a lot more effort should be placed on this topic.

It is understood that, *in situ* combustion should provoke two different types of channelling, namely

- channels due to viscous fingering
- channels due to macroscopic heterogeneity

The former type is expected due to high mobility contrast between injected oxygen and the reservoir oil. This is even more severe in the case of heavy oil reservoirs. Even though recent theories (Bentsen, 1982) have given insight into how to perform experiments in order to model viscous fingering, very little has been done in numerical simulation of such a phenomenon. Recently, Neighm *et al.* (1989) have shown some techniques for modelling viscous fingers.

Channelling due to macroscopic heterogeneity is more amenable to resolution if the reservoir is well defined. However, this is often not the case and numerical simulation of even known heterogeneity may impose absurd computational requirements.

Results can be greatly improved if dispersion and diffusion terms are included at least for the gaseous phases. This will effectively model modified reaction surface available to the reacting gases.

3.6 Non Equilibrium Phenomena

Most numerical simulators assume that both thermal and phase equilibria are achieved spontaneously. However, this assumption may not be valid, especially when channelling occurs in the reservoir. Ito (1984) introduced this phenomena through a super-upstream weighting method. A more rigorous technique should incorporate thermal as well as phase non-equilibrium (Lozada and Farouq Ali, 1987). Islam (1989; Islam and Farouq Ali, 1988) has shown that the effect of various non-equilibrium phenomena in the case of chemical injection. Almost all of these apply to *in situ* combustion processes for which *in situ* surfactant generation may lead to variable interfacial tension thereby varying the degree of emulsification, etc. Besides, there have been a few reports on time-dependent heat transfer coefficients (Satman *et al.*, 1984) even though no experimental results have been reported to support the numerical exercise.

3.7 Multiplicity of Flow Solutions

Another aspect of numerical simulation has been pointed out only recently by a series of papers by Islam and Nandakumar (1985,1986, 1988a, 1988b, 1988c, 1989). They pointed out that, due to non-linearity of the energy balance equation, there might be multiple solutions to one set of thermal fluid flow equations. Users of *in situ* combustion and steam-injection models have often cited examples of converging to the 'wrong root'. However, no one ever attempted to relate this phenomenon to true existence of multiple solutions. Some independent experimental studies have reported such multiple solutions for various thermal fluid flow problems (Elder, 1967). The implication of this phenomenon in multi-phase systems, such as, *in situ* combustion is yet to be investigated.

4.0 CONCLUSIONS

A state-of-the-art review of *in situ* combustion modeling is undertaken. On the basis of the review of numerical and experimental review, elements for an ideal *in situ* combustion simulator are proposed. The main difficulty in developing such a simulator is identified to be the lack of experimental data. Also lacking is mathematical models for various reactions actually taking place in the reservoir. With current knowledge, a guideline is provided for systematic experimental and numerical investigation in order to develop an ideal *in situ* combustion simulator.

5.0 NOMENCLATURE

C_{si}	surface concentration of component i
g	acceleration due to gravity
g_c	conversion factor
h_{ji}	partial molar enthalpy for comp. i in phase j
k	permeability
K_r	conductivity of reservoir rock
N_p	number of phases
p_i	pressure in phase i
p_c	capillary pressure
q	injection/production rate
T	temperature
t	time
ϕ	porosity
μ	viscosity
ρ	density
τ_j	stress-strain tensor for phase j

6.0 REFERENCES:

Abou-Kassem, J.H., and Farouq Ali, S.M., 1986, "Flow of Non-Newtonian Fluid in Porous Media", SPE paper no. 15954, presented at the SPE Eastern Regional Meet. held in Columbus, Ohio.

Abou-Kassem, J.H., and Farouq Ali, S.M., 1986, "A Mathematical Representation of Single Phase Emulsion Flow in Porous Media", paper presented at the First Int. Symp. on Enhanced Oil Rec., held in Maracaibo, Venezuela.

Abu-Khamsin, S.A., W.E. Brigham and H.J. Ramey, Jr., "Reaction Kinetics of Fuel Formation for In-Situ Combustion", SPE Reservoir Engineering, 1308-1316, November 1988.

Adegbesan, K.O., J.K. Donnely, R.G. Moore and D.W. Bennion, "Low Temperature Oxidation Kinetic Parameters for In Situ Combustion Numerical Simulation", SPE Reservoir Engineering, 573-582, November 1987.

Anis, M., Hwang, M.K., and Odeh, A.S., "A Sensitivity Study of the Effect of Parameters on Results From An In-Situ Combustion Simulator", Soc. Pet. Eng. J., April, (1983), 259-264.

Appelby, W.G., J.W. Gibson and G.M. Good, "Coke formation From Catalytic Cracking", Ind. Eng. Chem. Process Des. Dev., 1, 102-110, 1962.

Babu, D.R. and D.E. Cormack, "Effect of Low Temperature Oxidation on the Composition of Athabasca Bitumen", Fuel, 63, 858-861, June 1984.

Babu, D.R. and D.E. Cormack, "Effect of Oxidation on the Viscosity of Athabasca Bitumen", Can. J. Chem. Eng., 62, 562-564, August 1984.

Bailey, H.R., and Larkin, B.K., "Heat Conduction in Underground Combustion", Trans. AIME, vol. 216, (1959), 123.

Bailey, H.R., and Larkin, B.K., "Conduction - Convection in Underground Combustion", vol. 217, (1960), 321.

Baker, P.B., "Temperature Profiles in Underground Combustion", Soc. Pet. Eng. J., March, (1962), 21.

Bardon, C. and C. Gadelle, "Essai de Laboratoire Pour L'Etude de la Combustion In-Situ", paper presented at the French-Soviet Symposium on Enhanced Oil Recovery, Moscow, May 1977.

Bentsen, R.G., "A New Approach to Instability Theory in Porous Media", Soc. Pet. Eng. J., vol. 15, (Oct., 1985) 765-779.

Bousaid, I.S. and H.J. Ramey, Jr., "Oxidation of Crude Oils in Porous Media", Soc. Pet. Eng. J., 137-148, June 1968; Trans., AIME, 243.

Blouri, B., F. Hamdan and D. Herault, "Mild Cracking of High Molecular Weight Hydrocarbons", Ind. Eng. Chem. Process Des. Dev., 24, 30-37, 1985.

Burger, J.G. and B.C. Sahuquet, "Laboratory Research on Wet Combustion", J. Pet. Tech., 1137-1146, October 1973.

Camey, J.P., and Emanuel, A.S., "Effect of Grid Size in the Compositional Simulation of CO_2 Injection", paper SPE 6894, presented at the SPE Ann. Conf. and Exhib. held in Denver, CO, 1977.

Chakma, A., E. Chornet, R.P. Overend and W.H. Dawson,"Heavy Oil Upgrading Using Halide Catalysts in a Bubbling Microautoclave", Preprints of ACS Div. of Fuel Chemistry, 31(1), 355-363, June 1988.

Chakma, A., and Islam, M.R., "The Role of Asphaltenes in the Visbreaking of Heavy Oils/Bitumens", CIM paper no. 89-40- , to be presented at the 40th Ann. Tech. Meet. of the PS of the CIM, to be held in Banff, May, 1989.

Chornet, E., University of Sherbrooke, personal communication, 1988.

Chu, C., "Two-Dimensional Analysis of a Radial Heat Wave", J. Pet. Tech., Oct. (1972), 1137.

Chu, C., "The Vaporization - Condensation Phenomena in a Linear Heat Wave", Soc. Pet. Eng. J., June (1964), 85.

Chu, C., "The Curse of Grid Size In Combustion Modelling", paper presented at the AOSTRA Modelling Workshop, held in Edmonton, Jan., 1980.

Chu, C. and P.B. Crawford, "In Situ Combustion", in Improved Oil Recovery Interstate Oil Commission, Oklahoma City, Oklahoma, 1983, p 253.

Coats, K.H., "In-situ Combustion Model", Soc. Pet. Eng. J., Dec. (1980), 533-554.

Coats, K.H., "Some Observations on Field-Scale Simulation of the In-Situ Combustion Process", paper SPE 12247 presented at the 1983 SPE Reservoir Simulation Symposium, San Francisco, Nov. 15-18, 1983.

Cooperman, P., "Some Criteria for the In-situ Combustion of Crude Oil", J. App. Phys., vol. 30, Sept. (1959).

Couch, E.J., and Rodriguez, H.V., "Effects of Porosity and Permeability on In-situ Combustion Fuel Consumption", SPE paper no. 2873, presented at the 45th Ann. Fall Meet. of SPE, Houston, 1970.

Crawford, P.B. and W. A. Cunningham, "Carbon Formation in Cat Cracking", Pet. Refiner, 169-173, January 1956.

Crookston, H.B., W.E. Culham and W.H. Chen, "A Numerical Simulation Model For Thermal Recovery Processes", Soc. Pet. Eng. J., 37-58, February, 1979.

Dabbous, M.K., and Fulton, P.F., "Low-Temperature-Oxidation Reaction Kinetics and Effects on the In-situ Combustion Process", Soc. Pet. Eng. J., June (1974), 253-262.

Dietz, D.N. and J. Weijdema, "Wet and Partially Quenched Combustion", J. Pet. Tech., 411, April 1968.

Drici, O. and Vossoughi, S., "Study of Surface Effect on Crude Oil Combustion by Thermal Analysis Technique", JPT, (April,1985) 731-735.

Elder, J.W., "Steady Free Convection in a Porous Medium Heated From Below", J. Fluid Mech., vol. 27 (1), (1967), 29-48.

El-Khatib, N., "A Mathematical Model of Thermal Oil Recovery in a Forward In-Situ Combustion Process", Ph.D. Dissertation, U. of Pittsburgh, 1973.

Ewing, R.E., "Efficient Adaptive For Fluid Flow Applications", Comp. Meth. Appl. Mech. Eng., vol. 55 (1986), 89-103.

Ewing, R.E., and Lazarov, R.D., "Adaptive Local Grid Refinement", SPE paper no. 17806, presented at the SPE Rocky Mountain Regional Meet., held in Casper, WY, 1988.

Farouq Ali, S.M., "A Current Appraisal of In-Situ Combustion Field Test", JPT (April, 1972) 477-482.

Farouq Ali, S.M., "Multi-phase, Multidimensional Simulation of In-situ Combustion", paper SPE 6896, presented at the 52nd Ann. Fall Tech. Conf. and Exhib. of the SPE of AIME, held in Denver, CO, 1977.

Fassihi, M.R. and W.E. Brigham, "Analysis of Fuel Oxidation in In-Situ Combustion Oil Recovery", U.S. DOE publication, DOE/ET/12056-26 (DE 82019075), Aug. 1982.

Fassihi, M.R., W.E. Brigham and H.J. Ramey, Jr., "Reaction Kinetics of In Situ Combustion: Part 2 - Modelling", Soc. Pet. Eng. J., 408-416, August 1984.

Garon, A.M. and R.J. Wygal, "A Laboratory Investigation of Fire-Water-Flooding", Soc. Pet. Eng. J., 537, December 1974.

Gates, B.C., J.R. Katzer and G.C.A. Schuit, "Chemistry of Catalytic Processes", McGraw Hill Book Co., New York, 1979, p-9.

Geniesse, J.C. and R. Reuter, "Reaction Velocity Constants of Oil Cracking", Ind. Eng. Chem. 219-222, February 1932.

Gottfried, B.S., "A Mathematical Model of Thermal Recovery in Linear Systems", SPE J., (Sept., 1965) 196-210.

Grabowski, J.W., Vinsome, P.K., Lin, R.C., Behie, A., and Rubin, B., "A Fully Implicit General Purpose Finite Difference Thermal Model For In-Situ Combustion and Steam", paper SPE 8396, presented at the 54th Ann. Fall Tech. Conf. and Exhib., held in Las Vegas, NE, 1979.

Greaves, M., R.W. Field and V.A. Adewusi, "In Situ Combustion Kinetic Studies of Medium Heavy Crude Oil", Che. Eng. Res. Des., 66, 328-338, July 1988.

Han, D.K., Han, D.L., Yan, C.Z., and Peng, L.T., "A More Flexible Approach of Dynamic Local Refinement for Reservoir Modeling", SPE paper 16014, presented at the Nith SPE Symp. on Res. Sim. held in San Antonio, Texas, 1987.

Hardy, W.C. *et al*. "In-Situ Combustion in a Thin Reservoir Containing High Gravity Oil", JPT, 199-208, Feb. 1972; Trans., AIME, 253.

Henderson, J.H. and L. Weber, "Physical Upgrading of Heavy Crude Oils by the Application of Heat", J. Can. Pet. Tech., 206-212, Oct. 1965.

Hosoi, T. and H.G. Keister, "Ethylene From Crude Oil", Chem. Eng. Prog., 17(11), 63-67, 1975.

Hwang, M.K., W.R. Jines and A.S. Odeh, "An In-Situ Combustion Process Simulator With a Moving Front Presentation", Soc. Pet. Eng. J., April, (1982), 271-279.

Hwang, M.K., Jines, W.R., and Odeh, A.S., "An In-situ Combustion Process Simulator with a Moving Front Representation", Soc. Pet. Eng. J., April, (1982), 271-279.

Hayashitani, M., D.W. Bennion, J.K. Donnelly and R.G. Moore, "Thermal Cracking Models for Athabasca Oil Sands Oil", paper SPE 7549, presented at the 53rd Annual Fall Technical Conference and Exhib. of SPE-AIME, Houston, Texas, Oct. 1-3, 1978.

Heinemann, Z.E., Gerken, G., and von Hantelmann, G., "Using Local Grid Refinement in a Multiple-Application Reservoir Simulator", SPE paper no. 12255, presented at the Reservoir Simulation Symp. held in San francisco, CA, 1983.

Hughes, R., V.M. Kamath and D. Price, "Kinetics of In-Situ Combustion for Oil Recovery", Chem. Eng. Res. Des., 65, 23-28, January 1987.

Illes, V., K. Welther and I. Pleszkats, "Pyrolysis of Liquid Hydrocarbons, II. Overall Decomposition Rates For Liquid Hydrocarbons", Acta Chim. (Budapest), 78(4), 357, 1973.

Islam, M.R., and Erno, B.P., "The Role of Combustion Gases in Recovering Oil in In-situ Combustion Process", NHRC internal report, to appear in Feb., 1989.

Islam, M.R., and Farouq Ali, S.M., "An Experimental and Numerical Study of Blockage of a Mobile Water Zone by an Emulsion", paper no. 133, Proceeding of the UNITAR/UNDP Fourth Int. Conf. on Heavy Crude and Tar Sands, held in Edmonton, 1988.

Islam, M.R., and Farouq Ali, S.M., "Numerical Simulation of Alkaline/Polymer/ Cosurfactant Floodings" paper no. 163, Proceeding of the UNITAR/UNDP Fourth Int. Conf. on Heavy Crude and Tar Sands, held in Edmonton, 1988.

Islam, M.R., and Farouq Ali, S.M., "A Complete Scaling Technique For In-Situ Combustion Experiments", paper 25d, paper presented at the 38th Can. Chem. Eng. Conf., held in Edmonton, 1988.

Islam, M.R., Chakma, A., and Farouq Ali, S.M., "Non-Equilibrium Phenomena in Chemical Flooding: Experimental and Numerical Approach", to be presented at the Fifth European Conference on Improved Oil Recovery, Budapest, Hungary, April, 1989.

Islam, M.R., and Farouq Ali, S.M., "Numerical Simulation of Emulsion Flow Through Porous Media", CIM paper no. 89-40-68, to be presented at the 40th Ann. Tech. Meet. of the PS of the CIM, to be held in Banff, May, 1989.

Islam, M.R., and Nandakumar, "Mixed Convection Flow in Fluid Saturated Porous Media in the Non-Darcy Regime", proceeding of the Fourth Int. Conf. on Numerical Methods in Laminar and Turbulent Flow, held in Swansea, U.K., 1985.

Islam, M.R., and Nandakumar, K., "Multiple Solution For Buoyancy-Induced Flow in Saturated Porous Media For Large Peclet Numbers", ASME, J. Heat Transfer, vol. 108, (Nov., 1986), 866-871.

Islam, M.R., and Nandakumar, K., "Mixed Convection Heat Transfer in Porous Media in the Non-Darcy Regime", Can. J. Chem.Eng., (Jan., 1988), 68-74.

Islam, M.R., and Nandakumar, K., "Cellular Flow Pattern Evolution in a Porous Duct With Internal Heat Generation", paper 15a, presented at the 38th Ann. Conf. of the Can. Soc. Chem. Eng., held in Edmonton, 1988.

Islam, M.R., and Nandakumar, K., "Cellular Flow Pattern Evolution in a Porous Duct With Internal Heat Generation", paper submitted for publication in the Int. J. of Heat and Mass Transfer.

Islam, M.R., and Nandakumar, K., "Cellular Flow Pattern Evolution in An Inclined Porous Medium With Internal Heat Source", to be presented at the AIChE National Meeting to be held in Philadelphia, U.S.A., 1989.

Islam, M.R., "The Role of Combustion Gases in Recovering Oil in In-situ Combustion Process", NHRC Internal Report, 1989.

Ito, Y., "The Introduction of the Microchanneling Phenomenon to Cyclic Steam Stimulation and Its Application to the Numerical Simulator (Sand Deformation Concept), Soc. Pet. Eng. J. (Aug., 1984) 417-430.

Ito, Y. and A.K. Chow, "A Field Scale In-Situ Combustion Simulator With Channeling Considerations", SPE Reservoir Eng., 419-430, May 1988.

Kemp, R.R.D. and Wojciechowski, B.W., "The Kinetics of Mixed Feed Reactions", Ind. Eng. Chem. Fundam., 13, 332-336, 1974.

Kossiakoff, A., and Rice, F.O., J. Am. Chem. Soc., vol. 65, (1943) 519.

Kunzru, D., Y.T. Shah and E.B. Stuart, Ind. Eng. Chem. Process Des. Dev., 11, 605, 1972.

Lin, C.Y., W.H. Chen, S.T. Lee and W.E. Culham, "Numerical Simulation of Combustion Tube Experiments and the Associated Kinetics of In-Situ Combustion Processes", Soc. Pet. Eng. J., Dec. (1984), 657-666.

Lin, C.Y., W.H. Chen and W.E. Culham, "New Kinetic Models For Thermal Cracking of Crude Oils in In-Situ Combustion Processes", paper SPE 13074, presented at the 59th Annual Technical Conference and Exibition of SPE, held in Houston, Texas, September 16-19, 1984.

Lozada, D., and Farouq Ali, S.M., "New Sets of Scaling Criteria For Partial Equilibrium Immiscible Carbon Dioxide", CIM paper no. 87-38-23, presented at the 38th Ann. Tech. Meet. of the PS of the CIM, held in Calgary, 1987.

Madwick, G.G., C.H. Amberg and W.S. Peterson, "The Pyrolysis of a Heavy Crude Oil in a Fluidized Bed", Can. J. Chem. Eng., 65-70, April 1959.

Medorskii, S., "Thermal Decomposition of Organic Polymers", Mir Publications, Moscow, 1967.

Meyers, K.O., M.R. Fassihi and P.F. Basile, "Low Temperature Oxidation of Viscous Crude Oils", paper SPE 15648, presented at the 61st Annual Technical Meeting of SPE held in New Orleans, LA, October 5-8, 1986.

McNab, J.G., P.V. Smith, Jr. and R.L. Betts, "The Evolution of Petroleum", Ind. Eng. Chem., 2556-2563, November, 1952.

Miller, D.B., Ind. Eng. Chem. Process Des. Dev., 2, 220, 1963.

Millour, J.P., R.G. Moore, D.W. Bennion, M.G. Ursenbach and D.N. Gie, "A Simple Implicit Model for Thermal Cracking of Crude Oils", paper SPE 14226, presented at the 60th Annual Technical Conference and Exibition of SPE held in Las Vegas, NV, September 22-25, 1985.

Moore, R.G., D.W. Bennion, J.P. Millour, M.G. Ursenbach and D.N. Die, "Comparison of the Effect of Thermal Cracking and Low Temperature Oxidation on Fuel Deposition During In Situ Combustion", paper presented at the DOE Conference, Wyoming, 1986.

Moore, R.G, D.W. Bennion and M.G. Ursenbach, "A Review of In Situ Combustion Mechanisms", paper no. 50, preprints of the UNITAR/UNDP International Conference on Heavy Crudes and Tar Sands, Vol. V, Edmonton, Alberta, August 7-12, 1988.

Monin, J.C. and A. Audibert, "Laboratory Simulation of Thermal Changes of Crudes During Thermal Recovery", Proc. of the Third International Conference on Heavy Crude and Tar Sand held in Long Beach, CA, July 22-31, 1985.

Monin, J.C. and A. Audibert, "Thermal Cracking of Heavy Oil/Mineral Matrix Systems", Paper SPE 16269, presented at the SPE International Symposium on Oilfield Chemistry held in San Antonio, Texas, February 4-6, 1987.

Nghiem, L. and Li, Y.K., "A Method for Modeling Unstable Displacements in Compositional Simulation", SPE paper no. 18439, presented at the 1989 SPE Symp. on Res. Simulation, Houston, 1989.

Parish, D.R. and F.F. Craig, Jr., "Laboratory Study of a Combination of Forward Combustion and Waterflooding - the COFCAW Process", J. Pet. Tech. 735-761, June 1969.

Nace, D.M., S.E. Voltz and V.W. Weekman, Jr., "Application of a Kinetic Model for Catalytic Cracking", Ind. Eng. Chem. Process Des. Dev., 10, 530-538, 1971.

Phillips, C.R., N.I. Haidar and Y.C. Poon, "Kinetic Models For the Thermal Cracking of Athabasca Bitumen", Fuel, 64, 678-691, 1985.

Prats, M., Jones, R.F., and Truitt, N.E., "In-Situ Combustion Away From Thin, Horizontal Gas Channels", Soc. Pet. Eng. J., (March, 1968), 18-32.

Rice, F.O., "The Thermal Decomposition of Organic Compounds From the Standpoint of Free Radical III. The Calculation of the Products From Paraffin Hydrocarbons", J. Am. Chem. Soc., 55, 3035, 1933.

Rice, F.O. and E. Teller, "The Role of Free Radicals in Elementary Organic Reactions", J. Chem. Phys., 6,489, 1938, 7,199, 1939.

Rubin, B., and Buchannan, W.L., "A General Purpose Thermal Model", Soc. Pet. Eng. J., April (1985), 202-214.

Rubin, B., and Vinsome, P.K.W., "The Simulation of the In-Situ Combustion Process in One Dimension Using a Highly Implicit Finite Difference Scheme", J. Can. Pet., Oct.-Dec., (1980), 68-76.

Satman, A., Zolotukhin, A.B., and Soliman, M.Y., "Application of the Time-Dependent Overall Heat Transfer Coefficient Concept to Heat-Transfer Problems in Porous Media", Soc. Pet. Eng. J., (Feb., 1984) 107-112.

Severin, D., O. Glinzer, H. Killesreiter and H.J. Newman, "The Quiet Oxidation of a Crude Oil and the Effect on its Viscosity", Erdol und Kohl-Erdgas, 36(3), 127-130, March 1983.

Smith, J.T., and Farouq Ali, S.M., "Simulation of In-Situ Combustion in a Two-Dimensional System", paper SPE 3594, presented at the SPE-AIME 46th Ann. Fall Meet., Denver, CO, 1971.

Sukhonov, A.N. and M.D. Tilicheev, "Cracking in Liquid Phase", Neftianoe Izdatelstvo NTU VSNCh USSR, Moscow, 1928, p. 145.

Tanabe, K., Solid Acids and Bases - Their Catalytic Properties, Academic Press, New York, 1970. pp 105, 127.

Thiez, P.L., and Lemonnier, P., "An In-Situ Combustion Reservoir Simulator With a New Representation of Chemical Reactions", paper SPE 17416, presented at the SPE Calif. Reg. Meet., held in Long Beach, CA, 1988.

Thomas, G.W., "A Study of Forward Combustion in a Radial System Bounded by Permeable Media", J. Pet. Tech., Oct., (1963), 1145.

Vaughn, P., "Mathematical Modelling for In Situ Thermal Recovery Processes in Tar Sand: Model Description and Verification", *In Situ*, vol. 11, (1987) 169-189.

Venuto, P.B. and E.T. Habib, Jr., Fluid Catalytic Cracking With Zeolite Catalysts, Marcell Dekker Inc., New York, 1979, p 121.

Vossoughi, S. *et al.* "Automation of An In-Situ Combustion Tube and Study of the Effect of Clay on the In-Situ Combustion Process", Soc. Pet. Eng. J., 493-502, Aug., 1982.

Weekman, V.W., Jr., and D.M. Nace, "Kinetics of Catalytic Cracking Selectivity in Fixed, Moving and Fluid Bed Reactors", AIChE J., 16, 397-404, 1970.

Wilson, L.A. Reed, R.L., Reed, D.W., Clay, R.R., and Harrison, N.H., "Some Effects of Pressure on Forward and Reverse Combustion", Soc. Pet. Eng. J., June (1963), 127-137.

Wu, C.H. and P.F. Fulton, "Experimental Simulation of the Zones Preceding the Combustion Front of an In-Situ Combustion Process", Soc. Pet. Eng. J., 11, 38, 1971.

Youngren, G.K., "Development and Application of an In-Situ Combustion Reservoir Simulator", Soc. Pet. Eng. J., 39-51, February (1980), 39-51.